

Load Calculation Applications Manual

Second Edition

Jeffrey D. Spitler

SI Edition



ISBN 978-1-936504-76-3

©2009, 2014 ASHRAE
1791 Tullie Circle, NE
Atlanta, GA 30329
www.ashrae.org

All rights reserved.

Printed in the United States of America

Cover design by Tracy Becker.

ASHRAE is a registered trademark in the U.S. Patent and Trademark Office, owned by the American Society of Heating, Refrigerating and Air-Conditioning Engineers, Inc.

ASHRAE has compiled this publication with care, but ASHRAE has not investigated, and ASHRAE expressly disclaims any duty to investigate, any product, service, process, procedure, design, or the like that may be described herein. The appearance of any technical data or editorial material in this publication does not constitute endorsement, warranty, or guaranty by ASHRAE of any product, service, process, procedure, design, or the like. ASHRAE does not warrant that the information in the publication is free of errors, and ASHRAE does not necessarily agree with any statement or opinion in this publication. The entire risk of the use of any information in this publication is assumed by the user.

No part of this publication may be reproduced without permission in writing from ASHRAE, except by a reviewer who may quote brief passages or reproduce illustrations in a review with appropriate credit, nor may any part of this publication be reproduced, stored in a retrieval system, or transmitted in any way or by any means—electronic, photocopying, recording, or other—without permission in writing from ASHRAE. Requests for permission should be submitted at www.ashrae.org/permissions.

Library of Congress Cataloging-in-Publication Data

Spitler, Jeffrey D.

Load calculation applications manual / Jeffrey D. Spitler. -- Second edition, SI edition.
pages cm

Includes bibliographical references and index.

ISBN 978-1-936504-76-3 (hardcover : alk. paper) 1. Air conditioning--Efficiency. 2. Cooling load--Measurement. 3. Heating load--Measurement. 4. Heating. I. American Society of Heating, Refrigerating and Air-Conditioning Engineers. II. Title.
TH7687.5.S683 2014b
697.9'3--dc23

2014033520

ASHRAE STAFF

SPECIAL PUBLICATIONS

Mark S. Owen

Editor/Group Manager of Handbook and Special Publications

Cindy Sheffield Michaels

Managing Editor

James Madison Walker

Associate Editor

Sarah Boyle

Assistant Editor

Lauren Ramsdell

Editorial Assistant

Michshell Phillips

Editorial Coordinator

PUBLISHING SERVICES

David Soltis

Group Manager of Publishing Services and Electronic Communications

Jayne Jackson

Publication Traffic Administrator

Tracy Becker

Graphics Specialist

PUBLISHER

W. Stephen Comstock

This publication was supported by ASHRAE Research Project RP-1616 and was prepared under the auspices of TC 4.1, Load Calculation Data and Procedures.

Results of cooperative research between ASHRAE and Oklahoma State University.

About the Author

Jeffrey D. Spitler, PhD, PE, is Regents Professor and OG&E Energy Technology Chair in the School of Mechanical and Aerospace Engineering at Oklahoma State University, where he teaches classes and performs research in the areas of heat transfer, thermal systems, design cooling load calculations, HVAC systems, snow-melting systems, and ground-source heat pump systems. He is also the Fulbright Distinguished Chair of Alternative Energy Technology at Chalmers University of Technology in Gothenburg, Sweden for the 2014–2015 academic year.

He has worked with a wide range of research sponsors, including ASHRAE, the U.S. Department of Energy, the Federal Highway Administration, York International Corporation, and ClimateMaster. He is a past president of the International Building Performance Simulation Association and is an ASHRAE Fellow.

Spitler has served on several ASHRAE technical committees and standing committees. He currently serves on ASHRAE Technical Committee 6.8, Geothermal Heat Pump and Energy Recovery Applications, and the Conferences and Expositions Committee. He has authored or coauthored more than 120 technical papers and six books, including the *Annotated Guide to Load Calculation Models and Algorithms*.

Any updates/errata to this publication will be posted on the ASHRAE Web site at www.ashrae.org/publication_updates.

Preface to the Second Edition

To the casual observer, the need for a new load calculation manual may not be self-evident. Yet, changes in lighting and equipment commonly used in buildings require new data, new methods that are more widely applicable have become available, and other newer data have become available since the first edition was originally published in 2008. These new data and methods have been produced by ASHRAE-funded research and by volunteers working on ASHRAE technical committees (TCs). These effort include the following:

- TC 4.1, Load Calculation Data and Procedures, and their contractors (RP-1482) have produced new internal heat gain data for office equipment.
- TC 4.1 and TC 4.5, Fenestration, and their contractors (RP-1311) have developed new methods and data for computing the effects of internal shading on solar heat gains.
- TC 4.1 and TC 5.10, Kitchen Ventilation, and their contractors (RP-1326) have produced a complete new data set on heat gains from kitchen equipment based on experimental measurements.
- TC 4.2, Climatic Information, and their contractors have produced new weather data (RP-1613) for over 6000 stations worldwide based on the years 1986–2010. TC 4.2 also produced a new ASHRAE clear-sky model (RP-1453) that is applicable worldwide—a significant improvement over the old model, which was only valid for the continental United States. TC 4.2 has also developed improved methods (RP-1363) for generating design day temperature profiles.
- TC 4.4, Building Materials and Building Envelope Performance, has provided a major revision of the building thermal properties data.

In addition to acknowledging the members of the above technical committees and their contractors, I would also like to thank the members of the Project Monitoring Subcommittee who have overseen this work: Steve Bruning, Jim Pegues, Bob Doeffinger, Larry Sun, and Chris Wilkins. Their oversight and suggestions have been invaluable.

I have been assisted on this project by three students at Oklahoma State University: a graduate student, Laura Southard, and two undergraduate students, Jimmy Kim and Amy Wong, who have helped with developing revised examples and source code for the changes to the accompanying spreadsheets.

Putting together this book from a set of the author's Word files was a big task requiring quite a bit of attention to detail. I greatly appreciate the work of the ASHRAE staff, especially Sarah Boyle, assistant editor of Special Publications, in editing and typesetting the book. Cindy Michaels, Managing editor of Special Publications, was also very helpful in getting me access to handbook chapters as soon as they became available. Thanks to both of you!

I would like to take the author's prerogative to note three longtime ASHRAE TC 4.1 members who passed away during 2011 and 2012. Lynn G. Bellenger was not only an active TC 4.1 member, but very active in all areas of ASHRAE, serving as the first female ASHRAE President in 2010 and 2011. Lynn was an encouragement to many society members.

Two other TC 4.1 stalwarts, Thomas B. Romine, Jr. and Curtis O. Pedersen, both passed away in July of 2012. Tom was a consulting engineer in Fort Worth, Texas who ably represented the viewpoint of the consulting engineer on the technical committee and helped me keep the end user in mind when I was working on some of the earlier load calculation manuals. Curt was a professor at the University of Illinois at

Load Calculation Applications Manual (SI), Second Edition

Urbana-Champaign, my PhD advisor, an investigator on several load calculation-related research projects, and proponent of using fundamental methods—i.e., the heat balance method—for load calculations. Both men have had a great impact on the load calculation methodologies presented in this book.

Jeffrey D. Spitler, PhD, PE

Preface

This manual is the fourth in a series of load calculation manuals published by ASHRAE. The first in the series, *Cooling and Heating Load Calculation Manual*, by William Rudoy and Joseph Cuba, was published in 1980. A second edition, by Faye McQuiston and myself, was published in 1992 and focused on new developments in the transfer function method and the cooling load temperature difference method. Subsequent to the second edition, ASHRAE Technical Committee 4.1, Load Calculations Data and Procedures, commissioned additional research. This research led to the adaptation of the heat balance method for use in load calculation procedures and development of the radiant time series method (RTSM) as the recommended simplified procedure. Both methods were presented in the third volume of this series—*Cooling and Heating Load Calculation Principles*, by Curtis Pedersen, Daniel Fisher, Richard Liesen, and myself.

The *Load Calculation Applications Manual*, also sponsored by TC 4.1, builds on the past three, and some parts are taken directly from previous versions. New developments in data and methods have led to numerous revisions. This manual, intended to be more applications-oriented, includes extensive step-by-step examples for the RTSM.

This work, more so than many technical books, represents the work of many individuals, including the following:

- Authors, named above, of the previous three versions
- Numerous ASHRAE volunteers and researchers who have developed material for the ASHRAE Handbook that has now been incorporated
- Members of the Project Monitoring Subcommittee, including Chris Wilkins, Steve Bruning, Larry Sun, and Bob Doeffinger, who have provided extensive comments, guidance, and direction
- My graduate student, Bereket Nigusse, who has developed most of the spreadsheets underlying the examples and whose doctoral research has led to a number of developments in the RTSM that are incorporated into this manual

The contributions of all of these individuals are gratefully acknowledged.

Jeffrey D. Spitler, PhD, PE

Contents

Preface	vii
Preface to the Second Edition	ix
Chapter One	
Introduction	1
Chapter Two	
Fundamentals of Heat Transfer and Thermodynamics	5
Chapter Three	
Thermal Property Data	19
Chapter Four	
Environmental Design Conditions	79
Chapter Five	
Infiltration	93
Chapter Six	
Internal Heat Gain	117
Chapter Seven	
Fundamentals of the Radiant Time Series Method	139
Chapter Eight	
Application of the RTSM—Detailed Example	171
Chapter Nine	
Air Systems, Loads, IAQ, and Psychrometrics	207
Chapter Ten	
Heating Load Calculations	231
Chapter Eleven	
Heat Balance Method	241
Appendix A	
Psychrometric Processes—Basic Principles	251
Appendix B	
Spreadsheet Implementation of the RTSM	273
Appendix C	
Calculation of CTSFs and RTFs	301
Appendix D	
Solar Radiation and Heat Gain	307
Appendix E	
Treatment of Thermal Bridges	319
Appendix F	
Treatment of Uncontrolled Spaces	327
Appendix G	
Correction Factor for High-Conductance Surface Zones	333
Index	337

This manual focuses on two methods for calculating cooling loads in nonresidential buildings—the heat balance method (HBM) and the radiant time series method (RTSM). The two methods presented are based on fundamental heat balance principles, directly so in the case of the HBM, and less directly so in the case of the RTSM. Both methods were first fully presented for use in design load calculations in the predecessor to this volume, *Cooling and Heating Load Calculation Principles* (Pedersen et al. 1998). Since that time, there have been a number of developments in the RTSM. This publication attempts to bring the previous volume up to date, incorporate new developments, and provide a more in-depth treatment of the method. This edition incorporates recent improvements in available data for weather, building materials, fenestration, and internal heat gains and improved methods for predicting clear-sky radiation, design day temperatures, and solar heat gains from fenestration.

This publication is accompanied by a set of spreadsheets and a set of weather files, which can be found at ashrae.org/lcam. The spreadsheets support the more complex examples in the book; the weather files provided the needed weather information to perform load calculations around the world. If the files or information at the link are not accessible, please contact the publisher.

1.1 Definition of a Cooling Load

When an HVAC system is operating, the rate at which it removes heat from a space is the instantaneous heat extraction rate for that space. The concept of a design cooling load derives from the need to determine an HVAC system size that, under extreme conditions, will provide some specified condition within a space. The space served by an HVAC system commonly is referred to as a *thermal zone* or just a *zone*. Usually, the indoor boundary condition associated with a cooling load calculation is a constant interior dry-bulb temperature, but it could be a more complex function, such as a thermal comfort condition. What constitutes extreme conditions can be interpreted in many ways. Generally, for an office it would be assumed to be a clear sunlit day with high outdoor wet-bulb and dry-bulb temperatures, high office occupancy, and a correspondingly high use of equipment and lights. Design conditions assumed for a cooling load determination are subjective. However, after the design conditions are agreed upon, the design cooling load represents the maximum—or peak heat extraction—rate under those conditions.

1.2 The Basic Design Questions

In considering the problem of design from the HVAC system engineer's viewpoint, a designer needs to address the following three main questions:

1. What is the required equipment size?
2. How do the heating/cooling requirements vary spatially within the building?
3. What are the relative sizes of the various contributors to the heating/cooling load?

The cooling load calculation is performed primarily to answer the second question, that is, to provide a basis for specifying the required airflow to individual spaces within the

Load Calculation Applications Manual (SI), Second Edition

building. The calculation also is critical to professionally answering the first question. Answers to the third question help the designer make choices to improve the performance or efficiency of the design and occasionally may influence architectural designers regarding energy-sensitive consequences.

1.3 Overview of the ASHRAE Load Calculation Methods

1.3.1 Models and Reality

All calculation procedures involve some kind of model, and all models are approximate. The amount of detail involved in a model depends on the purpose of that model. This is the reality of modeling, which should describe only the variables and parameters that are significant to the problem at hand. The challenge is to ensure that no significant aspects of the process or device being modeled are excluded and, at the same time, that unnecessary detail is avoided.

A complete, detailed model of all of the heat transfer processes occurring in a building would be very complex and would be impractical as a computational model, even today. However, building physics researchers and practitioners generally agree that certain modeling simplifications are reasonable and appropriate under a broad range of situations. The most fundamental of these is that the air in the space can be modeled as well-stirred. This means there is an approximately uniform temperature throughout the space due to mixing. This modeling assumption is quite valid over a wide range of conditions. With that as a basis, it is possible to formulate fundamental models for the various heat transfer and thermodynamic processes that occur. The resulting formulation is called the HBM. There is an introduction to the general principles of the HBM in Chapter 2 and further description in Chapter 11.

1.3.2 The Heat Balance Method

The processes that make up the heat balance model can be visualized using the schematic shown in Figure 1.1. It consists of four distinct processes:

1. Outside face heat balance
2. Wall conduction process
3. Inside face heat balance
4. Air heat balance

Figure 1.1 shows the heat balance process in detail for a single opaque surface. The shaded part of the figure is replicated for each of the surfaces enclosing the zone.

The process for transparent surfaces is similar to that shown but does not have the absorbed solar component at the outside surface. Instead, it is split into two parts: an inward-flowing fraction and an outward-flowing fraction. These fractional parts participate in the inside and outside face heat balances. The transparent surfaces, of course, provide the transmitted solar component that contributes to the inside heat balance.

The double-ended arrows indicate schematically where there is a heat exchange, and the single-ended arrows indicate where the interaction is one way. The formulation of the heat balance consists of mathematically describing the four major processes, shown as rounded blocks in the figure.

1.3.3 The Radiant Time Series Method

The RTSM is a relatively new method for performing design cooling load calculations. It is derived directly from the HBM and effectively replaced all other simplified (non-heat-balance) methods such as the transfer function method (TFM), the cooling

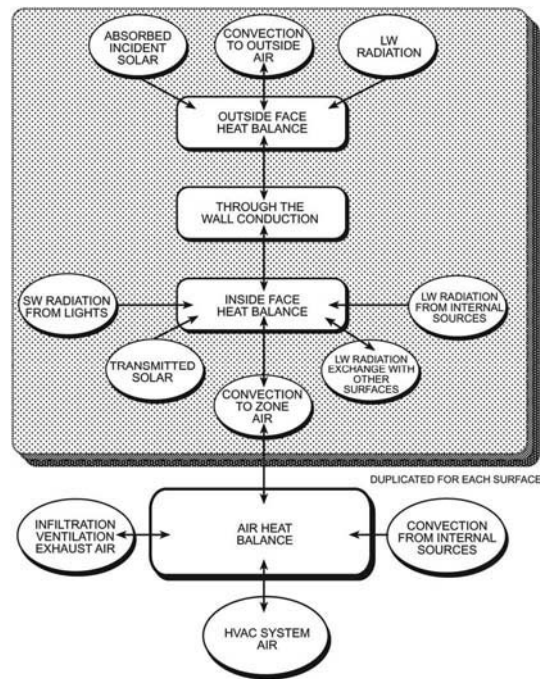


Figure 1.1 Schematic of heat balance process in a zone.

(Source: *Cooling and Heating Load Calculation Principles*, Figure 1.1).

load temperature difference/solar cooling load/cooling load factor method (CLTD/SCL/CLFM), and the total equivalent temperature difference/time averaging method (TETD/TAM). The RTSM was developed in response to a desire to offer a method that was rigorous yet did not require the iterative calculations of the previous methods. In addition, the periodic response factors and radiant time factors have clear physical meanings; when plotted, they allow the user to visually see the effects of damping and time delay on conduction heat gains and zone response.

The utility of the RTSM lies in the clarity, not the simplicity, of the procedure. Although the RTSM uses a “reduced” heat balance procedure to generate the radiant time series (RTS) coefficients, it is approximately as computationally intensive as the heat balance procedure upon which it is based. What the RTS method does offer is insight into the building physics without the computational rigor of the HBM, a sacrifice in accuracy that is surprisingly small in most cases. Previous simplified methods relied on room transfer function coefficients that completely obscured the actual heat transfer processes they modeled. The heat-balance-based RTS coefficients, on the other hand, provide some insight into the relationship between zone construction and the time dependence of the building heat transfer processes. The RTSM abstracts the building thermal response from the fundamentally rigorous heat balance and presents the effects of complex, interdependent physical processes in terms that are relatively easy to understand. The abstraction requires a number of simplifying assumptions and approximations. These are covered in Section 7.1. Figure 1.2 shows the computational procedure that defines the RTSM. A more detailed schematic is shown in Chapter 7.

In the RTSM, a conductive heat gain for each surface is first calculated using air-to-air response factors. The conductive heat gains and the internal heat gains are then split into radiant and convective portions. All convective portions are instantaneously converted to cooling loads and summed to obtain the fraction of the total hourly cooling load caused by convection.

Load Calculation Applications Manual (SI), Second Edition

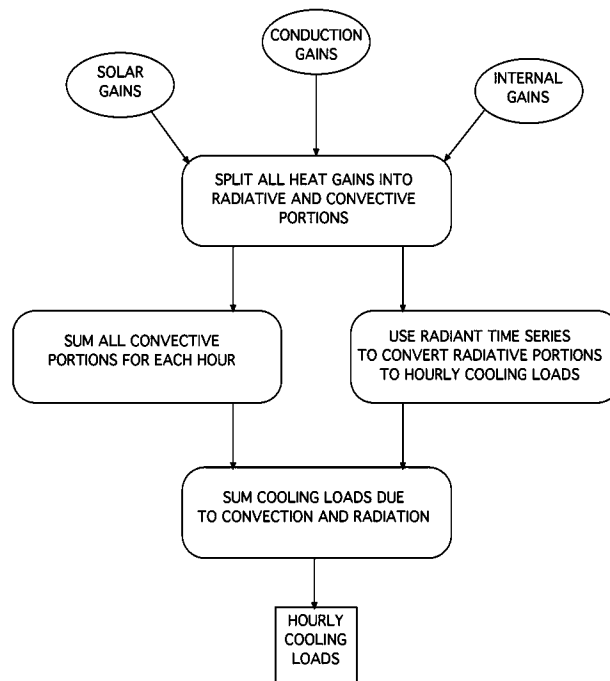


Figure 1.2 Schematic of the radiant time series method.

(Source: *Cooling and Heating Load Calculation Principles*, Figure 1.2).

Radiant heat gains from conduction, internal sources, and solar transmission are operated on by the RTS to determine the fraction of the heat gain that will be converted to a cooling load in current and subsequent hours. These fractional cooling loads are added to the previously calculated convective portions at the appropriate hour to obtain the total hourly cooling load.

1.4 Organization of the Manual

This manual is organized to roughly proceed from the general to the specific. Chapter 2 provides an overview of the heat transfer processes present in buildings and a brief discussion of how they are analyzed together in order to determine the building cooling load. Chapters 3–6 cover thermal properties, design conditions, infiltration, and internal heat gains—all of which are relevant to all load calculation methods. Chapters 7 and 8 cover the theory and application of the RTSM. Chapter 9 covers systems and psychrometrics, analyses of which are necessary to determine equipment sizes. Chapter 10 considers heating load calculations. Chapter 11 covers the HBM and its implementation.

Throughout the manual, numerous shaded examples are presented to illustrate various aspects of the RTSM. A number of the examples are performed using spreadsheets that are included in the supporting files online at www.ashrae.org/lcam.

References

Pedersen, C.O., D.E. Fisher, J.D. Spitler, and R.J. Liesen. 1998. *Cooling and Heating Load Calculation Principles*. Atlanta: ASHRAE.

Fundamentals of Heat Transfer and Thermodynamics

The cooling load is defined as the amount of heat that must be removed from the room air to maintain a constant room air temperature. Conversely, the heating load is the amount of heat that must be added to the room air. To determine these quantities, it is necessary to estimate the heat transmission into or out of the room. In turn, this requires analysis of all three modes of heat transfer—conduction, convection, and radiation—within the building envelope and between the building envelope and its surroundings. (Here, the term *building envelope* refers to the walls, roofs, floors, and fenestrations that make up the building.)

The three modes of heat transfer all occur simultaneously, and it is the simultaneous solution of all three modes of heat transfer that complicates the analysis. In practice, this simultaneous solution is done with a computer program either during the load calculation procedure (e.g., the heat balance method [HBM]) or prior to the load calculation procedure (all simplified load calculation procedures rely on tabulated factors that were developed with a simultaneous solution of all three modes of heat transfer).

Before concerning ourselves with the simultaneous solution, we should first consider the three modes independently. For convection and radiation, the treatment of the individual modes of heat transfer does not go far beyond what is taught in a first undergraduate course¹ in heat transfer. For steady-state conduction heat transfer, as used in heating load calculations, this is also the case. For transient conduction heat transfer, as used in cooling load calculations, the derivation of the solution procedure can be somewhat complex, although its application, in practice, is not very difficult.

Each of the three modes is discussed briefly below. Then, after considering the three modes of heat transfer, the simultaneous solution—based on the first law of thermodynamics—is briefly discussed.

2.1 Conduction—Steady State

Heat transfer through building walls and roofs is generally treated as a pure conduction heat transfer process, even though, for example, convection and radiation may be important in an internal air gap² in the wall. Conduction is the transfer of heat through a solid³ via random atomic and molecular motion in response to a temperature gradient. Elements of the building envelope such as thermal bridges and corners distort the temperature gradients so that the heat flows in directions other than purely perpendicular to the envelope surfaces. Such heat flow is said to be multidimensional. For building load calculations, multidimensional conduction heat transfer is generally approximated as being one-dimensional; however, the approximations do take into account the impact of thermal bridges.⁴ Heat loss from foundation elements is also multidimensional, but again, approximations are made that simplify the calculation procedure.

1. Cf. Incropera and DeWitt (2001).
2. Even though heat transfer in an air gap is due to convection and radiation, it is approximated as being a conduction process with a fixed thermal resistance that is independent of the temperatures of the gap surfaces.
3. Technically, conduction also occurs in liquids and gases, too. But here we are only concerned with conduction in solids.
4. Appendix E covers the treatment of thermal bridges.

Load Calculation Applications Manual (SI), Second Edition

One-dimensional steady-state heat conduction is described by the Fourier equation:

$$\dot{q} = -kA \frac{dt}{dx} \quad (2.1)$$

where

\dot{q} = heat transfer rate, W

k = thermal conductivity, W/(m·K)

A = area normal to the heat flow, m²

$\frac{dt}{dx}$ = temperature gradient, °C/m

For a single layer of a wall with heat flow in the x direction and with conductivity k and surface temperatures t_2 and t_1 , as shown in Figure 2.1, Equation 2.1 can be integrated to give

$$\dot{q} = -kA \frac{(t_2 - t_1)}{(x_2 - x_1)} \quad (2.2)$$

A convenient form of Equation 2.2 involves the definition of the unit thermal resistance R :

$$R = \frac{(x_2 - x_1)}{k} = \frac{\Delta x}{k} \quad (2.3)$$

where

R = unit thermal resistance, (m²·K)/W

Δx = thickness of the layer, units are consistent with k , mm

Then, the conduction heat transfer rate through the wall is given by

$$\dot{q} = A \frac{(t_1 - t_2)}{R} \quad (2.4)$$

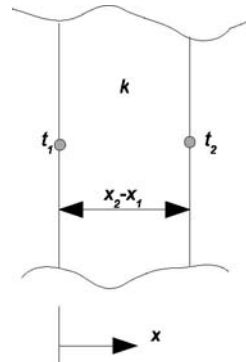


Figure 2.1 A single-layer plane wall.

Fundamentals of Heat Transfer and Thermodynamics

Example 2.1 Wall Heat Loss

A 0.1 m thick uninsulated wall with an area of 10 m² is made out of concrete with a conductivity of 1.15 W/(m·K). What is the R-value of the wall? Under steady-state conditions, with the exterior surface temperature of the wall at 0°C and the interior surface temperature of the wall at 15°C, what is the total heat loss through the wall?

Solution: The R-value is determined by dividing the thickness by the conductivity:

$$R = 0.1 \text{ m} / 1.15 \text{ W}/(\text{m}\cdot\text{K}) = 0.09 \text{ (m}^2\cdot\text{K)}/\text{W}$$

The conduction heat transfer rate through the wall is given by Equation 2.4:

$$\dot{q} = 10 \text{ m}^2 \frac{(15^\circ\text{C} - 0^\circ\text{C})}{0.09 \frac{\text{m}^2 \cdot \text{K}}{\text{W}}} = 1667 \text{ W}$$

A more common situation is that the wall has multiple layers, as shown in Figure 2.2. Here, the wall is made up of three layers with two exterior surfaces (one and four) and two interior interfaces (two and three). Each of the three layers is defined by a conductivity (e.g., k_{2-1} for the leftmost layer) and thickness (e.g., Δx_{2-1} for the leftmost layer).

Individual unit thermal resistances are determined for each layer:

$$R_{2-1} = \frac{\Delta x_{2-1}}{k_{2-1}} \quad (2.5a)$$

$$R_{3-2} = \frac{\Delta x_{3-2}}{k_{3-2}} \quad (2.5b)$$

$$R_{4-3} = \frac{\Delta x_{4-3}}{k_{4-3}} \quad (2.5c)$$

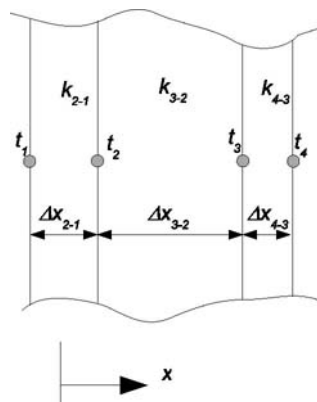


Figure 2.2 A multilayer wall.

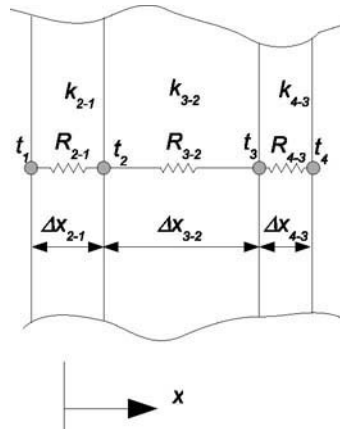


Figure 2.3 Multilayer wall analysis based on electrical analogy.

There is an analogy between conduction heat transfer and electricity, as illustrated in Figure 2.3, where the unit thermal resistances (analogous to electrical resistances⁵ per unit area) are shown connecting the surface temperatures (analogous to voltages). As a consequence, the total unit thermal resistance of the wall may be determined by simply adding the three individual unit thermal resistances (in series):

$$R_{4-1} = R_{2-1} + R_{3-2} + R_{4-3} \quad (2.6)$$

Then, the heat flux (analogous to current per unit area) may be determined as

$$q'' = \frac{(t_1 - t_4)}{R} \quad (2.7)$$

where

q'' = heat flux rate (heat transfer rate per unit area), W/m^2

Example 2.2 Series Resistances

The concrete wall of Example 2.1 is improved by adding a 0.05 m thick layer of expanded polystyrene, with an R-value of 1.76, and a layer of 0.013 m thick drywall, with an R-value of 0.08. With these additional layers, what is the R-value of the wall? Under steady-state conditions, with the exterior surface temperature of the wall at $0^\circ C$ and the interior surface temperature of the wall at $15^\circ C$, what is the total heat loss through the wall?

Solution: Because the three layers are in a series with each other, the total R-value is determined by adding the resistances of the three layers, as modeled in Equation 2.6:

5. The analogy is to discrete electrical resistors when expressed in thermal resistances ($R' = \Delta x/kA$) and heat transfer rates. For one-dimensional planar walls, it is often convenient to consider the analogy on a per-unit-area basis, in which case it may be expressed in terms of unit thermal resistances and heat fluxes (heat transfer rates per unit area).

Fundamentals of Heat Transfer and Thermodynamics

$$R = 0.09 + 1.76 + 0.08 = 1.93(\text{m}^2 \cdot \text{K})/\text{W}$$

The conduction heat transfer rate through the wall is given by Equation 2.4:

$$\dot{q} = 10 \text{ m}^2 \frac{(15^\circ\text{C} - 0^\circ\text{C})}{1.93 \frac{\text{m}^2 \cdot \text{K}}{\text{W}}} = 78 \text{ W}$$

A dramatic reduction in heat loss can generally be had when insulation is added to uninsulated walls.

Generally, heating load calculations are performed for conditions that are assumed to be approximately steady-state: that is, evening hours after the building occupants have gone home and the sun has gone down. In this case, the conduction heat transfer through the above-grade portion of the building envelope is determined by first calculating the overall thermal resistance and conductance (U-factor) of each surface, multiplying the U-factors by the surface areas, summing the UA (U-factor · area) values for each room, and multiplying the total UA for each room by the design temperature difference. For slab-on-grade floors, basement walls, and basement floors, a simple multidimensional analysis is used such that the solution is given in one-dimensional form.

2.2 Thermal Storage and Transient Conduction

The discussion of conduction heat transfer in Section 2.1 treated it as a steady-state phenomenon. While for heating load calculations this is generally sufficient, strong daily variations in incident solar radiation and outdoor air temperatures occurring under cooling load design conditions cannot be ignored in most cases. This is particularly true as the thermal capacitance of the wall or roof increases. Thermal capacitance of a wall or roof element may be defined as the amount of energy required to raise the temperature by one degree:

$$C_{th} = MC_p = \rho VC_p \quad (2.8)$$

where

C_{th} = thermal capacitance of a wall or roof layer, kJ/K

M = mass of the wall or roof layer, kg

C_p = specific heat of the wall or roof layer material, kJ/(kg·K)

ρ = density of the wall or roof layer material, kg/m³

V = volume of the wall or roof layer, m³

The energy required to raise the temperature of the layer is then given by

$$Q = C_{th}\Delta T = MC_p\Delta T = \rho VC_p\Delta T \quad (2.9)$$

where

ΔT = temperature increase, K

While a range of solution procedures (Spitler 1996) are possible (e.g., finite difference methods, finite volume methods, lumped parameter methods, frequency response methods, etc.), ASHRAE design cooling load calculations use either con-

Example 2.3 Thermal Storage

Consider the 0.1 m thick layer of concrete in the 10 m² wall in Example 2.2. During a design cooling day, it is warmed from a temperature of 21°C to a temperature of 27°C. If the concrete has a density of 2240 kg/m³ and a specific heat of 0.92 kJ/(kg·K), how much energy is absorbed in warming the concrete layer?

Solution: The total volume of the concrete is 1 m³; multiplying by the density gives the total mass of the concrete as 2240 kg. The required energy input is the mass multiplied by the specific heat multiplied by the rise in temperature:

$$Q = 2240 \text{ kg} \cdot 0.92 \text{ kJ/(kg}\cdot\text{K)} \cdot 6^\circ\text{C} = 12,365 \text{ kJ}$$

Comparing the amount of energy required to raise the temperature of the layer by 6°C to the expected heat transmission rate under steady-state conditions suggests that this heat storage effect will not be unimportant. However, because the thermal capacitance is distributed throughout each layer, there is no simple way to calculate the transient behavior. The distributed thermal capacitance is sometimes represented as shown in Figure 2.4, with the two parallel lines below each resistance representing the distributed capacitance.

duction transfer functions (CTFs) in the heat balance method or a form of periodic response factors, known as the conduction time series factors (CTSFs) in the radiant time series method (RTSM). The two methods are covered in Chapters 11 and 7, respectively. Software for calculating CTFs and CTSFs is included on the accompanying supporting files (online at www.ashrae.org/lcam) and is described in Appendix C.

To further illustrate the effects of thermal storage in the wall, consider what would happen if the three-layer (10 cm concrete, R-1.76 insulation, 1.3 cm drywall) wall described in Example 2.2 was placed in an office building in Atlanta, facing southwest. Under cooling load design conditions, the heat transmission through the wall may be calculated using two methods:

- A method that ignores the thermal mass in the wall, computing the conduction heat gain with Equation 2.4 at each hour of the day. In this case, the exterior temperature changing throughout the day gives conduction heat gains that change over the day. This method may be referred to as *quasi-steady-state* because it treats each hour of the day as if the wall comes immediately to steady-state conditions. (Labeled *Quasi-SS* in Figure 2.5.)
- The method described in Chapter 7, which takes into account the thermal capacitance of each layer. (Labeled *Transient* in Figure 2.5.)

Conduction heat gains computed with each method are shown in Figure 2.5. In this figure, two effects of the thermal mass may be observed:

- The first may be referred to as *time delay*—the peak heat gain, when calculated with the quasi-steady-state method, appears to occur at 5:00 p.m. When the thermal capacitance is accounted for in the calculation, we can see that the peak heat gain actually occurs at 9:00 p.m. This four-hour delay in the peak heat gain may be important, especially if the peak heat gain is delayed such that it occurs after the occupants have gone home.
- The second effect may be referred to as *damping*—the peak heat gain, when calculated with the transient method, is about 30% lower than that calculated with the quasi-steady-state method.

Fundamentals of Heat Transfer and Thermodynamics

Both effects are important, and this is why transient conduction calculations are typically performed as part of the cooling load calculation procedure.

2.3 Convection

Thermal convection is the transport of energy in a fluid or gas by mixing in addition to conduction. For load calculations, we are primarily interested in convection between an envelope surface (e.g., wall, roof) and the indoor or outdoor air. The rate of convection heat transfer depends on the temperature difference, whether the flow is laminar or turbulent, and whether it is buoyancy driven or driven by an external flow. The convection heat transfer rate is usually expressed⁶ as

$$\dot{q} = hA(t - t_s) \quad (2.10)$$

where

h = convection coefficient, W/(m²·K)

t = bulk temperature of the air, °C

t_s = surface temperature, °C

The convection coefficient, often referred to as the *film coefficient*, may be estimated with a convection correlation or, for design conditions, may be read from a table.

Example 2.4 Convection

A wall with a surface area of 10 m² is heated by the sun to a temperature of 60°C at a time when the outdoor air is at 21°C, and a light breeze results in a convection coefficient of 28 W/(m²·K). What is the heat lost by the surface due to convection?

Solution: Equation 2.10 gives the heat transferred to the surface by convection. The heat transferred away from the surface by convection would be given by

$$\dot{q} = hA(t_s - t) = 28 \frac{\text{W}}{\text{m}^2 \cdot \text{K}} (10 \text{ m}^2)(60^\circ\text{C} - 21^\circ\text{C}) = 10,920 \text{ W}$$

2.4 Radiation—Long Wave and Short Wave

Thermal radiation is the transfer of energy by electromagnetic waves. In building load calculations, thermal radiation is generally thought of as being a surface-to-surface phenomenon either between surfaces within the building or between the surface of the sun and the building surfaces. Gases, aerosols, and particulates also emit and absorb radiation between surfaces. However, for analysis of radiation heat transfer between surfaces within a building, the path lengths are short enough that emission and absorption of the indoor air can be neglected. For radiation heat transfer between the sun and the building surfaces, emission and absorption in the earth's atmosphere is accounted for in the models used to determine incident solar irradiation.

Thermal radiation emitted by any surface will have a range of wavelengths, depending upon the temperature of the emitting surface. The amount of thermal radi-

6. Also known as Newton's Law of Cooling.

Load Calculation Applications Manual (SI), Second Edition

ation absorbed, reflected, or emitted by any surface will depend on the wavelengths and direction in which the radiation is incident or emitted relative to the surface. Dependency on the wavelength is referred to as *spectral*; surfaces for which the properties are effectively independent of the wavelength are referred to as *gray* surfaces. Dependency on the direction is referred to as *specular*; surfaces for which the properties are effectively independent of the direction are referred to as *diffuse* surfaces. Properties of interest include the following:

- Absorptance,⁷ α , the ratio of radiation absorbed by a surface to that incident on the surface

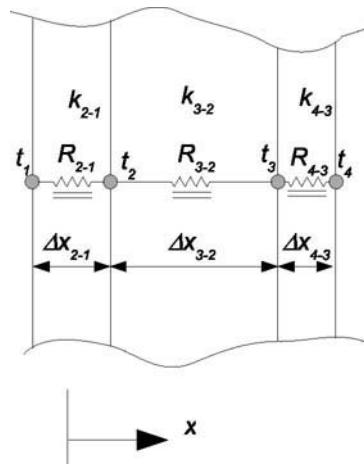


Figure 2.4 Electrical analogy with distributed thermal capacitance.

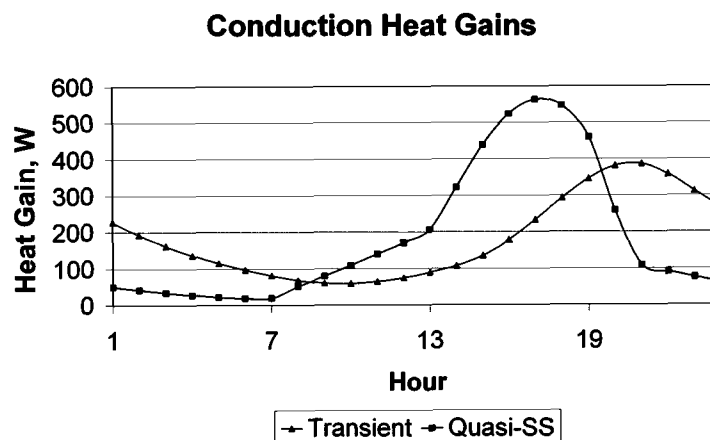


Figure 2.5 Comparison of transient and quasi-steady-state conduction heat gain calculations.

7. Despite some attempts to reserve the endings “-ivity” for optically pure surfaces and “-tance” for real-world surfaces, the terms *absorptivity*, *emissivity*, *reflectivity*, and *transmissivity* are often used interchangeably for *absorptance*, *emittance*, *reflectance*, and *transmittance*.

Fundamentals of Heat Transfer and Thermodynamics

- Emittance, ε , the ratio of radiation emitted by a surface to that emitted by an ideal “black” surface at the same temperature
- Reflectance, ρ , the ratio of radiation reflected by a surface to that incident on the surface
- Transmittance, τ , the ratio of radiation transmitted by a translucent surface to that incident on the surface

Analysis of thermal radiation is greatly simplified when the surfaces may be treated as gray and diffuse. With two exceptions, surfaces in buildings are treated as both gray and diffuse in load calculation procedures.

The first exception is based on the fact that thermal radiation wavelength distributions prevalent in buildings may be approximately lumped into two categories—short-wavelength radiation (solar radiation or visible radiation emitted by lighting) and long-wavelength radiation (radiation emitted by surfaces, people, equipment, etc. that is all at relatively low temperatures compared to the sun). Treatment of the two wavelength distributions separately in building load calculations might be referred to as a *two-band* model, but in practice this only means that surfaces may have different absorptances for short-wavelength radiation and long-wavelength radiation. As an example, consider that a surface painted white may have a short-wavelength absorptance of 0.4 and a long-wavelength absorptance of 0.9.

The second exception is for analysis of windows. Solar radiation is typically divided into specular (direct or beam) and diffuse components as described in Appendix D. Because the window absorptance, reflectance, and transmittance tend to be moderately strong functions of the incidence angle, these properties are generally calculated for the specific incidence angle each hour.

A notable feature of thermal radiation is that the emission is proportional to the fourth power of the absolute temperature (i.e., degrees Rankine or Kelvin.) As an example, consider a case with only two surfaces separated by a nonparticipating medium. The radiation heat transfer rate between surfaces 1 and 2 is given by

$$\dot{q}_{1-2} = \frac{\sigma(T_1^4 - T_2^4)}{\frac{1 - \varepsilon_1}{A_1 \varepsilon_1} + \frac{1}{A_1 F_{1-2}} + \frac{1 - \varepsilon_2}{A_2 \varepsilon_2}} \quad (2.11)$$

where

σ = Stefan-Boltzmann constant, $5.67 \cdot 10^{-8} \text{ W}/(\text{m}^2 \cdot \text{K}^4)$

T_1 and T_2 = surface temperatures of surfaces 1 and 2, K

ε_1 and ε_2 = emittances of surfaces 1 and 2

F_{1-2} = view factor from surface 1 to surface 2

In practice, rooms in buildings have more than two surfaces and, in general, every surface exchanges radiation heat transfer with every other surface. While it is possible to analyze the complete radiation network, load calculations typically adopt a simpler approximation. For the HBM, a mean radiant temperature approach, as described in Chapter 11, is usually adopted. For the RTSM, the analysis of the radiation heat transfer to/from inside and outside surfaces is combined with the analysis of convection, as described in the next section.

Example 2.5 Radiation

A 10 m² wall has an air gap separating a layer of brick and a layer of concrete block. At a time when the temperature of the brick surface adjacent to the air gap is -1.1°C and the temperature of the concrete block surface adjacent to the air gap is 7.2°C, what is the radiation heat transfer rate across the air gap?

Solution: The radiation heat transfer rate can be calculated with Equation 2.11. To use Equation 2.11, there are a few terms that must first be evaluated. First, the temperatures T_1 and T_2 are needed in absolute temperature or degrees Kelvin. Taking the concrete block as surface 1 and the brick as surface 2,

$$T_1 = t_1 + 273.15 = 72 + 273.15 = 280.35 \text{ K}$$

$$T_2 = t_2 + 273.15 = -1.1 + 273.15 = 272.05 \text{ K}$$

The surface emissivities are not given, but, in general, for building materials that are not polished metals, a value of 0.9 is a reasonable assumption.

The view factor between two parallel surfaces facing each other is approximately one. Equation 2.9 can then be evaluated as

$$\dot{q}_{1-2} = \frac{\sigma(280.35^4 - 272.05^4)}{\frac{1-0.9}{10 \cdot 0.9} + \frac{1}{10 \cdot 1} + \frac{1-0.9}{10 \cdot 0.9}} = 325 \text{ W}$$

If a low emissivity coating (e.g., a layer of aluminum foil) were applied to the concrete block layer and not compromised by being splattered with mortar or coated with dust during the bricklaying, the emittance might be as low as 0.05. (In practice, this would be nearly impossible, but just for purposes of example, we'll assume that it might be done.) The radiation heat transfer could then be calculated as

$$\dot{q}_{1-2} = \frac{\sigma(280.35^4 - 272.05^4)}{\frac{1-0.05}{10 \cdot 0.05} + \frac{1}{10 \cdot 1} + \frac{1-0.9}{10 \cdot 0.9}} = 20 \text{ W}$$

2.5 Combined Convection and Radiation

An important feature of simplified load calculation methods, like the RTSM, is that convection and radiation analysis are often combined into a single surface conductance. This requires a linear approximation of the radiation heat transfer. Considering that surface 2 in Equation 2.11 above could represent, in aggregate, the surroundings, then approximately $A_2 \gg A_1$ and Equation 2.11 can be simplified to

$$\dot{q}_{1-2} = A_1 \varepsilon_1 \sigma (T_1^4 - T_2^4) = A_1 h_r (T_1 - T_2) \quad (2.12)$$

$$h_r = \varepsilon_1 \sigma (T_1^2 + T_2^2)(T_1 + T_2) \approx 4 \varepsilon_1 \sigma \bar{T}^3 \quad (2.13)$$

where

h_r = radiation coefficient, W/(m²·K)

T = mean temperature, K

Note that while the linearized radiation coefficient is calculated with absolute temperatures, it is applied to a temperature difference, so it may just as easily be used to predict radiation heat transfer with the difference in, say, degrees Fahrenheit:

Fundamentals of Heat Transfer and Thermodynamics

$$\dot{q}_r = h_r A(t - t_w) \quad (2.14)$$

The surface conductance, which combines the radiation and convection coefficient, can then be defined as

$$h_o = h_c + h_r \quad (2.15)$$

This has the advantage of allowing the combined convection and radiation heat transfer rate to be expressed as

$$\dot{q} = h_o A(t - t_w) \quad (2.16)$$

Or, the inverse of the surface conductance can be treated as a conductive resistance, simplifying the analysis so that it appears as simply a conduction analysis. Though the surface conductance depends on both the value of the convection coefficient and the surface and surroundings temperatures, standard values for design purposes are tabulated in Chapter 3.

In the case of the exterior conductance, the problem is further complicated by the presence of solar radiation. For simplified load calculation procedures, an equivalent air temperature, or the sol-air temperature, is defined that gives approximately the same heat flux to the surface as the combined effects of solar radiation, convection, and radiation to the surroundings. It is given by

$$t_e = t_o + \alpha G_t / h_o - \varepsilon \delta R / h_o \quad (2.17)$$

where

t_e = sol-air temperature, °C

t_o = outdoor air temperature, °C

α = absorptance of the surface to solar radiation

G_t = total incident solar radiation flux, $W \cdot m^2$

h_o = exterior surface conductance, $W/(m^2 \cdot K)$

ε = exterior surface emittance

δR = difference between the thermal radiation incident on the surface from the sky or surroundings and the radiation emitted by a blackbody at the outdoor air temperature, $W \cdot m^2$

The last term, $\varepsilon \delta R / h_o$, is typically taken as 4°C for horizontal surfaces (i.e., facing the sky) and 0°C for vertical surfaces.

For the interior conductance, the indoor air temperature is taken as a suitable approximation to the actual effective temperature with which convection and radiation are exchanged.

The use of linearized radiation coefficients, combined with convection coefficients into surface conductances, allows the heat gains from each wall to be added without considering interaction between the surfaces or the possibility that heat may be conducted out under some circumstances by windows or other high-conductance surfaces. These effects are usually small but may be corrected for with the procedure described in Appendix G. In order to account for these effects more accurately, it is necessary to apply the HBM, which is introduced in the next section and more fully described in Chapter 11.

2.6 The First Law of Thermodynamics—Heat Balance

The HBM takes its name from the application of the first law of thermodynamics—energy is conserved—to the inner and outer surfaces of the building envelope and the zone air. All of the energy involved is in the form of heat, hence the term *heat balance*.

As an example, consider the exterior surface of a wall, as shown in Figure 2.6, where

- t_{es} = exterior surface temperature, °C
- t_{is} = interior surface temperature, °C
- t_o = outdoor air temperature, °C
- q''_{solar} = absorbed solar heat flux, W/m²
- t_{surr} = temperature of the surroundings, °C

Neglecting any transient effects, a heat balance on the exterior surface might be written as

$$q''_{conduction} = q''_{solar} + q''_{convection} + q''_{radiation} \quad (2.18)$$

with each component of the heat transfer defined as follows:

$$q''_{conduction} = U_{s-s}(t_{es} - t_{is}) \quad (2.19)$$

$$q''_{solar} = \alpha G_t \quad (2.20)$$

$$q''_{convection} = h_c(t_o - t_{es}) \quad (2.21)$$

$$q''_{radiation} = h_r(t_{surr} - t_{es}) \quad (2.22)$$

where

U_{s-s} = surface-to-surface conductance, W/(m²·K)

α = absorptance of the surface to solar radiation

G_t = total incident solar radiation flux, W/m²

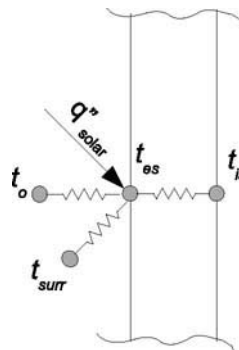


Figure 2.6 Exterior surface heat balance.

Fundamentals of Heat Transfer and Thermodynamics

h_c = exterior surface convection coefficient, W/(m²·K)

h_r = exterior surface radiation coefficient, W/(m²·K)

Here, the radiation heat transfer has been linearized, though in the heat balance solution procedure, the radiation heat transfer coefficient will be recalculated on an iterative basis. Substituting Equations 2.19–2.22 into Equation 2.18, the exterior surface temperature can then be determined:

$$t_{es} = \frac{\alpha G_t + U_{s-s} t_{is} + h_c t_o + h_r t_{surr}}{U_{s-s} + h_c + h_r} \quad (2.23)$$

A similar procedure for the interior surface yields a similar equation for the interior surface temperature. The interior and exterior surface temperatures would then be solved iteratively. When all interior surface temperatures are known, the cooling load can be calculated as the sum of the convective heat gains from the interior surfaces, lighting, equipment, people, and infiltration.

In practice, these calculations are further complicated by the transient conduction heat transfer and the need to analyze all modes of heat transfer simultaneously for all surfaces in a room. For more information, see Chapter 11.

References

- Incropera, F.P., and D.P. DeWitt. 2001. *Fundamentals of Heat and Mass Transfer*, 5th ed. New York: Wiley.
- Spitler, J.D. 1996. *Annotated Guide to Load Calculation Models and Algorithms*. Atlanta: ASHRAE.

Thermal Property Data

Analysis of walls and roofs for cooling or heating load calculations requires a layer-by-layer description of the wall or roof, specifying the thermal properties of each layer. Heating load calculations are typically performed with the assumption that the wall or roof is in steady-state conditions, and so only the thermal resistance of the wall or roof is needed. For cooling load calculations, unsteady or dynamic heat transfer will occur, so information on the heat storage capacity of each layer is also needed. Section 3.1 provides the necessary thermal property data. Section 3.2 gives the procedure for determining U-factors of walls and roofs for cases where there are no thermal bridges. For fenestration—windows, skylights, and doors—thermal and optical properties are given in Section 3.3. For walls and roofs with thermal bridges, consult Appendix E.

3.1 Thermal Property Data—Walls and Roofs

3.1.1 Thermal Properties of Building and Insulation Materials

The basic properties that determine the way in which a material will behave in the conductive mode of heat transfer are the thermal conductivity k , the density ρ , and the specific heat capacity C_p . The last two properties are important when unsteady heat transfer is occurring because of heat storage. These variables are discussed in Chapters 7, 8, and 11, where the unsteady nature of the load is covered. The thermal conductivity is basic to the determination of the thermal resistance component leading to the U-factor.

Table 3.1 lists the basic properties for many different construction and insulation materials. The data given are intended to be representative of materials generally available and are not intended for specification purposes. It is always advisable to use manufacturers' specification data when available.

Note that the data are given in two forms—for materials that may likely be used in any thickness, the density, thermal conductivity, and specific heat are given. For materials that come in fixed thicknesses, often only the unit thermal resistance is given in the column labeled Resistance R .

For materials where the unit thermal resistance is not given, it may be determined by

$$R = x/k, (\text{m}^2 \cdot \text{K})/\text{W} \quad (3.1)$$

where

k = thermal conductivity, $\text{W}/(\text{m} \cdot \text{K})$

x = thickness of material, m

The thermal resistance for the wall or roof section is then the summation of all of the layer unit thermal resistances divided by the wall or roof area. The thermal resistance for the wall or roof section is then

$$R' = \sum R/A, (\text{h} \cdot \text{F})/\text{Btu} \quad (3.2)$$

The unit thermal resistance per meter of material thickness is simply the reciprocal of the thermal conductivity. It should be noted that the data of Table 3.1 are for a mean temperature of 24°C. While these data are adequate for design load calculations, the thermal conductivity does depend on the temperature of the material.

Load Calculation Applications Manual (SI), Second Edition

For wall or roof constructions with an interior planar air space, thermal resistances can be found in Table 3.2, using effective emittances for the air space determined from Table 3.3a. Table 3.3b gives solar absorptance values needed for cooling load calculations as described in Section 7.3.

Table 3.1 Typical Thermal Properties of Common Building and Insulating Materials—Design Values^a

(Source: ASHRAE Handbook—Fundamentals [2013], Chapter 26, Table 1)

Description	Density, kg/m ³	Conductivity ^b k, W/(m·K)	Resistance R, (m ² ·K)/W	Specific Heat, kJ/(kg·K)	Reference ¹
Insulating Materials					
<i>Blanket and batt^{c,d}</i>					
Glass-fiber batts				0.8	Kumaran (2002)
	7.5 to 8.2	0.046 to 0.048	—	—	Four manufacturers (2011)
	9.8 to 12	0.040 to 0.043	—	—	Four manufacturers (2011)
	13 to 14	0.037 to 0.039	—	—	Four manufacturers (2011)
	22	0.033	—	—	Four manufacturers (2011)
Rock and slag wool batts				0.8	Kumaran (1996)
	32 to 37	0.036 to 0.037	—	—	One manufacturer (2011)
	45	0.033 to 0.035	—	—	One manufacturer (2011)
Mineral wool, felted	16 to 48	0.040	—	—	CIBSE (2006), NIST (2000)
	16 to 130	0.035	—	—	NIST (2000)
<i>Board and slabs</i>					
Cellular glass	120	0.042	—	0.8	One manufacturer (2011)
Cement fiber slabs, shredded wood with Portland cement binder	400 to 430	0.072 to 0.076	—	—	
with magnesia oxysulfide binder	350	0.082	—	1.3	
Glass fiber board				0.8	Kumaran (1996)
	24 to 96	0.033 to 0.035	—	—	One manufacturer (2011)
Expanded rubber (rigid)	64	0.029	—	1.7	Nottage (1947)
Extruded polystyrene, smooth skin				1.5	Kumaran (1996)
aged per Can/ULC Standard S770-2003	22 to 58	0.026 to 0.029	—	—	Four manufacturers (2011)
aged 180 days	22 to 58	0.029	—	—	One manufacturer (2011)
European product	30	0.030	—	—	One manufacturer (2011)
aged 5 years at 24°C	32 to 35	0.030	—	—	One manufacturer (2011)
blown with low global warming potential (GWP) (<5) blowing agent		0.035 to 0.036	—	—	One manufacturer (2011)
Expanded polystyrene, molded beads				1.5	Kumaran (1996)
	16 to 24	0.035 to 0.037	—	—	Independent test reports (2008)
	29	0.033	—	—	Independent test reports (2008)
Mineral fiberboard, wet felted	160	0.037	—	0.8	Kumaran (1996)
Rock wool board				0.8	Kumaran (1996)
floors and walls	64 to 130	0.033 to 0.036	—	—	Five manufacturers (2011)
roofing	160 to 180	0.039 to 0.042	—	0.8	Five manufacturers (2011)
Acoustical tile ^e	340 to 370	0.052 to 0.053	—	0.6 to 0.8	
Perlite board	140	0.052	—	—	One manufacturer (2010)
Polyisocyanurate				1.5	Kumaran (1996)
unfaced, aged per Can/ULC Standard S770-2003	26 to 37	0.023 to 0.025	—	—	Seven manufacturers (2011)
with foil facers, aged 180 days	—	0.022 to 0.023	—	—	Two manufacturers (2011)
Phenolic foam board with facers, aged	—	0.020 to 0.023	—	—	One manufacturer (2011)
<i>Loose fill</i>					
Cellulose fiber, loose fill				1.4	NIST (2000), Kumaran (1996)
attic application up to 100 mm	16 to 19	0.045 to 0.046	—	—	Four manufacturers (2011)
attic application > 100 mm	19 to 26	0.039 to 0.040	—	—	Four manufacturers (2011)
wall application, dense packed	56	0.039 to 0.040	—	—	One manufacturer (2011)
Perlite, expanded	32 to 64	0.039 to 0.045	—	1.1	(Manufacturer, pre 2001)
	64 to 120	0.045 to 0.052	—	—	(Manufacturer, pre 2001)
	120 to 180	0.052 to 0.061	—	—	(Manufacturer, pre 2001)
Glass fiber ^d					
attics, ~100 to 600 mm	6.4 to 8.0	0.052 to 0.055	—	—	Four manufacturers (2011)
attics, ~600 to 1100 mm	8 to 9.6	0.049 to 0.052	—	—	Four manufacturers (2011)
closed attic or wall cavities	29 to 37	0.035 to 0.036	—	—	Four manufacturers (2011)
Rock and slag wool ^d					
attics, ~90 to 115 mm	24 to 26	0.049	—	—	Three manufacturers (2011)
attics, ~125 to 430 mm	24 to 29	0.046 to 0.048	—	—	Three manufacturers (2011)
closed attic or wall cavities	64	0.039 to 0.042	—	—	Three manufacturers (2011)
Vermiculite, exfoliated	112 to 131	0.068	—	1.3	Sabine et al. (1975)

Thermal Property Data

Table 3.1 Typical Thermal Properties of Common Building and Insulating Materials—Design Values^a (continued)

(Source: ASHRAE Handbook—Fundamentals [2013], Chapter 26, Table 1)

Description	Density, kg/m ³	Conductivity ^b <i>k</i> , W/(m·K)	Resistance <i>R</i> , (m ² ·K)/W	Specific Heat, kJ/(kg·K)	Reference ¹
	64 to 96	0.063	—	—	Manufacturer (pre 2001)
<i>Spray-applied</i>					
Cellulose, sprayed into open wall cavities.....	26 to 42	0.039 to 0.040	—	—	Two manufacturers (2011)
Glass fiber, sprayed into open wall or attic cavities	16	0.039 to 0.042	—	—	Manufacturers' association (2011)
	29 to 37	0.033 to 0.037	—	—	Four manufacturers (2011)
Polyurethane foam	—	—	—	1.5	Kumaran (2002)
low density, open cell	7.2 to 10	0.037 to 0.042	—	—	Three manufacturers (2011)
medium density, closed cell, aged 180 days.....	30 to 51	0.020 to 0.029	—	—	Five manufacturers (2011)
Building Board and Siding					
<i>Board</i>					
Asbestos/cement board.....	1900	0.57	—	1.00	Nottage (1947)
Cement board.....	1150	0.25	—	0.84	Kumaran (2002)
Fiber/cement board	1400	0.25	—	0.84	Kumaran (2002)
	1000	0.19	—	0.84	Kumaran (1996)
	400	0.07	—	1.88	Kumaran (1996)
	300	0.06	—	1.88	Kumaran (1996)
Gypsum or plaster board.....	640	0.16	—	1.15	Kumaran (2002)
Oriented strand board (OSB)	650	—	0.11	1.88	Kumaran (2002)
..... 9 to 11 mm	650	—	0.12	1.88	Kumaran (2002)
..... 12.7 mm	460	—	0.14	1.88	Kumaran (2002)
Plywood (douglas fir).....	540	—	0.15	1.88	Kumaran (2002)
..... 12.7 mm	450	—	0.19	1.88	Kumaran (2002)
..... 15.9 mm	450	—	0.19	1.88	Kumaran (2002)
Plywood/wood panels	650	—	0.11	1.88	Kumaran (2002)
Vegetable fiber board	290	—	0.23	1.30	Lewis (1967)
sheathing, regular density	350	—	0.19	1.30	Lewis (1967)
intermediate density	400	—	0.19	1.30	
nail-based sheathing.....	290	—	0.17	1.30	
shingle backer	240	—	0.24	1.26	
sound deadening board	290	0.058	—	0.59	
tile and lay-in panels, plain or acoustic	480	0.072	—	1.38	Lewis (1967)
laminated paperboard	480	0.072	—	1.17	
homogeneous board from repulped paper	Hardboard				
medium density	800	0.105	—	1.30	Lewis (1967)
high density, service-tempered grade and service grade	880	0.12	—	1.34	Lewis (1967)
high density, standard-tempered grade.....	1010	0.144	—	1.34	Lewis (1967)
Particleboard					
low density	590	0.102	—	1.30	Lewis (1967)
medium density.....	800	0.135	—	1.30	Lewis (1967)
high density	1000	1.18	—	—	Lewis (1967)
underlayment.....	640	—	1.22	1.21	Lewis (1967)
15.9 mm	700	0.072	—	1.88	Kumaran (1996)
<i>Shingles</i>					
Asbestos/cement.....	1900	—	0.037	—	
Wood, 400 mm, 190 mm exposure	—	—	0.15	1.30	
Wood, double, 400 mm, 300 mm exposure.....	—	—	0.21	1.17	
Wood, plus ins. backer board	8 mm	—	0.25	1.30	
<i>Siding</i>					
Asbestos/cement, lapped	6.4 mm	—	0.037	1.01	
Asphalt roll siding	—	—	0.026	1.47	
Asphalt insulating siding (12.7 mm bed).....	—	—	0.26	1.47	
Hardboard siding.....	11 mm	—	—	0.12	1.17
Wood, drop, 200 mm.....	25 mm	—	0.14	1.17	
Wood, bevel	Building Membrane				
200 mm, lapped.....	13 mm	—	0.14	1.17	
250 mm, lapped.....	19 mm	—	0.18	1.17	
Wood, plywood, lapped.....	9.5 mm	—	0.10	1.22	
Aluminum, steel, or vinyl, ^{h, i} over sheathing	—	—	—	—	
hollow-backed.....	—	—	0.11	1.22 ⁱ	
insulating-board-backed.....	9.5 mm	—	0.32	1.34	
foil-backed.....	9.5 mm	—	0.52	—	
Architectural (soda-lime float) glass	2500	1.0	—	0.84	
Building Membrane					
Vapor-permeable felt.....	—	—	0.011	—	
Vapor: seal, 2 layers of mopped 0.73 kg/m ² felt.....	—	—	0.21	—	
Vapor: seal, plastic film.....	—	—	Negligible	—	

Load Calculation Applications Manual (SI), Second Edition

Table 3.1 Typical Thermal Properties of Common Building and Insulating Materials—Design Values^a (continued)

(Source: ASHRAE Handbook—Fundamentals [2013], Chapter 26, Table 1)

Description	Density, kg/m ³	Conductivity ^b <i>k</i> , W/(m·K)	Resistance <i>R</i> , (m ² ·K)/W	Specific Heat, kJ/(kg·K)	Reference ¹
Finish Flooring Materials					
Carpet and rebounded urethane pad..... 19 mm	110	—	0.42	—	NIST (2000)
Carpet and rubber pad (one-piece) 9.5 mm	320	—	0.12	—	NIST (2000)
Pile carpet with rubber pad 9.5 to 12.7 mm	290	—	0.28	—	NIST (2000)
Linoleum/cork tile..... 6.4 mm	465	—	0.09	—	NIST (2000)
PVC/rubber floor covering.....	—	0.40	—	—	CIBSE (2006)
rubber tile..... 25 mm	1900	—	0.06	—	NIST (2000)
terrazzo..... 25 mm	—	—	0.014	0.80	
Metals (See Chapter 33, Table 3)					
Roofing					
Asbestos/cement shingles.....	1920	—	0.037	1.00	
Asphalt (bitumen with inert fill)	1600	0.43	—	—	CIBSE (2006)
	1900	0.58	—	—	CIBSE (2006)
	2300	1.15	—	—	CIBSE (2006)
Asphalt roll roofing.....	920	—	0.027	1.51	
Asphalt shingles.....	920	—	0.078	1.26	
Built-up roofing..... 10 mm	920	—	0.059	1.47	
Mastic asphalt (heavy, 20% grit)	950	0.19	—	—	CIBSE (2006)
Reed thatch.....	270	0.09	—	—	CIBSE (2006)
Roofing felt.....	2250	1.20	—	—	CIBSE (2006)
Slate..... 13 mm	—	—	0.009	1.26	
Straw thatch.....	240	0.07	—	—	CIBSE (2006)
Wood shingles, plain and plastic-film-faced.....	—	—	0.166	1.30	
Plastering Materials					
Cement plaster, sand aggregate.....	1860	0.72	—	0.84	
Sand aggregate..... 10 mm	—	—	0.013	0.84	
..... 20 mm	—	—	0.026	0.84	
Gypsum plaster.....	1120	0.38	—	—	CIBSE (2006)
	1280	0.46	—	—	CIBSE (2006)
Lightweight aggregate..... 13 mm	—	720	—	0.056	—
..... 16 mm	—	720	—	0.066	—
on metal lath..... 19 mm	—	—	0.083	—	—
Perlite aggregate.....	720	0.22	—	1.34	
Sand aggregate.....	1680	0.81	—	0.84	
on metal lath..... 19 mm	—	—	0.023	—	
Vermiculite aggregate.....	480	0.14	—	—	CIBSE (2006)
	600	0.20	—	—	CIBSE (2006)
	720	0.25	—	—	CIBSE (2006)
	840	0.26	—	—	CIBSE (2006)
	960	0.30	—	—	CIBSE (2006)
Perlite plaster.....	400	0.08	—	—	CIBSE (2006)
	600	0.19	—	—	CIBSE (2006)
Pulpboard or paper plaster.....	600	0.07	—	—	CIBSE (2006)
Sand/cement plaster, conditioned.....	1560	0.63	—	—	CIBSE (2006)
Sand/cement/lime plaster, conditioned.....	1440	0.48	—	—	CIBSE (2006)
Sand/gypsum (3:1) plaster, conditioned.....	1550	0.65	—	—	CIBSE (2006)
Masonry Materials					
<i>Masonry units</i>					
Brick, fired clay.....	2400	1.21 to 1.47	—	—	Valore (1988)
	2240	1.07 to 1.30	—	—	Valore (1988)
	2080	0.92 to 1.12	—	—	Valore (1988)
	1920	0.81 to 0.98	—	0.80	Valore (1988)
	1760	0.71 to 0.85	—	—	Valore (1988)
	1600	0.61 to 0.74	—	—	Valore (1988)
	1440	0.52 to 0.62	—	—	Valore (1988)
	1280	0.43 to 0.53	—	—	Valore (1988)
	1120	0.36 to 0.45	—	—	Valore (1988)
Clay tile, hollow					
1 cell deep..... 75 mm	—	—	0.14	0.88	Rowley and Algren (1937)
..... 100 mm	—	—	0.20	—	Rowley and Algren (1937)
2 cells deep..... 150 mm	—	—	0.27	—	Rowley and Algren (1937)
..... 200 mm	—	—	0.33	—	Rowley and Algren (1937)
..... 250 mm	—	—	0.39	—	Rowley and Algren (1937)
3 cells deep..... 300 mm	—	—	0.44	—	Rowley and Algren (1937)
Lightweight brick.....	800	0.20	—	—	Kumaran (1996)

Thermal Property Data

Table 3.1 Typical Thermal Properties of Common Building and Insulating Materials—Design Values^a (continued)

(Source: ASHRAE Handbook—Fundamentals [2013], Chapter 26, Table 1)

Description	Density, kg/m ³	Conductivity ^b <i>k</i> , W/(m·K)	Resistance <i>R</i> , (m ² ·K)/W	Specific Heat, kJ/(kg·K)	Reference ¹
	770	0.22	—	—	Kumaran (1996)
<i>Concrete blocks^{f, g}</i>					
Limestone aggregate					
~200 mm, 16.3 kg, 2200 kg/m ³ concrete, 2 cores	—	—	—	—	
with perlite-filled cores	—	—	0.37	—	Valore (1988)
~300 mm, 25 kg, 2200 kg/m ³ concrete, 2 cores	—	—	—	—	
with perlite-filled cores	—	—	0.65	—	Valore (1988)
Normal-weight aggregate (sand and gravel)					
~200 mm, 16 kg, 2100 kg/m ³ concrete, 2 or 3 cores...	—	—	0.20 to 0.17	0.92	Van Geem (1985)
with perlite-filled cores	—	—	0.35	—	Van Geem (1985)
with vermiculite-filled cores	—	—	0.34 to 0.24	—	Valore (1988)
~300 mm, 22.7 kg, 2000 kg/m ³ concrete, 2 cores	—	—	0.217	0.92	Valore (1988)
Medium-weight aggregate (combinations of normal and lightweight aggregate)					
~200 mm, 13 kg, 1550 to 1800 kg/m ³ concrete, 2 or 3 cores	—	—	0.30 to 0.22	—	Van Geem (1985)
with perlite-filled cores	—	—	0.65 to 0.41	—	Van Geem (1985)
with vermiculite-filled cores	—	—	0.58	—	Van Geem (1985)
with molded-EPS-filled (beads) cores	—	—	0.56	—	Van Geem (1985)
with molded EPS inserts in cores	—	—	0.47	—	Van Geem (1985)
Low-mass aggregate (expanded shale, clay, slate or slag, pumice)					
~150 mm, 7 1/2 kg, 1400 kg/m ² concrete, 2 or 3 cores	—	—	0.34 to 0.29	—	Van Geem (1985)
with perlite-filled cores	—	—	0.74	—	Van Geem (1985)
with vermiculite-filled cores	—	—	0.53	—	Van Geem (1985)
200 mm, 8 to 10 kg, 1150 to 1380 kg/m ² concrete.....	—	—	0.56 to 0.33	0.88	Van Geem (1985)
with perlite-filled cores	—	—	1.20 to 0.77	—	Van Geem (1985)
with vermiculite-filled cores	—	—	0.93 to 0.69	—	Shu et al. (1979)
with molded-EPS-filled (beads) cores	—	—	0.85	—	Shu et al. (1979)
with UF foam-filled cores	—	—	0.79	—	Shu et al. (1979)
with molded EPS inserts in cores	—	—	0.62	—	Shu et al. (1979)
300 mm, 16 kg, 1400 kg/m ³ , concrete, 2 or 3 cores	—	—	0.46 to 0.40	—	Van Geem (1985)
with perlite-filled cores	—	—	1.6 to 1.1	—	Van Geem (1985)
with vermiculite-filled cores	—	—	1.0	—	Valore (1988)
Stone, lime, or sand	2880	10.4	—	—	Valore (1988)
Quartzitic and sandstone	2560	6.2	—	—	Valore (1988)
	2240	3.46	—	—	Valore (1988)
	1920	1.88	—	0.88	Valore (1988)
Calclitic, dolomitic, limestone, marble, and granite	2880	4.33	—	—	Valore (1988)
	2560	3.17	—	—	Valore (1988)
	2240	2.31	—	—	Valore (1988)
	1920	1.59	—	0.88	Valore (1988)
	1600	1.15	—	—	Valore (1988)
Gypsum partition tile					
75 by 300 by 760 mm, solid.....	—	—	0.222	0.79	Rowley and Algren (1937)
4 cells	—	—	0.238	—	Rowley and Algren (1937)
100 by 300 by 760 mm, 3 cells	—	—	0.294	—	Rowley and Algren (1937)
Limestone	2400	0.57	—	0.84	Kumaran (2002)
	2600	0.93	—	0.84	Kumaran (2002)
<i>Concretesⁱ</i>					
Sand and gravel or stone aggregate concretes.....	2400	1.4 to 2.9	—	—	Valore (1988)
(concretes with >50% quartz or quartzite sand have	2240	1.3 to 2.6	—	0.80 to 1.00	Valore (1988)
conductivities in higher end of range)	2080	1.0 to 1.9	—	—	Valore (1988)
Low-mass aggregate or limestone concretes.....	1920	0.9 to 1.3	—	—	Valore (1988)
expanded shale, clay, or slate; expanded slags; cinders;	1600	0.68 to 0.89	—	0.84	Valore (1988)
pumice (with density up to 1600 kg/m ³); scoria	1280	0.48 to 0.59	—	0.84	Valore (1988)
(sanded	960	0.30 to 0.36	—	—	Valore (1988)
concretes have conductivities in higher end of range)	640	0.18	—	—	Valore (1988)
Gypsum/fiber concrete (87.5% gypsum, 12.5% wood chips)	800	0.24	—	0.84	Rowley and Algren (1937)
Cement/lime, mortar, and stucco	1920	1.40	—	—	Valore (1988)
	1600	0.97	—	—	Valore (1988)
	1280	0.65	—	—	Valore (1988)
Perlite, vermiculite, and polystyrene beads	800	0.26 to 0.27	—	—	Valore (1988)
	640	0.20 to 0.22	—	0.63 to 0.96	Valore (1988)
	480	0.16	—	—	Valore (1988)
	320	0.12	—	—	Valore (1988)

Load Calculation Applications Manual (SI), Second Edition

Table 3.1 Typical Thermal Properties of Common Building and Insulating Materials—Design Values^a (continued)

(Source: ASHRAE Handbook—Fundamentals [2013], Chapter 26, Table 1)

Description	Density, kg/m ³	Conductivity ^b <i>k</i> , W/(m·K)	Resistance <i>R</i> , (m ² ·K)/W	Specific Heat, kJ/(kg·K)	Reference ¹
Foam concretes	1920	0.75	—	—	Valore (1988)
	1600	0.60	—	—	Valore (1988)
	1280	0.44	—	—	Valore (1988)
	1120	0.36	—	—	Valore (1988)
Foam concretes and cellular concretes	960	0.30	—	—	Valore (1988)
	640	0.20	—	—	Valore (1988)
	320	0.12	—	—	Valore (1988)
Aerated concrete (oven-dried)	430 to 800	0.20	—	0.84	Kumaran (1996)
Polystyrene concrete (oven-dried)	255 to 800	0.37	—	0.84	Kumaran (1996)
Polymer concrete	1950	1.64	—	—	Kumaran (1996)
	2200	1.03	—	—	Kumaran (1996)
Polymer cement	1870	0.78	—	—	Kumaran (1996)
Slag concrete	960	0.22	—	—	Touloukian et al. (1970)
	1280	0.32	—	—	Touloukian et al. (1970)
	1600	0.43	—	—	Touloukian et al. (1970)
	2000	1.23	—	—	Touloukian et al. (1970)
Woods (12% moisture content)^j					
<i>Hardwoods</i>					
Oak	—	—	—	1.63 ^k	Wilkes (1979)
Oak	660 to 750	0.16 to 0.18	—	—	Cardenas and Bible (1987)
Birch	680 to 725	0.17 to 0.18	—	—	Cardenas and Bible (1987)
Maple	635 to 700	0.16 to 0.17	—	—	Cardenas and Bible (1987)
Ash	615 to 670	0.15 to 0.16	—	—	Cardenas and Bible (1987)
<i>Softwoods</i>					
Southern pine	—	—	—	1.63 ^k	Wilkes (1979)
Southern pine	570 to 660	0.14 to 0.16	—	—	Cardenas and Bible (1987)
Southern yellow pine	500	0.13	—	—	Kumaran (2002)
Eastern white pine	400	0.10	—	—	Kumaran (2002)
Douglas fir/larch	535 to 580	0.14 to 0.15	—	—	Cardenas and Bible (1987)
Southern cypress	500 to 515	0.13	—	—	Cardenas and Bible (1987)
Hem/fir, spruce/pine/fir	390 to 500	0.11 to 0.13	—	—	Cardenas and Bible (1987)
Spruce	400	0.09	—	—	Kumaran (2002)
Western red cedar	350	0.09	—	—	Kumaran (2002)
West coast woods, cedars	350 to 500	0.10 to 0.13	—	—	Cardenas and Bible (1987)
Eastern white cedar	360	0.10	—	—	Kumaran (2002)
California redwood	390 to 450	0.11 to 0.12	—	—	Cardenas and Bible (1987)
Pine (oven-dried)	370	0.092	—	1.88	Kumaran (1996)
Spruce (oven-dried)	395	0.10	—	1.88	Kumaran (1996)

Thermal Property Data

Table 3.2 Thermal Resistances of Plane Air Spaces, ^{a,b,c} (m²·K)/W








(Source: ASHRAE Handbook—Fundamentals [2013], Chapter 26, Table 3)

Position of Air Space	Direction of Heat Flow	Air Space		Effective Emittance $\epsilon_{eff}^{d,e}$									
		Mean Temp. ^d , °C	Temp. Diff. ^d , K	13 mm Air Space ^c					20 mm Air Space ^c				
				0.03	0.05	0.2	0.5	0.82	0.03	0.05	0.2	0.5	0.82
Horiz.	Up ↑	32.2	5.6	0.37	0.36	0.27	0.17	0.13	0.41	0.39	0.28	0.18	0.13
		10.0	16.7	0.29	0.28	0.23	0.17	0.13	0.30	0.29	0.24	0.17	0.14
		10.0	5.6	0.37	0.36	0.28	0.20	0.15	0.40	0.39	0.30	0.20	0.15
		-17.8	11.1	0.30	0.30	0.26	0.20	0.16	0.32	0.32	0.27	0.20	0.16
		-17.8	5.6	0.37	0.36	0.30	0.22	0.18	0.39	0.38	0.31	0.23	0.18
		-45.6	11.1	0.30	0.29	0.26	0.22	0.18	0.31	0.31	0.27	0.22	0.19
45° Slope	Up ↗	32.2	5.6	0.43	0.41	0.29	0.19	0.13	0.52	0.49	0.33	0.20	0.14
		10.0	16.7	0.36	0.35	0.27	0.19	0.15	0.35	0.34	0.27	0.19	0.14
		10.0	5.6	0.45	0.43	0.32	0.21	0.16	0.51	0.48	0.35	0.23	0.17
		-17.8	11.1	0.39	0.38	0.31	0.23	0.18	0.37	0.36	0.30	0.23	0.18
		-17.8	5.6	0.46	0.45	0.36	0.25	0.19	0.48	0.46	0.37	0.26	0.20
		-45.6	11.1	0.37	0.36	0.31	0.25	0.21	0.36	0.35	0.31	0.25	0.20
Vertical	Horiz. →	32.2	5.6	0.43	0.41	0.29	0.19	0.14	0.62	0.57	0.37	0.21	0.15
		10.0	16.7	0.45	0.43	0.32	0.22	0.16	0.51	0.49	0.35	0.23	0.17
		10.0	5.6	0.47	0.45	0.33	0.22	0.16	0.65	0.61	0.41	0.25	0.18
		-17.8	11.1	0.50	0.48	0.38	0.26	0.20	0.55	0.53	0.41	0.28	0.21
		-17.8	5.6	0.52	0.50	0.39	0.27	0.20	0.66	0.63	0.46	0.30	0.22
		-45.6	11.1	0.51	0.50	0.41	0.31	0.24	0.51	0.50	0.42	0.31	0.24
45° Slope	Down ↘	32.2	5.6	0.44	0.41	0.29	0.19	0.14	0.62	0.58	0.37	0.21	0.15
		10.0	16.7	0.46	0.44	0.33	0.22	0.16	0.60	0.57	0.39	0.24	0.17
		10.0	5.6	0.47	0.45	0.33	0.22	0.16	0.67	0.63	0.42	0.26	0.18
		-17.8	11.1	0.51	0.49	0.39	0.27	0.20	0.66	0.63	0.46	0.30	0.22
		-17.8	5.6	0.52	0.50	0.39	0.27	0.20	0.73	0.69	0.49	0.32	0.23
		-45.6	11.1	0.56	0.54	0.44	0.33	0.25	0.67	0.64	0.51	0.36	0.28
Horiz.	Down ↓	32.2	5.6	0.44	0.41	0.29	0.19	0.14	0.62	0.58	0.37	0.21	0.15
		10.0	16.7	0.47	0.45	0.33	0.22	0.16	0.66	0.62	0.42	0.25	0.18
		10.0	5.6	0.47	0.45	0.33	0.22	0.16	0.68	0.63	0.42	0.26	0.18
		-17.8	11.1	0.52	0.50	0.39	0.27	0.20	0.74	0.70	0.50	0.32	0.23
		-17.8	5.6	0.52	0.50	0.39	0.27	0.20	0.75	0.71	0.51	0.32	0.23
		-45.6	11.1	0.57	0.55	0.45	0.33	0.26	0.81	0.78	0.59	0.40	0.30
Horiz.	Up ↑	32.2	5.6	0.45	0.42	0.30	0.19	0.14	0.50	0.47	0.32	0.20	0.14
		10.0	16.7	0.33	0.32	0.26	0.18	0.14	0.27	0.35	0.28	0.19	0.15
		10.0	5.6	0.44	0.42	0.32	0.21	0.16	0.49	0.47	0.34	0.23	0.16
		-17.8	11.1	0.35	0.34	0.29	0.22	0.17	0.40	0.38	0.32	0.23	0.18
		-17.8	5.6	0.43	0.41	0.33	0.24	0.19	0.48	0.46	0.36	0.26	0.20
		-45.6	11.1	0.34	0.34	0.30	0.24	0.20	0.39	0.38	0.33	0.26	0.21
45° Slope	Up ↗	32.2	5.6	0.51	0.48	0.33	0.20	0.14	0.56	0.52	0.35	0.21	0.14
		10.0	16.7	0.38	0.36	0.28	0.20	0.15	0.40	0.38	0.29	0.20	0.15
		10.0	5.6	0.51	0.48	0.35	0.23	0.17	0.55	0.52	0.37	0.24	0.17
		-17.8	11.1	0.40	0.39	0.32	0.24	0.18	0.43	0.41	0.33	0.24	0.19
		-17.8	5.6	0.49	0.47	0.37	0.26	0.20	0.52	0.51	0.39	0.27	0.20
		-45.6	11.1	0.39	0.38	0.33	0.26	0.21	0.41	0.40	0.35	0.27	0.22
Vertical	Horiz. →	32.2	5.6	0.70	0.64	0.40	0.22	0.15	0.65	0.60	0.38	0.22	0.15
		10.0	16.7	0.45	0.43	0.32	0.22	0.16	0.47	0.45	0.33	0.22	0.16
		10.0	5.6	0.67	0.62	0.42	0.26	0.18	0.64	0.60	0.41	0.25	0.18
		-17.8	11.1	0.49	0.47	0.37	0.26	0.20	0.51	0.49	0.38	0.27	0.20
		-17.8	5.6	0.62	0.59	0.44	0.29	0.22	0.61	0.59	0.44	0.29	0.22
		-45.6	11.1	0.46	0.45	0.38	0.29	0.23	0.50	0.48	0.40	0.30	0.24
Vertical	Horiz. →	32.2	5.6	0.45	0.42	0.30	0.19	0.14	0.50	0.47	0.32	0.20	0.14
		10.0	16.7	0.33	0.32	0.26	0.18	0.14	0.27	0.35	0.28	0.19	0.15
		10.0	5.6	0.44	0.42	0.32	0.21	0.16	0.49	0.47	0.34	0.23	0.16
		-17.8	11.1	0.35	0.34	0.29	0.22	0.17	0.40	0.38	0.32	0.23	0.18
		-17.8	5.6	0.43	0.41	0.33	0.24	0.19	0.48	0.46	0.36	0.26	0.20
		-45.6	11.1	0.34	0.34	0.30	0.24	0.20	0.39	0.38	0.33	0.26	0.21
45° Slope	Up ↗	32.2	5.6	0.51	0.48	0.33	0.20	0.14	0.56	0.52	0.35	0.21	0.14
		10.0	16.7	0.38	0.36	0.28	0.20	0.15	0.40	0.38	0.29	0.20	0.15
		10.0	5.6	0.51	0.48	0.35	0.23	0.17	0.55	0.52	0.37	0.24	0.17
		-17.8	11.1	0.40	0.39	0.32	0.24	0.18	0.43	0.41	0.33	0.24	0.19
		-17.8	5.6	0.49	0.47	0.37	0.26	0.20	0.52	0.51	0.39	0.27	0.20
		-45.6	11.1	0.39	0.38	0.33	0.26	0.21	0.41	0.40	0.35	0.27	0.22
Vertical	Horiz. →	32.2	5.6	0.70	0.64	0.40	0.22	0.15	0.65	0.60	0.38	0.22	0.15
		10.0	16.7	0.45	0.43	0.32	0.22	0.16	0.47	0.45	0.33	0.22	0.16
		10.0	5.6	0.67	0.62	0.42	0.26	0.18	0.64	0.60	0.41	0.25	0.18
		-17.8	11.1	0.49	0.47	0.37	0.26	0.20	0.51	0.49	0.38	0.27	0.20
		-17.8	5.6	0.62	0.59	0.44	0.29	0.22	0.61	0.59	0.44	0.29	0.22
		-45.6	11.1	0.46	0.45	0.38	0.29	0.23	0.50	0.48	0.40	0.30	0.24
Vertical	Horiz. →	32.2	5.6	0.45	0.42	0.30	0.19	0.14	0.50	0.47	0.32	0.20	0.14
		10.0	16.7	0.33	0.32	0.26	0.18	0.14	0.27	0.35	0.28	0.19	0.15
		10.0	5.6	0.44	0.42	0.32	0.21	0.16	0.49	0.47	0.34	0.23	0.16
		-17.8	11.1	0.35	0.34	0.29	0.22	0.17	0.40	0.38	0.32	0.23	0.18
		-17.8	5.6	0.43	0.41	0.33	0.24	0.19	0.48	0.46	0.36	0.26	0.20
		-45.6	11.1	0.34	0.34	0.30	0.24	0.20	0.39	0.38	0.33	0.26	0.21
45° Slope	Up ↗	32.2	5.6	0.51	0.48	0.33	0.20	0.14	0.56	0.52	0.35	0.21	0.14
		10.0	16.7	0.38	0.36	0.28	0.20	0.15	0.40	0.38	0.29	0.20	0.15
		10.0	5.6	0.51	0.48	0.35	0.23	0.17	0.55	0.52	0.37	0.24	0.17
		-17.8	11.1	0.40	0.39	0.32	0.24	0.18	0.43	0.41	0.33	0.24	0.19
		-17.8	5.6	0.49	0.47	0.37	0.26	0.20	0.52	0.51	0.39	0.27	0.20
		-45.6	11.1	0.39	0.38	0.33	0.26	0.21	0.41	0.40	0.35	0.27	0.22
Vertical	Horiz. →	32.2	5.6	0.70	0.64	0.40	0.22	0.15	0.65	0.60	0.38	0.22	0.15
		10.0	16.7	0.45	0.43	0.32	0.22	0.16	0.47	0.45	0.33	0.22	0.16
		10.0	5.6	0.67	0.62	0.42	0.26	0.18	0.64	0.60	0.41	0.25	0.18
		-17.8	11.1	0.49	0.47	0.37	0.26	0.20	0.51	0.49	0.38	0.27	0.20
		-17.8	5.6	0.62	0.59	0.44	0.29	0.22	0.61	0.59	0.44	0.29	0.22
		-45.6	11.1	0.46	0.45	0.38	0.29	0.23	0.50	0.48	0.40	0.30	0.24
Vertical	Horiz. →	32.2	5.6	0.45	0.42	0.30	0.19	0.14	0.50	0.47	0.32	0.20	0.14
		10.0	16.7	0.33	0.32	0.26	0.18	0.14	0.27	0.35	0.28	0.19	0.15
		10.0	5.6	0.44	0.42	0.32	0.21	0.16	0.49	0.47	0.34	0.23	0.16
		-17.8	11.1	0.35	0.34	0.29	0.22	0.17	0.40	0.38	0.32	0.23	0.18
		-17.8	5.6	0.43	0.41	0.33	0.24	0.19	0.48	0.46	0.36	0.26	0.20
		-45.6	11.1	0.34	0.34	0.30	0.24	0.20	0.39	0.38	0.33	0.26	0.21
45° Slope	Up ↗	32.2	5.6	0.51	0.48	0.33	0.20	0.14	0.56	0.52	0.35	0.21	0.14
		10.0</											

Load Calculation Applications Manual (SI), Second Edition

Table 3.2 Thermal Resistances of Plane Air Spaces, ^{a,b,c} (m²·K)/W (continued)

(Source: ASHRAE Handbook—Fundamentals [2013], Chapter 26, Table 3)

Air Space		Effective Emittance $\epsilon_{eff}^{d,e}$											
Position of Air Space	Direction of Heat Flow	Mean Temp. ^d , °C	Temp. Diff., ^d K	40 mm Air Space ^c					90 mm Air Space ^c				
				0.03	0.05	0.2	0.5	0.82	0.03	0.05	0.2	0.5	0.82
45° Slope	Down 	32.2	5.6	0.89	0.80	0.45	0.24	0.16	0.85	0.76	0.44	0.24	0.16
		10.0	16.7	0.63	0.59	0.41	0.25	0.18	0.62	0.58	0.40	0.25	0.18
		10.0	5.6	0.90	0.82	0.50	0.28	0.19	0.83	0.77	0.48	0.28	0.19
		-17.8	11.1	0.68	0.64	0.47	0.31	0.22	0.67	0.64	0.47	0.31	0.22
		-17.8	5.6	0.87	0.81	0.56	0.34	0.24	0.81	0.76	0.53	0.33	0.24
		-45.6	11.1	0.64	0.62	0.49	0.35	0.27	0.66	0.64	0.51	0.36	0.28
Horiz.	Down 	32.2	5.6	1.07	0.94	0.49	0.25	0.17	1.77	1.44	0.60	0.28	0.18
		10.0	16.7	1.10	0.99	0.56	0.30	0.20	1.69	1.44	0.68	0.33	0.21
		10.0	5.6	1.16	1.04	0.58	0.30	0.20	1.96	1.63	0.72	0.34	0.22
		-17.8	11.1	1.24	1.13	0.69	0.39	0.26	1.92	1.68	0.86	0.43	0.29
		-17.8	5.6	1.29	1.17	0.70	0.39	0.27	2.11	1.82	0.89	0.44	0.29
		-45.6	11.1	1.36	1.27	0.84	0.50	0.35	2.05	1.85	1.06	0.57	0.38
Horiz.	Up 	32.2	5.6	0.53	0.50	0.33	0.20	0.14					
		10.0	16.7	0.39	0.38	0.29	0.20	0.15					
		10.0	5.6	0.52	0.50	0.36	0.23	0.17					
		17.8	11.1	0.42	0.41	0.33	0.24	0.19					
		17.8	5.6	0.51	0.49	0.38	0.27	0.20					
		45.6	11.1	0.41	0.40	0.34	0.27	0.22					
45° Slope	Up 	32.2	5.6	0.57	0.54	0.35	0.21	0.15					
		10.0	16.7	0.39	0.37	0.29	0.20	0.15					
		10.0	5.6	0.56	0.53	0.37	0.24	0.17					
		17.8	11.1	0.41	0.40	0.33	0.24	0.18					
		17.8	5.6	0.53	0.51	0.39	0.27	0.20					
		45.6	11.1	0.38	0.37	0.32	0.26	0.21					
Vertical	Horiz. 	32.2	5.6	0.66	0.61	0.38	0.22	0.15					
		10.0	16.7	0.50	0.47	0.35	0.23	0.16					
		10.0	5.6	0.66	0.61	0.42	0.25	0.18					
		17.8	11.1	0.54	0.52	0.40	0.28	0.21					
		17.8	5.6	0.64	0.61	0.46	0.30	0.22					
		45.6	11.1	0.53	0.52	0.43	0.32	0.25					
45° Slope	Down 	32.2	5.6	0.865	0.78	0.44	0.24	0.16					
		10.0	16.7	0.68	0.64	0.43	0.26	0.18					
		10.0	5.6	0.87	0.80	0.49	0.28	0.19					
		17.8	11.1	0.75	0.71	0.50	0.32	0.23					
		17.8	5.6	0.87	0.82	0.56	0.34	0.24					
		45.6	11.1	0.75	0.73	0.56	0.39	0.29					
Horiz.	Down 	32.2	5.6	2.06	1.63	0.63	0.28	0.18					
		10.0	16.7	1.87	1.57	0.71	0.34	0.22					
		10.0	5.6	2.24	1.82	0.75	0.35	0.22					
		17.8	11.1	2.13	1.84	0.90	0.44	0.29					
		17.8	5.6	2.43	2.05	0.95	0.46	0.29					
		45.6	11.1	2.19	1.96	1.10	0.58	0.39					

^aSee Chapter 25. Thermal resistance values were determined from $R = 1/C$, where $C = h_c + \epsilon_{eff} h_r$, h_c is conduction/convection coefficient, $\epsilon_{eff} h_r$ is radiation coefficient $\approx 0.227 \epsilon_{eff} [(t_m + 273)/100]^3$, and t_m is mean temperature of air space. Values for h_c were determined from data developed by Robinson et al. (1954). Equations (5) to (7) in Yarbrough (1983) show data in this table in analytic form. For extrapolation from this table to air spaces less than 12.5 mm (e.g., insulating window glass), assume $h_c = 21.8(1 + 0.00274t_m)/l$, where l is air space thickness in mm, and h_c is heat transfer in W/(m²·K) through air space only.

^bValues based on data presented by Robinson et al. (1954). (Also see Chapter 4, Tables 5 and 6, and Chapter 33). Values apply for ideal conditions (i.e., air spaces of uniform thickness bounded by plane, smooth, parallel surfaces with no air leakage to or from the space). **This table should not be used for hollow siding or profiled cladding; see Table 1.** For greater accuracy, use overall U-factors determined through guarded hot box (ASTM Standard C1363) testing. Thermal resistance values for multiple air spaces must be based on careful estimates of mean temperature differences for each air space.

^cA single resistance value cannot account for multiple air spaces; each air space requires a separate resistance calculation that applies only for established boundary conditions. Resistances of horizontal spaces with heat flow downward are substantially independent of temperature difference.

^dInterpolation is permissible for other values of mean temperature, temperature difference, and effective emittance ϵ_{eff} . Interpolation and moderate extrapolation for air spaces greater than 90 mm are also permissible.

^eEffective emittance ϵ_{eff} of air space is given by $1/\epsilon_{eff} = 1/\epsilon_1 + 1/\epsilon_2 - 1$, where ϵ_1 and ϵ_2 are emittances of surfaces of air space (see Table 2). **Also, oxidation, corrosion, and accumulation of dust and dirt can dramatically increase surface emittance. Emittance values of 0.05 should only be used where the highly reflective surface can be maintained over the service life of the assembly.**

3.1.2 Surface Conductance and Resistances

The transfer of heat to surfaces such as walls and roofs is usually a combination of convection and radiation. For simplified calculation methods, (e.g., the radiant time series method [RTSM]) the two modes are combined into a combined-surface conductance or thermal resistance, even though the radiation component is quite sensitive to

Table 3.3a Emissivity of Various Surfaces and Effective Emittances of Facing Air Spaces^a

(Source: 2013 ASHRAE Handbook—Fundamentals, Chapter 26, Table 2)

Surface	Average Emissivity ϵ	Effective Emittance ϵ_{eff} of Air Space	
		One Surface's Emittance ϵ ; Other, 0.9	Both Surfaces' Emittance ϵ
Aluminum foil, bright	0.05	0.05	0.03
Aluminum foil, with condensate just visible (>0.7 g/ft ²)(>0.5 g/m ²)	0.30 ^b	0.29	—
Aluminum foil, with condensate clearly visible (>2.9 g/ft ²)(>2.0 g/m ²)	0.70 ^b	0.65	—
Aluminum sheet	0.12	0.12	0.06
Aluminum-coated paper, polished	0.20	0.20	0.11
Brass, nonoxidized	0.04	0.038	0.02
Copper, black oxidized	0.74	0.41	0.59
Copper, polished	0.04	0.038	0.02
Iron and steel, polished	0.2	0.16	0.11
Iron and steel, oxidized	0.58	0.35	0.41
Lead, oxidized	0.27	0.21	0.16
Nickel, nonoxidized	0.06	0.056	0.03
Silver, polished	0.03	0.029	0.015
Steel, galvanized, bright	0.25	0.24	0.15
Tin, nonoxidized	0.05	0.047	0.026
Aluminum paint	0.50	0.47	0.35
Building materials: wood, paper, masonry, nonmetallic paints	0.90	0.82	0.82
Regular glass	0.84	0.77	0.72

^aValues apply in 4 to 40 μm range of electromagnetic spectrum. Also, oxidation, corrosion, and accumulation of dust and dirt can dramatically increase surface emittance. Emittance values of 0.05 should only be used where the highly reflective surface can be maintained over the service life of the assembly. Except as noted, data from VDI (1999).

^bValues based on data in Bassett and Trethowen (1984).

Load Calculation Applications Manual (SI), Second Edition

Table 3.3b Solar Absorptance Values of Various Surfaces

Surface	Absorptance
Brick, red (Purdue) ^a	0.63
Paint, cardinal red ^b	0.63
Paint, matte black ^b	0.94
Paint, sandstone ^b	0.50
Paint, white acrylic ^a	0.26
Sheet metal, galvanized, new ^a	0.65
Sheet metal, galvanized, weathered ^a	0.80
Shingles, Aspen Gray ^b	0.82
Shingles, Autumn Brown ^b	0.91
Shingles, Onyx Black ^b	0.97
Shingles, Generic White ^b	0.75
Concrete ^{a,c}	0.60–0.83

^a Incropera and DeWitt (1990).

^b Parker et al. (2000).

^c Miller (1971).

surface type and temperature. Values of combined-surface conductances are given in Table 3.4.

The heat balance method (HBM) separates the radiative and convective heat transfer mechanisms, so the combined-surface conductance is not used. Rather, convection coefficients are determined with correlations and radiative heat transfer is analyzed with the mean radiant temperature method. These are discussed in Chapter 11.

3.2 Calculating Overall Thermal Resistance

For building constructions made out of homogeneous layers, the overall thermal resistance is calculated by summing the individual layer resistances:

$$R = R_i + \sum_{j=1}^N R_j + R_o \quad (3.3)$$

where

R_j = the j^{th} layer thermal resistance given by the ratio of the thickness to the thermal conductivity, $(\text{m}^2 \cdot \text{K})/\text{W}$

R_i = the inside air film thermal resistance, $(\text{m}^2 \cdot \text{K})/\text{W}$

R_o = the outdoor air film thermal resistance, $(\text{m}^2 \cdot \text{K})/\text{W}$

N = the number of layers in the construction

Thermal Property Data

The overall heat transfer coefficient U is the inverse of the overall thermal resistance:

$$U = \frac{1}{R} \quad (3.4)$$

The above example is relatively straightforward because each layer has only a single material. A more common case is for one or more layers to contain multiple materials (e.g., stud and insulation). In this case, the element with the higher conductance is often referred to as a *thermal bridge*. For such building constructions, the effects of the thermal bridge must be taken into account (see Appendix E).

3.3 Thermal and Optical Property Data—Fenestration

The term *fenestration* refers to the openings in the building envelope, such as doors and windows. The thermal properties of doors and windows can have a significant impact on the heating load, as they typically have a much higher conductance than the walls and roof. The optical properties of windows and doors (where glazed) often have a significant impact on the cooling load due to both direct transmission of solar radiation and convection into the space of solar radiation absorbed by the window or door.

When available, manufacturers' data for windows and doors should be used. It is typical for manufacturers of windows to provide U-factors and normal solar heat gain coefficients (SHGCs) for individual products. The manufacturer's U-factor should be used for calculating conductive heat gains, and the manufacturer's SHGC should be used with the RTSM (Chapter 7) or the HBM (Chapter 11) for calculating solar heat gains. If this information is not available, this chapter provides representative thermal and optical property data for a range of fenestration products.

Table 3.4 Surface Film Coefficients/Resistances

(Source: ASHRAE Handbook—Fundamentals [2013], Chapter 26, Table 10)

Position of Surface	Direction of Heat Flow	Surface Emittance, ε					
		Nonreflective $\varepsilon = 0.90$		Reflective			
		h_i	R_i	$\varepsilon = 0.20$		$\varepsilon = 0.05$	
		h_i	R_i	h_i	R_i	h_i	R_i
Indoor							
Horizontal	Upward	9.26	0.11	5.17	0.19	4.32	0.23
Sloping at 45°	Upward	9.09	0.11	5.00	0.20	4.15	0.24
Vertical	Horizontal	8.29	0.12	4.20	0.24	3.35	0.30
Sloping at 45°	Downward	7.50	0.13	3.41	0.29	2.56	0.39
Horizontal	Downward	6.13	0.16	2.10	0.48	1.25	0.80
Outdoor (any position)		h_o	R_o				
Wind (for winter) at 6.7 m/s	Any	34.0	0.030	—	—	—	—
Wind (for summer) at 3.4 m/s	Any	22.7	0.044	—	—	—	—

Notes:

1. Surface conductance h_i and h_o measured in $W/(m^2 \cdot K)$; resistance R_i and R_o in $(m^2 \cdot K)/W$.
2. No surface has both an air space resistance value and a surface resistance value.
3. Conductances are for surfaces of the stated emittance facing virtual blackbody surroundings at same temperature as ambient air. Values based on surface/air temperature difference of 5.6 K and surface temperatures of 21°C.
4. See Chapter 4 for more detailed information.
5. Condensate can have significant effect on surface emittance (see Table 2). Also, oxidation, corrosion, and accumulation of dust and dirt can dramatically increase surface emittance. Emittance values of 0.05 should only be used where highly reflective surface can be maintained over the service life of the assembly.

Example 3.1 Overall Thermal Resistance

Architectural plans for a building show a wall as being constructed from 0.1 m face brick, 0.025 m thick R-5 extruded polystyrene insulation, and 0.2 m concrete masonry unit (CMU, otherwise known as *concrete block*). The face brick is on the outside of the wall. The insulation is glued to the CMU, and there is an air gap (approximately 0.040 m) between the face brick and the insulation. Find the overall thermal resistance and the U-factor for the wall under winter conditions.

Solution: The first step is to find the thermal properties of each layer in the wall. As is often the case, architectural plans do not specify the materials with enough detail to precisely select every material from Table 3.1. In this situation, some engineering judgment is required. For this wall, the overall thermal resistance will depend strongly on the insulation resistance. Fortunately, this is specified. The layers, from outside to inside, are as follows:

- The outside surface resistance, under winter conditions (assumed 6.7 m/s wind) is taken from Table 3.4 as $0.03 \text{ (m}^2\cdot\text{K)/W}$.
- In Table 3.1, thermal properties are given for a range of brick densities, and for every density, variation in conductivity and resistance is given. Taking a median value for density (1760 kg/m^3), an intermediate value for conductivity for resistance would be $0.8 \text{ W/(m}\cdot\text{K)}$ or 0.125 for the 0.1 m thick brick layer ($0.1 \text{ m}/0.8 \text{ W/(m}\cdot\text{K}) = 0.125 \text{ (m}^2\cdot\text{K)/W}$).
- The resistance for the air gap between the brick and the extruded polystyrene insulation can be estimated from Table 3.2. To use Table 3.2, some estimate of the thermal emittance of the two surfaces must be made. From Table 3.3a, we can see that unless the surface is a polished metal, an estimate of 0.82 for emittance is reasonable, and with both surfaces having an emittance of 0.9, the effective emittance for the air gap is 0.82. Returning to Table 3.2, and knowing the air gap is 0.040 m thick, the effective emittance is 0.82, and the direction of heat flow is horizontal, we can then choose the resistance based on an estimate of the mean temperature and temperature difference. Since we are looking at winter conditions, a mean temperature of -17.8°C or 10°C and a temperature difference of 5.6°C or 11.1°C might be reasonable. Note that for the entire span of these combinations, the resistance only varies between 0.20 and 0.22. This will have a small effect on the overall resistance, and therefore we may choose an intermediate value of $0.21 \text{ (m}^2\cdot\text{K)/W}$.
- The resistance of the insulation is known to be $1 \text{ (m}^2\cdot\text{K)/W}$.
- For the concrete block there are even more entries in Table 3.1 than for brick. Lacking specific information for the concrete block, “normal weight aggregate” seems like a good first guess, and review of the table data for all types of unfilled block shows that its resistance ($0.217 - 0.17 \text{ [m}^2\cdot\text{K)/W}$) is at the low end. Hence, we will not go far wrong by choosing a value from within this range, say $0.2 \text{ (m}^2\cdot\text{K)/W}$.
- The inside surface resistance can be chosen from Table 3.4 for horizontal heat flow, nonreflective surface as $0.12 \text{ (m}^2\cdot\text{K)/W}$.

Thermal Property Data

The overall thermal resistance can then be determined by summing up the individual components: $R = 0.03 + 0.125 + 0.21 + 1 + 0.2 + 0.12 = 1.685 \text{ (m}^2\cdot\text{K)/W}$. The U-factor is then determined as the inverse of the overall thermal resistance: $U = 1/R = 1/1.685 = 0.59 \text{ W/(m}^2\cdot\text{K)}$.

With the final value in hand, we can see that small errors in the individual resistances, probably on the order of $0.02 \text{ (m}^2\cdot\text{K)/W}$, will have a fairly small influence on the U-factor. Thus, several of the informed guesses made for the individual layers have quite a small effect.

Tables 3.5a through Table 3.5d provide U-factors for doors that are glazed less than 50% by area. Tables 3.6a and 3.6b provide representative computed U-factors for a variety of generic fenestration products, including windows, skylights, and doors with glazing area in excess of 50%. U-factors, particularly for windows with multiple glazing layers, will vary with temperature. The values in Tables 3.6a and 3.6b are given for heating design conditions but are adequate for cooling design conditions, as conductive heat gain is usually a small fraction of the total heat gain for windows in direct sunlight.

Most of the total heat gain for windows is due to solar radiation transmitted into the space and solar radiation absorbed by the window before flowing into the space via convection and thermal radiation. To determine this heat gain, additional thermal and optical properties are needed. Table 3.7 gives angle-dependent SHGCs, transmittances, reflect-

Table 3.5a Design U-Factors of Swinging Doors in $\text{W}/(\text{m}^2\cdot\text{K})$

(Source: ASHRAE Handbook—Fundamentals [2013] Chapter 15, Table 6)

Door Type (Rough Opening = 970 × 2080 mm)	No Glazing	Single Glazing	Double	Double
			Glazing with 12.7 mm Air Space	Glazing with $e = 0.10$, 12.7 mm Argon
<i>Slab Doors</i>				
Wood slab in wood frame ^a	2.61			
6% glazing (560 × 200 lite)	—	2.73	2.61	2.50
25% glazing (560 × 910 lite)	—	3.29	2.61	2.38
45% glazing (560 × 1620 lite)	—	3.92	2.61	2.21
More than 50% glazing		Use Table 4 (operable)		
Insulated steel slab with wood edge in wood frame ^b	0.91			
6% glazing (560 × 200 lite)	—	1.19	1.08	1.02
25% glazing (560 × 910 lite)	—	2.21	1.48	1.31
45% glazing (560 × 1630 lite)	—	3.29	1.99	1.48
More than 50% glazing		Use Table 4 (operable)		
Foam-insulated steel slab with metal edge in steel frame ^c	2.10			
6% glazing (560 × 200 lite)	—	2.50	2.33	2.21
25% glazing (560 × 910 lite)	—	3.12	2.73	2.50
45% glazing (560 × 1630 lite)	—	4.03	3.18	2.73
More than 50% glazing		Use Table 4 (operable)		
Cardboard honeycomb slab with metal edge in steel frame	3.46			
<i>Stile-and-Rail Doors</i>				
Sliding glass doors/French doors		Use Table 4 (operable)		
<i>Site-Assembled Stile-and-Rail Doors</i>				
Aluminum in aluminum frame	—	7.49	5.28	4.49
Aluminum in aluminum frame with thermal break	—	6.42	4.20	3.58

Notes:

^aThermally broken sill [add $0.17 \text{ W}/(\text{m}^2\cdot\text{K})$ for nonthermally broken sill]

^bNonthermally broken sill

^cNominal U-factors are through center of insulated panel before consideration of thermal bridges around edges of door sections and because of frame.

Load Calculation Applications Manual (SI), Second Edition

Table 3.5b Design U-factors for Revolving Doors in W/(m²·K)

(Source: ASHRAE Handbook—Fundamentals [2013], Chapter 15, Table 7)

Type	Size (Width × Height)	U-Factor
3-wing	2.44 × 2.13 m	4.46
	3.28 × 2.44 m	4.53
4-wing	2.13 × 1.98 m	3.56
	2.13 × 2.29 m	3.63
Open*	2.08 × 2.13 m	7.49

*U-factor of Open door determined using NFRC *Technical Document* 100-91. It has not been updated to current rating methodology in NFRC *Technical Document* 100-2010.

Table 3.5c Design U-factors for Double-Skin Steel Emergency Exit Doors in W/(m²·K)

(Source: ASHRAE Handbook—Fundamentals [2013], Chapter 15, Table 8)

Core Insulation		Rough Opening Size	
Thickness, mm	Type	0.9 × 2 m	1.8 × 2 m
35*	Honeycomb kraft paper	3.23	2.97
	Mineral wool, steel ribs	2.50	2.05
	Polyurethane foam	1.92	1.60
44*	Honeycomb kraft paper	3.25	3.06
	Mineral wool, steel ribs	2.30	1.90
	Polyurethane foam	1.77	1.50
35	Honeycomb kraft paper	3.38	3.11
	Mineral wool, steel ribs	2.67	2.21
	Polyurethane foam	2.10	1.77
44	Honeycomb kraft paper	3.38	3.22
	Mineral wool, steel ribs	2.47	2.08
	Polyurethane foam	1.95	1.69

*With thermal break

Table 3.5d Design U-factors for Double-Skin Steel Garage and Aircraft Hanger Doors in W/(m²·K)

(Source: ASHRAE Handbook—Fundamentals [2013], Chapter 15, Table 9)

Insulation		One-Piece Tilt-Up ^a		Sectional Tilt-Up ^b	Aircraft Hangar	
Thickness, mm	Type	2.44 × 2.1 m	4.9 × 2.1 m	2.74 × 2.1 m	22 × 3.7 m ^c	73 × 15.2 m ^d
35	Extruded polystyrene, steel ribs	2.03	1.90	1.94 to 2.19		
	Expanded polystyrene, steel ribs	1.90	1.74	1.76 to 2.05		
50	Extruded polystyrene, steel ribs	1.74	1.58	1.66 to 1.87		
	Expanded polystyrene, steel ribs	1.62	1.46	1.53 to 1.77		
76	Extruded polystyrene, steel ribs	1.46	1.29	1.43 to 1.60		
	Expanded polystyrene, steel ribs	1.37	1.21	1.34 to 1.52		
102	Extruded polystyrene, steel ribs	1.29	1.13	1.29 to 1.43		
	Expanded polystyrene, steel ribs	1.22	1.06	1.22 to 1.36		
	Extruded polystyrene, steel ribs	1.11	0.93	1.13 to 1.22		
89	Expanded polystyrene, steel ribs	1.06	0.88	1.08 to 1.17		
	Expanded polystyrene				1.40	0.91
	Mineral wool, steel ribs				1.45	0.92
140	Extruded polystyrene				1.32	0.83
	Expanded polystyrene				1.18	0.72
	Mineral wool, steel ribs				1.28	0.73
—	Extruded polystyrene				1.14	0.67
	Uninsulated	6.53 ^e			6.27	7.00

Notes:

^aValues are for both thermally broken and thermally unbroken doors.

^bLower values are for thermally broken doors; higher values are for doors with no thermal break.

^cTypical size for a small private airplane (single or twin engine.)

^dTypical hangar door for a mid-sized commercial jet airliner.

^eU-factor determined using NFRC *Technical Document* 100-91. Not updated to current rating methodology in NFRC *Technical Document* 100-2010. U-factor determined for 3.05 × 3.05 m sectional door, but is representative of similar products of different size.

tances, and absorptances for representative fenestration products. These values may be used in the HBM as explained in Chapter 11. Table 3.8 contains angle correction factors that may be applied to the manufacturer's normal SHGC for use with the RTSM, as explained in Chapter 7. For windows with interior shading such as blinds and draperies, the interior attenuation coefficient (IAC), tabulated in Tables 3.9a through 3.9g, is multiplied by the solar heat gain through an unshaded window to determine the total solar heat gain with interior shading.

Thermal Property Data

Table 3.6a U-Factors for Various Fenestration Products in $W/(m^2 \cdot K)$

(Source: ASHRAE Handbook—Fundamentals [2013], Chapter 15, Table 4)

Product Type		Glass Only		Vertical Installation									
				Operable (including sliding and swinging glass doors)					Fixed				
Frame Type		Center of Glass	Edge of Glass	Aluminum Without Thermal Break	Aluminum With Thermal Break	Aluminum Reinforced Vinyl/Aluminum Clad Wood	Wood/Vinyl	Insulated Fiberglass/Vinyl	Aluminum Without Thermal Break	Aluminum With Thermal Break	Reinforced Vinyl/Aluminum Clad Wood	Wood/Vinyl	Insulated Fiberglass/Vinyl
ID	Glazing Type			Thermal Break	Thermal Break	Aluminum Clad Wood	Wood/Vinyl	Fiberglass/Vinyl	Thermal Break	Thermal Break	Aluminum Clad Wood	Wood/Vinyl	Fiberglass/Vinyl
Single Glazing													
1	3 mm glass	5.91	5.91	7.01	6.08	5.27	5.20	4.83	6.38	6.06	5.58	5.58	5.40
2	6 mm acrylic/polycarb	5.00	5.00	6.23	5.35	4.59	4.52	4.18	5.55	5.23	4.77	4.77	4.61
3	3.2 mm acrylic/polycarb	5.45	5.45	6.62	5.72	4.93	4.86	4.51	5.96	5.64	5.18	5.18	5.01
Double Glazing													
4	6 mm airspace	3.12	3.63	4.62	3.61	3.24	3.14	2.84	3.88	3.52	3.18	3.16	3.04
5	13 mm airspace	2.73	3.36	4.30	3.31	2.96	2.86	2.58	3.54	3.18	2.85	2.83	2.72
6	6 mm argon space	2.90	3.48	4.43	3.44	3.08	2.98	2.69	3.68	3.33	3.00	2.98	2.86
7	13 mm argon space	2.56	3.24	4.16	3.18	2.84	2.74	2.46	3.39	3.04	2.71	2.69	2.58
Double Glazing, e = 0.60 on Surface 2 or 3													
8	6 mm airspace	2.95	3.52	4.48	3.48	3.12	3.02	2.73	3.73	3.38	3.04	3.02	2.90
9	13 mm airspace	2.50	3.20	4.11	3.14	2.80	2.70	2.42	3.34	2.99	2.67	2.65	2.53
10	6 mm argon space	2.67	3.32	4.25	3.27	2.92	2.82	2.54	3.49	3.13	2.81	2.79	2.67
11	13 mm argon space	2.33	3.08	3.98	3.01	2.68	2.58	2.31	3.20	2.84	2.52	2.50	2.39
Double Glazing, e = 0.40 on Surface 2 or 3													
12	6 mm airspace	2.78	3.40	4.34	3.35	3.00	2.90	2.61	3.59	3.23	2.90	2.88	2.77
13	13 mm airspace	2.27	3.04	3.93	2.96	2.64	2.54	2.27	3.15	2.79	2.48	2.46	2.35
14	6 mm argon space	2.44	3.16	4.07	3.09	2.76	2.66	2.38	3.30	2.94	2.62	2.60	2.49
15	13 mm argon space	2.04	2.88	3.75	2.79	2.48	2.38	2.11	2.95	2.60	2.29	2.27	2.16
Double Glazing, e = 0.20 on Surface 2 or 3													
16	6 mm airspace	2.56	3.24	4.16	3.18	2.84	2.74	2.46	3.39	3.04	2.71	2.69	2.58
17	13 mm airspace	1.99	2.83	3.70	2.75	2.44	2.34	2.07	2.91	2.55	2.24	2.22	2.12
18	6 mm argon space	2.16	2.96	3.84	2.88	2.56	2.46	2.19	3.05	2.70	2.38	2.36	2.26
19	13 mm argon space	1.70	2.62	3.47	2.53	2.24	2.14	1.88	2.66	2.30	2.00	1.98	1.88
Double Glazing, e = 0.10 on Surface 2 or 3													
20	6 mm airspace	2.39	3.12	4.02	3.05	2.72	2.62	2.34	3.25	2.89	2.57	2.55	2.44
21	13 mm airspace	1.82	2.71	3.56	2.62	2.32	2.22	1.96	2.76	2.40	2.10	2.08	1.98
22	6 mm argon space	1.99	2.83	3.70	2.75	2.44	2.34	2.07	2.91	2.55	2.24	2.22	2.12
23	13 mm argon space	1.53	2.49	3.33	2.40	2.12	2.02	1.76	2.51	2.16	1.86	1.84	1.74
Double Glazing, e = 0.05 on Surface 2 or 3													
24	6 mm airspace	2.33	3.08	3.98	3.01	2.68	2.58	2.31	3.20	2.84	2.52	2.50	2.39
25	13 mm airspace	1.70	2.62	3.47	2.53	2.24	2.14	1.88	2.66	2.30	2.00	1.98	1.88
26	6 mm argon space	1.87	2.75	3.61	2.66	2.36	2.26	2.00	2.81	2.45	2.15	2.12	2.02
27	13 mm argon space	1.42	2.41	3.24	2.31	2.04	1.94	1.69	2.42	2.06	1.76	1.74	1.65
Triple Glazing													
28	6 mm airspace	2.16	2.96	3.78	2.78	2.46	2.42	2.17	3.02	2.68	2.36	2.36	2.25
29	13 mm airspace	1.76	2.67	3.46	2.47	2.18	2.14	1.90	2.68	2.34	2.03	2.03	1.92
30	6 mm argon space	1.93	2.79	3.60	2.60	2.30	2.26	2.02	2.82	2.49	2.17	2.17	2.06
31	13 mm argon space	1.65	2.58	3.36	2.39	2.10	2.06	1.83	2.58	2.24	1.93	1.93	1.83
Triple Glazing, e = 0.20 on Surface 2, 3, 4, or 5													
32	6 mm airspace	1.87	2.75	3.55	2.56	2.26	2.22	1.98	2.78	2.44	2.12	2.12	2.01
33	13 mm airspace	1.42	2.41	3.18	2.21	1.94	1.90	1.67	2.38	2.05	1.74	1.74	1.64
34	6 mm argon space	1.59	2.54	3.32	2.34	2.06	2.02	1.79	2.53	2.20	1.89	1.89	1.78
35	13 mm argon space	1.25	2.28	3.04	2.08	1.82	1.78	1.55	2.24	1.90	1.60	1.60	1.50
Triple Glazing, e = 0.20 on Surface 2 or 3 and 4 or 5													
36	6 mm airspace	1.65	2.58	3.36	2.39	2.10	2.06	1.83	2.58	2.24	1.93	1.93	1.83
37	13 mm airspace	1.14	2.19	2.95	1.99	1.74	1.69	1.48	2.14	1.80	1.50	1.50	1.40
38	6 mm argon space	1.31	2.32	3.09	2.12	1.86	1.82	1.59	2.29	1.95	1.65	1.65	1.55
39	13 mm argon space	0.97	2.05	2.81	1.86	1.62	1.57	1.36	1.99	1.65	1.36	1.36	1.26
Triple Glazing, e = 0.10 on Surface 2 or 3 and 4 or 5													
40	6 mm airspace	1.53	2.49	3.27	2.30	2.02	1.98	1.75	2.48	2.15	1.84	1.84	1.73
41	13 mm airspace	1.02	2.10	2.85	1.90	1.66	1.61	1.40	2.04	1.70	1.41	1.41	1.31
42	6 mm argon space	1.19	2.23	2.99	2.04	1.78	1.73	1.52	2.19	1.85	1.55	1.55	1.45
43	13 mm argon space	0.80	1.92	2.67	1.73	1.49	1.45	1.24	1.84	1.51	1.22	1.22	1.12
Quadruple Glazing, e = 0.10 on Surface 2 or 3 and 4 or 5													
44	6 mm airspaces	1.25	2.28	3.04	2.08	1.82	1.78	1.55	2.24	1.90	1.60	1.60	1.50
45	13 mm airspaces	0.85	1.96	2.71	1.77	1.54	1.49	1.28	1.89	1.55	1.26	1.26	1.17
46	6 mm argon spaces	0.97	2.05	2.81	1.86	1.62	1.57	1.36	1.99	1.65	1.36	1.36	1.26
47	13 mm argon spaces	0.68	1.83	2.57	1.64	1.41	1.37	1.16	1.74	1.41	1.12	1.12	1.03
48	6 mm krypton spaces	0.68	1.83	2.57	1.64	1.41	1.37	1.16	1.74	1.41	1.12	1.12	1.03

Notes:

1. All heat transmission coefficients in this table include film resistances and are based on winter conditions of -18°C outdoor air temperature and 21°C indoor air temperature, with 6.7 m/s outdoor air velocity and zero solar flux. Except for single glazing, small changes in the indoor and outdoor temperatures do not significantly affect overall U-factors. Coefficients are for vertical position except skylight values, which are for 20° from horizontal with heat flow up.
2. Glazing layer surfaces are numbered from outdoor to indoor. Double, triple, and quadruple refer to number of glazing panels. All data are based on 3 mm glass, unless otherwise noted. Thermal conductivities are: $0.917\text{ W/(m}\cdot\text{K)}$ for glass, and $0.19\text{ W/(m}\cdot\text{K)}$ for acrylic and polycarbonate.
3. Standard spacers are metal. Edge-of-glass effects are assumed to extend over the 63.5 mm band around perimeter of each glazing unit.

Load Calculation Applications Manual (SI), Second Edition

Table 3.6b U-Factors for Various Fenestration Products in W/(m²·K)

(Source: ASHRAE Handbook—Fundamentals [2013], Chapter 15, Table 4)

Vertical Installation					Sloped Installation									ID
Garden Windows		Curtainwall			Glass Only (Skylights)		Manufactured Skylight				Site-Assembled Sloped/Overhead Glazing			
Aluminum Without Thermal Break	Wood/Vinyl	Aluminum Without Thermal Break	Aluminum With Thermal Break	Structural Glazing	Center of Glass	Edge of Glass	Aluminum Without Thermal Break	Aluminum With Thermal Break	Reinforced Vinyl/Aluminum Clad	Wood/Vinyl	Aluminum Without Thermal Break	Aluminum With Thermal Break	Structural Glazing	
14.21	11.94	6.86	6.27	6.27	6.76	6.76	10.03	9.68	9.16	8.05	7.66	7.64	7.10	1
12.70	10.42	6.03	5.44	5.44	5.85	5.85	9.09	8.74	8.23	7.45	6.83	6.80	6.27	2
13.45	11.18	6.44	5.86	5.86	6.30	6.30	9.56	9.21	8.70	7.89	7.24	7.22	6.68	3
9.78	7.50	4.38	3.79	3.56	3.29	3.75	6.23	5.46	5.21	4.79	4.54	4.71	3.75	4
9.19	6.92	4.03	3.45	3.22	3.24	3.71	6.17	5.41	5.16	4.74	4.49	4.68	3.70	5
9.44	7.17	4.18	3.60	3.37	3.01	3.56	5.96	5.19	4.94	4.54	4.30	4.52	3.51	6
8.94	6.67	3.89	3.30	3.07	3.01	3.56	5.96	5.19	4.94	4.54	4.30	4.52	3.51	7
9.53	7.25	4.23	3.65	3.41	3.07	3.60	6.01	5.24	4.99	4.59	4.35	4.56	3.55	8
8.86	6.58	3.84	3.25	3.02	3.01	3.56	5.96	5.19	4.94	4.54	4.30	4.52	3.51	9
9.11	6.84	3.99	3.40	3.17	2.78	3.40	5.74	4.97	4.72	4.34	4.10	4.37	3.31	10
8.61	6.33	3.69	3.11	2.88	2.78	3.40	5.74	4.97	4.72	4.34	4.10	4.37	3.31	11
9.28	7.00	4.08	3.50	3.27	2.90	3.48	5.85	5.08	4.83	4.44	4.20	4.45	3.41	12
8.52	6.25	3.64	3.06	2.83	2.84	3.44	5.79	5.02	4.78	4.39	4.15	4.41	3.36	13
8.77	6.50	3.79	3.21	2.97	2.50	3.20	5.46	4.69	4.45	4.09	3.86	4.18	3.07	14
8.18	5.91	3.45	2.86	2.63	2.61	3.28	5.57	4.80	4.56	4.19	3.96	4.25	3.17	15
8.94	6.67	3.89	3.30	3.07	2.61	3.28	5.57	4.80	4.56	4.19	3.96	4.25	3.17	16
8.10	5.82	3.40	2.81	2.58	2.61	3.28	5.57	4.80	4.56	4.19	3.96	4.25	3.17	17
8.35	6.08	3.54	2.96	2.73	2.22	3.00	5.19	4.42	4.18	3.84	3.61	3.98	2.83	18
7.67	5.39	3.15	2.56	2.33	2.27	3.04	5.24	4.47	4.24	3.89	3.66	4.02	2.88	19
8.69	6.42	3.74	3.16	2.92	2.50	3.20	5.46	4.69	4.45	4.09	3.86	4.18	3.07	20
7.84	5.57	3.25	2.66	2.43	2.50	3.20	5.46	4.69	4.45	4.09	3.86	4.18	3.07	21
8.10	5.82	3.40	2.81	2.58	2.04	2.88	5.02	4.25	4.02	3.69	3.46	3.86	2.68	22
7.41	5.14	3.00	2.42	2.18	2.16	2.96	5.13	4.36	4.13	3.79	3.56	3.94	2.78	23
8.61	6.33	3.69	3.11	2.88	2.39	3.12	5.35	4.58	4.34	3.99	3.76	4.10	2.97	24
7.67	5.39	3.15	2.56	2.33	2.44	3.16	5.41	4.64	4.40	4.04	3.81	4.14	3.02	25
7.93	5.65	3.30	2.71	2.48	1.93	2.79	4.91	4.14	3.91	3.58	3.37	3.77	2.58	26
7.24	4.96	2.90	2.32	2.09	2.04	2.88	5.02	4.25	4.02	3.69	3.46	3.86	2.68	27
see note 7	see note 7	3.48	2.91	2.62	2.22	3.00	5.13	4.24	4.03	3.63	3.55	3.92	2.70	28
see note 7	see note 7	3.14	2.57	2.27	2.04	2.88	4.96	4.07	3.87	3.48	3.40	3.80	2.56	29
see note 7	see note 7	3.28	2.71	2.42	1.99	2.83	4.91	4.01	3.81	3.43	3.35	3.76	2.51	30
see note 7	see note 7	3.04	2.47	2.17	1.87	2.75	4.80	3.90	3.70	3.33	3.25	3.68	2.41	31
see note 7	see note 7	3.23	2.66	2.37	1.93	2.79	4.85	3.96	3.76	3.38	3.30	3.72	2.46	32
see note 7	see note 7	2.84	2.27	1.97	1.76	2.67	4.68	3.79	3.59	3.22	3.16	3.59	2.31	33
see note 7	see note 7	2.99	2.42	2.12	1.59	2.54	4.52	3.63	3.43	3.07	3.01	3.47	2.17	34
see note 7	see note 7	2.69	2.12	1.83	1.53	2.49	4.46	3.57	3.37	3.02	2.96	3.43	2.12	35
see note 7	see note 7	3.04	2.47	2.17	1.65	2.58	4.57	3.68	3.48	3.12	3.06	3.51	2.22	36
see note 7	see note 7	2.59	2.02	1.73	1.53	2.49	4.46	3.57	3.37	3.02	2.96	3.43	2.12	37
see note 7	see note 7	2.74	2.17	1.87	1.36	2.36	4.29	3.40	3.21	2.86	2.81	3.30	1.97	38
see note 7	see note 7	2.44	1.87	1.58	1.25	2.28	4.18	3.29	3.10	2.76	2.71	3.22	1.87	39
see note 7	see note 7	2.94	2.37	2.07	1.53	2.49	4.46	3.57	3.37	3.02	2.96	3.43	2.12	40
see note 7	see note 7	2.49	1.92	1.63	1.42	2.41	4.35	3.46	3.27	2.91	2.86	3.34	2.02	41
see note 7	see note 7	2.64	2.07	1.78	1.19	2.23	4.13	3.24	3.04	2.71	2.66	3.18	1.82	42
see note 7	see note 7	2.29	1.72	1.43	1.14	2.19	4.07	3.18	2.99	2.66	2.61	3.13	1.77	43
see note 7	see note 7	2.69	2.12	1.83	1.25	2.28	4.18	3.29	3.10	2.76	2.71	3.22	1.87	44
see note 7	see note 7	2.34	1.77	1.48	1.08	2.14	4.02	3.12	2.93	2.60	2.56	3.09	1.72	45
see note 7	see note 7	2.44	1.87	1.58	1.02	2.10	3.96	3.07	2.88	2.55	2.51	3.05	1.67	46
see note 7	see note 7	2.19	1.62	1.33	0.91	2.01	3.85	2.96	2.77	2.45	2.41	2.96	1.58	47
see note 7	see note 7	2.19	1.62	1.33	0.74	1.87	3.68	2.79	2.60	2.29	2.26	2.83	1.43	48

4. Product sizes are described in Figure 4, and frame U-factors are from Table 1.

5. Use $U = 3.40 \text{ W/(m}^2\cdot\text{K)}$ for glass block with mortar but without reinforcing or framing.

6. Use of this table should be limited to that of an estimating tool for early phases of design.

7. Values for triple- and quadruple-glazed garden windows are not listed, because these are not common products.

8. U-factors in this table were determined using NFRC 100-91. They have not been updated to the current rating methodology in NFRC 100-2010.

Table 3.7 Visible Transmittance (T_v), Solar Heat Gain Coefficient (SHGC), Solar Transmittance (T), Front Reflectance (R^f), Back Reflectance (R^b), and Layer Absorptance (A_n^f) for Glazing and Window Systems

(Source: ASHRAE Handbook—Fundamentals [2013], Chapter 15, Table 10)

ID	Glazing System		Center Glazing T_v		Center-of-Glazing Properties							Total Window SHGC at Normal Incidence				Total Window T_v at Normal Incidence			
					Incidence Angles							Aluminum		Other Frames		Aluminum		Other Frames	
	Glass Thick., mm				Normal 0.00	40.00	50.00	60.00	70.00	80.00	Hemis., Diffuse	Operable	Fixed	Operable	Fixed	Operable	Fixed	Operable	Fixed
<i>Uncoated Single Glazing</i>																			
1a	3	CLR	0.90	SHGC	0.86	0.84	0.82	0.78	0.67	0.42	0.78	0.78	0.79	0.70	0.76	0.80	0.81	0.72	0.79
				T	0.83	0.82	0.80	0.75	0.64	0.39	0.75								
				R^f	0.08	0.08	0.10	0.14	0.25	0.51	0.14								
				R^b	0.08	0.08	0.10	0.14	0.25	0.51	0.14								
1b	6	CLR	0.88	SHGC	0.81	0.80	0.78	0.73	0.62	0.39	0.73	0.74	0.74	0.66	0.72	0.78	0.79	0.70	0.77
				T	0.77	0.75	0.73	0.68	0.58	0.35	0.69								
				R^f	0.07	0.08	0.09	0.13	0.24	0.48	0.13								
				R^b	0.07	0.08	0.09	0.13	0.24	0.48	0.13								
1c	3	BRZ	0.68	SHGC	0.73	0.71	0.68	0.64	0.55	0.34	0.65	0.67	0.67	0.59	0.65	0.61	0.61	0.54	0.60
				T	0.65	0.62	0.59	0.55	0.46	0.27	0.56								
				R^f	0.06	0.07	0.08	0.12	0.22	0.45	0.12								
				R^b	0.06	0.07	0.08	0.12	0.22	0.45	0.12								
1d	6	BRZ	0.54	SHGC	0.62	0.59	0.57	0.53	0.45	0.29	0.54	0.57	0.57	0.50	0.55	0.48	0.49	0.43	0.48
				T	0.49	0.45	0.43	0.39	0.32	0.18	0.41								
				R^f	0.05	0.06	0.07	0.11	0.19	0.42	0.10								
				R^b	0.05	0.06	0.06	0.12	0.22	0.53	0.10								
1e	3	GRN	0.82	SHGC	0.70	0.68	0.66	0.62	0.53	0.33	0.63	0.64	0.64	0.57	0.62	0.73	0.74	0.66	0.72
				T	0.61	0.58	0.56	0.52	0.43	0.25	0.53								
				R^f	0.06	0.07	0.08	0.12	0.21	0.45	0.11								
				R^b	0.06	0.07	0.08	0.12	0.21	0.45	0.11								
1f	6	GRN	0.76	SHGC	0.60	0.58	0.56	0.52	0.45	0.29	0.54	0.55	0.55	0.49	0.53	0.68	0.68	0.61	0.67
				T	0.47	0.44	0.42	0.38	0.32	0.18	0.40								
				R^f	0.05	0.06	0.07	0.11	0.20	0.42	0.10								
				R^b	0.05	0.06	0.07	0.11	0.20	0.42	0.10								
1g	3	GRY	0.62	SHGC	0.70	0.68	0.66	0.61	0.53	0.33	0.63	0.64	0.64	0.57	0.62	0.55	0.56	0.50	0.55
				T	0.61	0.58	0.56	0.51	0.42	0.24	0.53								
				R^f	0.06	0.07	0.08	0.12	0.21	0.44	0.11								
				R^b	0.06	0.07	0.08	0.12	0.21	0.44	0.11								
				A_1^f	0.33	0.36	0.37	0.37	0.37	0.32	0.35								

Table 3.7 Visible Transmittance (T_v), Solar Heat Gain Coefficient (SHGC), Solar Transmittance (T), Front Reflectance (R^f), Back Reflectance (R^b), and Layer Absorptance (A_n^f) for Glazing and Window Systems (continued)

(Source: ASHRAE Handbook—Fundamentals [2013], Chapter 15, Table 10)

ID	Glazing System			Center Glazing T_v	Center-of-Glazing Properties							Total Window SHGC at Normal Incidence				Total Window T_v at Normal Incidence			
					Incidence Angles							Aluminum		Other Frames		Aluminum		Other Frames	
	Glass Thick., mm				Normal 0.00	40.00	50.00	60.00	70.00	80.00	Hemis., Diffuse	Operable	Fixed	Operable	Fixed	Operable	Fixed	Operable	Fixed
1h	6	GRY	0.46	SHGC	0.59	0.57	0.55	0.51	0.44	0.28	0.52	0.54	0.54	0.48	0.52	0.41	0.41	0.37	0.40
				T	0.46	0.42	0.40	0.36	0.29	0.16	0.38								
				R^f	0.05	0.06	0.07	0.10	0.19	0.41	0.10								
				R^b	0.05	0.06	0.07	0.10	0.19	0.41	0.10								
1i	6	BLUGRN	0.75	SHGC	0.49	0.52	0.54	0.54	0.52	0.43	0.51	0.57	0.57	0.50	0.55	0.67	0.68	0.60	0.66
				T	0.49	0.46	0.44	0.40	0.33	0.19	0.42								
				R^f	0.06	0.06	0.07	0.11	0.20	0.43	0.11								
				R^b	0.06	0.06	0.07	0.11	0.20	0.43	0.11								
				A_1^f	0.45	0.48	0.49	0.49	0.47	0.38	0.48								
Reflective Single Glazing																			
1j	6	SS on CLR 8%	0.08	SHGC	0.19	0.19	0.19	0.18	0.16	0.10	0.18	0.18	0.18	0.16	0.17	0.07	0.07	0.06	0.07
				T	0.06	0.06	0.06	0.05	0.04	0.03	0.05								
				R^f	0.33	0.34	0.35	0.37	0.44	0.61	0.36								
				R^b	0.50	0.50	0.51	0.53	0.58	0.71	0.52								
				A_1^f	0.61	0.61	0.60	0.58	0.52	0.37	0.57								
1k	6	SS on CLR 14%	0.14	SHGC	0.25	0.25	0.24	0.23	0.20	0.13	0.23	0.24	0.24	0.21	0.22	0.12	0.13	0.11	0.12
				T	0.11	0.10	0.10	0.09	0.07	0.04	0.09								
				R^f	0.26	0.27	0.28	0.31	0.38	0.57	0.30								
				R^b	0.44	0.44	0.45	0.47	0.52	0.67	0.46								
				A_1^f	0.63	0.63	0.62	0.60	0.55	0.39	0.60								
1l	6	SS on CLR 20%	0.20	SHGC	0.31	0.30	0.30	0.28	0.24	0.16	0.28	0.29	0.29	0.26	0.28	0.18	0.18	0.16	0.18
				T	0.15	0.15	0.14	0.13	0.11	0.06	0.13								
				R^f	0.21	0.22	0.23	0.26	0.34	0.54	0.25								
				R^b	0.38	0.38	0.39	0.41	0.48	0.64	0.41								
				A_1^f	0.64	0.64	0.63	0.61	0.56	0.40	0.60								
1m	6	SS on GRN 14%	0.12	SHGC	0.25	0.25	0.24	0.23	0.21	0.14	0.23	0.24	0.24	0.21	0.22	0.11	0.11	0.10	0.11
				T	0.06	0.06	0.06	0.06	0.04	0.03	0.06								
				R^f	0.14	0.14	0.16	0.19	0.27	0.49	0.18								
				R^b	0.44	0.44	0.45	0.47	0.52	0.67	0.46								
				A_1^f	0.80	0.80	0.78	0.76	0.68	0.48	0.75								
1n	6	TI on CLR 20%	0.20	SHGC	0.29	0.29	0.28	0.27	0.23	0.15	0.27	0.27	0.27	0.24	0.26	0.18	0.18	0.16	0.18
				T	0.14	0.13	0.13	0.12	0.09	0.06	0.12								
				R^f	0.22	0.22	0.24	0.26	0.34	0.54	0.26								
				R^b	0.40	0.40	0.42	0.44	0.50	0.65	0.43								
				A_1^f	0.65	0.65	0.64	0.62	0.57	0.40	0.62								

Table 3.7 Visible Transmittance (T_v), Solar Heat Gain Coefficient (SHGC), Solar Transmittance (T), Front Reflectance (R^f), Back Reflectance (R^b), and Layer Absorptance (A_n^f) for Glazing and Window Systems (continued)

(Source: ASHRAE Handbook—Fundamentals [2013], Chapter 15, Table 10)

ID	Glazing System			Center Glazing T_v	Center-of-Glazing Properties							Total Window SHGC at Normal Incidence				Total Window T_v at Normal Incidence			
					Incidence Angles							Aluminum		Other Frames		Aluminum		Other Frames	
	Glass Thick., mm				Normal 0.00	40.00	50.00	60.00	70.00	80.00	Hemis., Diffuse	Operable	Fixed	Operable	Fixed	Operable	Fixed	Operable	Fixed
1o	6	11 on CLR 30%	0.30	SHGC	0.39	0.38	0.37	0.35	0.30	0.20	0.35	0.36	0.36	0.32	0.35	0.27	0.27	0.24	0.26
				T	0.23	0.22	0.21	0.19	0.16	0.09	0.20								
				R^f	0.15	0.15	0.17	0.20	0.28	0.50	0.19								
				R^b	0.32	0.33	0.34	0.36	0.43	0.60	0.36								
				A_1^f	0.63	0.65	0.64	0.62	0.57	0.40	0.62								
Uncoated Double Glazing																			
5a	3	CLR CLR	0.81	SHGC	0.76	0.74	0.71	0.64	0.50	0.26	0.66	0.69	0.70	0.62	0.67	0.72	0.73	0.65	0.71
				T	0.70	0.68	0.65	0.58	0.44	0.21	0.60								
				R^f	0.13	0.14	0.16	0.23	0.36	0.61	0.21								
				R^b	0.13	0.14	0.16	0.23	0.36	0.61	0.21								
				A_1^f	0.10	0.11	0.11	0.12	0.13	0.13	0.11								
				A_2^f	0.07	0.08	0.08	0.08	0.07	0.05	0.07								
5b	6	CLR CLR	0.78	SHGC	0.70	0.67	0.64	0.58	0.45	0.23	0.60	0.64	0.64	0.57	0.62	0.69	0.70	0.62	0.69
				T	0.61	0.58	0.55	0.48	0.36	0.17	0.51								
				R^f	0.11	0.12	0.15	0.20	0.33	0.57	0.18								
				R^b	0.11	0.12	0.15	0.20	0.33	0.57	0.18								
				A_1^f	0.17	0.18	0.19	0.20	0.21	0.20	0.19								
				A_2^f	0.11	0.12	0.12	0.12	0.10	0.07	0.11								
5c	3	BRZ CLR	0.62	SHGC	0.62	0.60	0.57	0.51	0.39	0.20	0.53	0.57	0.57	0.50	0.55	0.55	0.56	0.50	0.55
				T	0.55	0.51	0.48	0.42	0.31	0.14	0.45								
				R^f	0.09	0.10	0.12	0.16	0.27	0.49	0.15								
				R^b	0.12	0.13	0.15	0.21	0.35	0.59	0.19								
				A_1^f	0.30	0.33	0.34	0.36	0.37	0.34	0.33								
				A_2^f	0.06	0.06	0.06	0.06	0.05	0.03	0.06								
5d	6	BRZ CLR	0.47	SHGC	0.49	0.46	0.44	0.39	0.31	0.17	0.41	0.45	0.45	0.40	0.43	0.42	0.42	0.38	0.41
				T	0.38	0.35	0.32	0.27	0.20	0.08	0.30								
				R^f	0.07	0.08	0.09	0.13	0.22	0.44	0.12								
				R^b	0.10	0.11	0.13	0.19	0.31	0.55	0.17								
				A_1^f	0.48	0.51	0.52	0.53	0.53	0.45	0.50								
				A_2^f	0.07	0.07	0.07	0.07	0.06	0.04	0.07								
5e	3	GRN CLR	0.75	SHGC	0.60	0.57	0.54	0.49	0.38	0.20	0.51	0.55	0.55	0.49	0.53	0.67	0.68	0.60	0.66
				T	0.52	0.49	0.46	0.40	0.30	0.13	0.43								
				R^f	0.09	0.10	0.12	0.16	0.27	0.50	0.15								
				R^b	0.12	0.13	0.15	0.21	0.35	0.60	0.19								
				A_1^f	0.34	0.37	0.38	0.39	0.39	0.35	0.37								
				A_2^f	0.05	0.05	0.05	0.04	0.04	0.03	0.04								

Table 3.7 Visible Transmittance (T_v), Solar Heat Gain Coefficient (SHGC), Solar Transmittance (T), Front Reflectance (R^f), Back Reflectance (R^b), and Layer Absorptance (A_n^f) for Glazing and Window Systems (continued)

(Source: ASHRAE Handbook—Fundamentals [2013], Chapter 15, Table 10)

ID	Glazing System			Center Glazing T_v	Center-of-Glazing Properties							Total Window SHGC at Normal Incidence				Total Window T_v at Normal Incidence			
	Glass Thick., mm	SHGC	SHGC		Incidence Angles							Aluminum		Other Frames		Aluminum		Other Frames	
					Normal 0.00	40.00	50.00	60.00	70.00	80.00	Hemis., Diffuse	Operable	Fixed	Operable	Fixed	Operable	Fixed	Operable	Fixed
5f	6	GRN CLR	0.68	SHGC	0.49	0.46	0.44	0.39	0.31	0.17	0.41	0.45	0.45	0.40	0.43	0.61	0.61	0.54	0.60
				T	0.39	0.36	0.33	0.29	0.21	0.09	0.31								
				R^f	0.08	0.08	0.10	0.14	0.23	0.45	0.13								
				R^b	0.10	0.11	0.13	0.19	0.31	0.55	0.17								
				A_1^f	0.49	0.51	0.05	0.53	0.52	0.43	0.50								
A_2^f	0.05	0.05	0.05	0.05	0.04	0.03	0.05												
5g	3	GRY CLR	0.56	SHGC	0.60	0.57	0.54	0.48	0.37	0.20	0.51	0.55	0.55	0.49	0.53	0.50	0.50	0.45	0.49
				T	0.51	0.48	0.45	0.39	0.29	0.12	0.42								
				R^f	0.09	0.09	0.11	0.16	0.26	0.48	0.14								
				R^b	0.12	0.13	0.15	0.21	0.34	0.59	0.19								
				A_1^f	0.34	0.37	0.39	0.40	0.41	0.37	0.37								
A_2^f	0.05	0.06	0.06	0.05	0.05	0.03	0.05												
5h	6	GRY CLR	0.41	SHGC	0.47	0.44	0.42	0.37	0.29	0.16	0.39	0.43	0.43	0.38	0.42	0.36	0.37	0.33	0.36
				T	0.36	0.32	0.29	0.25	0.18	0.07	0.28								
				R^f	0.07	0.07	0.08	0.12	0.21	0.43	0.12								
				R^b	0.10	0.11	0.13	0.18	0.31	0.55	0.17								
				A_1^f	0.51	0.54	0.56	0.57	0.56	0.47	0.53								
A_2^f	0.07	0.07	0.07	0.06	0.05	0.03	0.06												
5i	6	BLUGRN CLR	0.67	SHGC	0.50	0.47	0.45	0.40	0.32	0.17	0.43	0.46	0.46	0.41	0.44	0.60	0.60	0.54	0.59
				T	0.40	0.37	0.34	0.30	0.22	0.10	0.32								
				R^f	0.08	0.08	0.10	0.14	0.24	0.46	0.13								
				R^b	0.11	0.11	0.14	0.19	0.31	0.55	0.17								
				A_1^f	0.47	0.49	0.50	0.51	0.50	0.42	0.48								
A_2^f	0.06	0.06	0.06	0.05	0.04	0.03	0.05												
5j	6	HI-P GRN CLR	0.59	SHGC	0.39	0.37	0.35	0.31	0.25	0.14	0.33	0.36	0.36	0.32	0.35	0.53	0.53	0.47	0.52
				T	0.28	0.26	0.24	0.20	0.15	0.06	0.22								
				R^f	0.06	0.07	0.08	0.12	0.21	0.43	0.11								
				R^b	0.10	0.11	0.13	0.19	0.31	0.55	0.17								
				A_1^f	0.62	0.65	0.65	0.65	0.62	0.50	0.63								
A_2^f	0.03	0.03	0.03	0.03	0.02	0.01	0.03												
Reflective Double Glazing																			
5k	6	SS on CLR 8%, CLR	0.07	SHGC	0.13	0.12	0.12	0.11	0.10	0.06	0.11	0.13	0.13	0.11	0.12	0.06	0.06	0.06	0.06
				T	0.05	0.05	0.04	0.04	0.03	0.01	0.04								
				R^f	0.33	0.34	0.35	0.37	0.44	0.61	0.37								
				R^b	0.38	0.37	0.38	0.40	0.46	0.61	0.40								
				A_1^f	0.61	0.61	0.60	0.58	0.53	0.37	0.56								
A_2^f	0.01	0.01	0.01	0.01	0.01	0.01	0.01												
5l	6	SS on CLR 14%, CLR	0.13	SHGC	0.17	0.17	0.16	0.15	0.13	0.08	0.16	0.17	0.16	0.14	0.15	0.12	0.12	0.10	0.11

Table 3.7 Visible Transmittance (T_v), Solar Heat Gain Coefficient (SHGC), Solar Transmittance (T), Front Reflectance (R^f), Back Reflectance (R^b), and Layer Absorptance (A_n^f) for Glazing and Window Systems (continued)

(Source: ASHRAE Handbook—Fundamentals [2013], Chapter 15, Table 10)

ID	Glazing System			Center-of-Glazing Properties							Total Window SHGC at Normal Incidence				Total Window T_v at Normal Incidence					
				Incidence Angles							Aluminum		Other Frames		Aluminum		Other Frames			
	Glass Thick., mm	Center Glazing T_v		Normal 0.00	40.00	50.00	60.00	70.00	80.00	Hemis., Diffuse	Operable	Fixed	Operable	Fixed	Operable	Fixed	Operable	Fixed		
5m 6	SS on CLR 20%, CLR	0.18	T	0.08	0.08	0.08	0.07	0.05	0.02	0.07										
			R^f	0.26	0.27	0.28	0.31	0.38	0.57	0.30										
			R^b	0.34	0.33	0.34	0.37	0.44	0.60	0.36										
			A_1^f	0.63	0.64	0.64	0.63	0.61	0.56	0.60										
			A_2^f	0.02	0.02	0.02	0.02	0.02	0.02	0.02										
			SHGC	0.22	0.21	0.21	0.19	0.16	0.09	0.20	0.21	0.21	0.18	0.20	0.16	0.16	0.14	0.16		
			T	0.12	0.11	0.11	0.09	0.07	0.03	0.10										
			R^f	0.21	0.22	0.23	0.26	0.34	0.54	0.25										
			R^b	0.30	0.30	0.31	0.34	0.41	0.59	0.33										
			A_1^f	0.64	0.64	0.63	0.62	0.57	0.41	0.61										
5n 6	SS on GRN 14%, CLR	0.11	A_2^f	0.03	0.03	0.03	0.03	0.02	0.02	0.03										
			SHGC	0.16	0.16	0.15	0.14	0.12	0.08	0.14	0.16	0.16	0.14	0.14	0.10	0.10	0.09	0.10		
			T	0.05	0.05	0.05	0.04	0.03	0.01	0.04										
			R^f	0.14	0.14	0.16	0.19	0.27	0.49	0.18										
			R^b	0.34	0.33	0.34	0.37	0.44	0.60	0.36										
			A_1^f	0.80	0.80	0.79	0.76	0.69	0.49	0.76										
			A_2^f	0.01	0.01	0.01	0.01	0.01	0.01	0.01										
			SHGC	0.21	0.20	0.19	0.18	0.15	0.09	0.18	0.20	0.20	0.18	0.19	0.16	0.16	0.14	0.16		
			T	0.11	0.10	0.10	0.08	0.06	0.03	0.09										
			R^f	0.22	0.22	0.24	0.27	0.34	0.54	0.26										
5p 6	TI on CLR 30%, CLR	0.27	R^b	0.32	0.31	0.32	0.35	0.42	0.59	0.35										
			A_1^f	0.65	0.66	0.65	0.63	0.58	0.41	0.62										
			A_2^f	0.02	0.02	0.02	0.02	0.02	0.01	0.02										
			SHGC	0.29	0.28	0.27	0.25	0.20	0.12	0.25	0.27	0.27	0.24	0.26	0.24	0.24	0.22	0.24		
			T	0.18	0.17	0.16	0.14	0.10	0.05	0.15										
			R^f	0.15	0.15	0.17	0.20	0.29	0.51	0.19										
			R^b	0.27	0.27	0.28	0.31	0.40	0.58	0.31										
			A_1^f	0.64	0.64	0.63	0.62	0.58	0.43	0.61										
			A_2^f	0.04	0.04	0.04	0.04	0.03	0.02	0.04										
			Low-e Double Glazing, $e = 0.2$ on Surface 2																	
17a 3	LE CLR	0.76	SHGC	0.65	0.64	0.61	0.56	0.43	0.23	0.57	0.59	0.60	0.53	0.58	0.68	0.68	0.61	0.67		
			T	0.59	0.56	0.54	0.48	0.36	0.18	0.50										
			R^f	0.15	0.16	0.18	0.24	0.37	0.61	0.22										
			R^b	0.17	0.18	0.20	0.26	0.38	0.61	0.24										
			A_1^f	0.20	0.21	0.21	0.21	0.20	0.16	0.20										
			A_2^f	0.07	0.07	0.08	0.08	0.07	0.05	0.07										
17b 6	LE CLR	0.73	SHGC	0.60	0.59	0.57	0.51	0.40	0.21	0.53	0.55	0.55	0.49	0.53	0.65	0.66	0.58	0.64		
			T	0.51	0.48	0.46	0.41	0.30	0.14	0.43										

Table 3.7 Visible Transmittance (T_v), Solar Heat Gain Coefficient (SHGC), Solar Transmittance (T), Front Reflectance (R^f), Back Reflectance (R^b), and Layer Absorptance (A_n^f) for Glazing and Window Systems (continued)

(Source: ASHRAE Handbook—Fundamentals [2013], Chapter 15, Table 10)

ID	Glazing System		Center Glazing T_v		Center-of-Glazing Properties						Total Window SHGC at Normal Incidence				Total Window T_v at Normal Incidence				
					Incidence Angles						Aluminum		Other Frames		Aluminum		Other Frames		
	Glass Thick., mm				Normal 0.00	40.00	50.00	60.00	70.00	80.00	Hemis., Diffuse	Operable	Fixed	Operable	Fixed	Operable	Fixed	Operable	Fixed
			R^f	0.14	0.15	0.17	0.22	0.35	0.59	0.21									
			R^b	0.15	0.16	0.18	0.23	0.35	0.57	0.22									
			A_1^f	0.26	0.26	0.26	0.26	0.25	0.19	0.25									
			A_2^f	0.10	0.11	0.11	0.11	0.10	0.07	0.10									
<i>Low-e Double Glazing, e = 0.2 on Surface 3</i>																			
17c	3	CLR LE	0.76	SHGC	0.70	0.68	0.65	0.59	0.46	0.24	0.61	0.64	0.64	0.57	0.62	0.68	0.68	0.1	0.67
				T	0.59	0.56	0.54	0.48	0.36	0.18	0.50								
				R^f	0.17	0.18	0.20	0.26	0.38	0.61	0.24								
				R^b	0.15	0.16	0.18	0.24	0.37	0.61	0.22								
				A_1^f	0.11	0.12	0.13	0.13	0.14	0.15	0.12								
				A_2^f	0.14	0.14	0.14	0.13	0.11	0.07	0.13								
17d	6	CLR LE	0.73	SHGC	0.65	0.63	0.60	0.54	0.42	0.21	0.56	0.59	0.60	0.53	0.58	0.65	0.66	0.58	0.64
				T	0.51	0.48	0.46	0.41	0.30	0.14	0.43								
				R^f	0.15	0.16	0.18	0.23	0.35	0.57	0.22								
				R^b	0.14	0.15	0.17	0.22	0.35	0.59	0.21								
				A_1^f	0.17	0.19	0.20	0.21	0.22	0.22	0.19								
				A_2^f	0.17	0.17	0.17	0.15	0.13	0.07	0.16								
17e	3	BRZ LE	0.58	SHGC	0.57	0.54	0.51	0.46	0.35	0.18	0.48	0.52	0.52	0.46	0.51	0.52	0.52	0.46	0.51
				T	0.46	0.43	0.41	0.36	0.26	0.12	0.38								
				R^f	0.12	0.12	0.14	0.18	0.28	0.50	0.17								
				R^b	0.14	0.15	0.17	0.23	0.35	0.60	0.21								
				A_1^f	0.31	0.34	0.35	0.37	0.38	0.35	0.34								
				A_2^f	0.11	0.11	0.10	0.10	0.08	0.04	0.10								
17f	6	BRZ LE	0.45	SHGC	0.45	0.42	0.40	0.35	0.27	0.14	0.38	0.42	0.42	0.37	0.40	0.40	0.41	0.36	0.40
				T	0.33	0.30	0.28	0.24	0.17	0.07	0.26								
				R^f	0.09	0.09	0.10	0.14	0.23	0.44	0.13								
				R^b	0.13	0.14	0.16	0.21	0.34	0.58	0.20								
				A_1^f	0.48	0.51	0.52	0.54	0.53	0.45	0.50								
				A_2^f	0.11	0.11	0.10	0.09	0.07	0.04	0.09								
17g	3	GRN LE	0.70	SHGC	0.55	0.52	0.50	0.44	0.34	0.17	0.46	0.50	0.51	0.45	0.49	0.62	0.63	0.56	0.62
				T	0.44	0.41	0.38	0.33	0.24	0.11	0.36								
				R^f	0.11	0.11	0.13	0.17	0.27	0.48	0.16								
				R^b	0.14	0.15	0.17	0.23	0.35	0.60	0.21								
				A_1^f	0.35	0.38	0.39	0.41	0.42	0.37	0.38								
				A_2^f	0.11	0.10	0.10	0.09	0.07	0.04	0.09								
17h	6	GRN LE	0.61	SHGC	0.41	0.39	0.36	0.32	0.25	0.13	0.34	0.38	0.38	0.34	0.36	0.54	0.55	0.49	0.54

Table 3.7 Visible Transmittance (T_v), Solar Heat Gain Coefficient (SHGC), Solar Transmittance (T), Front Reflectance (R^f), Back Reflectance (R^b), and Layer Absorptance (A_n^f) for Glazing and Window Systems (continued)

(Source: ASHRAE Handbook—Fundamentals [2013], Chapter 15, Table 10)

ID	Glazing System			Center-of-Glazing Properties							Total Window SHGC at Normal Incidence				Total Window T_v at Normal Incidence						
				Incidence Angles							Aluminum		Other Frames		Aluminum		Other Frames				
	Glass Thick., mm	Center Glazing T_v		Normal 0.00	40.00	50.00	60.00	70.00	80.00	Hemis., Diffuse	Operable	Fixed	Operable	Fixed	Operable	Fixed	Operable	Fixed			
17i	3	GRY LE	0.53	T	0.29	0.26	0.24	0.21	0.15	0.06	0.23										
				R^f	0.08	0.08	0.09	0.13	0.22	0.43	0.13										
				R^b	0.13	0.14	0.16	0.21	0.34	0.58	0.20										
				A_1^f	0.53	0.57	0.58	0.59	0.58	0.48	0.56										
				A_2^f	0.10	0.09	0.09	0.08	0.06	0.03	0.08										
				SHGC	0.54	0.51	0.49	0.44	0.33	0.17	0.46	0.50	0.50	0.44	0.48	0.47	0.48	0.42	0.47		
				T	0.43	0.40	0.38	0.33	0.24	0.11	0.35										
				R^f	0.11	0.11	0.13	0.17	0.27	0.48	0.16										
				R^b	0.14	0.15	0.17	0.22	0.35	0.60	0.21										
				A_1^f	0.36	0.39	0.40	0.42	0.42	0.38	0.39										
				A_2^f	0.10	0.10	0.10	0.09	0.07	0.04	0.09										
17j	6	GRY LE	0.37	SHGC	0.39	0.37	0.35	0.31	0.24	0.13	0.33	0.36	0.36	0.32	0.35	0.33	0.33	0.30	0.33		
				T	0.27	0.25	0.23	0.20	0.14	0.06	0.21										
				R^f	0.09	0.09	0.11	0.14	0.23	0.44	0.14										
				R^b	0.13	0.14	0.16	0.22	0.34	0.58	0.20										
				A_1^f	0.55	0.58	0.59	0.59	0.58	0.48	0.56										
				A_2^f	0.09	0.09	0.08	0.07	0.06	0.03	0.08										
				SHGC	0.45	0.42	0.40	0.35	0.27	0.14	0.37	0.42	0.42	0.37	0.40	0.55	0.56	0.50	0.55		
				T	0.32	0.29	0.27	0.23	0.17	0.07	0.26										
				R^f	0.09	0.09	0.10	0.14	0.23	0.44	0.13										
				R^b	0.13	0.14	0.16	0.21	0.34	0.58	0.20										
17k	6	BLUGRN LE	0.62	A_1^f	0.48	0.51	0.53	0.54	0.54	0.45	0.51										
				A_2^f	0.11	0.10	0.10	0.09	0.07	0.03	0.09										
				SHGC	0.34	0.31	0.30	0.26	0.20	0.11	0.28	0.32	0.32	0.28	0.30	0.49	0.50	0.44	0.48		
				T	0.22	0.19	0.18	0.15	0.10	0.04	0.17										
				R^f	0.07	0.07	0.08	0.11	0.20	0.41	0.11										
				R^b	0.13	0.14	0.16	0.21	0.33	0.58	0.20										
				A_1^f	0.64	0.67	0.68	0.68	0.66	0.53	0.65										
				A_2^f	0.08	0.07	0.06	0.06	0.04	0.02	0.06										
Low-e Double Glazing, e = 0.1 on Surface 2																					
21a	3	LE CLR	0.76	SHGC	0.65	0.64	0.62	0.56	0.43	0.23	0.57	0.59	0.60	0.53	0.58	0.68	0.68	0.61	0.67		
				T	0.59	0.56	0.54	0.48	0.36	0.18	0.50										
				R^f	0.15	0.16	0.18	0.24	0.37	0.61	0.22										
				R^b	0.17	0.18	0.20	0.26	0.38	0.61	0.24										
				A_1^f	0.20	0.21	0.21	0.21	0.20	0.16	0.20										
				A_2^f	0.07	0.07	0.08	0.08	0.07	0.05	0.07										

Table 3.7 Visible Transmittance (T_v), Solar Heat Gain Coefficient (SHGC), Solar Transmittance (T), Front Reflectance (R^f), Back Reflectance (R^b), and Layer Absorptance (A_n^f) for Glazing and Window Systems (continued)

(Source: ASHRAE Handbook—Fundamentals [2013], Chapter 15, Table 10)

ID	Glazing System			Center Glazing T_v		Center-of-Glazing Properties							Total Window SHGC at Normal Incidence				Total Window T_v at Normal Incidence					
						Incidence Angles							Aluminum		Other Frames		Aluminum		Other Frames			
	Glass Thick., mm					Normal 0.00	40.00	50.00	60.00	70.00	80.00	Hemis., Diffuse	Operable	Fixed	Operable	Fixed	Operable	Fixed	Operable	Fixed		
21b	6	LE CLR	0.72	SHGC	0.60	0.59	0.57	0.51	0.40	0.21	0.53	0.55	0.55	0.49	0.53	0.64	0.65	0.58	0.63			
				T	0.51	0.48	0.46	0.41	0.30	0.14	0.43											
				R^f	0.14	0.15	0.17	0.22	0.35	0.59	0.21											
				R^b	0.15	0.16	0.18	0.23	0.35	0.57	0.22											
				A_1^f	0.26	0.26	0.26	0.26	0.25	0.19	0.25											
				A_2^f	0.10	0.11	0.11	0.11	0.10	0.07	0.10											
<i>Low-e Double Glazing, e = 0.1 on Surface 3</i>																						
21c	3	CLR LE	0.75	SHGC	0.60	0.58	0.56	0.51	0.40	0.22	0.52	0.55	0.55	0.49	0.53	0.67	0.68	0.60	0.66			
				T	0.48	0.45	0.43	0.37	0.27	0.13	0.40											
				R^f	0.26	0.27	0.28	0.32	0.42	0.62	0.31											
				R^b	0.24	0.24	0.26	0.29	0.38	0.58	0.28											
				A_1^f	0.12	0.13	0.14	0.14	0.15	0.15	0.13											
				A_2^f	0.14	0.15	0.15	0.16	0.16	0.10	0.15											
21d	6	CLR LE	0.72	SHGC	0.56	0.55	0.52	0.48	0.38	0.20	0.49	0.51	0.52	0.46	0.50	0.64	0.65	0.58	0.63			
				T	0.42	0.40	0.37	0.32	0.24	0.11	0.35											
				R^f	0.24	0.24	0.25	0.29	0.38	0.58	0.28											
				R^b	0.20	0.20	0.22	0.26	0.34	0.55	0.25											
				A_1^f	0.19	0.20	0.21	0.22	0.23	0.22	0.21											
				A_2^f	0.16	0.17	0.17	0.17	0.16	0.10	0.16											
21e	3	BRZ LE	0.57	SHGC	0.48	0.46	0.44	0.40	0.31	0.17	0.42	0.44	0.44	0.39	0.43	0.51	0.51	0.46	0.50			
				T	0.37	0.34	0.32	0.27	0.20	0.08	0.30											
				R^f	0.18	0.17	0.19	0.22	0.30	0.50	0.21											
				R^b	0.23	0.23	0.25	0.29	0.37	0.57	0.28											
				A_1^f	0.34	0.37	0.38	0.39	0.39	0.35	0.37											
				A_2^f	0.11	0.12	0.12	0.12	0.11	0.07	0.11											
21f	6	BRZ LE	0.45	SHGC	0.39	0.37	0.35	0.31	0.24	0.13	0.33	0.36	0.36	0.32	0.35	0.40	0.41	0.36	0.40			
				T	0.27	0.24	0.22	0.19	0.13	0.05	0.21											
				R^f	0.12	0.12	0.13	0.16	0.24	0.44	0.16											
				R^b	0.19	0.20	0.22	0.25	0.34	0.55	0.24											
				A_1^f	0.51	0.54	0.55	0.56	0.55	0.46	0.53											
				A_2^f	0.10	0.10	0.10	0.10	0.09	0.05	0.10											
21g	3	GRN LE	0.68	SHGC	0.46	0.44	0.42	0.38	0.30	0.16	0.40	0.42	0.43	0.38	0.41	0.61	0.61	0.54	0.60			
				T	0.36	0.32	0.30	0.26	0.18	0.08	0.28											
				R^f	0.17	0.16	0.17	0.20	0.29	0.48	0.20											
				R^b	0.23	0.23	0.25	0.29	0.37	0.57	0.27											

Table 3.7 Visible Transmittance (T_v), Solar Heat Gain Coefficient (SHGC), Solar Transmittance (T), Front Reflectance (R^f), Back Reflectance (R^b), and Layer Absorptance (A_n^f) for Glazing and Window Systems (continued)

(Source: ASHRAE Handbook—Fundamentals [2013], Chapter 15, Table 10)

ID	Glazing System			Center Glazing T_v	Center-of-Glazing Properties						Total Window SHGC at Normal Incidence				Total Window T_v at Normal Incidence						
					Incidence Angles						Aluminum		Other Frames		Aluminum		Other Frames				
	Glass Thick., mm				Normal 0.00	40.00	50.00	60.00	70.00	80.00	Hemis., Diffuse	Operable	Fixed	Operable	Fixed	Operable	Fixed	Operable	Fixed		
21h	6	GRN LE	0.61	A_1^f	0.38	0.41	0.42	0.43	0.43	0.38	0.40										
				A_2^f	0.10	0.11	0.11	0.11	0.10	0.06	0.10										
				SHGC	0.36	0.33	0.31	0.28	0.22	0.12	0.30	0.34	0.34	0.30	0.32	0.54	0.55	0.49	0.54		
				T	0.24	0.21	0.19	0.16	0.11	0.05	0.18										
				R^f	0.11	0.10	0.11	0.14	0.22	0.43	0.14										
				R^b	0.19	0.20	0.22	0.25	0.34	0.55	0.24										
21i	3	GRY LE	0.52	A_1^f	0.56	0.59	0.61	0.61	0.59	0.48	0.58										
				A_2^f	0.09	0.09	0.09	0.08	0.08	0.04	0.08										
				SHGC	0.46	0.44	0.42	0.38	0.30	0.16	0.39	0.42	0.43	0.38	0.41	0.46	0.47	0.42	0.46		
				T	0.35	0.32	0.30	0.25	0.18	0.08	0.28										
				R^f	0.16	0.16	0.17	0.20	0.28	0.48	0.20										
				R^b	0.23	0.23	0.25	0.29	0.37	0.57	0.27										
21j	6	GRY LE	0.37	A_1^f	0.39	0.42	0.43	0.44	0.44	0.38	0.41										
				A_2^f	0.10	0.11	0.11	0.11	0.10	0.06	0.10										
				SHGC	0.34	0.32	0.30	0.27	0.21	0.12	0.28	0.32	0.32	0.28	0.30	0.33	0.33	0.30	0.33		
				T	0.23	0.20	0.18	0.15	0.11	0.04	0.17										
				R^f	0.11	0.11	0.12	0.15	0.23	0.44	0.15										
				R^b	0.20	0.20	0.22	0.25	0.34	0.55	0.24										
21k	6	BLUGRN LE	0.62	A_1^f	0.58	0.60	0.61	0.61	0.59	0.48	0.59										
				A_2^f	0.08	0.08	0.08	0.08	0.07	0.04	0.08										
				SHGC	0.39	0.37	0.34	0.31	0.24	0.13	0.33	0.36	0.36	0.32	0.35	0.55	0.56	0.50	0.55		
				T	0.28	0.25	0.23	0.20	0.14	0.06	0.22										
				R^f	0.12	0.12	0.13	0.16	0.24	0.44	0.16										
				R^b	0.23	0.23	0.25	0.28	0.37	0.57	0.27										
21l	6	HI-P GRN W/LE CLR	0.57	A_1^f	0.51	0.54	0.56	0.56	0.55	0.46	0.53										
				A_2^f	0.08	0.09	0.08	0.08	0.08	0.05	0.08										
				SHGC	0.31	0.30	0.29	0.26	0.21	0.12	0.27	0.29	0.29	0.26	0.28	0.51	0.51	0.46	0.50		
				T	0.22	0.21	0.19	0.17	0.12	0.06	0.18										
				R^f	0.07	0.07	0.09	0.13	0.22	0.46	0.12										
				R^b	0.23	0.23	0.24	0.28	0.37	0.57	0.27										
Low-e Double Glazing, e = 0.05 on Surface 2																					
25a	3	LE CLR	0.72	SHGC	0.41	0.40	0.38	0.34	0.27	0.14	0.36	0.38	0.38	0.34	0.36	0.64	0.65	0.58	0.63		
				T	0.37	0.35	0.33	0.29	0.22	0.11	0.31										

Table 3.7 Visible Transmittance (T_v), Solar Heat Gain Coefficient (SHGC), Solar Transmittance (T), Front Reflectance (R^f), Back Reflectance (R^b), and Layer Absorptance (A_n^f) for Glazing and Window Systems (continued)

(Source: ASHRAE Handbook—Fundamentals [2013], Chapter 15, Table 10)

ID	Glazing System			Center Glazing T_v	Center-of-Glazing Properties						Total Window SHGC at Normal Incidence				Total Window T_v at Normal Incidence								
					Incidence Angles						Aluminum		Other Frames		Aluminum		Other Frames						
	Glass Thick., mm				Normal 0.00	40.00	50.00	60.00	70.00	80.00	Hemis., Diffuse	Operable	Fixed	Operable	Fixed	Operable	Fixed	Operable	Fixed				
25b	6	LE CLR	0.70	R^f	0.35	0.36	0.37	0.40	0.47	0.64	0.39												
				R^b	0.39	0.39	0.40	0.43	0.50	0.66	0.42												
				A_1^f	0.24	0.26	0.26	0.27	0.28	0.23	0.26												
				A_2^f	0.04	0.04	0.04	0.04	0.03	0.03	0.04												
				SHGC	0.37	0.36	0.34	0.31	0.24	0.13	0.32	0.34	0.34	0.30	0.33	0.62	0.63	0.56	0.62				
				T	0.30	0.28	0.27	0.23	0.17	0.08	0.25												
				R^f	0.30	0.30	0.32	0.35	0.42	0.60	0.34												
				R^b	0.35	0.35	0.35	0.38	0.44	0.60	0.37												
				A_1^f	0.34	0.35	0.35	0.36	0.35	0.28	0.34												
				A_2^f	0.06	0.07	0.07	0.06	0.06	0.04	0.06												
25c	6	BRZ W/LE CLR	0.42	SHGC	0.26	0.25	0.24	0.22	0.18	0.10	0.23	0.25	0.25	0.22	0.23	0.37	0.38	0.34	0.37				
				T	0.18	0.17	0.16	0.14	0.10	0.05	0.15												
				R^f	0.15	0.16	0.17	0.21	0.29	0.51	0.20												
				R^b	0.34	0.34	0.35	0.37	0.44	0.60	0.37												
				A_1^f	0.63	0.63	0.63	0.61	0.57	0.42	0.60												
				A_2^f	0.04	0.04	0.04	0.04	0.03	0.03	0.04												
				25d	6	GRN W/LE CLR	0.60	SHGC	0.31	0.30	0.28	0.26	0.21	0.12	0.27	0.29	0.29	0.26	0.28	0.53	0.54	0.48	0.53
								T	0.22	0.21	0.20	0.17	0.13	0.06	0.18								
								R^f	0.10	0.10	0.12	0.16	0.25	0.48	0.15								
								R^b	0.35	0.34	0.35	0.37	0.44	0.60	0.37								
A_1^f	0.64	0.64	0.64					0.63	0.59	0.43	0.62												
A_2^f	0.05	0.05	0.05					0.05	0.04	0.03	0.05												
25e	6	GRY W/LE CLR	0.35					SHGC	0.24	0.23	0.22	0.20	0.16	0.09	0.21	0.23	0.23	0.20	0.21	0.31	0.32	0.28	0.31
								T	0.16	0.15	0.14	0.12	0.09	0.04	0.13								
								R^f	0.12	0.13	0.15	0.18	0.26	0.49	0.17								
								R^b	0.34	0.34	0.35	0.37	0.44	0.60	0.37								
				A_1^f	0.69	0.69	0.68	0.67	0.62	0.45	0.66												
				A_2^f	0.03	0.03	0.03	0.03	0.03	0.02	0.03												
				25f	6	BLUE W/LE CLR	0.45	SHGC	0.27	0.26	0.25	0.23	0.18	0.11	0.24	0.26	0.25	0.22	0.24	0.40	0.41	0.36	0.40
								T	0.19	0.18	0.17	0.15	0.11	0.05	0.16								
								R^f	0.12	0.12	0.14	0.17	0.26	0.49	0.16								
								R^b	0.34	0.34	0.35	0.37	0.44	0.60	0.37								
A_1^f	0.66	0.66	0.65					0.64	0.60	0.44	0.63												
A_2^f	0.04	0.04	0.04					0.04	0.04	0.03	0.04												
25g	6	HI-P GRN W/LE CLR	0.53					SHGC	0.27	0.26	0.25	0.23	0.18	0.11	0.23	0.26	0.25	0.22	0.24	0.47	0.48	0.42	0.47

Table 3.7 Visible Transmittance (T_v), Solar Heat Gain Coefficient (SHGC), Solar Transmittance (T), Front Reflectance (R^f), Back Reflectance (R^b), and Layer Absorptance (A_n^f) for Glazing and Window Systems (continued)

(Source: ASHRAE Handbook—Fundamentals [2013], Chapter 15, Table 10)

ID	Glazing System			Center Glazing T_v	Center-of-Glazing Properties							Total Window SHGC at Normal Incidence				Total Window T_v at Normal Incidence			
					Incidence Angles							Aluminum		Other Frames		Aluminum		Other Frames	
	Glass Thick., mm				Normal 0.00	40.00	50.00	60.00	70.00	80.00	Hemis., Diffuse	Operable	Fixed	Operable	Fixed	Operable	Fixed	Operable	Fixed
				T	0.18	0.17	0.16	0.14	0.10	0.05	0.15								
				R^f	0.07	0.07	0.09	0.13	0.22	0.46	0.12								
				R^b	0.35	0.34	0.35	0.38	0.44	0.60	0.37								
				A_1^f	0.71	0.72	0.71	0.69	0.64	0.47	0.68								
				A_2^f	0.04	0.04	0.04	0.04	0.03	0.02	0.04								
Triple Glazing																			
29a	3	CLR CLR CLR	0.74	SHGC	0.68	0.65	0.62	0.54	0.39	0.18	0.57	0.62	0.62	0.55	0.60	0.66	0.67	0.59	0.65
				T	0.60	0.57	0.53	0.45	0.31	0.12	0.49								
				R^f	0.17	0.18	0.21	0.28	0.42	0.65	0.25								
				R^b	0.17	0.18	0.21	0.28	0.42	0.65	0.25								
				A_1^f	0.10	0.11	0.12	0.13	0.14	0.14	0.12								
				A_2^f	0.08	0.08	0.09	0.09	0.08	0.07	0.08								
				A_3^f	0.06	0.06	0.06	0.06	0.05	0.03	0.06								
29b	6	CLR CLR CLR	0.70	SHGC	0.61	0.58	0.55	0.48	0.35	0.16	0.51	0.56	0.56	0.50	0.54	0.62	0.63	0.56	0.62
				T	0.49	0.45	0.42	0.35	0.24	0.09	0.39								
				R^f	0.14	0.15	0.18	0.24	0.37	0.59	0.22								
				R^b	0.14	0.15	0.18	0.24	0.37	0.59	0.22								
				A_1^f	0.17	0.19	0.20	0.21	0.22	0.21	0.19								
				A_2^f	0.12	0.13	0.13	0.13	0.12	0.08	0.12								
				A_3^f	0.08	0.08	0.08	0.08	0.06	0.03	0.08								
29c	6	HI-P GRN CLR CLR	0.53	SHGC	0.32	0.29	0.27	0.24	0.18	0.10	0.26	0.30	0.30	0.26	0.29	0.47	0.48	0.42	0.47
				T	0.20	0.17	0.15	0.12	0.07	0.02	0.15								
				R^f	0.06	0.07	0.08	0.11	0.20	0.41	0.11								
				R^b	0.13	0.14	0.16	0.22	0.35	0.57	0.20								
				A_1^f	0.64	0.67	0.68	0.68	0.66	0.53	0.65								
				A_2^f	0.06	0.06	0.05	0.05	0.05	0.03	0.05								
				A_3^f	0.04	0.04	0.04	0.03	0.02	0.01	0.04								
Triple Glazing, $e = 0.2$ on Surface 2																			
32a	3	LE CLR CLR	0.68	SHGC	0.60	0.58	0.55	0.48	0.35	0.17	0.51	0.55	0.55	0.49	0.53	0.61	0.61	0.54	0.60
				T	0.50	0.47	0.44	0.38	0.26	0.10	0.41								
				R^f	0.17	0.19	0.21	0.27	0.41	0.64	0.25								
				R^b	0.19	0.20	0.22	0.29	0.42	0.63	0.26								
				A_1^f	0.20	0.20	0.20	0.21	0.21	0.17	0.20								
				A_2^f	0.08	0.08	0.08	0.09	0.08	0.07	0.08								

Table 3.7 Visible Transmittance (T_v), Solar Heat Gain Coefficient (SHGC), Solar Transmittance (T), Front Reflectance (R^f), Back Reflectance (R^b), and Layer Absorptance (A_n^f) for Glazing and Window Systems (continued)

(Source: ASHRAE Handbook—Fundamentals [2013], Chapter 15, Table 10)

ID	Glazing System		Center Glazing T_v		Center-of-Glazing Properties						Total Window SHGC at Normal Incidence				Total Window T_v at Normal Incidence				
					Incidence Angles						Aluminum		Other Frames		Aluminum		Other Frames		
					Normal 0.00	40.00	50.00	60.00	70.00	80.00	Hemis., Diffuse	Operable	Fixed	Operable	Fixed	Operable	Fixed	Operable	Fixed
32b	6	LE CLR CLR	0.64	A_3^f	0.06	0.06	0.06	0.06	0.05	0.03	0.06								
				SHGC	0.53	0.50	0.47	0.41	0.29	0.14	0.44	0.49	0.49	0.43	0.47	0.57	0.58	0.51	0.56
				T	0.39	0.36	0.33	0.27	0.17	0.06	0.30								
				R^f	0.14	0.15	0.17	0.21	0.31	0.53	0.20								
				R^b	0.16	0.16	0.19	0.24	0.36	0.57	0.22								
				A_1^f	0.28	0.31	0.31	0.34	0.37	0.31	0.31								
				A_2^f	0.11	0.11	0.11	0.11	0.10	0.08	0.11								
				A_3^f	0.08	0.08	0.08	0.07	0.05	0.03	0.07								
<i>Triple Glazing, e = 0.2 on Surface 5</i>																			
32c	3	CLR CLR LE	0.68	SHGC	0.62	0.60	0.57	0.49	0.36	0.16	0.52	0.57	0.57	0.50	0.55	0.61	0.61	0.54	0.60
				T	0.50	0.47	0.44	0.38	0.26	0.10	0.41								
				R^f	0.19	0.20	0.22	0.29	0.42	0.63	0.26								
				R^b	0.18	0.19	0.21	0.27	0.41	0.64	0.25								
				A_1^f	0.11	0.12	0.13	0.14	0.15	0.15	0.13								
				A_2^f	0.09	0.10	0.10	0.10	0.10	0.08	0.10								
				A_3^f	0.11	0.11	0.11	0.10	0.08	0.04	0.10								
32d	6	CLR CLR LE	0.64	SHGC	0.56	0.53	0.50	0.44	0.32	0.15	0.47	0.51	0.52	0.46	0.50	0.57	0.58	0.1	0.56
				T	0.39	0.36	0.33	0.27	0.17	0.06	0.30								
				R^f	0.16	0.16	0.19	0.24	0.36	0.57	0.22								
				R^b	0.14	0.15	0.17	0.21	0.31	0.53	0.20								
				A_1^f	0.17	0.19	0.20	0.21	0.22	0.22	0.19								
				A_2^f	0.13	0.14	0.14	0.14	0.13	0.10	0.13								
				A_3^f	0.15	0.16	0.15	0.14	0.12	0.05	0.14								
<i>Triple Glazing, e = 0.1 on Surface 2 and 5</i>																			
40a	3	LE CLR LE	0.62	SHGC	0.41	0.39	0.37	0.32	0.24	0.12	0.34	0.38	0.38	0.34	0.36	0.55	0.56	0.50	0.55
				T	0.29	0.26	0.24	0.20	0.13	0.05	0.23								
				R^f	0.30	0.30	0.31	0.34	0.41	0.59	0.33								
				R^b	0.30	0.30	0.31	0.34	0.41	0.59	0.33								
				A_1^f	0.25	0.27	0.28	0.30	0.32	0.27	0.28								
				A_2^f	0.07	0.08	0.08	0.08	0.07	0.06	0.07								
				A_3^f	0.08	0.09	0.09	0.09	0.07	0.04	0.08								
40b	6	LE CLR LE	0.59	SHGC	0.36	0.34	0.32	0.28	0.21	0.10	0.30	0.34	0.34	0.30	0.32	0.53	0.53	0.47	0.52
				T	0.24	0.21	0.19	0.16	0.10	0.03	0.18								
				R^f	0.34	0.34	0.35	0.38	0.44	0.61	0.37								
				R^b	0.23	0.23	0.25	0.28	0.36	0.56	0.27								
				A_1^f	0.24	0.25	0.26	0.28	0.30	0.25	0.26								

Table 3.7 Visible Transmittance (T_v), Solar Heat Gain Coefficient (SHGC), Solar Transmittance (T), Front Reflectance (R^f), Back Reflectance (R^b), and Layer Absorptance (A_n^f) for Glazing and Window Systems (continued)

(Source: ASHRAE Handbook—Fundamentals [2013], Chapter 15, Table 10)

ID	Glazing System		Center Glazing T_v		Center-of-Glazing Properties						Total Window SHGC at Normal Incidence				Total Window T_v at Normal Incidence				
					Incidence Angles						Aluminum		Other Frames		Aluminum		Other Frames		
	Glass Thick., mm				Normal 0.00	40.00	50.00	60.00	70.00	80.00	Hemis., Diffuse	Operable	Fixed	Operable	Fixed	Operable	Fixed	Operable	Fixed
			A_2^f		0.10	0.11	0.11	0.11	0.10	0.07	0.10								
			A_3^f		0.09	0.09	0.09	0.08	0.07	0.03	0.08								
<i>Triple Glazing, e = 0.05 on Surface 2 and 4</i>																			
49	3	LE LE CLR	0.58	SHGC	0.27	0.25	0.24	0.21	0.16	0.08	0.23	0.26	0.25	0.22	0.25	0.52	0.52	0.46	0.51
				T	0.18	0.17	0.16	0.13	0.08	0.03	0.14								
				R^f	0.41	0.41	0.42	0.44	0.50	0.65	0.44								
				R^b	0.46	0.45	0.46	0.48	0.53	0.68	0.47								
				A_1^f	0.27	0.28	0.28	0.29	0.30	0.24	0.28								
				A_2^f	0.12	0.12	0.12	0.12	0.11	0.07	0.12								
				A_3^f	0.02	0.02	0.02	0.02	0.01	0.01	0.02								
50	6	LE LE CLR	0.55	SHGC	0.26	0.25	0.23	0.21	0.16	0.08	0.22	0.25	0.25	0.21	0.24	0.49	0.0	0.44	0.48
				T	0.15	0.14	0.12	0.10	0.07	0.02	0.12								
				R^f	0.33	0.33	0.34	0.37	0.43	0.60	0.36								
				R^b	0.39	0.38	0.38	0.40	0.46	0.61	0.40								
				A_1^f	0.34	0.36	0.36	0.37	0.36	0.28	0.35								
				A_2^f	0.15	0.15	0.15	0.14	0.12	0.08	0.14								
				A_3^f	0.03	0.03	0.03	0.03	0.02	0.01	0.03								

KEY:
 CLR = clear, BRZ = bronze, GRN = green, GRY = gray, BLUGRN = blue green, SS = stainless steel
 reflective coating, TI = titanium reflective coating
 Reflective coating descriptors include percent visible transmittance as x%.
 HI-P GRN = high-performance green tinted glass, LE = low-emissivity coating

T_v = visible transmittance, T = solar transmittance, SHGC = solar heat gain coefficient, and H. = hemispherical SHGC
 ID #s refer to U-factors in Table 4, except for products 49 and 50.

Load Calculation Applications Manual (SI), Second Edition

Table 3.8 Angle Correction Factors for SHGC

ID	# of Layers	Description		SHGC Angle Correction Factors and Diffuse Correction Factor							
		Layer	Normal SHGC	T _v	0	40	50	60	70	80	Diffuse
1A	1	Clear	0.86	0.90	1.000	0.977	0.953	0.907	0.779	0.488	0.907
1B	1	Clear	0.81	0.88	1.000	0.988	0.963	0.901	0.765	0.481	0.901
1C	1	Bronze heat absorbing	0.73	0.68	1.000	0.973	0.932	0.877	0.753	0.466	0.890
1D	1	Bronze heat absorbing	0.62	0.54	1.000	0.952	0.919	0.855	0.726	0.468	0.871
1E	1	Green heat absorbing	0.70	0.82	1.000	0.971	0.943	0.886	0.757	0.471	0.900
1F	1	Green heat absorbing	0.60	0.76	1.000	0.967	0.933	0.867	0.867	0.750	0.483
1G	1	Gray	0.70	0.62	1.000	0.971	0.943	0.871	0.757	0.471	0.900
1H	1	Gray	0.59	0.46	1.000	0.966	0.932	0.864	0.746	0.475	0.881
1I	1	Reflective	0.62	0.75	1.000	0.952	0.919	0.871	0.742	0.484	0.887
1J	1	Stainless steel on clear 8%	0.19	0.08	1.000	1.000	1.000	0.947	0.842	0.526	0.947
1K	1	Stainless steel on clear 14%	0.25	0.14	1.000	1.000	0.960	0.920	0.800	0.520	0.920
1L	1	Stainless steel on clear 20%	0.31	0.20	1.000	0.968	0.968	0.903	0.774	0.516	0.903
1M	1	Stainless steel on green 14%	0.25	0.12	1.000	1.000	0.960	0.920	0.840	0.560	0.920
1N	1	Titanium reflective on clear 20%	0.29	0.20	1.000	1.000	0.966	0.931	0.793	0.517	0.931
1O	1	Titanium reflective on clear 30%	0.39	0.30	1.000	0.974	0.949	0.897	0.769	0.513	0.897
5A	2	Clear/clear	0.76	0.81	1.000	0.974	0.934	0.842	0.658	0.342	0.868
5B	2	Clear/clear	0.70	0.78	1.000	0.957	0.914	0.829	0.643	0.329	0.857
5C	2	Bronze heat absorbing/clear	0.62	0.62	1.000	0.968	0.919	0.823	0.629	0.323	0.855
5D	2	Bronze Heat Absorbing/clear	0.49	0.47	1.000	0.939	0.898	0.796	0.633	0.347	0.837
5E	2	Green heat absorbing/clear	0.60	0.75	1.000	0.950	0.900	0.817	0.633	0.333	0.850

Thermal Property Data

Table 3.8 Angle Correction Factors for SHGC (continued)

ID	# of Layers	Description		SHGC Angle Correction Factors and Diffuse Correction Factor							
		Layer	Normal SHGC	T _v	0	40	50	60	70	80	Diffuse
5F	2	Green heat absorbing/clear	0.49	0.68	1.000	0.939	0.898	0.796	0.633	0.347	0.837
5G	2	Gray/clear	0.60	0.56	1.000	0.950	0.900	0.800	0.617	0.333	0.850
5H	2	Gray/clear	0.47	0.41	1.000	0.936	0.894	0.787	0.617	0.340	0.830
5I	2	Reflective/clear	0.50	0.67	1.000	0.940	0.900	0.800	0.640	0.340	0.860
5J	2	Green heat absorbing/clear	0.39	0.59	1.000	0.949	0.897	0.795	0.641	0.359	0.846
5K	2	Stainless steel on clear 8%/clear	0.16	0.07	1.000	0.923	0.923	0.846	0.769	0.462	0.846
5L	2	Stainless steel on clear 14%/clear	0.17	0.13	1.000	1.000	0.941	0.882	0.765	0.471	0.941
5M	2	Stainless steel on clear 20%/clear	0.22	0.18	1.000	0.955	0.955	0.864	0.727	0.409	0.909
5N	2	Stainless steel on green 14%/clear	0.16	0.11	1.000	1.000	0.938	0.875	0.750	0.500	0.875
5O	2	Titanium reflective on clear 20%/clear	0.21	0.18	1.000	0.952	0.905	0.857	0.714	0.429	0.857
5P	2	Reflective/clear	0.29	0.27	1.000	0.966	0.931	0.862	0.690	0.414	0.862
17A	2	Low-e/clear	0.65	0.76	1.000	0.985	0.938	0.862	0.662	0.354	0.877
17B	2	Low-e/clear	0.60	0.73	1.000	0.983	0.950	0.850	0.667	0.350	0.883
17C	2	Clear/low-e ("high solar")	0.70	0.76	1.000	0.971	0.929	0.843	0.657	0.343	0.871
17D	2	Clear/low-e ("high solar")	0.65	0.73	1.000	0.969	0.923	0.831	0.646	0.323	0.862
17E	2	Bronze/low-e	0.57	0.58	1.000	0.947	0.895	0.807	0.614	0.316	0.842
17F	2	Bronze/low-e	0.45	0.45	1.000	0.933	0.889	0.778	0.600	0.311	0.844
17G	2	Green/low-e	0.55	0.70	1.000	0.945	0.909	0.800	0.618	0.309	0.836
17H	2	Green/low-e	0.41	0.61	1.000	0.951	0.878	0.780	0.610	0.317	0.829
17I	2	Gray/low-e	0.54	0.53	1.000	0.944	0.907	0.815	0.611	0.315	0.852
17J	2	Gray/low-e	0.39	0.37	1.000	0.949	0.897	0.795	0.615	0.333	0.846

Load Calculation Applications Manual (SI), Second Edition

Table 3.8 Angle Correction Factors for SHGC (continued)

ID	# of Layers	Description		SHGC Angle Correction Factors and Diffuse Correction Factor							
		Layer	Normal SHGC	T _v	0	40	50	60	70	80	Diffuse
17K	2	Blue-green/ low-e	0.45	0.62	1.000	0.933	0.889	0.778	0.600	0.311	0.822
17L	2	High-performance green/low-e	0.34	0.55	1.000	0.912	0.882	0.765	0.588	0.324	0.824
21A	2	Low-e/clear	0.65	0.76	1.000	0.985	0.954	0.862	0.662	0.354	0.877
21B	2	Low-e/clear	0.60	0.72	1.000	0.983	0.950	0.850	0.667	0.350	0.883
21C	2	Clear/low-e	0.60	0.75	1.000	0.967	0.933	0.850	0.667	0.367	0.867
21D	2	Clear/low-e	0.56	0.72	1.000	0.982	0.929	0.857	0.679	0.357	0.875
21E	2	Bronze/low-e	0.48	0.57	1.000	0.958	0.917	0.833	0.646	0.354	0.875
21F	2	Bronze/low-e	0.39	0.45	1.000	0.949	0.897	0.795	0.615	0.333	0.846
21G	2	Green/low-e	0.46	0.68	1.000	0.957	0.913	0.826	0.652	0.348	0.870
21H	2	Green/low-e	0.36	0.61	1.000	0.917	0.861	0.778	0.611	0.333	0.833
21I	2	Gray/low-e	0.46	0.52	1.000	0.957	0.913	0.826	0.652	0.348	0.848
21J	2	Gray/low-e	0.34	0.37	1.000	0.941	0.882	0.794	0.618	0.353	0.824
21K	2	Blue-green/ low-e	0.39	0.62	1.000	0.949	0.872	0.795	0.615	0.333	0.846
21L	2	High-performance green with low-e/clear	0.31	0.57	1.000	0.968	0.935	0.839	0.677	0.387	0.871
25A	2	Low-e/clear ("low solar")	0.41	0.72	1.000	0.976	0.927	0.829	0.659	0.341	0.878
25B	2	Low-e/clear ("low solar")	0.37	0.70	1.000	0.973	0.919	0.838	0.649	0.351	0.865
25C	2	Bronze with low-e/clear	0.26	0.42	1.000	0.962	0.923	0.846	0.692	0.385	0.885
25D	2	Green with low-e/clear	0.31	0.60	1.000	0.968	0.903	0.839	0.677	0.387	0.871
25E	2	Gray with low-e/clear	0.24	0.35	1.000	0.958	0.917	0.833	0.667	0.375	0.875
25F	2	Blue with low-e/clear	0.27	0.45	1.000	0.963	0.926	0.852	0.667	0.407	0.889

Thermal Property Data

Table 3.8 Angle Correction Factors for SHGC (continued)

ID	# of Layers	Description		SHGC Angle Correction Factors and Diffuse Correction Factor							
		Layer	Normal SHGC	T _v	0	40	50	60	70	80	Diffuse
25G	2	High-performance green with low-e/clear	0.27	0.53	1.000	0.963	0.926	0.852	0.667	0.407	0.852
29A	3	Clear/clear/clear	0.68	0.74	1.000	0.956	0.912	0.794	0.574	0.265	0.838
29B	3	Clear/clear/clear	0.61	0.70	1.000	0.951	0.902	0.787	0.574	0.262	0.836
29C	3	Green heat absorbing/clear/clear	0.32	0.53	1.000	0.906	0.844	0.750	0.563	0.313	0.813
32A	3	Low-e/clear/clear	0.60	0.68	1.000	0.967	0.917	0.800	0.583	0.283	0.850
32B	3	Low-e/clear/clear	0.53	0.64	1.000	0.943	0.887	0.774	0.547	0.264	0.830
32C	3	Clear/clear/low-e ("high solar")	0.62	0.68	1.000	0.968	0.919	0.790	0.581	0.258	0.839
32D	3	Clear/clear/low-e ("high solar")	0.56	0.64	1.000	0.946	0.893	0.786	0.571	0.268	0.839
40A	3	Low-e/clear/low-e	0.41	0.62	1.000	0.951	0.902	0.780	0.585	0.293	0.829
40B	3	Low-e/clear/low-e	0.36	0.59	1.000	0.944	0.889	0.778	0.583	0.278	0.833
40C	3	Low-e/low-e/clear ("low solar")	0.27	0.58	1.000	0.926	0.889	0.778	0.593	0.296	0.852
40D	3	Low-e/low-e/clear ("low solar")	0.26	0.55	1.000	0.962	0.885	0.808	0.615	0.308	0.846

Table 3.9a IAC Values for Louvered Shades: Uncoated Single Glazings

(Source: ASHRAE Handbook—Fundamentals [2013], Chapter 15, Table 13A)

Glazing ID:			1a	1b	1c	1d	1e	1f	1g	1h	1i	
Louver Location	Louver Reflection	ϕ	IAC ₀ (IAC ₆₀)/IAC _{diff} , F _R ^d									
Indoor Side	0.15	Worst ^a	0.98 (0.97)/ 0.86	0.98 (0.97)/ 0.86	0.98 (0.96)/ 0.86	0.97 (0.95)/ 0.87	0.98 (0.96)/ 0.87	0.97 (0.95)/ 0.87	0.98 (0.96)/ 0.87	0.97 (0.95)/ 0.87	0.97 (0.95)/ 0.87	
			0.92	0.91	0.88	0.82	0.87	0.82	0.87	0.81	0.83	
		0°	0.98 (0.78)/ 0.87	0.98 (0.79)/ 0.87	0.98 (0.80)/ 0.88	0.97 (0.82)/ 0.88	0.98 (0.80)/ 0.88	0.97 (0.82)/ 0.89	0.98 (0.80)/ 0.88	0.97 (0.82)/ 0.89	0.98 (0.80)/ 0.88	0.97 (0.82)/ 0.89
			0.69	0.68	0.66	0.64	0.66	0.63	0.66	0.63	0.64	
		Excluded Beam ^b	0.73 (0.78)/ 0.87	0.74 (0.79)/ 0.87	0.75 (0.80)/ 0.88	0.77 (0.82)/ 0.88	0.76 (0.80)/ 0.88	0.77 (0.82)/ 0.88	0.76 (0.80)/ 0.88	0.78 (0.82)/ 0.88	0.77 (0.82)/ 0.88	
			0.43	0.43	0.42	0.41	0.42	0.41	0.42	0.41	0.41	
	45°	0.80 (0.74)/ 0.83	0.80 (0.75)/ 0.83	0.81 (0.76)/ 0.84	0.82 (0.78)/ 0.85	0.81 (0.77)/ 0.84	0.83 (0.79)/ 0.85	0.81 (0.77)/ 0.84	0.83 (0.79)/ 0.85	0.82 (0.78)/ 0.85		
		0.47	0.46	0.45	0.44	0.45	0.43	0.45	0.43	0.44		
	Closed	0.70 (0.70)/ 0.73	0.70 (0.70)/ 0.74	0.72 (0.72)/ 0.75	0.74 (0.74)/ 0.76	0.72 (0.72)/ 0.75	0.74 (0.74)/ 0.77	0.72 (0.72)/ 0.75	0.74 (0.74)/ 0.77	0.74 (0.74)/ 0.77		
		0.44	0.44	0.42	0.4	0.42	0.4	0.42	0.4	0.4		
	Indoor Side	0.50	Worst ^a	0.98 (0.96)/ 0.80	0.97 (0.96)/ 0.80	0.97 (0.96)/ 0.81	0.97 (0.95)/ 0.83	0.97 (0.96)/ 0.82	0.97 (0.95)/ 0.83	0.97 (0.96)/ 0.82	0.97 (0.95)/ 0.83	0.97 (0.95)/ 0.83
				0.94	0.93	0.89	0.83	0.88	0.83	0.88	0.82	0.84
0°			0.98 (0.70)/ 0.83	0.97 (0.70)/ 0.84	0.97 (0.72)/ 0.84	0.97 (0.75)/ 0.86	0.97 (0.73)/ 0.85	0.97 (0.76)/ 0.86	0.97 (0.73)/ 0.85	0.97 (0.76)/ 0.86	0.97 (0.75)/ 0.86	
			0.74	0.73	0.71	0.67	0.7	0.67	0.7	0.66	0.67	
Excluded Beam ^b			0.59 (0.70)/ 0.82	0.60 (0.70)/ 0.83	0.63 (0.72)/ 0.84	0.67 (0.75)/ 0.85	0.64 (0.73)/ 0.84	0.67 (0.76)/ 0.85	0.64 (0.73)/ 0.84	0.67 (0.76)/ 0.85	0.67 (0.75)/ 0.85	
			0.5	0.5	0.48	0.46	0.48	0.46	0.48	0.46	0.46	
45°		0.69 (0.58)/ 0.74	0.70 (0.59)/ 0.75	0.72 (0.62)/ 0.76	0.75 (0.66)/ 0.79	0.73 (0.63)/ 0.77	0.75 (0.67)/ 0.79	0.73 (0.63)/ 0.77	0.75 (0.67)/ 0.79	0.75 (0.66)/ 0.79		
		0.53	0.52	0.5	0.48	0.5	0.47	0.5	0.47	0.48		
Closed		0.51 (0.49)/ 0.58	0.52 (0.50)/ 0.58	0.55 (0.53)/ 0.61	0.60 (0.58)/ 0.65	0.56 (0.54)/ 0.62	0.60 (0.59)/ 0.65	0.56 (0.54)/ 0.62	0.61 (0.59)/ 0.66	0.60 (0.58)/ 0.65		
		0.46	0.45	0.43	0.4	0.42	0.4	0.42	0.39	0.4		
Indoor Side		0.80	Worst ^a	0.97 (0.96)/ 0.73	0.97 (0.96)/ 0.74	0.97 (0.95)/ 0.76	0.96 (0.95)/ 0.78	0.97 (0.95)/ 0.79	0.96 (0.95)/ 0.79	0.97 (0.95)/ 0.76	0.96 (0.95)/ 0.79	0.96 (0.95)/ 0.78
				0.95	0.94	0.9	0.85	0.89	0.84	0.89	0.83	0.85
	0°		0.97 (0.60)/ 0.78	0.97 (0.61)/ 0.79	0.97 (0.64)/ 0.80	0.96 (0.68)/ 0.82	0.97 (0.65)/ 0.81	0.96 (0.69)/ 0.83	0.97 (0.65)/ 0.81	0.96 (0.69)/ 0.83	0.96 (0.68)/ 0.82	
			0.82	0.81	0.78	0.73	0.77	0.72	0.77	0.72	0.73	
	Excluded Beam ^b		0.45 (0.60)/ 0.77	0.47 (0.61)/ 0.77	0.51 (0.64)/ 0.79	0.57 (0.68)/ 0.81	0.52 (0.65)/ 0.81	0.57 (0.69)/ 0.81	0.52 (0.65)/ 0.81	0.58 (0.69)/ 0.82	0.57 (0.68)/ 0.81	
			0.66	0.65	0.61	0.56	0.59	0.55	0.59	0.55	0.56	
	45°	0.59 (0.42)/ 0.66	0.60 (0.43)/ 0.67	0.63 (0.48)/ 0.69	0.67 (0.54)/ 0.73	0.64 (0.49)/ 0.73	0.68 (0.55)/ 0.73	0.64 (0.49)/ 0.70	0.68 (0.56)/ 0.73	0.68 (0.54)/ 0.73		
		0.66	0.65	0.61	0.56	0.59	0.55	0.59	0.55	0.56		
	Closed	0.33 (0.29)/ 0.43	0.35 (0.31)/ 0.44	0.40 (0.37)/ 0.49	0.47 (0.44)/ 0.54	0.42 (0.38)/ 0.50	0.48 (0.45)/ 0.55	0.42 (0.38)/ 0.50	0.49 (0.46)/ 0.55	0.47 (0.44)/ 0.54		
		0.52	0.51	0.46	0.41	0.45	0.41	0.45	0.41	0.42		

Table 3.9a IAC Values for Louvered Shades: Uncoated Single Glazings (continued)

(Source: ASHRAE Handbook—Fundamentals [2013], Chapter 15, Table 13A)

Glazing ID:			1a	1b	1c	1d	1e	1f	1g	1h	1i
Outdoor Side	0.15	Worst ^a	0.93 (0.89)/	0.93 (0.89)/	0.93 (0.89)/	0.93 (0.89)/	0.93 (0.89)/	0.93 (0.89)/	0.93 (0.89)/	0.93 (0.89)/	0.93 (0.89)/
			0.36	0.36	0.36	0.37	0.36	0.37	0.36	0.37	0.37
			0.98	0.97	0.95	0.92	0.94	0.91	0.94	0.91	0.92
		0°	0.93 (0.05)/	0.93 (0.06)/	0.93 (0.06)/	0.93 (0.06)/	0.93 (0.06)/	0.93 (0.06)/	0.93 (0.06)/	0.93 (0.07)/	0.93 (0.06)/
			0.41	0.41	0.42	0.42	0.42	0.42	0.42	0.42	0.42
			0.9	0.89	0.87	0.84	0.87	0.84	0.87	0.83	0.84
		Excluded Beam ^b	0.04 (0.05)/	0.04 (0.06)/	0.04 (0.06)/	0.05 (0.06)/	0.04 (0.06)/	0.05 (0.06)/	0.04 (0.06)/	0.05 (0.07)/	0.05 (0.06)/
			0.39	0.40	0.40	0.40	0.40	0.40	0.40	0.40	0.40
			0.77	0.76	0.74	0.72	0.74	0.72	0.74	0.72	0.72
		45°	0.20 (0.04)/	0.20 (0.04)/	0.21 (0.04)/	0.21 (0.05)/	0.21 (0.04)/	0.21 (0.05)/	0.21 (0.04)/	0.21 (0.05)/	0.21 (0.05)/
			0.29	0.30	0.30	0.30	0.30	0.30	0.30	0.30	0.30
			0.83	0.82	0.81	0.78	0.8	0.78	0.8	0.77	0.78
		Closed	0.03 (0.03)/	0.03 (0.04)/	0.04 (0.04)/	0.04 (0.05)/	0.04 (0.04)/	0.05 (0.05)/	0.04 (0.04)/	0.05 (0.05)/	0.04 (0.05)/
			0.11	0.11	0.11	0.12	0.11	0.12	0.11	0.12	0.12
			0.65	0.65	0.65	0.64	0.64	0.64	0.64	0.64	0.64
Outdoor Side	0.50	Worst ^a	0.94 (0.95)/	0.94 (0.95)/	0.94 (0.95)/	0.94 (0.95)/	0.94 (0.95)/	0.94 (0.95)/	0.94 (0.95)/	0.94 (0.95)/	0.94 (0.95)/
			0.44	0.44	0.44	0.44	0.44	0.44	0.44	0.44	0.44
			0.98	0.97	0.95	0.92	0.94	0.91	0.94	0.91	0.92
		0°	0.94 (0.15)/	0.94 (0.15)/	0.94 (0.15)/	0.94 (0.15)/	0.94 (0.15)/	0.94 (0.15)/	0.94 (0.15)/	0.94 (0.15)/	0.94 (0.15)/
			0.50	0.50	0.50	0.50	0.50	0.50	0.50	0.50	0.50
			0.96	0.96	0.93	0.9	0.92	0.89	0.92	0.89	0.9
		Excluded Beam ^b	0.08 (0.15)/	0.08 (0.15)/	0.09 (0.15)/	0.09 (0.15)/	0.09 (0.15)/	0.09 (0.15)/	0.09 (0.15)/	0.09 (0.15)/	0.09 (0.15)/
			0.48	0.48	0.48	0.48	0.48	0.48	0.48	0.48	0.48
			0.92	0.91	0.89	0.85	0.88	0.85	0.88	0.84	0.85
		45°	0.26 (0.07)/	0.26 (0.07)/	0.26 (0.07)/	0.26 (0.07)/	0.26 (0.07)/	0.26 (0.07)/	0.26 (0.07)/	0.26 (0.07)/	0.26 (0.07)/
			0.36	0.36	0.36	0.37	0.36	0.37	0.36	0.37	0.37
			0.93	0.92	0.89	0.86	0.89	0.85	0.89	0.85	0.86
		Closed	0.05 (0.03)/	0.05 (0.03)/	0.05 (0.03)/	0.05 (0.04)/	0.05 (0.04)/	0.06 (0.04)/	0.05 (0.04)/	0.06 (0.04)/	0.05 (0.04)/
			0.14	0.14	0.14	0.15	0.14	0.15	0.14	0.15	0.15
			0.8	0.8	0.77	0.75	0.77	0.74	0.77	0.74	0.75
Outdoor Side	0.80	Worst ^a	0.95 (1.02)/	0.95 (1.02)/	0.95 (1.01)/	0.95 (1.00)/	0.95 (1.01)/	0.95 (1.00)/	0.95 (1.01)/	0.95 (1.00)/	0.95 (1.01)/
			0.54	0.54	0.54	0.54	0.54	0.54	0.54	0.54	0.54
			0.98	0.98	0.95	0.92	0.95	0.91	0.95	0.91	0.92
		0°	0.95 (0.28)/	0.95 (0.28)/	0.95 (0.28)/	0.95 (0.28)/	0.95 (0.28)/	0.95 (0.28)/	0.95 (0.28)/	0.95 (0.28)/	0.95 (0.28)/
			0.61	0.61	0.61	0.61	0.61	0.61	0.61	0.61	0.61
			0.98	0.97	0.95	0.91	0.94	0.91	0.94	0.91	0.91
		Excluded Beam ^b	0.17 (0.28)/	0.17 (0.28)/	0.17 (0.28)/	0.17 (0.28)/	0.17 (0.28)/	0.17 (0.28)/	0.17 (0.28)/	0.17 (0.28)/	0.17 (0.28)/
			0.59	0.59	0.58	0.58	0.58	0.58	0.58	0.59	0.59
			0.97	0.96	0.94	0.9	0.93	0.89	0.93	0.89	0.9
		45°	0.34 (0.12)/	0.34 (0.12)/	0.34 (0.12)/	0.34 (0.12)/	0.34 (0.12)/	0.34 (0.12)/	0.34 (0.12)/	0.34 (0.12)/	0.35 (0.12)/
			0.46	0.46	0.46	0.46	0.46	0.46	0.46	0.46	0.46
			0.97	0.96	0.94	0.9	0.93	0.9	0.93	0.89	0.9
		Closed	0.08 (0.04)/	0.08 (0.04)/	0.09 (0.04)/	0.09 (0.04)/	0.09 (0.04)/	0.09 (0.04)/	0.09 (0.04)/	0.09 (0.04)/	0.09 (0.04)/
			0.21	0.21	0.20	0.21	0.21	0.21	0.21	0.21	0.21
			0.93	0.92	0.89	0.86	0.89	0.85	0.89	0.85	0.86
Sheer	100%		0.7	0.71	0.72	0.74	0.72	0.74	0.72	0.74	0.74
			0.5	0.49	0.47	0.45	0.47	0.44	0.47	0.44	0.47

^aNotes: Louvers track so that profile angle equals negative slat angle and maximum direct beam is admitted.

^bLouvers track to block direct beam radiation. When negative slat angles result, slat defaults to 0°.

^cGlazing cavity width equals original cavity width plus slat width.

^d F_R is radiant fraction; ratio of radiative heat transfer to total heat transfer, on room side of glazing system.

Table 3.9b IAC Values for Louvered Shades: Uncoated Double Glazings

(Source: ASHRAE Handbook—Fundamentals [2013], Chapter 15, Table 13B)

Glazing ID:		5a	5b	5c	5d	5e	5f	5g	5h	5i		
Louver Location	Louver Reflection	ϕ	IAC ₀ (IAC ₆₀)/IAC _{diff} , F _R ^d									
Indoor Side	0.15	Worst ^a	0.99 (0.98)/ 0.92 0.87	0.99 (0.98)/ 0.92 0.84	0.99 (0.97)/ 0.92 0.84	0.98 (0.97)/ 0.93 0.79	0.99 (0.97)/ 0.92 0.83	0.98 (0.97)/ 0.93 0.78	0.99 (0.97)/ 0.92 0.83	0.98 (0.97)/ 0.93 0.78	0.98 (0.97)/ 0.93 0.79	
		0°	0.99 (0.88)/ 0.93 0.67	0.99 (0.89)/ 0.93 0.65	0.99 (0.89)/ 0.93 0.65	0.98 (0.90)/ 0.93 0.62	0.99 (0.89)/ 0.93 0.65	0.98 (0.90)/ 0.94 0.62	0.99 (0.89)/ 0.93 0.65	0.98 (0.90)/ 0.94 0.62	0.98 (0.90)/ 0.93 0.62	
		Excluded Beam ^b	0.84 (0.88)/ 0.93 0.42	0.84 (0.89)/ 0.93 0.41	0.84 (0.89)/ 0.93 0.41	0.86 (0.90)/ 0.93 0.4	0.85 (0.89)/ 0.93 0.41	0.86 (0.90)/ 0.93 0.4	0.85 (0.89)/ 0.93 0.41	0.86 (0.90)/ 0.93 0.41	0.86 (0.90)/ 0.93 0.4	0.86 (0.90)/ 0.93 0.4
		45°	0.88 (0.85)/ 0.90 0.45	0.88 (0.85)/ 0.90 0.44	0.88 (0.85)/ 0.90 0.44	0.89 (0.87)/ 0.91 0.42	0.88 (0.86)/ 0.90 0.44	0.89 (0.87)/ 0.91 0.42	0.88 (0.86)/ 0.90 0.42	0.89 (0.87)/ 0.91 0.42	0.88 (0.86)/ 0.90 0.42	0.89 (0.87)/ 0.91 0.42
		Closed	0.81 (0.81)/ 0.83 0.41	0.82 (0.82)/ 0.84 0.4	0.82 (0.82)/ 0.84 0.4	0.83 (0.84)/ 0.85 0.38	0.82 (0.82)/ 0.84 0.4	0.83 (0.84)/ 0.85 0.38	0.82 (0.82)/ 0.84 0.4	0.83 (0.84)/ 0.85 0.38	0.82 (0.82)/ 0.84 0.4	0.83 (0.84)/ 0.85 0.38
		Indoor Side	0.50	Worst ^a	0.98 (0.97)/ 0.86 0.88	0.98 (0.97)/ 0.87 0.86	0.98 (0.97)/ 0.87 0.85	0.98 (0.97)/ 0.88 0.8	0.98 (0.97)/ 0.87 0.84	0.98 (0.97)/ 0.89 0.79	0.98 (0.97)/ 0.87 0.84	0.98 (0.97)/ 0.89 0.79
Indoor Side	0.50	0°	0.98 (0.80)/ 0.89 0.71	0.98 (0.82)/ 0.90 0.69	0.98 (0.81)/ 0.90 0.69	0.98 (0.84)/ 0.91 0.65	0.98 (0.82)/ 0.90 0.68	0.98 (0.84)/ 0.91 0.65	0.98 (0.82)/ 0.90 0.68	0.98 (0.84)/ 0.91 0.65	0.98 (0.84)/ 0.91 0.65	
		Excluded Beam ^b	0.70 (0.80)/ 0.88 0.48	0.72 (0.82)/ 0.89 0.47	0.72 (0.81)/ 0.89 0.47	0.75 (0.84)/ 0.90 0.45	0.73 (0.82)/ 0.89 0.46	0.76 (0.84)/ 0.90 0.45	0.73 (0.82)/ 0.89 0.46	0.76 (0.84)/ 0.90 0.45	0.75 (0.84)/ 0.90 0.45	
		45°	0.78 (0.70)/ 0.82 0.5	0.80 (0.72)/ 0.83 0.49	0.79 (0.72)/ 0.83 0.48	0.82 (0.76)/ 0.85 0.46	0.80 (0.73)/ 0.84 0.48	0.82 (0.76)/ 0.85 0.46	0.80 (0.73)/ 0.84 0.48	0.82 (0.76)/ 0.85 0.46	0.80 (0.73)/ 0.84 0.48	0.82 (0.76)/ 0.85 0.46
		Closed	0.63 (0.63)/ 0.69 0.42	0.66 (0.65)/ 0.71 0.4	0.65 (0.65)/ 0.71 0.4	0.70 (0.70)/ 0.74 0.38	0.66 (0.66)/ 0.71 0.4	0.70 (0.70)/ 0.75 0.38	0.66 (0.66)/ 0.71 0.4	0.70 (0.70)/ 0.75 0.38	0.66 (0.66)/ 0.71 0.4	0.70 (0.70)/ 0.74 0.38
		Indoor Side	0.80	Worst ^a	0.97 (0.96)/ 0.80 0.9	0.97 (0.96)/ 0.81 0.87	0.97 (0.96)/ 0.81 0.87	0.97 (0.96)/ 0.84 0.81	0.97 (0.96)/ 0.82 0.86	0.97 (0.96)/ 0.84 0.86	0.97 (0.96)/ 0.82 0.86	0.97 (0.96)/ 0.84 0.81
		Indoor Side	0.80	0°	0.97 (0.71)/ 0.84 0.78	0.97 (0.73)/ 0.85 0.75	0.97 (0.73)/ 0.85 0.75	0.97 (0.77)/ 0.87 0.7	0.97 (0.73)/ 0.85 0.74	0.97 (0.77)/ 0.87 0.7	0.97 (0.73)/ 0.85 0.74	0.97 (0.77)/ 0.87 0.7
Excluded Beam ^b	0.57 (0.71)/ 0.83 0.6			0.60 (0.73)/ 0.84 0.58	0.60 (0.73)/ 0.84 0.58	0.65 (0.77)/ 0.86 0.54	0.61 (0.73)/ 0.84 0.57	0.66 (0.77)/ 0.86 0.53	0.61 (0.73)/ 0.84 0.57	0.66 (0.77)/ 0.86 0.53	0.65 (0.77)/ 0.86 0.54	
45°	0.68 (0.56)/ 0.74 0.6			0.71 (0.60)/ 0.76 0.58	0.70 (0.59)/ 0.76 0.58	0.74 (0.65)/ 0.79 0.54	0.71 (0.60)/ 0.76 0.57	0.75 (0.66)/ 0.79 0.53	0.71 (0.60)/ 0.76 0.57	0.75 (0.66)/ 0.79 0.53	0.71 (0.60)/ 0.76 0.57	0.74 (0.65)/ 0.79 0.54
Closed	0.47 (0.45)/ 0.55 0.46			0.51 (0.50)/ 0.59 0.43	0.50 (0.49)/ 0.58 0.43	0.57 (0.56)/ 0.64 0.4	0.51 (0.50)/ 0.59 0.43	0.57 (0.57)/ 0.64 0.39	0.51 (0.50)/ 0.59 0.43	0.57 (0.57)/ 0.64 0.39	0.51 (0.50)/ 0.59 0.43	0.57 (0.56)/ 0.64 0.4
Between Glazings ^c	0.15			Worst ^a	0.97 (0.98)/ 0.66 0.93	0.97 (0.99)/ 0.67 0.91	0.96 (0.97)/ 0.67 0.91	0.95 (0.96)/ 0.69 0.88	0.95 (0.97)/ 0.67 0.91	0.95 (0.95)/ 0.69 0.88	0.95 (0.97)/ 0.67 0.91	0.95 (0.96)/ 0.69 0.88

Table 3.9b IAC Values for Louvered Shades: Uncoated Double Glazings (continued)

(Source: ASHRAE Handbook—Fundamentals [2013], Chapter 15, Table 13B)

Glazing ID:		5a	5b	5c	5d	5e	5f	5g	5h	5i
	0°	0.97 (0.50)/ 0.70	0.97 (0.51)/ 0.71	0.96 (0.52)/ 0.70	0.95 (0.55)/ 0.72	0.95 (0.52)/ 0.70	0.95 (0.55)/ 0.72	0.95 (0.52)/ 0.70	0.95 (0.55)/ 0.72	0.95 (0.55)/ 0.72
		0.81	0.8	0.8	0.78	0.79	0.78	0.79	0.78	0.78
	Excluded Beam ^b	0.43 (0.50)/ 0.69	0.45 (0.51)/ 0.69	0.46 (0.52)/ 0.69	0.49 (0.55)/ 0.71	0.46 (0.52)/ 0.69	0.49 (0.55)/ 0.71	0.46 (0.52)/ 0.69	0.49 (0.55)/ 0.71	0.49 (0.55)/ 0.71
		0.66	0.66	0.66	0.65	0.65	0.65	0.65	0.65	0.65
	45°	0.54 (0.47)/ 0.62	0.55 (0.48)/ 0.63	0.56 (0.49)/ 0.63	0.58 (0.52)/ 0.65	0.56 (0.49)/ 0.63	0.58 (0.52)/ 0.65	0.56 (0.49)/ 0.63	0.59 (0.52)/ 0.65	0.58 (0.52)/ 0.65
		0.7	0.7	0.7	0.69	0.69	0.68	0.69	0.68	0.69
	Closed	0.42 (0.45)/ 0.50	0.44 (0.47)/ 0.51	0.44 (0.47)/ 0.52	0.47 (0.50)/ 0.54	0.45 (0.48)/ 0.52	0.48 (0.51)/ 0.54	0.45 (0.48)/ 0.52	0.48 (0.51)/ 0.54	0.47 (0.50)/ 0.54
		0.65	0.65	0.65	0.64	0.64	0.64	0.64	0.64	0.64
Between Glazings ^c	0.50	Worst ^d	0.97 (1.01)/ 0.67	0.97 (1.02)/ 0.67	0.96 (1.00)/ 0.67	0.95 (0.98)/ 0.69	0.95 (0.99)/ 0.68	0.95 (0.98)/ 0.68	0.95 (0.98)/ 0.69	0.95 (0.98)/ 0.69
		0.94	0.92	0.92	0.89	0.92	0.89	0.92	0.89	0.89
	0°	0.97 (0.49)/ 0.71	0.97 (0.50)/ 0.72	0.96 (0.51)/ 0.72	0.95 (0.54)/ 0.73	0.95 (0.52)/ 0.73	0.95 (0.55)/ 0.73	0.95 (0.52)/ 0.73	0.95 (0.55)/ 0.73	0.95 (0.54)/ 0.73
		0.84	0.83	0.83	0.8	0.82	0.8	0.82	0.8	0.8
	Excluded Beam ^b	0.38 (0.49)/ 0.70	0.39 (0.50)/ 0.70	0.40 (0.51)/ 0.70	0.44 (0.54)/ 0.72	0.41 (0.52)/ 0.72	0.45 (0.55)/ 0.72	0.41 (0.52)/ 0.72	0.45 (0.55)/ 0.72	0.44 (0.54)/ 0.72
		0.72	0.71	0.71	0.69	0.71	0.69	0.71	0.69	0.69
	45°	0.51 (0.38)/ 0.61	0.52 (0.40)/ 0.62	0.53 (0.41)/ 0.62	0.56 (0.45)/ 0.64	0.53 (0.42)/ 0.64	0.56 (0.46)/ 0.64	0.53 (0.42)/ 0.62	0.56 (0.46)/ 0.64	0.56 (0.45)/ 0.64
		0.75	0.74	0.73	0.72	0.73	0.71	0.73	0.71	0.72
	Closed	0.32 (0.32)/ 0.42	0.33 (0.33)/ 0.43	0.35 (0.35)/ 0.44	0.39 (0.39)/ 0.47	0.36 (0.36)/ 0.45	0.39 (0.40)/ 0.48	0.36 (0.36)/ 0.45	0.40 (0.40)/ 0.48	0.39 (0.39)/ 0.47
		0.67	0.66	0.66	0.65	0.66	0.65	0.66	0.65	0.66
Between Glazings ^c	0.80	Worst ^d	0.97 (1.04)/ 0.68	0.97 (1.04)/ 0.68	0.96 (1.02)/ 0.69	0.95 (1.01)/ 0.70	0.96 (1.02)/ 0.69	0.95 (1.00)/ 0.70	0.96 (1.02)/ 0.69	0.95 (1.01)/ 0.70
		0.94	0.93	0.93	0.9	0.93	0.9	0.93	0.89	0.9
	0°	0.97 (0.49)/ 0.73	0.97 (0.50)/ 0.74	0.96 (0.51)/ 0.74	0.95 (0.55)/ 0.75	0.96 (0.52)/ 0.74	0.95 (0.55)/ 0.75	0.96 (0.52)/ 0.74	0.95 (0.55)/ 0.75	0.95 (0.55)/ 0.75
		0.89	0.88	0.87	0.84	0.87	0.84	0.87	0.84	0.84
	Excluded Beam ^b	0.35 (0.49)/ 0.72	0.36 (0.50)/ 0.72	0.37 (0.51)/ 0.72	0.42 (0.55)/ 0.74	0.38 (0.52)/ 0.74	0.42 (0.55)/ 0.74	0.38 (0.52)/ 0.72	0.42 (0.55)/ 0.74	0.42 (0.55)/ 0.74
		0.82	0.81	0.8	0.76	0.79	0.76	0.79	0.76	0.77
	45°	0.50 (0.32)/ 0.60	0.51 (0.33)/ 0.61	0.52 (0.35)/ 0.62	0.55 (0.40)/ 0.64	0.53 (0.36)/ 0.62	0.55 (0.41)/ 0.64	0.53 (0.36)/ 0.62	0.56 (0.41)/ 0.64	0.55 (0.40)/ 0.64
		0.83	0.81	0.8	0.77	0.8	0.77	0.8	0.77	0.77
	Closed	0.24 (0.20)/ 0.36	0.25 (0.22)/ 0.37	0.27 (0.25)/ 0.39	0.32 (0.30)/ 0.43	0.28 (0.26)/ 0.40	0.33 (0.31)/ 0.43	0.28 (0.26)/ 0.40	0.33 (0.31)/ 0.43	0.32 (0.30)/ 0.43
		0.74	0.73	0.71	0.69	0.71	0.69	0.71	0.69	0.69
Outdoor Side	0.15	Worst ^d	0.93 (0.89)/ 0.35	0.93 (0.89)/ 0.36	0.93 (0.89)/ 0.36	0.93 (0.89)/ 0.36	0.93 (0.89)/ 0.36	0.93 (0.89)/ 0.36	0.93 (0.89)/ 0.36	0.93 (0.89)/ 0.36
		0.95	0.94	0.93	0.9	0.93	0.89	0.93	0.89	0.9
	0°	0.93 (0.05)/ 0.41	0.93 (0.05)/ 0.41	0.93 (0.05)/ 0.41	0.93 (0.05)/ 0.41	0.93 (0.05)/ 0.41	0.93 (0.06)/ 0.41	0.93 (0.05)/ 0.41	0.93 (0.06)/ 0.41	0.93 (0.05)/ 0.41
		0.9	0.88	0.88	0.84	0.87	0.84	0.87	0.84	0.84
	Excluded Beam ^b	0.03 (0.05)/ 0.39	0.03 (0.05)/ 0.39	0.03 (0.05)/ 0.39	0.03 (0.05)/ 0.39	0.03 (0.05)/ 0.39	0.03 (0.06)/ 0.39	0.03 (0.05)/ 0.39	0.04 (0.06)/ 0.40	0.03 (0.05)/ 0.39
		0.78	0.77	0.76	0.73	0.76	0.73	0.76	0.73	0.73

Table 3.9b IAC Values for Louvered Shades: Uncoated Double Glazings (continued)

(Source: ASHRAE Handbook—Fundamentals [2013], Chapter 15, Table 13B)

Glazing ID:		5a	5b	5c	5d	5e	5f	5g	5h	5i
	45°	0.19 (0.03)/ 0.29 0.84	0.19 (0.03)/ 0.29 0.82	0.20 (0.03)/ 0.29 0.82	0.20 (0.04)/ 0.29 0.79	0.20 (0.03)/ 0.29 0.81	0.20 (0.04)/ 0.29 0.78	0.20 (0.03)/ 0.29 0.81	0.20 (0.04)/ 0.30 0.78	0.20 (0.04)/ 0.29 0.79
	Closed	0.02 (0.02)/ 0.10 0.66	0.02 (0.02)/ 0.10 0.66	0.02 (0.03)/ 0.10 0.65	0.03 (0.03)/ 0.11 0.64	0.03 (0.03)/ 0.10 0.65	0.03 (0.03)/ 0.11 0.64	0.03 (0.03)/ 0.10 0.65	0.03 (0.03)/ 0.11 0.64	0.03 (0.03)/ 0.11 0.64
Outdoor Side	0.50	Worst ^a	0.94 (0.98)/ 0.44 0.95	0.94 (0.98)/ 0.44 0.94	0.94 (0.97)/ 0.44 0.93	0.94 (0.96)/ 0.44 0.9	0.94 (0.96)/ 0.44 0.93	0.94 (0.95)/ 0.44 0.9	0.94 (0.96)/ 0.44 0.93	0.94 (0.95)/ 0.44 0.89
	0°	0.94 (0.14)/ 0.50 0.94	0.94 (0.14)/ 0.50 0.93	0.94 (0.15)/ 0.50 0.92	0.94 (0.15)/ 0.50 0.89	0.94 (0.15)/ 0.50 0.92	0.94 (0.15)/ 0.50 0.88	0.94 (0.15)/ 0.50 0.92	0.94 (0.15)/ 0.50 0.88	0.94 (0.15)/ 0.50 0.89
	Excluded Beam ^b	0.07 (0.14)/ 0.48 0.91	0.07 (0.14)/ 0.48 0.9	0.08 (0.15)/ 0.48 0.89	0.08 (0.15)/ 0.48 0.85	0.08 (0.15)/ 0.48 0.88	0.08 (0.15)/ 0.48 0.85	0.08 (0.15)/ 0.48 0.88	0.08 (0.15)/ 0.48 0.84	0.08 (0.15)/ 0.48 0.85
	45°	0.25 (0.06)/ 0.36 0.92	0.25 (0.06)/ 0.36 0.9	0.25 (0.06)/ 0.36 0.9	0.25 (0.07)/ 0.36 0.86	0.25 (0.06)/ 0.36 0.89	0.25 (0.07)/ 0.36 0.85	0.25 (0.06)/ 0.36 0.89	0.25 (0.06)/ 0.36 0.85	0.25 (0.07)/ 0.36 0.86
	Closed	0.04 (0.02)/ 0.14 0.82	0.04 (0.03)/ 0.14 0.81	0.04 (0.03)/ 0.14 0.8	0.04 (0.03)/ 0.14 0.76	0.04 (0.03)/ 0.14 0.79	0.05 (0.03)/ 0.14 0.76	0.04 (0.03)/ 0.14 0.79	0.05 (0.03)/ 0.14 0.76	0.04 (0.03)/ 0.14 0.76
Outdoor Side	0.80	Worst ^a	0.95 (1.08)/ 0.55 0.95	0.95 (1.07)/ 0.55 0.94	0.95 (1.04)/ 0.55 0.93	0.95 (1.02)/ 0.54 0.9	0.95 (1.04)/ 0.55 0.93	0.95 (1.02)/ 0.54 0.9	0.95 (1.04)/ 0.55 0.93	0.95 (1.02)/ 0.54 0.89
	0°	0.95 (0.29)/ 0.62 0.95	0.95 (0.29)/ 0.61 0.94	0.95 (0.28)/ 0.61 0.94	0.95 (0.28)/ 0.61 0.9	0.95 (0.28)/ 0.61 0.93	0.95 (0.28)/ 0.61 0.9	0.95 (0.28)/ 0.61 0.93	0.95 (0.28)/ 0.61 0.89	0.95 (0.28)/ 0.61 0.9
	Excluded Beam ^b	0.16 (0.29)/ 0.59 0.94	0.16 (0.29)/ 0.59 0.93	0.16 (0.28)/ 0.59 0.92	0.16 (0.28)/ 0.59 0.89	0.16 (0.28)/ 0.59 0.92	0.16 (0.28)/ 0.59 0.88	0.16 (0.28)/ 0.59 0.92	0.16 (0.28)/ 0.59 0.88	0.16 (0.28)/ 0.59 0.89
	45°	0.34 (0.12)/ 0.47 0.95	0.34 (0.12)/ 0.47 0.93	0.33 (0.12)/ 0.47 0.93	0.33 (0.12)/ 0.46 0.89	0.33 (0.12)/ 0.46 0.92	0.33 (0.12)/ 0.46 0.88	0.33 (0.12)/ 0.46 0.92	0.33 (0.12)/ 0.46 0.88	0.34 (0.12)/ 0.46 0.89
	Closed	0.08 (0.04)/ 0.21 0.92	0.08 (0.04)/ 0.21 0.9	0.08 (0.04)/ 0.21 0.89	0.08 (0.04)/ 0.21 0.86	0.08 (0.04)/ 0.21 0.89	0.08 (0.04)/ 0.21 0.85	0.08 (0.04)/ 0.21 0.89	0.08 (0.04)/ 0.21 0.85	0.08 (0.04)/ 0.21 0.86

^aNotes: ^aLouvers track so that profile angle equals negative slat angle and maximum direct beam is admitted.

^bLouvers track to block direct beam radiation. When negative slat angles result, slat defaults to 0°.

^cGlazing cavity width equals original cavity width plus slat width.

^d F_R is radiant fraction; ratio of radiative heat transfer to total heat transfer, on room side of glazing system.

Table 3.9c IAC Values for Louvered Shades: Coated Double Glazings with 0.2 Low-E

(Source: ASHRAE Handbook—Fundamentals [2013], Chapter 15, Table 13C)

Glazing ID:		17a	17b	17c	17d	17e	17f	17g	17h	17i	17j	17k		
Louver Location	Louver Reflection	IAC ₀ (IAC ₆₀)/IAC _{diff} · F _R ^d												
φ	φ													
Indoor Side	0.15	Worst ^d	0.99 (0.98)/0.94 0.86	0.99 (0.98)/0.94 0.83	0.99 (0.98)/0.94 0.83	0.99 (0.98)/0.94 0.79	0.99 (0.98)/0.94 0.81	0.99 (0.98)/0.95 0.76	0.99 (0.98)/0.94 0.8	0.99 (0.98)/0.95 0.75	0.99 (0.98)/0.94 0.8	0.99 (0.98)/0.95 0.75	0.99 (0.98)/0.95 0.76	
		0°	0.99 (0.91)/0.95 0.66	0.99 (0.91)/0.95 0.64	0.99 (0.91)/0.95 0.65	0.99 (0.92)/0.95 0.63	0.99 (0.92)/0.95 0.63	0.99 (0.93)/0.95 0.61	0.99 (0.92)/0.95 0.63	0.99 (0.93)/0.95 0.6	0.99 (0.92)/0.95 0.63	0.99 (0.93)/0.95 0.6	0.99 (0.93)/0.95 0.61	
		Excluded Beam ^b	0.87 (0.91)/0.94 0.41	0.88 (0.91)/0.95 0.41	0.88 (0.91)/0.95 0.41	0.89 (0.92)/0.95 0.41	0.88 (0.92)/0.95 0.41	0.90 (0.93)/0.95 0.4	0.88 (0.92)/0.95 0.41	0.90 (0.93)/0.95 0.4	0.88 (0.92)/0.95 0.41	0.90 (0.93)/0.95 0.4	0.88 (0.92)/0.95 0.41	0.90 (0.93)/0.95 0.4
		45°	0.90 (0.88)/0.92 0.44	0.91 (0.89)/0.93 0.43	0.91 (0.89)/0.93 0.44	0.92 (0.89)/0.93 0.43	0.91 (0.89)/0.93 0.43	0.92 (0.90)/0.93 0.42	0.91 (0.89)/0.93 0.43	0.92 (0.90)/0.93 0.42	0.91 (0.89)/0.93 0.43	0.92 (0.90)/0.93 0.42	0.91 (0.89)/0.93 0.43	0.92 (0.90)/0.93 0.42
		Closed	0.85 (0.85)/0.87 0.4	0.86 (0.86)/0.88 0.39	0.85 (0.86)/0.88 0.4	0.86 (0.87)/0.88 0.39	0.86 (0.86)/0.88 0.37	0.87 (0.88)/0.89 0.37	0.86 (0.86)/0.88 0.39	0.87 (0.88)/0.89 0.37	0.86 (0.86)/0.88 0.39	0.87 (0.88)/0.89 0.37	0.86 (0.86)/0.88 0.39	0.87 (0.88)/0.89 0.37
Indoor Side	0.50	Worst ^d	0.98 (0.98)/0.88 0.87	0.98 (0.98)/0.89 0.84	0.98 (0.98)/0.89 0.84	0.98 (0.98)/0.90 0.8	0.98 (0.98)/0.90 0.82	0.98 (0.98)/0.91 0.76	0.98 (0.98)/0.90 0.81	0.98 (0.98)/0.91 0.76	0.98 (0.98)/0.90 0.81	0.98 (0.98)/0.91 0.76	0.98 (0.98)/0.91 0.77	
		0°	0.98 (0.83)/0.91 0.7	0.98 (0.85)/0.91 0.68	0.98 (0.85)/0.91 0.68	0.98 (0.86)/0.92 0.66	0.98 (0.85)/0.92 0.67	0.98 (0.87)/0.93 0.63	0.98 (0.85)/0.92 0.66	0.98 (0.87)/0.93 0.63	0.98 (0.85)/0.92 0.66	0.98 (0.87)/0.93 0.63	0.98 (0.87)/0.93 0.64	
		Excluded Beam ^b	0.74 (0.83)/0.90 0.47	0.76 (0.85)/0.91 0.46	0.76 (0.85)/0.91 0.46	0.79 (0.86)/0.92 0.45	0.77 (0.85)/0.91 0.45	0.80 (0.87)/0.92 0.44	0.77 (0.85)/0.91 0.45	0.80 (0.87)/0.92 0.44	0.77 (0.85)/0.91 0.45	0.81 (0.87)/0.92 0.44	0.77 (0.85)/0.91 0.45	0.80 (0.87)/0.92 0.44
		45°	0.81 (0.74)/0.85 0.49	0.83 (0.76)/0.86 0.48	0.83 (0.76)/0.86 0.48	0.84 (0.79)/0.87 0.47	0.83 (0.77)/0.86 0.47	0.86 (0.81)/0.88 0.45	0.83 (0.77)/0.87 0.47	0.86 (0.81)/0.88 0.45	0.83 (0.77)/0.87 0.47	0.86 (0.81)/0.88 0.45	0.83 (0.77)/0.87 0.47	0.86 (0.81)/0.88 0.45
		Closed	0.67 (0.67)/0.73 0.41	0.70 (0.70)/0.75 0.39	0.70 (0.70)/0.75 0.4	0.73 (0.73)/0.78 0.38	0.71 (0.71)/0.76 0.39	0.75 (0.75)/0.79 0.37	0.72 (0.71)/0.76 0.38	0.76 (0.75)/0.79 0.37	0.72 (0.71)/0.76 0.38	0.76 (0.76)/0.80 0.37	0.75 (0.75)/0.79 0.37	0.73 (0.73)/0.78 0.38
Indoor Side	0.80	Worst ^d	0.98 (0.97)/0.82 0.88	0.98 (0.97)/0.83 0.85	0.98 (0.97)/0.83 0.85	0.98 (0.97)/0.85 0.82	0.98 (0.97)/0.84 0.83	0.98 (0.97)/0.86 0.78	0.98 (0.97)/0.84 0.83	0.98 (0.97)/0.87 0.77	0.98 (0.97)/0.84 0.83	0.98 (0.97)/0.87 0.77	0.98 (0.97)/0.87 0.78	
		0°	0.98 (0.74)/0.86 0.76	0.98 (0.76)/0.87 0.74	0.98 (0.76)/0.87 0.74	0.98 (0.79)/0.88 0.71	0.98 (0.77)/0.88 0.72	0.98 (0.81)/0.89 0.68	0.98 (0.77)/0.88 0.72	0.98 (0.81)/0.89 0.68	0.98 (0.77)/0.88 0.72	0.98 (0.81)/0.89 0.68	0.98 (0.81)/0.89 0.68	
		Excluded Beam ^b	0.61 (0.74)/0.84 0.59	0.64 (0.76)/0.86 0.56	0.64 (0.76)/0.86 0.56	0.68 (0.79)/0.87 0.54	0.66 (0.77)/0.86 0.55	0.71 (0.81)/0.88 0.51	0.66 (0.77)/0.87 0.54	0.71 (0.81)/0.89 0.51	0.66 (0.77)/0.87 0.54	0.72 (0.81)/0.89 0.51	0.66 (0.77)/0.87 0.54	0.71 (0.81)/0.88 0.51
		45°	0.71 (0.60)/0.77 0.59	0.74 (0.64)/0.79 0.56	0.74 (0.64)/0.79 0.56	0.77 (0.68)/0.81 0.54	0.75 (0.66)/0.80 0.55	0.79 (0.71)/0.83 0.51	0.75 (0.66)/0.80 0.54	0.79 (0.71)/0.83 0.51	0.75 (0.66)/0.80 0.54	0.79 (0.72)/0.83 0.51	0.75 (0.66)/0.80 0.54	0.79 (0.71)/0.83 0.51
		Closed	0.51 (0.50)/0.59 0.44	0.55 (0.54)/0.63 0.42	0.55 (0.55)/0.63 0.42	0.60 (0.60)/0.67 0.4	0.57 (0.57)/0.65 0.41	0.64 (0.64)/0.70 0.38	0.58 (0.57)/0.65 0.4	0.64 (0.64)/0.70 0.38	0.58 (0.57)/0.65 0.4	0.64 (0.64)/0.70 0.38	0.58 (0.57)/0.65 0.4	0.64 (0.64)/0.70 0.38
Between Glazings ^c	0.15	Worst ^d	0.97 (1.02)/0.78 0.92	0.98 (1.02)/0.78 0.9	0.96 (0.96)/0.59 0.91	0.96 (0.96)/0.60 0.89	0.95 (0.95)/0.60 0.9	0.95 (0.95)/0.62 0.87	0.95 (0.95)/0.60 0.9	0.95 (0.95)/0.62 0.87	0.95 (0.95)/0.60 0.9	0.95 (0.95)/0.62 0.87	0.95 (0.95)/0.62 0.87	
		0°	0.97 (0.66)/0.80 0.8	0.98 (0.67)/0.81 0.79	0.96 (0.39)/0.63 0.79	0.96 (0.40)/0.64 0.78	0.95 (0.41)/0.64 0.79	0.95 (0.44)/0.65 0.77	0.95 (0.41)/0.64 0.79	0.95 (0.44)/0.65 0.77	0.95 (0.41)/0.64 0.79	0.95 (0.44)/0.65 0.77	0.95 (0.44)/0.65 0.77	
		45°	0.66	0.66	0.66	0.66	0.65	0.65	0.65	0.65	0.65	0.65	0.65	
		Closed	0.67 (0.62)/0.74 0.69	0.68 (0.63)/0.75 0.69	0.46 (0.36)/0.54 0.7	0.46 (0.37)/0.55 0.7	0.47 (0.38)/0.55 0.7	0.50 (0.41)/0.57 0.69	0.47 (0.38)/0.56 0.7	0.50 (0.41)/0.57 0.69	0.47 (0.38)/0.56 0.7	0.50 (0.41)/0.58 0.69	0.49 (0.41)/0.57 0.69	
Between Glazings ^c	0.50	Worst ^d	0.97 (1.03)/0.75 0.92	0.97 (1.03)/0.75 0.91	0.96 (1.01)/0.61 0.91	0.96 (1.01)/0.62 0.89	0.96 (1.00)/0.62 0.91	0.95 (0.99)/0.64 0.87	0.95 (0.99)/0.62 0.9	0.95 (0.98)/0.64 0.87	0.95 (0.99)/0.62 0.9	0.95 (0.98)/0.64 0.87	0.95 (0.99)/0.64 0.88	
		0°	0.97 (0.66)/0.80 0.8	0.98 (0.67)/0.81 0.79	0.96 (0.39)/0.63 0.79	0.96 (0.40)/0.64 0.78	0.95 (0.41)/0.64 0.79	0.95 (0.44)/0.65 0.77	0.95 (0.41)/0.64 0.79	0.95 (0.44)/0.65 0.77	0.95 (0.41)/0.64 0.79	0.95 (0.44)/0.65 0.77	0.95 (0.44)/0.65 0.77	
		45°	0.66	0.66	0.66	0.66	0.65	0.65	0.65	0.65	0.65	0.65	0.65	
		Closed	0.57 (0.60)/0.64 0.65	0.58 (0.61)/0.65 0.65	0.32 (0.34)/0.40 0.64	0.33 (0.35)/0.41 0.64	0.34 (0.36)/0.42 0.64	0.37 (0.40)/0.44 0.64	0.35 (0.37)/0.42 0.64	0.38 (0.40)/0.45 0.64	0.35 (0.37)/0.42 0.64	0.38 (0.40)/0.45 0.64	0.37 (0.39)/0.44 0.64	

Table 3.9c IAC Values for Louvered Shades: Coated Double Glazings with 0.2 Low-E (continued)

(Source: ASHRAE Handbook—Fundamentals [2013], Chapter 15, Table 13C)

Glazing ID:	17a	17b	17c	17d	17e	17f	17g	17h	17i	17j	17k
0°	0.97 (0.61)/0.79 0.83	0.97 (0.62)/0.79 0.82	0.96 (0.41)/0.66 0.83	0.96 (0.42)/0.67 0.82	0.96 (0.43)/0.67 0.82	0.95 (0.45)/0.68 0.8	0.95 (0.43)/0.67 0.82	0.95 (0.46)/0.68 0.8	0.95 (0.43)/0.67 0.82	0.95 (0.46)/0.69 0.8	0.95 (0.45)/0.68 0.8
Excluded Beam ^b	0.49 (0.61)/0.77 0.7	0.50 (0.62)/0.78 0.7	0.31 (0.41)/0.65 0.72	0.32 (0.42)/0.65 0.72	0.33 (0.43)/0.65 0.71	0.36 (0.45)/0.67 0.7	0.33 (0.43)/0.66 0.71	0.37 (0.46)/0.67 0.7	0.33 (0.43)/0.66 0.71	0.37 (0.46)/0.67 0.7	0.36 (0.45)/0.67 0.7
45°	0.61 (0.49)/0.69 0.73	0.62 (0.50)/0.70 0.72	0.45 (0.31)/0.55 0.75	0.46 (0.32)/0.56 0.74	0.47 (0.33)/0.56 0.74	0.49 (0.37)/0.58 0.72	0.47 (0.34)/0.56 0.74	0.50 (0.37)/0.58 0.72	0.47 (0.34)/0.56 0.74	0.50 (0.37)/0.58 0.72	0.49 (0.37)/0.58 0.72
Closed	0.42 (0.42)/0.52 0.66	0.43 (0.43)/0.53 0.66	0.25 (0.25)/0.35 0.67	0.26 (0.26)/0.36 0.66	0.28 (0.27)/0.37 0.66	0.31 (0.31)/0.40 0.66	0.28 (0.28)/0.38 0.66	0.32 (0.32)/0.41 0.65	0.28 (0.28)/0.38 0.66	0.32 (0.32)/0.41 0.65	0.31 (0.31)/0.40 0.66
Between Glazings ^c	0.80	0.80	0.80	0.80	0.80	0.80	0.80	0.80	0.80	0.80	0.80
Worst ^a	0.97 (1.05)/0.72 0.94	0.97 (1.05)/0.72 0.92	0.97 (1.05)/0.65 0.92	0.97 (1.05)/0.66 0.9	0.96 (1.04)/0.66 0.91	0.96 (1.02)/0.67 0.88	0.96 (1.03)/0.66 0.91	0.95 (1.02)/0.67 0.88	0.96 (1.03)/0.66 0.91	0.95 (1.02)/0.68 0.88	0.96 (1.02)/0.67 0.88
0°	0.97 (0.55)/0.77 0.88	0.97 (0.56)/0.78 0.86	0.97 (0.45)/0.71 0.88	0.97 (0.46)/0.72 0.86	0.96 (0.46)/0.72 0.87	0.96 (0.49)/0.73 0.84	0.96 (0.47)/0.72 0.86	0.95 (0.49)/0.73 0.83	0.96 (0.47)/0.72 0.86	0.95 (0.50)/0.73 0.83	0.96 (0.49)/0.73 0.84
Excluded Beam ^b	0.40 (0.55)/0.75 0.8	0.41 (0.56)/0.76 0.78	0.31 (0.45)/0.69 0.82	0.32 (0.46)/0.70 0.81	0.33 (0.46)/0.70 0.8	0.37 (0.49)/0.71 0.77	0.34 (0.47)/0.70 0.8	0.37 (0.49)/0.71 0.77	0.34 (0.47)/0.70 0.8	0.37 (0.50)/0.71 0.77	0.37 (0.49)/0.71 0.77
45°	0.55 (0.37)/0.65 0.81	0.56 (0.39)/0.65 0.79	0.47 (0.28)/0.58 0.83	0.48 (0.29)/0.58 0.81	0.49 (0.31)/0.59 0.81	0.51 (0.34)/0.61 0.77	0.49 (0.31)/0.59 0.8	0.51 (0.35)/0.61 0.77	0.49 (0.31)/0.59 0.8	0.52 (0.35)/0.61 0.77	0.51 (0.34)/0.61 0.78
Closed	0.29 (0.25)/0.41 0.72	0.30 (0.27)/0.42 0.71	0.21 (0.17)/0.33 0.75	0.22 (0.18)/0.34 0.73	0.24 (0.20)/0.35 0.72	0.27 (0.25)/0.38 0.7	0.24 (0.21)/0.36 0.72	0.28 (0.25)/0.39 0.7	0.24 (0.21)/0.36 0.72	0.28 (0.26)/0.39 0.69	0.27 (0.25)/0.38 0.7
Outdoor Side	0.15	0.15	0.15	0.15	0.15	0.15	0.15	0.15	0.15	0.15	0.15
Worst ^a	0.93 (0.89)/0.35 0.95	0.93 (0.89)/0.35 0.93	0.93 (0.89)/0.35 0.93	0.93 (0.89)/0.35 0.91	0.93 (0.89)/0.35 0.92	0.93 (0.89)/0.35 0.88	0.93 (0.89)/0.35 0.91	0.93 (0.89)/0.35 0.88	0.93 (0.89)/0.35 0.91	0.93 (0.89)/0.36 0.88	0.93 (0.89)/0.35 0.88
0°	0.93 (0.04)/0.41 0.9	0.93 (0.04)/0.41 0.88	0.93 (0.04)/0.41 0.89	0.93 (0.04)/0.41 0.87	0.93 (0.04)/0.41 0.87	0.93 (0.05)/0.41 0.84	0.93 (0.04)/0.41 0.87	0.93 (0.05)/0.41 0.83	0.93 (0.04)/0.41 0.87	0.93 (0.05)/0.41 0.83	0.93 (0.05)/0.41 0.84
Excluded Beam ^b	0.02 (0.04)/0.39 0.8	0.02 (0.04)/0.39 0.79	0.02 (0.04)/0.39 0.8	0.02 (0.04)/0.39 0.78	0.02 (0.04)/0.39 0.77	0.03 (0.05)/0.39 0.74	0.02 (0.04)/0.39 0.77	0.03 (0.05)/0.39 0.74	0.02 (0.04)/0.39 0.77	0.03 (0.05)/0.39 0.74	0.03 (0.05)/0.39 0.74
45°	0.19 (0.02)/0.28 0.84	0.19 (0.02)/0.29 0.83	0.19 (0.02)/0.28 0.84	0.19 (0.02)/0.29 0.82	0.19 (0.02)/0.29 0.82	0.19 (0.03)/0.29 0.79	0.19 (0.03)/0.29 0.81	0.20 (0.03)/0.29 0.78	0.19 (0.03)/0.29 0.81	0.20 (0.03)/0.29 0.78	0.19 (0.03)/0.29 0.79
Closed	0.02 (0.02)/0.09 0.67	0.02 (0.02)/0.09 0.66	0.02 (0.02)/0.09 0.67	0.02 (0.02)/0.09 0.66	0.02 (0.02)/0.09 0.66	0.02 (0.02)/0.10 0.65	0.02 (0.02)/0.09 0.66	0.02 (0.03)/0.10 0.65	0.02 (0.02)/0.09 0.66	0.02 (0.03)/0.10 0.65	0.02 (0.02)/0.10 0.65
Outdoor Side	0.50	0.50	0.50	0.50	0.50	0.50	0.50	0.50	0.50	0.50	0.50
Worst ^a	0.94 (0.98)/0.43 0.95	0.94 (0.98)/0.43 0.93	0.94 (0.99)/0.44 0.93	0.94 (0.98)/0.44 0.91	0.94 (0.97)/0.43 0.92	0.94 (0.95)/0.43 0.88	0.94 (0.96)/0.43 0.91	0.94 (0.95)/0.43 0.88	0.94 (0.96)/0.43 0.91	0.94 (0.95)/0.43 0.88	0.94 (0.96)/0.43 0.88
0°	0.94 (0.14)/0.50 0.94	0.94 (0.14)/0.50 0.92	0.94 (0.14)/0.50 0.92	0.94 (0.14)/0.50 0.9	0.94 (0.14)/0.49 0.91	0.94 (0.14)/0.49 0.87	0.94 (0.14)/0.49 0.91	0.94 (0.14)/0.49 0.87	0.94 (0.14)/0.49 0.91	0.94 (0.14)/0.49 0.87	0.94 (0.14)/0.49 0.88
Excluded Beam ^b	0.07 (0.14)/0.47 0.91	0.07 (0.14)/0.47 0.9	0.07 (0.14)/0.48 0.9	0.07 (0.14)/0.48 0.88	0.07 (0.14)/0.47 0.88	0.07 (0.14)/0.47 0.85	0.07 (0.14)/0.47 0.88	0.07 (0.14)/0.47 0.84	0.07 (0.14)/0.47 0.88	0.08 (0.14)/0.47 0.84	0.07 (0.14)/0.47 0.85
45°	0.25 (0.06)/0.36 0.92	0.25 (0.06)/0.36 0.9	0.25 (0.06)/0.36 0.91	0.25 (0.06)/0.36 0.88	0.25 (0.06)/0.36 0.89	0.25 (0.06)/0.36 0.85	0.25 (0.06)/0.36 0.88	0.25 (0.06)/0.36 0.85	0.25 (0.06)/0.36 0.88	0.25 (0.06)/0.36 0.85	0.25 (0.06)/0.36 0.85
Closed	0.04 (0.02)/0.13 0.84	0.04 (0.02)/0.13 0.82	0.04 (0.02)/0.13 0.83	0.04 (0.02)/0.13 0.81	0.04 (0.02)/0.13 0.81	0.04 (0.03)/0.13 0.77	0.04 (0.02)/0.13 0.8	0.04 (0.03)/0.14 0.77	0.04 (0.02)/0.13 0.8	0.04 (0.03)/0.14 0.77	0.04 (0.03)/0.14 0.77
Outdoor Side	0.80	0.80	0.80	0.80	0.80	0.80	0.80	0.80	0.80	0.80	0.80
Worst ^a	0.95 (1.07)/0.55 0.95	0.95 (1.07)/0.55 0.93	0.95 (1.08)/0.55 0.93	0.95 (1.08)/0.55 0.91	0.95 (1.04)/0.55 0.92	0.95 (1.02)/0.54 0.88	0.95 (1.04)/0.54 0.91	0.95 (1.02)/0.54 0.88	0.95 (1.04)/0.54 0.91	0.95 (1.02)/0.54 0.88	0.95 (1.03)/0.54 0.88
0°	0.95 (0.28)/0.61 0.95	0.95 (0.28)/0.61 0.93	0.95 (0.29)/0.62 0.93	0.95 (0.28)/0.61 0.91	0.95 (0.28)/0.61 0.92	0.95 (0.28)/0.61 0.88	0.95 (0.28)/0.61 0.91	0.95 (0.28)/0.61 0.88	0.95 (0.28)/0.61 0.91	0.95 (0.28)/0.61 0.88	0.95 (0.28)/0.61 0.88

Table 3.9c IAC Values for Louvered Shades: Coated Double Glazings with 0.2 Low-E (continued)

(Source: ASHRAE Handbook—Fundamentals [2013], Chapter 15, Table 13C)

Glazing ID:	17a	17b	17c	17d	17e	17f	17g	17h	17i	17j	17k
Excluded Beam ^b	0.16 (0.28)/0.59 0.94	0.16 (0.28)/0.59 0.92	0.16 (0.29)/0.59 0.92	0.16 (0.28)/0.59 0.9	0.16 (0.28)/0.59 0.91	0.16 (0.28)/0.58 0.87	0.16 (0.28)/0.59 0.9	0.16 (0.28)/0.58 0.87	0.16 (0.28)/0.59 0.9	0.16 (0.28)/0.58 0.87	0.16 (0.28)/0.59 0.87
45°	0.34 (0.12)/0.47 0.94	0.34 (0.12)/0.47 0.92	0.34 (0.12)/0.47 0.92	0.34 (0.12)/0.47 0.9	0.33 (0.12)/0.46 0.91	0.33 (0.12)/0.46 0.88	0.33 (0.12)/0.46 0.91	0.33 (0.12)/0.46 0.87	0.33 (0.12)/0.46 0.91	0.33 (0.12)/0.46 0.87	0.33 (0.12)/0.46 0.88
Closed	0.08 (0.04)/0.21 0.92	0.08 (0.04)/0.21 0.9	0.08 (0.04)/0.21 0.91	0.08 (0.04)/0.21 0.88	0.08 (0.04)/0.21 0.89	0.08 (0.04)/0.20 0.85	0.08 (0.04)/0.21 0.88	0.08 (0.04)/0.20 0.85	0.08 (0.04)/0.21 0.88	0.08 (0.04)/0.20 0.85	0.08 (0.04)/0.20 0.85

^aNotes:^aLouvers track so that profile angle equals negative slat angle and maximum direct beam is admitted.

^bLouvers track to block direct beam radiation. When negative slat angles result, slat defaults to 0°.

^cGlazing cavity width equals original cavity width plus slat width.

^d F_R is radiant fraction; ratio of radiative heat transfer to total heat transfer, on room side of glazing system.

Table 3.9d IAC Values for Louvered Shades: Coated Double Glazings with 0.1 Low-E

(Source: ASHRAE Handbook—Fundamentals [2013], Chapter 15, Table 13D)

Glazing ID:	21a	21b	21c	21d	21e	21f	21g	21h	21i	21j	21k
Louver Location Louver Reflection ϕ	IAC₀ (IAC₆₀)/IAC_{diff}, F_R^d										
Indoor Side 0.15 Worst ^a	0.99 (0.98)/0.94 0.85	0.99 (0.98)/0.95 0.82	0.99 (0.98)/0.95 0.82	0.99 (0.98)/0.95 0.8	0.99 (0.98)/0.95 0.8	0.99 (0.98)/0.95 0.75	0.99 (0.98)/0.95 0.79	0.99 (0.98)/0.95 0.75	0.99 (0.98)/0.95 0.79	0.99 (0.98)/0.95 0.75	0.99 (0.98)/0.95 0.76
0°	0.99 (0.92)/0.95 0.66	0.99 (0.92)/0.95 0.64	0.99 (0.93)/0.96 0.64	0.99 (0.93)/0.96 0.63	0.99 (0.93)/0.96 0.63	0.99 (0.93)/0.96 0.61	0.99 (0.93)/0.96 0.63	0.99 (0.94)/0.96 0.6	0.99 (0.93)/0.96 0.63	0.99 (0.94)/0.96 0.6	0.99 (0.93)/0.96 0.61
Excluded Beam ^b	0.89 (0.92)/0.95 0.41	0.89 (0.92)/0.95 0.41	0.90 (0.93)/0.95 0.41	0.90 (0.93)/0.96 0.41	0.90 (0.93)/0.95 0.4	0.91 (0.93)/0.96 0.4	0.90 (0.93)/0.96 0.4	0.91 (0.94)/0.96 0.4	0.90 (0.93)/0.96 0.4	0.91 (0.94)/0.96 0.4	0.91 (0.93)/0.96 0.4
45°	0.92 (0.89)/0.93 0.44	0.92 (0.90)/0.93 0.43	0.92 (0.90)/0.93 0.43	0.93 (0.91)/0.94 0.43	0.92 (0.91)/0.94 0.43	0.93 (0.91)/0.94 0.42	0.93 (0.91)/0.94 0.42	0.93 (0.91)/0.94 0.41	0.93 (0.91)/0.94 0.42	0.93 (0.91)/0.94 0.41	0.93 (0.91)/0.94 0.42
Closed	0.86 (0.87)/0.88 0.4	0.87 (0.87)/0.89 0.39	0.87 (0.88)/0.89 0.39	0.88 (0.88)/0.90 0.39	0.88 (0.88)/0.89 0.38	0.89 (0.89)/0.90 0.37	0.88 (0.88)/0.90 0.38	0.89 (0.89)/0.90 0.37	0.88 (0.88)/0.90 0.38	0.89 (0.89)/0.90 0.37	0.89 (0.89)/0.90 0.37
Indoor Side 0.50 Worst ^a	0.99 (0.98)/0.89 0.86	0.99 (0.98)/0.90 0.84	0.99 (0.98)/0.91 0.83	0.99 (0.98)/0.91 0.81	0.99 (0.98)/0.91 0.81	0.99 (0.98)/0.92 0.76	0.99 (0.98)/0.91 0.8	0.99 (0.98)/0.92 0.76	0.99 (0.98)/0.91 0.8	0.99 (0.98)/0.92 0.76	0.99 (0.98)/0.92 0.76
0°	0.99 (0.85)/0.92 0.7	0.99 (0.86)/0.92 0.68	0.99 (0.87)/0.93 0.67	0.99 (0.87)/0.93 0.66	0.99 (0.87)/0.93 0.66	0.99 (0.89)/0.94 0.63	0.99 (0.87)/0.93 0.66	0.99 (0.89)/0.94 0.63	0.99 (0.87)/0.93 0.66	0.99 (0.89)/0.94 0.63	0.99 (0.89)/0.94 0.64
Excluded Beam ^b	0.77 (0.85)/0.91 0.47	0.79 (0.86)/0.92 0.46	0.79 (0.87)/0.92 0.46	0.81 (0.87)/0.92 0.45	0.80 (0.87)/0.92 0.45	0.82 (0.89)/0.93 0.44	0.80 (0.87)/0.92 0.45	0.82 (0.89)/0.93 0.44	0.80 (0.87)/0.92 0.45	0.82 (0.89)/0.93 0.44	0.82 (0.89)/0.93 0.44
45°	0.83 (0.77)/0.86 0.49	0.84 (0.79)/0.87 0.48	0.85 (0.79)/0.88 0.48	0.86 (0.81)/0.88 0.47	0.85 (0.80)/0.88 0.47	0.87 (0.82)/0.89 0.45	0.86 (0.80)/0.88 0.47	0.87 (0.83)/0.89 0.45	0.86 (0.80)/0.88 0.47	0.87 (0.83)/0.89 0.45	0.87 (0.82)/0.89 0.45
Closed	0.71 (0.70)/0.75 0.41	0.73 (0.73)/0.77 0.39	0.74 (0.73)/0.78 0.39	0.75 (0.75)/0.79 0.38	0.75 (0.75)/0.79 0.39	0.77 (0.77)/0.81 0.37	0.75 (0.75)/0.79 0.38	0.78 (0.78)/0.81 0.37	0.75 (0.75)/0.79 0.38	0.78 (0.78)/0.81 0.37	0.77 (0.77)/0.81 0.37
Indoor Side 0.80 Worst ^a	0.98 (0.97)/0.84 0.88	0.98 (0.97)/0.85 0.85	0.98 (0.97)/0.86 0.84	0.98 (0.97)/0.87 0.82	0.98 (0.97)/0.86 0.82	0.98 (0.97)/0.88 0.77	0.98 (0.97)/0.86 0.81	0.98 (0.97)/0.88 0.77	0.98 (0.97)/0.86 0.81	0.98 (0.97)/0.88 0.77	0.98 (0.97)/0.88 0.78
0°	0.98 (0.76)/0.87 0.76	0.98 (0.78)/0.88 0.74	0.98 (0.79)/0.89 0.73	0.98 (0.81)/0.89 0.71	0.98 (0.80)/0.89 0.72	0.98 (0.83)/0.90 0.68	0.98 (0.81)/0.89 0.71	0.98 (0.83)/0.90 0.68	0.98 (0.81)/0.89 0.71	0.98 (0.83)/0.90 0.68	0.98 (0.83)/0.90 0.68
Excluded Beam ^b	0.64 (0.76)/0.86 0.59	0.67 (0.78)/0.87 0.56	0.69 (0.79)/0.88 0.56	0.71 (0.81)/0.89 0.54	0.70 (0.80)/0.88 0.55	0.73 (0.83)/0.90 0.52	0.70 (0.81)/0.88 0.54	0.74 (0.83)/0.90 0.52	0.70 (0.81)/0.88 0.54	0.74 (0.83)/0.90 0.52	0.73 (0.83)/0.90 0.52
45°	0.74 (0.64)/0.79 0.59	0.76 (0.67)/0.81 0.57	0.77 (0.68)/0.81 0.56	0.79 (0.71)/0.83 0.54	0.78 (0.70)/0.82 0.55	0.80 (0.74)/0.84 0.52	0.78 (0.70)/0.82 0.55	0.81 (0.74)/0.84 0.52	0.78 (0.70)/0.82 0.55	0.81 (0.74)/0.84 0.51	0.81 (0.74)/0.84 0.52
Closed	0.54 (0.53)/0.62	0.59 (0.58)/0.66	0.60 (0.59)/0.67	0.63 (0.62)/0.69	0.62 (0.61)/0.68	0.66 (0.66)/0.72	0.62 (0.62)/0.69	0.67 (0.66)/0.72	0.62 (0.62)/0.69	0.67 (0.67)/0.72	0.66 (0.66)/0.72

Table 3.9d IAC Values for Louvered Shades: Coated Double Glazings with 0.1 Low-E (continued)

(Source: ASHRAE Handbook—Fundamentals [2013], Chapter 15, Table 13D)

Glazing ID:	21a	21b	21c	21d	21e	21f	21g	21h	21i	21j	21k
	0.45	0.42	0.42	0.4	0.41	0.38	0.41	0.38	0.41	0.38	0.38
Between Glazings ^c 0.15 Worst ^a	0.98 (1.01)/0.80 0.91	0.98 (1.01)/0.80 0.9	0.96 (0.99)/0.60 0.9	0.96 (0.99)/0.61 0.9	0.96 (0.98)/0.61 0.89	0.95 (0.97)/0.63 0.87	0.95 (0.98)/0.61 0.89	0.95 (0.97)/0.63 0.86	0.95 (0.98)/0.61 0.89	0.95 (0.97)/0.63 0.86	0.95 (0.97)/0.62 0.87
0°	0.98 (0.69)/0.82 0.8	0.98 (0.70)/0.83 0.79	0.96 (0.40)/0.64 0.79	0.96 (0.40)/0.65 0.78	0.96 (0.42)/0.65 0.78	0.95 (0.44)/0.66 0.77	0.95 (0.42)/0.65 0.78	0.95 (0.45)/0.66 0.77	0.95 (0.42)/0.65 0.78	0.95 (0.45)/0.66 0.77	0.95 (0.44)/0.66 0.77
Excluded Beam ^b	0.63 (0.69)/0.81 0.66	0.64 (0.70)/0.82 0.66	0.34 (0.40)/0.63 0.66	0.35 (0.40)/0.63 0.65	0.36 (0.42)/0.64 0.65	0.39 (0.44)/0.65 0.65	0.37 (0.42)/0.64 0.65	0.39 (0.45)/0.65 0.65	0.37 (0.42)/0.64 0.65	0.40 (0.45)/0.65 0.65	0.39 (0.44)/0.65 0.65
45°	0.71 (0.66)/0.77 0.69	0.71 (0.67)/0.78 0.69	0.47 (0.36)/0.55 0.7	0.47 (0.37)/0.56 0.7	0.48 (0.38)/0.56 0.69	0.50 (0.41)/0.58 0.69	0.49 (0.39)/0.57 0.69	0.51 (0.42)/0.58 0.68	0.49 (0.39)/0.57 0.69	0.51 (0.42)/0.58 0.68	0.50 (0.41)/0.58 0.69
Closed	0.61 (0.64)/0.68 0.65	0.63 (0.65)/0.69 0.65	0.33 (0.35)/0.41 0.64	0.34 (0.36)/0.41 0.64	0.35 (0.37)/0.42 0.64	0.38 (0.40)/0.45 0.64	0.35 (0.37)/0.43 0.64	0.38 (0.40)/0.45 0.64	0.35 (0.37)/0.43 0.64	0.38 (0.40)/0.45 0.64	0.38 (0.40)/0.45 0.64
Between Glazings ^c 0.50 Worst ^a	0.97 (1.03)/0.77 0.92	0.97 (1.03)/0.78 0.9	0.97 (1.06)/0.63 0.91	0.97 (1.06)/0.63 0.89	0.96 (1.05)/0.64 0.9	0.95 (1.03)/0.65 0.87	0.96 (1.04)/0.64 0.89	0.95 (1.03)/0.65 0.87	0.96 (1.04)/0.64 0.89	0.95 (1.03)/0.65 0.87	0.95 (1.03)/0.65 0.87
0°	0.97 (0.65)/0.81 0.83	0.97 (0.66)/0.81 0.82	0.97 (0.42)/0.68 0.83	0.97 (0.42)/0.68 0.82	0.96 (0.44)/0.69 0.82	0.95 (0.46)/0.69 0.8	0.96 (0.44)/0.69 0.81	0.95 (0.46)/0.70 0.8	0.96 (0.44)/0.69 0.81	0.95 (0.47)/0.70 0.79	0.95 (0.46)/0.69 0.8
Excluded Beam ^b	0.54 (0.65)/0.80 0.7	0.55 (0.66)/0.80 0.7	0.32 (0.42)/0.66 0.72	0.32 (0.42)/0.67 0.71	0.34 (0.44)/0.67 0.71	0.37 (0.46)/0.68 0.7	0.34 (0.44)/0.67 0.71	0.37 (0.46)/0.68 0.7	0.34 (0.44)/0.67 0.71	0.38 (0.47)/0.68 0.7	0.37 (0.46)/0.68 0.7
45°	0.64 (0.54)/0.72 0.73	0.65 (0.55)/0.73 0.72	0.47 (0.31)/0.56 0.75	0.47 (0.32)/0.57 0.74	0.48 (0.34)/0.58 0.74	0.50 (0.37)/0.59 0.72	0.49 (0.34)/0.58 0.73	0.51 (0.37)/0.59 0.72	0.49 (0.34)/0.58 0.73	0.51 (0.38)/0.59 0.72	0.50 (0.37)/0.59 0.72
Closed	0.47 (0.47)/0.56 0.66	0.48 (0.48)/0.57 0.66	0.26 (0.25)/0.36 0.67	0.27 (0.26)/0.37 0.66	0.28 (0.28)/0.38 0.66	0.32 (0.32)/0.41 0.65	0.29 (0.29)/0.39 0.66	0.32 (0.32)/0.41 0.65	0.29 (0.29)/0.39 0.66	0.33 (0.32)/0.42 0.65	0.32 (0.32)/0.41 0.66
Between Glazings ^c 0.80 Worst ^a	0.97 (1.04)/0.74 0.93	0.97 (1.04)/0.75 0.92	0.97 (1.12)/0.67 0.91	0.97 (1.12)/0.68 0.9	0.96 (1.11)/0.68 0.9	0.96 (1.09)/0.69 0.88	0.96 (1.11)/0.68 0.9	0.96 (1.09)/0.69 0.88	0.96 (1.11)/0.68 0.9	0.95 (1.09)/0.69 0.88	0.96 (1.09)/0.69 0.88
0°	0.97 (0.60)/0.79 0.88	0.97 (0.60)/0.80 0.86	0.97 (0.46)/0.73 0.87	0.97 (0.46)/0.73 0.86	0.96 (0.47)/0.73 0.86	0.96 (0.50)/0.74 0.84	0.96 (0.48)/0.73 0.86	0.96 (0.50)/0.74 0.83	0.96 (0.48)/0.73 0.86	0.95 (0.50)/0.74 0.83	0.96 (0.50)/0.74 0.84
Excluded Beam ^b	0.45 (0.60)/0.78 0.8	0.46 (0.60)/0.78 0.79	0.33 (0.46)/0.71 0.82	0.33 (0.46)/0.71 0.81	0.35 (0.47)/0.71 0.8	0.38 (0.50)/0.72 0.77	0.35 (0.48)/0.72 0.79	0.38 (0.50)/0.72 0.77	0.35 (0.48)/0.72 0.79	0.39 (0.50)/0.72 0.77	0.38 (0.50)/0.72 0.77
45°	0.59 (0.43)/0.68 0.81	0.59 (0.44)/0.68 0.8	0.49 (0.29)/0.60 0.82	0.50 (0.30)/0.60 0.81	0.51 (0.31)/0.61 0.8	0.53 (0.35)/0.62 0.78	0.51 (0.32)/0.61 0.8	0.53 (0.35)/0.63 0.77	0.51 (0.32)/0.61 0.8	0.53 (0.36)/0.63 0.77	0.53 (0.35)/0.62 0.78
Closed	0.33 (0.30)/0.44 0.73	0.34 (0.31)/0.45 0.72	0.22 (0.17)/0.34 0.75	0.23 (0.18)/0.35 0.74	0.25 (0.21)/0.37 0.72	0.28 (0.25)/0.40 0.7	0.25 (0.22)/0.37 0.72	0.29 (0.26)/0.40 0.7	0.25 (0.22)/0.37 0.72	0.29 (0.26)/0.41 0.7	0.28 (0.25)/0.40 0.7
Outdoor Side 0.15 Worst ^a	0.93 (0.90)/0.35 0.94	0.93 (0.90)/0.35 0.93	0.93 (0.90)/0.35 0.92	0.93 (0.90)/0.35 0.91	0.93 (0.89)/0.35 0.91	0.93 (0.89)/0.35 0.88	0.93 (0.89)/0.35 0.9	0.93 (0.89)/0.36 0.88	0.93 (0.89)/0.35 0.9	0.93 (0.89)/0.36 0.88	0.93 (0.89)/0.35 0.88
0°	0.93 (0.04)/0.41 0.9	0.93 (0.04)/0.41 0.88	0.93 (0.04)/0.41 0.88	0.93 (0.04)/0.41 0.87	0.93 (0.04)/0.41 0.87	0.93 (0.05)/0.41 0.84	0.93 (0.04)/0.41 0.86	0.93 (0.05)/0.41 0.84	0.93 (0.04)/0.41 0.86	0.93 (0.05)/0.41 0.83	0.93 (0.05)/0.41 0.84
Excluded Beam ^b	0.02 (0.04)/0.39 0.8	0.02 (0.04)/0.39 0.79	0.02 (0.04)/0.39 0.79	0.02 (0.04)/0.39 0.78	0.02 (0.04)/0.39 0.77	0.03 (0.05)/0.39 0.74	0.02 (0.04)/0.39 0.77	0.03 (0.05)/0.39 0.74	0.02 (0.04)/0.39 0.77	0.03 (0.05)/0.39 0.74	0.03 (0.05)/0.39 0.74
45°	0.19 (0.02)/0.29 0.84	0.19 (0.02)/0.29 0.83	0.19 (0.02)/0.29 0.83	0.19 (0.02)/0.29 0.82	0.19 (0.02)/0.29 0.81	0.20 (0.03)/0.29 0.79	0.19 (0.03)/0.29 0.81	0.20 (0.03)/0.29 0.78	0.19 (0.03)/0.29 0.81	0.20 (0.03)/0.29 0.78	0.20 (0.03)/0.29 0.79
Closed	0.02 (0.02)/0.09 0.67	0.02 (0.02)/0.09 0.66	0.02 (0.02)/0.09 0.67	0.02 (0.02)/0.09 0.66	0.02 (0.02)/0.09 0.66	0.02 (0.02)/0.10 0.65	0.02 (0.02)/0.09 0.66	0.02 (0.03)/0.10 0.65	0.02 (0.02)/0.09 0.66	0.02 (0.03)/0.10 0.65	0.02 (0.02)/0.10 0.65
Outdoor Side 0.50 Worst ^a	0.94 (1.02)/0.44	0.94 (1.01)/0.44	0.94 (1.01)/0.44	0.94 (1.01)/0.44	0.94 (0.98)/0.44	0.94 (0.96)/0.44	0.94 (0.98)/0.44	0.94 (0.96)/0.44	0.94 (0.98)/0.44	0.94 (0.96)/0.44	0.94 (0.97)/0.44

Table 3.9d IAC Values for Louvered Shades: Coated Double Glazings with 0.1 Low-E (continued)

(Source: ASHRAE Handbook—Fundamentals [2013], Chapter 15, Table 13D)

Glazing ID:			21a	21b	21c	21d	21e	21f	21g	21h	21i	21j	21k
			0.94	0.93	0.92	0.91	0.91	0.88	0.91	0.88	0.91	0.88	0.88
0°			0.94 (0.14)/0.50 0.94	0.94 (0.14)/0.50 0.92	0.94 (0.14)/0.50 0.92	0.94 (0.14)/0.50 0.9	0.94 (0.14)/0.50 0.9	0.94 (0.14)/0.50 0.87	0.94 (0.14)/0.50 0.9	0.94 (0.14)/0.50 0.87	0.94 (0.14)/0.50 0.9	0.94 (0.14)/0.50 0.87	0.94 (0.14)/0.50 0.88
Excluded Beam ^b			0.07 (0.14)/0.48 0.91	0.07 (0.14)/0.48 0.9	0.07 (0.14)/0.48 0.89	0.07 (0.14)/0.48 0.88	0.07 (0.14)/0.48 0.88	0.08 (0.14)/0.48 0.85	0.07 (0.14)/0.48 0.87	0.08 (0.14)/0.48 0.84	0.07 (0.14)/0.48 0.87	0.08 (0.14)/0.48 0.84	0.08 (0.14)/0.48 0.85
45°			0.25 (0.06)/0.37 0.92	0.25 (0.06)/0.37 0.9	0.25 (0.06)/0.37 0.9	0.25 (0.06)/0.37 0.89	0.25 (0.06)/0.36 0.88	0.25 (0.06)/0.36 0.85	0.25 (0.06)/0.36 0.88	0.25 (0.06)/0.36 0.85	0.25 (0.06)/0.36 0.88	0.25 (0.06)/0.36 0.85	0.25 (0.06)/0.36 0.85
Closed			0.04 (0.02)/0.14 0.84	0.04 (0.02)/0.14 0.82	0.04 (0.02)/0.14 0.83	0.04 (0.02)/0.14 0.81	0.04 (0.02)/0.14 0.8	0.04 (0.03)/0.14 0.77	0.04 (0.02)/0.14 0.8	0.04 (0.03)/0.14 0.77	0.04 (0.02)/0.14 0.8	0.04 (0.03)/0.14 0.77	0.04 (0.03)/0.14 0.77
Outdoor Side	0.80	Worst ^a	0.95 (1.14)/0.56 0.94	0.95 (1.12)/0.56 0.93	0.95 (1.13)/0.56 0.92	0.95 (1.12)/0.56 0.91	0.95 (1.07)/0.55 0.91	0.95 (1.04)/0.55 0.88	0.95 (1.07)/0.55 0.91	0.95 (1.04)/0.54 0.88	0.95 (1.07)/0.55 0.91	0.95 (1.03)/0.54 0.88	0.95 (1.05)/0.55 0.88
0°			0.95 (0.29)/0.62 0.95	0.95 (0.29)/0.62 0.93	0.95 (0.29)/0.62 0.92	0.95 (0.29)/0.62 0.91	0.95 (0.28)/0.61 0.91	0.95 (0.28)/0.61 0.88	0.95 (0.28)/0.61 0.91	0.95 (0.28)/0.61 0.88	0.95 (0.28)/0.61 0.91	0.95 (0.28)/0.61 0.88	0.95 (0.28)/0.61 0.88
Excluded Beam ^b			0.17 (0.29)/0.60 0.94	0.17 (0.29)/0.60 0.92	0.17 (0.29)/0.60 0.91	0.17 (0.29)/0.60 0.9	0.16 (0.28)/0.59 0.9	0.16 (0.28)/0.59 0.87	0.16 (0.28)/0.59 0.9	0.16 (0.28)/0.59 0.87	0.16 (0.28)/0.59 0.9	0.16 (0.28)/0.59 0.87	0.16 (0.28)/0.59 0.87
45°			0.35 (0.13)/0.49 0.94	0.35 (0.13)/0.48 0.92	0.35 (0.13)/0.48 0.92	0.35 (0.13)/0.48 0.9	0.34 (0.12)/0.47 0.9	0.34 (0.12)/0.46 0.88	0.34 (0.12)/0.47 0.9	0.34 (0.12)/0.46 0.87	0.34 (0.12)/0.47 0.9	0.34 (0.12)/0.46 0.87	0.34 (0.12)/0.47 0.88
Closed			0.08 (0.04)/0.22 0.92	0.08 (0.04)/0.22 0.9	0.08 (0.04)/0.22 0.9	0.08 (0.04)/0.22 0.89	0.08 (0.04)/0.21 0.88	0.08 (0.04)/0.21 0.85	0.08 (0.04)/0.21 0.88	0.08 (0.04)/0.21 0.85	0.08 (0.04)/0.21 0.88	0.08 (0.04)/0.21 0.85	0.08 (0.04)/0.21 0.85

^aNotes: ^aLouvers track so that profile angle equals negative slat angle and maximum direct beam is admitted.
^bLouvers track to block direct beam radiation. When negative slat angles result, slat defaults to 0°.

^cGlazing cavity width equals original cavity width plus slat width.
^d F_R is radiant fraction; ratio of radiative heat transfer to total heat transfer, on room side of glazing system.

Table 3.9e IAC Values for Louvered Shades: Double Glazings with 0.05 Low-E

(Source: ASHRAE Handbook—Fundamentals [2013], Chapter 15, Table 13E)

Glazing ID:			25a	25b	25c	25d	25e	25f
Louver Location	Louver Reflection	ϕ	IAC ₀ (IAC ₆₀)/IAC _{diff} , F_R^d					
Indoor Side	0.15	Worst ^a	0.99 (0.99)/0.95 0.84	0.99 (0.98)/0.95 0.81	0.99 (0.98)/0.96 0.74	0.99 (0.98)/0.96 0.76	0.99 (0.98)/0.96 0.72	0.99 (0.98)/0.96 0.76
		0°	0.99 (0.93)/0.96 0.65	0.99 (0.93)/0.96 0.64	0.99 (0.94)/0.96 0.6	0.99 (0.94)/0.96 0.61	0.99 (0.95)/0.96 0.59	0.99 (0.94)/0.96 0.61
		Excluded Beam ^b	0.90 (0.93)/0.96 0.41	0.91 (0.93)/0.96 0.4	0.92 (0.94)/0.96 0.39	0.92 (0.94)/0.96 0.4	0.92 (0.95)/0.96 0.39	0.92 (0.94)/0.96 0.4
		45°	0.93 (0.91)/0.94 0.43	0.93 (0.91)/0.94 0.43	0.94 (0.93)/0.95 0.41	0.94 (0.92)/0.95 0.42	0.94 (0.93)/0.95 0.41	0.94 (0.92)/0.95 0.42
		Closed	0.88 (0.88)/0.90 0.39	0.89 (0.89)/0.90 0.39	0.90 (0.90)/0.91 0.36	0.90 (0.90)/0.91 0.37	0.90 (0.91)/0.92 0.36	0.90 (0.90)/0.91 0.37
Indoor Side	0.50	Worst ^a	0.99 (0.98)/0.91 0.86	0.99 (0.98)/0.92 0.82	0.99 (0.98)/0.93 0.75	0.99 (0.98)/0.93 0.77	0.99 (0.98)/0.93 0.73	0.99 (0.98)/0.93 0.77
		0°	0.99 (0.87)/0.93 0.69	0.99 (0.89)/0.94 0.67	0.99 (0.91)/0.95 0.63	0.99 (0.90)/0.94 0.64	0.99 (0.91)/0.95 0.62	0.99 (0.90)/0.94 0.64
		Excluded Beam ^b	0.80 (0.87)/0.92	0.82 (0.89)/0.93	0.85 (0.91)/0.94	0.85 (0.90)/0.94	0.86 (0.91)/0.94	0.84 (0.90)/0.94

Table 3.9e IAC Values for Louvered Shades: Double Glazings with 0.05 Low-E (continued)

(Source: ASHRAE Handbook—Fundamentals [2013], Chapter 15, Table 13E)

Glazing ID:			25a	25b	25c	26d	25e	25f
			0.47	0.46	0.44	0.44	0.43	0.45
45°			0.85 (0.80)/0.88	0.87 (0.83)/0.90	0.89 (0.85)/0.91	0.89 (0.85)/0.91	0.89 (0.86)/0.91	0.89 (0.85)/0.91
			0.49	0.48	0.45	0.46	0.45	0.46
Closed			0.74 (0.74)/0.79	0.77 (0.77)/0.81	0.81 (0.81)/0.84	0.80 (0.80)/0.83	0.82 (0.82)/0.85	0.80 (0.80)/0.83
			0.4	0.39	0.37	0.37	0.36	0.38
Indoor Side	0.80	Worst ^a	0.98 (0.98)/0.86	0.98 (0.98)/0.88	0.98 (0.97)/0.90	0.98 (0.98)/0.90	0.98 (0.97)/0.90	0.98 (0.98)/0.89
			0.87	0.84	0.76	0.78	0.74	0.78
0°			0.98 (0.80)/0.89	0.98 (0.83)/0.91	0.98 (0.86)/0.92	0.98 (0.85)/0.92	0.98 (0.86)/0.92	0.98 (0.85)/0.92
			0.76	0.73	0.68	0.69	0.66	0.69
Excluded Beam ^b			0.69 (0.80)/0.88	0.73 (0.83)/0.90	0.78 (0.86)/0.91	0.77 (0.85)/0.91	0.78 (0.86)/0.92	0.77 (0.85)/0.91
			0.59	0.56	0.52	0.53	0.51	0.53
45°			0.78 (0.69)/0.82	0.81 (0.73)/0.84	0.84 (0.78)/0.87	0.83 (0.77)/0.86	0.84 (0.79)/0.87	0.83 (0.77)/0.86
			0.59	0.57	0.52	0.53	0.51	0.54
Closed			0.60 (0.59)/0.67	0.65 (0.65)/0.71	0.71 (0.71)/0.76	0.70 (0.70)/0.75	0.72 (0.72)/0.77	0.70 (0.69)/0.75
			0.45	0.42	0.39	0.4	0.38	0.4
Between Glazings ^c	0.15	Worst ^a	0.97 (1.00)/0.80	0.97 (0.99)/0.81	0.95 (0.96)/0.80	0.95 (0.96)/0.80	0.94 (0.95)/0.80	0.96 (0.96)/0.80
			0.91	0.89	0.86	0.86	0.85	0.86
0°			0.97 (0.71)/0.82	0.97 (0.72)/0.82	0.95 (0.73)/0.82	0.95 (0.73)/0.82	0.94 (0.73)/0.82	0.96 (0.73)/0.82
			0.79	0.78	0.76	0.77	0.76	0.77
Excluded Beam ^b			0.66 (0.71)/0.82	0.67 (0.72)/0.82	0.69 (0.73)/0.81	0.69 (0.73)/0.81	0.70 (0.73)/0.81	0.69 (0.73)/0.81
			0.65	0.65	0.65	0.65	0.64	0.65
45°			0.73 (0.69)/0.78	0.73 (0.69)/0.78	0.75 (0.71)/0.78	0.75 (0.71)/0.78	0.75 (0.72)/0.79	0.75 (0.71)/0.78
			0.68	0.68	0.67	0.67	0.67	0.67
Closed			0.65 (0.67)/0.70	0.66 (0.68)/0.71	0.68 (0.70)/0.72	0.68 (0.70)/0.72	0.69 (0.71)/0.73	0.68 (0.70)/0.72
			0.65	0.65	0.64	0.64	0.64	0.64
Between Glazings ^c	0.50	Worst ^a	0.97 (1.01)/0.79	0.97 (1.00)/0.79	0.95 (0.97)/0.80	0.95 (0.98)/0.80	0.94 (0.96)/0.80	0.95 (0.98)/0.80
			0.92	0.9	0.86	0.87	0.85	0.87
0°			0.97 (0.68)/0.82	0.97 (0.69)/0.82	0.95 (0.71)/0.82	0.95 (0.71)/0.82	0.94 (0.72)/0.82	0.95 (0.71)/0.82
			0.82	0.81	0.79	0.79	0.78	0.79
Excluded Beam ^b			0.58 (0.68)/0.81	0.60 (0.69)/0.81	0.64 (0.71)/0.81	0.63 (0.71)/0.81	0.65 (0.72)/0.81	0.63 (0.71)/0.81
			0.7	0.7	0.68	0.69	0.68	0.69
45°			0.68 (0.59)/0.74	0.69 (0.61)/0.75	0.71 (0.65)/0.76	0.71 (0.64)/0.76	0.72 (0.66)/0.77	0.71 (0.64)/0.76
			0.73	0.72	0.7	0.71	0.7	0.71
Closed			0.52 (0.52)/0.60	0.54 (0.54)/0.61	0.59 (0.59)/0.65	0.58 (0.58)/0.64	0.60 (0.60)/0.65	0.58 (0.58)/0.64
			0.66	0.66	0.65	0.66	0.65	0.66
Between Glazings ^c	0.80	Worst ^a	0.97 (1.02)/0.77	0.97 (1.01)/0.78	0.95 (0.98)/0.79	0.95 (0.98)/0.79	0.94 (0.97)/0.79	0.95 (0.99)/0.79
			0.93	0.91	0.87	0.88	0.86	0.88
0°			0.97 (0.65)/0.81	0.97 (0.67)/0.82	0.95 (0.70)/0.82	0.95 (0.69)/0.82	0.94 (0.71)/0.82	0.95 (0.69)/0.82
			0.87	0.86	0.83	0.83	0.82	0.84
Excluded Beam ^b			0.51 (0.65)/0.80	0.53 (0.67)/0.81	0.59 (0.70)/0.81	0.58 (0.69)/0.81	0.60 (0.71)/0.81	0.58 (0.69)/0.81
			0.8	0.79	0.76	0.76	0.75	0.76
45°			0.64 (0.50)/0.71	0.65 (0.53)/0.73	0.69 (0.59)/0.74	0.68 (0.58)/0.74	0.69 (0.60)/0.75	0.68 (0.58)/0.74

Table 3.9e IAC Values for Louvered Shades: Double Glazings with 0.05 Low-E (continued)

(Source: ASHRAE Handbook—Fundamentals [2013], Chapter 15, Table 13E)

Glazing ID:			25a	25b	25c	26d	25e	25f
			0.81	0.8	0.76	0.77	0.76	0.77
Closed			0.39 (0.36)/0.49 0.73	0.42 (0.39)/0.51 0.73	0.49 (0.47)/0.57 0.7	0.48 (0.46)/0.56 0.71	0.51 (0.49)/0.58 0.7	0.48 (0.46)/0.56 0.71
Outdoor Side	0.15	Worst ^a	0.93 (0.92)/0.36 0.94	0.93 (0.92)/0.36 0.92	0.93 (0.90)/0.36 0.87	0.93 (0.89)/0.36 0.88	0.93 (0.90)/0.36 0.86	0.93 (0.89)/0.36 0.89
0°			0.93 (0.05)/0.41 0.89	0.93 (0.05)/0.41 0.87	0.93 (0.06)/0.41 0.82	0.93 (0.05)/0.41 0.83	0.93 (0.06)/0.42 0.81	0.93 (0.05)/0.41 0.84
Excluded Beam ^b			0.03 (0.05)/0.39 0.78	0.03 (0.05)/0.39 0.77	0.04 (0.06)/0.40 0.72	0.03 (0.05)/0.39 0.73	0.04 (0.06)/0.40 0.71	0.03 (0.05)/0.39 0.74
45°			0.20 (0.03)/0.29 0.83	0.20 (0.03)/0.29 0.82	0.20 (0.04)/0.30 0.77	0.20 (0.03)/0.29 0.78	0.20 (0.04)/0.30 0.76	0.20 (0.03)/0.29 0.78
Closed			0.02 (0.02)/0.10 0.66	0.02 (0.02)/0.10 0.66	0.03 (0.03)/0.11 0.64	0.03 (0.03)/0.10 0.65	0.03 (0.04)/0.11 0.64	0.03 (0.03)/0.10 0.65
Outdoor Side	0.50	Worst ^a	0.94 (1.08)/0.45 0.94	0.94 (1.06)/0.45 0.92	0.94 (1.06)/0.44 0.87	0.94 (0.96)/0.44 0.88	0.94 (0.98)/0.44 0.86	0.94 (0.97)/0.44 0.89
0°			0.94 (0.15)/0.51 0.93	0.94 (0.15)/0.51 0.91	0.94 (0.15)/0.50 0.86	0.94 (0.15)/0.50 0.87	0.94 (0.15)/0.50 0.85	0.94 (0.15)/0.50 0.88
Excluded Beam ^b			0.08 (0.15)/0.49 0.9	0.08 (0.15)/0.49 0.88	0.08 (0.15)/0.48 0.83	0.08 (0.15)/0.48 0.84	0.08 (0.15)/0.48 0.82	0.08 (0.15)/0.48 0.85
45°			0.26 (0.06)/0.38 0.91	0.26 (0.06)/0.38 0.89	0.26 (0.07)/0.37 0.84	0.25 (0.06)/0.36 0.85	0.26 (0.07)/0.37 0.82	0.25 (0.06)/0.36 0.85
Closed			0.04 (0.03)/0.15 0.82	0.04 (0.03)/0.15 0.81	0.05 (0.03)/0.14 0.75	0.04 (0.03)/0.14 0.76	0.05 (0.03)/0.14 0.74	0.04 (0.03)/0.14 0.76
Outdoor Side	0.80	Worst ^a	0.95 (1.25)/0.59 0.94	0.95 (1.21)/0.58 0.92	0.95 (1.08)/0.56 0.87	0.95 (1.04)/0.55 0.88	0.95 (1.06)/0.55 0.86	0.95 (1.05)/0.55 0.89
0°			0.95 (0.30)/0.64 0.94	0.95 (0.30)/0.64 0.92	0.95 (0.29)/0.62 0.88	0.95 (0.28)/0.61 0.88	0.95 (0.29)/0.61 0.86	0.95 (0.28)/0.61 0.89
Excluded Beam ^b			0.18 (0.30)/0.62 0.93	0.18 (0.30)/0.62 0.91	0.17 (0.29)/0.60 0.86	0.16 (0.28)/0.59 0.87	0.17 (0.29)/0.59 0.85	0.17 (0.28)/0.59 0.88
45°			0.37 (0.13)/0.51 0.93	0.37 (0.13)/0.50 0.91	0.35 (0.13)/0.48 0.86	0.34 (0.12)/0.47 0.87	0.35 (0.13)/0.47 0.85	0.34 (0.12)/0.47 0.88
Closed			0.09 (0.04)/0.24 0.91	0.09 (0.04)/0.24 0.89	0.09 (0.04)/0.22 0.83	0.08 (0.04)/0.21 0.85	0.09 (0.04)/0.21 0.82	0.08 (0.04)/0.21 0.85

^aNotes: Louvers track so that profile angle equals negative slat angle and maximum direct beam is admitted.

^bLouvers track to block direct beam radiation. When negative slat angles result, slat defaults to 0°.

^cGlazing cavity width equals original cavity width plus slat width.

^d F_{R} is radiant fraction; ratio of radiative heat transfer to total heat transfer, on room side of glazing system.

Table 3.9f IAC Values for Louvered Shades: Triple Glazing

(Source: ASHRAE Handbook—Fundamentals [2013], Chapter 15, Table 13F)

Glazing ID:		29a	29b	32a	32b	32c	32d	40a	40b	40c	40d	
Louver Location	Louver Reflection	ϕ	IAC ₀ (IAC ₆₀)/IAC _{diff} , F _R ^d									
Indoor Side	0.15	Worst ^a	0.99 (0.98)/0.94 0.82	0.99 (0.98)/0.95 0.78	0.99 (0.98)/0.95 0.8	0.99 (0.98)/0.96 0.75	1.00 (1.00)/0.97 0.76	1.00 (1.00)/0.97 0.71	1.00 (1.00)/0.98 0.73	1.00 (1.00)/0.98 0.67	0.99 (0.99)/0.96 0.78	0.99 (0.99)/0.96 0.73
		0°	0.99 (0.92)/0.95 0.65	0.99 (0.93)/0.95 0.62	0.99 (0.94)/0.96 0.64	0.99 (0.94)/0.96 0.61	1.00 (0.96)/0.98 0.6	1.00 (0.96)/0.98 0.56	1.00 (0.96)/0.98 0.58	1.00 (0.97)/0.99 0.54	0.99 (0.95)/0.97 0.63	0.99 (0.95)/0.97 0.6
	Excluded Beam ^b	0.88 (0.92)/0.95 0.41	0.89 (0.93)/0.95 0.4	0.90 (0.94)/0.96 0.41	0.91 (0.94)/0.96 0.4	0.93 (0.96)/0.97 0.39	0.93 (0.96)/0.98 0.36	0.94 (0.96)/0.98 0.37	0.95 (0.97)/0.98 0.35	0.92 (0.95)/0.97 0.4	0.93 (0.95)/0.97 0.4	
	45°	0.91 (0.89)/0.93 0.43	0.92 (0.90)/0.93 0.43	0.93 (0.91)/0.94 0.43	0.93 (0.92)/0.95 0.42	0.95 (0.93)/0.96 0.41	0.95 (0.94)/0.97 0.38	0.95 (0.94)/0.97 0.39	0.96 (0.95)/0.97 0.37	0.94 (0.92)/0.95 0.42	0.94 (0.93)/0.96 0.41	
	Closed	0.86 (0.87)/0.88 0.39	0.87 (0.88)/0.89 0.38	0.88 (0.89)/0.90 0.39	0.89 (0.90)/0.91 0.37	0.91 (0.91)/0.93 0.37	0.92 (0.92)/0.94 0.35	0.92 (0.93)/0.94 0.36	0.93 (0.94)/0.95 0.33	0.90 (0.90)/0.92 0.38	0.91 (0.91)/0.92 0.37	
Indoor Side	0.50	Worst ^a	0.98 (0.98)/0.90 0.83	0.98 (0.98)/0.91 0.79	0.99 (0.98)/0.91 0.81	0.99 (0.98)/0.92 0.76	0.99 (0.99)/0.92 0.77	1.00 (1.00)/0.93 0.72	0.99 (1.00)/0.93 0.74	1.00 (1.00)/0.95 0.68	0.99 (0.98)/0.92 0.79	0.99 (0.98)/0.93 0.74
		0°	0.98 (0.86)/0.92 0.68	0.98 (0.87)/0.93 0.65	0.99 (0.88)/0.93 0.67	0.99 (0.90)/0.94 0.64	0.99 (0.89)/0.94 0.62	1.00 (0.91)/0.95 0.58	0.99 (0.91)/0.95 0.6	1.00 (0.92)/0.96 0.56	0.99 (0.89)/0.94 0.66	0.99 (0.91)/0.95 0.63
	Excluded Beam ^b	0.77 (0.86)/0.91 0.46	0.80 (0.87)/0.92 0.45	0.80 (0.88)/0.93 0.45	0.83 (0.90)/0.94 0.44	0.81 (0.89)/0.94 0.42	0.83 (0.91)/0.95 0.39	0.83 (0.91)/0.95 0.4	0.86 (0.92)/0.96 0.37	0.82 (0.89)/0.93 0.45	0.84 (0.91)/0.94 0.44	
	45°	0.83 (0.78)/0.87 0.48	0.85 (0.81)/0.88 0.46	0.85 (0.81)/0.89 0.47	0.87 (0.84)/0.90 0.45	0.86 (0.82)/0.90 0.43	0.88 (0.84)/0.91 0.4	0.88 (0.84)/0.91 0.41	0.90 (0.87)/0.93 0.38	0.87 (0.83)/0.90 0.46	0.89 (0.85)/0.91 0.45	
	Closed	0.71 (0.72)/0.77 0.39	0.74 (0.75)/0.79 0.38	0.75 (0.76)/0.80 0.37	0.78 (0.79)/0.82 0.37	0.76 (0.76)/0.81 0.35	0.79 (0.80)/0.83 0.33	0.78 (0.80)/0.83 0.34	0.82 (0.83)/0.86 0.31	0.77 (0.78)/0.81 0.38	0.80 (0.81)/0.84 0.36	
Indoor Side	0.80	Worst ^a	0.98 (0.97)/0.85 0.84	0.98 (0.97)/0.87 0.8	0.98 (0.97)/0.86 0.82	0.98 (0.97)/0.88 0.77	0.99 (0.99)/0.87 0.79	0.99 (0.99)/0.89 0.73	0.99 (0.99)/0.88 0.75	0.99 (0.99)/0.90 0.69	0.98 (0.98)/0.87 0.8	0.98 (0.98)/0.89 0.75
		0°	0.98 (0.78)/0.88 0.74	0.98 (0.81)/0.89 0.7	0.98 (0.81)/0.89 0.72	0.98 (0.84)/0.91 0.68	0.99 (0.81)/0.90 0.67	0.99 (0.83)/0.91 0.62	0.99 (0.83)/0.91 0.64	0.99 (0.86)/0.93 0.59	0.98 (0.82)/0.90 0.71	0.98 (0.85)/0.92 0.67
	Excluded Beam ^b	0.66 (0.78)/0.87 0.56	0.70 (0.81)/0.89 0.53	0.69 (0.81)/0.88 0.55	0.74 (0.84)/0.90 0.52	0.69 (0.81)/0.89 0.49	0.73 (0.83)/0.90 0.45	0.72 (0.83)/0.90 0.46	0.77 (0.86)/0.92 0.42	0.71 (0.82)/0.89 0.54	0.76 (0.85)/0.91 0.51	
	45°	0.75 (0.67)/0.80 0.56	0.78 (0.71)/0.83 0.53	0.77 (0.71)/0.82 0.55	0.81 (0.75)/0.85 0.52	0.77 (0.70)/0.83 0.49	0.80 (0.74)/0.85 0.44	0.80 (0.74)/0.85 0.46	0.83 (0.78)/0.87 0.42	0.79 (0.73)/0.84 0.54	0.82 (0.77)/0.86 0.51	
	Closed	0.57 (0.58)/0.65 0.42	0.62 (0.64)/0.70 0.4	0.61 (0.63)/0.69 0.41	0.67 (0.68)/0.74 0.38	0.60 (0.62)/0.69 0.35	0.66 (0.67)/0.73 0.31	0.65 (0.66)/0.72 0.33	0.71 (0.72)/0.77 0.29	0.64 (0.65)/0.71 0.4	0.69 (0.71)/0.76 0.38	
Between Glazings ^c	0.15	Worst ^a	0.97 (1.01)/0.63 0.9	0.97 (1.02)/0.64 0.87	0.98 (1.05)/0.76 0.88	0.98 (1.05)/0.77 0.85	0.97 (1.01)/0.60 0.79	0.98 (1.02)/0.62 0.74	0.98 (1.05)/0.73 0.75	0.99 (1.05)/0.75 0.7	0.98 (1.04)/0.71 0.87	0.99 (1.04)/0.73 0.84
		0°	0.97 (0.44)/0.66 0.79	0.97 (0.46)/0.68 0.78	0.98 (0.62)/0.78 0.78	0.98 (0.63)/0.80 0.77	0.97 (0.40)/0.64 0.59	0.98 (0.42)/0.66 0.56	0.98 (0.57)/0.76 0.57	0.99 (0.60)/0.78 0.54	0.98 (0.55)/0.74 0.78	0.99 (0.58)/0.76 0.76
	Excluded Beam ^b	0.36 (0.44)/0.65 0.66	0.38 (0.46)/0.67 0.65	0.52 (0.62)/0.77 0.66	0.54 (0.63)/0.79 0.65	0.32 (0.40)/0.63 0.34	0.35 (0.42)/0.65 0.33	0.48 (0.57)/0.75 0.33	0.50 (0.60)/0.77 0.33	0.46 (0.55)/0.73 0.65	0.49 (0.58)/0.75 0.65	
	45°	0.48 (0.41)/0.59 0.7	0.50 (0.43)/0.60 0.69	0.62 (0.58)/0.72 0.69	0.64 (0.60)/0.73 0.68	0.45 (0.37)/0.56 0.43	0.47 (0.40)/0.58 0.41	0.58 (0.54)/0.69 0.4	0.60 (0.57)/0.71 0.39	0.57 (0.52)/0.68 0.69	0.59 (0.55)/0.69 0.68	
	Closed	0.36 (0.41)/0.46 0.64	0.38 (0.43)/0.48 0.64	0.51 (0.57)/0.61 0.65	0.53 (0.58)/0.63 0.65	0.32 (0.37)/0.43 0.31	0.34 (0.40)/0.45 0.31	0.46 (0.53)/0.57 0.32	0.49 (0.55)/0.60 0.32	0.45 (0.51)/0.56 0.64	0.48 (0.53)/0.58 0.64	

Table 3.9f IAC Values for Louvered Shades: Triple Glazing (continued)

(Source: ASHRAE Handbook—Fundamentals [2013], Chapter 15, Table 13F)

Glazing ID:		29a	29b	32a	32b	32c	32d	40a	40b	40c	40d		
Between Glazings ^c	0.50	Worst ^a	0.97 (1.06)/0.65 0.9	0.98 (1.06)/0.66 0.88	0.98 (1.08)/0.74 0.89	0.98 (1.08)/0.75 0.86	0.97 (1.07)/0.63 0.8	0.98 (1.07)/0.65 0.75	0.98 (1.09)/0.72 0.77	0.99 (1.09)/0.74 0.71	0.98 (1.08)/0.71 0.88	0.99 (1.08)/0.72 0.85	
		0°	0.97 (0.45)/0.69 0.83	0.98 (0.47)/0.71 0.81	0.98 (0.58)/0.78 0.81	0.98 (0.60)/0.79 0.79	0.97 (0.42)/0.68 0.66	0.98 (0.44)/0.69 0.62	0.98 (0.55)/0.77 0.62	0.99 (0.57)/0.78 0.59	0.98 (0.54)/0.75 0.81	0.99 (0.56)/0.77 0.79	
	Excluded Beam ^b	45°	0.33 (0.45)/0.68 0.71	0.34 (0.47)/0.69 0.7	0.44 (0.58)/0.77 0.7	0.46 (0.60)/0.78 0.69	0.30 (0.42)/0.66 0.46	0.32 (0.44)/0.68 0.43	0.41 (0.55)/0.75 0.42	0.43 (0.57)/0.77 0.4	0.40 (0.54)/0.74 0.7	0.42 (0.56)/0.75 0.69	
		Closed	0.28 (0.29)/0.39 0.66	0.29 (0.31)/0.41 0.66	0.38 (0.40)/0.50 0.66	0.40 (0.41)/0.51 0.66	0.25 (0.27)/0.37 0.36	0.27 (0.29)/0.39 0.35	0.35 (0.37)/0.48 0.35	0.37 (0.39)/0.49 0.34	0.34 (0.36)/0.46 0.66	0.36 (0.38)/0.48 0.65	
	Between Glazings ^c	0.80	Worst ^a	0.97 (1.11)/0.68 0.91	0.98 (1.11)/0.69 0.89	0.97 (1.11)/0.73 0.9	0.98 (1.11)/0.73 0.87	0.98 (1.12)/0.67 0.81	0.98 (1.12)/0.69 0.76	0.98 (1.12)/0.72 0.79	0.99 (1.12)/0.73 0.73	0.98 (1.11)/0.71 0.89	0.99 (1.11)/0.72 0.86
			0°	0.97 (0.48)/0.74 0.87	0.98 (0.49)/0.75 0.85	0.97 (0.55)/0.78 0.85	0.98 (0.56)/0.79 0.83	0.98 (0.47)/0.73 0.75	0.98 (0.48)/0.74 0.7	0.98 (0.54)/0.78 0.71	0.99 (0.55)/0.79 0.66	0.98 (0.53)/0.77 0.85	0.99 (0.54)/0.78 0.82
Excluded Beam ^b		45°	0.32 (0.48)/0.72 0.81	0.33 (0.49)/0.73 0.79	0.38 (0.55)/0.76 0.78	0.39 (0.56)/0.77 0.76	0.31 (0.47)/0.71 0.63	0.32 (0.48)/0.72 0.59	0.37 (0.54)/0.76 0.58	0.38 (0.55)/0.77 0.54	0.36 (0.53)/0.75 0.78	0.38 (0.54)/0.76 0.76	
		Closed	0.22 (0.19)/0.36 0.73	0.23 (0.21)/0.37 0.72	0.27 (0.24)/0.41 0.71	0.29 (0.26)/0.42 0.7	0.21 (0.18)/0.35 0.49	0.22 (0.20)/0.37 0.46	0.26 (0.23)/0.40 0.45	0.28 (0.25)/0.41 0.43	0.25 (0.23)/0.39 0.72	0.27 (0.24)/0.40 0.7	
Outdoor Side		0.15	Worst ^a	0.93 (0.90)/0.35 0.92	0.93 (0.90)/0.35 0.9	0.93 (0.90)/0.35 0.91	0.93 (0.89)/0.35 0.88	0.93 (0.90)/0.35 0.83	0.93 (0.90)/0.35 0.78	0.93 (0.90)/0.35 0.81	0.93 (0.89)/0.35 0.75	0.93 (0.89)/0.35 0.9	0.93 (0.89)/0.35 0.87
			0°	0.93 (0.04)/0.41 0.88	0.93 (0.05)/0.41 0.86	0.93 (0.04)/0.40 0.88	0.93 (0.04)/0.41 0.85	0.93 (0.04)/0.41 0.77	0.93 (0.04)/0.41 0.72	0.93 (0.04)/0.40 0.76	0.93 (0.04)/0.41 0.7	0.93 (0.04)/0.40 0.87	0.93 (0.04)/0.40 0.84
	Excluded Beam ^b	45°	0.02 (0.04)/0.39 0.78	0.02 (0.05)/0.39 0.76	0.02 (0.04)/0.39 0.79	0.02 (0.04)/0.39 0.77	0.02 (0.04)/0.39 0.59	0.02 (0.04)/0.39 0.55	0.02 (0.04)/0.39 0.59	0.02 (0.04)/0.39 0.55	0.02 (0.04)/0.39 0.79	0.02 (0.04)/0.39 0.77	
		Closed	0.02 (0.02)/0.09 0.66	0.02 (0.02)/0.09 0.66	0.01 (0.02)/0.09 0.67	0.02 (0.02)/0.09 0.66	0.02 (0.02)/0.09 0.36	0.02 (0.02)/0.09 0.35	0.01 (0.01)/0.09 0.37	0.01 (0.02)/0.09 0.35	0.01 (0.01)/0.09 0.67	0.01 (0.02)/0.09 0.66	
	Outdoor Side	0.50	Worst ^a	0.94 (1.00)/0.44 0.92	0.94 (0.99)/0.44 0.9	0.94 (0.99)/0.44 0.91	0.94 (0.99)/0.44 0.88	0.94 (1.00)/0.44 0.84	0.94 (1.00)/0.44 0.79	0.94 (1.00)/0.44 0.81	0.94 (0.99)/0.44 0.75	0.94 (0.99)/0.44 0.9	0.94 (0.99)/0.43 0.87
			0°	0.94 (0.14)/0.50 0.92	0.94 (0.14)/0.50 0.89	0.94 (0.14)/0.50 0.91	0.94 (0.14)/0.50 0.88	0.94 (0.14)/0.50 0.83	0.94 (0.14)/0.50 0.78	0.94 (0.14)/0.50 0.81	0.94 (0.14)/0.50 0.75	0.94 (0.14)/0.50 0.9	0.94 (0.14)/0.50 0.87
Excluded Beam ^b		45°	0.07 (0.14)/0.48 0.89	0.07 (0.14)/0.48 0.86	0.07 (0.14)/0.48 0.88	0.07 (0.14)/0.48 0.85	0.07 (0.14)/0.48 0.78	0.07 (0.14)/0.48 0.73	0.07 (0.14)/0.48 0.76	0.07 (0.14)/0.48 0.7	0.07 (0.14)/0.48 0.88	0.07 (0.14)/0.47 0.85	
		Closed	0.04 (0.02)/0.14 0.82	0.04 (0.02)/0.14 0.79	0.03 (0.02)/0.13 0.82	0.04 (0.02)/0.13 0.79	0.03 (0.02)/0.14 0.65	0.04 (0.02)/0.14 0.61	0.03 (0.02)/0.13 0.65	0.03 (0.02)/0.13 0.6	0.03 (0.02)/0.13 0.82	0.03 (0.02)/0.13 0.79	
Outdoor Side		0.80	Worst ^a	0.95 (1.11)/0.56 0.92	0.95 (1.10)/0.56 0.9	0.95 (1.10)/0.56 0.91	0.95 (1.08)/0.55 0.88	0.95 (1.11)/0.56 0.84	0.95 (1.10)/0.56 0.79	0.95 (1.10)/0.56 0.81	0.95 (1.09)/0.55 0.75	0.95 (1.10)/0.55 0.9	0.95 (1.08)/0.55 0.87
			0°	0.95 (0.29)/0.62	0.95 (0.29)/0.62	0.95 (0.29)/0.62	0.95 (0.29)/0.62	0.95 (0.29)/0.62	0.95 (0.29)/0.62	0.95 (0.29)/0.62	0.95 (0.29)/0.62	0.95 (0.29)/0.62	0.95 (0.29)/0.62

Table 3.9f IAC Values for Louvered Shades: Triple Glazing (continued)

(Source: ASHRAE Handbook—Fundamentals [2013], Chapter 15, Table 13F)

Glazing ID:	29a	29b	32a	32b	32c	32d	40a	40b	40c	40d
	0.93	0.9	0.92	0.89	0.84	0.79	0.82	0.76	0.9	0.87
Excluded Beam ^b	0.16 (0.29)/0.60 0.91	0.16 (0.29)/0.60 0.88	0.16 (0.29)/0.60 0.9	0.16 (0.29)/0.59 0.87	0.15 (0.29)/0.60 0.82	0.15 (0.29)/0.60 0.76	0.15 (0.29)/0.60 0.79	0.15 (0.29)/0.60 0.73	0.15 (0.29)/0.60 0.89	0.15 (0.29)/0.59 0.86
45°	0.33 (0.13)/0.48 0.92	0.33 (0.13)/0.48 0.89	0.33 (0.12)/0.48 0.91	0.33 (0.12)/0.47 0.88	0.33 (0.13)/0.48 0.83	0.33 (0.13)/0.48 0.77	0.33 (0.12)/0.48 0.8	0.33 (0.12)/0.47 0.74	0.33 (0.12)/0.48 0.9	0.33 (0.12)/0.47 0.87
Closed	0.08 (0.04)/0.22 0.89	0.08 (0.04)/0.22 0.87	0.08 (0.04)/0.21 0.89	0.08 (0.04)/0.21 0.86	0.08 (0.04)/0.22 0.79	0.08 (0.04)/0.22 0.74	0.08 (0.04)/0.21 0.77	0.08 (0.04)/0.21 0.71	0.08 (0.04)/0.21 0.88	0.08 (0.04)/0.21 0.85

Notes:^aLouvers track so that profile angle equals negative slat angle and maximum direct beam is admitted.

^bLouvers track to block direct beam radiation. When negative slat angles result, slat defaults to 0°.

^cGlazing cavity width equals original cavity width plus slat width.

^d F_R is radiant fraction; ratio of radiative heat transfer to total heat transfer, on room side of glazing system.

Table 3.9g IAC Values for Draperies, Roller Shades, and Insect Screens

(Source: ASHRAE Handbook—Fundamentals [2013], Chapter 15, Table 13F)

Drapery

Glazing ID:			1a	1b	1c	1d	1e	1f	1g	1h	1i		
Shade	Fabric Designator	Fullness	IAC, FR _d										
Dark Closed Weave	IIID	100%	0.71, 0.50	0.71, 0.49	0.72, 0.47	0.74, 0.45	0.72, 0.47	0.74, 0.44	0.72, 0.47	0.74, 0.44	0.74, 0.45		
Medium Closed Weave	IIIM	100%	0.59, 0.53	0.60, 0.52	0.62, 0.49	0.65, 0.46	0.63, 0.49	0.66, 0.46	0.63, 0.49	0.66, 0.45	0.65, 0.46		
Light Closed Weave	IIIL	100%	0.45, 0.62	0.46, 0.60	0.50, 0.56	0.55, 0.50	0.51, 0.54	0.56, 0.50	0.51, 0.54	0.56, 0.49	0.55, 0.51		
Dark Semiopen Weave	IID	100%	0.75, 0.55	0.75, 0.54	0.76, 0.52	0.78, 0.49	0.76, 0.52	0.78, 0.49	0.76, 0.52	0.78, 0.49	0.78, 0.49		
Medium Semiopen Weave	IIM	100%	0.65, 0.63	0.66, 0.62	0.68, 0.59	0.70, 0.55	0.68, 0.58	0.71, 0.54	0.68, 0.58	0.71, 0.54	0.70, 0.55		
Light Semiopen Weave	IIL	100%	0.56, 0.79	0.57, 0.77	0.60, 0.71	0.64, 0.65	0.61, 0.70	0.65, 0.64	0.61, 0.70	0.65, 0.63	0.64, 0.65		
Dark Open Weave	ID	100%	0.80, 0.63	0.80, 0.62	0.81, 0.60	0.82, 0.57	0.82, 0.59	0.83, 0.56	0.82, 0.59	0.83, 0.56	0.82, 0.57		
Medium Open Weave	IM	100%	0.71, 0.73	0.72, 0.72	0.73, 0.69	0.76, 0.64	0.74, 0.68	0.76, 0.63	0.74, 0.68	0.76, 0.63	0.76, 0.64		
Light Open Weave	IL	100%	0.64, 0.87	0.65, 0.85	0.68, 0.80	0.71, 0.73	0.68, 0.78	0.71, 0.72	0.68, 0.78	0.72, 0.71	0.71, 0.73		
Sheer		100%	0.73, 0.89	0.73, 0.88	0.75, 0.83	0.77, 0.77	0.75, 0.82	0.78, 0.76	0.75, 0.82	0.78, 0.75	0.77, 0.77		

Table 3.9g IAC Values for Draperies, Roller Shades, and Insect Screens (continued)

(Source: ASHRAE Handbook—Fundamentals [2013], Chapter 15, Table 13F)

Glazing ID:		5a	5b	5c	5d	5e	5f	5g	5h	5i			
Dark Closed Weave	IIID	100%	0.81, 0.46	0.82, 0.45	0.82, 0.44	0.83, 0.42	0.82, 0.44	0.83, 0.42	0.82, 0.44	0.84, 0.42	0.83, 0.42		
Medium Closed Weave	IIIM	100%	0.70, 0.48	0.72, 0.46	0.72, 0.46	0.75, 0.43	0.72, 0.46	0.75, 0.43	0.72, 0.46	0.75, 0.43	0.75, 0.43		
Light Closed Weave	IIIL	100%	0.57, 0.54	0.60, 0.52	0.59, 0.52	0.64, 0.47	0.60, 0.51	0.65, 0.47	0.60, 0.51	0.65, 0.47	0.64, 0.47		
Dark Semiopen Weave	IID	100%	0.84, 0.51	0.85, 0.50	0.85, 0.49	0.86, 0.47	0.85, 0.49	0.86, 0.47	0.85, 0.49	0.86, 0.46	0.86, 0.47		
Medium Semiopen Weave	IIM	100%	0.75, 0.57	0.76, 0.55	0.76, 0.55	0.79, 0.51	0.76, 0.55	0.79, 0.51	0.76, 0.55	0.79, 0.51	0.79, 0.52		
Light Semiopen Weave	IIL	100%	0.65, 0.70	0.68, 0.67	0.67, 0.67	0.71, 0.61	0.68, 0.66	0.72, 0.60	0.68, 0.66	0.72, 0.60	0.72, 0.61		
Dark Open Weave	ID	100%	0.88, 0.59	0.88, 0.57	0.88, 0.57	0.89, 0.54	0.88, 0.57	0.89, 0.54	0.88, 0.57	0.89, 0.54	0.89, 0.54		
Medium Open Weave	IM	100%	0.79, 0.68	0.80, 0.65	0.80, 0.65	0.82, 0.61	0.80, 0.65	0.82, 0.60	0.80, 0.65	0.82, 0.60	0.82, 0.61		
Light Open Weave	IL	100%	0.72, 0.79	0.74, 0.76	0.73, 0.76	0.77, 0.69	0.74, 0.75	0.77, 0.69	0.74, 0.75	0.77, 0.68	0.77, 0.69		
Sheer		100%	0.78, 0.83	0.8, 0.8	0.8, 0.8	0.82, 0.73	0.8, 0.79	0.82, 0.73	0.8, 0.79	0.82, 0.73	0.82, 0.74		
Glazing ID:		17a	17b	17c	17d	17e	17f	17g	17h	17i	17j	17k	
Dark Closed Weave	IIID	100%	0.85, 0.45	0.86, 0.43	0.86, 0.44	0.87, 0.43	0.86, 0.43	0.88, 0.41	0.87, 0.42	0.88, 0.40	0.87, 0.42	0.88, 0.40	0.88, 0.41
Medium Closed Weave	IIIM	100%	0.74, 0.47	0.76, 0.45	0.76, 0.45	0.79, 0.44	0.77, 0.44	0.80, 0.42	0.78, 0.44	0.80, 0.41	0.78, 0.44	0.80, 0.41	0.80, 0.42
Light Closed Weave	IIIL	100%	0.60, 0.52	0.64, 0.50	0.64, 0.50	0.68, 0.47	0.66, 0.48	0.71, 0.44	0.66, 0.48	0.71, 0.44	0.66, 0.48	0.71, 0.44	0.71, 0.45
Dark Semiopen Weave	IID	100%	0.88, 0.50	0.89, 0.48	0.88, 0.49	0.89, 0.47	0.89, 0.48	0.90, 0.45	0.89, 0.47	0.90, 0.45	0.89, 0.47	0.90, 0.45	0.90, 0.45
Medium Semiopen Weave	IIM	100%	0.78, 0.56	0.8, 0.54	0.8, 0.54	0.82, 0.52	0.81, 0.52	0.83, 0.49	0.81, 0.52	0.83, 0.49	0.81, 0.52	0.83, 0.49	0.83, 0.49
Light Semiopen Weave	IIL	100%	0.68, 0.68	0.71, 0.64	0.71, 0.64	0.74, 0.61	0.72, 0.62	0.76, 0.57	0.73, 0.62	0.77, 0.57	0.73, 0.62	0.77, 0.57	0.76, 0.57

Table 3.9g IAC Values for Draperies, Roller Shades, and Insect Screens (continued)

(Source: ASHRAE Handbook—Fundamentals [2013], Chapter 15, Table 13F)

Dark Open Weave	ID	100%	0.90, 0.58	0.91, 0.56	0.91, 0.56	0.91, 0.55	0.91, 0.55	0.92, 0.52	0.91, 0.55	0.92, 0.52	0.91, 0.55	0.92, 0.52	0.92, 0.52
Medium Open Weave	IM	100%	0.81, 0.66	0.83, 0.64	0.83, 0.64	0.85, 0.61	0.84, 0.62	0.86, 0.58	0.84, 0.62	0.86, 0.58	0.84, 0.62	0.86, 0.58	0.86, 0.58
Light Open Weave	IL	100%	0.74, 0.77	0.76, 0.73	0.76, 0.73	0.79, 0.69	0.77, 0.71	0.81, 0.65	0.78, 0.71	0.81, 0.65	0.78, 0.71	0.81, 0.65	0.81, 0.65
Sheer		100%	0.8, 0.81	0.82, 0.77	0.82, 0.78	0.84, 0.74	0.83, 0.75	0.85, 0.7	0.83, 0.75	0.85, 0.69	0.83, 0.75	0.85, 0.69	0.85, 0.7
Glazing ID:			21a	21b	21c	21d	21e	21f	21g	21h	21i	21j	21k
Dark Closed Weave	IIID	100%	0.87, 0.44	0.88, 0.43	0.88, 0.43	0.88, 0.42	0.88, 0.42	0.89, 0.40	0.88, 0.42	0.89, 0.40	0.88, 0.42	0.89, 0.40	0.89, 0.40
Medium Closed Weave	IIIM	100%	0.77, 0.46	0.79, 0.45	0.79, 0.45	0.81, 0.43	0.80, 0.43	0.82, 0.41	0.80, 0.43	0.82, 0.41	0.80, 0.43	0.82, 0.41	0.82, 0.41
Light Closed Weave	IIIL	100%	0.64, 0.52	0.67, 0.49	0.68, 0.49	0.70, 0.47	0.69, 0.47	0.73, 0.45	0.70, 0.47	0.73, 0.44	0.70, 0.47	0.73, 0.44	0.73, 0.45
Dark Semiopen Weave	IID	100%	0.89, 0.49	0.90, 0.48	0.90, 0.48	0.90, 0.47	0.90, 0.47	0.91, 0.45	0.90, 0.47	0.91, 0.45	0.90, 0.47	0.91, 0.45	0.91, 0.45
Medium Semiopen Weave	IIM	100%	0.8, 0.55	0.82, 0.53	0.82, 0.53	0.83, 0.51	0.83, 0.52	0.85, 0.49	0.83, 0.51	0.85, 0.49	0.83, 0.51	0.85, 0.49	0.85, 0.49
Light Semiopen Weave	IIL	100%	0.71, 0.67	0.74, 0.64	0.74, 0.63	0.76, 0.61	0.75, 0.61	0.78, 0.57	0.76, 0.61	0.78, 0.57	0.76, 0.61	0.78, 0.57	0.78, 0.57
Dark Open Weave	ID	100%	0.92, 0.57	0.92, 0.56	0.92, 0.55	0.92, 0.54	0.92, 0.54	0.93, 0.52	0.92, 0.54	0.93, 0.52	0.92, 0.54	0.93, 0.52	0.93, 0.52
Medium Open Weave	IM	100%	0.83, 0.65	0.85, 0.63	0.85, 0.63	0.86, 0.61	0.86, 0.61	0.87, 0.58	0.86, 0.61	0.87, 0.58	0.86, 0.61	0.87, 0.58	0.87, 0.58
Light Open Weave	IL	100%	0.76, 0.77	0.78, 0.73	0.79, 0.72	0.81, 0.69	0.80, 0.70	0.82, 0.65	0.80, 0.69	0.82, 0.65	0.80, 0.69	0.82, 0.65	0.82, 0.66
Sheer		100%	0.82, 0.81	0.83, 0.77	0.84, 0.76	0.85, 0.74	0.85, 0.74	0.86, 0.7	0.85, 0.74	0.86, 0.69	0.85, 0.74	0.86, 0.69	0.86, 0.7
IAC Values for Draperies, Roller Shades, and Insect Screens (Continued)													
Glazing ID:			25a	25b	25c	26d	25e	25f	Glazing ID:			29a	29b
Dark Closed Weave	IIID	100%	0.88, 0.43	0.89, 0.42	0.90, 0.40	0.90, 0.40	0.91, 0.39	0.90, 0.40	Dark Closed Weave	IIID	100%	0.86, 0.44	0.87, 0.42

Table 3.9g IAC Values for Draperies, Roller Shades, and Insect Screens (continued)

(Source: ASHRAE Handbook—Fundamentals [2013], Chapter 15, Table 13F)

Medium Closed Weave	IIM	100%	0.80, 0.45	0.82, 0.44	0.85, 0.41	0.84, 0.41	0.85, 0.40	0.84, 0.42	Medium Closed Weave	IIM	100%	0.77, 0.45	0.80, 0.43
Light Closed Weave	IIIL	100%	0.68, 0.51	0.72, 0.48	0.76, 0.44	0.76, 0.45	0.77, 3	0.76, 0.45	Light Closed Weave	IIIL	100%	0.65, 0.50	0.69, 0.47
Dark Semiopen Weave	IID	100%	0.91, 0.48	0.91, 0.47	0.92, 0.44	0.92, 0.45	0.92, 0.43	0.92, 0.45	Dark Semiopen Weave	IID	100%	0.89, 0.48	0.90, 0.47
Medium Semiopen Weave	IIM	100%	0.83, 0.54	0.85, 0.52	0.87, 0.48	0.86, 0.49	0.87, 0.47	0.86, 0.49	Medium Semiopen Weave	IIM	100%	0.81, 0.54	0.83, 0.51
Light Semiopen Weave	IIL	100%	0.75, 0.66	0.78, 0.63	0.81, 0.57	0.81, 0.58	0.82, 0.55	0.81, 0.58	Light Semiopen Weave	IIL	100%	0.72, 0.65	0.76, 0.60
Dark Open Weave	ID	100%	0.93, 0.56	0.93, 0.55	0.94, 0.51	0.94, 0.52	0.94, 0.50	0.94, 0.52	Dark Open Weave	ID	100%	0.91, 0.56	0.92, 0.54
Medium Open Weave	IM	100%	0.86, 0.65	0.87, 0.62	0.89, 0.57	0.89, 0.58	0.89, 0.56	0.89, 0.59	Medium Open Weave	IM	100%	0.84, 0.64	0.85, 0.60
Light Open Weave	IL	100%	0.79, 0.75	0.82, 0.72	0.85, 0.65	0.84, 0.66	0.85, 0.63	0.84, 0.67	Light Open Weave	IL	100%	0.77, 0.73	0.80, 0.69
Sheer		100%	0.84, 0.8	0.86, 0.76	0.88, 0.69	0.88, 0.7	0.89, 0.67	0.88, 0.71	Sheer		100%	0.83, 0.78	0.85, 0.73
Glazing ID:			32a	32b	32c	32d	40a	40b	40c	40d			
Dark Closed Weave	IIID	100%	0.89, 0.43	0.90, 0.41	0.91, 0.42	0.92, 0.39	0.93, 0.41	0.94, 0.37	0.90, 0.42	0.91, 0.40			
Medium Closed Weave	IIM	100%	0.80, 0.44	0.83, 0.42	0.82, 0.42	0.84, 0.39	0.84, 0.40	0.87, 0.37	0.82, 0.43	0.85, 0.41			
Light Closed Weave	IIIL	100%	0.69, 0.48	0.73, 0.45	0.69, 0.44	0.73, 0.40	0.73, 0.42	0.77, 0.38	0.71, 0.47	0.76, 0.44			
Dark Semiopen Weave	IID	100%	0.91, 0.47	0.92, 0.46	0.93, 0.46	0.94, 0.43	0.94, 0.45	0.95, 0.41	0.92, 0.46	0.93, 0.45			
Medium Semiopen Weave	IIM	100%	0.83, 0.52	0.85, 0.50	0.84, 0.50	0.86, 0.46	0.86, 0.48	0.89, 0.44	0.85, 0.51	0.87, 0.48			

Table 3.9g IAC Values for Draperies, Roller Shades, and Insect Screens (continued)

(Source: ASHRAE Handbook—Fundamentals [2013], Chapter 15, Table 13F)

Light Semiopen Weave	IIL	100%	0.75, 0.62	0.79, 0.58	0.75, 0.58	0.79, 0.52	0.78, 0.55	0.82, 0.49	0.77, 0.60	0.80, 0.56			
Dark Open Weave	ID	100%	0.93, 0.55	0.93, 0.53	0.95, 0.53	0.95, 0.50	0.96, 0.51	0.96, 0.47	0.94, 0.54	0.94, 0.52			
Medium Open Weave	IM	100%	0.86, 0.62	0.87, 0.59	0.87, 0.59	0.88, 0.54	0.88, 0.56	0.90, 0.51	0.87, 0.60	0.89, 0.57			
Light Open Weave	IL	100%	0.80, 0.71	0.83, 0.66	0.80, 0.66	0.82, 0.60	0.82, 0.63	0.85, 0.57	0.81, 0.69	0.84, 0.64			
Sheer		100%	0.84, 0.75	0.87, 0.7	0.85, 0.71	0.87, 0.65	0.86, 0.68	0.89, 0.61	0.86, 0.73	0.88, 0.68			
<i>Roller Shades and Insect Screens</i>													
Shade/Screen	Openness	Refl./Trans.											
Glazing ID:			1a	1b	1c	1d	1e	1f	1g	1h	1i		
Light Translucent	0.14	0.60/0.25	0.44, 0.74	0.45, 0.72	0.49, 0.66	0.55, 0.59	0.51, 0.65	0.56, 0.59	0.51, 0.65	0.57, 0.58	0.55, 0.6		
White Opaque	0	0.65/0.00	0.34, 0.45	0.35, 0.44	0.4, 0.41	0.47, 0.38	0.42, 0.4	0.48, 0.38	0.42, 0.4	0.49, 0.38	0.47, 0.38		
Dark Opaque	0	0.20/0.00	0.64, 0.48	0.65, 0.47	0.67, 0.45	0.69, 0.43	0.67, 0.45	0.7, 0.42	0.67, 0.45	0.7, 0.42	0.69, 0.43		
Light Gray Translucent	0.1	0.31/0.15	0.61, 0.57	0.62, 0.57	0.64, 0.54	0.68, 0.51	0.65, 0.53	0.68, 0.5	0.65, 0.53	0.69, 0.5	0.68, 0.51		
Dark Gray Translucent	0.14	0.17/0.19	0.71, 0.58	0.72, 0.58	0.73, 0.55	0.76, 0.52	0.74, 0.55	0.76, 0.52	0.74, 0.55	0.76, 0.52	0.76, 0.52		
Reflective White Opaque	0	0.84/0.00	0.3, 0.71	0.32, 0.68	0.38, 0.6	0.45, 0.53	0.39, 0.58	0.46, 0.52	0.39, 0.58	0.47, 0.52	0.45, 0.53		
Reflective White Translucent	0.07	0.75/0.16	0.23, 0.42	0.25, 0.41	0.31, 0.38	0.39, 0.36	0.33, 0.37	0.4, 0.35	0.33, 0.37	0.41, 0.35	0.39, 0.36		
Outdoor Insect Screen			0.64, 0.98	0.64, 0.98	0.64, 0.95	0.64, 0.92	0.64, 0.95	0.64, 0.91	0.64, 0.95	0.64, 0.91	0.64, 0.92		
Indoor Insect Screen			0.88, 0.81	0.88, 0.8	0.89, 0.78	0.9, 0.75	0.89, 0.78	0.9, 0.75	0.89, 0.78	0.9, 0.75	0.9, 0.76		
Glazing ID:			5a	5b	5c	5d	5e	5f	5g	5h	5i		
Light Translucent	0.14	0.60/0.25	0.55, 0.65	0.58, 0.62	0.58, 0.62	0.63, 0.56	0.58, 0.61	0.64, 0.56	0.58, 0.61	0.64, 0.56	0.63, 0.56		

Table 3.9g IAC Values for Draperies, Roller Shades, and Insect Screens (continued)

(Source: ASHRAE Handbook—Fundamentals [2013], Chapter 15, Table 13F)

White Opaque	0	0.65/0.00	0.48, 0.4	0.52, 0.39	0.51, 0.39	0.57, 0.37	0.52, 0.39	0.58, 0.37	0.52, 0.39	0.58, 0.36	0.57, 0.37		
Dark Opaque	0	0.20/0.00	0.76, 0.44	0.77, 0.43	0.77, 0.43	0.8, 0.41	0.78, 0.43	0.8, 0.41	0.78, 0.43	0.8, 0.4	0.8, 0.41		
Light Gray Translucent	0.1	0.31/0.15	0.72, 0.53	0.74, 0.51	0.74, 0.51	0.77, 0.48	0.74, 0.51	0.77, 0.48	0.74, 0.51	0.77, 0.48	0.77, 0.48		
Dark Gray Translucent	0.14	0.17/0.19	0.81, 0.54	0.82, 0.53	0.82, 0.53	0.84, 0.5	0.82, 0.52	0.84, 0.5	0.82, 0.52	0.84, 0.5	0.84, 0.5		
Reflective White Opaque	0	0.84/0.00	0.43, 0.6	0.47, 0.55	0.46, 0.56	0.54, 0.5	0.47, 0.55	0.55, 0.49	0.47, 0.55	0.55, 0.49	0.54, 0.5		
Reflective White Translucent	0.07	0.75/0.16	0.37, 0.38	0.42, 0.36	0.41, 0.36	0.49, 0.34	0.42, 0.36	0.5, 0.34	0.42, 0.36	0.5, 0.34	0.49, 0.34		
Outdoor Insect Screen			0.64, 0.96	0.64, 0.94	0.64, 0.94	0.64, 0.91	0.64, 0.94	0.64, 0.9	0.64, 0.94	0.64, 0.9	0.64, 0.91		
Indoor Insect Screen			0.92, 0.78	0.93, 0.77	0.93, 0.76	0.93, 0.74	0.93, 0.76	0.93, 0.74	0.93, 0.76	0.93, 0.73	0.93, 0.74		
IAC Values for Draperies, Roller Shades, and Insect Screens (Continued)													
Glazing ID:			17a	17b	17c	17d	17e	17f	17g	17h	17i	17j	17k
Light Translucent	0.14	0.60/0.25	0.58, 0.63	0.62, 0.6	0.62, 0.6	0.67, 0.56	0.64, 0.58	0.69, 0.53	0.64, 0.57	0.7, 0.53	0.64, 0.57	0.7, 0.53	0.7, 0.53
White Opaque	0	0.65/0.00	0.52, 0.39	0.56, 0.38	0.57, 0.38	0.61, 0.37	0.59, 0.37	0.65, 0.36	0.59, 0.37	0.65, 0.36	0.59, 0.37	0.65, 0.35	0.65, 0.36
Dark Opaque	0	0.20/0.00	0.8, 0.43	0.82, 0.42	0.82, 0.42	0.83, 0.41	0.82, 0.41	0.84, 0.39	0.82, 0.41	0.84, 0.39	0.82, 0.41	0.84, 0.39	0.84, 0.39
Light Gray Translucent	0.1	0.31/0.15	0.76, 0.52	0.78, 0.5	0.78, 0.5	0.8, 0.48	0.78, 0.49	0.81, 0.46	0.79, 0.49	0.82, 0.46	0.79, 0.49	0.82, 0.46	0.81, 0.46
Dark Gray Translucent	0.14	0.17/0.19	0.84, 0.53	0.85, 0.52	0.85, 0.52	0.86, 0.5	0.86, 0.51	0.87, 0.48	0.86, 0.51	0.88, 0.48	0.86, 0.51	0.88, 0.48	0.87, 0.48
Reflective White Opaque	0	0.84/0.00	0.46, 0.57	0.52, 0.53	0.52, 0.53	0.58, 0.5	0.54, 0.51	0.61, 0.47	0.55, 0.51	0.62, 0.46	0.55, 0.51	0.62, 0.46	0.61, 0.47
Reflective White Translucent	0.07	0.75/0.16	0.41, 0.37	0.47, 0.36	0.47, 0.36	0.53, 0.35	0.49, 0.35	0.57, 0.34	0.5, 0.35	0.58, 0.34	0.5, 0.35	0.58, 0.33	0.57, 0.34

Table 3.9g IAC Values for Draperies, Roller Shades, and Insect Screens (continued)

(Source: ASHRAE Handbook—Fundamentals [2013], Chapter 15, Table 13F)

Outdoor Insect Screen			0.64, 0.95	0.64, 0.93	0.64, 0.94	0.64, 0.91	0.64, 0.92	0.64, 0.89	0.64, 0.92	0.64, 0.89	0.64, 0.92	0.64, 0.89	0.64, 0.89
Indoor Insect Screen			0.94, 0.77	0.94, 0.76	0.94, 0.76	0.94, 0.74	0.94, 0.75	0.95, 0.72	0.94, 0.75	0.95, 0.72	0.94, 0.75	0.95, 0.72	0.95, 0.72
Glazing ID:			21a	21b	21c	21d	21e	21f	21g	21h	21i	21j	21k
Light Translucent	0.14	0.60/0.25	0.61, 0.63	0.65, 0.59	0.66, 0.59	0.69, 0.56	0.68, 0.57	0.72, 0.53	0.68, 0.57	0.72, 0.53	0.68, 0.57	0.72, 0.53	0.72, 0.53
White Opaque	0	0.65/0.00	0.55, 0.39	0.6, 0.38	0.61, 0.38	0.64, 0.37	0.63, 0.37	0.67, 0.36	0.63, 0.37	0.67, 0.36	0.63, 0.37	0.68, 0.35	0.67, 0.36
Dark Opaque	0	0.20/0.00	0.82, 0.43	0.84, 0.42	0.84, 0.42	0.85, 0.41	0.85, 0.41	0.86, 0.39	0.85, 0.41	0.86, 0.39	0.85, 0.41	0.86, 0.39	0.86, 0.39
Light Gray Translucent	0.1	0.31/0.15	0.78, 0.51	0.8, 0.5	0.8, 0.5	0.82, 0.48	0.81, 0.48	0.83, 0.46	0.81, 0.48	0.83, 0.46	0.81, 0.48	0.83, 0.46	0.83, 0.46
Dark Gray Translucent	0.14	0.17/0.19	0.86, 0.53	0.87, 0.51	0.87, 0.51	0.88, 0.5	0.88, 0.5	0.89, 0.48	0.88, 0.5	0.89, 0.48	0.88, 0.5	0.89, 0.48	0.89, 0.48
Reflective White Opaque	0	0.84/0.00	0.5, 0.56	0.55, 0.53	0.56, 0.52	0.6, 0.5	0.58, 0.51	0.63, 0.47	0.59, 0.5	0.64, 0.47	0.59, 0.5	0.64, 0.47	0.64, 0.47
Reflective White Translucent	0.07	0.75/0.16	0.44, 0.36	0.5, 0.35	0.51, 0.35	0.56, 0.35	0.54, 0.35	0.6, 0.34	0.54, 0.35	0.6, 0.34	0.54, 0.35	0.6, 0.33	0.6, 0.34
Outdoor Insect Screen			0.64, 0.95	0.64, 0.93	0.64, 0.93	0.64, 0.91	0.64, 0.92	0.64, 0.89	0.64, 0.91	0.64, 0.89	0.64, 0.91	0.64, 0.89	0.64, 0.89
Indoor Insect Screen			0.94, 0.77	0.95, 0.75	0.95, 0.75	0.95, 0.74	0.95, 0.74	0.95, 0.72	0.95, 0.74	0.95, 0.72	0.95, 0.74	0.95, 0.72	0.95, 0.72
Glazing ID:			25a	25b	25c	26d	25e	25f	Glazing ID:			29a	29b
Light Translucent	0.14	0.60/0.25	0.66, 0.62	0.71, 0.58	0.75, 0.53	0.75, 0.54	0.77, 0.52	0.74, 0.55	Light Translucent	0.14	0.60/0.25	0.64, 0.6	0.68, 0.56
White Opaque	0	0.65/0.00	0.6, 0.38	0.66, 0.37	0.71, 0.35	0.7, 0.36	0.72, 0.35	0.7, 0.36	White Opaque	0	0.65/0.00	0.58, 0.38	0.63, 0.37
Dark Opaque	0	0.20/0.00	0.85, 0.42	0.86, 0.41	0.88, 0.39	0.88, 0.39	0.88, 0.38	0.87, 0.39	Dark Opaque	0	0.20/0.00	0.82, 0.42	0.84, 0.41
Light Gray Translucent	0.1	0.31/0.15	0.81, 0.5	0.83, 0.49	0.86, 0.46	0.85, 0.46	0.86, 0.45	0.85, 0.47	Light Gray Translucent	0.1	0.31/0.15	0.78, 0.5	0.81, 0.48
Dark Gray Translucent	0.14	0.17/0.19	0.88, 0.52	0.89, 0.51	0.9, 0.47	0.9, 0.48	0.91, 0.47	0.9, 0.48	Dark Gray Translucent	0.14	0.17/0.19	0.86, 0.52	0.87, 0.5

Table 3.9g IAC Values for Draperies, Roller Shades, and Insect Screens (continued)

(Source: ASHRAE Handbook—Fundamentals [2013], Chapter 15, Table 13F)

Reflective White Opaque	0	0.84/0.00	0.55, 0.55	0.61, 0.52	0.68, 0.47	0.67, 0.48	0.69, 0.46	0.66, 0.48	Reflective White Opaque	0	0.84/0.00	0.53, 0.53	0.59, 0.49
Reflective White Translucent	0.07	0.75/0.16	0.5, 0.36	0.57, 0.35	0.64, 0.33	0.62, 0.34	0.65, 0.33	0.62, 0.34	Reflective White Translucent	0.07	0.75/0.16	0.48, 0.36	0.55, 0.35
Outdoor Insect Screen			0.65, 0.95	0.65, 0.93	0.64, 0.88	0.64, 0.89	0.64, 0.87	0.64, 0.89	Outdoor Insect Screen			0.64, 0.94	0.64, 0.91
Indoor Insect Screen			0.95, 0.76	0.96, 0.75	0.96, 0.72	0.96, 0.72	0.96, 0.71	0.96, 0.72	Indoor Insect Screen			0.94, 0.76	0.95, 0.74
Glazing ID:			32a	32b	32c	32d	40a	40b	40c	40d			
Light Translucent	0.14	0.60/0.25	0.67, 0.58	0.72, 0.54	0.67, 0.52	0.71, 0.46	0.7, 0.49	0.75, 0.43	0.69, 0.56	0.74, 0.52			
White Opaque	0	0.65/0.00	0.62, 0.37	0.68, 0.36	0.62, 0.33	0.67, 0.3	0.67, 0.31	0.72, 0.29	0.65, 0.37	0.71, 0.36			
Dark Opaque	0	0.20/0.00	0.85, 0.41	0.87, 0.4	0.87, 0.4	0.89, 0.38	0.89, 0.39	0.91, 0.36	0.87, 0.41	0.88, 0.39			
Light Gray Translucent	0.1	0.31/0.15	0.81, 0.49	0.84, 0.47	0.82, 0.46	0.85, 0.43	0.85, 0.44	0.87, 0.41	0.83, 0.48	0.85, 0.46			
Dark Gray Translucent	0.14	0.17/0.19	0.88, 0.51	0.89, 0.49	0.9, 0.49	0.91, 0.45	0.91, 0.47	0.92, 0.43	0.89, 0.5	0.91, 0.48			
Reflective White Opaque	0	0.84/0.00	0.57, 0.51	0.64, 0.47	0.57, 0.44	0.63, 0.39	0.61, 0.41	0.68, 0.36	0.6, 0.5	0.67, 0.46			
Reflective White Translucent	0.07	0.75/0.16	0.53, 0.35	0.61, 0.34	0.52, 0.28	0.59, 0.26	0.58, 0.27	0.65, 0.25	0.56, 0.35	0.64, 0.34			
Outdoor Insect Screen			0.64, 0.92	0.64, 0.9	0.64, 0.86	0.64, 0.8	0.64, 0.83	0.64, 0.77	0.64, 0.91	0.64, 0.88			
Indoor Insect Screen			0.95, 0.75	0.96, 0.73	0.95, 0.7	0.95, 0.67	0.96, 0.68	0.96, 0.64	0.96, 0.74	0.96, 0.72			

Notes:

- ^a Louvers track so that profile angle equals negative slat angle and maximum direct beam is admitted.
- ^b Louvers track to block direct beam radiation. When negative slat angles result, slat defaults to 0°.
- ^c Glazing cavity width equals original cavity width plus slat width.
- ^d FR is radiant fraction; ratio of radiative heat transfer to total heat transfer, on room side of glazing system.

Table 3.9g IAC Values for Draperies, Roller Shades, and Insect Screens (continued)

(Source: ASHRAE Handbook—Fundamentals [2013], Chapter 15, Table 13F)

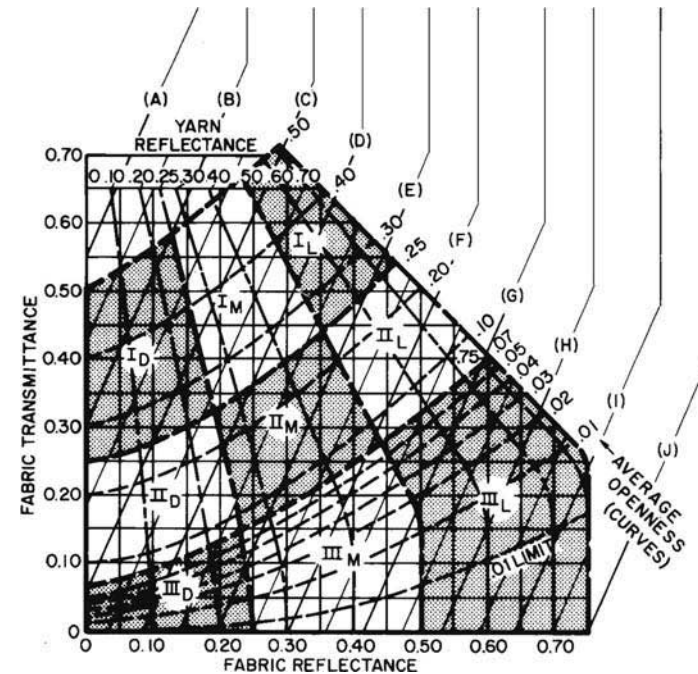
Interior Attenuation Coefficient (IAC)

Notes:

1. Interior attenuation coefficients are for draped fabrics.
2. Other properties are for fabrics in flat orientation.
3. Use fabric reflectance and transmittance to obtain accurate IAC values.
4. Use openness and yarn reflectance to obtain the various environmental characteristics, or to obtain approximate IAC values.

Classification of Fabrics

- I = Open weave
- II = Semiopen weave
- III = Closed weave
- D = Dark color
- M = Medium color
- L = Light color



To obtain fabric designator (III_L, II_M, etc.). Using either (1) fabric transmittance and fabric reflectance coordinates or (2) openness and yarn reflectance coordinates, find a point on the chart and note the designator for that area. If properties are not known, the classification may be approximated by eye as described in the note in Figure 19 in the ASHRAE Handbook—Fundamentals (2013), Chapter 15.

IAC values are tabulated by glass type, shading type, and profile angle. The profile angle Ω for louvered or slat-type sunshades (e.g., Venetian blinds) is illustrated in Figure 3.1. The glass type will determine which of Tables 3.9a through Table 3.9f are used and, specifically, which column is selected. Then, the louver location and louver reflectance will determine which set of IACs are chosen. Within each set, several values of IAC are given for different profile angles. Computation of the profile angle depends on the solar angles, which are described in Appendix D, Section D.1. For horizontal blinds, the profile angle Ω is given as

$$\tan(\Omega) = \frac{\tan(\beta)}{\cos(\gamma)} \quad 3.5$$

where β is the solar altitude angle and γ is the surface solar azimuth angle.

For vertical blinds, the profile angle is the surface solar azimuth angle. Figure 3.1 shows the geometry assumed for the data given in the tables with the slat width w , slat crown c , slat spacing s , and slat angle ϕ . The values given in the tables assume ratios w/s and w/c of 1.2 and 1.6, respectively. The slat angle includes *worst*, where the shades are opened to maximize the solar heat gain; 0° ; *excluded beam*, where the blinds are adjusted to eliminate transmission of beam radiation; 45° ; and *closed*. For each combination of glass type, shade location and type, and slat angle, four values are given:



Figure 3.1 Geometry of Slat-Type Sunshades

(Source: *ASHRAE Handbook—Fundamentals* [2013], Chapter 15, Figure 18).

Load Calculation Applications Manual (SI), Second Edition

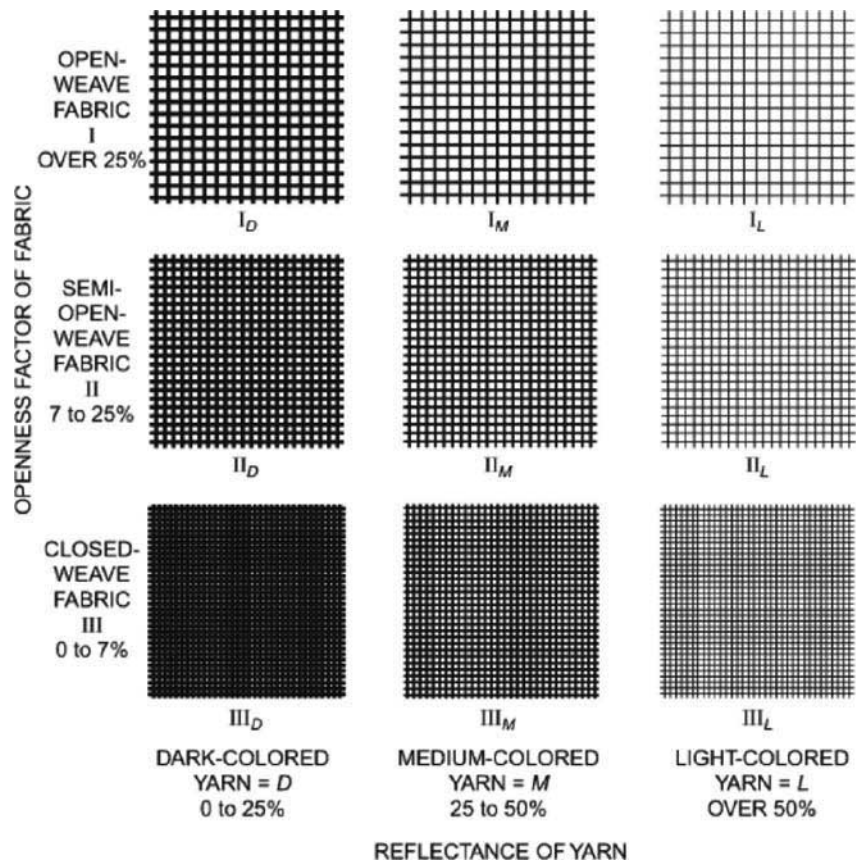
- IAC_0 —corresponding to a profile angle of 0°
- IAC_{60} —corresponding to a profile angle of 60°
- IAC_{diff} —the IAC applied to diffuse irradiation
- F_R —the fraction of the solar heat gain that is radiant

For profile angles other than 0° or 60° , the IAC can be estimated as

$$IAC(\theta, \Omega) = IAC_0 + IAC_x \cdot \min(1, 0.02 \cdot \Omega) \quad (3.6)$$

where $IAC_x = IAC_{60} - IAC_0$.

For roller blinds, insect screens, and draperies, IAC values are given in Table 3.9g. Drapery fabrics may be characterized using Figures 3.2 and 3.3. Draperies are also characterized by their fullness—100% fullness corresponds to the



NOTE: Classes may be approximated by eye. With closed fabrics, no objects are visible through the material, but large light or dark areas may show. Semiopen fabrics do not allow details to be seen, and large objects are clearly defined. Open fabrics allow details to be seen, and the general view is relatively clear with no confusion of vision. The yarn color or shade of light or dark may be observed to determine whether the fabric is light, medium, or dark.

Figure 3.2 Designation of drapery fabrics.

(Source: *ASHRAE Handbook—Fundamentals* [2013], Chapter 15, Figure 19).

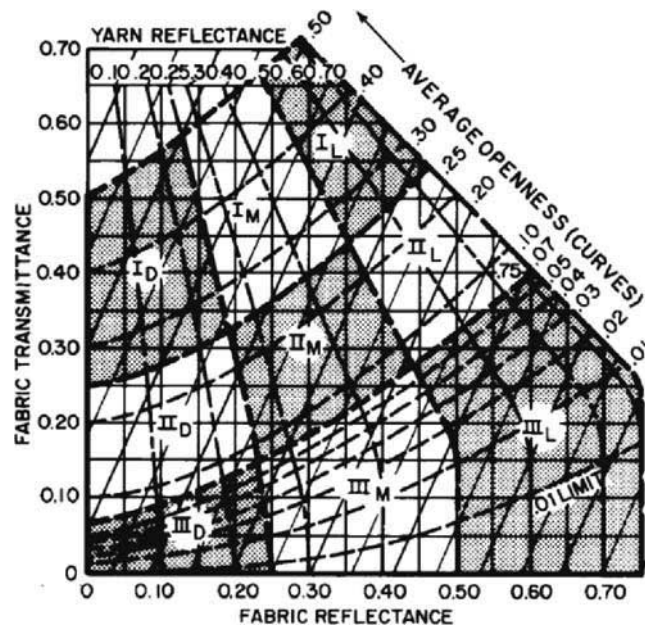


Figure 3.3 Drapery fabric properties.

(Source: *ASHRAE Handbook—Fundamentals* [2013], Chapter 15, Figure 20).

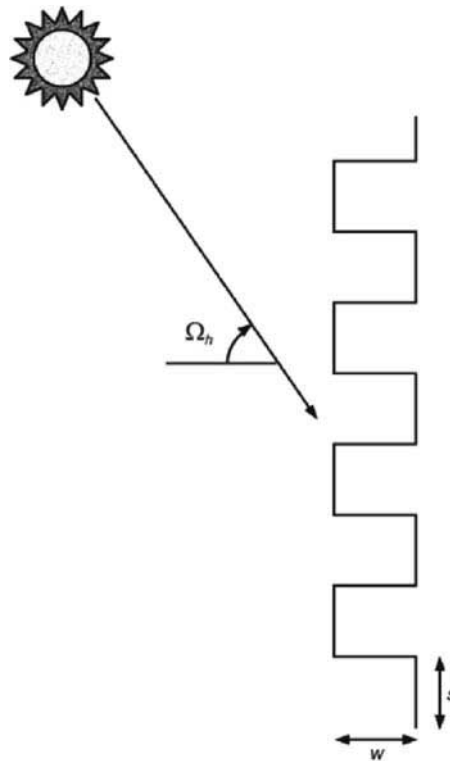


Figure 3.4 Drapery fabric geometry,

(Source: *ASHRAE Handbook—Fundamentals* [2013], Chapter 15, Figure 21).

Load Calculation Applications Manual (SI), Second Edition

fabric (i.e., if stretched out horizontally) being twice as wide as the window; 0% fullness would correspond to the fabric being the same width as the window, such as a roller blind. The tables only treat the 100% and 0% fullness cases (i.e., draperies are assumed to have 100% fullness; roller blinds and insect screens are assumed to have 0% fullness).

Use of the IAC to compute solar heat gain is described in Section 7.7 of Chapter 7 and demonstrated in Example 7.2.

With the exception of Tables 3.3b and 3.8, the tables in this section all come from Chapter 15 of the *ASHRAE Handbook—Fundamentals* (ASHRAE 2013) and for further information the reader should consult that chapter.

References

- Adams, L. 1971. Supporting cryogenic equipment with wood. *Chemical Engineering* (May): 156–58.
- ASHRAE. 2013. *ASHRAE Handbook—Fundamentals*. Atlanta: ASHRAE.
- Bassett, M.R., and H.A. Trethowen. 1984. Effect of condensation on emittance of reflective insulation. *Journal of Thermal Insulation* 8(October):127.
- Incropera, F.P., and D.P. DeWitt. 1990. *Fundamentals of Heat and Mass Transfer*, 3rd ed. New York: Wiley.
- Lewis, W.C. 1967. Thermal conductivity of wood-base fiber and particle panel materials. Forest Products Laboratory, Research Paper FPL 77, Madison, Wisconsin.
- MacLean, J.D. 1941. Thermal conductivity of wood. *ASHVE Transactions* 47:323.
- Miller, A. 1971. *Meteorology*, 2nd ed. Columbus: Charles E. Merrill Publishing.
- NFRC. 2004. Procedure for determining fenestration product U-factors. *Technical Document 100-2004*, National Fenestration Rating Council, Silver Spring, MD.
- Parker, D.S., J.E.R. Mellvaine, S.F. Barkaszi, D.J. Beal, and M.T. Anello. 2000. Laboratory testing of the reflectance properties of roofing material. FSEC-CR670-00, Florida Solar Energy Center, Cocoa, FL.
- Robinson, H.E., F.J. Powlitch, and R.S. Dill. 1954. The thermal insulation value of airspaces. Housing and Home Finance Agency. *Housing Research Paper*, 32. Washington, DC.
- USDA. 1974. *Wood Handbook: Wood as an Engineering Material*. Forest Product Laboratory, U.S. Department of Agriculture, Handbook No. 72, Tables 3-7 and 4-2 and Figures 3-4 and 3-5.
- Van Dyke, R.L., and T.P. Konen. 1982. Energy conservation through interior shading of windows: An analysis, test and evaluation of reflective Venetian blinds. LBL-14369. Lawrence Berkeley Laboratory, Berkeley, CA. March.
- VDI. 1999. Standard 3789 Part 2, *Environmental Meteorology—Interactions between Atmosphere and Surfaces—Calculation of Short-Wave and Long-Wave Radiation*. Verein Deutscher Ingenieure (Association of German Engineers), Dusseldorf.
- Wilkes, K.E. 1979. Thermophysical properties data base activities at Owens-Corning Fiberglass. *Proceedings of the ASHRAE/DOE-ORNL Conference, Thermal Performance of the Exterior Envelopes of Buildings* 28:662–77.
- Yarbrough, E.W. 1983. Assessment of reflective insulations for residential and commercial applications. ORNL/TM-8891, October. Oak Ridge, TN: Oak Ridge National Laboratory.

Environmental Design Conditions

This chapter describes the weather data for locations around the world (which can be found in supporting files online at www.ashrae.org/lcam), the application of the weather data, and recommended interior and exterior design conditions. The data come from the *ASHRAE Handbook—Fundamentals* (2013) and are based on long-term hourly observations. For additional information on the basis for the weather data and its application, consult Chapter 14 of the *ASHRAE Handbook—Fundamentals* (2013).

4.1 Indoor Design Conditions

The primary purpose of a heating and air-conditioning system is to maintain the space in a comfortable and healthy condition. To do this, the system must generally maintain the dry-bulb temperature and the relative humidity within an acceptable range.

ANSI/ASHRAE Standard 55-2010, *Thermal Environmental Conditions for Human Occupancy*, gives thermal comfort values at selected conditions in the building environment. Physiological principles, comfort, and health are addressed in Chapter 9 of the *ASHRAE Handbook—Fundamentals* (2013). The *ASHRAE Handbook—HVAC Applications* (2011) gives specific recommendations for indoor design conditions for such applications as hospitals and other special cases.

ANSI/ASHRAE/ACCA Standard 183-2007, *Peak Cooling and Heating Load Calculations in Buildings Except Low-Rise Residential Buildings*, states that “Indoor design conditions shall be established by owner criteria, local codes, or comfort criteria.” This gives considerable latitude in selecting design conditions. Experience has shown that, except in critical cases, the indoor design temperature and relative humidity should be selected on the high side of the comfort envelope to avoid overdesign of the system.

For cooling load calculations, a design dry-bulb temperature of 24°C to 26°C with a design relative humidity of approximately 50% is widely used in practice for usual occupied spaces. For heating load, a dry-bulb temperature of 21°C with relative humidity less than or equal to 30% is common.

4.2 Outdoor Design Conditions

The annual climatic design conditions for Atlanta, Georgia, are shown in Table 4.1 to illustrate the format of the data. Data for five additional sites are shown in Tables 4.4–4.8 at the end of the chapter. Data in the same format for 6443 stations worldwide are given in the online supplementary files. Not all of the data are immediately useful for design load calculations; application of the data for cooling and heating load calculations is discussed in the following sections. Data needed for load calculations are, for almost all of the stations, incorporated in the accompanying online spreadsheets. Columns are numbered and described as follows:

Station Information

Station Identifiers

- Name of the observing station
- World Meteorological Organization (WMO) station identifier
- Latitude of station, °N/S
- Longitude of station, °E/W

Load Calculation Applications Manual (SI), Second Edition

Elevation of station, m

Standard pressure at elevation, in kPa

Time zone, h \pm coordinated universal time (UTC)

Time zone code (e.g., NAE = Eastern Time, United States, and Canada)

- The supporting files online contain a list of all time zone codes used in the tables.

Period analyzed (e.g., 72–01 = data from 1972 to 2001 were used)

Weather Bureau Army Navy (WBAN) station identifier

Annual Heating and Humidification Design Conditions

- 1a. Coldest month (i.e., month with lowest average dry-bulb temperature; 1 = January, 12 = December)
- 1b. and 1c. Dry-bulb temperature corresponding to 99.6% and 99.0% annual cumulative frequency of occurrence (cold conditions), °C
- 1d.–1i. Dew-point temperature corresponding to 99.6% and 99.0% annual cumulative frequency of occurrence, °C; corresponding humidity ratio, calculated at standard atmospheric pressure at elevation of station, grains of moisture per lb of dry air; mean coincident dry-bulb temperature, °C
- 1j. – 1m. Wind speed corresponding to 0.4% and 1.0% cumulative frequency of occurrence for coldest month (column 1a), m/s; mean coincident dry-bulb temperature, °C
- 1n.–1o. Mean wind speed coincident with 99.6% dry-bulb temperature (column 1b), m/s; corresponding most frequent wind direction, degrees from north (east = 90°)

Annual Cooling, Dehumidification, and Enthalpy Design Conditions

- 2a. Hottest month (i.e., month with highest average dry-bulb temperature; 1 = January, 12 = December)
- 2b. Daily temperature range for hottest month, °C (defined as mean of the difference between daily maximum and daily minimum dry-bulb temperatures for hottest month [column 2a])
- 2c.–2h. Dry-bulb temperature corresponding to 0.4%, 1.0%, and 2.0% annual cumulative frequency of occurrence (warm conditions), °C; mean coincident wet-bulb temperature, °C
- 2i.–2n. Wet-bulb temperature corresponding to 0.4%, 1.0%, and 2.0% annual cumulative frequency of occurrence, °C; mean coincident dry-bulb temperature, °C
- 2o.–2p. Mean wind speed coincident with 0.4% dry-bulb temperature (column 2c), in m/s; corresponding most frequent wind direction, degrees from north
- 3a.–3i. Dew-point temperature corresponding to 0.4%, 1.0%, and 2.0% annual cumulative frequency of occurrence, °C; corresponding humidity ratio, calculated at the standard atmospheric pressure at elevation of station, grains of moisture per kg of dry air; mean coincident dry-bulb temperature, °C

Environmental Design Conditions

Table 4.1 Design Conditions for Atlanta, Georgia

(Source: ASHRAE Handbook—Fundamentals [2013], Chapter 14, Table 1)

2013 ASHRAE Handbook - Fundamentals (SI)

© 2013 ASHRAE, Inc.

ATLANTA MUNICIPAL, GA, USA

WMO#: 722190

Lat: **33.64N** Long: **84.43W** Elev: **313** StdP: **97.62** Time Zone: **-5.00 (NAE)** Period: **86-10** WBAN: **13874**

Annual Heating and Humidification Design Conditions

Coldest Month	Heating DB			Humidification DP/MCDB and HR						Coldest month WS/MCDB				MCWS/PCWD to 99.6% DB	
	99.6%	99%		99.6%		99%		99%		0.4%		1%		MCWS	PCWD
(a)	(b)	(c)	(d)	(e)	(f)	(g)	(h)	(i)	(j)	(k)	(l)	(m)	(n)	(o)	
1	-5.8	-3.1	-15.5	1.0	-1.9	-12.7	1.3	0.1	11.1	4.4	10.5	4.4	5.3	320	

Annual Cooling, Dehumidification, and Enthalpy Design Conditions

Hottest Month	Hottest Month DB Range	Cooling DB/MCWB						Evaporation WB/MCDB						MCWS/PCWD to 0.4% DB	
		0.4%		1%		2%		0.4%		1%		2%		MCWS	PCWD
(a)	(b)	(c)	(d)	(e)	(f)	(g)	(h)	(i)	(j)	(k)	(l)	(m)	(n)	(o)	(p)
7	9.4	34.4	23.4	33.1	23.3	32.1	23.0	25.2	31.4	24.7	30.4	24.1	29.4	3.9	300

DP	HR	MCDB	Dehumidification DP/MCDB and HR						Enthalpy/MCDB						Hours 8 to 4 & 12.8/20.6
			0.4%		1%		2%		0.4%		1%		2%		
(a)	(b)	(c)	(d)	(e)	(f)	(g)	(h)	(i)	(j)	(k)	(l)	(m)	(n)	(o)	(p)
23.5	19.0	27.4	23.0	18.4	26.8	22.6	17.9	26.5	78.3	31.4	76.0	30.4	74.0	29.8	800

Extreme Annual Design Conditions

Extreme Annual WS			Extreme Max WB	Extreme Annual DB				n-Year Return Period Values of Extreme DB							
1%	2.5%	5%		Mean		Standard deviation		n=5 years		n=10 years		n=20 years		n=50 years	
(a)	(b)	(c)	(d)	(e)	(f)	(g)	(h)	(i)	(j)	(k)	(l)	(m)	(n)	(o)	(p)
9.6	8.5	7.7	28.0	-10.0	35.9	2.5	1.8	-11.7	37.3	-13.2	38.3	-14.5	39.4	-16.3	40.7

Monthly Climatic Design Conditions

		Annual (d)	Jan (e)	Feb (f)	Mar (g)	Apr (h)	May (i)	Jun (j)	Jul (k)	Aug (l)	Sep (m)	Oct (n)	Nov (o)	Dec (p)	
(5)	Temperatures, Degree-Days and Degree-Hours	Tavg	17.1	6.9	8.7	12.7	16.9	21.4	25.1	26.8	26.4	23.2	17.3	12.3	7.6
(6)		Sd		5.23	5.06	4.95	4.27	3.27	2.51	1.92	2.18	3.08	3.94	4.52	4.95
(7)		HDD10.0	373	123	77	31	4	0	0	0	0	2	29	107	
(8)		HDD18.3	1484	354	269	183	75	12	1	0	0	4	66	186	334
(9)		CDD10.0	2983	28	42	113	210	352	454	521	509	396	230	97	32
(10)		CDD18.3	1052	0	1	7	31	106	204	263	251	151	35	4	1
(11)		CDH23.3	9169	0	3	54	259	807	1851	2548	2342	1103	186	15	1
(12)	CDH26.7	3477	0	0	5	47	217	744	1116	978	348	21	1	0	
(13)	Precipitation	PrecAvg	1289	121	122	147	108	109	90	127	93	87	77	98	110
(14)		PrecMax	1649	258	324	296	301	213	187	216	220	154	191	182	252
(15)		PrecMin	958	44	20	62	38	10	25	19	13	18	2	23	17
(16)		PrecSD	182.9	53.7	69.8	68.5	61.4	59.2	45.6	56.0	56.9	40.7	52.7	39.5	60.1
(17)	Monthly Design Dry Bulb and Mean Coincident Wet Bulb Temperatures	0.4%	DB	21.4	23.0	27.1	29.9	32.2	34.7	36.6	36.3	33.7	28.7	25.4	22.3
(18)			MCWB	15.4	16.5	16.9	18.9	22.0	22.8	23.7	23.9	22.5	20.8	17.7	17.2
(19)		2%	DB	18.9	20.7	24.8	28.0	30.5	33.2	34.7	34.1	31.6	27.1	23.1	19.7
(20)			MCWB	14.5	15.0	15.6	17.9	21.0	22.7	23.7	23.7	21.9	19.2	16.7	16.1
(21)		5%	DB	17.1	18.8	22.9	26.4	29.0	32.2	33.3	32.7	30.1	25.6	21.6	17.6
(22)			MCWB	13.6	14.0	14.9	17.1	20.4	22.5	23.5	23.6	21.6	18.2	16.1	14.7
(23)		10%	DB	15.1	17.1	21.0	24.5	27.6	30.9	32.0	31.4	28.7	23.8	19.8	15.7
(24)			MCWB	11.7	12.7	14.1	16.4	19.7	22.1	23.5	23.2	21.4	17.8	15.2	12.2
(25)	Monthly Design Wet Bulb and Mean Coincident Dry Bulb Temperatures	0.4%	WB	17.8	18.6	19.1	21.6	23.9	25.1	26.0	25.8	24.6	22.6	20.7	18.9
(26)			MCDB	19.6	19.8	22.9	26.2	28.6	31.4	32.1	32.3	29.9	26.6	22.4	20.6
(27)		2%	WB	16.1	17.0	17.8	20.0	22.7	24.3	25.2	25.2	23.6	21.4	19.2	17.3
(28)			MCDB	17.8	19.2	22.0	24.6	28.0	30.3	31.4	31.5	28.3	24.5	21.3	18.8
(29)		5%	WB	14.4	15.5	16.7	19.0	21.8	23.8	24.7	24.6	23.1	20.5	17.8	15.5
(30)			MCDB	16.4	17.9	20.8	23.4	26.9	29.4	30.5	30.3	27.3	23.1	20.0	17.5
(31)		10%	WB	12.5	13.6	15.5	17.9	21.0	23.2	24.1	24.1	22.5	19.4	16.3	12.9
(32)			MCDB	14.5	15.9	19.1	22.3	25.7	28.3	29.5	29.2	26.5	22.2	18.8	14.7
(33)	Mean Daily Temperature Range	5% DB	MDBR	9.6	10.1	10.8	11.2	10.3	9.6	9.4	9.2	9.1	10.1	10.2	9.3
(34)			MCDBR	11.3	11.6	12.8	12.7	11.3	11.2	11.4	10.8	10.6	11.3	11.5	11.0
(35)			MCWBR	7.9	7.2	6.3	5.4	4.3	3.6	3.5	3.3	3.8	5.0	6.5	7.7
(36)		5% WB	MCDBR	9.3	9.6	10.0	10.2	9.6	9.6	9.8	9.5	8.6	8.2	9.1	9.5
(37)			MCWBR	7.8	7.4	6.4	5.6	4.3	3.8	3.6	3.4	3.9	4.9	6.9	7.9
(38)			taub	0.334	0.324	0.355	0.383	0.379	0.406	0.440	0.427	0.388	0.358	0.354	0.335
(39)	taud	2.614	2.580	2.474	2.328	2.324	2.270	2.202	2.269	2.428	2.514	2.523	2.618		
(40)	Clear Sky Solar Irradiance	Ebn,noon	884	932	922	904	907	877	846	852	875	879	847	861	
(41)		Edh,noon	77	87	105	127	129	136	144	133	109	92	84	73	

Nomenclature: See separate page

Load Calculation Applications Manual (SI), Second Edition

- 3j.–3o. Enthalpy corresponding to 0.4%, 1.0%, and 2.0% annual cumulative frequency of occurrence, kJ/kg; mean coincident dry-bulb temperature, °C
- 3p. Number of hours between 8 a.m. and 4 p.m. (inclusive) with dry-bulb temperature between 12.8 °C and 20.6 °C

Extreme Annual Design Conditions

- 4a.–4c. Wind speed corresponding to 1.0%, 2.5%, and 5.0% annual cumulative frequency of occurrence, m/s
- 4d. Extreme maximum wet-bulb temperature, °C
- 4e.–4h. Mean and standard deviation of extreme annual maximum and minimum dry-bulb temperature, °C
- 4i.–4p. 5-, 10-, 20-, and 50-year return period values for maximum and minimum extreme dry-bulb temperature, °C

Monthly Design Conditions

A range of monthly design conditions for Atlanta, Georgia are provided in rows 5 through 41 of Table 4.1. These values are derived from the same analysis that results in the annual design conditions.

The monthly summaries are useful when seasonal variations in solar geometry and intensity, building or facility occupancy, or building use patterns require consideration. In particular, these values can be used when determining air-conditioning loads during periods of maximum solar heat gain. The monthly information in Table 4.1 is identified by the following column numbers:

- 5.–12. Monthly average temperatures, standard deviation of monthly average temperatures, both in °C. Heating degree days for base temperatures of 10°C and 18.3°C. Cooling degree days for base temperatures of 10°C, 18.3°C, 23.3°C, and 26.7°C. Not typically used in design load calculations.
- 13.–16. Monthly average precipitation, maximum, minimum, and standard deviation of precipitation, all in millimeters.
- 17.–24. Dry-bulb temperature corresponding to 0.4%, 2.0%, 5.0%, and 10.0% cumulative frequency of occurrence for indicated month, °C; mean coincident wet-bulb temperature, °C. For a 30-day month, the 0.4%, 2.0%, 5.0%, and 10.0% values of occurrence represent the value that occurs or is exceeded for a total of 3, 14, 36 and 72 hours, respectively, per month on average over the period of record.
- 25.–32. Wet-bulb temperature corresponding to 0.4%, 2.0%, 5.0%, and 10.0% cumulative frequency of occurrence for indicated month, °C; mean coincident dry-bulb temperature, °C.
- 33.–37. Mean daily temperature range for month indicated, °C (defined as mean of difference between daily maximum/minimum dry-bulb temperatures). Mean daily dry- and wet-bulb temperature ranges coincident with the 5% monthly design dry-bulb temperature. Mean daily dry- and wet-bulb temperature ranges coincident with the 5% monthly design wet-bulb temperature.

Environmental Design Conditions

- 38.–41. Clear-sky optical depths for beam (τ_{aub}) and diffuse (τ_{aud}) solar irradiation corresponding to the 21st day of each month. Also, clear-sky normal beam irradiation and horizontal diffuse irradiation at solar noon for the same days, W/m^2 .

Monthly percentile values of dry- or wet-bulb temperature may be higher or lower than the design conditions corresponding to the same nominal percentile, depending on the month and the seasonal distribution of the parameter at that location. Generally, for the hottest or most humid months of the year, the monthly percentile value exceeds the design condition corresponding to the same annual percentile. For example, in Table 4.1, the annual 0.4% design dry-bulb temperature (row 2, column c) in Atlanta, GA is 34.4°C . Row 17 shows that the 0.4% monthly dry-bulb temperature exceeds 34.4°C for June, July, and August, with values of 34.7°C , 36.6°C , and 36.3°C , respectively. A general, approximate rule of thumb is that the $n\%$ annual cooling design value is roughly equivalent to the $5n\%$ monthly cooling condition for the hottest month. For example, the 0.4% annual design dry bulb temperature is roughly equivalent to the 2% monthly design dry bulb for the hottest month.

4.2.1 Cooling Load Design Conditions

Design cooling load calculations are typically performed first for annual design conditions—a design day with a statistically high peak temperature. This peak day is assumed to occur in the month with the highest mean dry-bulb temperature, shown in column 2a of Table 4.1. The month information is used to determine the incident solar radiation, assuming clear-sky conditions, as described in Appendix D. The peak temperature would be the annual 0.4%, 1%, or 2% dry-bulb temperatures shown in columns 2c, 2e, and 2g, respectively, of Table 4.1. The daily dry-bulb temperature range for this day is given in column 2b and is used as described in the next section to determine the hourly dry-bulb temperatures for the design day. The mean coincident wind speed and direction corresponding to the 0.4% design condition are given in columns 2o and 2p and may be used to help estimate infiltration.

The above information is used to define a peak temperature design day that may often be sufficient for determining peak room cooling loads. However, peak room cooling loads may occur on days that are not peak temperature days for rooms with cooling loads dominated by solar radiation. For example, rooms with a significant amount of south-facing glass in temperate climates (e.g., Atlanta) might have peak cooling loads in the fall or winter. For this reason, peak temperatures are specified on a monthly basis, along with the mean coincident wet-bulb temperature in rows 17 to 24. As it is difficult beforehand to know in which month the cooling load will peak, it is recommended that months other than the peak temperature month be checked for rooms with significant amounts of glazing.

Finally, although peak room cooling load generally follows either peak temperatures or peak solar gains, peak system loads can often occur at peak wet-bulb temperatures. Therefore, it may also be prudent to calculate cooling loads for design wet-bulb conditions given in rows 25 to 32 of Table 4.1. Here, peak wet-bulb temperatures are given for each month, at four different percentiles. In this analysis, the peak dry-bulb temperature would be the mean coincident dry bulb given in rows 25 to 32.

4.2.2 Daily Temperature Profiles for Cooling Load Calculations

Table 4.1 gives peak design temperatures, but cooling load calculation procedures require hourly temperatures. However, with peak design temperatures and the corresponding daily temperature range taken from Table 4.1, hourly dry-bulb temperatures can be obtained by subtracting the daily temperature range multiplied by the fractions given in Table 4.2.

Load Calculation Applications Manual (SI), Second Edition

For example, as shown in Table 4.1, the 1% design condition in Atlanta is 33.1°C; the hottest month is July and the corresponding daily range (in column 2b) is 9.4°C. From Table 4.2, the fraction of daily range at 5:00 p.m. (hour 17) apparent solar time is 0.14, and the temperature at 5:00 p.m. would be 33.1°C – 0.14 · 9.4°C = 31.8°C. If, as is often the case, the load calculation is being performed on the basis of local standard time or local daylight savings time, the values in Table 4.2 can be interpolated using the corresponding apparent solar time at each hour.

Alternatively, an equation fit to the fraction-of-daily-range data in Table 4.2 can be used. This equation can be given as:

$$t = t_{peak} - DR \sum_{i=0}^{11} \left[a_i \cos\left(\frac{2\pi i \theta}{24}\right) + b_i \sin\left(\frac{2\pi i \theta}{24}\right) \right] \quad (4.1)$$

where

t = air temperature, °C

t_{peak} = peak design temperature, °C

DR = daily range, °C

a_i, b_i = equation-fit coefficients given in Table 4.3, dimensionless

θ = the apparent solar time in decimal form, dimensionless

Note that the argument for the cosine and sine functions are in units of radians. This equation has been used in the examples in Chapters 7 and 8.

Table 4.2 Fraction of Daily Temperature Range

(Source: ASHRAE Handbook—Fundamentals [2005], Chapter 28)

Time, h	f	Time, h	f	Time, h	f
1	0.88	9	0.55	17	0.14
2	0.92	10	0.38	18	0.24
3	0.95	11	0.23	19	0.39
4	0.98	12	0.13	20	0.5
5	1	13	0.05	21	0.59
6	0.98	14	0	22	0.68
7	0.91	15	0	23	0.75
8	0.74	16	0.06	24	0.82

Table 4.3 Coefficients for Equation 4.1

i	a_i	b_i
0	0.5363	0
1	0.3482	0.3426
2	-0.0732	-0.0491
3	0.002	-0.0194
4	0.0104	0.0123
5	-0.0041	0.0049
6	0.0025	-0.0017
7	-0.0004	-0.0027
8	-0.0038	0.0036
9	-0.0003	0.0006
10	0.0032	0
11	-0.0005	0.0002

Environmental Design Conditions

Hourly wet-bulb temperatures are also needed (e.g., for calculating hourly latent loads from infiltration or outdoor ventilation air). The peak wet-bulb temperatures would be taken from rows 17 to 24 or rows 25 to 32 of Table 4.1, depending on whether the analysis is using design dry-bulb or design wet-bulb conditions. The mean coincident wet-bulb range would be taken from row 35 (for design dry-bulb conditions) or row 37 (for design wet-bulb conditions) of Table 4.1. Hourly fractions from Table 4.2 are applied to the daily temperature range to find the hourly wet-bulb temperature. Alternatively, Equation 4.1 may be used with the appropriate inputs for peak wet-bulb temperature and wet-bulb daily range. Note that the temperature ranges apply to the 5% conditions; use at other peak temperature conditions may require some engineering judgment. Specifically, the wet-bulb temperature cannot be higher than the dry-bulb temperature. Other moist air properties can be determined using a psychrometric chart or the equations in Chapter 1 of the *ASHRAE Handbook—Fundamentals* (2013).

4.2.3 Heating Load Design Conditions

Like cooling loads, heating loads are transient because outdoor conditions are continuously changing. However, during the winter months, sustained periods of very cold and cloudy weather with relatively low levels of solar radiation may occur. In this situation, heat loss from the space will be relatively constant and, in the absence of internal heat gains, is likely to peak during the early morning hours. Therefore, for design purposes, heating losses are usually estimated based on steady-state heat transfer for some reasonable design temperature and solar radiation is neglected.

The 99.6% and 99.0% design conditions are given in columns 1b and 1c of Table 4.1. To calculate infiltration under the minimum temperature condition, columns 1n and 1o provide the mean wind speed and direction coincident to the 99.6% design dry-bulb temperature in column 1b. If the peak load were dominated by infiltration, it would also be useful to perform a heating load calculation under peak wind conditions. Columns 1j through 1m provide extreme wind speeds for the coldest month, with the mean coincident dry-bulb temperatures. To calculate the maximum latent loads due to infiltration, columns 1d through 1i provide 99.6% and 99.0% dew-point temperatures, the corresponding humidity ratios, and the mean coincident dry-bulb temperatures.

Minimum temperatures usually occur between 6:00 a.m. and 8:00 a.m. solar time on clear days when the daily range is greatest. Studies at several stations have found that the duration of extremely cold temperatures can continue below the 99% level for three days and below the 97.5% level for five days or more (ECP 1980; Snelling 1985; Crow 1963). This fact should be carefully considered in selecting the design temperature.

ASHRAE/IES Standard 90.1 stipulates that design temperatures shall not be less than the 99% temperatures. The mean of annual extremes, column 4e, may be used under unusual conditions to ensure the prevention of damage to the building or its contents. Generally, it is recommended that the 99% values be used and the 99.6% and mean of extremes be reserved for exceptionally harsh cases.

Load Calculation Applications Manual (SI), Second Edition

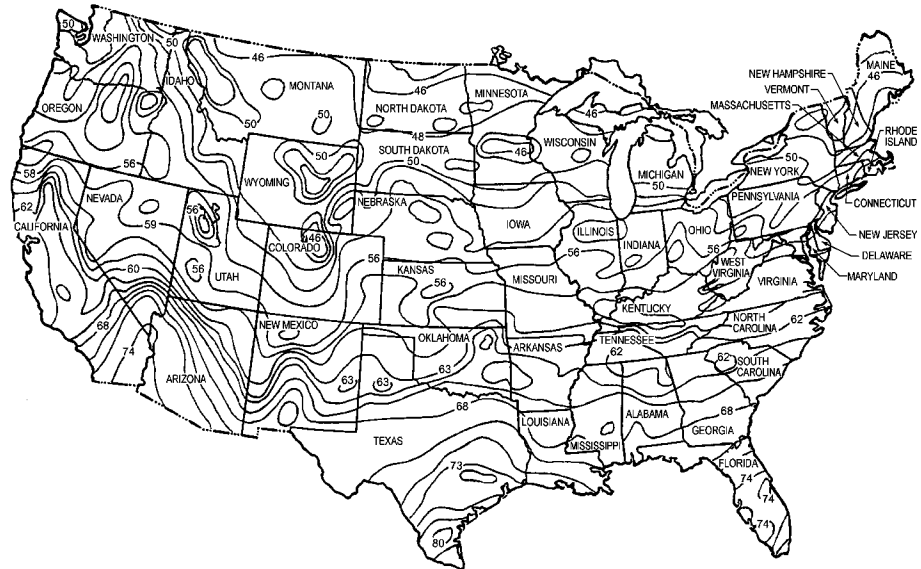


Figure 4.1. Approximate groundwater temperatures (°C) in the continental United States.

(Source: *ASHRAE Handbook—HVAC Applications* (2011), Chapter 34, Figure 17).

4.2.4 Data for Ground Heat Transfer

For below-grade walls and floors, the external design temperature is different than the design air temperatures because of the heat capacity of the soil. For the procedure described in Chapter 10, the external design temperature is the ground surface temperature. The ground surface temperature varies about a mean value by an amplitude A , which varies with geographic location and surface cover. Therefore, suitable external design temperatures can be obtained by subtracting A for the location from the mean ground temperature. The mean ground temperature may be approximated from the annual average air temperature or from well-water temperatures, which are shown in Figure 4.1 for the continental United States. The amplitude A can be estimated from the map in Figure 4.2. This map is part of one prepared by Chang (1958) giving annual ranges in ground temperature at a depth of 0.1 m.

References

- ASHRAE. 2010a. ANSI/ASHRAE/IES Standard 90.1-2010, *Energy Standard for Buildings Except Low-Rise Residential Buildings*. Atlanta: ASHRAE.
- ASHRAE. 2010b. ANSI/ASHRAE Standard 55-2004, *Thermal Environmental Conditions for Human Occupancy*. Atlanta: ASHRAE.
- ASHRAE. 2013. *ASHRAE Handbook—Fundamentals*. Atlanta: ASHRAE.
- ASHRAE. 2011. *ASHRAE Handbook—HVAC Applications*. Atlanta: ASHRAE.
- Chang, J.H. 1958. *Ground temperature*. Bluehill Meteorological Observatory, Harvard University, Cambridge, MA.

Environmental Design Conditions

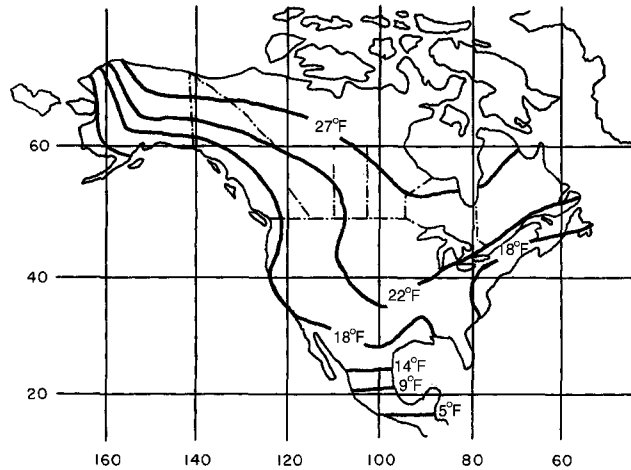


Figure 4.2. Ground temperature amplitude.

(Source: *ASHRAE Handbook—Fundamentals* [2013], Chapter 18, Figure 13).

Crow, L.W. 1963. *Research study of weather design conditions*. ASHRAE RP-23. Atlanta: ASHRAE.

Ecodyne Cooling. 1980. *Weather data handbook: For HVAC and cooling equipment/design*, 1st ed. New York: McGraw-Hill.

Snelling, H.J. 1985. Duration study for heating and air-conditioning design temperatures. *ASHRAE Transactions* 91(2b):242–47.

Load Calculation Applications Manual (SI), Second Edition

Table 4.4 Design Conditions for Chicago, Illinois

(Source: ASHRAE Handbook—Fundamentals [2013], accompanying CD)

2013 ASHRAE Handbook - Fundamentals (SI)

© 2013 ASHRAE, Inc.

CHICAGO/O'HARE ARPT, IL, USA

WMO#: 725300

Lat: 41.99N Long: 87.91W Elev: 205 StdP: 98.89 Time Zone: -6.00 (NAC) Period: 86-10 WBAN: 94846

Annual Heating and Humidification Design Conditions

Coldest Month	Heating DB			Humidification DP/MCDB and HR						Coldest month WS/MCDB				MCWS/PCWD to 99.6% DB	
	99.6%	99%		99.6%		99%				0.4%		1%		MCWS	PCWD
(a)	(b)	(c)	(d)	(e)	(f)	(g)	(h)	(i)	(j)	(k)	(l)	(m)	(n)	(o)	(p)
1	-18.6	-15.7	-24.0	0.4	-17.8	-21.1	0.6	-14.8	12.1	-0.5	11.1	-0.6	4.9	270	

Annual Cooling, Dehumidification, and Enthalpy Design Conditions

Hottest Month	Hottest Month DB Range	Cooling DB/MCWB						Evaporation WB/MCDB						MCWS/PCWD to 0.4% DB	
		0.4%		1%		2%		0.4%		1%		2%		MCWS	PCWD
(a)	(b)	(c)	(d)	(e)	(f)	(g)	(h)	(i)	(j)	(k)	(l)	(m)	(n)	(o)	(p)
7	10.2	33.0	23.5	31.5	22.9	30.0	22.1	25.4	31.0	24.4	29.4	23.5	28.0	5.1	220

DP	HR	MCDB	Dehumidification DP/MCDB and HR						Enthalpy/MCDB						Hours 8 to 4 & 12.8/20.6
			0.4%		1%		2%		0.4%		1%		2%		
(a)	(b)	(c)	(d)	(e)	(f)	(g)	(h)	(i)	(j)	(k)	(l)	(m)	(n)	(o)	(p)
23.7	19.0	28.7	22.8	18.0	27.6	22.0	17.0	26.5	78.8	31.1	74.8	29.4	70.8	28.1	619

Extreme Annual Design Conditions

Extreme Annual WS			Extreme Max WB	Extreme Annual DB				n-Year Return Period Values of Extreme DB							
1%	2.5%	5%		Mean	Standard deviation	n=5 years		n=10 years		n=20 years		n=50 years			
(a)	(b)	(c)	(d)	(e)	(f)	(g)	(h)	(i)	(j)	(k)	(l)	(m)	(n)	(o)	(p)
11.0	9.4	8.5	28.5	-22.2	35.6	3.2	2.0	-24.5	37.0	-26.4	38.1	-28.2	39.2	-30.5	40.7

Monthly Climatic Design Conditions

		Annual (d)	Jan	Feb	Mar	Apr	May	Jun	Jul	Aug	Sep	Oct	Nov	Dec
			(e)	(f)	(g)	(h)	(i)	(j)	(k)	(l)	(m)	(n)	(o)	(p)
Temperatures, Degree-Days and Degree-Hours	Tavg	10.2	-3.9	-2.1	3.5	9.6	15.2	20.7	23.4	22.5	18.3	11.5	4.8	-1.9
	Sd	6.35	5.86	5.90	5.24	4.81	4.24	3.23	3.29	4.19	4.92	5.25	5.89	
	HDD10.0	1648	432	341	216	68	7	0	0	0	1	42	170	372
	HDD18.3	3449	691	573	459	267	123	24	2	5	52	219	406	628
	CDD10.0	1723	1	1	16	57	169	322	417	388	250	87	14	1
	CDD18.3	480	0	0	1	5	27	97	160	134	51	6	0	0
	CDH23.3	4353	0	0	6	59	281	961	1512	1085	396	54	0	0
CDH26.7	1476	0	0	1	13	79	343	572	354	104	9	0	0	
Precipitation	PrecAvg	910	39	35	68	93	84	96	93	107	97	61	74	63
	PrecMax	1159	104	80	150	140	181	222	193	217	360	119	128	136
	PrecMin	528	7	6	26	25	35	40	30	17	1	5	16	8
	PrecSD	177.5	30.2	19.4	31.2	32.7	37.7	47.1	46.6	67.5	89.3	29.3	28.2	34.6
Monthly Design Dry Bulb and Mean Coincident Wet Bulb Temperatures	0.4%	DB	13.6	15.3	23.5	28.4	31.3	34.1	35.7	34.7	32.0	28.0	20.8	15.2
		MCWB	11.7	10.7	16.3	18.1	21.2	22.5	24.3	25.1	22.1	19.6	14.3	13.7
	2%	DB	9.1	11.2	19.8	24.7	28.9	32.3	33.4	32.2	29.4	24.5	17.7	11.1
		MCWB	6.8	7.8	14.1	16.4	20.3	22.3	24.3	24.0	20.8	17.4	13.6	8.6
	5%	DB	6.2	7.6	16.2	22.0	26.7	30.4	31.5	30.2	27.5	22.2	15.7	8.0
		MCWB	4.2	4.8	11.5	14.6	18.8	21.7	23.3	23.1	19.7	16.0	12.4	5.8
	10%	DB	3.9	5.3	12.8	18.8	24.0	28.5	29.9	28.4	25.7	19.6	13.0	5.5
		MCWB	2.4	3.2	8.9	12.7	17.4	21.0	22.5	21.9	18.9	14.9	9.7	3.6
Monthly Design Wet Bulb and Mean Coincident Dry Bulb Temperatures	0.4%	WB	12.0	11.8	17.6	19.3	23.5	25.2	26.9	26.5	23.9	21.1	16.4	13.9
		MCDB	13.0	12.9	22.5	26.0	29.1	31.0	32.7	32.4	28.7	25.7	18.4	15.0
	2%	WB	7.6	8.0	15.0	17.5	21.8	24.0	25.6	25.4	22.4	18.9	14.7	9.3
		MCDB	8.7	10.4	18.6	22.4	26.6	29.9	31.2	30.8	26.7	22.8	17.2	10.3
	5%	WB	4.5	5.2	12.1	15.5	20.2	23.0	24.7	24.2	21.4	17.1	12.6	5.9
		MCDB	5.9	7.4	15.9	21.2	24.7	28.2	29.8	28.4	25.4	21.0	15.2	7.7
	10%	WB	2.6	3.2	9.0	13.3	18.5	21.9	23.6	23.2	20.3	15.3	10.3	3.7
		MCDB	3.9	5.1	12.7	18.2	23.0	27.0	28.3	26.9	24.1	18.8	12.8	5.3
Mean Daily Temperature Range	5% DB	MDBR	7.4	7.7	9.1	10.4	11.1	11.1	10.2	9.5	10.4	9.9	8.0	7.1
		MCDBR	9.2	10.9	13.8	14.9	13.9	13.0	11.8	11.1	12.4	13.3	11.0	9.4
	5% WB	MCWBR	7.9	8.3	9.4	8.6	7.2	6.0	5.3	4.9	5.6	7.4	8.4	7.7
		MCDDBR	8.9	10.1	13.1	13.2	12.2	11.5	10.7	9.6	10.2	11.3	10.0	8.9
Clear Sky Solar Irradiance	taub	taub	0.288	0.305	0.325	0.359	0.369	0.383	0.415	0.416	0.392	0.344	0.306	0.294
		taud	2.524	2.474	2.473	2.343	2.310	2.285	2.209	2.242	2.343	2.487	2.629	2.584
	Ebn,noon	Ebn,noon	871	906	924	909	905	889	855	843	838	847	848	836
		Edh,noon	70	87	98	120	127	131	140	131	111	85	64	62

Nomenclature: See separate page

Environmental Design Conditions

Table 4.5 Design Conditions for Dallas, Texas

(Source: ASHRAE Handbook—Fundamentals [2013], accompanying CD)

2013 ASHRAE Handbook - Fundamentals (SI)

© 2013 ASHRAE, Inc.

DALLAS-FORT WORTH/F, TX, USA

WMO#: 722590

Lat: **32.90N** Long: **97.04W** Elev: **182** StdP: **99.16** Time Zone: **-6.00 (NAC)** Period: **86-10** WBAN: **03927**

Annual Heating and Humidification Design Conditions

Coldest Month	Heating DB		Humidification DP/MCDB and HR						Coldest month WS/MCDB				MCWS/PCWD to 99.6% DB	
	99.6%	99%	99.6%		99%		99%		0.4%		1%		MCWS	PCWD
	(a)	(b)	DP	HR	MCDB	DP	HR	MCDB	WS	MCDB	WS	MCDB		
(1) 1	(b) -5.0	(c) -2.6	(d) -12.8	(e) 1.3	(f) -1.1	(g) -10.3	(h) 1.6	(i) 1.4	(j) 12.9	(k) 11.0	(l) 11.9	(m) 11.3	(n) 5.3	(o) 350

Annual Cooling, Dehumidification, and Enthalpy Design Conditions

Hottest Month	Hottest Month DB Range	Cooling DB/MCWB						Evaporation WB/MCDB						MCWS/PCWD to 0.4% DB	
		0.4%		1%		2%		0.4%		1%		2%		MCWS	PCWD
		DB	MCWB	DB	MCWB	DB	MCWB	WB	MCDB	WB	MCDB	WB	MCDB		
(2) 7	(b) 10.7	(c) 38.0	(d) 23.6	(e) 37.0	(f) 23.7	(g) 35.8	(h) 23.9	(i) 25.9	(j) 33.1	(k) 25.5	(l) 32.7	(m) 25.1	(n) 32.1	(o) 4.5	(p) 180

	Dehumidification DP/MCDB and HR						Enthalpy/MCDB						Hours 8 to 4 & 12.820.6		
	0.4%		1%		2%		0.4%		1%		2%				
	DP	HR	MCDB	DP	HR	MCDB	DP	HR	MCDB	Enth	MCDB	Enth		MCDB	Enth
(3) 24.1	(b) 19.4	(c) 28.7	(d) 23.6	(e) 18.8	(f) 28.2	(g) 23.1	(h) 18.2	(i) 27.8	(j) 81.1	(k) 33.1	(l) 78.8	(m) 32.7	(n) 76.9	(o) 32.1	(p) 700

Extreme Annual Design Conditions

	Extreme Annual WS			Extreme Max WB	Extreme Annual DB						n-Year Return Period Values of Extreme DB					
	1%	2.5%	5%		Mean		Standard deviation		n=5 years		n=10 years		n=20 years		n=50 years	
	(a)	(b)	(c)		Min	Max	Min	Max	Min	Max	Min	Max	Min	Max	Min	Max
(4) 11.6	(b) 10.5	(c) 9.2	(d) 28.3	(e) -8.1	(f) 39.9	(g) 3.1	(h) 1.9	(i) -10.3	(j) 41.3	(k) -12.1	(l) 42.4	(m) -13.8	(n) 43.5	(o) -16.0	(p) 45.0	

Monthly Climatic Design Conditions

		Annual	Jan	Feb	Mar	Apr	May	Jun	Jul	Aug	Sep	Oct	Nov	Dec	
		(d)	(e)	(f)	(g)	(h)	(i)	(j)	(k)	(l)	(m)	(n)	(o)	(p)	
(5)	Tavg	19.2	8.3	10.3	14.3	18.8	23.5	27.5	29.7	29.7	25.7	19.9	13.8	8.8	
(6)	Std		5.45	5.64	5.17	4.07	3.42	2.44	2.08	2.65	3.60	4.35	5.19	5.37	
(7)	HDD10.0	286	97	59	21	1	0	0	0	0	0	1	21	86	
(8)	HDD18.3	1218	313	229	142	43	4	0	0	2	34	151	299		
(9)	CDD10.0	3658	45	68	154	264	418	526	610	612	471	307	136	48	
(10)	CDD18.3	1547	2	4	17	56	164	276	352	353	223	82	16	2	
(11)	CDH23.3	17941	13	41	134	437	1474	3194	4694	4740	2379	719	103	13	
(12)	CDH26.7	8851	1	8	23	100	539	1552	2603	2682	1093	233	15	2	
(13)	PrecAvg	886	52	60	77	85	118	83	59	55	76	93	63	58	
(14)	PrecMax	1048	91	157	162	273	228	176	283	174	242	194	158	177	
(15)	PrecMin	587	3	4	3	34	25	10	2	1	22	6	5	6	
(16)	PrecSD	146.5	30.3	38.5	47.5	55.3	61.0	55.5	65.7	45.0	60.9	57.4	39.8	37.3	
(17)	Monthly Design Dry Bulb and Mean Coincident Wet Bulb Temperatures	0.4%	DB	25.1	27.5	29.3	32.4	35.1	37.4	39.4	40.0	37.6	33.2	28.6	25.2
(18)			MCWB	15.7	15.8	18.5	19.7	23.4	24.0	23.5	23.4	23.2	21.3	19.0	16.7
(19)		2%	DB	22.1	24.0	26.5	29.1	33.0	36.0	37.9	38.4	35.3	31.3	26.2	22.1
(20)			MCWB	14.7	15.2	17.4	19.9	22.9	24.2	23.7	23.6	23.1	21.0	18.2	16.2
(21)		5%	DB	19.8	21.8	24.6	27.5	31.3	34.5	36.8	37.3	33.8	29.2	24.1	19.8
(22)			MCWB	14.7	15.1	17.0	19.3	22.6	24.0	23.8	23.7	22.9	20.1	17.7	15.2
(23)	10%	DB	17.6	19.4	22.6	25.9	29.7	33.2	35.4	36.0	32.3	27.4	22.2	17.7	
(24)		MCWB	12.7	14.2	16.3	18.6	22.1	23.9	24.0	23.8	22.5	19.4	17.0	13.3	
(25)	Monthly Design Wet Bulb and Mean Coincident Dry Bulb Temperatures	0.4%	WB	19.0	19.3	21.1	23.4	25.7	26.9	26.8	26.2	25.5	24.3	21.7	19.6
(26)			MCDB	21.4	22.7	25.9	28.1	31.6	33.6	33.7	33.7	32.1	28.6	24.7	22.3
(27)		2%	WB	17.6	18.1	20.0	22.0	24.6	25.9	25.8	25.6	24.8	23.2	20.3	18.2
(28)			MCDB	19.8	21.2	24.0	26.5	30.1	32.6	33.3	33.3	31.2	27.8	23.9	20.6
(29)		5%	WB	15.7	16.7	18.8	21.1	23.9	25.3	25.4	25.1	24.3	22.2	19.1	16.4
(30)			MCDB	18.7	20.5	22.5	25.1	29.0	31.8	32.9	32.9	30.2	26.6	22.8	18.9
(31)	10%	WB	13.3	14.7	17.6	20.3	23.1	24.7	24.9	24.7	23.8	21.1	17.8	13.8	
(32)		MCDB	16.3	18.6	21.3	24.1	28.1	30.9	32.2	32.4	29.5	25.5	21.2	17.0	
(33)	Mean Daily Temperature Range	MDBR	10.8	10.9	11.3	11.2	10.1	10.3	10.7	10.8	10.8	11.5	10.8	10.5	
(34)		5% DB	MCDBR	14.7	14.7	13.6	12.6	11.5	11.4	12.0	12.2	11.9	13.3	12.7	
(35)			MCWBR	9.1	8.6	7.3	6.5	4.5	3.5	3.1	3.1	3.8	5.8	6.9	
(36)		5% WB	MCDBR	11.1	11.9	10.5	10.1	9.9	10.4	10.5	10.8	9.8	10.2	10.4	
(37)	MCWBR		8.5	8.7	7.4	6.4	5.0	3.9	3.4	3.2	3.6	5.6	7.2		
(38)	Clear Sky Solar Irradiance	taub	0.332	0.329	0.359	0.367	0.376	0.384	0.403	0.385	0.373	0.361	0.338	0.333	
(39)		taud	2.588	2.570	2.431	2.379	2.350	2.348	2.326	2.405	2.465	2.494	2.578	2.586	
(40)		Ebn,noon	890	929	919	921	910	898	879	893	892	878	874	867	
(41)		Edb,noon	80	89	110	121	125	125	128	116	105	95	80	76	

Nomenclature: See separate page

Load Calculation Applications Manual (SI), Second Edition

Table 4.6 Design Conditions for Los Angeles, California

(Source: ASHRAE Handbook—Fundamentals [2013], accompanying CD)

2013 ASHRAE Handbook - Fundamentals (SI)

© 2013 ASHRAE, Inc.

LOS ANGELES INTL, CA, USA

WMO#: 722950

Lat: 33.94N Long: 118.41W Elev: 99 StdP: 100.14 Time Zone: -8.00 (NAP) Period: 86-10 WBAN: 23174

Annual Heating and Humidification Design Conditions																
Coldest Month	Heating DB		Humidification DP/MCDB and HR						Coldest month WS/MCDB				MCWS/PCWD to 99.6% DB			
	99.6%	99%	99.6%		99%		0.4%		1%		MCWS	PCWD				
(a)	(b)	(c)	DP	HR	MCDB	DP	HR	MCDB	WS	MCDB	WS	MCDB	(n)	(o)		
(1) 12	7.0	8.0	-11.3	1.4	15.4	-8.0	1.9	15.3	11.2	12.8	9.3	13.5	2.2	80		
Annual Cooling, Dehumidification, and Enthalpy Design Conditions																
Hottest Month	Hottest DB Range	Cooling DB/MCWB						Evaporation WB/MCDB						MCWS/PCWD to 0.4% DB		
		0.4%		1%		2%		0.4%		1%		2%		MCWS	PCWD	
(a)	(b)	DB	MCWB	DB	MCWB	DB	MCWB	WB	MCDB	WB	MCDB	WB	MCDB	(n)	(p)	
(2) 8	5.9	28.7	17.4	26.9	17.5	25.3	17.9	21.1	25.1	20.4	24.2	19.8	23.4	4.0	250	
Dehumidification DP/MCDB and HR																
		0.4%						1%						Hours 8 to 4 & 12.8/20.6		
		DP	HR	MCDB	DP	HR	MCDB	DP	HR	MCDB	Enth	MCDB	Enth	MCDB	Enth	MCDB
(3) 19.6	14.5	23.2	18.9	13.9	22.5	18.3	13.3	21.8	61.4	25.3	58.9	24.1	56.8	23.5	1874	
Extreme Annual Design Conditions																
Extreme Annual WS			Extreme Max WB	Extreme Annual DB						n-Year Return Period Values of Extreme DB						
1%	2.5%	5%		Mean	Standard deviation	n=5 years		n=10 years		n=20 years		n=50 years				
(a)	(b)	(c)	(d)	(e)	(f)	(g)	(h)	(i)	(j)	(k)	(l)	(m)	(n)	(o)	(p)	
(4) 8.9	7.8	7.1	24.0	4.3	34.5	1.5	2.7	3.2	36.4	2.4	38.0	1.5	39.5	0.5	41.4	
Monthly Climatic Design Conditions																
		Annual	Jan	Feb	Mar	Apr	May	Jun	Jul	Aug	Sep	Oct	Nov	Dec		
(5) Temperatures, Degree-Days and Degree-Hours	Tavg	(d) 17.2	(e) 14.2	(f) 14.2	(g) 14.8	(h) 16.0	(i) 17.3	(j) 18.8	(k) 20.5	(l) 20.9	(m) 20.4	(n) 19.0	(o) 16.7	(p) 14.1		
	Sd	2.69	2.63	2.28	2.58	1.78	1.57	1.57	1.74	2.06	2.37	2.67	2.47			
	HDD10.0	4	1	1	0	0	0	0	0	0	0	0	0	2		
	HDD18.3	719	134	119	113	81	42	11	1	2	17	64	134			
	CDD10.0	2649	129	119	151	179	226	264	325	337	313	279	199	127		
	CDD18.3	323	4	4	4	10	9	25	68	79	66	37	14	2		
	CDH23.3	914	30	29	31	66	25	38	98	166	171	156	90	15		
	CDH26.7	188	4	6	7	22	5	6	8	22	36	48	24	1		
	(13) Precipitation	PrecAvg	317	68	78	49	19	2	2	1	1	6	10	35	45	
		PrecMax	2225	162	162	161	175	192	205	227	234	235	203	183	161	
		PrecMin	1854	106	10	1	3	1	164	3	159	159	156	136	100	
		PrecSD	93.0	12.4	31.5	34.4	45.2	50.6	11.8	46.3	17.5	17.8	13.9	13.6	16.9	
(17) Monthly Design Dry Bulb and Mean Coincident Wet Bulb Temperatures	0.4%	DB	27.0	27.2	27.2	29.4	26.5	27.1	27.7	29.1	30.6	31.8	29.7	25.4		
		MCWB	13.0	14.2	13.7	15.2	17.6	19.2	21.4	20.8	18.7	15.9	15.1	12.0		
	2%	DB	23.2	23.0	22.6	24.5	22.9	24.0	25.6	26.6	27.1	27.4	25.9	22.4		
		MCWB	12.3	12.8	12.9	14.9	17.6	18.3	20.0	20.3	19.5	15.6	13.7	11.8		
	5%	DB	20.9	20.3	20.0	21.8	21.5	22.7	24.2	25.0	25.1	24.3	23.1	20.2		
		MCWB	11.5	12.2	13.2	14.9	16.8	17.9	19.5	19.8	19.4	16.3	12.9	11.3		
	10%	DB	18.4	17.9	18.1	19.6	20.3	21.7	23.2	23.8	23.6	22.3	21.0	18.2		
		MCWB	11.2	12.0	13.3	14.7	16.3	17.4	19.0	19.3	18.8	16.4	13.0	11.1		
	(25) Monthly Design Wet Bulb and Mean Coincident Dry Bulb Temperatures	0.4%	WB	16.1	16.4	16.6	18.1	20.0	20.0	21.9	21.9	21.8	20.0	17.9	15.9	
			MCDB	18.9	20.6	20.4	23.7	23.7	25.2	25.9	27.3	26.7	24.9	21.8	18.1	
		2%	WB	15.1	15.3	15.6	16.8	18.3	19.0	20.9	21.0	20.7	19.0	16.8	15.1	
			MCDB	17.6	18.0	18.9	21.3	21.7	23.3	24.2	25.1	24.7	22.8	20.0	17.1	
5%		WB	14.3	14.6	15.0	15.8	17.5	18.3	20.1	20.3	20.0	18.3	16.1	14.3		
		MCDB	16.6	17.0	17.8	19.6	20.6	22.1	23.4	24.0	23.9	21.4	19.0	16.4		
10%		WB	13.6	13.9	14.3	15.2	16.8	17.8	19.4	19.6	19.2	17.7	15.4	13.6		
		MCDB	16.0	16.3	16.8	18.6	19.6	21.1	22.6	23.1	22.8	20.5	18.4	15.9		
(33) Mean Daily Temperature Range		5% DB	MDBR	8.5	7.6	6.9	6.9	6.0	5.6	5.6	5.9	6.2	7.1	8.7	8.6	
			MCDDBR	13.0	12.2	10.8	10.9	7.7	7.0	6.6	7.3	8.6	11.6	12.9	12.1	
		5% WB	MCWBR	6.6	6.2	5.6	5.2	3.7	3.2	2.9	3.1	3.5	5.2	6.7	6.8	
			MCDWBR	7.9	8.0	7.3	8.2	6.7	6.7	6.3	6.9	7.6	8.1	8.8	8.3	
	5% WB	MCWBR	4.9	4.7	4.3	4.4	3.5	3.2	2.9	3.0	3.3	4.0	5.3	5.4		
		MCDWBR	4.9	4.7	4.3	4.4	3.5	3.2	2.9	3.0	3.3	4.0	5.3	5.4		
(38) Clear Sky Solar Irradiance	tau _{0.1}		0.334	0.344	0.338	0.326	0.338	0.337	0.349	0.359	0.346	0.344	0.333	0.330		
	tau _{0.2}		2.634	2.570	2.541	2.512	2.448	2.413	2.428	2.444	2.535	2.542	2.620	2.621		
	E _{bn,noon}		883	908	939	960	945	941	928	915	917	894	876	865		
	E _{dn,noon}		76	88	98	105	114	117	115	111	97	89	76	73		

Nonindicated: See separate page

Environmental Design Conditions

Table 4.7 Design Conditions for New York City, New York

(Source: ASHRAE Handbook—Fundamentals [2013], accompanying CD)

2013 ASHRAE Handbook - Fundamentals (SI)

© 2013 ASHRAE, Inc.

NEW YORK/JOHN F. KE, NY, USA

WMO#: 744860

Lat: **40.66N** Long: **73.80W** Elev: **7** StP: **101.24** Time Zone: **-5.00 (NAE)** Period: **86-10** WBAN: **94789**

Annual Heating and Humidification Design Conditions

Coldest Month	Heating DB			Humidification DP/MCDB and HR						Coldest month WS/MCDB				MCWS/PCWD to 99.6% DB	
	99.6%	99%	(c)	99.6%			99%			0.4%		1%		MCWS	PCWD
				DP	HR	MCDB	DP	HR	MCDB	WS	MCDB	WS	MCDB		
(1) 1	(b) -10.1	(e) -7.9	(d) -20.9	(o) 0.6	(f) -8.5	(g) -18.7	(h) 0.7	(i) -6.2	(j) 14.2	(k) -1.3	(l) 12.8	(m) -0.9	(n) 7.4	(p) 310	

Annual Cooling, Dehumidification, and Enthalpy Design Conditions

Hottest Month	Hottest DB Range	Cooling DB/MCWB						Evaporation WB/MCDB						MCWS/PCWD to 0.4% DB	
		0.4%		1%		2%		0.4%		1%		2%		MCWS	PCWD
		DB	MCWB	DB	MCWB	DB	MCWB	WB	MCDB	WB	MCDB	WB	MCDB		
(2) 7	7.4	32.1	22.7	30.3	22.1	28.7	21.7	24.8	28.8	24.1	27.6	23.5	26.7	5.8	230

	Dehumidification DP/MCDB and HR						Enthalpy/MCDB						Hours 8 to 4 & 12 R/20.6		
	0.4%		1%		2%		0.4%		1%		2%				
	DP	HR	MCDB	DP	HR	MCDB	DP	HR	MCDB	Enth	MCDB	Enth		MCDB	Enth
(3) 23.6	18.5	26.7	23.0	17.7	25.9	22.4	17.1	25.3	75.2	29.0	72.3	27.8	69.7	26.6	753

Extreme Annual Design Conditions

	Extreme Annual WS			Extreme Max WB	Extreme Annual DB				n-Year Return Period Values of Extreme DB							
	1%	2.5%	5%		Mean		Standard deviation		n=5 years		n=10 years		n=20 years		n=50 years	
					Min	Max	Min	Max	Min	Max	Min	Max	Min	Max	Min	Max
(4) 12.2	11.0	9.7	28.0	-12.9	35.4	2.5	1.8	-14.7	36.7	-16.1	37.7	-17.5	38.7	-19.4	40.0	

Monthly Climatic Design Conditions

		Annual (d)	Jan	Feb	Mar	Apr	May	Jun	Jul	Aug	Sep	Oct	Nov	Dec
			(e)	(f)	(g)	(h)	(i)	(j)	(k)	(l)	(m)	(n)	(o)	(p)
(5) Temperatures, Degree-Days and Degree-Hours	Tavg	12.5	0.8	1.5	5.3	10.6	15.8	21.2	24.2	23.8	20.1	13.8	8.6	3.1
	Sd	5.05	4.32	4.32	3.62	3.60	3.30	2.67	2.66	3.18	3.81	4.05	4.52	
	HDD10.0	1013	286	240	154	34	1	0	0	0	9	74	217	
	HDD18.3	2691	543	473	403	233	98	11	0	1	18	147	293	471
	CDD10.0	1912	1	1	9	52	179	337	441	427	302	128	31	4
	CDD18.3	547	0	0	0	2	18	97	183	169	70	8	0	0
	CDH23.3	3412	0	0	2	15	123	564	1310	1096	278	24	0	0
	CDH26.7	921	0	0	0	3	34	161	399	276	43	4	0	0
(13) Precipitation	PrecAvg	1056	81	77	91	99	97	93	97	87	84	73	93	87
	PrecMax	1440	212	124	207	191	164	179	215	211	245	127	242	156
	PrecMin	649	14	27	34	32	16	5	14	11	24	4	8	23
	PrecSD	186.3	51.0	28.4	37.2	41.9	38.4	42.9	58.9	54.8	58.0	30.5	61.6	42.6
(17) Monthly Design Dry Bulb and Mean Coincident Wet Bulb Temperatures	0.4%	DB	13.5	15.3	20.6	25.4	30.5	33.2	35.3	33.7	30.4	26.5	19.7	16.1
	MCWB	10.7	8.8	12.6	15.6	20.6	22.9	24.6	23.6	21.5	19.6	15.1	12.2	
	2%	DB	11.3	11.0	15.9	21.3	26.7	30.8	32.4	31.2	27.7	23.0	17.4	13.0
	MCWB	9.7	7.3	9.8	13.4	18.6	22.0	23.0	22.7	20.5	18.3	14.2	10.8	
	5%	DB	9.4	9.1	13.1	18.5	23.8	28.3	30.5	29.4	26.2	21.3	16.0	11.3
	MCWB	7.4	6.3	8.5	11.7	17.2	20.7	22.2	22.5	20.3	17.4	13.6	9.4	
	10%	DB	7.6	7.5	11.2	16.2	21.7	26.4	28.7	28.0	24.8	19.7	14.7	9.6
	MCWB	5.4	5.1	7.8	10.6	16.1	20.1	21.9	21.8	19.9	16.3	12.5	7.4	
(25) Monthly Design Wet Bulb and Mean Coincident Dry Bulb Temperatures	0.4%	WB	12.0	10.6	14.2	17.2	22.0	24.6	26.0	25.7	24.2	21.5	17.0	13.5
	MCDB	12.7	12.3	17.9	23.0	27.9	30.2	31.5	30.5	26.5	23.9	18.0	15.0	
	2%	WB	10.2	8.5	11.4	15.0	20.1	23.4	25.0	24.8	23.1	20.0	15.4	11.5
	MCDB	11.0	10.1	13.8	19.1	24.8	28.1	29.2	28.3	25.0	22.2	16.5	12.6	
	5%	WB	7.9	6.9	10.0	13.2	18.5	22.4	24.2	24.1	22.4	18.5	14.2	9.9
	MCDB	9.1	8.4	12.3	16.7	22.4	26.3	28.0	27.1	24.3	20.4	15.6	11.1	
	10%	WB	5.8	5.3	8.5	11.8	17.1	21.4	23.5	23.5	21.5	17.0	12.9	7.8
	MCDB	7.3	7.4	10.5	14.5	20.5	24.8	26.9	26.4	23.7	18.9	14.4	9.1	
(33) Mean Daily Temperature Range	5% DB	MDBR	6.6	7.1	7.7	8.0	8.2	7.9	7.4	7.2	7.4	7.6	6.9	6.4
	MCDBR	8.1	8.9	10.6	11.7	11.8	10.7	9.5	8.5	8.3	8.9	7.9	8.3	
	MCWBR	7.0	6.9	6.6	6.1	5.8	4.8	4.1	4.2	4.4	5.8	6.6	7.7	
	5% WB	MDBR	8.0	8.4	9.6	9.9	10.8	9.3	7.9	7.1	6.7	7.7	7.1	7.8
	MCWBR	7.8	7.6	7.3	6.2	6.1	4.9	3.9	3.9	4.5	6.1	6.9	8.4	
(38) Clear Sky Solar Irradiance	taob	0.339	0.333	0.363	0.391	0.418	0.458	0.434	0.439	0.403	0.352	0.329	0.325	
	taod	2.470	2.481	2.402	2.297	2.179	2.079	2.188	2.197	2.331	2.498	2.567	2.568	
	Ebrnoon	815	882	888	881	861	824	841	825	833	848	825	807	
	Edlnoon	78	89	107	127	146	162	144	138	113	86	71	67	

Nomenclature: See separate page

Load Calculation Applications Manual (SI), Second Edition

Table 4.8 Design Conditions for Seattle, Washington

(Source: ASHRAE Handbook—Fundamentals [2013], accompanying CD)

2013 ASHRAE Handbook - Fundamentals (SI)

© 2013 ASHRAE, Inc.

SEATTLE-TACOMA INTL, WA, USA

WMO#: 727930

Lat: 47.46N Long: 122.31W Elev: 132 StDp: 99.75 Time Zone: -8.00 (NAP) Period: 86-10 WBAN: 24233

Annual Heating and Humidification Design Conditions

Coldest Month	Heating DB		Humidification DP/MCDB and HR							Coldest month WS/MCDB				MCWS/PCWD to 99.6% DB	
	99.6%	99%	99.6%			99%				0.4%		1%		MCWS	PCWD
			DP	HR	MCDB	DP	HR	MCDB	WS	MCDB	WS	MCDB			
(a)	(b)	(c)	(d)	(e)	(f)	(g)	(h)	(i)	(j)	(k)	(l)	(m)	(n)	(o)	(p)
(1) 12	-3.8	-1.3	-12.4	1.3	0.0	-8.7	1.8	1.9	12.0	6.8	10.8	7.3	4.0	10	

Annual Cooling, Dehumidification, and Enthalpy Design Conditions

Hottest Month	Hottest Month DB Range	Cooling DB/MCWB						Evaporation WB/MCDB						MCWS/PCWD to 0.4% DB	
		0.4%		1%		2%		0.4%		1%		2%		MCWS	PCWD
		DB	MCWB	DB	MCWB	DB	MCWB	WB	MCDB	WB	MCDB	WB	MCDB		
(a)	(b)	(c)	(d)	(e)	(f)	(g)	(h)	(i)	(j)	(k)	(l)	(m)	(n)	(o)	(p)
(2) 8	10.4	29.6	18.4	27.6	17.6	25.7	17.0	19.3	28.1	18.3	26.1	17.4	24.5	4.1	350

Dehumidification DP/MCDB and HR											Enthalpy/MCDB					Hours 8 to 4 & 12.8/20.6
0.4%			1%			2%					0.4%		1%		2%	
DP	HR	MCDB	DP	HR	MCDB	DP	HR	MCDB	Enth	MCDB	Enth	MCDB	Enth	MCDB		
(a)	(b)	(c)	(d)	(e)	(f)	(g)	(h)	(i)	(j)	(k)	(l)	(m)	(n)	(o)	(p)	
(3) 16.1	11.6	21.1	15.2	11.0	20.0	14.5	10.5	19.5	55.2	28.3	52.0	25.9	49.3	24.4	1107	

Extreme Annual Design Conditions

Extreme Annual WS			Extreme Max WB	Extreme Annual DB				n-Year Return Period Values of Extreme DB									
1%	2.5%	5%		Mean	Standard deviation	n=5 years		n=10 years		n=20 years		n=50 years					
(a)	(b)	(c)		(d)	(e)	(f)	(g)	(h)	(i)	(j)	(k)	(l)	(m)	(n)	(o)	(p)	
(4) 9.1	8.1	7.3	28.4	-6.0	34.0	3.1	2.4	-8.2	35.7	-10.0	37.0	-11.8	38.4	-14.0	40.1		

Monthly Climatic Design Conditions

		Annual (d)	Jan	Feb	Mar	Apr	May	Jun	Jul	Aug	Sep	Oct	Nov	Dec		
			(e)	(f)	(g)	(h)	(i)	(j)	(k)	(l)	(m)	(n)	(o)	(p)		
(5)	Temperatures, Degree-Days and Degree-Hours	Tavg	11.5	5.6	6.3	7.9	10.2	13.3	16.0	18.7	18.8	16.3	11.6	7.6	5.0	
(6)		Sd	3.17	3.05	2.60	2.77	3.07	2.92	2.92	2.39	2.63	2.61	2.94	3.20		
(7)		HDD10.0	606	140	107	74	30	4	0	0	0	13	81	156		
(8)		HDD18.3	2614	396	338	323	245	161	84	30	22	71	208	323	413	
(9)		CDD10.0	1140	2	3	10	35	106	179	268	272	191	63	9	2	
(10)		CDD18.3	104	0	0	0	0	3	13	40	37	12	0	0	0	
(11)		CDH23.3	1019	0	0	0	6	47	148	391	316	107	4	0	0	
(12)		CDH26.7	280	0	0	0	0	8	43	127	81	21	1	0	0	
(13)		Precipitation	PrecAvg	95.2	141	95	92	66	45	37	18	29	41	84	157	146
(14)			PrecMax	1243	248	231	181	106	94	97	38	117	151	197	246	301
(15)	PrecMin		58.2	45	40	14	14	10	11	2	1	5	18	19	35	
(16)	PrecSD		165.6	58.2	51.1	42.6	26.0	22.1	24.0	11.0	35.1	40.2	46.5	64.2	60.9	
(17)	Monthly Design Dry Bulb and Mean Coincident Wet Bulb Temperatures	0.4%	DB	13.8	16.4	18.9	23.8	27.7	31.3	33.8	31.5	28.9	22.8	16.1	13.4	
(18)			MCWB	9.9	9.8	11.0	13.4	16.9	17.8	20.3	19.5	17.8	14.2	12.5	11.6	
(19)		2%	DB	12.2	13.7	16.0	20.0	24.2	27.4	29.9	28.8	26.4	19.3	13.9	11.5	
(20)			MCWB	9.2	9.0	10.1	12.4	15.7	17.0	18.9	18.4	16.8	13.5	11.6	9.3	
(21)		5%	DB	10.9	12.1	13.8	17.4	21.5	24.4	27.4	27.0	23.9	17.3	12.6	10.2	
(22)			MCWB	8.8	8.7	9.3	11.3	14.2	15.9	17.9	17.7	16.3	13.0	10.7	8.3	
(23)		10%	DB	9.8	10.6	12.2	15.2	18.9	22.0	25.1	24.7	21.8	15.6	11.6	9.1	
(24)			MCWB	7.9	7.7	8.7	10.3	13.3	15.1	17.1	17.0	15.3	12.4	9.9	7.4	
(25)		Monthly Design Wet Bulb and Mean Coincident Dry Bulb Temperatures	0.4%	WB	12.2	12.1	12.5	15.1	17.8	19.1	21.3	20.5	18.9	16.2	13.6	12.1
(26)				MCDB	12.9	13.6	16.0	20.2	25.5	28.8	31.8	29.0	26.7	19.4	14.7	13.0
(27)	2%		WB	10.3	10.6	11.2	13.2	16.3	17.5	19.7	19.1	17.6	14.8	12.3	10.1	
(28)			MCDB	11.2	12.2	14.0	18.1	22.7	25.8	28.9	27.3	24.6	17.6	13.3	11.0	
(29)	5%		WB	9.2	9.2	10.3	12.0	15.1	16.4	18.5	18.2	16.7	13.8	11.3	8.9	
(30)			MCDB	10.2	11.0	13.0	16.0	20.5	23.3	26.4	25.6	22.8	16.1	12.3	9.9	
(31)	10%		WB	8.0	8.1	9.2	10.9	13.8	15.4	17.4	17.3	15.8	12.8	10.3	7.8	
(32)			MCDB	9.2	9.9	11.6	14.2	18.2	21.2	24.3	23.9	20.8	14.9	11.4	8.8	
(33)	Mean Daily Temperature Range		MDBR	4.9	6.5	7.1	8.1	8.7	9.1	10.4	10.4	9.4	6.8	5.3	4.8	
(34)				MCDDBR	5.8	8.6	10.2	12.0	13.3	13.9	14.4	14.2	13.4	9.8	6.1	5.2
(35)		5% DB	MCWBR	4.1	5.1	5.6	6.1	6.3	6.0	5.8	5.7	5.1	4.1	4.0		
(36)			MCDWBR	4.8	6.9	8.5	10.4	11.7	12.6	13.6	12.9	12.1	8.0	5.1	4.7	
(37)		5% WB	MCWBR	4.1	4.7	5.2	5.5	6.1	5.8	5.8	5.5	5.4	4.6	4.1	4.2	
(38)			MCDWBR	4.8	6.9	8.5	10.4	11.7	12.6	13.6	12.9	12.1	8.0	5.1	4.7	
(39)	Clear Sky Solar Irradiance	taub	0.312	0.313	0.321	0.329	0.330	0.323	0.318	0.323	0.341	0.322	0.320	0.312		
(40)		taud	2.600	2.586	2.526	2.459	2.440	2.464	2.512	2.546	2.522	2.603	2.615	2.585		
(41)		Ebn,noon	787	866	907	926	933	938	939	922	872	841	770	740		
		Edb,noon	59	72	88	103	109	107	101	93	87	70	57	54		

Nomenclature: See separate page

5 Infiltration

It is practically impossible to accurately predict infiltration on theoretical grounds. However, it is possible to develop relationships to describe the general nature of the problem. With experience and some experimental data, it is possible to put these relations in convenient tabular and graphical form, which can be useful in estimating infiltration rates. Much of the following material describes how the graphs herein were made and the restrictions placed upon them.

Infiltration is caused by a greater air pressure on the outside of the building than on the inside. The amount of infiltrated air depends on this pressure difference; the number, the size, and the shape of the cracks involved; the number, the length, and the width of the perimeter gaps of windows and doors; and the nature of the flow in the crack or gap (laminar or turbulent). The relation connecting these quantities is

$$Q = C(\Delta p)^n \quad (5.1)$$

where

Q = flow rate of leaking air, L/s

Δp = pressure difference between the inside and the outside surfaces of the building, Pa. When the outside pressure is greater than the inside pressure, Q , a positive value, is the flow rate of air leaking into the building. If the inside pressure exceeds the outside pressure, Q is the flow rate of exfiltrating air.

n = flow exponent. If the flow in the crack is laminar, $n = 1.0$; if turbulent, $n = 0.50$. Usually, the flow will be transitional, thus, n will be between 0.5 and 1.0. Small hairline cracks tend to have values of n of 0.8 to 0.9, whereas cracks or openings of 3 mm or greater will have complete turbulent flow, thus, n will be 0.5.

C = flow coefficient. C is determined experimentally and includes the crack or opening size (area).

The pressure difference Δp is given by

$$\Delta p = \Delta p_s + \Delta p_w + \Delta p_p \quad (5.2)$$

where

Δp_s = pressure difference caused by the stack effect, Pa

Δp_w = pressure difference caused by wind, Pa

Δp_p = pressure difference caused by pressurizing the building, Pa

The pressure differences Δp_s , Δp_w , and Δp_p are positive when, acting separately, each would cause infiltration ($p_{out} - p_{in}) > 0$.

Experienced engineers and designers often estimate infiltration by the air change method. This method simply requires an estimation of the number of air changes per hour (ACH) that a space will experience based on their appraisal of the building type, construction, and use. The infiltration rate is related to ACH and space volume as follows:

$$Q = \text{ach} \cdot \text{VOL} \cdot (1000/3600) \quad (5.3)$$

where

Q = infiltration rate, L/s

VOL = gross space volume, m³

Load Calculation Applications Manual (SI), Second Edition

Once the flow rate of infiltration has been determined, the resulting loads can be determined as discussed in Section 5.1. To use the detailed approach represented by Equations 5.1 and 5.2, the pressure differences that drive infiltration must be determined as described in Section 5.2. Coefficients for Equation 5.1 appropriate for various infiltration paths are summarized in Section 5.3. Section 5.4 discusses considerations for low-rise buildings.

5.1 Infiltration and Outdoor Ventilation Air Loads

Infiltration is the uncontrolled flow of air through unintentional openings such as cracks in the walls and ceilings and through the perimeter gaps of windows and doors driven by wind, temperature difference, and internally induced pressures. The flow of the air into a building through doorways resulting from normal opening and closing also is generally considered infiltration. The flow of air leaving the building by these means is called exfiltration. There are situations where outdoor air is intentionally supplied directly to the space for ventilation purposes. In this case, the outdoor air produces a heating or cooling load on the space in the same way as infiltration air.

In most modern systems, however, outdoor air is introduced through the air heating and cooling system where it is mixed with recirculated air, conditioned, and then supplied to the space. Confusion often results when both the air from outdoors and the air supplied to the space are referred to as *ventilation air*. It is becoming more common to associate ventilation with indoor air quality, and this usage, which is compatible with ANSI/ASHRAE Standard 62.1-2007, *Ventilation for Acceptable Indoor Air Quality*, will be used herein. *Ventilation* is the intentional distribution of air throughout a building and is generally a mixture of filtered outdoor and recirculated air. Infiltration air produces a load on the space while the outdoor air introduced through the air heating and cooling system produces a load on the heating or cooling coil. Therefore, the load due to outdoor air introduced through the system should be considered during the psychrometric analysis when supply air quantities, coil sizes, etc. are computed. This procedure is discussed in Chapter 9 and Appendix A.

For summer conditions, the infiltrating air has to be cooled to the desired space temperature. This represents a cooling load and must be included in the room cooling load. Assuming standard air, the equation for the sensible load is

$$q_s = C_s Q \Delta t \quad (5.4)$$

where

C_s = sensible heat factor, (W · s)/(L · K); 1.23 is a typical value

Δt = temperature difference between outdoor air and indoor air, °C

A more complete explanation of this equation, which accounts for local pressure and temperature, is given in Chapter 9. By a similar analysis, Equation 5.4 can be used to determine the heating load caused by infiltrating air. For low-humidity winter weather at standard conditions, the value of 1.23 is usually replaced by 1.21.

For summer conditions, some of the water vapor in the infiltrating air is ultimately condensed on the cooling system coils and, thus, constitutes a part of the space-cooling load. The equation for this latent load assuming standard air is

$$q_l = C_l Q \Delta W \quad (5.5)$$

where

C_l = air latent heat factor, (W · s)/(L · K); a typical value is 3010

ΔW = humidity ratio difference between outdoor and indoor air, kg/kg

A complete explanation of Equation 5.5 is also given in Chapter 9.

If humidification of a space is required, such as in the heating season or to maintain higher humidities, heat must be supplied to a humidifier to vaporize the amount of water that is deficient in the infiltrating air. Equation 5.5 gives this required latent heating load for humidification, a negative number representing a heating load.

5.2 Determination of Pressure Differences

To use Equation 5.1, it is necessary to be able to estimate the pressure difference based on the contributions of the three components—stack effect, wind effect, and mechanical pressurization. These are discussed in Sections 5.2.1, 5.2.2, and 5.2.3.

5.2.1 Pressure Difference Due to Stack Effect

The stack effect occurs when the air densities are different on the inside and outside of a building. The air density decreases with increasing temperature and decreases slightly with increasing humidity. Because the pressure of the air is due to the weight of a column of air, on winter days the air pressure at ground level will be less inside the building due to warm inside air and the cold air outside the building. As a result of this pressure difference, air will infiltrate into a building at ground level and flow upward inside the building. Under summer conditions when the air is cooler in the building, outdoor air enters the top of the building and flows downward on the inside.

Under the influence of the stack effect, there will be a vertical location in the building where the inside pressure equals the outside pressure. This location is defined as the neutral pressure level of the building. In theory, if cracks and other openings are uniformly distributed vertically, the neutral pressure level will be exactly at the mid-height of the building. If larger openings predominate in the upper portions of the building, this will raise the neutral pressure level. Likewise, large openings in the lower part will lower the neutral pressure level. The neutral pressure level in tall buildings typically varies between 30% and 70% of the total building height (Tamura and Wilson 1966, 1967). Unless there is information to the contrary, it is assumed that the neutral pressure will be at the building mid-height when under the influence of the stack effect acting alone.

The theoretical pressure difference for a horizontal leak at any vertical location, neglecting vertical density gradients, resulting from the stack effect can be found using

$$\Delta p_{st} = C_1(\rho_o - \rho)g(H_{NPL} - H) \quad (5.6a)$$

or

$$\Delta p_{st} = C_1\rho_o\left(\frac{T_i - T_o}{T_i}\right)g(H_{NPL} - H) \quad (5.6b)$$

where

- T_o = outdoor temperature, degrees K
- T_i = indoor temperature, degrees K
- ρ_o = outdoor air density, kg/m³
- ρ_i = indoor air density, kg/m³
- g = gravitational acceleration, 9.81 m/s²

H = height above reference plane, m

H_{NPL} = height of neutral pressure level above reference plane without any other driving forces, m

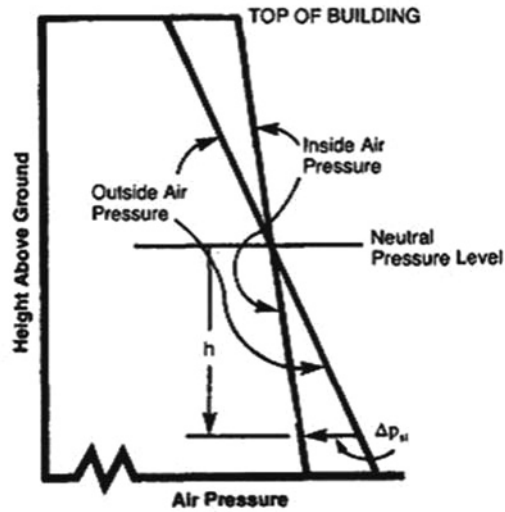


Figure 5.1 Winter stack effect showing theoretical pressure difference versus height.

(Source: *Cooling and Heating Load Calculation Principles*, Figure 6.1).

Figure 5.1 shows the stack effect pressure variations for cold outdoor air. When the outside pressure is greater than the inside pressure, as in the lower half of the building, Δp_{st} is positive and the airflow is into the building. When the outside temperature is greater than the inside air temperature, then the situation is reversed and Δp_{st} is positive for the upper half of the building.

The Δp_{st} given by Equation 5.6 is valid only for buildings with no vertical separations, that is, no floors—as, for example, an atrium, an auditorium, or fire stair towers. Floors in conventional buildings offer a resistance to the vertical flow of air caused by the stack effect. There are pressure drops from one story to the next. If these resistances, such as doors, can be assumed uniform for every floor, then a single correction, called the *thermal draft coefficient*, C_d , can be used to relate Δp_{st} and Δp_s , the actual pressure difference:

$$C_d = \left(\frac{\Delta p_s}{\Delta p_{st}} \right) \quad (5.7)$$

Figure 5.2 shows the effect of the pressure differences between floors for winter conditions. The flow of air upward through the building causes the pressure to decrease at each floor. For this reason, Δp_s is less than Δp_{st} ; thus, C_d will be a number less than 1.0. Note that the slope of the actual inside pressure curve within each floor is the same as the theoretical curve.

Equations 5.6 and 5.7 are combined to yield

$$\frac{\Delta p_s}{C_d} = C_1 \left(\frac{T_o - T_i}{T_i} \right) \rho_o g (H_{NPL} - H) \quad (5.8)$$

Equation 5.8 is plotted in Figure 5.3 with an inside temperature of 24°C and $P_b = 101.325$ kPa (sea level pressure). The values of Δt were obtained by using decreasing values of T_o for winter conditions. Figure 5.3 can, however, be used for the summer stack effect with little loss in accuracy.

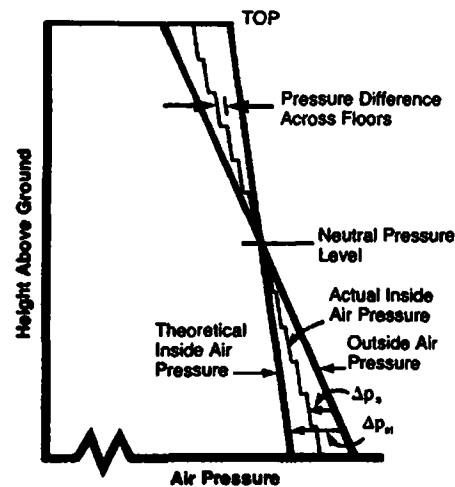


Figure 5.2 Winter stack effect showing actual pressure difference versus height for a 12-story building.

(Source: *Cooling and Heating Load Calculation Principles*, Figure 6.2).

The value of the thermal draft coefficient C_d depends on the resistance to the vertical flow of air (that is, the tightness of stair doors, etc.) and to the quantity of vertical airflow. In this last regard, the larger the vertical flow, the larger the pressure drop per floor and thus the smaller the value of C_d (see Figure 5.3). For this reason, loose-fitting exterior walls that produce large amounts of infiltration and, thus vertical flow, tend to lower the values of C_d , whereas loose-fitting stair floors, etc. tend to raise the value of C_d by reducing pressure drops. With no doors in the stairwells, C_d has a value of 1.0. Values of C_d determined experimentally for a few modern office buildings ranged from 0.63 to 0.82 (Tamura and Wilson 1967). Values of C_d for apartment buildings are not available. However, as apartment buildings have fewer elevator shafts and leakier exteriors, resulting in higher vertical resistance and lower horizontal resistance, the values of C_d probably will be lower than those for office buildings.

5.2.2 Pressure Difference Due to Wind Effect

The wind pressure or velocity pressure is given by

$$P_w = C_p \rho \frac{U^2}{2} \quad (5.9)$$

where

P_w = wind surface pressure relative to outdoor static pressure in undisturbed flow, Pa

ρ = outdoor air density, kg/m³ (about 1.2)

U = wind speed, m/s

C_p = wind surface pressure coefficient, dimensionless

C_p is a function of location of the building envelope and wind direction (see Chapter 24, *ASHRAE Handbook—Fundamentals* [2013]). The pressure coefficient will always have a value of less than 1.0 and can be negative when the wind causes outdoor pressures below atmospheric on some surfaces of a building.

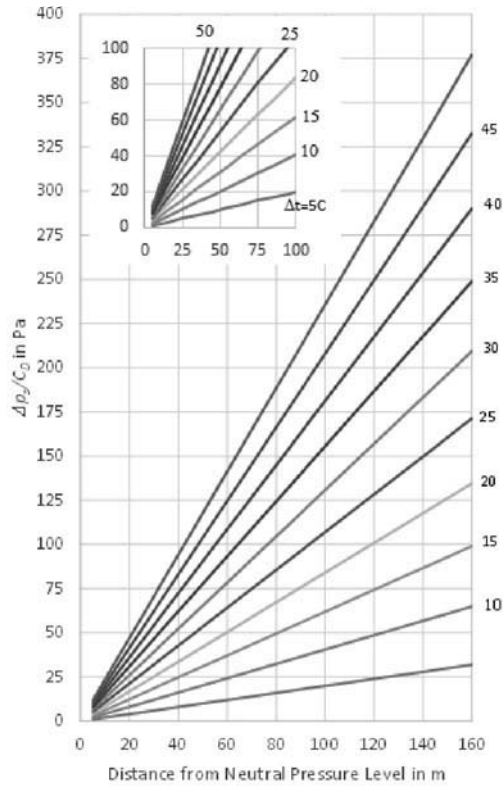


Figure 5.3 Pressure difference due to stack effect.
 (Source: *Cooling and Heating Load Calculation Principles*, Figure 6.3).

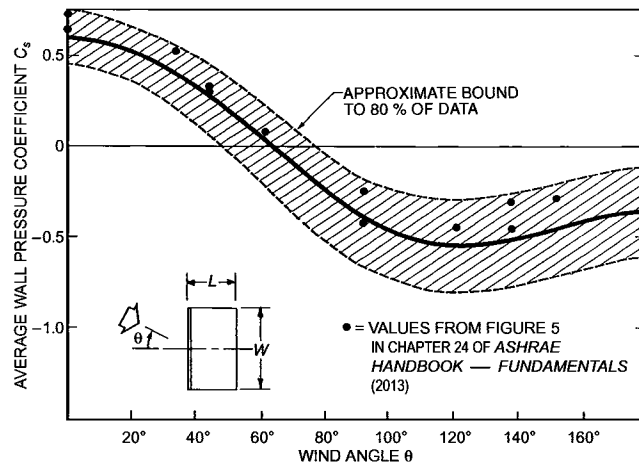


Figure 5.4 Variation of surface-averaged wall pressure coefficients for low-rise buildings.
 (Source: *ASHRAE Handbook—Fundamentals* [2013], Chapter 24, Figure 6).

Figure 5.4 gives average wall pressure coefficients for low-rise buildings (Swami and Chandra 1987). Note that the windward side corresponds to an angle of zero and the leeward side corresponds to an angle of 180°. The average roof pressure coefficient for a low-rise building with a roof inclined less than 20° is approximately 0.5 (Holmes 1986).

An alternative approximation for the surface-averaged wall pressure coefficient for low-rise buildings (three stories or less in height) is given by

$$C_p(\theta) = 0.15(\cos^2\theta)^{1/4} + 0.45(\cos\theta) - 0.65(\sin^2\theta)^2 \quad (5.10)$$

Figures 5.5 and 5.6 give average pressure coefficients for tall buildings (Akins et al. 1979). Pressure coefficient generally increases with height; however, the variation is well within the approximations of the data in general.

For nonrectangular low-rise buildings, Swami and Chandra (1988) have made recommendations for pressure coefficients. Grosso (1992) gives a more general model for determining pressure coefficients.

Effective Wind Speed

The reference wind speed used to determine pressure coefficients and infiltration rates is usually the wind speed at the eave height for low-rise buildings and the building height for high-rise buildings. However, measured meteorological data are usually

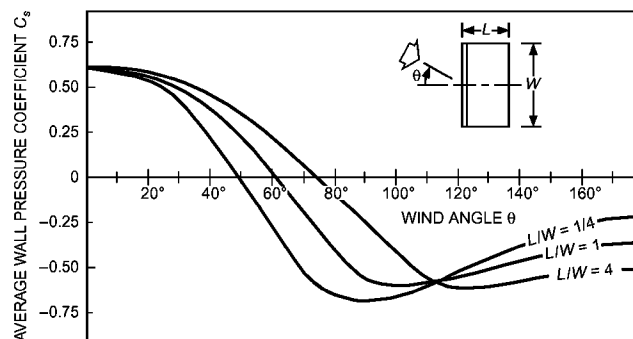


Figure 5.5 Surface-averaged wall pressure coefficients for tall buildings (Akins et al. 1979).

(Source: *ASHRAE Handbook—Fundamentals* [2013], Chapter 24, Figure 7).

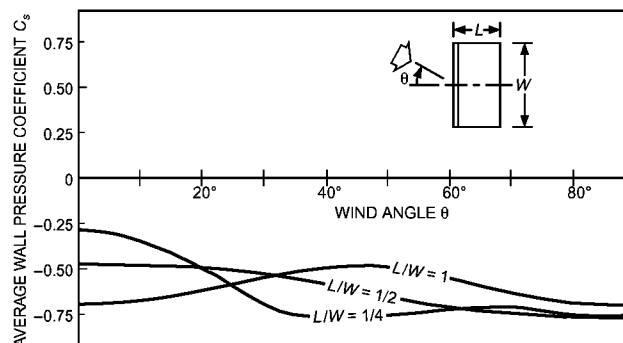


Figure 5.6 Surface-averaged roof pressure coefficients for tall buildings (Akins et al. 1979).

(Source: *ASHRAE Handbook—Fundamentals* [2013], Chapter 24, Figure 9).

Load Calculation Applications Manual (SI), Second Edition

available at 10 m. This wind speed needs to be corrected for reductions caused by the difference between the height where the wind speed is measured and the height of the building.

The effective wind speed U_H can be computed from the reference wind speed U_{met} using boundary layer theory, and an estimate of terrain effect is given by

$$U_H = U_{met} \left(\frac{\delta_{met}}{H_{met}} \right)^{a_{met}} \left(\frac{H}{\delta} \right)^a \quad (5.11)$$

where

δ = boundary layer thickness of the local terrain in Table 5.1, m

a = exponent for the local terrain in Table 5.1, dimensionless

δ_{met} = boundary layer thickness for the meteorological station in Table 5.1, m

a_{met} = exponent for the meteorological station in Table 5.1, dimensionless

H = average height above local obstacles, weighted by the area plan, m

H_{met} = the height at which the wind speed was measured, m

The wind boundary layer thickness δ and exponent a used in Equation 5.11 are determined from Table 5.1. Typical values for meteorological stations, generally measured in flat, open terrain (category 3 in Table 5.1), are $a_{met} = 0.14$ and $\delta_{met} = 270$ m. Equation 5.11 is less reliable at heights below the average obstacle height (see Chapter 24, *ASHRAE Handbook—Fundamentals [2013]*).

Calculation of Wind Pressure Difference

The wind-induced pressure difference is found using the coefficient:

$$C_{p(in-out)} = C_p - C_{in} \quad (5.12)$$

Table 5.1 Atmospheric Boundary Layer Parameters

(Source: *ASHRAE Handbook—Fundamentals [2013]*, Chapter 24, Table 1)

Terrain Category	Description	Exponent a	Layer Thickness δ , m
1	Large city centers, in which at least 50% of buildings are higher than 25 m, over a distance of at least 0.8 km or 10 times the height of the structure upwind, whichever is greater	0.33	460
2	Urban and suburban areas, wooded areas, or other terrain with numerous closely spaced obstructions having the size of single-family dwellings or larger, over a distance of at least 460 m or 10 times the height of the structure upwind, whichever is greater	0.22	370
3	Open terrain with scattered obstructions having heights generally less than 9 m, including flat open country typical of meteorological station surroundings	0.14	270
4	Flat, unobstructed areas exposed to wind flowing over water for at least 1.6 km, over a distance of 460 m or 10 times the height of the structure inland, whichever is greater	0.10	210

For uniformly distributed air leakage sites in all walls, C_{in} is about -0.2 . Then, the wind-induced pressure difference is given by

$$\Delta P_w = C_{p(in-out)} \rho \frac{U_H^2}{2} \tag{5.13}$$

5.2.3 Pressure Difference Due to Building Pressurization

The pressure inside a building p_p and the corresponding pressure difference Δp_p depend on the air distribution and ventilation system design and are not a result of natural phenomena. A building can be pressurized by bringing in more outdoor air through the air-handling system than is allowed to exhaust. This results in a negative pressure difference Δp_p and a reduction in infiltration from wind and stack effect. On the other hand, adjustment or design of the air-handling system may be such that more air is exhausted than supplied from outdoors. This generally results in a lower pressure inside the building, a positive pressure difference Δp_p , and increased infiltration from wind and stack effect. This latter case is usually undesirable.

Although building pressurization often is desired and assumed to occur, it is emphasized that the air circulation system must be carefully designed and adjusted in the field to achieve this effect. For purposes of design calculations, the designer must assume a value for ΔP_p . Take care to assume a realistic value that can actually be achieved by the system.

Example 5.1 Estimating Building Pressure Differences

Estimate the indoor/outdoor pressure differences for the first and twelfth floors of a 12-story office building located in Atlanta, Georgia, under 99.6% design heating conditions. A plan view of the building is shown in Figure 5.7. It is 36 by 9 m with floor-to-floor heights of 3 m. Consider only wind and stack effect—with limited information available, assume neutral pressure level at 1/2 of building height. The indoor design temperature is 21°C. The building is in a suburban area, with mixed single family dwellings, single-story retail buildings, and small office buildings.

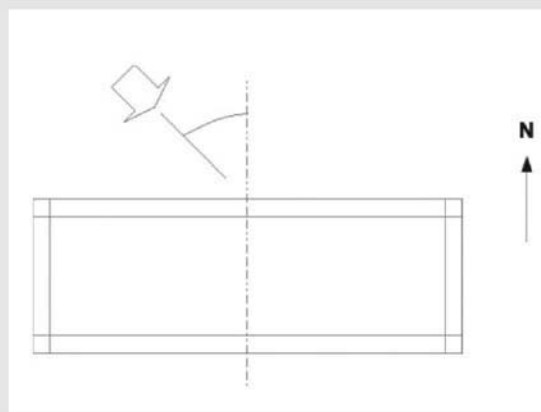


Figure 5.7 Building orientation and wind direction for Example 5.1.

Solution:

Item	Equation/Figure	Explanation
Building height, m		36.0
Neutral pressure height, m		18.0
Wind speed, m/s	Table 4.1	5.3

Load Calculation Applications Manual (SI), Second Edition

Outdoor air temperature, °C		-5.8
Indoor air temperature, °C		21.0
H (application height of the first floor), m		1.5
H (application height of the twelfth floor), m		34.5
H (application height of roof), m		36.0
Wind Speed Correction Parameters Taken from Table 5.1		
δ_{met} , m		270.0
a_{met} (-)		0.14
H_{met} (reference height of wind speed), m	Table 5.1	10.0
δ (application site), m		370.0
a (application site coefficient)		0.22
Wind speed correction	Equation 5.11	$U_H = U_{met} (\delta_{met}/H_{met})^{a_{met}} (H/\delta)^a$
Wind speed (twelfth floor), m/s	Equation 5.11	4.99
Wind speed (first floor), m/s		2.50
Surface Average Pressure Coefficients		
Wind-induced internal pressure coefficient		Assumes equal wind-induced internal pressure coefficient $C_{in} = -0.20$
Surface average pressure coefficients		$L/W = 9/36 = 0.25$
North wall, windward, $\theta = 40^\circ$		$C_{pN} = 0.46$
West wall, windward, $\theta = 50^\circ$	Figure 5.5	$C_{pW} = 0.38$
South wall, leeward, $\theta = 140^\circ$		$C_{pS} = -0.60$
East wall, leeward, $\theta = 130^\circ$		$C_{pE} = -0.63$
Roof, slope less than 20° , (-)	Figure 5.6	$C_{pR} = -0.50$
Effective average surface pressure coefficient	Equation 5.12	$C_p = C_{pout} - C_{in}$
North wall, windward, $\theta = 40^\circ$		$C_{pN} = 0.66$
West wall, windward, $\theta = 50^\circ$		$C_{pW} = 0.58$
South wall, leeward, $\theta = 140^\circ$	Equation 5.12	$C_{pS} = -0.40$
East wall, leeward, $\theta = 130^\circ$		$C_{pE} = -0.43$
Roof, slope less than 20°		$C_{pR} = -0.30$
Wind pressure difference calculation	Equation 5.13	$\Delta p_w = C_p \rho U^2 / 2$
Average air density, kg/m^3		$\rho = 1.2$
Wind Pressure Difference (First Floor)		
North wall, windward, $\theta = 40^\circ$		$\Delta p_N = 2.475$
West wall, windward, $\theta = 0^\circ$	Equation 5.13	$\Delta p_W = 2.175$
South wall leeward, $\theta = 140^\circ$		$\Delta p_S = -1.5$
East wall, leeward, $\theta = 130^\circ$		$\Delta p_E = -1.613$

Wind Pressure Difference (Twelfth Floor)		
North wall, windward, $\theta = 40^\circ$		$\Delta p_N = 9.86$
West wall, windward, $\theta = 50^\circ$		$\Delta p_W = 8.665$
South wall, leeward, $\theta = 140^\circ$	Equation 5.13	$\Delta p_S = -5.976$
East wall, leeward, $\theta = 140^\circ$		$\Delta p_E = -6.424$
Roof, slope less than 20°		$\Delta p_R = -4.482$
Stack Pressure Difference Calculation		
Design indoor temperature, Kelvin		$t_i = 294.15$
Design outdoor air temperature, Kelvin		$t_o = 267.35$
Gravitational acceleration, m/s^2		$g = 9.81$
Net Height Difference ($H_{NPL} - H$)		
Walls (first floor), m		$H_{NPL} - H = 16.5$
Walls (twelfth floor), m		$H_{NPL} - H = -16.5$
Roof, m		$H_{NPL} - H = -18.0$
Draft Coefficient, (-)	Assumed	$C_d = 0.800$
Theoretical stack pressure difference	Equation 5.6b	$\Delta p_{st} = C_1 \rho_o \left(\frac{t_i - t_o}{t_i} \right) g (H_{NPL} - H)$
Walls (first floor)		$\Delta p_{st} = 17.697$
Walls (twelfth floor)	Equation 5.6b	$\Delta p_{st} = -17.697$
Roof		$\Delta p_{st} = -19.31$
Actual stack pressure difference	Equation 5.7	$\Delta p_s = C_d \Delta p_{st}$
Walls (first floor)		$\Delta p_s = 0.8 \times (17.697) = 14.16$
Walls (twelfth floor)		$\Delta p_s = 0.8 \times (-17.697) = -14.16$
Roof		$\Delta p_s = 0.8 \times (-19.31) = -15.45$
Total pressure difference across the surfaces	Equation 5.2	$\Delta p = \Delta p_s + \Delta p_w$
Surfaces	First Floor	Twelfth Floor
North wall, windward, $\theta = 40^\circ$, Pa	$\Delta p = 16.63$	$\Delta p = -4.3$
West wall, windward, $\theta = 50^\circ$, Pa	$\Delta p = 16.33$	$\Delta p = -5.49$
South wall, leeward, $\theta = 140^\circ$, Pa	$\Delta p = 12.66$	$\Delta p = -20.13$
East wall, leeward, $\theta = 130^\circ$, Pa	$\Delta p = 12.55$	$\Delta p = -20.58$
Roof, slope less than 20° , Pa		$\Delta p = -19.93$

Note: Results show that air will tend to infiltrate on the first nine floors on the windward side. The first floor will have infiltration on all sides and the twelfth floor will have exfiltration on all sides. Recall that these calculations are based on a relatively low wind velocity. A higher wind velocity could cause infiltration on the top floor.

5.3 Infiltration Through Building Envelope

With the pressure differences established, infiltration through the building envelope can be estimated. Different approaches, as discussed below, are used for curtain walls, cracks, and operable doors.

Load Calculation Applications Manual (SI), Second Edition

5.3.1 Curtain Wall Infiltration per Floor or Room

For purposes of design load calculations, it is desirable to have the infiltration rate for each room or floor of the building. Depending on the location of the room, with respect to the wind direction and the neutral pressure level, air may be infiltrating or exfiltrating. By estimating the pressure differential between inside and outside, the direction of the air leakage may be determined. It is possible that air leaking into the building on one floor may leave the building on a different floor. For the space to be comfortable, it must be assumed that the load due to infiltration is absorbed in the space where the air enters. Therefore, exfiltration does not directly cause a load and only infiltration is of interest in this regard. It is possible that some exfiltrated air enters the space by way of the air-conditioning system, but the load is absorbed by the heating or cooling coil. Calculation aids and procedures are described below. It is assumed that curtain walls are used in high-rise construction.

The flow coefficient C in Equation 5.1 has a particular value for each crack and each window and door perimeter gap. Although values of C are determined experimentally for window and door gaps, this same procedure will not work for cracks. Cracks occur at random in fractures of building materials and at the interface of similar or dissimilar materials. The number and size of the cracks depend on the type of construction, the workmanship during construction, and the maintenance of the building after construction. To determine a value of C for each crack would be impractical; however, an overall leakage coefficient can be used by changing Equation 5.1 into the following form:

$$Q = KA(\Delta p)^n \quad (5.14)$$

where

A = wall area, m^2

K = leakage coefficient ($C = KA$)

When Equation 5.14 is applied to a wall area having cracks, the leakage coefficient K can then be determined experimentally. If very large wall areas are used in the test, the averaging effect of a very large number of cracks is taken advantage of. Tests have been made on entire buildings by pressurizing them with fans. Measurements are made of the flow through the fan, which is equal to the exfiltration, and the pressure difference due to pressurization (Shaw et al. 1973; Tamura and Shaw 1976). Air leakage through doors and other openings is not included in the wall leakage. Seven tall office-type buildings tested were of curtain wall construction of metal or precast concrete panels and had nonoperable windows. The results of these tests are presented in Table 5.2 and Figure 5.8. The equation of the three curves in Figure 5.8 is $Q/A = K(\Delta p)^{0.65}$ for $K = 0.031, 0.093,$ and 0.183 . One masonry building was tested and was found to obey the relation $Q/A = 0.56(\Delta p)^{0.65}$, which is for a very loose-fitting wall. Because only one such building was tested, this equation was not plotted in Figure 5.8.

Table 5.2 Curtain Wall Classification

(Source: *Cooling and Heating Load Calculation Principles*, Table 6.1)

Leakage Coefficient	Description	Curtain Wall Construction
$K = 0.031$	Tight-fitting wall	Constructed under close supervision of workmanship on wall joints. When joints seals appear inadequate, they must be redone.
$K = 0.093$	Average-fitting wall	Conventional construction procedures are used.
$K = 0.183$	Loose-fitting wall	Poor construction quality control or an older building having separated joints.

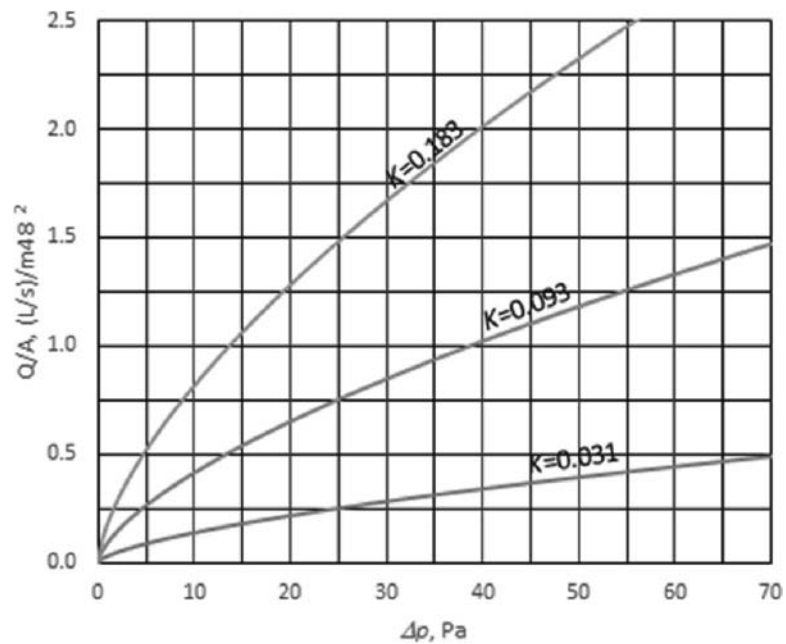


Figure 5.8. Curtain wall infiltration for one room or one floor.

(Source: *Cooling and Heating Load Calculation Principles*, Figure 6.5).

**Example 5.2
Infiltration Through
Curtain Wall—High
Rise**

Estimate the curtain wall infiltration rate for the first and twelfth floors of the building described in Example 5.1. The curtain wall may be classified as “average-fitting.”

Solution:

Item	Figure/Equation	Explanation
Infiltration rate	Figure 5.8	$Q = (Q/A)A$ $A = \text{wall surface area}$
First floor		From Example 5.1, Δp_1 indicates air will infiltrate on all sides
	Figure 5.8	North wall (windward): $\Delta p_1 = 17.11 \text{ Pa}$
	Table 5.2	$K = 0.093$
	Equation 5.14	$(Q/A)_n = 0.589 \text{ (L/s)/m}^2$ $A = 36 \cdot 3 = 108 \text{ m}^2$ $Q_n = 0.589 \cdot 108 = 6 \text{ L/s}$
		West wall (windward): $\Delta p_1 = 16.79 \text{ Pa}, K = 0.093$

Load Calculation Applications Manual (SI), Second Edition

	$(Q/A)_w = 0.582 \text{ (L/s)/m}^2$ $A = 9 \cdot 3 = 27 \text{ m}^2$ $Q_w = 0.582 \cdot 27 = 16 \text{ L/s}$ South wall (leeward): $\Delta p_1 = 13 \text{ Pa}, K = 0.093$
	$(Q/A)_s = 0.493 \text{ (L/s)/m}^2$ $A = 36 \cdot 3 = 108 \text{ m}^2$ $Q_s = 0.493 \cdot 108 = 53 \text{ L/s}$ East wall (leeward): $\Delta p_1 = 12.88 \text{ Pa}, K = 0.093$
	$(Q/A)_l = 0.49 \text{ (L/s)/m}^2$ $A = 9 \cdot 3 = 27 \text{ m}^2$ $Q_l = 0.49 \cdot 27 = 13 \text{ L/s}$
Total, first floor	$Q_1 = Q_n + Q_w + Q_s + Q_l$ $Q_1 = 64 + 16 + 53 + 13$ $= 146 \text{ L/s}$
Twelfth floor	From Example 5.1, all pressure differences are negative, indicating exfiltration on all sides, $Q_{12} = 0$

5.3.2 Crack Infiltration for Doors and Movable Windows

Door infiltration depends on the type of door, room, and building. In residences and small buildings where doors are used infrequently, the air changes associated with a door can be estimated based on air leakage through cracks between the door and the frame. Infiltration through windows and all types of doors can be determined by altering Equation 5.1 to the form

$$Q = KP(\Delta p)^n \quad (5.15)$$

where

P = perimeter of the window or door, m

K = perimeter leakage coefficient, $C = KP$

Experiments may be carried out on windows and residential-type doors, and the values of the leakage coefficient K and the exponent n are determined using Equation 5.15. The results of some tests are presented in Tables 5.3 and 5.4 and Figure 5.9 (Sabine and Lacher 1975; Sasaki and Wilson 1965). The equation of the three curves in Figure 5.9 is $Q/P = K(\Delta P)^{0.65}$ for $K = 0.043, 0.086,$ and 0.257 . In using Tables 5.3 and 5.4 to select the

proper category, remember that movable sashes and doors will develop larger cracks over the life of the unit. Therefore, care should be taken to select a category representative of the period over which the unit will be used.

5.3.3 Infiltration Through Commercial-Type Doors

Commercial-type doors differ from those described in Section 5.6 in that they have larger cracks and they are used more often. Therefore, different data are required.

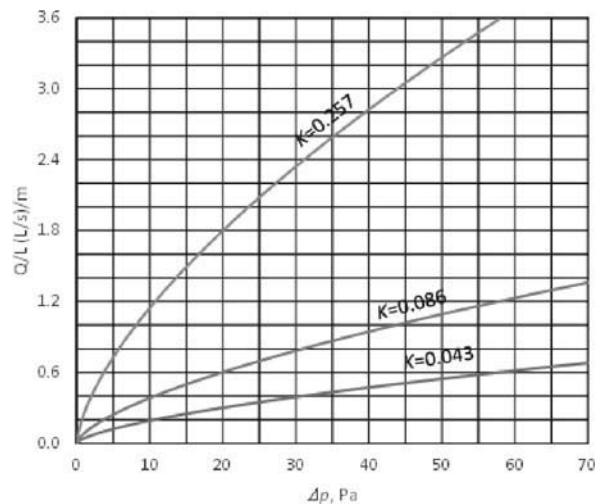


Figure 5.9 Window and door infiltration characteristics.

(Source: *Cooling and Heating Load Calculation Principles*, Figure 6.9).

Table 5.3 Windows Classification

(Source: *Cooling and Heating Load Calculation Principles*, Table 6.2)

	Wood Double-Hung (Locked)	Other Types
Tight-fitting window, $K = 0.043$	Weatherstripped average gap (0.4 mm crack)	Wood casement and awning windows; weatherstripped. Metal casement windows; weatherstripped
Average-fitting window, $K = 0.086$	Nonweatherstripped average gap (0.4 mm crack) or Weatherstripped large gap (2.5 mm crack)	All types of vertical and horizontal sliding windows; weatherstripped. Note: If average gap (0.4 mm crack) this could be tight-fitting window. Metal casement windows; nonweatherstripped. Note: If large gap (2.4 mm crack) this could be a loose-fitting window.
Loose-fitting window, $K = 0.257$	Nonweatherstripped large gap (2.5 mm crack)	Vertical and horizontal sliding windows, nonweatherstripped.

Load Calculation Applications Manual (SI), Second Edition

Swinging Doors

Data for swinging doors are given in Figure 5.10 where $Q/P = K(\Delta P)^{0.50}$ for $K = 0.86, 1.72, 3.44, \text{ and } 6.88$. The corresponding crack width is given opposite each value of K . Note that for these large cracks the exponent n is 0.50.

Commercial buildings often have a rather large number of people entering and leaving, which can increase infiltration significantly. Figures 5.11 and 5.12 have been developed to estimate this kind of infiltration for swinging doors. The infiltration rate per door is given in Figure 5.11 as a function of the pressure difference and a traffic coefficient that depends on the traffic rate and the door arrangement. Figure 5.12 gives the traffic coefficients as a function of the traffic rate and two door types. Single-bank doors open directly into the space; however, there may be two or more doors at one location. Vestibule-type doors are best characterized as two doors in series so as to form an air lock between them. These doors often appear as two pairs of doors in series, which amounts to two vestibule-type doors.

The equation for the four curves in Figure 5.11 is $Q = C(\Delta P)^{0.5}$ for flow coefficients $C = 80, 160, 320, \text{ and } 480$. This is the same equation as would be used for flow through a sharp-edged orifice. These values of C in Figures 5.11 and 5.12 were obtained from model tests and observing traffic under actual conditions (Min 1958). The values of C obtained from Figure 5.12 are based on a standard-sized (1 · 2.1 m)

Table 5.4 Residential-Type Door Classification

(Source: *Cooling and Heating Load Calculation Principles*, Table 6.3)

Tight-fitting door, $K = 0.043$	Very small perimeter gap and perfect fit weatherstripping—often characteristic of new doors.
Average-fitting door, $K = 0.086$	Small perimeter gap having stop trim fitting properly around door and weatherstripped.
Loose-fitting door, $K = 0.257$	Large perimeter gap having poor fitting stop trim and weatherstripped, or small perimeter gap with no weatherstripping.

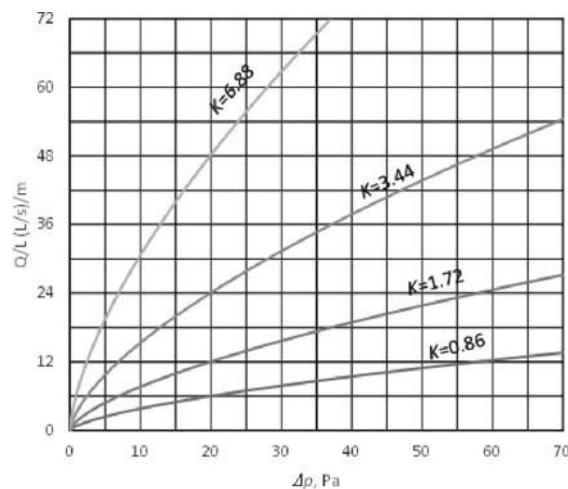


Figure 5.10 Infiltration through closed swinging door cracks.

(Source: *Cooling and Heating Load Calculation Principles*, Figure 6.10).

door. Care must be taken to not overestimate the traffic rate. The traffic rate may be extremely high for short periods of time and not representative of most of the day.

Revolving Doors

Figure 5.13 shows the infiltration due to a pressure difference across the door seals of a standard-sized revolving door (Schutrum et al. 1961). The results are for seals that are typically worn but have good contact with adjacent surfaces.

Figures 5.14 and 5.15 account for infiltration due to a mechanical interchange of air caused by the rotation of the standard-sized door (Schutrum et al. 1961). The amount of air interchanged depends on the inside-outside temperature difference and the rotational speed of the door.

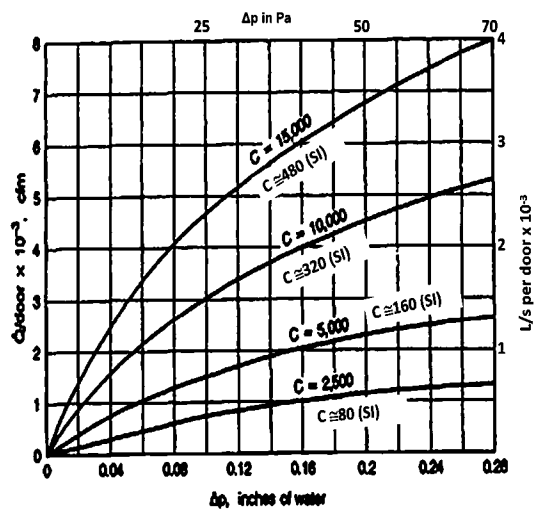


Figure 5.11 Swinging door infiltration characteristics with traffic.

(Source: *Cooling and Heating Load Calculation Principles*, Figure 6.11).

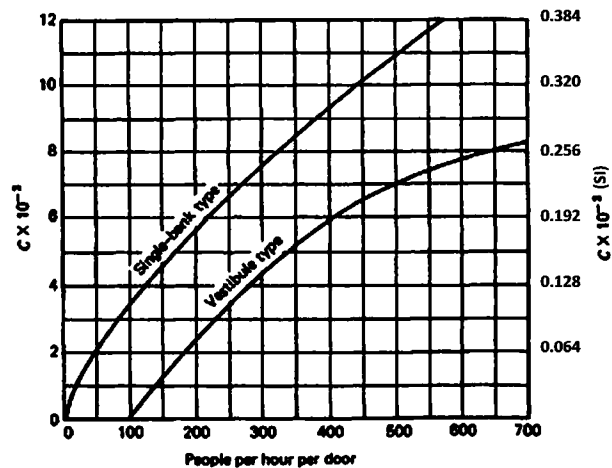


Figure 5.12 Flow coefficient dependence on traffic rates.

(Source: *Cooling and Heating Load Calculation Principles*, Figure 6.12).

Load Calculation Applications Manual (SI), Second Edition

The total infiltration is the infiltration due to leakage through the door seals plus the infiltration due to the mechanical interchange of air due to the rotation of the door.

Air Leakage Through Automatic Doors

Automatic doors are a major source of air leakage in buildings. For automatic doors, because the opening area changes with time, a combined coefficient that accounts for the discharge coefficient and the fraction of time the door remains open was developed by Yuill et al. (2000). This is related to the people use rate per hour, as is shown in Figure 5.16. The infiltration rate is given as

$$Q = C_A A \sqrt{\Delta p} \quad (5.16)$$

where

Q = airflow rate, L/s

C_A = airflow coefficient from Figure 5.16, L/(s·m²·Pa^{0.5})

A = area of the door, m²

Δp = pressure difference across the door, Pa

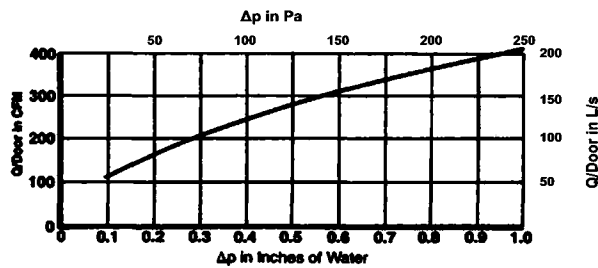


Figure 5.13 Infiltration through seals of revolving doors not revolving.

(Source: *Cooling and Heating Load Calculation Principles*, Figure 6.13).

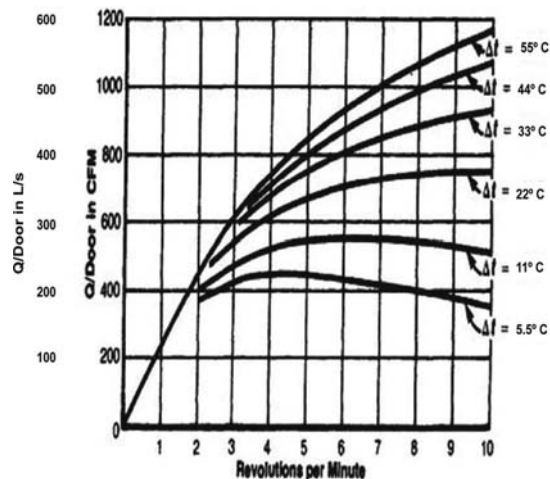


Figure 5.14 Infiltration for motor-operated revolving door.

(Source: *Cooling and Heating Load Calculation Principles*, Figure 6.14).

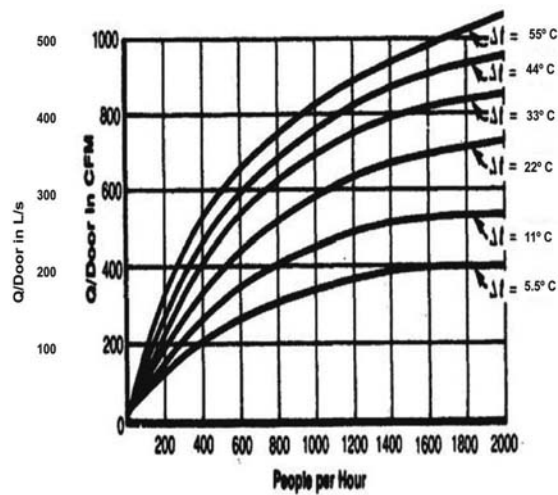


Figure 5.15 Infiltration for manually operated revolving door.
 (Source: *Cooling and Heating Load Calculation Principles*, Figure 6.15).

**Example 5.3
 Infiltration Through
 Swinging
 Commercial-Type
 Door**

The 12-story office building described in Example 5.1 has a two-door vestibule-type entrance on the north side (windward side) of the building. The two doors handle 500 people per hour during afternoon hours. There is a 3 mm perimeter air gap around each door. The doors have dimensions of 1 · 2.1 m. Estimate the infiltration rate for the entrance.

Solution:

Item	Figure/Example	Explanation
Crack infiltration		$Q = (Q/L)L$
	Equation 5.15	$Q = (Q/L)L = LK(\Delta P)^n, n = 0.50$
Pressure difference	Example 5.1	$\Delta p_w = 16.6 \text{ Pa}$ (windward side)
	Figure 5.10	$K = 4.0$
	Equation 5.15 or Figure 5.10	$Q/L = 4.0 \cdot (16.6)^{0.50} = 16.3 \text{ L/(s}\cdot\text{m)}$
Crack length		$L = 2(2.1 + 1) \cdot 2 = 12.4 \text{ m}$
Crack infiltration		$Q_c = 16.3 \cdot 12.4 = 202 \text{ L/s}$
		Note: Since doors are vestibule-type, crack infiltration will be reduced; assume 30% reduction, $Q_c = 0.7 \cdot 202 = 141 \text{ L/s}$
Infiltration due to traffic	Figure 5.12	250 people per door, vestibule-type
		$C = 110$
	Figure 5.11	$\Delta p = 16.6 \text{ Pa}, C = 110$
		$Q/\text{door} = 457 \text{ L/s}$

Total infiltration $Q = Q_c + Q_t$

$Q = 144 + 914$

$Q = 1058 \text{ L/s}$

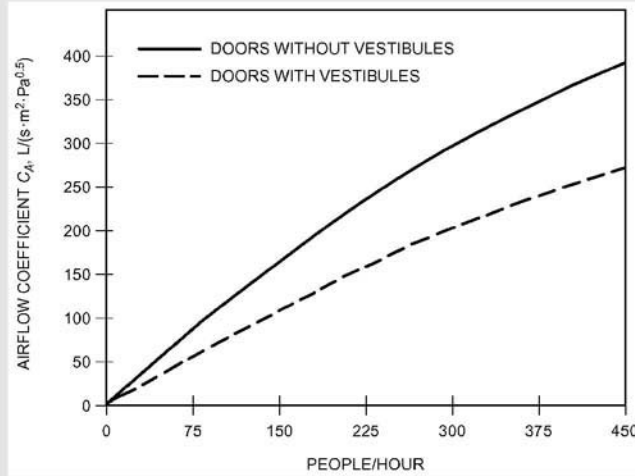


Figure 5.16 Airflow coefficient for automatic doors (Yuill et al. 2000).
 (Source: *ASHRAE Handbook—Fundamentals* [2013], Chapter 16, Figure 16).

**Example 5.4
 Infiltration Through
 Revolving Doors**

Assume the door system of Example 5.3 is replaced by a manually operated revolving door, and estimate the infiltration rate.

Solution:

Item	Figure/Example	Explanation
Crack infiltration	Figure 5.13 Example 5.1 The lower end of the curve is used.	$Q_c = (Q/\text{door}) \cdot 1$ $\Delta_p = 16.6 \text{ Pa}$ $Q_c = 50 \text{ L/s}$
Infiltration due to traffic	Figure 5.15	500 people / hour $\Delta_t = 26.8^\circ\text{C}$ $Q/\text{door} = 225 \text{ L/s}$ $Q_t = 225 \text{ L/s}$
Total infiltration		$Q = Q_c + Q_t = 50 + 225$ $Q = 275 \text{ L/s}$

5.4 Infiltration for Low-Rise Buildings

Low-rise buildings do not often utilize curtain-wall construction. This is especially true of light commercial structures where frame or masonry construction is prevalent. These structures often have movable windows, have cracks or other openings in the ceil-

ing, and generally resemble residential construction. Stack effect, although present, is much less important than the wind in producing infiltration. Therefore, stack effect can be neglected in most cases. The air distribution systems used in light commercial buildings usually will not pressurize the space. Therefore, infiltration must be considered.

It is common practice to use the air change method, previously discussed, where a reasonable estimate of the air changes per hour (ACH) is made based on experience. The range is usually from about 0.3 to 1.5 ach. Newer, well-constructed buildings tend to be at the lower end of the range; older buildings tend to be at the higher end.

A method similar to that described for curtain walls can be applied to this class of buildings where the infiltration rate is related to crack length and size. Considerable data are available for the cracks associated with windows and doors (Figures 5.9 and 5.10), but other cracks, such as those around electrical outlets, between the floor and the wall, etc., are very difficult to identify and describe.

A suggested approach to estimating infiltration in low-rise, light, commercial buildings by the crack method follows.

Assume that air infiltrates on all sides and exfiltrates through ceiling openings and cracks near the ceiling. Base the crack length on double the identifiable cracks around windows and doors to account for other obscure cracks. Compute the pressure difference based on wind alone for the windward side, but use the same value on all sides because the wind direction will vary randomly. Compute the infiltration for each room as $Q = (Q/P)P$, where Q/P is obtained from data given in Section 5.6 and P is crack length. Finally, check the results to see if the ACH are between about 0.5 and 2.0 to be sure of a reasonable result.

For cases where the air-moving system does have provisions for makeup and exhaust, it is good practice to consider the effect on infiltration. Obviously, if the system does pressurize the space, infiltration will be greatly reduced or eliminated. On the other hand, separate exhaust fans in restrooms, kitchens, or other spaces without suitable makeup air may reduce the space pressure and increase infiltration significantly. Such situations must be evaluated individually.

Example 5.5 Design Infiltration Rate

Estimate the design infiltration rate for a 6 · 6 m room with a 2.4 m ceiling in the northwest corner of a light commercial building, as shown in Figure 5.17. The room has four average-fitting ($K = 0.086$) 1 · 1.5 m movable-sash windows with weather stripping. Two windows are on the north wall and two windows are on the west wall. The environmental conditions are those given in Example 5.1, and the wind speed from Example 5.1 for the first floor (2.5 m/s) may be used. The building is not pressurized.

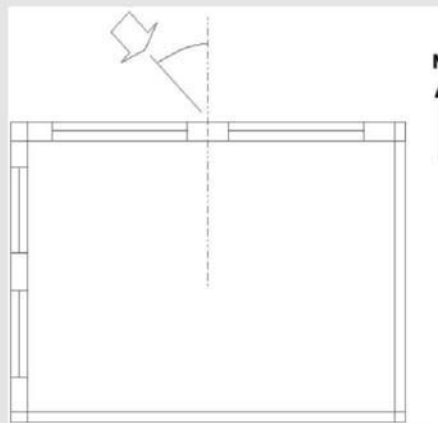


Figure 5.17 Northwest corner zone with two exterior façades.

Load Calculation Applications Manual (SI), Second Edition

Solution:		
Items	Equation / Figure	Explanation
Building height, m		3.0
Wind speed (at the walls), m/s	Example 5.1	2.5
Surface Average Pressure Coefficients		
Wind-induced internal pressure coefficient		Assumes equal wind induced internal pressure coefficient. $C_{in} = -0.200$
Surface Average Pressure Coefficients, Low-Rise Building		
Windward, (-)	Figure 5.4	$C_{Pw} = 0.350$
Effective average surface pressure coefficient	Equation 5.12	$C_p = C_{pout} - C_{in}$
Windward, (-)		$C_{Pw} = 0.550$
Wind pressure difference calculation	Equation 5.13	$\Delta P_w = C_p \rho U^2 / 2$
Average air density, kg/m ³		$\rho = 1.2$
Wind pressure difference (first floor)		
Windward	Equation 5.13	$\Delta P_w = 2.1 \text{ Pa}$
Infiltration data	Figure 5.9	Assume: average-fitting windows, $K = 0.086$
Pressure difference		$\Delta P_w = 2.1$ (windward)
Infiltration rate	Equation 5.15	$Q = (Q/L)L = LK(P)^n, n = 0.65$ $K = 0.086$
	Equation 5.15 or Figure 5.9	$Q/L = 0.086 \cdot (2.1)^{0.65} = 0.14 \text{ L/s per m}$
Crack length per window		$L = 2H + 3W = (2 \cdot 1.5) + (3 \cdot 1) = 6 \text{ m}$
Total crack length		$TL = 4 \cdot L \cdot 2$ (taking double the identifiable crack length) $= 48 \text{ m}$
Infiltration rate		$Q = (Q/L) L_t = 0.14 \cdot 48 = 6.7 \text{ L/s}$
ACH		$\text{ach} = Q/1000 / (\text{Volume}/3600)$ $= 6.7/1000 \cdot 3600 / (6 \cdot 6 \cdot 2.4) = 0.28 \text{ ach}$

References

- ASHRAE. 2013. *ASHRAE Handbook—Fundamentals*. Atlanta: ASHRAE.
- ASHRAE. 2007. *ANSI/ASHRAE Standard 62.1-2007, Ventilation for Acceptable Indoor Air Quality*. Atlanta: ASHRAE.
- Akins, R.E., J.A. Peterka, and J.E. Cermak. 1979. Averaged pressure coefficients for rectangular buildings. *Proceedings of the Fifth International Conference on Wind Engineering, Fort Collins, CO*, 7:369–80.
- Grosso, M. 1992. Wind pressure distribution around buildings: A parametrical model. *Energy and Buildings* 18(2):101–31.

- Holmes, J.D. 1986. Wind loads on low-rise buildings: The structural and environmental effects of wind on buildings and structures. Faculty of Engineering, Monash University, Melbourne, Australia.
- Min, T.C. 1958. Winter infiltration through swinging-door entrances in multistory building. *ASHAE Transactions* 64:421–46.
- Pedersen, C.O., D.E. Fisher, J.D. Spitler, and R.J. Liesen. 1998. *Cooling and Heating Load Calculation Principles*. Atlanta: ASHRAE.
- Sabine, H.J., and M.B. Lacher. 1975. Acoustical and thermal performance of exterior residential walls, doors, and windows. U.S. Department of Commerce, Washington, DC.
- Sasaki, J.R., and A.G. Wilson. 1965. Air leakage values for residential windows. *ASHRAE Transactions* 71(2):81–88.
- Schutrum, L.F., N. Ozisik, C.M. Humphrey, and J.T. Baker. 1961. Air infiltration through revolving doors. *ASHRAE Transactions* 67:488–506.
- Shaw, C.Y., D.M. Sander, and G.T. Tamura. 1973. Air leakage measurements of the exterior walls of tall buildings. *ASHRAE Transactions* 79(2):40–48.
- Swami, M.V., and S. Chandra. 1987. Procedures for calculating natural ventilation airflow rates in buildings. Final Report FSEC-CR-163-86, Florida Solar Energy Center, Cape Canaveral, FL.
- Swami, M.V., and S. Chandra. 1988. Correlations for pressure distribution on buildings and calculation of natural-ventilation airflow. *ASHRAE Transactions* 94(1):243–66.
- Tamura, G.T., and A.G. Wilson. 1966. Pressure differences for a nine-story building as a result of chimney effect and ventilation system operation. *ASHRAE Transactions* 72(1):180–89.
- Tamura, G.T., and A.G. Wilson. 1967. Pressure differences caused by chimney effect in three high buildings. *ASHRAE Transactions* 73(2):1–10.
- Tamura, G.T., and C.Y. Shaw. 1976. Studies on exterior wall air tightness and air infiltration of tall buildings. *ASHRAE Transactions* 82(1):122–34.
- Yuill, G.K., R. Upham, and C. Hui. 2000. Air leakage through automatic doors. *ASHRAE Transactions* 106(2):145–60.

6

Internal Heat Gain

Internal sources of heat energy may contribute significantly to the total heat gain for a space. In the case of a completely isolated interior room, the total heat gain is due entirely to internal sources. These internal sources fall into the general categories of people, lights, and equipment, such as office equipment, cooking appliances, hospital equipment, and powered machinery.

For people and some types of equipment, the heat gain may be made up of sensible and latent portions. The latent portion is generally assumed to instantaneously become part of the latent cooling load. The sensible heat gain is usually made up of both radiative and convective fractions. While the convective fraction becomes part of the cooling load instantaneously, the radiant fraction interacts with surfaces in the zone and may be absorbed and then later convected to the room air. In the radiant time series method (RTSM), the entire radiant fraction of the heat gain eventually appears as a cooling load distributed over the 24-hour period. In the heat balance method (HBM), all or almost all of the radiant heat gains will eventually appear as cooling loads, depending on the thermal response characteristics of the zone. In contrast to the RTSM, in the HBM there is the possibility that part of the radiant heat gains will be conducted to the outside environment. This limitation in the RTSM sometimes leads to slight overpredictions of peak cooling load by the RTSM.

Both the HBM and the RTSM rely on estimated radiative/convective splits to characterize the contribution of internal heat gains to the radiant exchange. Accordingly, in addition to information about the quantity of heat gain, the radiative/convective split is also important. For lighting, the split between short-wavelength and long-wavelength radiation has some effect on the peak cooling load, but it is typically ignored. The distribution of internal radiant heat gains to the various room surfaces also has an effect, but it is typically assumed to be distributed uniformly by area to all internal surfaces.

Failure to identify all internal heat sources can lead to gross undersizing, while an overly conservative approach may lead to significant oversizing. Both cases are undesirable. The most serious problem in making accurate estimates of internal heat gain is lack of information on the exact schedule of occupancy, light usage, and equipment operation.

For example, it may not be reasonable to assume that all occupants are present, all lights are on, and all equipment is operating in a large office building. However, for a particular room in the building, the total occupancy, light, and equipment load usually should be used to compute the room's heat gain. In brief, it is probable that any particular room will be fully loaded but the complete building will never experience a full internal load. The assumption here is that the air-cooling and delivery systems would be sized to accommodate the space loads, but the central cooling plant would be sized for a lower capacity, based on the diversified load. Every building must be examined using available information, experience, and judgment to determine the internal load diversity and schedule.

People

The heat gain from human beings has two components, sensible and latent. The total and relative amounts of sensible and latent heat vary depending on the level of activity, and in general, the relative amount of latent heat gain increases with the level of activity. Table 6.1 gives heat gain data from occupants in conditioned spaces. The latent heat gain is assumed to instantly become cooling load, while the sensible heat gain is partially delayed, depending on the nature of the conditioned space. This delay depends on the radiative and convective fractions. Typical radiative fractions are given in Table 6.1; the remainder of the sensible heat gain will be convective.

Load Calculation Applications Manual (SI), Second Edition

Table 6.1 Representative Rates at Which Heat and Moisture Are Given Off by Human Beings in Different States of Activity

(Source: *ASHRAE Handbook—Fundamentals* [2013], Chapter 18, Table 1)

Degree of Activity	Location	Total Heat, W		Sensible Heat, W	Latent Heat, W	% Sensible Heat that is Radiant ^b	
		Adult Male	Adjusted, M/F ^a			Low <i>V</i>	High <i>V</i>
Seated at theater	Theater, matinee	115	95	65	30		
Seated at theater, night	Theater, night	115	105	70	35	60	27
Seated, very light work	Offices, hotels, apartments	130	115	70	45		
Moderately active office work	Offices, hotels, apartments	140	130	75	55		
Standing, light work; walking	Department store; retail store	160	130	75	55	58	38
Walking, standing	Drug store, bank	160	145	75	70		
Sedentary work	Restaurant ^c	145	160	80	80		
Light bench work	Factory	235	220	80	140		
Moderate dancing	Dance hall	265	250	90	160	49	35
Walking 4.8 km/h; light machine work	Factory	295	295	110	185		
Bowling ^d	Bowling alley	440	425	170	255		
Heavy work	Factory	440	425	170	255	54	19
Heavy machine work; lifting	Factory	470	470	185	285		
Athletics	Gymnasium	585	525	210	315		

Notes:

1. Tabulated values are based on 24°C room dry-bulb temperature. For 27°C room dry bulb, the total heat remains the same, but the sensible heat values should be decreased by approximately 20% and the latent heat values increased accordingly.
2. Also refer to the *ASHRAE Handbook—Fundamentals* (2013) Chapter 9, Table 4, for additional rates of metabolic heat generation.
3. All values are rounded to nearest 5 W.

^aAdjusted heat gain is based on normal percentage of men, women, and children for the application listed, and assumes that gain from an adult female is 85% of that for an adult male, and gain from a child is 75% of that for an adult male.

^bValues approximated from data in the *ASHRAE Handbook—Fundamentals* (2013) Chapter 9, Table 6, where *V* is air velocity with limits shown in that table.

^cAdjusted heat gain includes 18 W for food per individual (9 W sensible and 9 W latent).

^dFigure one person per alley actually bowling, and all others as sitting (117 W) or standing or walking slowly (231 W).

Lighting

Since lighting is often the major internal load component, an accurate estimate of the space heat gain it imposes is needed. The rate of heat gain at any given moment can be quite different from the heat equivalent of power supplied instantaneously to those lights.

The primary source of heat from lighting comes from the light-emitting elements, or lamps, although significant additional heat may be generated from associated components in the light fixtures housing such lamps. Generally, the instantaneous rate of heat gain from electric lighting may be calculated from

$$q_{el} = WF_{ul}F_{sa} \quad (6.1)$$

where

q_{el} = heat gain, W

W = total installed light wattage, W

F_{ul} = use factor, ratio of wattage in use to total installed wattage

F_{sa} = special allowance factor

Internal Heat Gain

The total light wattage is obtained from the ratings of all lamps installed, both for general illumination and for display use.

The use factor is the ratio of the wattage in use, for the conditions under which the load estimate is being made, to the total installed wattage. For commercial applications such as stores, the use factor would generally be unity.

The special allowance factor is the ratio of the power consumption of the lighting fixture, including lamps and ballast, to the nominal power consumption of the lamps. For incandescent lights, the special allowance factor is one. For fluorescent lights, the special allowance factor accounts for the power consumed by the ballast as well as the effect of the ballast on the lamp power consumption. The special allowance factor can be less than one for electronic ballasts that lower the electricity consumption below the rated power consumption for the lamp. It is suggested that engineers use manufacturer values for system (lamps + ballast) power, when available.

For high-intensity discharge lamps (e.g., metal halide, mercury vapor, and high- and low-pressure sodium vapor lamps), the actual lighting system power consumption should be available from the manufacturer of the fixture or ballast. At the time of writing, a very limited check of ballasts available for metal halide and high-pressure sodium vapor lamps showed special allowance factors ranging from about 1.3 for low-wattage lamps down to 1.1 for high-wattage lamps.

An alternative procedure is to estimate the lighting heat gain on a per-square meter basis. Such an approach may be required when final lighting plans are not available. Table 6.2 shows the maximum lighting power density (lighting heat gain per square meter) permitted by ASHRAE/IES Standard 90.1-2010 for a range of space types. There are several cases where these values may be exceeded; examples include the following:

- Decorative lighting or lighting for highlighting art or exhibits, which may add additional heat gain
- Retail sales display areas, for which additional allowances depend on the type of merchandise
- Spaces with extra lighting controls
- Corridors and transition spaces with widths less than 8 feet

For more detailed information, consult Chapter 9 of ASHRAE/IESNA Standard 90.1-2010.

In addition to determining the lighting heat gain, the fraction of the lighting heat gain that enters the conditioned space may need to be distinguished from the fraction that enters an unconditioned space (e.g., return air plenum) and, of the lighting heat gain that enters the conditioned space, the distribution between radiative and convective heat gain must be established.

ASHRAE RP-1282 (Fisher and Chantrasrisalai 2006) experimentally studied 12 luminaire types and recommended 5 different categories of luminaires, as shown in Table 6.3. This table provides a range of design data for the conditioned space fraction, the shortwave radiative fraction, and the longwave radiative fraction under typical operating conditions: airflow rate of $5 \text{ L}/(\text{s}\cdot\text{m}^2)$, supply air temperature between 15°C and 17°C , and room air temperature between 22°C and 24°C . The recommended fractions in Table 6.3 are based on lighting heat input rates ranging from $9 \text{ W}/\text{m}^2$ to $26 \text{ W}/\text{m}^2$. For design power input higher than $26 \text{ W}/\text{m}^2$, the lower bounds of the space and shortwave fractions should be used, and for design power input less than $9 \text{ W}/\text{m}^2$, the upper bounds of the space and shortwave fractions should be used. The space fraction in the table is the fraction of lighting heat gain that goes to the room; the fraction going to the plenum can be computed as one minus the space fraction. The radiative fraction is the fraction of the lighting heat gain that goes to the room that is radiative. The convective fraction of the lighting heat gain that goes to the room is one minus the radiative frac-

Load Calculation Applications Manual (SI), Second Edition

tion. Using values in the middle of the range yields sufficiently accurate results. However, selection of values that better suit a specific situation may be determined according to notes given in the *Notes* column in Table 6.3.

The data presented in Table 6.3 are applicable for both ducted and nonducted returns. However, the application of the data, particularly the ceiling plenum fraction, may vary for different return configurations. For instance, for a room with a ducted return, although a portion of the lighting energy initially dissipated to the ceiling plenum is quantitatively equal to the plenum fraction, a large portion of this energy would likely end up as the conditioned space cooling load. A small

Table 6.2 Lighting Power Densities Using the Space-by-Space Method

(Source: ASHRAE/IES Standard 90.1-2010, Table 9.6.1)

Common Space Types ^a	LPD, W/m ²	RCR Threshold
Atrium		
First 13 m height	1.059 per m (height)	NA
Height above 13 m	0.706 per m (height)	NA
Audience/Seating Area—Permanent		
For auditorium	8.5	6
For Performing Arts Theater	26.2	8
For Motion Picture Theater	12.3	4
Classroom/Lecture/Training	13.3	4
Conference/Meeting/Multipurpose	13.2	6
Corridor/Transition	7.1	Width < 2.4 m
Dining Area		
For Bar Lounge/Leisure Dining	14.1	4
For Family Dining	9.6	4
Dressing/Fitting Room for Performing Arts Theater	4.3	6
Electrical/Mechanical	10.2	6
Food Preparation	10.7	6
Laboratory		
For Classrooms	13.8	6
For Medical/Industrial/Research	19.5	6
Lobby		
For Elevator	6.88	6
For Performing Arts Theater	21.5	6
For Motion Picture Theater	5.6	4
Locker Room	8.1	6
Lounge/Recreation	7.9	4
Office		
Enclosed	11.9	8
Open Plan	10.5	4
Restrooms	10.5	8

Internal Heat Gain

**Table 6.2 Lighting Power Densities Using the Space-by-Space Method
(continued)**

Building-Specific Space Types	LPD, W/m ²	RCR Threshold
Sales Area (for accent lighting, see Section 9.6.2(b))	18.1	6
Stairway	7.4	10
Storage	6.8	6
Workshop	17.1	6
Automotive		
Service/Repair	7.2	4
Bank/Office		
Banking Activity Area	14.9	6
Convention Center		
Audience Seating	8.8	4
Exhibit Space	15.6	4
Courthouse/Police Station/Penitentiary		
Courtroom	18.5	6
Confinement Cells	11.8	6
Judges' Chambers	12.6	8
Penitentiary Audience Seating	4.6	4
Penitentiary Classroom	14.4	4
Penitentiary Dining	11.5	6
Dormitory		
Living Quarters	4.1	8
Fire Stations		
Engine Room	6.0	4
Sleeping Quarters	2.7	6
Gymnasium/Fitness Center		
Fitness Area	7.8	4
Gymnasium Audience Seating	4.6	6
Playing Area	12.9	4
Hospital		
Corridor/Transition	9.6	Width < 2.4 m
Emergency	24.3	6
Exam/Treatment	17.9	8
Laundry/Washing	6.5	4
Lounge/Recreation	11.5	6
Medical Supply	13.7	6
Nursery	9.5	6
Nurses' Station	9.4	6
Operating Room	20.3	6

Load Calculation Applications Manual (SI), Second Edition

Table 6.2 Lighting Power Densities Using the Space-by-Space Method (continued)

Building-Specific Space Types	LPD, W/m ²	RCR Threshold
Patient Room	6.7	6
Pharmacy	12.3	6
Physical Therapy	9.8	6
Radiology/Imaging	14.2	6
Recovery	12.4	6
Hotel/Highway Lodging		
Hotel Dining	8.8	4
Hotel Guest Rooms	11.9	6
Hotel Lobby	11.4	4
Highway Lodging Dining	9.5	4
Highway Lodging Guest Rooms	8.1	6
Library		
Card File and Cataloging	7.8	4
Reading Area	10	4
Stacks	18.4	4
Manufacturing		
Corridor/Transition	4.4	Width < 2.4 m
Detailed Manufacturing	13.9	4
Equipment Room	10.2	6
Extra High Bay (>15.2 m Floor to Ceiling Height)	11.3	4
High Bay (7.6–15.2 m Floor to Ceiling Height)	13.2	4
Low Bay (<7.6 m Floor to Ceiling Height)	12.8	4
Museum		
General Exhibition	11.3	6
Restoration	11.0	6
Parking Garage		
Garage Area	2.0	4
Post Office		
Sorting Area	10.1	4
Religious Buildings		
Audience Seating	16.5	4
Fellowship Hall	6.9	4
Worship Pulpit, Choir	16.5	4

Table 6.2 Lighting Power Densities Using the Space-by-Space Method (continued)

Building-Specific Space Types	LPD, W/m ²	RCR Threshold
Retail		
Dressing/Fitting Room	9.4	8
Mall Concourse	11.8	4
Sports Arena		
Audience Seating	4.6	4
Court Sports Arena—Class 4	7.8	4
Court Sports Arena—Class 3	12.9	4
Court Sports Arena—Class 2	20.7	4
Court Sports Arena—Class 1	32.4	4
Ring Sports Arena	28.8	4
Transportation		
Air/Train/Bus—Baggage Area	8.2	4
Airport—Concourse	3.9	4
Audience Seating	5.8	4
Terminal—Ticket Counter	11.6	4
Warehouse		
Fine Material Storage	10.2	6
Medium/Bulky Material Storage	6.2	4

^a In cases where both a common space type and a building-specific type are listed, the building specific space type shall apply.

portion would end up as the cooling load to the return air. Treatment of such cases is discussed in Appendix F and an example is given in Chapter 8.

If the space airflow rate is different from the typical condition (i.e., about 5 L/(s · m²), Figure 6.1 can be used to estimate the lighting heat gain parameters. Design data shown in Figure 6.1 are only applicable for the recessed fluorescent luminaire without lens.

Although design data presented in Table 6.3 and Figure 6.1 can be used for a vented luminaire with side-slot returns, they are likely not applicable for a vented luminaire with lamp-compartment returns, because all heat convected in the vented luminaire with lamp-compartment returns would likely go directly to the ceiling plenum, resulting in a zero convective fraction and a much lower space fraction than that for a vented luminaire with side-slot returns. Therefore, the design data should only be used for a configuration where the conditioned air is returned through the ceiling grille or the luminaire side slots.

For other luminaire types not covered by ASHRAE RP-1282 (Fisher and Chant-rasrisalai 2006), it may be necessary to estimate the heat gain for each component as a fraction of the total lighting heat gain by using judgment to estimate heat-to-space and heat-to-return percentages.

Because of the directional nature of downlight luminaires, a large portion of the shortwave radiation typically falls on the floor. When converting heat gains to cooling loads in the RTSM, solar radiant time factors (RTFs) may be more appropriate than non-solar RTFs. (Solar RTFs are calculated assuming most of the solar radiation is intercepted by the floor; nonsolar RTFs assume a uniform distribution by area over all interior surfaces.) This effect may be significant for rooms where the lighting heat gain is high and for which the solar RTFs are significantly different from the nonsolar RTFs.

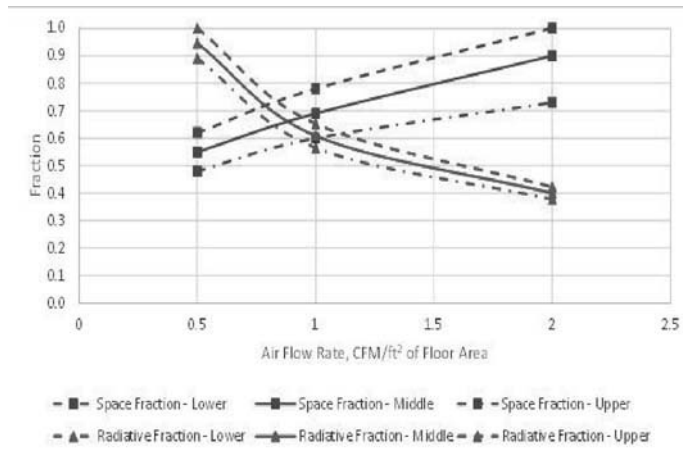


Figure 6.1 Lighting heat gain parameters for recessed fluorescent luminaire without lens.

(Source: *Lighting heat gain distribution in buildings*, RP-1282, 2006).

Table 6.3 Lighting Heat Gain Parameters for Typical Operating Conditions

(Source: *Lighting heat gain distribution in buildings*, RP-1282, 2006)

Luminaire Category	Space Fraction	Radiative Fraction	Notes
Recessed fluorescent luminaire without lens	0.64–0.74	0.48–0.68	Use middle values in most situations. May use higher space fraction and lower radiative fraction for luminaire with side-slot returns. May use lower values of both fractions for direct/indirect luminaire. May use higher values of both fractions for ducted returns.
Recessed fluorescent luminaire with lens	0.40–0.50	0.61–0.73	May adjust values in the same way as for recessed fluorescent luminaire without lens.
Downlight compact fluorescent luminaire	0.12–0.24	0.95–1.0	Use middle or high values if detailed features are unknown. Use low value for space fraction and high value for radiative fraction if there are large holes in the reflector of the luminaire.
Downlight incandescent luminaire	0.70–0.80	0.95–1.0	Use middle values if lamp type is unknown. Use low value for space fraction if a standard lamp (e.g., A-lamp) is used. Use high value for space fraction if a reflector lamp (e.g., BR-lamp) is used.
Non-in-ceiling fluorescent luminaire	1.0	0.5–0.57	Use lower value for radiative fraction for surface-mounted luminaire. Use higher value for radiative fraction for pendant luminaire.

Miscellaneous Equipment

Estimates of heat gain in this category tend to be even more subjective than for people and lights. However, considerable data are available that, when used judiciously, will yield reliable results. Careful evaluation of the operating schedule and the load factor for each piece of equipment is essential.

Power

When equipment is operated by electric motor within a conditioned space, the heat equivalent is calculated as

$$q_{em} = (P/E_m)F_{UM}F_{LM} \quad (6.2)$$

where

- q_{em} = heat equivalent of equipment operation, W
- P = motor power rating, kW
- E_m = motor efficiency, as decimal fraction < 1.0
- F_{UM} = motor-use factor, 1.0 or decimal < 1.0
- F_{LM} = motor-load factor, 1.0 or decimal < 1.0

The motor-use factor may be applied when motor use is known to be intermittent with significant nonuse during all hours of operation—for example, in the case of an overhead door operator. In these cases, the motor-use factor in any hour is equal to the fraction of time the motor is operated during the hour. For conventional applications, its value is 1.0.

The motor-load factor is the fraction of the rated motor load delivered under the conditions of the cooling-load estimate. Heat output of a motor generally is proportional to the motor load, within the overload limits. Because of typically high no-load motor current, fixed losses, and other reasons, F_{LM} is assumed to be unity, and no adjustment should be made for underloading or overloading unless the situation is fixed and can be accurately established and unless the reduced load efficiency data can be obtained from the motor manufacturer.

In Equation 6.2, both the motor and the driven equipment are assumed to be within the conditioned space. If the motor is outside the space or airstreams and the driven equipment is within the conditioned space, use

$$q_{em} = (P)F_{UM}F_{LM} \quad (6.3)$$

When the motor is inside the conditioned space or airstream but the driven machine is outside, use

$$q_{em} = P\left(\frac{1.0 - E_m}{E_m}\right)F_{UM}F_{LM} \quad (6.4)$$

Equation 6.4 also applies to a fan or pump in the conditioned space that exhausts air or pumps fluid outside that space.

Table 6.4 gives minimum efficiencies for typical electric motors of recent manufacture from ASHRAE/IES Standard 90.1-2010. If electric-motor heat gain is an appreciable portion of cooling load, the motor efficiency should be obtained from the manufacturer. Also, depending on design, the maximum efficiency might occur anywhere between 75% and 110% of full load. If underloaded or overloaded, the efficiency could vary from the manufacturer's listing.

Unless the manufacturer's technical literature indicates otherwise, the heat gain should be divided about 50% radiant and 50% convective for subsequent cooling load calculations.

Food Preparation Appliances

In a cooling-load estimate, heat gain from all appliances—electric, gas, or steam—should be taken into account. The tremendous variety of appliances, applications, usage schedules, and installations makes estimates very subjective. To establish

Load Calculation Applications Manual (SI), Second Edition

a heat gain value, actual input data values and various factors, efficiencies, or other judgmental modifiers are preferred. However, where specific rating data are not available, recommended heat gains tabulated in this chapter may be used as an alternative approach. In estimating the appliance load, probabilities of simultaneous use and operation of different appliances located in the same space must be considered.

In commercial kitchens, appliances are typically on and “up to temperature” for the entire day, though the actual amount of time that they are actually used for cooking is often less than 25% (Swierczyna et al. 2009.) Therefore, measured values of heat gains under idle conditions are often used for cooling load calculations. Recommended rates of heat gain corresponding to idle conditions are given in Tables 6.5a to 6.5a. For unhooded electric appliances, recommended rates of sensible radiant heat gain, sensible convective heat gain, and latent heat gain are given in the fourth, fifth, and sixth columns of Table 6.5a. A usage factor, F_U , is also given—it is the ratio of the standby heat gain to the rated energy. The radiation factor F_R given in the last column is the fraction of sensible heat gain that is radiant. These values have already been applied to the rates of heat gain that are given.

For hooded appliances, recommended heat gain rates are given in Tables 6.5b, 6.5c, and 6.5d. For hooded appliances, the convective and latent heat gains are

**Table 6.4 Minimum Nominal Full-Load Efficiency
for 60 HZ NEMA General Purpose Electric Motors (Subtype I) Rated
600 Volts or Less (Random Wound)**

(Source: ASHRAE/IES Standard 90.1-2010)

Minimum Nominal Full Load Efficiency (%) for Motors Manufactured on or after December 19, 2010							
		Open Drip-Proof Motors			Totally Enclosed Fan-Cooled Motors		
Number of Poles ⇒		2	4	6	2	4	6
Synchronous Speed (RPM) ⇒		3600	1800	1200	3600	1800	1200
Kilowatts							
	0.8	77.0	85.5	82.5	77.0	85.5	82.5
	1.1	84.0	86.5	86.5	84.0	86.5	87.5
	1.5	85.5	86.5	87.5	85.5	86.5	88.5
	2.2	85.5	89.5	88.5	86.5	89.5	89.5
	3.7	86.5	89.5	89.5	88.5	89.5	89.5
	5.6	88.5	91.0	90.2	89.5	91.7	91.0
	7.5	89.5	91.7	91.7	90.2	91.7	91.0
	11.1	90.2	93.0	91.7	91.0	92.4	91.7
	14.9	91.0	93.0	92.4	91.0	93.0	91.7
	18.7	91.7	93.6	93.0	91.7	93.6	93.0
	22.4	91.7	94.1	93.6	91.7	93.6	93.0
	29.8	92.4	94.1	94.1	92.4	94.1	94.1
	37.3	93.0	94.5	94.1	93.0	94.5	94.1
	44.8	93.6	95.0	94.5	93.6	95.0	94.5
	56.0	93.6	95.0	94.5	93.6	95.4	94.5
	74.6	93.6	95.4	95.0	94.1	95.4	95.0
	93.3	94.1	95.4	95.0	95.0	95.4	95.0
	111.9	94.1	95.8	95.4	95.0	95.8	95.8
	149.2	95.0	95.8	95.4	95.4	96.2	95.8
	186.5	95.0	95.8	95.4	95.8	96.2	95.8
	223.8	95.4	95.8	95.4	95.8	96.2	95.8
	261.1	95.4	95.8	95.4	95.8	96.2	95.8
	298.4	95.8	95.8	95.8	95.8	96.2	95.8
	357.7	95.8	96.2	96.2	95.8	96.2	95.8
	373.0	95.8	96.2	96.2	95.8	96.2	95.8

Source: ASHRAE/IES Standard 90.1-2010

*Nominal efficiencies established in accordance with NEMA Standard MG1. Design A and Design B are National Electric Manufacturers Association (NEMA) design class designations for fixed-frequency small and medium AC squirrel-cage induction motors.

assumed to be removed by the hood, so the remaining heat gain shown in the fourth column of each table is 100% radiant. As before, the usage factor and radiation factor have already been applied.

Hospital and Laboratory Equipment

As with large kitchen installations, hospital and laboratory equipment is a major source of heat gain in conditioned spaces. Care must be taken in evaluating the probability and duration of simultaneous usage when many components are concentrated in one area, as in a laboratory, operating room, etc. The chapters related to health facilities and laboratories in the *ASHRAE Handbook—HVAC Applications* (2011) should be consulted for further information.

Tables 6.6 and 6.7 give recommended rates of heat gain for hospital equipment (Alereza and Breen 1984) and laboratory equipment (Hosni et al. 1999). These data are recommended where specific heat gain data and use schedules are not available.

As a general rule, for equipment that does not have significantly elevated surface temperatures, Hosni et al. (1999) recommend a radiative/convective split of 10%/90% for fan-cooled equipment and 30%/70% for non-fan-cooled equipment.

Office Appliances

Computers, printers, copiers, and other office equipment can generate significant internal heat gains, and so it is important to adequately account for these heat gains when computing the cooling load. Past research has shown that nameplate data are not reliable indicators of actual heat gain, significantly overstating

Table 6.5a Recommended Rates of Radiant and Convective Heat Gain from Unhooded Electric Appliances During Idle (Ready-to-Cook) Conditions

(Source: *ASHRAE Handbook—Fundamentals* [2013], Chapter 18, Table 5A)

Appliance	Energy Rate, W		Rate of Heat Gain, W				Usage Factor F_U	Radiation Factor F_R
	Rated	Standby	Sensible Radiant	Sensible Convective	Latent	Total		
Cabinet: hot serving (large), insulated*	1993	352	117	234	0	352	0.18	0.33
hot serving (large), uninsulated	1993	1026	205	821	0	1026	0.51	0.20
proofing (large)*	5099	410	352	0	59	410	0.08	0.86
proofing (small 15-shelf)	4191	1143	0	264	879	1143	0.27	0.00
Coffee brewing urn	3810	352	59	88	205	352	0.08	0.17
Drawer warmers, 2-drawer (moist holding)*	1202	147	0	0	59	59	0.12	0.00
Egg cooker	3194	205	88	117	0	205	0.06	0.43
Espresso machine*	2403	352	117	234	0	352	0.15	0.33
Food warmer: steam table (2-well-type)	1495	1026	88	176	762	1026	0.69	0.08
Freezer (small)	791	322	147	176	0	322	0.41	0.45
Hot dog roller*	996	703	264	440	0	703	0.71	0.38
Hot plate: single burner, high speed	1114	879	264	615	0	879	0.79	0.30
Hot-food case (dry holding)*	9115	733	264	469	0	733	0.08	0.36
Hot-food case (moist holding)*	9115	967	264	528	176	967	0.11	0.27
Microwave oven: commercial (heavy duty)	3194	0	0	0	0	0	0	0.00
Oven: countertop conveyorized bake/finishing*	6008	3693	645	3048	0	3693	0.61	0.17
Panini*	1700	938	352	586	0	938	0.55	0.38
Popcorn popper*	586	59	29	29	0	59	0.1	0.50
Rapid-cook oven (quartz-halogen)*	12 016	0	0	0	0	0	0	0.00
Rapid-cook oven (microwave/convection)*	7297	1202	293	909	0	4,100	0.16	0.24
Reach-in refrigerator*	1407	352	88	264	0	352	0.25	0.25
Refrigerated prep table*	586	264	176	88	0	264	0.45	0.67
Steamer (bun)	1495	205	176	29	0	205	0.14	0.86
Toaster: 4-slice pop up (large): cooking	1788	879	59	410	293	762	0.49	0.07
contact (vertical)	3312	1553	791	762	0	1553	0.47	0.51
conveyor (large)	9613	3019	879	2139	0	3019	0.31	0.29
small conveyor	1700	1084	117	967	0	1084	0.64	0.11
Waffle iron	909	352	234	117	0	352	0.39	0.67

*Items with an asterisk appear only in Swierczyna et al. (2009); all others appear in both Swierczyna et al. (2008) and (2009).

Load Calculation Applications Manual (SI), Second Edition

Table 6.5b Recommended Rates of Radiant Heat Gain from Hooded Electric Appliances During Idle (Ready-to-Cook) Conditions

(Source: ASHRAE Handbook—Fundamentals [2013], Chapter 18, Table 5B)

Appliance	Energy Rate, W		Rate of Heat Gain, W		Usage Factor F_U	Radiation Factor F_R
	Rated	Standby	Sensible Radiant			
Broiler: underfired 900 mm	10 814	9056	3165		0.84	0.35
Cheesemelter*	3605	3488	1348		0.97	0.39
Fryer: kettle	29 014	528	147		0.02	0.28
Fryer: open deep-fat, 1-vat	14 008	821	293		0.06	0.36
Fryer: pressure	13 511	791	147		0.06	0.19
Griddle: double sided 900 mm (clamshell down)*	21 218	2022	410		0.10	0.20
Griddle: double sided 900 mm (clamshell up)*	21 218	3370	1055		0.16	0.31
Griddle: flat 900 mm	17 115	3370	1319		0.20	0.39
Griddle-small 900 mm*	8997	1788	791		0.20	0.44
Induction cooktop*	21 013	0	0		0.00	0.00
Induction wok*	3488	0	0		0.00	0.00
Oven: combi: combi-mode*	16 411	1612	234		0.10	0.15
Oven: combi: convection mode	16 412	1612	410		0.10	0.25
Oven: convection full-size	12 103	1964	440		0.16	0.22
Oven: convection half-size*	5510	1084	147		0.20	0.14
Pasta cooker*	22 010	2491	0		0.11	0.00
Range top: top off/oven on*	4865	1172	293		0.24	0.25
Range top: 3 elements on/oven off	15 005	4513	1846		0.30	0.41
Range top: 6 elements on/oven off	15 005	9730	4074		0.65	0.42
Range top: 6 elements on/oven on	19 870	10 668	4250		0.54	0.40
Range: hot-top	15 826	15 035	3458		0.95	0.23
Rotisserie*	11 107	4044	1319		0.36	0.33
Salamander*	7004	6829	2051		0.97	0.30
Steam kettle: large (225 L), simmer lid down*	32 414	762	29		0.02	0.04
Steam kettle: small (150 L), simmer lid down*	21 599	528	88		0.02	0.17
Steamer: compartment: atmospheric*	9789	4484	59		0.46	0.01
Tilting skillet/braising pan	9642	1553	0		0.16	0.00

* Items with an asterisk appear only in Swierczyna et al. (2009); all others appear in both Swierczyna et al. (2008) and (2009).

Table 6.5c Recommended Rates of Radiant Heat Gain from Hooded Gas Appliances During Idle (Ready-to-Cook) Conditions

(Source: ASHRAE Handbook—Fundamentals [2013], Chapter 18, Table 5C)

Appliance	Energy Rate, W		Rate of Heat Gain, W		Usage Factor F_U	Radiation Factor F_R
	Rated	Standby	Sensible Radiant			
Broiler: batch*	27 842	20 280	2374		0.73	0.12
Broiler: chain (conveyor)	38 685	28 340	3869		0.73	0.14
Broiler: overfired (upright)*	29 307	25 761	733		0.88	0.03
Broiler: underfired 900 mm	28 135	21 658	2638		0.77	0.12
Fryer: doughnut	12 895	3634	850		0.28	0.23
Fryer: open deep-fat, 1 vat	23 446	1377	322		0.06	0.23
Fryer: pressure	23 446	2638	234		0.11	0.09
Griddle: double sided 900 mm (clamshell down)*	31 710	2345	528		0.07	0.23
Griddle: double sided 900 mm (clamshell up)*	31 710	4308	1436		0.14	0.33
Griddle: flat 900 mm	26 376	5979	1084		0.23	0.18
Oven: combi: combi-mode*	22 185	1758	117		0.08	0.07
Oven: combi: convection mode	22 185	1700	293		0.08	0.17
Oven: convection full-size	12 895	3488	293		0.27	0.08
Oven: conveyor (pizza)	49 822	20 017	2286		0.40	0.11
Oven: deck	30 772	6008	1026		0.20	0.17
Oven: rack mini-rotating*	16 500	1319	322		0.08	0.24
Pasta cooker*	23 446	6946	0		0.30	0.00
Range top: top off/oven on*	7327	2169	586		0.30	0.27
Range top: 3 burners on/oven off	35 169	17 614	2081		0.50	0.12
Range top: 6 burners on/oven off	35 169	35 403	3370		1.01	0.10
Range top: 6 burners on/oven on	42 495	36 018	3986		0.85	0.11
Range: wok*	29 014	25 614	1524		0.88	0.06
Rethermalizer*	26 376	6829	3370		0.26	0.49
Rice cooker*	10 257	147	88		0.01	0.60
Salamander*	10 257	9759	1553		0.95	0.16
Steam kettle: large (225 L) simmer lid down*	42 495	1583	0		0.04	0.00
Steam kettle: small (38 L) simmer lid down*	15 240	967	88		0.06	0.09

Table 6.5c Recommended Rates of Radiant Heat Gain from Hooded Gas Appliances During Idle (Ready-to-Cook) Conditions (continued)

(Source: ASHRAE Handbook—Fundamentals [2013], Chapter 18, Table 5C)

Appliance	Energy Rate, W		Rate of Heat Gain, W		Usage Factor F_U	Radiation Factor F_R
	Rated	Standby	Sensible Radiant			
Steam kettle: small (150 L) simmer lid down	29 307	1260	0		0.04	0.00
Steamer: compartment: atmospheric*	7620	2432	0		0.32	0.00
Tilting skillet/braising pan	30 479	3048	117		0.10	0.04

*Items with an asterisk appear only in Swierczyna et al. (2009); all others appear in both Swierczyna et al. (2008) and (2009).

Table 6.5d Recommended Rates of Radiant Heat Gain from Hooded Solid Fuel Appliances During Idle (Ready-to-Cook) Conditions

(Source: ASHRAE Handbook—Fundamentals [2013], Chapter 18, Table 5D)

Appliance	Energy Rate, W	Rate of Heat Gain, W		Usage Factor F_U	Radiation Factor F_R
	Rated	Standby	Sensible		
Broiler: solid fuel: charcoal	18 kg	12 309	1817	N/A	0.15
Broiler: solid fuel: wood (mesquite)*	18 kg	14 536	2051	N/A	0.14

*Items with an asterisk appear only in Swierczyna et al. (2009); all others appear in both Swierczyna et al. (2008) and (2009).

Table 6.5e Recommended Rates of Radiant and Convective Heat Gain from Warewashing Equipment During Idle (Standby) or Washing Conditions

(Source: ASHRAE Handbook—Fundamentals [2013], Chapter 18, Table 5E)

Appliance	Energy Rate, W		Rate of Heat Gain, W						
			Unhooded				Hooded	Usage Factor F_U	Radiation Factor F_R
	Rated	Standby/Washing	Sensible Radiant	Sensible Convective	Latent	Total	Sensible Radiant		
Dishwasher (conveyor type, chemical sanitizing)	13 716	1671/12 778	0	1304	3954	5258	0	0.36	0
Dishwasher (conveyor type, hot-water sanitizing) standby	13 716	1671/N/A	0	1392	4973	6366	0	N/A	0
Dishwasher (door-type, chemical sanitizing) washing	5393	352/3898	0	580	818	1398	0	0.26	0
Dishwasher (door-type, hot-water sanitizing) washing	5393	352/3898	0	580	818	1398	0	0.26	0
Dishwasher* (under-counter type, chemical sanitizing) standby	7796	352/5480	0	668	1222	1890	0	0.35	0.00
Dishwasher* (under-counter type, hot-water sanitizing) standby	7796	498/5774	234	305	882	1421	234	0.27	0.34
Booster heater*	38 099	0	147	0	0	0	147	0	N/A

*Items with an asterisk appear only in Swierczyna et al. (2009); all others appear in both Swierczyna et al. (2008) and (2009).

Note: Heat load values are prorated for 30% washing and 70% standby.

the heat gain. There are two approaches that may be taken to estimate office heat gains. The first approach involves estimating the heat gains on a piece-by-piece basis—a certain amount of heat gain is allocated to each appliance anticipated in the space. To use this approach, Tables 6.8, 6.9, and 6.10 give recommended rates of heat gain for computers, printers, and miscellaneous office equipment (ASHRAE Handbook—Fundamentals [2013]). For larger spaces with many pieces of equipment, diversity should be considered. That is, not all of the equipment is likely to be on at any given time.

Diversity varies with occupancy—different types of businesses are likely to have different diversity factors. ASHRAE Research Project 1093 (Abushakra et al. 2004; Claridge et al. 2004) derived diversity profiles for a variety of office buildings.

A second approach simply estimates likely heat gain per unit area. Recommendations based on work by Wilkins and Hosni (2011) can be found in Table 6.11. The medium-load density should be sufficient for most standard office spaces. The heavy-load densities are likely to be conservative estimates even for densely populated spaces.

Like other internal heat gains, it is necessary to split the heat gain into radiant and convective components. Recommendations for specific office equipment are given in the footnotes of Tables 6.8 and 6.9. For other office equipment, Hosni et al. (1999) recommend a radiative/convective split of 10%/90% for fan-cooled equipment and 30%/70% for non-fan-cooled equipment.

Load Calculation Applications Manual (SI), Second Edition

Table 6.6 Recommended Heat Gain from Typical Medical Equipment

(Source: ASHRAE Handbook—Fundamentals [2013], Chapter 18, Table 6)

Equipment	Nameplate, W	Peak, W	Average, W
Anesthesia system	250	177	166
Blanket warmer	500	504	221
Blood pressure meter	180	33	29
Blood warmer	360	204	114
ECG/RESP	1440	54	50
Electrosurgery	1000	147	109
Endoscope	1688	605	596
Harmonical scalpel	230	60	59
Hysteroscopic pump	180	35	34
Laser sonics	1200	256	229
Optical microscope	330	65	63
Pulse oximeter	72	21	20
Stress treadmill	N/A	198	173
Ultrasound system	1800	1063	1050
Vacuum suction	621	337	302
		968	82
X-ray system	1725	534	480
	2070		18

Source: Hosni et al. 1999.

Table 6.7 Recommended Heat Gain from Typical Laboratory Equipment

(Source: ASHRAE Handbook—Fundamentals [2013], Chapter 18, Table 7)

Equipment	Nameplate, W	Peak, W	Average, W
Analytical balance	7	7	7
Centrifuge	138	89	87
	288	136	132
	5500	1176	730
Electrochemical analyzer	50	45	44
	100	85	84
Flame photometer	180	107	105
Fluorescent microscope	150	144	143
	200	205	178
Function generator	58	29	29
Incubator	515	461	451
	600	479	264
	3125	1335	1222
Orbital shaker	100	16	16
Oscilloscope	72	38	38
	345	99	97
Rotary evaporator	75	74	73
	94	29	28
Spectronics	36	31	31
	575	106	104
Spectrophotometer	200	122	121
	N/A	127	125
	340	405	395
Spectro fluorometer	1840	965	641
Thermocycler	N/A	233	198
	475	132	46
Tissue culture	2346	1178	1146

Source: Hosni et al. (1999).

Load Calculation Applications Manual (SI), Second Edition

Table 6.8 Recommended Heat Gain from Typical Computer Equipment

(Source: ASHRAE Handbook—Fundamentals [2013], Chapter 18, Table 8)

Equipment	Description	Nameplate Power, W	Average Power, W	Radiant Fraction
Desktop computer ^a	Manufacturer A (model A); 2.8 GHz processor, 1 GB RAM	480	73	0.10 ^a
	Manufacturer A (model B); 2.6 GHz processor, 2 GB RAM	480	49	0.10 ^a
	Manufacturer B (model A); 3.0 GHz processor, 2 GB RAM	690	77	0.10 ^a
	Manufacturer B (model B); 3.0 GHz processor, 2 GB RAM	690	48	0.10 ^a
	Manufacturer A (model C); 2.3 GHz processor, 3 GB RAM	1200	97	0.10 ^a
Laptop computer ^b	Manufacturer 1; 2.0 GHz processor, 2 GB RAM, 430 mm screen	130	36	0.25 ^b
	Manufacturer 1; 1.8 GHz processor, 1 GB RAM, 430 mm screen	90	23	0.25 ^b
	Manufacturer 1; 2.0 GHz processor, 2 GB RAM, 355 mm screen	90	31	0.25 ^b
	Manufacturer 2; 2.13 GHz processor, 1 GB RAM, 355 mm screen, tablet PC	90	29	0.25 ^b
	Manufacturer 2; 366 MHz processor, 130 MB RAM (355 mm screen)	70	22	0.25 ^b
Flat-panel monitor ^c	Manufacturer 3; 900 MHz processor, 256 MB RAM (265 mm screen)	50	12	0.25 ^b
	Manufacturer X (model A); 760 mm screen	383	90	0.40 ^c
	Manufacturer X (model B); 560 mm screen	360	36	0.40 ^c
	Manufacturer Y (model A); 480 mm screen	288	28	0.40 ^c
	Manufacturer Y (model B); 430 mm screen	240	27	0.40 ^c
Flat-panel monitor ^c	Manufacturer Z (model A); 430 mm screen	240	29	0.40 ^c
	Manufacturer Z (model C); 380 mm screen	240	19	0.40 ^c

Source: Hosni and Beck (2008).

^aPower consumption for newer desktop computers in operational mode varies from 50 to 100 W, but a conservative value of about 65 W may be used. Power consumption in sleep mode is negligible. Because of cooling fan, approximately 90% of load is by convection and 10% is by radiation. Actual power consumption is about 10 to 15% of nameplate value.

^bPower consumption of laptop computers is relatively small: depending on processor speed and screen size, it varies from about 15 to 40 W. Thus, differentiating between radiative and convective parts of the cooling load is unnecessary and the entire load may be classified as convective. Otherwise, a 75/25% split between convective and radiative components may be used. Actual power consumption for laptops is about 25% of nameplate values.

^cFlat-panel monitors have replaced cathode ray tube (CRT) monitors in many workplaces, providing better resolution and being much lighter. Power consumption depends on size and resolution, and ranges from about 20 W (for 380 mm size) to 90 W (for 760 mm). The most common sizes in workplaces are 480 and 560 mm, for which an average 30 W power consumption value may be used. Use 60/40% split between convective and radiative components. In idle mode, monitors have negligible power consumption. Nameplate values should not be used.

Table 6.9 Recommended Heat Gain from Typical Laser Printers and Copiers

(Source: ASHRAE Handbook—Fundamentals [2013], Chapter 18, Table 9)

Equipment	Description	Nameplate Power, W	Average Power, W	Radiant Fraction
Laser printer, typical desktop, small-office type ^a	Printing speed up to 10 pages per minute	430	137	0.30 ^a
	Printing speed up to 35 pages per minute	890	74	0.30 ^a
	Printing speed up to 19 pages per minute	508	88	0.30 ^a
	Printing speed up to 17 pages per minute	508	98	0.30 ^a
	Printing speed up to 19 pages per minute	635	110	0.30 ^a
	Printing speed up to 24 page per minute	1344	130	0.30 ^a
Multifunction (copy, print, scan) ^b	Small, desktop type	600	30	d
	Medium, desktop type	40	15	d
Scanner ^b	Small, desktop type	700	135	d
	Small, desktop type	19	16	d
Copy machine ^c	Large, multiuser, office type	1750	800 (idle 260 W)	d (idle 0.00 ^c)
		1440	550 (idle 135 W)	d (idle 0.00 ^c)
		1850	1060 (idle 305 W)	d (idle 0.00 ^c)
Fax machine	Medium	936	90	d
	Small	40	20	d
Plotter	Manufacturer A	400	250	d
	Manufacturer B	456	140	d

Source: Hosni and Beck (2008).

^aVarious laser printers commercially available and commonly used in personal offices were tested for power consumption in print mode, which varied from 75 to 140 W, depending on model, print capacity, and speed. Average power consumption of 110 W may be used. Split between convection and radiation is approximately 70/30%.

^bSmall multifunction (copy, scan, print) systems use about 15 to 30 W; medium-sized ones use about 135 W. Power consumption in idle mode is negligible. Nameplate values do not represent actual power consumption and should not be used. Small, single-sheet scanners consume less than 20 W and do not contribute significantly to building cooling load.

^cPower consumption for large copy machines in large offices and copy centers ranges from about 550 to 1100 W in copy mode. Consumption in idle mode varies from about 130 to 300 W. Count idle-mode power consumption as mostly convective in cooling load calculations.

^dSplit between convective and radiant heat gain was not determined for these types of equipment.

Internal Heat Gain

Table 6.10 Recommended Heat Gain from Miscellaneous Office Equipment

Equipment	Maximum Input Rating, W	Recommended Rate of Heat Gain, W
Mail-processing equipment		
Folding machine	125	80
Inserting machine, 3600 to 6800 pieces/h	600 to 3300	390 to 2150
Labeling machine, 1500 to 30 000 pieces/h	600 to 6600	390 to 4300
Postage meter	230	150
Vending machines		
Cigarette	72	72
Cold food/beverage	1150 to 1920	575 to 960
Hot beverage	1725	862
Snack	240 to 275	240 to 275
Other		
Bar code printer	440	370
Cash registers	60	48
Check processing workstation, 12 pockets	4800	2470
Coffee maker, 10 cups	1500	1050 sens., 450 latent
Microfiche reader	85	85
Microfilm reader	520	520
Microfilm reader/printer	1150	1150
Microwave oven, 28 L	600	400
Paper shredder	250 to 3000	200 to 2420
Water cooler, 30 L/h	700	350

Load Calculation Applications Manual (SI), Second Edition

Table 6.11 Recommended Load Factors for Various Types of Offices

(Source: ASHRAE Handbook—Fundamentals [2013], Chapter 18, Table 11)

Type of Use	Load Factor, W/m ²	Description
100% laptop, light	2.69	15.5 m ² /workstation, all laptop use, 1 printer per 10, speakers, misc.
medium	3.55	11.6 m ² /workstation, all laptop use, 1 printer per 10, speakers, misc.
50% laptop, light	4.31	15.5 m ² /workstation, 50% laptop / 50% desktop, 1 printer per 10, speakers, misc.
medium	5.38	11.6 m ² /workstation, 50% laptop / 50% desktop, 1 printer per 10, speakers, misc.
100% desktop, light	6.46	15.5 m ² /workstation, all desktop use, 1 printer per 10, speakers, misc.
medium	8.61	11.6 m ² /workstation, all desktop use, 1 printer per 10, speakers, misc.
100% desktop, two monitors	10.76	11.6 m ² /workstation, all desktop use, 2 monitors, 1 printer per 10, speakers, misc.
100% desktop, heavy	16.15	7.9 m ² /workstation, all desktop use, 2 monitors, 1 printer per 8, speakers, misc.
100% desktop, full on	21.52	7.9 m ² /workstation, all desktop use, 2 monitors, 1 printer per 8, speakers, misc, no diversity.

Source: Wilkins and Hosni (2011).

Example 6.1 Heat Gain from Occupants

Determine the heat gain from eight people in a retail store. Divide the heat gain into components for cooling load calculation.

Solution:

Items	Table/Equation	Explanation
Heat gain per person	Table 6.1	For degree of activity, use “Standing, light work; walking.” Sensible and latent heat gains for the adjusted M/F group are: $q'_s = 75 \text{ W per person}$ $q'_l = 55 \text{ W per person}$
Total latent heat gain		$q_l = Nq'_l = 8 \cdot 55 = 440 \text{ W}$
Total sensible heat gain		$q_s = Nq'_s = 8 \cdot 75 = 600 \text{ W}$
Radiant component of sensible heat gain		Assuming low air velocity, the radiant fraction is 58%. $q_r = 0.58q_s = 0.58 \cdot 600 = 348 \text{ W}$
Convective component of sensible heat gain		The convective fraction is 100% – 58% = 42%. $q_c = 0.42q_s = 0.42 \cdot 600 = 252 \text{ W}$

Example 6.2 Heat Gain from Lights for Single Room

A 16 m² office is illuminated with four fixtures recessed in the ceiling. Each fixture contains three 1.2 m T-8 lamps that are covered by a lens and utilize an electronic ballast. The ceiling air space is a return air plenum. Estimate the heat gain and determine the various components for cooling load calculation.

Solution:

Item	Table/Equation	Explanation
Total installed wattage		$W = (4 \text{ fixtures})(3 \text{ lamps/fixture})(32 \text{ W/lamp}) = 384 \text{ W}$
Use factor, F_{ul}		Assume $F_{ul} = 1$ for single room
Special allowance factor, F_{sa}		$F_{sa} = 0.94$, determined from manufacturer's data
Heat gain	Eqn. 6.1	$q_{el} = 384 \text{ W} \cdot 1 \cdot 0.94 = 361 \text{ W}$
Heat gain to the space (sensible)	Table 6.3	Space fraction = 45%, taking a mean value of the range, as recommended in the text. $q = 0.45 \cdot 361 \text{ W} = 162 \text{ W}$
Radiant component of heat gain to the space	Table 6.3	Again taking a mean value of the range, radiative fraction = 67% $q_r = 162 \cdot 0.67 = 108 \text{ W}$
Convective component of heat gain to the space		Convective fraction is 100% – 67% = 33% $q_c = 162 \cdot 0.33 = 53 \text{ W}$
Heat gain to return air		Plenum fraction is 1-space fraction or 55%. $q_{ra} = 0.55 \cdot 361 \text{ W} = 199 \text{ W}$ q_{ra} is assumed to be all convective and an immediate load on the coil

Example 6.3 Heat Gain from Motor-Driven Equipment

An air-conditioned machine shop has a motor-driven milling machine with a 2.2 kW motor estimated to be in operation 30% of the time. Estimate the heat gain and determine the various components for cooling load calculation.

Solution:

Item	Table/Equation	Explanation
Heat gain	Equation 6.2	Both the motor and the driven equipment are in the conditioned space
Motor use factor, F_{UM}		From given information, $F_{um} = 0.3$
Motor load factor, F_{LM}		The motor will usually be at partial load, but the underloading is indeterminate; therefore assume $F_{LM} = 1$
Motor efficiency, E_M	Table 6.4	Without additional information about the specific motor, take the efficiency from Table 6.4 $E_M = 85.5\%$
Heat gain to the space (sensible)	Equation 6.2	$q_{em} = (2200 \text{ W} / 0.855) \times 0.3 \times 1 = 772 \text{ W}$

Load Calculation Applications Manual (SI), Second Edition

Item	Table/Equation	Explanation
Radiant component of heat gain to the space		Without additional information, take radiant/convective split as 50%/50%, as recommended in the text $q_r = 772 \times 0.5 = 386 \text{ W}$
Convective component of heat gain to the space		$q_c = 772 \times 0.5 = 386 \text{ W}$

Example 6.4 Heat Gain from Restaurant Equipment

Consider a flat, 900mm electric griddle with rated heat input of 17,115 W. While it will be hooded, consider both the hooded and unhooded cases. Estimate the heat gain and determine the various components for cooling load calculation.

Solution:

Item	Table/Equations	Explanation
Hooded case		
Heat gain	Table 6.5b	With the hood in operation, there will only be sensible heat gain of 1319W <i>all of which is radiant.</i> $q = 1319 \text{ W}$
Radiant component, q_r		For hooded appliances, all heat gain to the space is radiant. $q_r = 1319 \text{ W}$
Convective component, q_c		$q_c = 0 \text{ W}$
Unhooded case		
Heat gain	Table 6.5b	Without a hood in operation, the total heat gain is given in the 3 rd column of Table 6.5bq $= 3370 \text{ W}$
Sensible heat gain, q_s		The total sensible heat gain including convection may be determined by dividing the sensible radiant heat gain by the radiation factor $q_s = 1319 \text{ W} / 0.39 = 3370$ (actually, the calculation gives 3382 since the radiation factor is only given to two decimal places, but the sensible heat gain cannot be more than the total heat gain.)
Latent heat gain, q_L		$q_L = q - q_s = 0$ How can the latent heat gain be zero? The heat gains in Table 6.5b are for standby conditions when no food will be on the griddle. In the event there is food on the griddle, we anticipate the hood being on.
Radiant component, q_r , of sensible heat gain		The radiant heat gain without the hood is the same as that with the hood. $q_r = 1319 \text{ W}$
Convective component, q_c , of sensible heat gain		$q_c = q_s - q_r = 3370 - 1319 = 2051 \text{ W}$

References

- Abushakra, B., J.S. Haberl, and D.E. Claridge. 2004. Overview of literature on diversity factors and schedules for energy and cooling load calculations (RP-1093). *ASHRAE Transactions* 110(1):164–76.
- Alereza, T., and J.P. Breen, III. 1984. Estimates of recommended heat gains due to commercial appliances and equipment. *ASHRAE Transactions* 90(2A):25–58.
- ASHRAE. 2013. *ASHRAE Handbook—Fundamentals*. Atlanta: ASHRAE.
- ASHRAE. 2011. *ASHRAE Handbook—HVAC Applications*. Atlanta: ASHRAE.
- ASHRAE. 2010. ANSI/ASHRAE/IES Standard 90.1-2010, *Energy Standard for Buildings Except Low-Rise Residential Buildings*. Atlanta: ASHRAE.
- Claridge, D.E., B. Abushakra, J.S. Haberl, and A. Sreshthaputra. 2004. Electricity diversity profiles for energy simulation of office buildings (RP-1093). *ASHRAE Transactions* 110(1):365–77.
- Fisher, D.E., and C. Chantrasrisalai. 2006. *Lighting heat gain distribution in buildings*. RP-1282. Final Report. Atlanta: ASHRAE.
- Hosni, M.H., and B.T. Beck. 2008. *Update to measurements of office equipment heat gain data*. RP-1482. ASHRAE Research Project, Progress Report. Atlanta: ASHRAE.
- Hosni, M.H., B.W. Jones, and H. Xu. 1999. Experimental results for heat gain and radiant/convective split from equipment in buildings. *ASHRAE Transactions* 105(2):527–39.
- Swierczyna, R., P. Sobiski, and D. Fisher. 2008. *Revised heat gain and capture and containment exhaust rates from typical commercial cooking appliances*. RP-1362. Final Report. Atlanta: ASHRAE.
- Swierczyna, R., P.A. Sobiski, and D.R. Fisher. 2009. Revised heat gain rates from typical commercial cooking appliances from RP- 1362. *ASHRAE Transactions* 115(2):138–60.
- Wilkins, C.K., and M. Hosni. 2011. Plug load design factors. *ASHRAE Journal* 53(5):30–4.

Fundamentals of the Radiant Time Series Method

The radiant time series method (RTSM) is a simplified method for performing design cooling load calculations. It is derived from the heat balance method (HBM) and, when used within its limitations, gives results that are slightly conservative—that is, it overpredicts the cooling load by a small amount when compared to the HBM.

The RTSM was developed to be rigorous, without requiring iteration (as does the HBM) to determine conduction heat gains and cooling loads. The RTSM produces individual component heat gains and cooling loads that can be readily examined by the designer. In addition, the coefficients that are used to compute transient conduction heat gain and cooling loads have a physical meaning that can be understood by the user of the method. These characteristics allow the use of engineering judgment during the cooling load calculation process.

The RTSM is well suited for use in a spreadsheet. Although it is simple in concept, there are too many calculations required to be practical as a manual method. In the supporting files online (at www.ashrae.org/lcam) that accompany this manual are several different spreadsheets that implement the RTSM. In addition, each example in this chapter has an accompanying spreadsheet that implements the relevant part of the method.

7.1 Assumptions and Limitations of the RTSM

To develop the RTSM as a simplified replacement for the HBM, several key assumptions are required. These assumptions and the resulting limitations in the RTSM are as follows:

1. *Calculation period*—the RTSM assumes that the design day cooling load calculation is for a single day, with the previous days having the same conditions. In other words, any energy stored in the building overnight will be consistent with the previous days, having been identical in weather and internal heat gains. In practice, the HBM also uses this assumption, though the HBM also may be used with non-periodic conditions. Accordingly, while the HBM may be adapted for use in multi-day and annual energy calculation simulations, the RTSM is not appropriate for this use.
2. *Exterior surface heat balance*—the RTSM replaces the exterior surface heat balance by assuming that the exterior surface exchanges heat with an exterior boundary condition known as the *sol-air temperature*. The heat exchange is governed by the surface conductance, which is a combined radiative and convective coefficient. The HBM balances the heat flows (convective, radiative, and conductive) at the exterior surface and computes its temperature.
3. *Interior surface heat balance and room air heat balance*—the energy stored and later released by each surface dampens and delays the peak cooling load, so it is important to include in the analysis. The RTSM uses another approach that involves simplifying the radiation heat exchange and using data (radiant time factors) derived from the HBM to make a reasonably accurate estimate of the damping and delay. The HBM balances the heat flows (convective, radiative, and conductive) at the interior surface and all of the convective flows to and from the room air. This allows the HBM to account for all of the radiative exchanges and to keep track of the energy being stored and later released by each surface. The

Load Calculation Applications Manual (SI), Second Edition

RTSM simplification of the radiation exchange relies on two approximations: first, that the other surface temperatures can be reasonably approximated as being the same as the indoor air temperature, and second, that the fourth-order dependency on absolute surface temperatures can be approximated with a simple linear relationship. This, in turn, allows the radiation and convection to be combined and calculated with a single combined coefficient (called the *surface conductance*) multiplied by the difference between the interior surface temperature and the air temperature. Or, even more conveniently, they can be combined into a single resistance, becoming part of the total resistance of the wall.

The above assumptions allow the RTSM to proceed sequentially, without iteration. The latter two assumptions result in the RTSM not being able to give exactly the same answer as the HBM. For most cases, these differences are relatively unimportant, as the difference is generally a small percentage. One significant exception is the case of buildings with large amounts of low thermal resistance envelope area (e.g., single-pane glazing or possibly a fabric structure) (Rees et al. 1998). Similar to earlier simplified methods, the RTSM moderately overpredicts cooling loads in buildings with high fractions of single-pane exterior fenestration.

7.2 Overview of the RTSM

The RTSM has two basic steps: calculation of heat gains and calculation of cooling loads. In practice, additional steps are needed to prepare for calculation of the heat gains, and when breaking out all of the heat gain calculations by component type, the

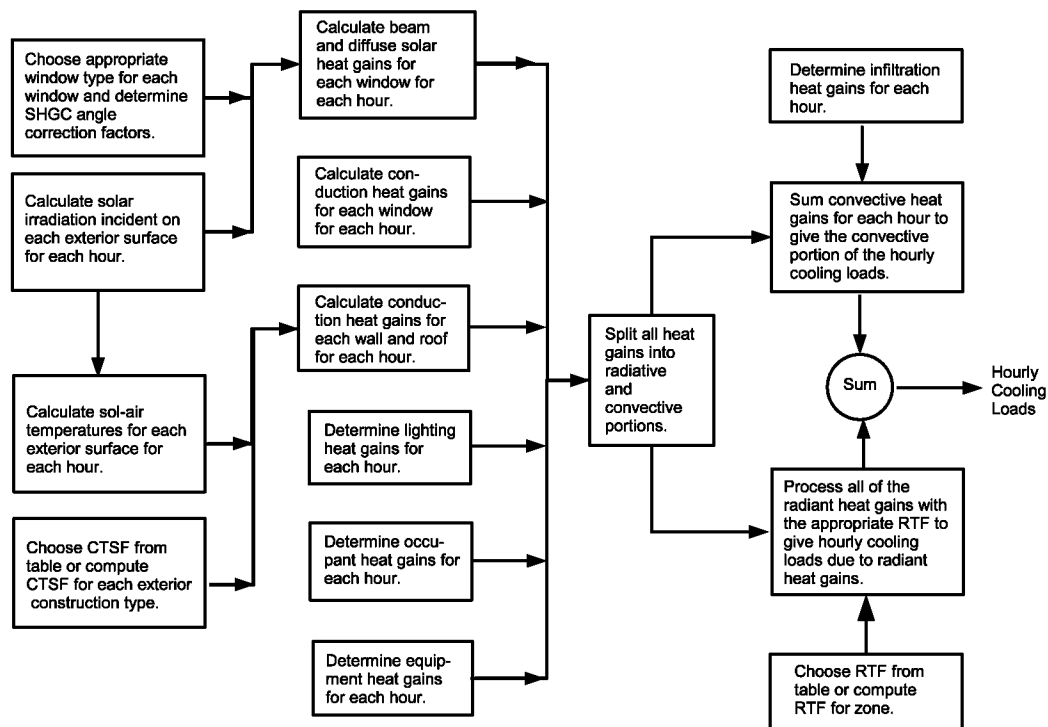


Figure 7.1 Overview of the RTSM for a single zone.

(Source: ASHRAE Handbook—Fundamentals [2013], Chapter 18, Figure 8).

Fundamentals of the Radiant Time Series Method

overall procedure looks slightly more complex, as shown in Figure 7.1. Furthermore, Figure 7.1 assumes initial data gathering has already been done—meaning that geometry, constructions, environmental design conditions, peak internal heat gains and schedules, etc. have already been determined.

7.3 Computation of Solar Irradiation and Sol-Air Temperatures

The computation of solar radiation incident on each surface is an important first step in computing cooling loads in any cooling load calculation procedure. (Solar *irradiation* is simply the radiation incident on a surface.) For the RTSM, it is also necessary to compute sol-air temperatures. The methodology for these computations and a spreadsheet implementation are described in Appendix D.

Using the spreadsheet *7-1-solar.xls* (in the online supporting files accompanying this manual) with location, orientations, clearness number, etc. as inputs, the solar irradiation for vertical surfaces facing the cardinal and intercardinal directions are determined for each hour of the day and given in Table 7.1. With the additional information of the peak temperature, daily range, surface solar absorptivity, and surface conductance, the spreadsheet will also compute the sol-air temperatures, which are given in Table 7.2.

Table 7.1 Solar Irradiation, Atlanta, July 21

Solar Irradiation (W/m ²) for July 21, 33.65°N Latitude, 84.42°W Longitude, Time Zone: NAE Daylight Savings Time									
USA - GA - ATLANTA MUNICIPAL, Ground Reflectance: rhog = 0.2									
Local Time	N	NE	E	SE	S	SW	W	NW	Horizontal
1.0	0.0	0.0	0.0	0.0	0.0	0.0	0.0	0.0	0.0
2.0	0.0	0.0	0.0	0.0	0.0	0.0	0.0	0.0	0.0
3.0	0.0	0.0	0.0	0.0	0.0	0.0	0.0	0.0	0.0
4.0	0.0	0.0	0.0	0.0	0.0	0.0	0.0	0.0	0.0
5.0	0.0	0.0	0.0	0.0	0.0	0.0	0.0	0.0	0.0
6.0	0.0	0.0	0.0	0.0	0.0	0.0	0.0	0.0	0.0
7.0	39.0	78.1	77.5	37.6	10.6	10.6	10.6	10.6	21.4
8.0	166.5	438.5	482.4	268.0	45.0	45.0	45.0	45.0	167.0
9.0	169.2	568.0	687.7	447.0	83.2	78.5	78.5	78.5	367.9
10.0	121.8	554.3	738.2	550.8	119.3	108.1	108.1	108.1	568.9
11.0	139.9	456.9	676.2	578.5	228.0	132.2	132.2	132.2	743.9
12.0	154.4	312.6	532.4	534.5	317.4	154.6	149.7	149.7	875.3
13.0	159.7	172.3	336.1	429.0	371.0	198.2	164.3	159.7	951.6
14.0	161.5	161.5	172.0	277.7	381.4	364.0	236.2	169.5	966.1
15.0	158.9	155.3	155.3	164.9	347.1	492.8	447.0	238.6	917.7
16.0	147.3	141.1	141.1	141.1	272.8	566.7	618.5	394.5	810.5
17.0	129.7	119.9	119.9	119.9	169.5	572.8	721.7	517.4	653.7
18.0	150.7	92.7	92.7	92.7	100.1	504.2	727.1	575.1	462.1
19.0	177.8	60.8	60.8	60.8	62.8	359.4	599.8	521.4	257.0
20.0	117.0	26.0	26.0	26.0	26.0	143.0	283.1	271.8	75.0
21.0	0.0	0.0	0.0	0.0	0.0	0.0	0.0	0.0	0.0
22.0	0.0	0.0	0.0	0.0	0.0	0.0	0.0	0.0	0.0
23.0	0.0	0.0	0.0	0.0	0.0	0.0	0.0	0.0	0.0
24.0	0.0	0.0	0.0	0.0	0.0	0.0	0.0	0.0	0.0

Load Calculation Applications Manual (SI), Second Edition

Table 7.2 Sol-Air Temperatures, Atlanta, July 21

Sol-Air Temperature (°C) for July 21, 33.64°N Latitude, 84.43°W Longitude, Time Zone:
NAE Daylight Savings Time

USA - GA - ATLANTA MUNICIPAL, 5% Design Condition, Surface Color: alpha/ho = 0.05

Local Time	Air Temperature	N	NE	E	SE	S	SW	W	NW	Horizontal
1.0	24.5	24.5	24.5	24.5	24.5	24.5	24.5	24.5	24.5	20.7
2.0	23.7	23.7	23.7	23.7	23.7	23.7	23.7	23.7	23.7	19.9
3.0	23.1	23.1	23.1	23.1	23.1	23.1	23.1	23.1	23.1	19.2
4.0	22.7	22.7	22.7	22.7	22.7	22.7	22.7	22.7	22.7	18.8
5.0	22.4	22.4	22.4	22.4	22.4	22.4	22.4	22.4	22.4	18.5
6.0	22.0	22.0	22.0	22.0	22.0	22.0	22.0	22.0	22.0	18.1
7.0	21.9	24.0	26.1	26.0	23.9	22.5	22.5	22.5	22.5	19.2
8.0	22.3	31.1	45.4	47.8	36.4	24.6	24.6	24.6	24.6	27.2
9.0	23.3	32.3	53.4	59.7	47.0	27.7	27.5	27.5	27.5	38.9
10.0	25.5	31.9	54.8	64.5	54.6	31.8	31.2	31.2	31.2	51.7
11.0	27.6	35.0	51.7	63.3	58.1	39.6	34.6	34.6	34.6	63.0
12.0	29.5	37.6	46.0	57.6	57.7	46.2	37.6	37.4	37.4	71.8
13.0	31.0	39.5	40.1	48.8	53.7	50.6	41.5	39.7	39.5	77.4
14.0	32.1	40.6	40.6	41.2	46.8	52.2	51.3	44.6	41.0	79.2
15.0	32.9	41.3	41.1	41.1	41.6	51.3	59.0	56.6	45.5	77.5
16.0	33.4	41.1	40.8	40.8	40.8	47.8	63.3	66.0	54.2	72.3
17.0	33.2	40.0	39.5	39.5	39.5	42.1	63.5	71.3	60.5	63.8
18.0	32.4	40.3	37.3	37.3	37.3	37.6	59.0	70.8	62.7	52.9
19.0	31.5	40.9	34.7	34.7	34.7	34.8	50.5	63.2	59.0	41.2
20.0	30.1	36.3	31.5	31.5	31.5	31.5	37.7	45.1	44.5	30.2
21.0	28.4	28.4	28.4	28.4	28.4	28.4	28.4	28.4	28.4	24.6
22.0	27.3	27.3	27.3	27.3	27.3	27.3	27.3	27.3	27.3	23.4
23.0	26.3	26.3	26.3	26.3	26.3	26.3	26.3	26.3	26.3	22.4
24.0	25.3	25.3	25.3	25.3	25.3	25.3	25.3	25.3	25.3	21.4

7.4 Computation of Conductive Heat Gains from Opaque Surfaces

Conductive heat gain is calculated for each wall and roof type with the use of a conduction time series (CTS). The 24 coefficients of the CTS are periodic response factors referred to as *conduction time series factors* (CTSFs). This formulation gives a time series solution to the transient, periodic, one-dimensional conductive heat transfer problem. For any hour, θ , the conductive heat gain for the surface q_{θ} is given by the summation of the CTSFs multiplied by the UA value multiplied by the temperature difference across the surface, as shown in Equation 7.1:

$$q_{\theta} = \sum_{j=0}^{23} c_j UA (t_{e,\theta-j\delta} - t_{rc}) \quad (7.1)$$

Fundamentals of the Radiant Time Series Method

or

$$q_0 = c_0 UA(t_{e,\theta} - t_{rc}) + c_1 UA(t_{e,\theta-\delta} - t_{rc}) + c_2 UA(t_{e,\theta-2\delta} - t_{rc}) + \dots + c_{23} UA(t_{e,\theta-23\delta} - t_{rc}) \quad (7.2)$$

where

- q_0 = hourly conductive heat gain, W, for the surface
- U = overall heat transfer coefficient for the surface, W/(m²·K)
- A = surface area, m²
- c_j = j^{th} conduction time series factor
- $t_{e,\theta-j\delta}$ = sol-air temperature, °C, j hours ago
- t_{rc} = presumed constant room air temperature, °C
- θ = the current hour
- δ = the time step (one hour)

Note that the quantity $UA(t_{e,\theta-j\delta} - t_{rc})$ would be the heat transfer at each hour if steady-state conditions prevailed. The conduction time factors may be thought of as an adjustment to the steady-state heat transfer calculation, telling us how much heat that was previously stored in the wall or roof is released this hour. Figure 7.2 illustrates conduction time series for three different walls ranging from light to very heavy. As can be seen, the CTSFs for the very light wall are large for the first few hours and nearly zero for the remaining hours—relatively little heat is stored in this lightweight wall. On the other hand, the heavier walls have smaller values of CTSFs early on but they remain nonzero for many hours, indicating the long time delay inherent in the heavier walls.

7.4.1 Obtaining CTSFs

CTSFs may be obtained in several different ways. They are given for sample walls and roofs in Tables 7.3a, 7.3b, and 7.4, they may be determined with the spreadsheet in the online supporting files that accompany this manual and that contain the contents of Tables 7.3 and 7.4 (*7-3_tabulated_CTSF.xls*), or they may be determined with the spreadsheet interface to a program implemented in Visual Basic for Applications (VBA) (*7-4_generate_CTSF.xls*). Thermal properties of the materials used for the walls and roofs in Tables 7.3a, 7.3b, and 7.4 are given in Table 7.5.

In the case of using the tables, engineering judgment is required to select a similar wall type. In questionable cases, particularly where the conduction heat gain may form a significant part of the cooling load, it may be desirable to use the *7-4_generate_CTSF.xls* spreadsheet, which allows the user to specify the wall or roof in a layer-by-layer fashion. For walls or roofs with studs or other thermal bridges, consult Appendix E for the appropriate methodology.

7.5 Computation of Fenestration Heat Gains

Fenestration (e.g., windows and skylights) allow heat gains via transmitted solar radiation, absorbed solar radiation, and conduction. While the inward-flowing fraction of the absorbed solar radiation and the conduction are interrelated, a reasonable approximation is to calculate them separately.

A problem in computing fenestration heat gains is the lack of data generally available in practice. Whereas Chapter 15 of *ASHRAE Handbook—Fundamentals* (2013) gives angle-dependent values of solar heat gain coefficients (SHGCs), transmittances, absorptances, etc., in many situations it will be difficult or impossible to choose the correct window from the tables in Chapter 15.

Load Calculation Applications Manual (SI), Second Edition

Table 7.3a Wall Conduction Time Series (CTS)

(Source: ASHRAE Handbook—Fundamentals [2013], Chapter 18, Table 16)

Wall Number =	Curtain Walls			Stud Walls				EIFS			Brick Walls									
	1	2	3	4	5	6	7	8	9	10	11	12	13	14	15	16	17	18	19	20
U-Factor, W/(m ² ·K)	0.428	0.429	0.428	0.419	0.417	0.406	0.413	0.668	0.305	0.524	0.571	0.377	0.283	0.581	0.348	0.628	0.702	0.514	0.581	0.389
Total R	2.3	2.3	2.3	2.4	2.4	2.5	2.4	1.5	3.3	1.9	1.7	2.7	3.5	1.7	2.9	1.6	1.4	1.9	1.7	2.6
Mass, kg/m ²	31.0	20.9	80.0	25.5	84.6	25.6	66.7	36.6	38.3	130.9	214.1	214.7	215.8	290.6	304.0	371.7	391.5	469.3	892.2	665.1
Thermal Capacity, kJ/(m ² ·K)	30.7	20.4	67.5	24.5	73.6	32.7	61.3	36.7	38.8	120.6	177.8	177.8	177.8	239.1	253.5	320.9	312.7	388.4	784.9	580.5
Hour	Conduction Time Factors, %																			
0	18	25	8	19	6	7	5	11	2	1	0	0	0	1	2	2	1	3	4	3
1	58	57	45	59	42	44	41	50	25	2	5	4	1	1	2	2	1	3	4	3
2	20	15	32	18	33	32	34	26	31	6	14	13	7	2	2	2	3	3	4	3
3	4	3	11	3	13	12	13	9	20	9	17	17	12	5	3	4	6	3	4	4
4	0	0	3	1	4	4	4	3	11	9	15	15	13	8	5	5	7	3	4	4
5	0	0	1	0	1	1	2	1	5	9	12	12	13	9	6	6	8	4	4	4
6	0	0	0	0	1	0	1	0	3	8	9	9	11	9	7	6	8	4	4	5
7	0	0	0	0	0	0	0	0	2	7	7	7	9	9	7	7	8	5	4	5
8	0	0	0	0	0	0	0	0	1	6	5	5	7	8	7	7	8	5	4	5
9	0	0	0	0	0	0	0	0	0	6	4	4	6	7	7	6	7	5	4	5
10	0	0	0	0	0	0	0	0	0	5	3	3	5	7	6	6	6	5	4	5
11	0	0	0	0	0	0	0	0	0	5	2	2	4	6	6	6	6	5	5	5
12	0	0	0	0	0	0	0	0	0	4	2	2	3	5	5	5	5	5	5	5
13	0	0	0	0	0	0	0	0	0	4	1	2	2	4	5	5	4	5	5	5
14	0	0	0	0	0	0	0	0	0	3	1	2	2	4	5	5	4	5	5	5
15	0	0	0	0	0	0	0	0	0	3	1	1	1	3	4	4	3	5	4	4
16	0	0	0	0	0	0	0	0	0	3	1	1	1	3	4	4	3	5	4	4
17	0	0	0	0	0	0	0	0	0	2	1	1	1	2	3	4	3	4	4	4
18	0	0	0	0	0	0	0	0	0	2	0	0	1	2	3	3	2	4	4	4
19	0	0	0	0	0	0	0	0	0	2	0	0	1	2	3	3	2	4	4	4
20	0	0	0	0	0	0	0	0	0	2	0	0	0	1	3	3	2	4	4	4
21	0	0	0	0	0	0	0	0	0	1	0	0	0	1	2	2	1	4	4	4
22	0	0	0	0	0	0	0	0	0	1	0	0	0	1	2	2	1	4	4	3
23	0	0	0	0	0	0	0	0	0	0	0	0	0	0	1	1	1	3	4	3
Total Percentage	100	100	100	100	100	100	100	100	100	100	100	100	100	100	100	100	100	100	100	100
Layer ID from outdoors to indoors (see Table 18)	F01 F09 F04 I02 F04 G01 F02 F02 0	F01 F08 F04 I02 F04 G01 F02 F02 0	F01 F10 F04 I02 F04 G01 F02 F02 0	F01 F08 G03 I04 G01 F02 0 0 0	F01 F10 G03 I04 G01 F02 0 0 0	F01 F11 G02 I04 G04 F02 0 0 0	F01 F07 G03 I04 G01 F02 0 0 0	F01 F06 I01 G03 F04 G01 F02 0 0	F01 F06 I01 G03 I04 G01 F02 F02 0	F01 F06 I01 G03 M03 F04 G01 G01 F02	F01 M01 F04 I01 G03 I04 G01 F02 0	F01 M01 F04 I01 M03 I04 G01 F02 0	F01 M01 F04 I01 M03 I04 M05 G01 F02 0	F01 M01 F04 I01 M03 I04 M05 G01 F02 0	F01 M01 F04 I01 M03 I04 M05 G01 F02 0	F01 M01 F04 I01 M03 I04 M05 G01 F02 0	F01 M01 F04 I01 M03 I04 M05 G01 F02 0	F01 M01 F04 I01 M03 I04 M05 G01 F02 0	F01 M01 F04 I01 M03 I04 M05 G01 F02 0	F01 M01 F04 I01 M03 I04 M05 G01 F02 0

Wall Number Descriptions

Spandrel glass, insulation board, gyp board	Brick, insulation board, sheathing, gyp board
Metal wall panel, insulation board, gyp board	Brick, sheathing, batt insulation, gyp board
25 mm stone, insulation board, gyp board	Brick, insulation board, sheathing, batt insulation, gyp board
Metal wall panel, sheathing, batt insulation, gyp board	Brick, insulation board, 200 mm LW CMU
25 mm stone, sheathing, batt insulation, gyp board	Brick, 200 mm LW CMU, batt insulation, gyp board
Wood siding, sheathing, batt insulation, 13 mm wood	Brick, insulation board, 200 mm HW CMU, gyp board
25 mm stucco, sheathing, batt insulation, gyp board	Brick, insulation board, brick
EIFS finish, insulation board, sheathing, gyp board	Brick, insulation board, 200 mm LW concrete, gyp board
EIFS finish, insulation board, sheathing, batt insulation, gyp board	Brick, insulation board, 300 mm HW concrete, gyp board
EIFS finish, insulation board, sheathing, 200 mm LW CMU, gyp board	Brick, 200 mm HW concrete, batt insulation, gyp board

Fundamentals of the Radiant Time Series Method

Table 7.3b Wall Conduction Time Series (CTS)

(Source: ASHRAE Handbook—Fundamentals [2013], Chapter 18, Table 16)

Wall Number =	Concrete Block Wall						Precast and Cast-in-Place Concrete Walls								
	21	22	23	24	25	26	27	28	29	30	31	32	33	34	35
U-Factor, W/(m²·K)	0.383	0.335	0.414	1.056	0.834	0.689	0.673	0.418	0.434	0.650	0.387	0.467	0.434	0.266	3.122
Total R	2.6	3.0	2.4	0.9	1.2	1.5	1.5	2.4	2.3	1.5	2.6	2.1	2.3	3.8	0.3
Mass, kg/m²	108.8	108.8	224.3	94.3	107.1	168.9	143.9	144.6	262.5	291.8	274.7	488.1	469.9	698.9	683.2
Thermal Capacity, kJ/(m²·K)	98.1	98.1	204.4	83.8	96.1	151.3	124.7	124.7	220.8	247.3	233.0	441.5	425.2	631.6	615.2
Hour	Conduction Time Factors, %														
0	0	1	0	1	0	1	1	0	1	2	1	3	1	2	1
1	4	1	2	11	3	1	10	8	1	2	2	3	2	2	2
2	13	5	8	21	12	2	20	18	3	3	3	4	5	3	4
3	16	9	12	20	16	5	18	18	6	5	6	5	8	3	7
4	14	11	12	15	15	7	14	14	8	6	7	6	9	5	8
5	11	10	11	10	12	9	10	11	9	6	8	6	9	5	8
6	9	9	9	7	10	9	7	8	9	6	8	6	8	6	8
7	7	8	8	5	8	8	5	6	9	6	7	5	7	6	8
8	6	7	7	3	6	8	4	4	8	6	7	5	6	6	7
9	4	6	6	2	4	7	3	3	7	6	6	5	6	6	6
10	3	5	5	2	3	6	2	2	7	5	6	5	5	6	6
11	3	4	4	1	3	6	2	2	6	5	5	5	5	5	5
12	2	4	3	1	2	5	1	2	5	5	5	4	4	5	4
13	2	3	2	1	2	4	1	1	4	5	4	4	4	5	4
14	2	3	2	0	1	4	1	1	4	4	4	4	3	4	4
15	1	3	2	0	1	3	1	1	3	4	3	4	3	4	3
16	1	2	1	0	1	3	0	1	2	4	3	4	3	4	3
17	1	2	1	0	1	2	0	0	2	3	3	4	2	4	3
18	1	2	1	0	0	2	0	0	1	3	2	4	2	4	2
19	0	1	1	0	0	2	0	0	1	3	2	3	2	3	2
20	0	1	1	0	0	2	0	0	1	3	2	3	2	3	2
21	0	1	1	0	0	2	0	0	1	3	2	3	2	3	1
22	0	1	1	0	0	1	0	0	1	3	2	3	1	3	1
23	0	1	0	0	0	1	0	0	1	2	2	2	1	3	1
Total Percentage	100	100	100	100	100	100	100	100	100	100	100	100	100	100	100
Layer ID from outdoors to indoors (see Table 18)	F01 M03 I04 G01 F02 —	F01 M08 I04 G01 F02 —	F01 F07 M05 I04 G01 F02	F01 M08 F02 — — —	F01 M08 F04 G01 F02 —	F01 M09 F04 G01 F02 —	F01 M11 I01 F04 G01 F02 F02	F01 M11 I04 G01 F02 —	F01 M11 I02 M11 G01 F02 —	F01 F06 I01 M13 G01 G01 F02	F01 M13 I04 G01 F02 —	F01 F06 I02 M15 G01 F02 F02	F01 M15 I04 G01 F02 —	F01 M16 I05 G01 F02 —	F01 M16 I05 G01 F02 —

Wall Number Descriptions

- | | |
|---|--|
| 1. 200 mm LW CMU, batt insulation, gyp board | 9. 100 mm LW concrete, board insulation, 100 mm LW concrete |
| 2. 200 mm LW CMU with fill insulation, batt insulation, gyp board | 10. EIFS finish, insulation board, 200 mm LW concrete, gyp board |
| 3. 25 mm stucco, 200 mm HW CMU, batt insulation, gyp board | 11. 200 mm LW concrete, batt insulation, gyp board |
| 4. 200 mm LW CMU with fill insulation | 12. EIFS finish, insulation board, 200 mm HW concrete, gyp board |
| 5. 200 mm LW CMU with fill insulation, gyp board | 13. 200 mm HW concrete, batt insulation, gyp board |
| 6. 300 mm LW CMU with fill insulation, gyp board | 14. 300 mm HW concrete, batt insulation, gyp board |
| 7. 100 mm LW concrete, board insulation, gyp board | 15. 300 mm HW concrete |
| 8. 100 mm LW concrete, batt insulation, gyp board | |

Understanding this, the method presented here (Barnaby et al. 2004) incorporates some approximations that allow it to rely solely on the data that are actually provided by window manufacturers, including the following:

- Number of layers—is the window single-pane, double-pane, or triple-pane?
- Some description of the glass type—coloration and whether or not it has a low-e coating, for example. This information is often vague when compared to the tabulated layer description.
- U-factor (NFRC 2004a).

Load Calculation Applications Manual (SI), Second Edition

- SHGCs at normal-incidence-angle SHGC (NFRC 2004b).
- Visual transmittance (NFRC 2004b).

Using the manufacturer's information, the engineer chooses a window type from the tabulated set of windows in Tables 7.9 or 3.8. (Table 7.9 is a subset of Table 3.8.) The designer should look for a window that has a matching number of layers, the closest possible match to the tabulated values of normal SHGC and visual transmittance T_v , and a reasonably close match to the description of the layers, if possible.

Table 7.4 Roof Conduction Time Series (CTS)

(Source: ASHRAE Handbook—Fundamentals [2013], Chapter 18, Table 17)

Roof Number	Sloped Frame Roofs						Wood Deck		Metal Deck Roofs					Concrete Roofs					
	1	2	3	4	5	6	7	8	9	10	11	12	13	14	15	16	17	18	19
U-Factor, W/(m²·K)	0.249	0.227	0.255	0.235	0.239	0.231	0.393	0.329	0.452	0.370	0.323	0.206	0.297	0.304	0.296	0.288	0.315	0.313	0.239
Total R	4.0	4.4	3.9	4.2	4.2	4.3	2.5	3.0	2.2	2.7	3.1	4.9	3.4	3.3	3.4	3.5	3.2	3.2	4.2
Mass, kg/m²	26.7	21.0	14.0	34.7	55.5	34.9	48.9	55.9	23.9	30.9	25.0	27.2	57.6	149.2	214.3	279.3	360.7	474.5	362.3
Thermal Capacity, kJ/(m²·K)	26.6	16.4	12.3	47.0	73.5	47.0	75.6	79.7	28.6	32.7	28.6	32.7	57.2	134.9	190.1	245.2	333.2	437.4	331.1
Hour	Conduction Time Factors, %																		
0	6	10	27	1	1	1	0	1	18	4	8	1	0	1	2	2	2	3	1
1	45	57	62	17	17	12	7	3	61	41	53	23	10	2	2	2	2	3	2
2	33	27	10	31	34	25	18	8	18	35	30	38	22	8	3	3	5	3	6
3	11	5	1	24	25	22	18	10	3	14	7	22	20	11	6	4	6	5	8
4	3	1	0	14	13	15	15	10	0	4	2	10	14	11	7	5	7	6	8
5	1	0	0	7	6	10	11	9	0	1	0	4	10	10	8	6	7	6	8
6	1	0	0	4	3	6	8	8	0	1	0	2	7	9	8	6	6	6	7
7	0	0	0	2	1	4	6	7	0	0	0	0	5	7	7	6	6	6	7
8	0	0	0	0	0	2	5	6	0	0	0	0	4	6	7	6	6	6	6
9	0	0	0	0	0	1	3	5	0	0	0	0	3	5	6	6	5	5	5
10	0	0	0	0	0	1	3	5	0	0	0	0	2	5	5	6	5	5	5
11	0	0	0	0	0	1	2	4	0	0	0	0	1	4	5	5	5	5	5
12	0	0	0	0	0	0	1	4	0	0	0	0	1	3	5	5	4	5	4
13	0	0	0	0	0	0	1	3	0	0	0	0	1	3	4	5	4	4	4
14	0	0	0	0	0	0	1	3	0	0	0	0	0	3	4	4	4	4	3
15	0	0	0	0	0	0	1	3	0	0	0	0	0	2	3	4	4	4	3
16	0	0	0	0	0	0	0	2	0	0	0	0	0	2	3	4	3	4	3
17	0	0	0	0	0	0	0	2	0	0	0	0	0	2	3	4	3	4	3
18	0	0	0	0	0	0	0	2	0	0	0	0	0	1	3	3	3	3	2
19	0	0	0	0	0	0	0	2	0	0	0	0	0	1	2	3	3	3	2
20	0	0	0	0	0	0	0	1	0	0	0	0	0	1	2	3	3	3	2
21	0	0	0	0	0	0	0	1	0	0	0	0	0	1	2	3	3	3	2
22	0	0	0	0	0	0	0	1	0	0	0	0	0	1	2	3	2	2	2
23	0	0	0	0	0	0	0	0	0	0	0	0	0	1	1	2	2	2	2
	100	100	100	100	100	100	100	100	100	100	100	100	100	100	100	100	100	100	100
Layer ID from outdoors to indoors (see Table 18)	F01	F01	F01	F01	F01	F01	F01	F01	F01	F01	F01	F01	F01	F01	F01	F01	F01	F01	F01
	F08	F08	F08	F12	F14	F15	F13	F13	F13	F13	F13	F13	M17	F13	F13	F13	F13	F13	F13
	G03	G03	G03	G05	G05	G05	G03	G03	G03	G03	G03	G03	F13	G03	G03	G03	G03	G03	M14
	F05	F05	F05	F05	F05	F05	I02	I02	I02	I02	I03	I02	G03	I03	I03	I03	I03	I03	F05
	I05	I05	I05	I05	I05	I05	G06	G06	F08	F08	F08	I03	I03	M11	M12	M13	M14	M15	I05
	G01	F05	F03	F05	F05	F05	F03	F05	F03	F05	F03	F08	F08	F03	F03	F03	F03	F03	F16
	F03	F16	—	G01	G01	G01	—	F16	—	F16	—	—	F03	—	—	—	—	—	F03
	—	F03	—	F03	F03	F03	—	F03	—	F03	—	—	—	—	—	—	—	—	—

Roof Number Descriptions

- | | |
|--|--|
| 1. Metal roof, batt insulation, gyp board | 11. Membrane, sheathing, insulation board, metal deck |
| 2. Metal roof, batt insulation, suspended acoustical ceiling | 12. Membrane, sheathing, plus insulation boards, metal deck |
| 3. Metal roof, batt insulation | 13. 50 mm concrete roof ballast, membrane, sheathing, insulation board, metal deck |
| 4. Asphalt shingles, wood sheathing, batt insulation, gyp board | 14. Membrane, sheathing, insulation board, 100 mm LW concrete |
| 5. Slate or tile, wood sheathing, batt insulation, gyp board | 15. Membrane, sheathing, insulation board, 150 mm LW concrete |
| 5. Wood shingles, wood sheathing, batt insulation, gyp board | 16. Membrane, sheathing, insulation board, 200 mm LW concrete |
| 7. Membrane, sheathing, insulation board, wood deck | 17. Membrane, sheathing, insulation board, 150 mm HW concrete |
| 8. Membrane, sheathing, insulation board, wood deck, suspended acoustical ceiling | 18. Membrane, sheathing, insulation board, 200 mm HW concrete |
| 9. Membrane, sheathing, insulation board, metal deck | 19. Membrane, 150 mm HW concrete, batt insulation, suspended acoustical ceiling |
| 9. Membrane, sheathing, insulation board, metal deck, suspended acoustical ceiling | |

Fundamentals of the Radiant Time Series Method

Table 7.5 Thermal Properties and Code Numbers of Layers Used in Wall and Roof Descriptions for Tables 7.3a, 7.3b, and 7.4

(Source: ASHRAE Handbook—Fundamentals [2013], Chapter 18, Table 18)

Layer ID	Description	Thickness, mm	Conductivity, W/(m·K)	Density, kg/m ³	Specific Heat, kJ/(kg·K)	Resistance, (m ² ·K)/W	R	Mass, kg/m ²	Thermal Capacity, kJ/(m ² ·K)	Notes
F01	Outdoor surface resistance	—	—	—	—	0.04	0.04	—	—	1
F02	Indoor vertical surface resistance	—	—	—	—	0.12	0.12	—	—	2
F03	Indoor horizontal surface resistance	—	—	—	—	0.16	0.16	—	—	3
F04	Wall air space resistance	—	—	—	—	0.15	0.15	—	—	4
F05	Ceiling air space resistance	—	—	—	—	0.18	0.18	—	—	5
F06	EIFS finish	9.5	0.72	1856	0.84	—	0.01	17.7	14.92	6
F07	25 mm stucco	25.4	0.72	1856	0.84	—	0.04	47.2	39.45	6
F08	Metal surface	0.8	45.28	7824	0.50	—	0.00	6.0	3.07	7
F09	Opaque spandrel glass	6.4	0.99	2528	0.88	—	0.01	16.1	14.10	8
F10	25 mm stone	25.4	3.17	2560	0.79	—	0.01	65.1	51.71	9
F11	Wood siding	12.7	0.09	592	1.17	—	0.14	7.5	8.79	10
F12	Asphalt shingles	3.2	0.04	1120	1.26	—	0.08	3.6	4.50	
F13	Built-up roofing	9.5	0.16	1120	1.46	—	0.06	10.7	15.74	
F14	Slate or tile	12.7	1.59	1920	1.26	—	0.01	24.4	30.67	
F15	Wood shingles	6.4	0.04	592	1.30	—	0.17	3.8	4.91	
F16	Acoustic tile	19.1	0.06	368	0.59	—	0.31	7.0	4.09	11
F17	Carpet	12.7	0.06	288	1.38	—	0.22	3.7	5.11	12
F18	Terrazzo	25.4	1.80	2560	0.79	—	0.01	65.1	51.71	13
G01	16 mm gyp board	15.9	0.16	800	1.09	—	0.10	12.7	13.90	
G02	16 mm plywood	15.9	0.12	544	1.21	—	0.14	8.6	10.42	
G03	13 mm fiberboard sheathing	12.7	0.07	400	1.30	—	0.19	5.1	6.54	14
G04	13 mm wood	12.7	0.15	608	1.63	—	0.08	7.7	12.67	15
G05	25 mm wood	25.4	0.15	608	1.63	—	0.17	15.5	25.35	15
G06	50 mm wood	50.8	0.15	608	1.63	—	0.33	30.9	50.49	15
G07	100 mm wood	101.6	0.15	608	1.63	—	0.66	61.8	100.97	15
I01	25 mm insulation board	25.4	0.03	43	1.21	—	0.88	1.1	1.43	16
I02	50 mm insulation board	50.8	0.03	43	1.21	—	1.76	2.2	2.66	16
I03	75 mm insulation board	76.2	0.03	43	1.21	—	2.64	3.3	4.09	16
I04	89 mm batt insulation	89.4	0.05	19	0.96	—	1.94	1.7	1.64	17
I05	154 mm batt insulation	154.4	0.05	19	0.96	—	3.34	3.0	2.86	17
I06	244 mm batt insulation	243.8	0.05	19	0.96	—	5.28	4.7	4.50	17
M01	100 mm brick	101.6	0.89	1920	0.79	—	0.11	195.2	155.34	18
M02	150 mm LW concrete block	152.4	0.49	512	0.88	—	0.31	78.1	68.68	19
M03	200 mm LW concrete block	203.2	0.50	464	0.88	—	0.41	94.3	82.99	20
M04	300 mm LW concrete block	304.8	0.71	512	0.88	—	0.43	156.2	137.36	21
M05	200 mm concrete block	203.2	1.11	800	0.92	—	0.18	162.7	149.83	22
M06	300 mm concrete block	304.8	1.40	800	0.92	—	0.22	244.0	224.84	23
M07	150 mm LW concrete block (filled)	152.4	0.29	512	0.88	—	0.53	78.1	68.68	24
M08	200 mm LW concrete block (filled)	203.2	0.26	464	0.88	—	0.78	94.3	82.99	25
M09	300 mm LW concrete block (filled)	304.8	0.29	512	0.88	—	1.04	156.2	137.36	26
M10	200 mm concrete block (filled)	203.2	0.72	800	0.92	—	0.28	162.7	149.83	27
M11	100 mm lightweight concrete	101.6	0.53	1280	0.84	—	0.19	130.1	108.95	
M12	150 mm lightweight concrete	152.4	0.53	1280	0.84	—	0.29	195.2	163.52	
M13	200 mm lightweight concrete	203.2	0.53	1280	0.84	—	0.38	260.3	218.10	
M14	150 mm heavyweight concrete	152.4	1.95	2240	0.90	—	0.08	341.6	307.62	
M15	200 mm heavyweight concrete	203.2	1.95	2240	0.90	—	0.10	455.5	410.23	
M16	300 mm heavyweight concrete	304.8	1.95	2240	0.90	—	0.16	683.2	615.24	
M17	50 mm LW concrete roof ballast	50.8	0.19	640	0.84	—	0.27	32.5	27.19	28

Notes: The following notes give sources for the data in this table.

- Chapter 26, Table 1 for 3.4 m/s wind
- Chapter 26, Table 1 for still air, horizontal heat flow
- Chapter 26, Table 1 for still air, downward heat flow
- Chapter 26, Table 3 for 40 mm space, 32.2°C, horizontal heat flow, 0.82 emittance
- Chapter 26, Table 3 for 90 mm space, 32.2°C, downward heat flow, 0.82 emittance
- EIFS finish layers approximated by Chapter 26, Table 4 for 10 mm cement plaster, sand aggregate
- Chapter 33, Table 3 for steel (mild), 22 gage
- Chapter 26, Table 4 for architectural glass
- Chapter 26, Table 4 for marble and granite
- Chapter 26, Table 4, density assumed same as Southern pine
- Chapter 26, Table 4 for mineral fiberboard, wet molded, acoustical tile
- Chapter 26, Table 4 for carpet and rubber pad, density assumed same as fiberboard
- Chapter 26, Table 4, density assumed same as stone
- Chapter 26, Table 4 for nail-base sheathing
- Chapter 26, Table 4 for Southern pine
- Chapter 26, Table 4 for expanded polystyrene
- Chapter 26, Table 4 for glass fiber batt, specific heat per glass fiber board
- Chapter 26, Table 4 for clay fired brick
- Chapter 26, Table 4, 7.3 kg block, 200 × 400 mm face
- Chapter 26, Table 4, 8.6 kg block, 200 × 400 mm face
- Chapter 26, Table 4, 14.5 kg block, 200 × 400 mm face
- Chapter 26, Table 4, 15 kg normal weight block, 200 × 400 mm face
- Chapter 26, Table 4, 22.7 kg normal weight block, 200 × 400 mm face
- Chapter 26, Table 4, 7.3 kg block, vermiculite fill
- Chapter 26, Table 4, 8.6 kg block, 200 × 400 mm face, vermiculite fill
- Chapter 26, Table 4, 14.5 kg block, 200 × 400 mm face, vermiculite fill
- Chapter 26, Table 4, 15 kg normal weight block, 200 × 400 mm face, vermiculite fill
- Chapter 26, Table 4 for 640 kg/m³ LW concrete

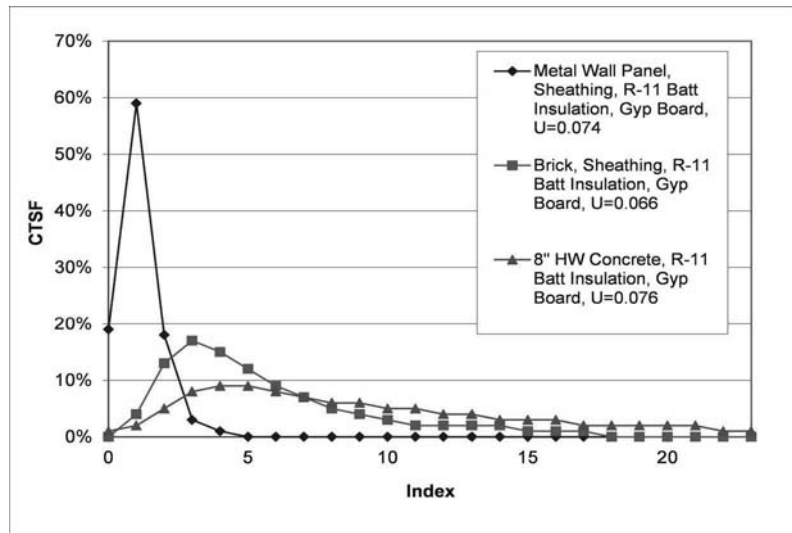


Figure 7.2 Conduction time series factors for light and heavy walls.

Example 7.1 Conduction Heat Gain

Consider a 10 m² SE-facing wall in Atlanta, Georgia, on July 21. From the materials list in Table 7.5, the material layers, from outside to inside, are given as M01, F04, I01, M03, I01, and G01. (To this, outside and inside surface resistances will be added.) The outer layer of brick is red and the solar absorptivity may be taken from Table 3.3b as 0.63. Using the ASHRAE July 5% design weather data, find the conduction heat gain for the wall at 5:00 p.m., EDST. The indoor air temperature is 24°C.

Solution:

Weather data for Atlanta are found in Table 4.1. The peak daily temperature is 33.3°C, and the mean coincident dry-bulb range for July is 11.4°C. The wind speed is not known exactly, but the mean coincident wind speed for the annual 0.4% design condition is 3.9 m/s. Taking this as the wind speed, the actual surface conductance can be interpolated from Table 3.4 as 24.41 W/m²·°C and the resulting resistance as 0.04 m²·°C/W. Alternatively, the standard value for summer conditions, equivalent to Layer F01 in Table 7.5 (0.044 m²·°C/W), may be used with little loss of accuracy. The interior surface resistance may be taken from Table 3.4 as 0.12 m²·°C/W; this is equivalent to Layer F02 in Table 7.5. Using F01 and F02 for the exterior and interior surface conductances, the wall may be summarized as shown in Table 7.6, with a total resistance of 2.69 m²·°C/W and a U-factor of 0.372 W/m²·°C.

In reviewing Tables 7.3a and 7.3b, it is clear that this wall (mentioned in Table 7.6) is similar to wall 14 except it has an extra layer of R-0.88 insulation board covered by 16 mm gypsum added to the inside. It is also similar to wall 15, except this wall has an extra layer of insulation board between the brick and concrete block and R-0.88 insulation board instead of the R-1.94 batt between the concrete block and the gypsum layer. A challenge of using the tables in practice is matching the actual wall construction to a wall with a similar thermal response. For this example, conduction time factors given in Table 7.3a for both wall 14 and wall 15 will be used. For comparison purposes, conduction time factors for the actual wall will also be computed using a spreadsheet, *Example 7.1 Compute CTSF.xls*, which is available online in the supporting files that accompany this manual. All three sets of conduction time factors are shown in Table 7.7.

Fundamentals of the Radiant Time Series Method

Table 7.6 Example Wall

Layer Code	Layer Description	Thickness, mm	Conductivity, W/(m ² -K)	Density, kg/m ³	Specific Heat, kJ/(kg-K)	Resistance, (m ² -K)/W
F01	Outside surface resistance					0.04
M01	100 mm brick	101.6	0.89	1920	0.79	0.11
F04	Wall air space resistance	0	—	—	—	0.15
I01	25 mm insulation board	25.4	0.03	43	1.21	0.88
M03	200 mm LW concrete block	203.2	0.50	464	0.88	0.41
I01	25 mm insulation board	25.4	0.03	43	1.21	0.88
G01	16 mm gyp board	15.9	0.16	800	1.09	0.10
F02	Inside vertical surface resistance					0.12
Sum of the Resistances						2.69

Table 7.7 Computer and Tabulated CTSFs (%)

CTSF Index	Tabulated CTSFs (Wall 14)	Tabulated CTSFs (Wall 15)	Computed CTSFs (Actual)	CTSF Index	Tabulated CTSFs (Wall 14)	Tabulated CTSFs (Wall 15)	Computed CTSFs (Actual)
0	1	2	3	12	5	5	5
1	1	2	2	13	4	5	5
2	2	2	2	14	4	5	5
3	5	3	3	15	3	4	5
4	8	5	4	16	3	4	4
5	9	6	5	17	2	3	4
6	9	7	5	18	2	3	4
7	9	7	6	19	2	3	4
8	8	7	6	20	1	3	3
9	7	7	6	21	1	2	3
10	7	6	6	22	1	2	3
11	6	6	5	23	0	1	3

Total incident solar radiation, outdoor air temperatures, and sol-air temperatures for each hour are given in Table 7.8. The conduction heat gain, using the tabulated CTSFs for wall 14 with Equation 7.1, is:

$$\begin{aligned}
 q_{17} = & \left. \begin{aligned}
 & 0.01(0.372)(100)(36.5 - 24.0) + 0.01(0.372)(100)(37.3 - 24.0) \\
 & + 0.02(0.372)(100)(37.5 - 24.0) + 0.05(0.372)(100)(39.8 - 24.0) \\
 & + 0.08(0.372)(100)(42.9 - 24.0) + 0.09(0.372)(100)(44.3 - 24.0) \\
 & \vdots \\
 & + 0.01(0.372)(100)(33.1 - 24.0) + 0.0(0.372)(100)(34.9 - 24.0)
 \end{aligned} \right\}
 \end{aligned}$$

$$q_{17} = 34.4 \text{ W}$$

$$q_{\theta} = \sum_{j=0}^{23} c_j UA(t_{e,\theta-j\delta} - t_{rc})$$

Load Calculation Applications Manual (SI), Second Edition

Table 7.8 Intermediate Values and Conduction Heat Gains for Wall in Example 7.1

Hour	Total Incident Radiation on Surface, W/m ²	Outdoor Air Temperature, °C	Sol Air Temperature, °C	Heat Gain (W), Computed CTSFs	Heat Gain (W), Tabulated CTSFs (Wall 14)	Heat Gain (W), Tabulated CTSFs (Wall 15)
1	0.0	24.5	24.5	34.0	38.1	36.6
2	0.0	23.7	23.7	33.5	35.2	35.2
3	0.0	23.1	23.1	32.7	32.1	33.5
4	0.0	22.7	22.7	31.7	28.7	31.5
5	0.0	22.4	22.4	30.4	25.2	29.3
6	0.0	22.0	22.0	29.0	21.7	27.0
7	37.6	21.9	23.0	27.4	18.1	24.4
8	268.0	22.3	29.7	25.8	14.8	21.9
9	447.0	23.3	35.8	24.1	11.9	19.6
10	550.8	25.5	40.8	22.5	9.9	17.5
11	578.5	27.6	43.6	21.2	9.3	16.1
12	534.5	29.5	44.3	20.4	10.8	15.9
13	429.0	31.0	42.9	20.4	14.3	16.8
14	277.7	32.1	39.8	21.1	19.1	18.9
15	164.9	32.9	37.5	22.4	24.6	21.6
16	141.1	33.4	37.3	24.1	29.9	24.9
17	119.9	33.2	36.5	26.0	34.4	28.3
18	92.7	32.4	34.9	27.8	38.0	31.2
19	60.8	31.5	33.1	29.6	40.6	33.6
20	26.0	30.1	30.8	31.1	42.4	35.4
21	0.0	28.4	28.4	32.3	43.3	36.7
22	0.0	27.3	27.3	33.3	43.3	37.5
23	0.0	26.3	26.3	33.9	42.4	37.8
24	0.0	25.3	25.3	34.1	40.6	37.5

The same computation, using the tabulated CTSFs for wall 15 and the computed CTSFs, give heat gains of 28.3 and 26.0 W, respectively. Using the CTSFs for wall 14 overpredicts the conduction heat gain at 5:00 p.m. by 32%, while the CTSFs for wall 15 give a closer result. (In both cases, the comparison is to the value determined with the computed CTSFs, which will be correct to the degree that the sol-air temperatures and thermal properties of the wall layers are correct.) The heat gains vary more significantly for some other hours. If the computation is repeated for every hour of the day using the spreadsheet Example 7.1 Conduction.xls, the resulting heat gains are shown in Table 7.8 and plotted in Figure 7.3. It might also be noted that while the solar irradiation and outdoor air temperature follow Tables 7.1 and 7.2 exactly, the sol-air temperatures are lower than those shown in Table 7.2. This is due to the difference in solar absorptivity and exterior surface conductance for this wall. (The ratio α/h_o is $0.63/22.7 = 0.03$ for this example; Table 7.2 was developed for a wall with $\alpha/h_o = 0.9/17 = 0.05$.)

The same computation, using the tabulated CTSFs for wall 15 and the computed CTSFs, give heat gains of 28.3 and 26.0 W, respectively. Using the CTSFs for wall 14 overpredicts the conduction heat gain at 5:00 P.M. by 32%, while the CTSFs for wall 15 give a closer result. (In both cases, the comparison is to the value determined with the computed CTSFs, which will be correct to the degree that the sol-air temperatures and thermal properties of the wall layers are correct.) The heat gains vary more significantly for some other hours. If the computation is repeated for every hour of the day using the spreadsheet *Example 7.1 Conduction.xls*, the resulting heat gains are shown in Table 7.8 and plotted in Figure 7.3. Note that, while the solar irradiation and outdoor air temperature follow Tables 7.1 and 7.2 exactly, the sol-air temperatures are lower than those shown in Table 7.2. This is due to the difference in solar absorptivity and exterior surface conductance for this wall. (The ratio α/h_o is $0.63/22.7 = 0.03$ for this example; Table 7.2 was developed for a wall with $\alpha/h_o = 0.9/17 = 0.05$.)

The differences in the results illustrate the importance of choosing the correct wall type. The conduction heat gains can be quite sensitive to the wall type. In many cases,

Fundamentals of the Radiant Time Series Method

the conduction heat gain will be a small part of the overall cooling load, and a rough approximation may have little effect on the overall cooling load, particularly for well-insulated buildings with significant amounts of fenestration and/or internal heat gains. However, for buildings where conduction heat gain through the walls and/or roof forms a significant part of the cooling load, it is best to calculate CTSFs for the actual construction rather than relying on tabulated values for the closest construction.

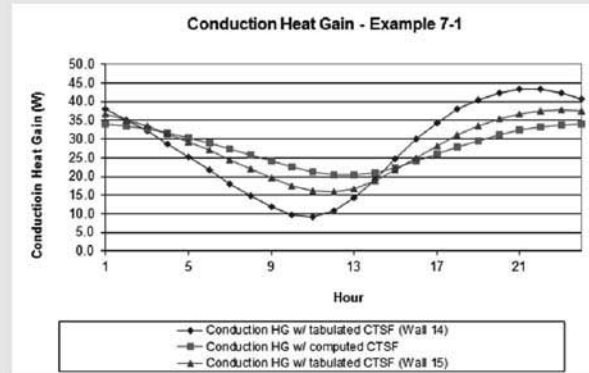


Figure 7.3 Hourly conduction heat gains using three different sets of CTSFs.

Once the best match has been found, the angle-dependent SHGCs are determined by multiplying the manufacturer-specified SHGC by the angle correction factors in Tables 7.9 or 3.8. A SHGC value for any incidence angle can then be determined with linear interpolation. These values, along with the manufacturer-specified U-factor, are used as demonstrated in Example 7.2 to compute the heat gains due to fenestration.

Conduction heat gain is computed separately from the transmitted and absorbed solar heat gain. Because the thermal mass of the glass is very low, the conduction is approximately steady state. Accordingly, for each hour, the conduction heat gain may be calculated as

$$q_{\theta} = UA(t_{o,\theta} - t_{rc}) \quad (7.3)$$

where

- q_{θ} = hourly conductive heat gain, W, for the window
- U = overall heat transfer coefficient for the window, W/(m²·K)
as specified by the window manufacturer
- A = window area—including frame, m²
- $t_{o,\theta}$ = outdoor air temperature, °C
- t_{rc} = presumed constant room air temperature, °C
- θ = the current hour

Transmitted and absorbed solar heat gains are calculated for each hour with a step-by-step procedure, as follows:

1. Compute incident angle, surface azimuth angle, incident direct (beam) irradiation, and diffuse irradiation on window, as described in Appendix D.
2. If exterior shading exists, determine sunlit area and shaded area, as described in Appendix D.
3. With no interior shading, the beam, diffuse, and total transmitted and absorbed solar heat gains are given by

Load Calculation Applications Manual (SI), Second Edition

Table 7.9 Angle Correction Factors for SHGC

ID	# of layers	SHGC Angle Correction Factors and Diffuse Correction Factor							Description		
		0	40	50	60	70	80	Diffuse	Layer	Normal SHGC	T_v
1A	1	1.000	0.977	0.953	0.907	0.779	0.488	0.907	Clear	0.86	0.90
1C	1	1.000	0.973	0.932	0.877	0.753	0.466	0.890	Bronze Heat Absorbing	0.73	0.68
1I	1	1.000	0.952	0.919	0.871	0.742	0.484	0.887	Reflective	0.62	0.75
5A	2	1.000	0.974	0.934	0.842	0.658	0.342	0.868	Clear/Clear	0.76	0.81
5C	2	1.000	0.968	0.919	0.823	0.629	0.323	0.855	Bronze Heat Absorbing/Clear	0.62	0.62
5P	2	1.000	0.966	0.931	0.862	0.690	0.414	0.862	Reflective/Clear	0.29	0.27
17C	2	1.000	0.971	0.929	0.843	0.657	0.343	0.871	Clear/Low-e ("high solar")	0.70	0.76
25A	2	1.000	0.976	0.927	0.829	0.659	0.341	0.878	Low-e/Clear ("low solar")	0.41	0.72
25E	2	1.000	0.958	0.917	0.833	0.667	0.375	0.875	Gray Low-e/Clear	0.24	0.35
29A	3	1.000	0.956	0.912	0.794	0.574	0.265	0.838	Clear/Clear/Clear	0.68	0.74
29C	3	1.000	0.906	0.844	0.750	0.563	0.313	0.813	Green Heat Absorbing/Clear/Clear	0.32	0.53
32C	3	1.000	0.968	0.919	0.790	0.581	0.258	0.839	Clear/Clear/Low-e ("high solar")	0.62	0.68
40C	3	1.000	0.926	0.889	0.778	0.593	0.296	0.852	Low-e/Low-e/Clear ("low solar")	0.27	0.58

Note: See Table 3.8 for a more complete list.

$$q_{SHG,D} = E_D A_{sunlit} SHGC(\theta) \quad (7.4a)$$

$$q_{SHG,d} = (E_{dV} + E_r) A \cdot SHGC_{diffuse} \quad (7.4b)$$

$$q_{SHG} = q_{SHG,D} + q_{SHG,d} \quad (7.4c)$$

where

- $q_{SHG,D}$ = direct (beam) solar heat gain, W/m^2
- $q_{SHG,d}$ = diffuse solar heat gain, W/m^2
- q_{SHG} = total solar heat gain, W/m^2
- E_D = incident direct (beam) irradiation, W/m^2
- E_{dV} = incident diffuse irradiation from sky on a vertical surface, W/m^2
- E_r = incident diffuse reflected irradiation, W/m^2
- $SHGC(\theta)$ = angle-dependent SHGC determined from manufacturer's normal SHGC corrected by correction factors in Table 7.9 or 3.8
- $SHGC_{diffuse}$ = the SHGC for diffuse irradiation, determined by multiplying the manufacturer's normal SHGC by the diffuse correction factor in Table 7.9 or 3.8
- IAC_{diff} = interior attenuation coefficient applying to diffuse irradiation on a specific window/shade combination, as tabulated in Tables 3.9a – 3.9g
- A_{sunlit} = the unshaded area of the window, m^2

Fundamentals of the Radiant Time Series Method

A = the total area of the window, including the frame, m^2

If there is no interior shading, the window heat gain calculation is complete.

4. With interior shading, such as Venetian blinds or draperies, the effects on solar heat gain may be estimated with interior attenuation coefficients (IACs), which are tabulated in Tables 3.9a through 3.9g. Use of the tables to obtain IACs is described in Chapter 3. The direct and diffuse solar heat gains determined with Equations 7.4a through 7.4c are multiplied by angle-dependent and diffuse IACs to determine the solar heat gain with the interior shading layer. For the direct (beam) solar heat gain, the IAC depends on the profile angle as given by Equation 3.6. Then, the total solar heat gain is given by

$$q_{SHG} = E_D A_{\text{sunlit}} SHGC(\theta) IAC(\theta, \Omega) + (E_{dV} + E_r) A \cdot SHGC_{\text{diffuse}} IAC_{\text{diff}} \quad (7.5)$$

The first line of Equation 7.5 is the direct part of the solar heat gain; the second line represents the diffuse portion.

7.6 Computation of Internal and Infiltration Heat Gains

As with any load calculation procedure, internal heat gains due to occupants, lighting, and equipment must be estimated for each hour. Chapter 6 covers procedures and data for estimating internal heat gains.

Likewise, heat gains due to infiltration must also be estimated. Procedures and data for estimating infiltration flow rates are given in Chapter 5.

7.7 Splitting Heat Gains into Radiative and Convective Portions

The instantaneous cooling load is defined as the rate at which heat energy is connected to the zone air at a given point in time. The computation of convective heat gains is complicated by the radiant exchange between surfaces, furniture, partitions, and other mass in the zone. Radiative heat transfer introduces a time dependency into the process that is not easily quantified. Heat balance procedures calculate the radiant exchange between surfaces based on their surface temperatures and emissivities but typically rely on estimated radiative/convective splits to determine the contribution of internal heat sinks and sources to the radiant exchange. The radiant time series procedure simplifies the heat balance procedure by splitting all heat gains into radiative and convective portions instead of simultaneously solving for the instantaneous convection and radiative heat transfer from each surface. Table 7.10 contains recommendations for splitting each of the heat gain components.

According to the radiant time series procedure, once each heat gain is split into radiative and convective portions, the heat gains can be converted to cooling loads. The radiative portion is absorbed by the thermal mass in the zone and then convected into the space. This process creates a time lag and dampening effect. The convective portion, on the other hand, is assumed to instantly become cooling load and, therefore, only needs to be summed to find its contribution to the hourly cooling load. The method for converting the radiative portion to cooling loads is discussed in the next sections.

7.8 Conversion of Radiative Heat Gains into Cooling Loads

The RTSM converts the radiant portion of hourly heat gains to hourly cooling loads using radiant time factors (RTFs). Radiant time series calculate the cooling load

Load Calculation Applications Manual (SI), Second Edition

Example 7.2 Solar Heat Gain Calculation

Compute the solar heat gain for a window facing 30° east of south in Atlanta, Georgia, at 33.64°N latitude and 84.43°W longitude on July 21 at 12:00 p.m. EDT. The room temperature is 24°C. The window is 1.2 m high and 1.2 m wide; the exterior surface is flush with the outside of the building wall, and it has a horizontal shading surface at the top of the window that extends out from the building 0.3 m. The window manufacturer gives the following information:

- Double-pane window with a low-e coating and a soft gray tint. Neither the location of the coating nor the degree of window tinting is specified.
- The U-factor is given as 1.82 W/(m²·K).
- The normal SHGC is given as 0.26.
- The visual transmittance is given as 0.32.

Compute the solar heat gain for the case where the window has no internal shading and for the case where it has light-colored interior miniblinds.

**Table 7.10 Recommended Radiative/Convective Splits
for Internal Heat Gains**

(Source: Nigusse 2007)

Heat Gain Type	Recommended Radiative Fraction	Recommended Convective Fraction	Comments
Occupants—typical office conditions	0.6	0.4	See Table 6.1 for other conditions.
Equipment	0.1–0.8	0.9–0.2	See Chapter 6 for detailed coverage of equipment heat gain and recommended radiative/convective splits for motors, cooking appliances, laboratory equipment, medical equipment, office equipment, etc.
Office equipment with fan	0.10	0.9	
Office equipment without fan	0.3	0.7	
Lighting			Varies—see Table 6.3.
Conduction heat gain through walls and floors	0.46	0.54	
Conduction heat gain through roofs	0.60	0.40	
Conduction heat gain through windows	0.33 (SHGC > 0.5) 0.46 (SHGC ≤ 0.5)	0.67 (SHGC > 0.5) 0.54 (SHGC ≤ 0.5)	
Solar heat gain through fenestration w/o interior shading	1.0	0.0	
Solar heat gain through fenestration w/interior shading			Varies; see Tables 3.9a to 3.9c
Infiltration	0.0	1.0	

Fundamentals of the Radiant Time Series Method

Solution: First, the incident angles, shading, and incident irradiation are determined using the procedures described in Appendix D. Then, the window properties, including appropriate values of SHGC, are determined. Lastly, the solar heat gains with and without internal shading are calculated.

Conduction Heat Gain. The U-factor is given by the manufacturer as 1.82 W/(m²·K). The area of the window is 1.44 m². The air temperature at noon is 29.5°C. From Equation 7.3, the conduction heat gain at noon is

$$q_{cond,12} = 1.82 \cdot (1.44) \cdot (29.5 - 24) = 14.4 \text{ W}$$

Incident Angle Calculation. The local standard time for Atlanta in the summer is one hour before the local daylight savings time:

$$12:00 - 1:00 = 11:00$$

The equation of time for July from Table D.1 in Appendix D is -6.20 min. From Equation D.2, the local solar time to the nearest minute then becomes

$$11:00 - 6.2/60 + (75 - 84.43)/15 = 10.268, \text{ or } 10:16 \text{ a.m.}$$

The hour angle (Equation D.3) 1 hour and 44 minutes before solar noon is equal to -26.0°. The declination for July, from Table D.1, is 20.6°. Here, we use the value calculated with Equation D.7, 20.64°. The solar altitude angle is given by Equation D.4:

$$\beta = \sin^{-1}[\cos(33.64^\circ) \cos(-26.0^\circ) \cos(20.64^\circ) + \sin(33.64^\circ) \sin(20.64^\circ)] = 63.56^\circ$$

The solar azimuth angle is calculated from Equation D.5b:

$$\phi = \cos^{-1}\left(\frac{\sin(20.64^\circ) \cos(33.64^\circ) - \cos(20.64^\circ) \sin(33.64^\circ) \cos(-26.0^\circ)}{\cos(63.56^\circ)}\right) = 112.79^\circ$$

The surface solar azimuth angle is calculated using Equation D.6:

$$\gamma = |112.79^\circ - 150^\circ| = 37.21^\circ$$

The angle of incidence can then be calculated using Equation D.7:

$$\theta = \cos^{-1}[\cos(63.56^\circ) \cos(37.21^\circ) \sin(90^\circ) + \sin(63.56^\circ) \cos(90^\circ)] = 69.23^\circ$$

Solar Radiation Calculation. The ASHRAE clear-sky model (covered in Section D.2 of Appendix D) is used to calculate the beam and diffuse irradiation. Equation D.15 is used to determine the extraterrestrial solar irradiation, E_o . The relative air mass, m , is calculated with Equation D.16. The beam and diffuse optical depths (τ_b and τ_d) are taken from the July column of rows 38 and 39 of Table 4.1. Then the air mass exponents, ab and ad , are calculated with Equations D.17 and D.18. The normal beam irradiation E_b is then calculated with Equation D.19. The direct (beam) radiation incident on the wall $E_{b,t}$ is then calculated with Equation D.21:

Load Calculation Applications Manual (SI), Second Edition

$$E_0 = 1367 \cdot \left\{ 1 + 0.033 \cos \left[360^\circ \frac{(202-3)}{365} \right] \right\} = 1323.7 \text{ W/m}^2$$

$$m = \frac{1}{\sin 63.56^\circ + 0.50572 \cdot 6.07995 + 63.56^\circ - 1.6364} = 1.116$$

$$ab = 1.454 - 0.406 \cdot 0.440 - 0.268 \cdot 2.202 + 0.021 \cdot 0.440 \cdot 2.202 = 0.706$$

$$ad = 0.507 + 0.205 \cdot 0.440 - 0.080 \cdot 2.202 - 0.190 \cdot 0.440 \cdot 2.202 = 0.237$$

$$E_b = 1323.7 \cdot e^{[-0.440 \times (1.116^{0.706})]} = 822.8 \text{ W/m}^2$$

$$E_{t,b} = 822.8 \cdot \cos(69.23^\circ) = 291.8 \text{ Btu/h-ft}^2$$

The diffuse radiation on a horizontal surface is given by Equation D.20, and the resulting diffuse radiation on the vertical wall is given by Equations D.22 and D.23:

$$E_d = 1323.7 \cdot e^{[-2.202 \cdot (1.116^{0.237})]} = 138.1 \text{ W/m}^2$$

$$Y = 0.55 + 0.437 \cos(69.23^\circ) + 0.313 \cos^2(69.23^\circ) = 0.744$$

$$E_{d,t} = 0.744 \cdot 138.1 = 102.7 \text{ W/m}^2$$

The reflected radiation on the window is given by Equation D.26:

$$E_r = (822.8 \cdot \sin 63.56^\circ + 138.1) \cdot 0.2 \cdot 0.5 = 87.5 \text{ W/m}^2$$

External Shading Calculation. The window has a horizontal overhang only. The profile angle for the horizontal projection is given by Equation D.28:

$$\tan \Omega = \frac{\tan \beta}{\cos \gamma} = \frac{\tan(63.56^\circ)}{\cos(37.21^\circ)} = 2.525$$

$$\Omega = \tan^{-1}(2.525^\circ) = 68.39^\circ$$

The height of the horizontal overhang projection is given by Equation D.29:

$$S_H = 0.3 \cdot \tan(68.39^\circ) = 0.76 \text{ m}$$

The window sunlit and shaded areas from Equations D.31 and D.32, respectively, are given by

$$A_{SL} = [1.2 - (0 - 0)] \cdot [1.2 - (0.76 - 0)] = 0.53 \text{ m}^2$$

$$A_{SH} = 1.2^2 - 0.53 = 0.91 \text{ m}^2$$

The horizontal projection is 0.76 m, so the window will be partially shaded, with 36.9% (the lower 0.44 m) exposed to direct and diffuse radiation covers and 63.1% (the upper 0.76 m) exposed only to diffuse solar radiation.

Fundamentals of the Radiant Time Series Method

Solar Heat Gain Calculation. The SHGC angle correction factor is taken from Table 7.9 or 3.8. The most similar window in terms of number of panes, description, normal SHGC, and visual transmittance is window 25E. The angle-dependent SHGC is then determined as the product of the normal SHGC (0.24) and the SHGC angle correction factor 0.680 determined by interpolation between angle 60° and 70° in row 25E of Table 7.9. The diffuse SHGC is similarly obtained by multiplying the normal SHGC by the diffuse angle correction factor taken from row 25E of Table 7.9. The SHGCs are then

$$\text{SHGC}(69.23^\circ) = 0.24 \cdot 0.680 = 0.163$$

$$\text{SHGC}_{\text{diffuse}} = 0.24 \cdot 0.875 = 0.210$$

If the window has no internal shading, the beam, diffuse, and total solar heat gains can be calculated directly using Equation 7.4:

$$q_{SHG,D,12} = 291.8 \cdot 0.53 \cdot 0.163 = 25.2 \text{ W}$$

$$q_{SHG,d,12} = (102.7 + 87.5) \cdot 1.44 \cdot 0.210 = 57.5 \text{ W}$$

$$q_{SHG,12} = 25.2 + 57.5 = 82.7 \text{ W}$$

To determine the solar heat gains with the light-colored miniblind, it is necessary to look up the IAC values. Here, we interpret light-colored miniblinds to have a reflectance of 0.8 and we choose the blinds to be oriented at a 45° angle. From Table 3.9e, in the glazing type 25e column, $IAC_0 = 0.84$, $IAC_{60} = 0.79$, and $IAC_{diff} = 0.87$. The profile angle is the same as computed for the external shading above, 68.4°. Using Equation 3.6, the $IAC(\theta, \Omega) = 0.79$. The solar heat gains corrected for the light-colored miniblind interior shading element become

$$q_{SHG,12} = 291.8 \cdot 0.53 \cdot 0.163 \cdot 0.79 + (102.7 + 87.5) \cdot 1.44 \cdot 0.210 \cdot 0.87 = 70 \text{ W}$$

The total heat gain for the window is obtained by adding the solar heat gain and the conduction heat gain:

$$q_{12} = q_{cond,12} + q_{SHG,12}$$

$$q_{12} = 14.4 + 70 = 84.4 \text{ W}$$

Example 7.2 Window.xls, included on the online supporting files that accompany this manual, demonstrates this computation for all hours of the day.

for the current hour on the basis of current and past heat gains. The radiant time series for a particular zone gives the time-dependent response of the zone to a single, steady, periodic pulse of radiant energy. The series shows the portion of the radiant pulse that is convected to the zone air for each hour. Thus, r_0 represents the fraction of the radiant pulse convected to the zone air in the current hour, r_1 in the previous hour, and so on. The radiant time series thus generated is used to convert the radiant portion of hourly heat gains to hourly cooling loads according to Equation 7.6:

$$Q_0 = r_0 q_0 + r_1 q_{0-8} + r_2 q_{0-28} + r_3 q_{0-38} + \dots + r_{23} q_{0-238} \quad (7.6)$$

Load Calculation Applications Manual (SI), Second Edition

where

Q_0 = cooling load (Q) for the current hour θ
 q_0 = heat gain for the current hour
 $q_{0-n\delta}$ = heat gain n hours ago
 $r_0, r_1, \text{ etc.}$ = RTFs

RTFs are unique to each zone and depend on the zone geometry, envelope constructions, internal partitions and thermal mass, etc. Furthermore, they also depend on the distribution of the radiant energy entering the zone. In many cases, beam solar radiation transmitted through windows will primarily strike the floor. Radiation emitted by occupants, equipment, etc. will tend to be distributed to all surfaces in the zone. In the common case where the floor is thermally massive while the walls and ceiling are lightweight, this can lead to a significant difference in thermal response between solar radiation and nonsolar radiation. As a result, two different sets of RTFs are utilized—one set that applies to transmitted solar radiation and another set that applies to radiation from internal heat gains and building envelope surfaces. The second set is labeled *nonsolar radiation*.

A representative set of RTFs for a range of zones is given in Tables 7.11 and 7.12. The test zone geometry and construction details used to generate the RTFs in Tables 7.11 and 7.12 are described in Table 7.13. It should be noted that the test zone has a single external wall, hence the percentage glass figures given in Tables 7.11 and 7.12 are based on a percentage of the single external wall.

To use these tables, the zone that most closely matches the room must be selected. In cases where the zone does not clearly match any of the sample zones, the engineer may wish to calculate RTFs for the specific zone in question. Spreadsheet tools for doing this are the files *7-6 RTF_tabulated.xls* (a standalone version) and *Example 7.3 RTF Generation.xls*, both in the online supporting files accompanying this manual. Use of the second spreadsheet is demonstrated in Example 7.3.

When considering how closely the actual zone should match a zone in Tables 7.11 and 7.12, or when considering how to specify a zone with the RTF generation tool, some engineering judgment is required. The primary purpose of the RTFs is to quantify how fast the zone responds to heat gains. Consider Figure 7.4, where the RTFs applying to transmitted solar heat gain are plotted for three sample zones—a lightweight zone without carpeting, a heavyweight zone with carpeting, and a heavyweight zone without carpeting—all with 10% glazing on one wall. The curves represent the response of the zone: the higher the value at the beginning, the faster the zone responds and the more closely the cooling loads follow the heat gains. Generally speaking, the zone responds more slowly when either the thermal mass of the zone is increased or when any resistance between the heat gain and the thermal mass is decreased. For example, in Figure 7.4, when comparing the lightweight and heavyweight zones without carpeting, the heavyweight zone responds much more slowly than the lightweight zone, due to a significant amount of heat gain being stored in the heavyweight zone's structure. The third curve, for a heavyweight zone with carpeting, reveals that the zone now acts much more like a lightweight zone than a heavyweight zone. Additional factors that might be considered include the following:

- *Furniture*—furniture acts as an internal thermal mass that can store energy, so it can slow the response of the zone. However, furniture that intercepts solar or thermal radiation and is less thermally massive than the floor can speed the response of the zone; this is usually the dominant factor. The RTFs tabulated in Tables 7.11 and 7.12 assumed the presence of furniture with a surface area of 21 m² or 1/2 of the floor area. In turn, 50% of the beam solar radiation was assumed to be intercepted by the furniture, and the remainder was incident on the floor. This has a mitigating effect on the energy stored in the floor. With the RTF generation spreadsheet, it is

Fundamentals of the Radiant Time Series Method

possible to set any level of furniture. For rooms with significant window area and an uncarpeted massive floor, eliminating the furniture may noticeably reduce the peak cooling load. However, given the limited knowledge of future placement of furniture in the space, prudence is suggested.

- *Carpeting*—carpeting limits the amount of energy that can be stored in the floor, speeding the response of the zone.
- *Zone geometry and construction*—for purposes of computing the RTF, specification of the zone geometry and construction controls the response of the zone only. For example, choosing a higher percentage of fenestration replaces the wall, which

Table 7.11 Representative Nonsolar RTS Values for Light to Heavy Construction

(Source: ASHRAE Handbook—Fundamentals [2013], Chapter 18, Table 19)

% Glass	Light						Medium						Heavy						Interior Zones					
	With Carpet			No Carpet			With Carpet			No Carpet			With Carpet			No Carpet			Light		Medium		Heavy	
	10	50	90	10	50	90	10	50	90	10	50	90	10	50	90	10	50	90	With Carpet	With No Carpet	With Carpet	With No Carpet	With Carpet	With No Carpet
Hour	Radiant Time Factor, %																							
0	47	50	53	41	43	46	46	49	52	31	33	35	34	38	42	22	25	28	46	40	46	31	33	21
1	19	18	17	20	19	19	18	17	16	17	16	15	9	9	9	10	9	9	19	20	18	17	9	9
2	11	10	9	12	11	11	10	9	8	11	10	10	6	6	5	6	6	6	11	12	10	11	6	6
3	6	6	5	8	7	7	6	5	5	8	7	7	4	4	4	5	5	5	6	8	6	8	5	5
4	4	4	3	5	5	5	4	3	3	6	5	5	4	4	4	5	5	4	4	5	3	6	4	5
5	3	3	2	4	3	3	2	2	2	4	4	4	4	3	3	4	4	4	3	4	2	4	4	4
6	2	2	2	3	3	2	2	2	2	4	3	3	3	3	3	4	4	4	2	3	2	4	3	4
7	2	1	1	2	2	2	1	1	1	3	3	3	3	3	3	4	4	4	2	2	1	3	3	4
8	1	1	1	1	1	1	1	1	1	3	2	2	3	3	3	4	3	3	1	1	1	3	3	4
9	1	1	1	1	1	1	1	1	1	2	2	2	3	3	2	3	3	3	1	1	1	2	3	3
10	1	1	1	1	1	1	1	1	1	2	2	2	3	2	2	3	3	3	1	1	1	2	3	3
11	1	1	1	1	1	1	1	1	1	2	2	2	2	2	2	3	3	3	1	1	1	2	2	3
12	1	1	1	1	1	1	1	1	1	1	1	1	2	2	2	3	3	3	1	1	1	1	2	3
13	1	1	1	0	1	0	1	1	1	1	1	1	2	2	2	3	3	2	1	1	1	1	2	3
14	0	0	1	0	1	0	1	1	1	1	1	1	2	2	2	3	2	2	1	0	1	1	2	3
15	0	0	1	0	0	0	1	1	1	1	1	1	2	2	2	2	2	2	0	0	1	1	2	3
16	0	0	0	0	0	0	1	1	1	1	1	1	2	2	2	2	2	2	0	0	1	1	2	3
17	0	0	0	0	0	0	1	1	1	1	1	1	2	2	2	2	2	2	0	0	1	1	2	2
18	0	0	0	0	0	0	1	1	1	1	1	1	2	2	1	2	2	2	0	0	1	1	2	2
19	0	0	0	0	0	0	0	1	0	0	1	1	2	2	1	2	2	2	0	0	1	0	2	2
20	0	0	0	0	0	0	0	0	0	0	1	1	2	1	1	2	2	2	0	0	0	0	2	2
21	0	0	0	0	0	0	0	0	0	0	1	1	2	1	1	2	2	2	0	0	0	0	2	2
22	0	0	0	0	0	0	0	0	0	0	1	0	1	1	1	2	2	2	0	0	0	0	1	2
23	0	0	0	0	0	0	0	0	0	0	0	0	1	1	1	2	2	1	0	0	0	0	1	2
	100	100	100	100	100	100	100	100	100	100	100	100	100	100	100	100	100	100	100	100	100	100	100	100

Load Calculation Applications Manual (SI), Second Edition

may be thermally massive, with glazing, which has negligible thermal mass. This would speed the response of the zone.

7.9 Implementing the RTSM

The RTSM method may be implemented in a spreadsheet or as a separate computer program. The spreadsheet may be constructed in an infinite number of ways, to be more or less automated, depending on the desires of the user. The use of macros can simplify the implementation by eliminating the need for coding individual equations in each cell.

The implementation follows the flow chart shown in Figure 7.1. After geometry, constructions, environmental design conditions, peak internal heat gains and schedules, etc. have been determined, the steps may be summarized as follows:

Table 7.12 Representative Solar RTS Values for Light to Heavy Construction

(Source: ASHRAE Handbook—Fundamentals [2013], Chapter 18, Table 20)

% Glass	Light						Medium						Heavy					
	With Carpet			No Carpet			With Carpet			No Carpet			With Carpet			No Carpet		
	10	50	90	10	50	90	10	50	90	10	50	90	10	50	90	10	50	90
Hour	Radiant Time Factor, %																	
0	53	55	56	44	45	46	52	54	55	28	29	29	47	49	51	26	27	28
1	17	17	17	19	20	20	16	16	15	15	15	15	11	12	12	12	13	13
2	9	9	9	11	11	11	8	8	8	10	10	10	6	6	6	7	7	7
3	5	5	5	7	7	7	5	4	4	7	7	7	4	4	3	5	5	5
4	3	3	3	5	5	5	3	3	3	6	6	6	3	3	3	4	4	4
5	2	2	2	3	3	3	2	2	2	5	5	5	2	2	2	4	4	4
6	2	2	2	3	2	2	2	1	1	4	4	4	2	2	2	3	3	3
7	1	1	1	2	2	2	1	1	1	4	3	3	2	2	2	3	3	3
8	1	1	1	1	1	1	1	1	1	3	3	3	2	2	2	3	3	3
9	1	1	1	1	1	1	1	1	1	3	3	3	2	2	2	3	3	3
10	1	1	1	1	1	1	1	1	1	2	2	2	2	2	2	3	3	3
11	1	1	1	1	1	1	1	1	1	2	2	2	2	2	1	3	3	2
12	1	1	1	1	1	0	1	1	1	2	2	2	2	1	1	2	2	2
13	1	1	0	1	0	0	1	1	1	2	2	2	2	1	1	2	2	2
14	1	0	0	0	0	0	1	1	1	1	1	1	2	1	1	2	2	2
15	1	0	0	0	0	0	1	1	1	1	1	1	1	1	1	2	2	2
16	0	0	0	0	0	0	1	1	1	1	1	1	1	1	1	2	2	2
17	0	0	0	0	0	0	1	1	1	1	1	1	1	1	1	2	2	2
18	0	0	0	0	0	0	1	1	1	1	1	1	1	1	1	2	2	2
19	0	0	0	0	0	0	0	0	0	1	1	1	1	1	1	2	2	2
20	0	0	0	0	0	0	0	0	0	1	1	1	1	1	1	2	2	2
21	0	0	0	0	0	0	0	0	0	0	0	0	1	1	1	2	2	2
22	0	0	0	0	0	0	0	0	0	0	0	0	1	1	1	2	1	1
23	0	0	0	0	0	0	0	0	0	0	0	0	1	1	1	2	1	1
	100	100	100	100	100	100	100	100	100	100	100	100	100	100	100	100	100	100

Fundamentals of the Radiant Time Series Method

1. Determine conduction time series factors (CTSFs) for exterior walls and roofs. There are two approaches for determining the CTSFs:
 - a. If a sufficiently close match to one of the walls or roofs in Tables 7.3 and 7.4 can be found, CTSFs may be taken directly from the tables. To avoid retyping the numbers, spreadsheet *7-3_tabulated_CTSF.xls* contains a simple database that can extract any set of CTSFs from the tables.
 - b. Alternatively, CTSFs may be computed for any combination of one-dimensional layers using the methodology utilized in the spreadsheet

Table 7.13 Representative Zone Construction for Tables 7.11 and 7.12

(Source: ASHRAE Handbook—Fundamentals [2013], Chapter 18, Table 21)

Construction Class	Exterior Wall	Roof/Ceiling	Partition	Floor	Furnishing
Light	Steel siding, 50 mm insulation, air space, 19 mm gyp	100 mm LW concrete, ceiling air space, acoustic tile	19 mm gyp, air space, 19 mm gyp	Acoustic tile, ceiling air space, 100 mm LW concrete	25 mm wood @ 50% of floor area
Medium	100 mm face brick, 50 mm insulation, air space, 19 mm gyp	100 mm LW concrete, ceiling air space, acoustic tile	19 mm gyp, air space, 19 mm gyp	Acoustic tile, ceiling air space, 100 mm LW concrete	25 mm wood @ 50% of floor area
Heavy	100 mm face brick, 50 mm insulation, 200 mm HW concrete, 19 mm gyp	200 mm LW concrete, ceiling air space, acoustic tile	19 mm gyp, 200 mm HW concrete block, 19 mm gyp	Acoustic tile, ceiling air space, 200 mm LW concrete	25 mm wood @ 50% of floor area

1. Surface layers are listed in order from the outside of the room to the inside of the room.
2. Carpet, when specified in Tables 7.11 and 7.12, has no thermal mass and a resistance of 0.48 (m²·K)/W.
3. The test zone is 4.55 · 9.1 · 2.75 m high. Zones labeled Interior Zones in Table 7.11 have only interior partitions and no exterior walls or fenestration. The other RTFs are based on a test zone with one exterior wall, 9.1 m long. The % glazing is the % of area on the exterior wall covered by glazing.

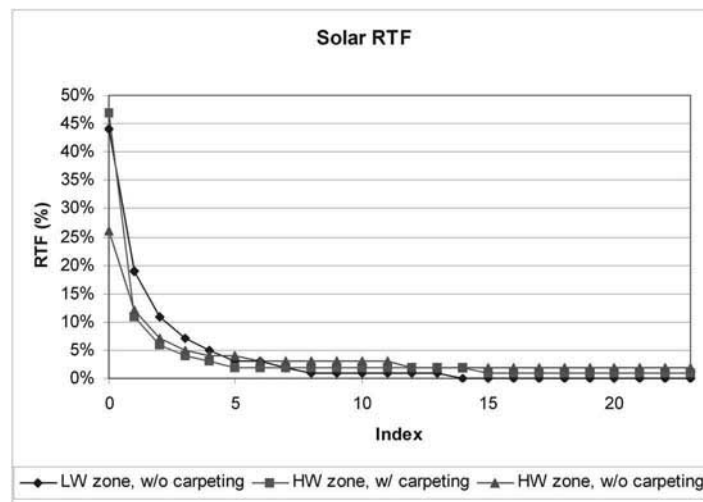


Figure 7.4 RTFs (solar) for three zones.

Example 7.3 RTF Determination

The ASHRAE headquarters building in Atlanta, Georgia has a 12.1 m² office in the southwest corner of the second floor. Figure 7.5 shows a plan view of the office. Figure 7.6 shows two elevation views of the building. The exterior vertical walls are composed of a spandrel curtain wall construction, a brick wall construction, and windows. The acoustical tile is approximately even with the top of the second-floor windows, and the space above the acoustical tile serves as a return air plenum. Layer-by-layer descriptions of all constructions are given in Table 7.14; surface areas and absorptivities are summarized in Table 7.15. (Note: There is additional discussion of the zone and building in Chapter 8.) The southeast façade has a glazing fraction of 34%, and the southwest façade has a glazing fraction of 44%.

Determine the RTFs from Tables 7.11 and 7.12 and then using the spreadsheet RTF generation tool.

Solution: When viewing Figure 7.5, immediately note that, from the exterior, the geometry of the room is relatively complex, with the brick-clad portion of the façade being oriented at 45° angles to the other surfaces. Furthermore, as shown in Figure 7.6, there is a large overhang around the building. The first choice the engineer has to make is how to draw the boundary of the zone (i.e., will the surface areas be determined at the inside of the room, the outside of the room, or an intermediate point?). Secondly, how will the brick-clad portion of the façade be represented? The following two important considerations should be kept in mind.

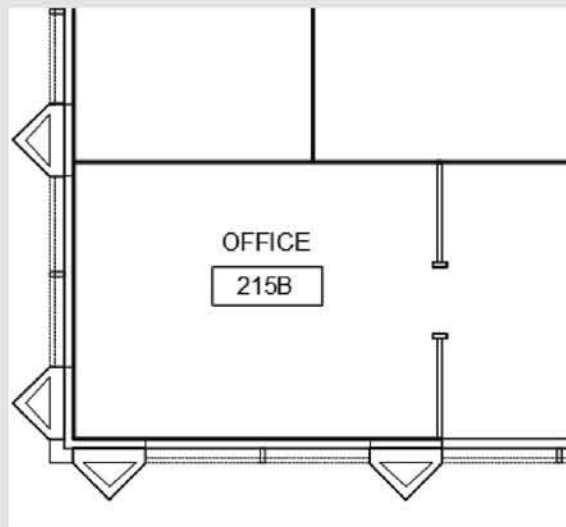


Figure 7.5 ASHRAE headquarters building office plan view.

Fundamentals of the Radiant Time Series Method

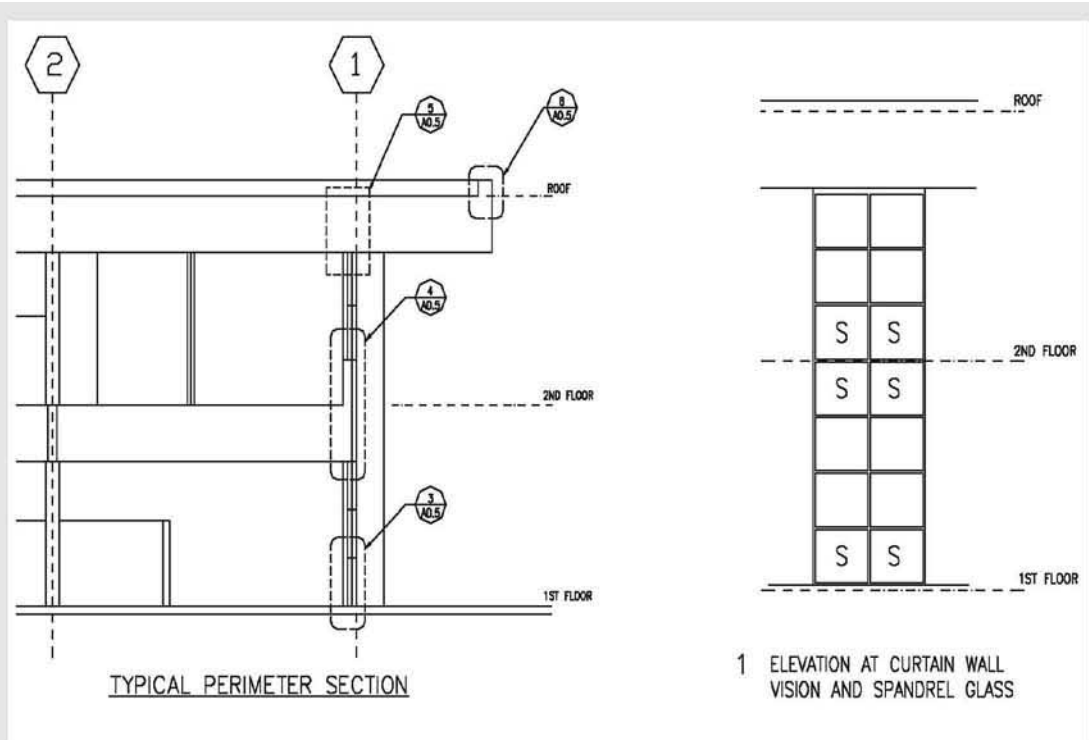


Figure 7.6 Elevation views of the ASHRAE headquarters building.

Table 7.14 Summary of Constructions for Example 7.3

Layer Number	Brick Clad	Spandrel	Partition	Furniture	Roof	Floor
1	F01	F01	F02	F02	F01	F03
2	M01	F09	G01	G05	F13	F16
3	M02	F04	F04	F02	I06	F05
4	I07*	I07*	G01		F03	F08
5	G01	G01	F02			M18*
6	M02	F02				F17
7	F02					F03

1. Layer codes are taken from Table 7.5, except where marked with an asterisk (*). These surfaces are as follows:

I07 is R-2.2 insulation board, otherwise equivalent to I02.

M18 is 125 mm of lightweight concrete, otherwise equivalent to M11.

2. Layers are specified from outside to inside.

Table 7.15 Office Surface Areas

Surface Name	SE Brick	SE Spandrel	SW Brick	SW Spandrel	NW Partition	NE Partition	SE Window	SW Window	Roof	Floor	Furniture
Area (m ²) based on room inside	5.6	1.5	3.1	1.5	10.9	8.4	3.7	3.7	12.1	12.1	12.1
Area (m ²) based on room outside	8.0	1.5	4.4	1.5	10.9	8.4	3.7	3.7	12.1	12.1	12.1

Load Calculation Applications Manual (SI), Second Edition

First, at this point in the load calculation process, we are seeking the response of the zone to heat gains. The overhang and the construction of the building above the acoustical ceiling tile have little or no effect on the zone response. The two-dimensional nature of the brick-clad portion may have a slight effect on the response, yet neither the RTF generation procedure nor any of the cooling load calculation procedures presented in this manual have an explicit way to account for such a construction. If desired, the limiting cases (area of brick-clad construction based on inside area and area of brick-clad construction based on outside area) could be examined with the one-dimensional RTF generation procedure.

Second, conduction heat gains will have a relatively small impact on the zone cooling load compared to solar heat gains through fenestration and internal heat gains. At the point where conduction heat gains are calculated, the same choices must be made. Again, the relative sensitivity to the choice of zone boundary can be checked with one-dimensional procedures, but engineering judgment should be used with regard to the time and effort spent on the representation of the zone. For example, the shading of the windows by the overhang will be considerably more important than conduction heat gain through the overhang side walls, and effort should be spent accordingly.

Given all of the above, for purposes of the example, the areas are calculated based on the inside room boundary, with the room being 2.74 m, measured from the top of the floor to the bottom of the acoustical tile. As a check, the RTFs will also be computed using the outside surface areas.

To choose the correct set of RTFs from Tables 7.11 and 7.12, it is necessary to compare the constructions. The office has a 125 mm lightweight (LW) concrete floor, which would be closest to the lightweight construction in Tables 7.11 and 7.12. However, as the floor is carpeted and the room has furniture, matching it exactly will be less important. The brick portion of the exterior wall is relatively close to the medium-weight construction. The window and spandrel are both very lightweight constructions. As a percentage of the total vertical wall area, the office is approximately 50% lightweight partition, 27% window and spandrel, and 23% brick, or, lumping the partition, window, and spandrel together as lightweight constructions, about 77% lightweight/23% brick. For the medium-weight tabulated zone with 50% glazing on one exterior wall, the total vertical wall area would be 66% lightweight partition, 17% window, and 17% brick, or 83% lightweight/17% brick. The office roof construction matches the tabulated lightweight zone best, though the fact that the mass in the roof is separated from the room by the acoustical tile and air space renders the match less important.

The above considerations suggest that a tabulated zone with 50% glazing (on the one exterior wall) and carpeting would be appropriate, and either the medium-weight or lightweight zone would be the best choice, with the medium-weight zone perhaps being the slightly better choice.

For generating custom RTFs, the spreadsheet *Example 7.3 RTF Generation.xls* may be used. Sample input parameters are shown in Figure 7.7. After entering the input parameters, the RTFs are computed by clicking on the button labeled *GENERATE RTF*. In order to check the sensitivity to the choice of inside area versus outside area, two different worksheets are included, *Example 7.3 Inside A* and *Example 7.3 Outside A*, respectively.

Fundamentals of the Radiant Time Series Method

Finally, the various sets of RTFs may be compared. Figure 7.8 shows the nonsolar RTFs: generated with the outside areas (RTFG-O), generated with the inside areas (RTFG-I), determined from Table 7.11 for a carpeted room with 50% exterior glazing on the one exterior wall and assuming the medium-weight construction (Tables-MW), and assuming a lightweight construction (Tables-LW). An equivalent comparison is shown for the solar RTFs in Figure 7.9. As can be seen, there is essentially no difference between the two different methods of calculating the surface areas. The approximations that are inevitable when choosing an equivalent zone from the tables do result in an observable but small difference. In the next example, the sensitivity of the cooling load to these small differences in RTFs will be examined.

Example 7.3 RTF generation - Microsoft Excel

Surface ID	1	2	3	4	5	6	7	8	9	10	11
Surface Name	SE Brick	SE Spandrel	SW Brick	SW Spandrel	NW Partition	NE Partition	SE Window	SW Window	Ceiling	Floor	Furniture
Facing	150.0	150.0	240.0	240.0	330.0	60.0	150.0	240.0	0.0	0.0	0
Tilt Angle	90.0	90.0	90.0	90.0	90.0	90.0	90.0	90.0	0.0	180.0	180
Area	60.75	16.25	33.75	16.25	117.0	90.0	40.0	40.0	130.0	130.0	130
LW Emissivity In	0.9	0.9	0.9	0.9	0.9	0.9	0.9	0.9	0.9	0.9	0.9
Boundary Cond	T05	T05	T05	T05	TA	TA	T05	T05	T05	TA	TA
Number of Layers	7	6	7	6	5	5	5	5	4	7	3
Layer1	F01	F01	F01	F01	F02	F02	F01	F01	F01	F03	F02
Layer2	M01	F09	M01	F09	G01	G01	W2	W2	F13	F16	G05
Layer3	M02	F04	M02	F04	F04	F04	B1	B1	I06	F05	F02
Layer4	I04	I04	I04	I04	G01	G01	W2	W2	F03	F08	
Layer5	G01	G01	G01	G01	F02	F02	F02	F02		M11	
Layer6	M02	F02	M02	F02						F17	
Layer7	F02		F02							F03	
Layer8											
Layer9											
Layer10											

GENERATE RTF

Figure 7.7 RTF generation input parameters with inside areas for Example 7.3 (ASHRAE headquarters building office).

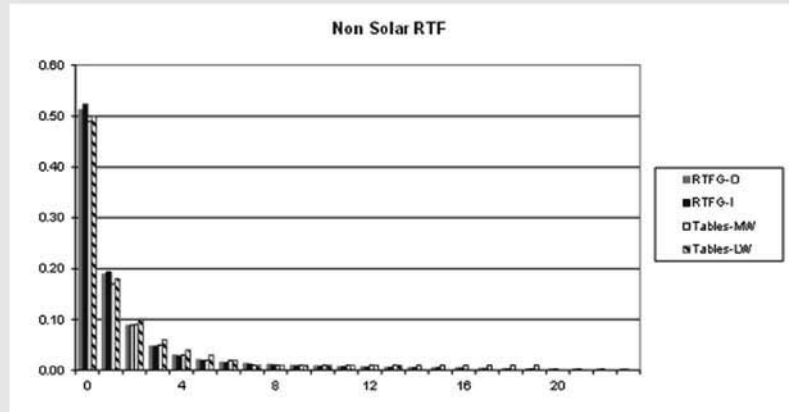


Figure 7.8 Nonsolar RTFs for Example 7.3.

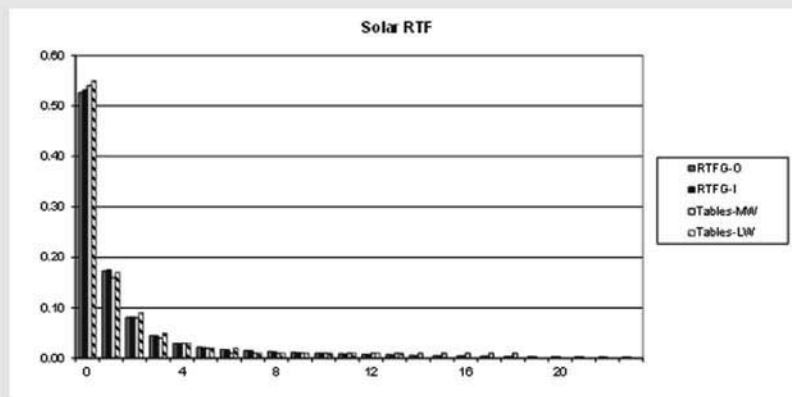


Figure 7.9 Solar RTFs for Example 7.3.

Example 7.4 Cooling Load Calculation

For the office described in Example 7.3, determine the cooling load resulting from a 11 m² equipment heat gain (computers and video projectors—assume 20% radiative) occurring between 8:00 a.m. and 5:00 p.m. Compare the cooling loads resulting from the four slightly different sets of nonsolar RTFs developed in Example 7.3.

Solution: The hourly equipment heat gains are split into radiative and convective portions. Based on the given radiative/convective split, during the hours between 8:00 a.m. and 5:00 p.m., the hourly radiative heat gain is 48 W and the hourly convective heat gain is 224 W. The radiative heat gains are converted to cooling loads with the RTFs and then added to the convective heat gains to determine the total cooling load for each hour. As an example, consider the cooling load at 2:00 p.m., using the RTFs for the medium-weight zone (Tables-MW in Figure 7.8). The radiative portion of the cooling load is determined with Equation 7.4:

Fundamentals of the Radiant Time Series Method

$$Q_{14, radiative} = \left. \begin{aligned} &0.49(56.1) + 0.17(56.1) + 0.09(56.1) + 0.05(56.1) \\ &+ 0.03(56.1) + 0.02(56.1) + 0.02(0.0) + 0.01(0.0) \\ &+ 0.01(0.0) + 0.01(0.0) + 0.01(0.0) + 0.01(0.0) \\ &\vdots \\ &+ 0.0(56.1) + 0.0(56.1) + 0.00(56.1) + 0.0(56.1) \end{aligned} \right\}$$

resulting in a value of $Q_{14, radiative} = 48 \text{ W}$.

The convective portion of the cooling load is equivalent to the convective portion of the heat gain: 224 W. Then, the total cooling load is simply the summation of the radiative and convective portions:

$$Q_{14} = Q_{14, radiative} + Q_{14, convective} = 48 + 224 = 272 \text{ W}$$

Calculations for every hour and all four sets of RTFs developed in Example 7.3 are performed in the spreadsheet *Example 7.4 ClgLoad from heat gain-SI.xls*. These results are summarized in Table 7.16. All four sets of RTFs give approximately the same peak loads, with the tabulated RTFs giving peak cooling loads within about 2% of the custom-generated RTFs in this case. Figure 7.10 illustrates the hourly heat gains and cooling loads calculated with the custom-generated RTFs and tabulated RTFs corresponding to the medium-weight zone.

While it would be rash to reach a conclusion on the accuracy of the tabulated RTFs based on a single case, the accuracy is certainly acceptable for this case. For cases where there is no clear match to the tables, users should consider using the RTF generation spreadsheet.

Table 7.16 Summary of Results for the Four Sets of RTFs Developed in Example 7.3

Hour	Heat Gain, W	Cooling Load, W			
		RTFG-I	RTFG-O	Tables-MW	Tables-LW
1	0	2	2	5	3
2	0	1	1	5	3
3	0	1	1	5	2
4	0	1	1	5	2
5	0	0	0	4	1
6	0	0	0	4	1
7	0	0	0	3	0
8	0	0	0	3	0
9	281	251	251	254	252
10	281	263	263	263	263
11	281	269	269	268	268
12	281	273	273	270	272
13	281	276	276	271	274
14	281	277	277	272	275
15	281	278	278	273	277
16	281	279	279	274	277

Load Calculation Applications Manual (SI), Second Edition

Table 7.16 Summary of Results for the Four Sets of RTFs Developed in Example 7.3 (continued)

Hour	Heat Gain, W	Cooling Load, W			
		RTFG-I	RTFG-O	Tables-MW	Tables-LW
17	281	279	279	274	278
18	0	29	29	23	26
19	0	17	17	14	16
20	0	11	11	10	11
21	0	7	7	7	8
22	0	5	5	6	7
23	0	3	3	6	5
24	0	2	2	5	4

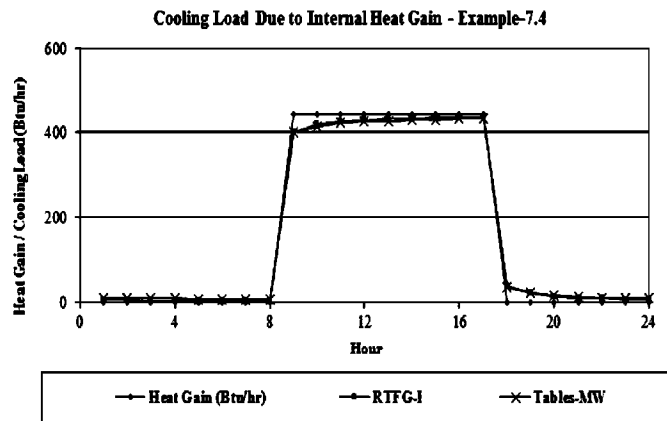


Figure 7.10 Space radiant heat gain and cooling load for Example 7.4.

- 7-4_generate_CTSF.xls*. If the wall or roof has thermal bridges, the methodology in Appendix E should be used to determine an equivalent layer-by-layer description.
- Based on the number of panes, the normal SHGC, and the U-factor and window description provided by the manufacturer, determine the appropriate window types and resulting angle correction factors from Table 7.9 or 3.8.
 - Determine RTFs for the zone. There are two approaches:
 - Choose an approximately equivalent zone in Tables 7.11 and 7.12 and use the tabulated sets of RTFs. Spreadsheet *7-6 RTF_tabulated.xls* contains a simple database that can extract any set of RTFs from the tables.
 - Compute custom RTFs for the zone using the methodology demonstrated in the spreadsheet *Example 7.3 RTF Generation.xls*.
 - Calculate hourly solar irradiation incident on each exterior surface and the hourly sol-air temperature for each surface using the methodology described in Appendix D and demonstrated in the spreadsheet *7-1-solar.xls*.
 - Compute hourly conductive heat gains from exterior walls and roofs using Equation 7.2 for each hour and the 24 hourly values of sol-air temperature. This is demonstrated in the spreadsheet *Example 7.1 Conduction.xls*.

Fundamentals of the Radiant Time Series Method

6. Compute hourly heat gains from fenestration. This includes:
 - a. Compute the conduction heat gains using Equation 7.3 and the outdoor air temperature for each hour.
 - b. Compute the solar heat gain corresponding to beam and diffuse irradiation for each hour using the procedure described in Section 7.5.
7. Compute hourly internal heat gains from occupants, equipment, and lighting, based on peak heat gains and schedules determined in the initial data-gathering phase.
8. Compute infiltration heat gains based on the procedures described in Chapter 5.
9. Split all heat gains into radiative and convective portions using the recommendations in Table 7.10.
10. Convert radiative portion of internal heat gains to hourly cooling loads using Equation 7.5. The beam solar heat gain will be converted using the solar RTFs; all other heat gains will be converted with the nonsolar RTFs.
11. For each hour, sum convective portions of heat gains with radiative cooling loads. This will be the hourly sensible cooling.

The above steps are suitable for most zones for which the RTSM is suitable. All surfaces are assumed to be of two types: exterior, with associated heat gains, or interior, with no net heat gains. A common exception is the zone with an adjacent uncontrolled space, such as a return air plenum, attic, basement, etc. Treatment of uncontrolled spaces is covered in Appendix F. Chapter 8 demonstrates two approaches to the use of the RTSM for a case with a return air plenum. A general-purpose RTSM spreadsheet is described in Appendix B.

References

- ASHRAE. 2013. *ASHRAE Handbook—Fundamentals*. Atlanta: ASHRAE.
- Barnaby, C.S., J.D. Spitler, and D. Xiao. 2004. Updating the ASHRAE/ACCA Residential Heating and Cooling Load Calculation Procedures and Data, RP-1199 Final Report. Atlanta: ASHRAE.
- Nigusse, B.A. 2007. Improvements to the radiant time series method cooling load calculation procedure. PhD thesis, School of Mechanical and Aerospace Engineering, Oklahoma State University.
- NFRC. 2004a. Procedure for determining fenestration product U-factors. NFRC 100-2004, National Fenestration Rating Council, Silver Spring, MD.
- NFRC. 2004b. Procedure for determining fenestration product solar heat gain coefficient and visible transmittance at normal incidence. NFRC 200-2004, National Fenestration Rating Council, Silver Spring, MD.
- Rees, S.J., J.D. Spitler, and P. Haves. 1998. Quantitative comparison of North American and U.K. cooling load calculation procedures—Results. *ASHRAE Transactions* 104(2):47–61.

Application of the RTSM—Detailed Example

This chapter gives a start-to-finish example of applying the radiant time series method (RTSM) for a single zone in the ASHRAE headquarters building—the office introduced in Chapter 7. The headquarters building underwent substantial renovation starting in 2007, and the description here is largely based on the post-renovation state of the building.

The chapter is organized by first presenting the building (Section 8.1) and office (Section 8.2), then presenting the application of the RTSM for the following cases:

1. First, for the case with no interior shading, all of the steps are presented with intermediate values (Section 8.3). In this section, the return air plenum is treated by use of an estimate regarding the percentage of roof heat gain that goes directly to the return air.
2. Second, the case with light-colored venetian blinds (Section 8.4) is considered.
3. An alternative approach to calculating the effect of the return air plenum (Section 8.5) is presented. Here, the hourly air temperature in the return air plenum is estimated and used to estimate the heat gain through the acoustic tile to the room.

8.1 Building Overview

The ASHRAE headquarters building is a two-story, approximately 3252 m² office building located in Atlanta, Georgia, at 33.8°N latitude and 84.5°W longitude. Figures 8.1 and 8.2 show floor plans for the building. Figures 8.3 and 8.4 show elevation views.

The building has a curtain wall construction, with the exterior walls alternating between brick pilasters and window/spandrel glass sections.

The following information for the windows is interpreted from the original manufacturer's data; the windows are similar to glass type 5D in Table 3.7, but not exactly the same:

- Double-glazed window with a 6 mm bronze-tinted outer pane, 13 mm air space, and 6 mm clear indoor pane.
- The windows are nonoperable and mounted in aluminum frames with thermal breaks. The overall combined U-factor is estimated to be 3.18 W/(m²·K).
- The normal solar heat gain coefficient (SHGC) is given as 0.56.
- The visual transmittance is given as 0.48.
- Light-colored interior miniblinds are installed.

The values for U-factor, normal SHGC, and visual transmittance have all been given without reference to window sizes, so they may be inferred to be center-of-glass values.

Lighting is done with pendant fluorescent fixtures.

8.2 Office Details

The ASHRAE headquarters building in Atlanta has a 13.3 m² office in the southwest corner of the second floor. Figure 8.7 shows elevation views of the office roof overhang and windows. Figure 8.5 shows a plan view of the office.

The geometry of the building was discussed in Example 7.3. Because of the complex geometry, some approximations will be made, particularly for the brick-clad pilasters. The office has southeast- and southwest-facing exterior vertical walls composed of spandrel curtain wall construction, brick-clad pilasters, and windows. The

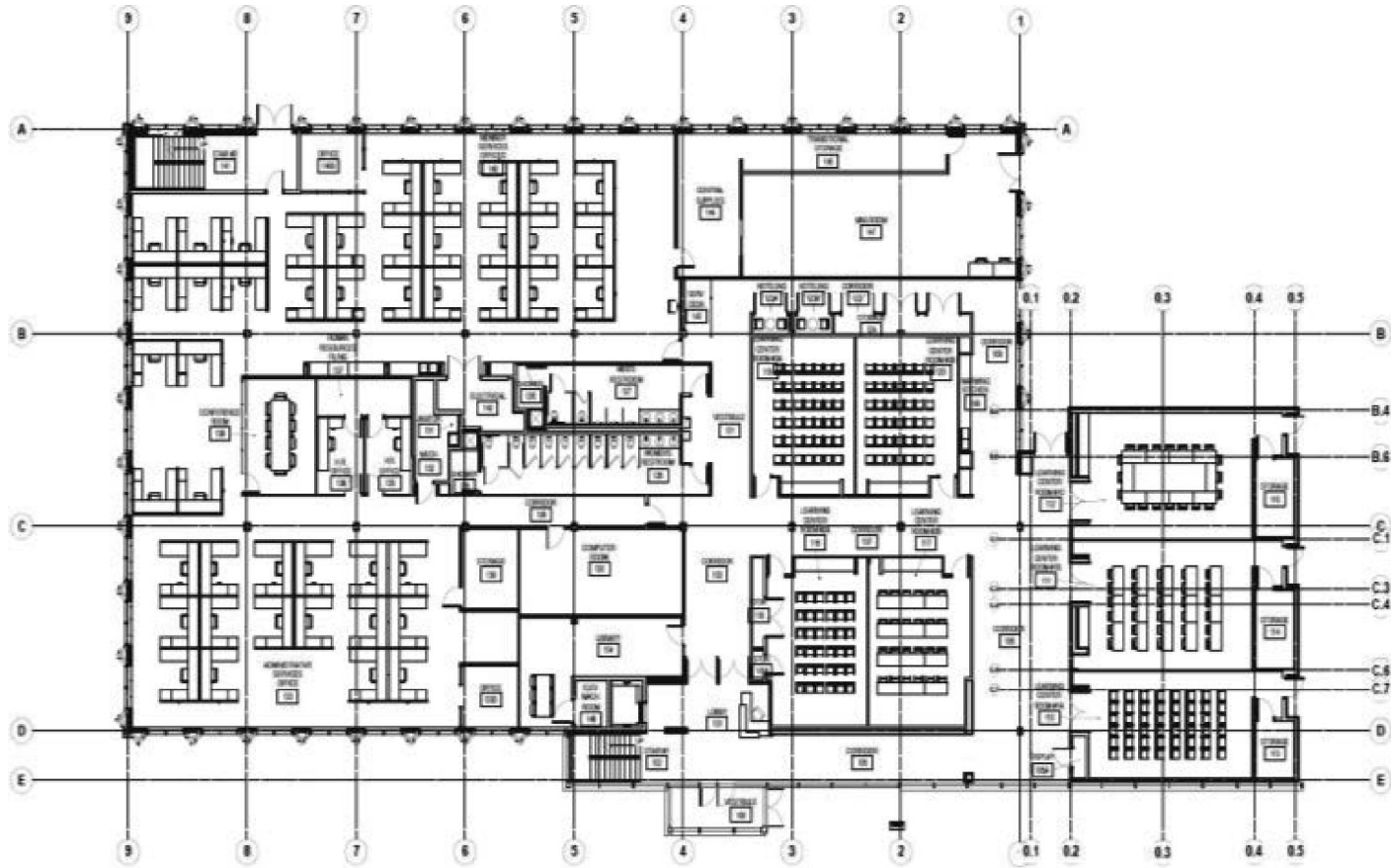


Figure 8.1 Floor plan for the first floor (not to scale).
(Source: *ASHRAE Handbook—Fundamentals* [2013], Chapter 18, Figure 20).

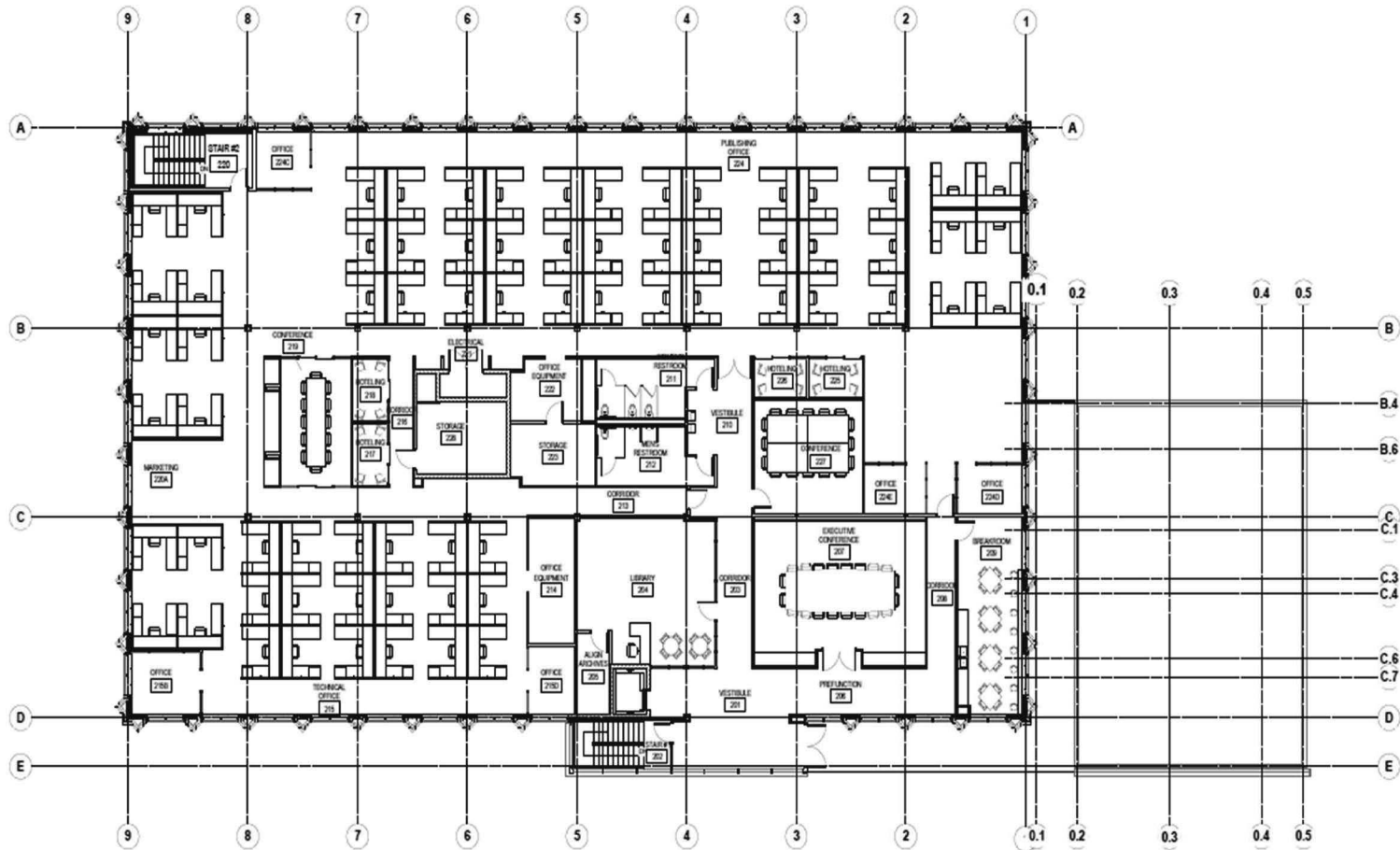


Figure 8.2 Floor plan for the second floor (not to scale).

(Source: *ASHRAE Handbook—Fundamentals* [2013], Chapter 18, Figure 21).

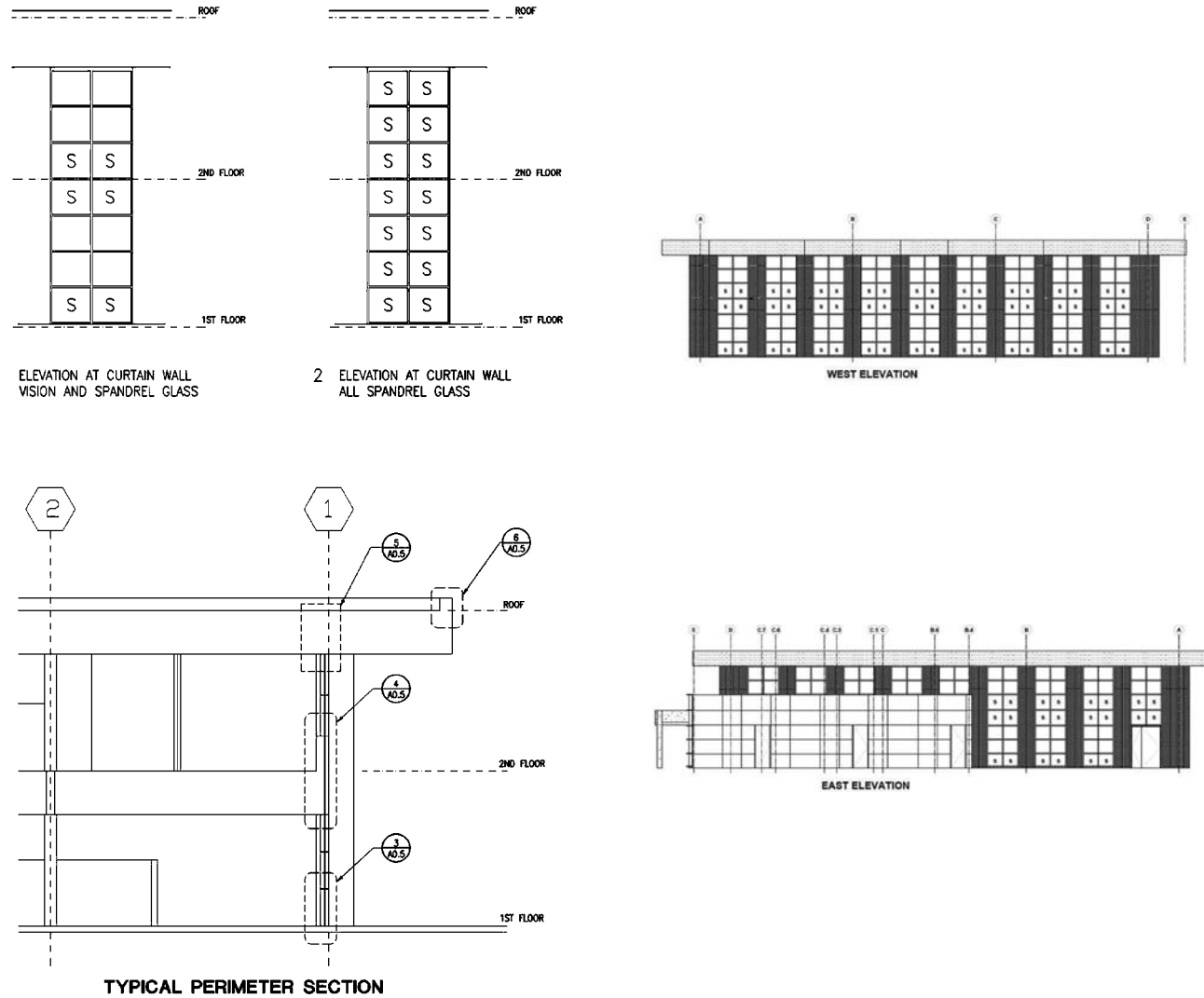


Figure 8.3 East/west elevations, elevation details, and perimeter section (not to scale).

(Source: ASHRAE Handbook—Fundamentals [2013], Chapter 18, Figure 19).

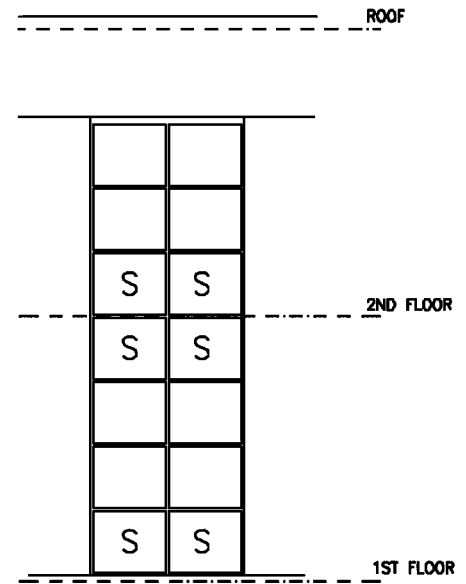
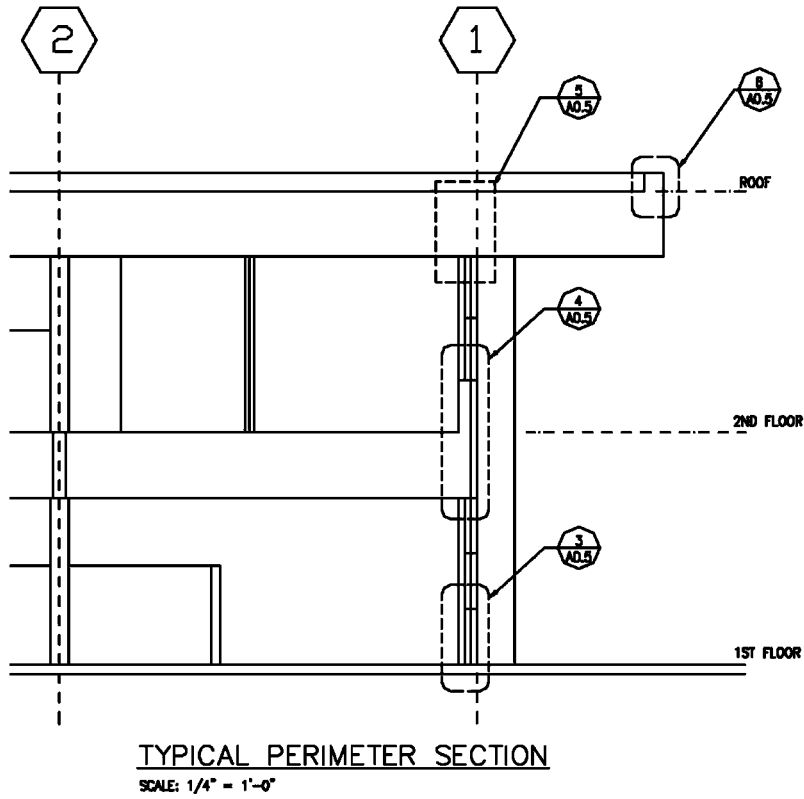


Figure 8.4 Elevation views of the building.

Load Calculation Applications Manual (SI), Second Edition

southeast façade has a glazing fraction of 25%, and the southwest façade has a glazing fraction of 32%. The acoustical tile is approximately even with the top of the second floor windows, and the space above the acoustical tile serves as a return air plenum. The return air plenum complicates the load calculation. An initial approximation is that the return air plenum removes 30% of the cooling load due to roof heat gains. In many cases, return air plenums will also remove a fraction of the lighting heat gain, but with pendant fixtures no fraction of the lighting heat gain will be removed.

Layer-by-layer descriptions of all constructions are given in Table 8.1; surface areas are summarized in Tables 8.2a and 8.2b. A few notes on how the drawings shown in Figure 8.5 are represented by the layer-by-layer descriptions in Table 8.1 may be helpful:

- *Brick-clad pilaster*—The complex geometry of the brick pilaster must be rendered in one-dimensional form before it can be analyzed with standard load calculation methods. A detailed numerical analysis could possibly be used to come up with

Table 8.1 Office Construction Data

Layer No.	Brick Clad	Spandrel	Partition	Furniture	Roof	Floor
1	F01	F01	F02	F02	F01	F03
2	M01	F09	G01	G05	F13	F16
3	M02	F04	F04	F02	I06	F05
4	I07*	I07*	G01		F03	F08
5	G01	G01	F02			M18*
6	M02	F02				F17
7	F02					F03

Notes:

1. Layer codes are taken from Table 7.5, except where marked with (*). These surfaces are as follows:
I07 is R-2.2 insulation board, otherwise equivalent to I04.
M18 is 125 mm of lightweight concrete, otherwise equivalent to M11.
2. Layers are specified from outside to inside.

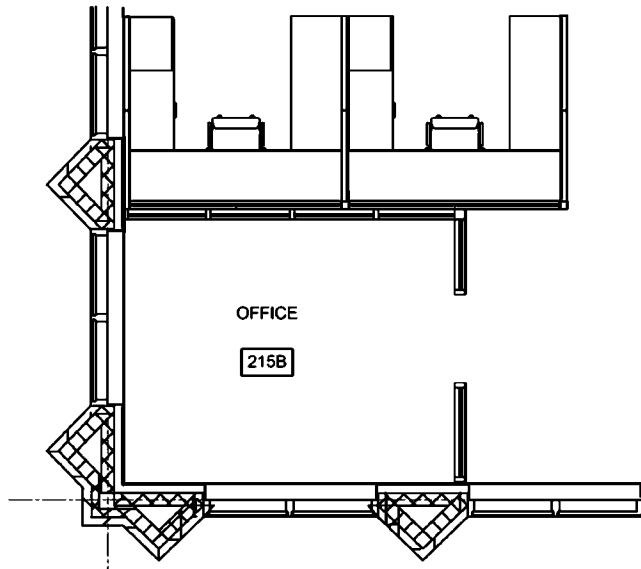


Figure 8.5 Office plan view.

Application of the RTSM—Detailed Example

Table 8.2a Surface Geometry, Absorptance, and Boundary Condition

Surface Name	Facing Direction, °	Tilt Angle, °	Area, m ²	Solar Absorptance Out	Boundary Condition
SE brick	150	90	7.8	0.9	TOS
SE spandrel	150	90	3.5	0.9	TOS
SW brick	240	90	4.4	0.9	TOS
SW spandrel	240	90	3.5	0.9	TOS
NE partition	60	90	8.4	0.9	TA
NW partition	330	90	10.9	0.9	TA
Roof	0	0	12	0.9	TOS
Floor	0	180	12	0.0	TA
Furniture	0	180	12	0.9	TA

Note:

TOS = the outside of the surface is exposed to the outside sol-air temperature

TA = the outside of the surface is exposed to another conditioned space

Table 8.2b Window Area and Optical Properties

Surface Name	Area, m ²	Normal SHGC
SE window	3.73	0.49
SW window	3.73	0.49

Table 8.2c Window and External Shading Geometry

Surface Name	Window Width, m	Window Height, m	Horizontal Overhang, m		Vertical Overhang, m	
			P _H	R _H	P _V	R _W
SE window	1.91	1.95	0.91	0.0	0.0	0.0
SW window	1.91	1.95	0.91	0.0	0.0	0.0

Note: Horizontal and vertical overhang dimensions correspond to Figure D.3 in Appendix D.

the best possible one-dimensional representation of the wall, but it is hard to imagine a situation where that would be feasible. Instead, given the expected small heat gains due to conduction through exterior walls (compared to internal heat gains and fenestration heat gains), this will be approximated as a one-dimensional wall of area equivalent to the inside area but with material layers based on the actual construction. Furthermore, the inside of the column is filled with insulation, but in an irregular shape. The insulation is rated at R-0.21 cm per inch of thickness, and an estimate of a mean thickness of around 75 mm or a little more suggests treating the insulation as being about R-1.6. Note that, when choosing between insulation layers given in Table 7.5, the thermal mass of the insulation is insignificant. Thus, choosing any insulation type that gives a unit thermal resistance of R-1.6 should be sufficient.

- *Spandrel wall*—The spandrel wall is relatively simple compared to the brick-clad pilaster, but it presents its own minor difficulties. Specifically, the placement of the batt insulation is a little unclear in the original drawings. Furthermore, the steel studs will create thermal bridges for which we might be justified in using the

Load Calculation Applications Manual (SI), Second Edition

approach described in Appendix E to account for their effect. However, considering the relatively small effect of conduction on the total cooling load and the presence of rigid board insulation that covers the studs and reduces the impact of the thermal bridges, the simple approximation shown in Table 8.1 is made. The approximation includes neglecting the impact of the thermal bridge, combining the two layers of insulation into one R-1.6 layer, and neglecting two additional air spaces that may or may not exist everywhere the spandrel glass construction is used.

- *Partition*—The partitions, which consist of gypsum board screwed to steel studs, are modeled as two layers of gypsum board separated by an air space. Since they are not exterior surfaces, their only influence is on the thermal storage of the zone.
- *Furniture*—The furniture is almost always an unknown. Even if there is some knowledge of what will be initially installed, occupants are likely to move or change it over time. Given this uncertainty, coupled with the difficulty in precisely describing even the simplest furniture and the small influence that furniture generally has on the cooling load, a simple approach is taken here. A 2.5 cm thick layer of wood with surface area equal to the floor area would be approximately equivalent to a table taking up one half of the floor area or a smaller table and chairs. (The area specified is the exposed area of the table, meaning both the top and bottom sides.)
- *Roof*—Since we are using the simple approximation that the effect of the return air plenum is simply to move 30% of the cooling load due to the roof from the zone to the return air, we will treat the return air plenum as part of the zone. Hence, the description shown in Table 8.1 does not include the air space or acoustical tile. Also, the exterior wall areas include the wall portions above the acoustical tile, in the return air plenum, which is approximately 1 m high.
- *Floor*—The floor is a carpeted 125 mm concrete slab poured on a metal deck above an air space and acoustical tile.

As discussed in Example 7.3, the geometry of the room is, from the exterior, relatively complex, with the brick-clad portion of the façade being oriented at 45° angles to the other surfaces. Noting that the brick façade will represent a fairly small part of the overall heat gains, a simple approximation of treating the brick façade as if it has a surface area corresponding to the inside surface area can be justified. Therefore, the inside areas taken from Example 7.3 will be used to represent each of the surfaces, with the exception that gross wall areas will include those parts above the acoustical tile. On the outside of the building, above the level of the acoustic tile, there is an overhang. For simplicity in this example, we have simply computed the gross outside surface areas as if the spandrel and brick extend to the roof. These areas are summarized in Tables 8.2a and 8.2b. Table 8.2a shows the surface facing directions (degrees clockwise from north), tilt angles (degrees from horizontal), surface solar absorptances, and surface boundary conditions (TOS = outside of surface is exposed to the outside sol-air temperature; TA = outside of surface is exposed to another conditioned space).

Table 8.2b summarizes the window properties and Table 8.2c summarizes the exterior shading geometry.

8.3 Office Example— RTSM

Figure 7.1 shows a flowchart for application of the RTSM. The method might broadly be divided into five steps:

1. Preliminary selection of coefficients (conduction time series factors [CTSFs], radiant time factors [RTFs], and solar heat gain coefficients [SHGC] and angle correc-

Application of the RTSM—Detailed Example

tion factors); determination of outdoor environmental conditions (hourly air temperatures, sol-air temperatures, and incident solar radiation); determination of indoor environmental conditions

2. Computation of heat gains
3. Splitting of heat gains into radiative and convective components
4. Conversion of radiative heat gains to cooling loads
5. Summation of cooling loads due to radiative and convective heat gains

Sections 8.3.1–8.3.5 discuss each of the steps in turn.

8.3.1 Selection of Coefficients and Determination of Environmental Conditions

Conduction Time Series Factors (CTSFs)

The office has three exterior construction types: brick-clad wall on the southeast and southwest façades, spandrel wall on the southeast and southwest façades, and the roof. Several different approaches for determining CTSFs were used in Example 7.1. In this case, compute the CTSFs using the spreadsheet *Example 8.1 Compute CTSF.xls* available on the online supporting files accompanying this manual. The resulting CTSFs are summarized in Table 8.3. Note that rounding the CTSFs to two or three significant digits will often result in the CTSFs not summing to one. Using three significant digits, as in Table 8.3, gives summations that are within 0.1% of one; this is equivalent to an error in the U-factor of 0.1%. This is insignificant compared to other uncertainties in the load calculation.

Radiant Time Factors (RTFs)

The RTFs for this zone were computed in Example 7.3. Two approaches, determination of RTFs from look-up tables and use of a spreadsheet to generate RTFs for the specific zone, were examined. In addition, the zone geometry was specified based on both outside areas and inside areas. As shown in the example, all approaches gave similar results. Here, we will adopt custom-generated RTFs based on the zone inside areas, as shown in Table 8.4. These are taken from the spreadsheet *Example 8.1 Compute RTF.xls*.

Solar Heat Gain Coefficients (SHGCs) and Angle Correction Factors

The windows, as described in Section 8.1, have a normal SHGC of 0.56, and the closest fenestration type in Table 3.7 is 5d. The angle correction factors are taken from Table 3.8 and are summarized in Table 8.5. We will consider the cooling load both with and without interior shading using light-colored venetian blinds. With no interior shading, the interior attenuation coefficient (IAC) is 1, and the radiative fraction for beam and diffuse solar heat gains is 100%. With light-colored venetian blinds, the IAC can be taken from Table 3.9b for glass type 5D. While heat gains may be chosen for a range of louver positions, here we are assuming the louvers positioned at 45°. In that case, $IAC_0 = 0.74$, $IAC_{60} = 0.65$, $IAC_{diff} = 0.79$ and the radiative fraction can be taken from the same table as 0.54.

Design Air Temperatures

For this example, we will use the Atlanta 5% July design conditions. Atlanta design conditions are taken from Table 4.1. Information taken from Table 4.1 includes the following:

- Latitude: 33.64°N
- Longitude: 84.43°W

Load Calculation Applications Manual (SI), Second Edition

- Peak dry-bulb temperature: 33.3°C (5% monthly cooling condition for July, which is the hottest month)
- Mean coincident wet-bulb temperature: 23.6°C
- Mean daily temperature range: 11.4°C

Knowing the peak dry-bulb temperature and mean daily temperature range, Table 4.2 can be used to determine the hourly air temperatures. Instead, Equation 4.1 is used here and the resulting air temperatures are summarized along with sol-air temperatures in Table 8.7.

The inside design air temperature is chosen to be 24°C, with a relative humidity of 50%.

Incident Solar Radiation and Sol-Air Temperatures

Table 8.3 CTSFs for Office Constructions

U-factor W/(m ² ·K)	Brick-Clad Wall	Spandrel Wall	Roof
	0.313	0.383	0.180
Hour			
0	0.022	0.141	0.081
1	0.020	0.555	0.479
2	0.018	0.236	0.306
3	0.020	0.054	0.096
4	0.026	0.012	0.027
5	0.035	0.002	0.008
6	0.045	0.001	0.002
7	0.053	0.000	0.001
8	0.059	0.000	0.000
9	0.063	0.000	0.000
10	0.063	0.000	0.000
11	0.063	0.000	0.000
12	0.061	0.000	0.000
13	0.059	0.000	0.000
14	0.056	0.000	0.000
15	0.052	0.000	0.000
16	0.048	0.000	0.000
17	0.044	0.000	0.000
18	0.041	0.000	0.000
19	0.037	0.000	0.000
20	0.034	0.000	0.000
21	0.030	0.000	0.000
22	0.027	0.000	0.000
23	0.025	0.000	0.000

Application of the RTSM—Detailed Example

Table 8.4 Radiant Time Factors for the Office

Index	Nonsolar RTFs	Solar RTFs
0	0.50	0.52
1	0.19	0.17
2	0.09	0.08
3	0.05	0.04
4	0.03	0.03
5	0.02	0.02
6	0.02	0.02
7	0.01	0.01
8	0.01	0.01
9	0.01	0.01
10	0.01	0.01
11	0.01	0.01
12	0.01	0.01
13	0.01	0.01
14	0.01	0.01
15	0.00	0.01
16	0.00	0.01
17	0.00	0.00
18	0.00	0.00
19	0.00	0.00
20	0.00	0.00
21	0.00	0.00
22	0.00	0.00
23	0.00	0.00

Table 8.5 Angle Correction Factors for Window

ID	SHGC Angle Correction Factors and Diffuse Correction Factor						
	0	40	50	60	70	80	Diffuse
5D	1.000	0.939	0.898	0.796	0.633	0.347	0.837

Outdoor air temperature is computed with Equation 4.1. Incident solar radiation and sol-air temperatures are computed using the procedures described in Appendix D, where all relevant equations are given. The spreadsheet *Example 8.1 solar.xls* is used to determine incident solar radiation, shown in Table 8.6, for the southeast-facing wall, the southwest-facing wall, and the horizontal roof. It also determines hourly air temperature, and sol-air temperatures on the same three surfaces, as shown in Table 8.7.

To determine the values in Tables 8.6 and 8.7, it is necessary to choose the following parameters in addition to those listed immediately above:

Load Calculation Applications Manual (SI), Second Edition

- Time convention: can be chosen as local time or solar time. Local time is used here. For convenience when specifying internal heat gain schedules, it is best to use local time.
- The solar absorptance affects the results in Table 8.7 only. (Table 3.3 gives typical values.) For spaces such as this, where the walls and roof have moderate amounts of insulation and where most of the cooling loads will come from fenestration and internal heat gains, the solar absorptances will have a relatively small effect on the cooling load. The solar absorptance of the roof will have the greatest effect. The roof has a low solar absorptance (0.45) but given the possibility that, over time, the roof will become soiled regardless of the roof coating, a value of 0.9 is chosen. The walls may also have slightly lower absorptances, but a value of 0.9 is chosen as a conservative estimate.
- An exterior surface conductance of $22.7 \text{ W}/(\text{m}^2\cdot\text{K})$, corresponding to summer design conditions, was selected.
- Optical depths τ_{aub} and τ_{aud} are taken from Table 4.1 as 0.440 and 2.202, respectively.
- Ground reflectance: a typical value of 0.2 is taken.

8.3.2 Computation of Heat Gains

With all of the preliminaries out of the way, we are ready to begin computing the heat gains. Most of the difficulties requiring engineering judgment are now over, and what remains is mostly straightforward calculation. First, conduction heat gains for each surface are computed, then solar heat gains from fenestration, internal heat gains, and finally, infiltration heat gains.

Conduction Heat Gain from Opaque Surfaces

The conduction heat gain from each surface is computed with Equation 7.1 as illustrated in Example 7.1. The values required to evaluate Equation 7.1 are taken from the following:

- Areas: Table 8.2
- U-factors: Table 8.3
- CTSFs: Table 8.3
- Sol-air temperatures: Table 8.7

The spreadsheet *Example 8.1 Conduction HG.xls* is used to perform the calculation. The resulting heat gains are shown in Table 8.8. A comparison of the numbers shows that the roof, because of its large area, has significantly higher heat gains than the other surfaces.

Fenestration Heat Gains

There are two types of heat gains associated with the windows—conduction heat gains and solar heat gains. Because the thin layers of glass used in windows have relatively low thermal capacitance, the conduction heat gain can be analyzed on a steady-state basis. As noted earlier, the manufacturer's data are all for center-of-glass only. Ideally, framing effects would be included; they would tend to increase heat loss under heating load conditions and increase conduction heat gain under cooling loads but decrease solar heat gains under cooling load conditions. Tables 3.6a and 3.6b give corrected U-factors for a range of glass and frame combinations. This may be used to roughly estimate the combined U-factor if manufacturer's data are not available.

For this example, the manufacturer's data are simply applied to the total window area (including the frame). Under cooling load conditions, where the solar heat gains are considerably larger than the window conduction heat gains, this approximation is expected to slightly overpredict the peak cooling load. The U-factor given by the manufacturer—

Application of the RTSM—Detailed Example

Table 8.6 Incident Solar Radiation for Office Exterior Surfaces

Incident Solar Radiation (W/m^2) for July 21, 33.64 N Latitude, 84.43 W Longitude, Time Zone: NAE Daylight Savings Time Ground Reflectance $\rho_g = 0.2$			
Local Time	SE (150°)-Facing Wall	SW (240°)-Facing Wall	Horizontal Roof
1.0	0.0	0.0	0.0
2.0	0.0	0.0	0.0
3.0	0.0	0.0	0.0
4.0	0.0	0.0	0.0
5.0	0.0	0.0	0.0
6.0	0.0	0.0	0.0
7.0	20.4	10.6	21.4
8.0	160.8	45.0	167.0
9.0	309.4	78.5	367.9
10.0	421.3	108.1	568.9
11.0	480.7	132.2	743.9
12.0	481.9	149.7	875.3
13.0	426.6	171.2	951.6
14.0	323.0	330.9	966.1
15.0	185.1	500.0	917.7
16.0	146.9	616.5	810.5
17.0	119.9	660.3	653.7
18.0	92.7	615.5	462.1
19.0	60.8	468.5	257.0
20.0	26.0	202.1	75.0
21.0	0.0	0.0	0.0
22.0	0.0	0.0	0.0
23.0	0.0	0.0	0.0
24.0	0.0	0.0	0.0

Table 8.7 Air Temperatures and Sol-Air Temperatures for Conference Room Exterior Surfaces

Air Temperatures and Sol-Air Temperature ($^{\circ}C$) for July 21, 33.65 N Latitude, 84.42 W Longitude, Time Zone: Eastern Daylight Savings Time Clearness Index: CN = 0.93; Surface Color: $\alpha/h_o = 0.04$				
Local Time	Air Temperature	SE (150°)-Facing Wall	SW (240°)-Facing Wall	Horizontal Roof
1.0	24.5	24.5	24.5	20.7
2.0	23.7	23.7	23.7	19.9
3.0	23.1	23.1	23.1	19.2
4.0	22.7	22.7	22.7	18.8

Load Calculation Applications Manual (SI), Second Edition

Table 8.7 Air Temperatures and Sol-Air Temperatures for Conference Room Exterior Surfaces (continued)

Local Time	Air Temperature	SE (150°)-Facing Wall	SW (240°)-Facing Wall	Horizontal Roof
5.0	22.4	22.4	22.4	18.5
6.0	22.0	22.0	22.0	18.1
7.0	21.9	22.7	22.3	18.9
8.0	22.3	28.6	24.0	25.0
9.0	23.3	35.6	26.5	34.0
10.0	25.5	42.2	29.8	44.1
11.0	27.6	46.6	32.8	53.2
12.0	29.5	48.6	35.4	60.3
13.0	31.0	47.9	37.8	64.9
14.0	32.1	44.9	45.2	66.5
15.0	32.9	40.3	52.8	65.4
16.0	33.4	39.2	57.8	61.6
17.0	33.2	37.9	59.4	55.2
18.0	32.4	36.0	56.8	46.8
19.0	31.5	33.9	50.0	37.8
20.0	30.1	31.2	38.1	29.2
21.0	28.4	28.4	28.4	24.6
22.0	27.3	27.3	27.3	23.4
23.0	26.3	26.3	26.3	22.4
24.0	25.3	25.3	25.3	21.4

Table 8.8 Conduction Heat Gains for Opaque Exterior Surfaces, W

Hour	SE Brick	SE Spandrel	SW Brick	SW Spandrel	Roof
1	28	2	18	2	-4
2	28	1	19	1	-6
3	27	0	19	0	-8
4	26	-1	19	-1	-9
5	25	-2	19	-2	-11
6	24	-2	18	-2	-11
7	23	-2	17	-2	-12
8	21	-1	16	-2	-11
9	19	5	15	0	-2
10	17	13	14	3	13
11	16	22	13	7	32
12	14	28	11	11	52
13	13	31	10	14	69
14	13	31	9	19	81
15	13	28	9	27	88

Application of the RTSM—Detailed Example

Table 8.8 Conduction Heat Gains for Opaque Exterior Surfaces, W (continued)

Hour	SE Brick	SE Spandrel	SW Brick	SW Spandrel	Roof
16	14	24	8	36	89
17	16	21	8	43	84
18	18	19	8	46	73
19	20	17	9	43	58
20	22	14	10	36	40
21	24	10	12	23	22
22	25	7	13	11	9
23	26	5	15	6	2
24	27	3	17	4	-2

1.82 W/(m²·K)—coupled with the window areas given in Table 8.2b, the outdoor air temperatures given in Table 8.7, and an inside room air temperature of 24°C are used with Equation 7.3 to determine the window conduction heat gains given in Table 8.9.

The solar heat gains are computed with the procedure illustrated in Example 7.2, although they are for a window of different size and different shading geometry. Table 8.10a shows the solar angle calculations and incident beam and diffuse radiation for daylight hours. The apparent solar time, hour angle, solar altitude angle, solar azimuth angle, surface solar azimuth angle, and incident angle are computed with the referenced equations from Appendix D. The incident beam and diffuse radiation values are calculated with the ASHRAE clear-sky model, covered in Section D.2 of Appendix D, with the same assumptions as discussed in conjunction with Table 8.6.

Table 8.10b gives the intermediate results for the exterior shading calculations. Up to the point of finding the sunlit and shaded areas of the window, the procedure follows Appendix D, using the referenced equations. The beam SHGC is determined by interpolating the angle correction factors in Table 8.5 for the corresponding incidence angles given in Table 8.10a, then multiplying by the normal SHGC taken from Table 8.2b. Then, the beam solar heat gains (next-to-last column) are calculated by multiplying the sunlit area by the incident beam radiation and the interpolated SHGC, as described in Section 7.5. The diffuse solar heat gains (last column) are calculated by multiplying the total window area by the incident diffuse radiation and the diffuse SHGC given in Table 8.6. Without interior shading, the last two columns of Table 8.10b give the beam and diffuse solar heat gains.

The calculations are repeated for the southeast-facing windows; the results are given in Tables 8.11a and 8.11b.

Internal Heat Gains

Internal heat gains are typically specified for each hour as a combination of a peak heat gain rate and an hourly, fractional schedule. First, a reasonable estimate of the maximum number of people for the office must be made. We will assume that there is one person with a sensible heat gain of 75 W and a latent heat gain of 55 W. This corresponds to moderately active office work adjusted for a typical male/female ratio, as shown in Table 6.1. The peak occupancy rate (in this case, one person) is then adjusted on an hour-by-hour basis, according to the schedule shown in Table 8.12. For purposes of making the load calculation, some reasonable assumptions must be made about the schedule of operation. Here, we have assumed that the building will be fully in operation between about 7:30 a.m. and 5:30 p.m. and, as a result, the people, lighting, and equipment fractions are set to be 1 for hours 9–17 and

Load Calculation Applications Manual (SI), Second Edition

Table 8.9 Fenestration Conduction Heat Gains

Local Time	SE Windows Conduction Heat Gain, W	SW Windows Conduction Heat Gain, W	Total Windows Conduction Heat Gain, W
1	5	5	10
2	-2	-2	-5
3	-9	-9	-18
4	-16	-16	-31
5	-21	-21	-42
6	-24	-24	-49
7	-25	-25	-49
8	-21	-21	-42
9	-13	-13	-26
10	1	1	2
11	19	19	39
12	41	41	81
13	64	64	128
14	84	84	168
15	99	99	198
16	108	108	216
17	110	110	220
18	104	104	209
19	93	93	186
20	77	77	155
21	59	59	119
22	43	43	85
23	28	28	56
24	15	15	30

Table 8.10a Solar Heat Gain Calculations for the Southwest-Facing Windows, Part 1

Local Time	Apparent Solar Time (Eq. D.5)	Hour Angle, ° (Eq. D.6)	Solar Altitude Angle, ° (Eq. D.9)	Solar Azimuth Angle, ° (Eq. D.10)	Surface Solar Azimuth Angle, ° (Eq. D.13)	Incident Angle, ° (Eq. D.27)	Incident Beam Radiation, W/m ² (Eq. D.21)	Incident Diffuse Radiation, W/m ² (Eq. D.24 and D.26)
7	5.27	-100.9	2.7	66.9	-173.1	172.6	0.0	10.4
8	6.27	-85.9	14.5	74.6	-165.4	159.5	0.0	45.1
9	7.27	-70.9	26.7	82.0	-158.0	145.9	0.0	78.5
10	8.27	-55.9	39.2	89.8	-150.2	132.3	0.0	108.2
11	9.27	-40.9	51.6	99.1	-140.9	118.8	0.0	132.2
12	10.27	-25.9	63.6	112.9	-127.1	105.6	0.0	149.8
13	11.27	-10.9	73.8	140.5	-99.5	92.6	0.0	171.3
14	12.27	4.1	76.5	196.5	-43.5	80.3	142.9	188.0
15	13.27	19.1	68.7	237.2	-2.8	68.7	302.5	197.5
16	14.27	34.1	57.2	255.4	15.4	58.6	420.2	196.2
17	15.27	49.1	44.9	266.2	26.2	50.6	479.2	181.1
18	16.27	64.1	32.4	274.5	34.5	45.9	465.3	149.8
19	17.27	79.1	20.1	282.0	42.0	45.7	364.4	104.1
20	18.27	94.1	8.1	289.5	49.5	50.0	154.9	47.0

Application of the RTSM—Detailed Example

Table 8.10b Solar Heat Gain Calculations for the Southwest-Facing Windows, Part 2

Local Time	Profile Angle, ° (Eq. D.28)	Shadow Height, m (Eq. D.29)	Sunlit Area, m ² (Eq. D.31)	Shaded Area, m ² (Eq. D.32)	Beam SHGC (Normal SHGC with Angle Correction from Table 8.5)	Beam SHG (without Internal Shading), W (Eq. 7.4a)	Diffuse SHG (without Internal Shading), W (Eq. 7.4b)
7			0.0	3.7		0	16
8			0.0	3.7		0	69
9			0.0	3.7		0	120
10			0.0	3.7		0	165
11			0.0	3.7		0	202
12			0.0	3.7		0	229
13			0.0	3.7		0	262
14	80.1	5.2	0.0	3.7	0.308	0	287
15	68.7	2.3	0.0	3.7	0.320	0	302
16	58.2	1.5	0.9	2.8	0.397	154	300
17	48.0	1.0	1.8	1.9	0.437	376	277
18	37.6	0.7	2.4	1.3	0.448	497	229
19	26.2	0.5	2.9	0.9	0.449	469	159
20	12.3	0.2	3.3	0.4	0.440	228	72

Table 8.11a Solar Heat Gain Calculations for the Southeast-Facing Windows, Part 1

Local Time	Apparent Solar Time (Eq. D.2)	Hour Angle, ° (Eq. D.3)	Solar Altitude Angle, ° (Eq. D.4)	Solar Azimuth Angle, ° (Eq. D.5)	Surface Solar Azimuth Angle, ° (Eq. D.6)	Incident Angle, ° (Eq. D.7)	Incident Beam Radiation, W/m ² (Eq. D.9)	Incident Diffuse Radiation, W/m ² (Eq. D.10 and D.13)
7	5.27	-100.9	2.7	66.9	-83.1	83.1	6.9	13.5
8	6.27	-85.9	14.5	74.6	-75.4	75.9	101.7	59.2
9	7.27	-70.9	26.7	82.0	-68.0	70.4	204.9	104.6
10	8.27	-55.9	39.2	89.8	-60.2	67.4	277.5	143.8
11	9.27	-40.9	51.6	99.1	-50.9	66.9	307.5	173.2
12	10.27	-25.9	63.6	112.9	-37.1	69.2	291.6	190.3
13	11.27	-10.9	73.8	140.5	-9.5	74.0	231.9	194.6
14	12.27	4.1	76.5	196.5	46.5	80.8	135.8	187.3
15	13.27	19.1	68.7	237.2	87.2	89.0	14.6	170.5
16	14.27	34.1	57.2	255.4	105.4	98.3	0.0	146.9
17	15.27	49.1	44.9	266.2	116.2	108.3	0.0	119.9
18	16.27	64.1	32.4	274.5	124.5	118.6	0.0	92.7
19	17.27	79.1	20.1	282.0	132.0	128.9	0.0	60.8
20	18.27	94.1	8.1	289.5	139.5	138.8	0.0	26.0

0.5 for hours 8 and 18. During the remainder of the day, it is assumed that there will be no occupants present but that lighting and equipment will have about 10% of their peak heat gain from some lights and equipment remaining on and/or being in standby condition.

Load Calculation Applications Manual (SI), Second Edition

Table 8.11b Solar Heat Gain Calculations for the Southeast-Facing Windows, Part 2

Local Time	Profile Angle, ° (Eq. D.14)	Shadow Height, m (Eq. D.15)	Sunlit Area, m ² (Eq. D.17)	Shaded Area, m ² (Eq. D.18)	Beam SHGC (Normal SHGC with Angle Correction from Table 8.5)	Beam SHG (without Internal Shading), W (Eq. 7.4a)	Diffuse SHG (without Internal Shading), W (Eq. 7.4b)
7	21.5	0.4	3.0	0.7	0.285	6	21
8	45.7	0.9	1.9	1.8	0.228	45	91
9	53.3	1.2	1.4	2.3	0.304	87	160
10	58.6	1.5	0.9	2.9	0.331	80	220
11	63.4	1.8	0.2	3.5	0.335	25	265
12	68.4	2.3	0.0	3.7	0.316	0	291
13	74.0	3.2	0.0	3.7	0.254	0	298
14	80.6	5.5	0.0	3.7	0.304	0	286
15	88.9	48.4	0.0	3.7	0.238	0	261
16			0.0	3.7	0.000	0	225
17			0.0	3.7	0.000	0	183
18			0.0	3.7	0.000	0	142
19			0.0	3.7	0.000	0	93
20			0.0	3.7	0.000	0	40

Table 8.12 Internal Heat Gain Schedules

Hour	People	Lighting	Equipment
1	0.0	0.1	0.0
2	0.0	0.1	0.1
3	0.0	0.1	0.1
4	0.0	0.1	0.1
5	0.0	0.1	0.1
6	0.0	0.1	0.1
7	0.0	0.1	0.1
8	0.5	0.5	0.5
9	1.0	1.0	1.0
10	1.0	1.0	1.0
11	1.0	1.0	1.0
12	1.0	1.0	1.0
13	1.0	1.0	1.0
14	1.0	1.0	1.0
15	1.0	1.0	1.0
16	1.0	1.0	1.0
17	1.0	1.0	1.0
18	0.5	0.5	0.5
19	0.0	0.1	0.1
20	0.0	0.1	0.1
21	0.0	0.1	0.1
22	0.0	0.1	0.1
23	0.0	0.1	0.1
24	0.0	0.1	0.1

Application of the RTSM—Detailed Example

Lighting heat gain has been set at 110 W, based on the specified lighting fixture. As discussed above, an equipment heat gain of 130 W, based on a desktop computer, flat-panel monitor, and multifunction personal printer has been determined. We have assumed no equipment latent heat gain, as would be expected for office equipment. Like occupant heat gains, the peak values are modified by the fractional schedules given in Table 8.12. A single occupant is expected for this office. Multiplying the peak heat gains by the fractional schedules in Table 8.12 gives the hourly internal heat gains shown in Table 8.13.

Infiltration Heat Gains

An infiltration rate of 12.7 L/s has already been determined. Then, the sensible heat gain is determined with Equation 5.4, and the latent heat gain is determined with Equation 5.5. The resulting heat gains are summarized in Table 8.14. For purposes of determining the latent heat gain, the indoor design condition of 24°C, 50% relative humidity corresponds to a humidity ratio of 0.0096 kg_w/kg_a. The outside humidity ratio is calculated for each hour, based on the hourly dry-bulb and wet-bulb temperatures shown in the table. For both states, the humidity ratios have been computed based on barometric pressure (97.62 kPa) taken from Table 4.1.

Summary

Table 8.15 summarizes the sensible heat gains presented in Tables 8.8–8.13 for the initial case of no interior shading (venetian blinds) on the windows. The wall conduction is simply the sum of the conduction heat gains for the four walls presented in Table 8.8. The roof conduction heat gain comes from Table 8.8 but is only the 70% presumed to reach the space. (The other 30% is presumed to be transferred directly to the return air.) The window conduction heat gain comes from Table 8.9. The window beam solar heat gain and diffuse solar heat gain are found from adding the last two columns of Tables 8.10b and 8.11b. The people and equipment heat gains come directly from Table 8.13. The lighting heat gains in Table 8.13 represent the total heat gain to the space and the return air plenum. In Table 8.15, the values from Table 8.13 have been multiplied by the fraction going to the space, 100% for pendant-type lighting. The infiltration heat gains come from Table 8.14.

Table 8.16 summarizes the latent heat gains from Tables 8.13 and 8.14. Because the latent heat gains are all assumed to be met by the cooling system during the hour in which they occur, these are equivalent to the latent cooling loads.

8.3.3 Splitting of Sensible Heat Gains into Radiative and Convective Components

Once all of the sensible heat gains have been determined, the next step in the RTSM is to split them into radiative and convective components. The radiative fractions for each component are as follows:

- Wall conduction: 46%, from Table 7.10
- Roof conduction: 60%, from Table 7.10
- Window conduction: 46%, from Table 7.10

Window beam and diffuse solar: 100%, from Table 7.10 (for windows without interior shading. For the case with light-colored venetian blinds, the radiative fraction will be 54%.)

- People: 60%, from Table 7.10 (Table 6.1 covers a range of conditions.)
- Office equipment: 15%. It is expected that the equipment will be predominantly fan-cooled (computers and video projector). However, flat-panel display monitors will not be fan-cooled, so the value of 15% represents an intermediate value between the two options (10% radiative for fan-cooled, 30% radiative for non-fan-cooled, as shown in Table 7.10).

Load Calculation Applications Manual (SI), Second Edition

Table 8.13 Internal Heat Gains, W

Hour	People (Sensible)	Lighting	Equipment	People (Latent)
1	0	11	13	0
2	0	11	13	0
3	0	11	13	0
4	0	11	13	0
5	0	11	13	0
6	0	11	13	0
7	0	11	13	0
8	75	55	65	55
9	150	110	130	110
10	150	110	130	110
11	150	110	130	110
12	150	110	130	110
13	150	110	130	110
14	150	110	130	110
15	150	110	130	110
16	150	110	130	110
17	150	110	130	110
18	75	55	65	55
19	0	11	13	0
20	0	11	13	0
21	0	11	13	0
22	0	11	13	0
23	0	11	13	0
24	0	11	13	0

Table 8.14 Infiltration Heat Gains

Hour	Outdoor Air Temperature, °C	Outdoor Air Wet-bulb Temperature, °C	Sensible Heat Gain, W (Eq. 5.4)	Latent Heat Gain, W (Eqn. 5.5)
1	24.4	14.6	7	-111
2	23.8	14.0	-3	-128
3	23.2	13.4	-12	-142
4	22.7	12.9	-21	-156
5	22.2	12.4	-27	-166
6	22.0	12.2	-32	-173
7	21.9	12.1	-32	-174
8	22.3	12.5	-27	-166
9	22.9	13.1	-17	-150
10	24.1	14.3	1	-120
11	25.6	15.8	26	-78
12	27.4	17.6	54	-23
13	29.4	19.6	84	42
14	31.1	21.3	111	107

Application of the RTSM—Detailed Example

Table 8.14 Infiltration Heat Gains

Hour	Outdoor Air Temperature, °C	Outdoor Air Wet-bulb Temperature, °C	Sensible Heat Gain, W (Eq. 5.4)	Latent Heat Gain, W (Eqn. 5.5)
15	32.3	22.5	130	158
16	33.1	23.3	143	192
17	33.3	23.5	145	198
18	32.8	23.0	137	177
19	31.9	22.1	123	138
20	30.5	20.7	102	85
21	29.0	19.2	78	29
22	27.6	17.8	56	-18
23	26.4	16.6	37	-56
24	25.3	15.5	20	-88

Table 8.15 Summary of Sensible Heat Gains to Room, Without Interior Shading, W

Hour	Wall Conduction	Roof Conduction (Space Fraction Only)	Window Conduction	Window Beam Solar	Window Diffuse Solar	People (Sensible)	Equipment (Sensible)	Lighting (Space Fraction Only)	Infiltration (Sensible)
1	50	-3	10	0	0	0	13	11	7
2	49	-4	-5	0	0	0	13	11	-3
3	47	-6	-18	0	0	0	13	11	-12
4	44	-7	-31	0	0	0	13	11	-21
5	41	-7	-42	0	0	0	13	11	-27
6	38	-8	-49	0	0	0	13	11	-32
7	35	-8	-49	6	37	0	13	11	-32
8	34	-7	-42	45	159	38	65	55	-27
9	39	-2	-26	87	280	75	130	110	-17
10	48	9	2	80	385	75	130	110	1
11	57	23	39	25	467	75	130	110	26
12	65	36	81	0	520	75	130	110	54
13	70	48	128	0	560	75	130	110	84
14	73	57	168	0	574	75	130	110	111
15	77	61	198	0	563	75	130	110	130
16	82	62	216	154	525	75	130	110	143
17	88	59	220	376	460	75	130	110	145
18	91	51	209	497	371	38	65	55	137
19	89	40	186	469	252	0	13	11	123
20	81	28	155	228	112	0	13	11	102
21	68	15	119	0	0	0	13	11	78
22	57	6	85	0	0	0	13	11	56
23	53	1	56	0	0	0	13	11	37
24	51	-1	30	0	0	0	13	11	20

Load Calculation Applications Manual (SI), Second Edition

Table 8.16 Latent Heat Gains and Cooling Loads, W

Hour	People	Infiltration	Total Latent
1	0	-111	-111
2	0	-128	-128
3	0	-142	-142
4	0	-156	-156
5	0	-166	-166
6	0	-173	-173
7	0	-174	-174
8	28	-166	-138
9	55	-150	-95
10	55	-120	-65
11	55	-78	-23
12	55	-23	32
13	55	42	97
14	55	107	162
15	55	158	213
16	55	192	247
17	55	198	253
18	28	177	205
19	0	138	138
20	0	85	85
21	0	29	29
22	0	-18	-18
23	0	-56	-56
24	0	-88	-88

- Lighting: 57% for pendant fixtures (non-in-ceiling fluorescent luminaire from Table 6.3). This is 57% of the space fraction, which here is 100% of the lighting heat gain.
- Infiltration: 0%, from Table 7.10

Applying these radiative fractions to the heat gains given in Table 8.15 yields the values given in Table 8.17. The rest of the heat gains are convective and summarized in Table 8.18

8.3.4 Conversion of Radiative Heat Gains to Cooling Loads

The next step in the RTSM is to convert the radiative heat gains into cooling loads by application of Equation 7.5 with the appropriate set of RTFs from Table 8.4. In short, the nonsolar RTFs are applied to every heat gain type except beam solar radiation. This includes diffuse solar heat gains. The solar RTFs are applied only to the beam solar radiation heat gain. The resulting cooling loads from the radiative heat gains are given in Table 8.19.

8.3.5 Summation of Cooling Loads

Now that the radiative heat gains have been converted to cooling loads, the cooling loads for each component can be determined by adding the convective heat gains, which are equivalent to the convective portion of the cooling loads, to the radiative

Application of the RTSM—Detailed Example

Table 8.17 Radiative Components of the Heat Gains, W

Hour	Wall Conduction	Roof Conduction (Space Fraction Only)	Window Conduction	Window Beam Solar	Window Diffuse Solar	People (Sensible)	Equipment (Sensible)	Lighting (Space Fraction Only)	Infiltration (Sensible)
1	24	-2	5	0	0	0	2	6	0
2	23	-3	-2	0	0	0	2	6	0
3	23	-3	-8	0	0	0	2	6	0
4	22	-4	-14	0	0	0	2	6	0
5	21	-4	-19	0	0	0	2	6	0
6	20	-5	-22	0	0	0	2	6	0
7	19	-5	-23	6	37	0	2	6	0
8	20	-4	-19	45	159	23	10	31	0
9	22	-1	-12	87	280	45	20	63	0
10	26	5	1	80	385	45	20	63	0
11	31	14	18	25	467	45	20	63	0
12	35	22	37	0	520	45	20	63	0
13	38	29	59	0	560	45	20	63	0
14	40	34	77	0	574	45	20	63	0
15	42	37	91	0	563	45	20	63	0
16	45	37	100	154	525	45	20	63	0
17	48	35	101	376	460	45	20	63	0
18	50	31	96	497	371	23	10	31	0
19	50	24	86	469	252	0	2	6	0
20	47	17	71	228	112	0	2	6	0
21	41	9	55	0	0	0	2	6	0
22	36	4	39	0	0	0	2	6	0
23	35	1	26	0	0	0	2	6	0
24	35	-1	14	0	0	0	2	6	0

portion of the cooling loads. Once the cooling loads from radiative heat gains are added to the cooling loads from convective heat gains for each component, the resulting sensible cooling loads are given in Table 8.20.

In addition to the sensible cooling loads on the room, there are the latent cooling loads, previously summarized in Table 8.16, and the heat gains to the return air plenum, which are assumed to be instantaneous. These heat gains include 30% of the roof heat gains and 55% of the lighting heat gains and are summarized in the first two columns of Table 8.21. The third column gives the total presumed heat gains to the return air. The fourth column gives the system sensible cooling load, which is the room sensible cooling load from Table 8.20 plus the heat gains to the return air. This represents the load on the system from this room. The room sensible cooling load in Table 8.20 would be used to determine the required airflow at a given supply temperature to keep the room at the design temperature, 24°C. The system sensible cooling load in Table 8.21 would be used to determine the required coil capacity.

Load Calculation Applications Manual (SI), Second Edition

Table 8.18 Convective Components of the Heat Gains, W

Hour	Wall Conduction	Roof Conduction (Space Fraction Only)	Window Conduction	Window Beam Solar	Window Diffuse Solar	People (Sensible)	Equipment (Sensible)	Lighting (Space Fraction Only)	Infiltration (Sensible)
1	28	-1	6	0	0	0	11	5	7
2	27	-2	-3	0	0	0	11	5	-3
3	27	-2	-10	0	0	0	11	5	-12
4	26	-3	-17	0	0	0	11	5	-21
5	25	-3	-22	0	0	0	11	5	-27
6	24	-3	-26	0	0	0	11	5	-32
7	23	-3	-27	0	0	0	11	5	-32
8	23	-3	-22	0	0	15	55	24	-27
9	26	-1	-14	0	0	30	111	47	-17
10	31	4	1	0	0	30	111	47	1
11	37	9	21	0	0	30	111	47	26
12	41	15	44	0	0	30	111	47	54
13	45	19	69	0	0	30	111	47	84
14	47	23	91	0	0	30	111	47	111
15	50	25	107	0	0	30	111	47	130
16	53	25	117	0	0	30	111	47	143
17	57	23	119	0	0	30	111	47	145
18	59	20	113	0	0	15	55	24	137
19	58	16	101	0	0	0	11	5	123
20	55	11	84	0	0	0	11	5	102
21	48	6	64	0	0	0	11	5	78
22	43	2	46	0	0	0	11	5	56
23	41	1	30	0	0	0	11	5	37
24	41	0	16	0	0	0	11	5	20

8.4 RTSM Calculation with Light-Colored Venetian Blinds

Section 8.3 carried the office-cooling load calculation from start to finish for the office without any interior shading of the windows. In this section, the changes in the calculation procedure and results will be briefly discussed.

First, with venetian blinds some assumption must be made regarding their position; here they are assumed to be oriented at 45°. Then the interior attenuation coefficients (IAC) can be taken from Table 3.9b (value varies) and the radiative fraction is 0.54. From Table 3.9b, in the glazing type 5D column, $IAC_0 = 0.74$, $IAC_{60} = 0.65$, and $IAC_{diff} = 0.79$. The IAC for the beam radiation is computed each hour with Equation 3.2; it varies with solar position and the resulting profile angle.

With IAC values determined, the beam and diffuse solar heat gains given in the last two columns of Tables 8.10b and 8.11b are multiplied by the IAC, giving the values shown in Table 8.22. The beam and diffuse solar heat gains are added for both windows to get the total heat gains shown in the last two columns of Table 8.22.

Application of the RTSM—Detailed Example

Table 8.19 Radiative Components of the Cooling Load, W

Hour	Wall Conduction	Roof Conduction	Window Conduction	Window Beam Solar	Window Diffuse Solar	People (Sensible)	Equipment (Sensible)	Lighting (Space Fraction Only)
1	30	2	19	28	50	3	3	10
2	28	0	10	24	44	3	3	10
3	26	-1	1	21	40	2	3	9
4	25	-2	-7	19	36	2	3	9
5	24	-3	-13	17	32	2	3	9
6	23	-3	-17	15	29	2	3	8
7	22	-4	-18	17	45	2	3	8
8	22	-3	-15	37	112	13	6	21
9	23	0	-8	64	197	28	13	41
10	25	4	4	70	281	34	15	49
11	28	9	12	45	355	37	16	53
12	32	15	25	24	412	39	17	55
13	34	21	41	16	458	40	18	56
14	36	26	57	12	486	41	18	57
15	39	30	70	10	495	41	18	58
16	41	32	81	89	483	42	18	59
17	44	32	86	229	450	42	18	59
18	46	30	87	341	395	31	14	44
19	47	26	82	371	316	16	8	25
20	46	21	74	263	217	10	6	18
21	43	15	63	115	123	7	5	15
22	39	10	51	66	87	5	4	13
23	37	6	39	44	69	4	4	12
24	36	4	29	34	58	4	3	11

The total solar heat gains shown in Table 8.22 must be split into radiative and convective components. A key difference, as can be seen in Table 7.10, is that the radiative fraction for solar heat gains is not 100% when interior shading is present. Rather, radiative fractions are given for each combination of fenestration and shading in Tables 3.9a–3.9g. For this specific case, a value of 0.54 is given by Table 3.9b. Applying this fraction to both the beam and diffuse solar heat gains in Table 8.22 gives the radiative and convective components shown in Table 8.23.

Next, the radiative heat gains are converted to the radiative components of the cooling loads (second and third columns of Table 8.24), and the radiative and convective portions of the cooling loads are added together (fourth and fifth columns of Table 8.24). Finally, all of the cooling load components are summed to get the zone-sensible cooling loads, as shown in the sixth column of Table 8.24. Note that all other cooling load components are as shown in Tables 8.19 and 8.20.

Load Calculation Applications Manual (SI), Second Edition

**Table 8.20 Component-by-Component Breakdown
of the Room Cooling Load, W (Without Interior Shading)**

Hour	Wall Conduction	Roof Conduction	Window Conduction	Window Beam Solar	Window Diffuse Solar	People (Sensible)	Equipment (Sensible)	Lighting (Space Fraction Only)	Infiltration	Total
1	58	0	25	28	50	3	14	15	7	200
2	55	-2	8	24	44	3	14	14	-3	158
3	53	-3	-9	21	40	2	14	14	-12	120
4	51	-5	-24	19	36	2	14	14	-21	86
5	49	-6	-35	17	32	2	14	13	-27	59
6	47	-6	-43	15	29	2	14	13	-32	38
7	45	-7	-44	17	45	2	14	13	-32	51
8	44	-6	-37	37	112	28	62	44	-27	256
9	49	0	-22	64	197	58	123	88	-17	540
10	56	7	5	70	281	64	126	96	1	708
11	65	18	33	45	355	67	127	100	26	836
12	73	29	69	24	412	69	128	102	54	960
13	79	40	110	16	458	70	128	104	84	1088
14	83	49	148	12	486	71	128	105	111	1192
15	88	54	177	10	495	71	129	105	130	1260
16	94	57	197	89	483	72	129	106	143	1369
17	100	55	205	229	450	72	129	106	145	1491
18	105	50	199	341	395	46	69	67	137	1410
19	105	42	183	371	316	16	19	30	123	1205
20	100	32	158	263	217	10	17	23	102	921
21	91	21	127	115	123	7	16	19	78	597
22	82	13	97	66	87	5	15	17	56	437
23	78	7	70	44	69	4	15	16	37	340
24	77	3	45	34	58	4	14	16	20	270

Comparison of the solar heat gains between the case without blinds (Table 8.15) and the case with blinds (Table 8.22) shows a reduction in diffuse heat gains of 21% and reductions in beam heat gains from 28% to 35%. However, comparison of the cooling loads between the two cases does not show a precisely corresponding reduction. For example, the peak cooling load due to beam solar heat gains is 371 W at hour 19 without blinds and 290 W at hour 19 with blinds—a 22% reduction. Physically speaking, this is a consequence of the blinds absorbing the incoming solar radiation and releasing much of it by convection to the room air. This portion of the solar radiation becomes part of the cooling load instantaneously. From the viewpoint of the RTSM calculation, this is accomplished by choosing a lower radiative fraction when the blinds are present. In either case, because the window cooling loads are only about half of the total cooling loads at the peak hour, the overall effect on the zone-sensible cooling load is relatively small (about 117 W at hour 17, as shown in Figure 8.6).

Application of the RTSM—Detailed Example

**Table 8.21 Return Air Cooling Load and System Cooling Load, W
(without Interior Shading)**

Hour	Lighting to Return Air	Roof Heat Gain to Return Air	Total Heat Gain to Return Air	System Sensible Cooling Load
1	0	-1	-1	199
2	0	-2	-2	156
3	0	-2	-2	117
4	0	-3	-3	83
5	0	-3	-3	56
6	0	-3	-3	34
7	0	-4	-4	47
8	0	-3	-3	253
9	0	-1	-1	539
10	0	4	4	712
11	0	10	10	846
12	0	16	16	975
13	0	21	21	1109
14	0	24	24	1216
15	0	26	26	1286
16	0	27	27	1395
17	0	25	25	1516
18	0	22	22	1432
19	0	17	17	1222
20	0	12	12	933
21	0	7	7	604
22	0	3	3	440
23	0	1	1	340
24	0	-1	-1	269

8.5 RTSM Calculation with Separate Treatment of Return Air Plenum

The office has a return air plenum above the suspended acoustic-tile ceiling. In Sections 8.3 and 8.4, this was addressed by treating the entire space as one thermal zone, with an assumption that 30% of the roof heat gains were transferred directly to the return air without becoming part of the room cooling load. These heat gains do, however, show up as part of the system cooling load. The 30% assumption is fairly arbitrary, and it may be checked with an alternative approach. As discussed in Appendix F, uncontrolled spaces may be analyzed with a quasi-steady-state heat balance. This approach is relatively simple, but its accuracy decreases as the thermal mass in the uncontrolled space envelope increases. In this particular case, there is relatively little thermal mass in either the roof or floor of the return air plenum, and therefore the quasi-steady-state approach is quite adequate.

In this section, a quasi-steady-state heat balance on the return air plenum will be used to estimate the hourly space air temperature in the return air plenum and then to find the resulting heat gain to the occupied space. This example will use windows without interior shading (i.e., the room as described in Section 8.3 will serve as the

Load Calculation Applications Manual (SI), Second Edition

Table 8.22 Solar Heat Gains with Light-Colored Venetian Blinds

Local Time	SW Windows		SE Windows		Total	
	Beam SHG (with Interior Shading), W	Diffuse SHG (with Interior Shading), W	Beam SHG (with Interior Shading), W	Diffuse SHG (with Interior Shading), W	Beam SHG (with Interior Shading), W	Diffuse SHG (with Interior Shading), W
7	0	13	4	16	4	29
8	0	54	30	72	30	126
9	0	95	57	126	57	221
10	0	131	52	174	52	304
11	0	160	16	209	16	369
12	0	181	0	230	0	411
13	0	207	0	235	0	442
14	0	227	0	226	0	453
15	0	239	0	206	0	445
16	101	237	0	178	101	415
17	251	219	0	145	251	364
18	340	181	0	112	340	293
19	329	126	0	73	329	199
20	165	57	0	31	165	88

Table 8.23 Radiative and Convective Components of Solar Heat Gains with Light-Colored Venetian Blinds

Local Time	Radiative Component of Beam SHG (with Interior Shading), W	Radiative Component of Diffuse SHG (with Interior Shading), W	Convective Component of Beam SHG (with Interior Shading), W	Convective Component of Diffuse SHG (with Interior Shading), W
7	2	16	2	13
8	16	68	14	58
9	31	119	26	102
10	28	164	24	140
11	9	199	8	170
12	0	222	0	189
13	0	239	0	203
14	0	245	0	209
15	0	240	0	205
16	54	224	46	191
17	136	196	116	167
18	184	158	156	135
19	177	108	151	92
20	89	48	76	41

Application of the RTSM—Detailed Example

**Table 8.24 Cooling Load Components
with Light-Colored Venetian Blinds, W**

Hour	Radiative		Radiative + Convective		Zone Sensible Cooling Loads
	Window Beam Solar	Window Diffuse Solar	Window Beam Solar	Window Diffuse Solar	
1	10	18	10	18	151
2	9	16	9	16	114
3	8	14	8	14	81
4	7	12	7	12	51
5	6	11	6	11	27
6	6	10	6	10	9
7	6	16	8	30	27
8	13	45	27	103	237
9	23	81	49	183	512
10	25	119	49	259	664
11	16	152	23	321	781
12	9	178	9	367	899
13	6	198	6	401	1021
14	4	211	4	419	1118
15	4	215	4	420	1178
16	31	211	78	402	1276
17	83	196	198	364	1374
18	125	173	282	308	1263
19	139	139	290	230	1038
20	100	95	176	136	753
21	44	54	44	54	456
22	25	36	25	36	345
23	17	27	17	27	270
24	13	22	13	22	213

base case). Treatment of the return air plenum will be described first, in Section 8.5.1. Then, calculation of loads for the room will be described in Section 8.5.2.

8.5.1 Computation of Air Temperature in the Return Air Plenum

Finding air temperatures in the return air plenum is similar to the procedure described in Appendix F for an unheated mechanical room. A steady-state heat balance is performed by balancing all of the heat flows into and out of the return air plenum. These include the following:

- Conduction heat transfer from the outdoors through the roof
- Conduction heat transfer from the outdoors through the side walls
- Conduction heat transfer to the room below through the acoustic tile ceiling
- Heat transfer to/from return air from the room
- Heat transfer to/from infiltration air
- Heat gain from the room lighting

Load Calculation Applications Manual (SI), Second Edition

Conduction Heat Transfer from the Outside via the Roof and Exterior Walls

For each of the exterior surfaces, conduction heat gain to the space is simply given by

$$q_{c, ext} = UA \cdot \Delta t = UA \cdot (t_{SA} - t_p) \quad (8.1)$$

where

t_{SA} = the sol-air temperature applying to the surface, °C

t_p = the plenum air temperature, °C

UA values are summarized for each surface in Table 8.25. The value for the roof is taken from Table 8.3. As before, it does not include the acoustic tile or ceiling air space resistances. For the side walls, actual computation of the UA value might include the parapet, but it has been ignored here. The U-factor has been computed for two vertical surface resistances, two layers of gypsum board, and two layers of R-0.9 insulation, as taken from the original building drawings.

Conduction Heat Transfer from the Plenum to the Room via the Acoustic Tile Ceiling

Conduction heat loss from the plenum to the room below is given by

$$q_{c, int} = UA \cdot \Delta t = UA \cdot (t_p - t_{rc}) \quad (8.2)$$

where t_{rc} is the constant room-air temperature, 24°C.

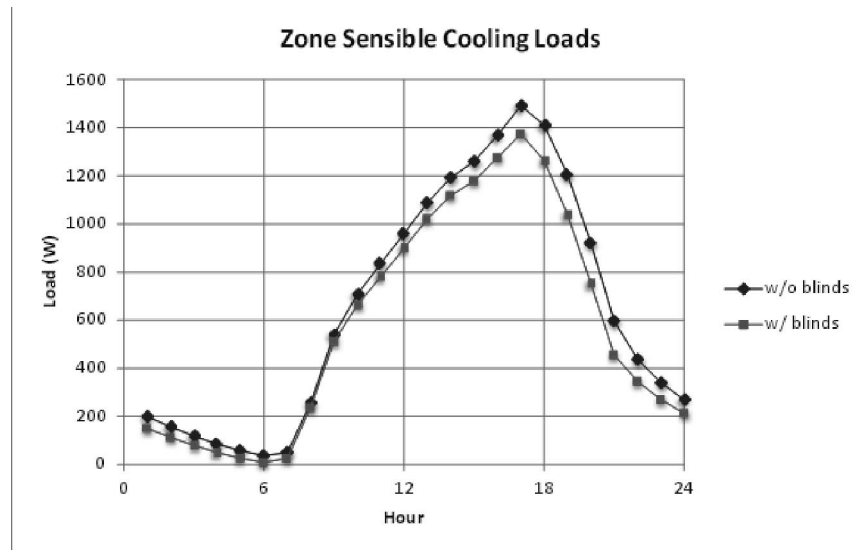


Figure 8.6 Comparison of zone-sensible cooling loads, with and without light-colored venetian blinds.

Table 8.25 UA Values for the Return Air Plenum

Surface	$U, W/(m^2K)$	A, m^2	UA, WK
Roof	0.18	12.0	2.16
SE side wall	0.45	4.2	1.92
SW side wall	0.45	3.3	1.48
Acoustic tile ceiling	1.56	12.0	18.74

Application of the RTSM—Detailed Example

The U-factor of the plenum floor, given in Table 8.25, has been computed for two horizontal surface resistances and a single layer of acoustic tile.

Heat Transfer from the Room to the Plenum via Return Air and Lighting Heat Gain

There is a significant flow of return air from the room into the return air plenum. This air may be heated by the lights while in transit from the room to the plenum. However, the two effects may be treated separately. Return air will be assumed to enter the plenum at the room air temperature, and the lighting heat gain will be added separately. The fact that some of the lighting heat gain may be transferred to the return air then to the plenum, rather than directly to the plenum, has no effect on the plenum air temperature.

There is a significant flow of return air from the room into the return air plenum. The amount of return air has not been determined. For this room, it will be equal to the supply airflow rate, which will depend on the supply air temperature. If a supply air temperature of 15°C is chosen, with the peak sensible room cooling load calculated in Section 8.3 (1598 W, shown in Table 8.20), a supply airflow rate of about 145 L/s will be required. Adapting Equation 5.4, the heat gain to the plenum via return air will be

$$q_{ra} = C_s Q \Delta t = C_s Q (t_{rc} - t_p) \quad (8.3)$$

where

C_s = sensible heat factor, (W·s)/(L·K), 1.23 is a typical value

Δt = temperature difference between the outdoor air and the indoor air, °C

Although this is written as a heat gain to the plenum, it will usually be negative, resulting in a heat loss to the plenum. With a flow rate of 145 L/s and using a value of 1.23 for the sensible heat factor, Equation 8.3 can be reduced to

$$q_{ra} = 178(t_{rc} - t_p) \quad (8.4)$$

The lighting heat gain q_{ltg} to the return air plenum has already been determined and can be taken directly from Table 8.21.

Heat Transfer to/from the Outdoors via Infiltration

For sea-level conditions, the infiltration heat gain is given by Equation 5.4 and is adapted to our situation:

$$q_{inf} = C_s Q \Delta t = C_s Q (t_o - t_p) \quad (8.5)$$

The infiltration rate to the plenum will be approximately volume weighted and taken to be 3.6 L/s, in which case Equation 8.5 reduces to

$$q_{inf} = 4.37(11)(t_o - t_p) \quad (8.6)$$

Heat Balance

The steady-state heat balance can now be expressed in words as “the heat transfer rate into the plenum is equal to the heat transfer rate out of the plenum.” Or, it can be expressed in equation form as

$$\Sigma q_{c, ext} + q_{inf} + q_{ra} + q_{ltg} = q_{c, int} \quad (8.7)$$

Substituting Equations 8.1, 8.2, 8.4, and 8.6 into Equation 8.7 then solving for t_p gives

Load Calculation Applications Manual (SI), Second Edition

$$t_p = \frac{\Sigma UA_{\text{ext}}t_{\text{SA}} + UA_{\text{int}}t_{\text{rc}} + 7.7 \cdot t_o + 314 \cdot t_{\text{rc}} + q_{\text{ltg}}}{\Sigma UA_{\text{ext}} + UA_{\text{int}} + 7.7 + 314} \quad (8.8)$$

In both Equations 8.7 and 8.8, the summation simply represents the inclusion of each of the three exterior surfaces: roof, southeast end wall, and southwest end wall. Note that Equation 8.8 is essentially a weighted average of the different boundary temperatures with which the plenum exchanges heat, with the addition of the lighting heat gain to the numerator. The weights are either UA values or sensible heat factors.

The calculation is summarized in Table 8.26. The second row contains the numerical values of the weights for each of the heat transfers. The second through fourth columns hold the sol-air temperatures for each of the three exterior surfaces for each hour. The fifth column is the temperature on the other side of the plenum floor (i.e., the constant room air temperature). The sixth column holds the outdoor air temperatures for each hour; the seventh column holds the return air temperature (again, the constant room air temperature). The eighth column holds the lighting heat gain to the plenum for each hour. Finally, the ninth column holds the calculated plenum temperatures for each hour, based on Equation 8.8.

Table 8.26 Summary of Heat Balance Calculation

Hour	Boundary Temperatures (Weight, W/°C)						Heat Gain	Plenum
	Roof (2.2)	SE Wall (1.9)	SW Wall (1.5)	Plenum Floor (18.7)	Infiltration (4.4)	Return Air (178.3)	q_{ltg}	t_p
1	20.7	24.5	24.5	24.0	24.5	24.0	0	24.0
2	19.9	23.7	23.7	24.0	23.7	24.0	0	23.9
3	19.2	23.1	23.1	24.0	23.1	24.0	0	23.9
4	18.8	22.7	22.7	24.0	22.7	24.0	0	23.9
5	18.5	22.4	22.4	24.0	22.4	24.0	0	23.9
6	18.1	22.0	22.0	24.0	22.0	24.0	0	23.9
7	18.9	22.7	22.3	24.0	21.9	24.0	0	23.9
8	25.0	28.6	24.0	24.0	22.3	24.0	0	24.0
9	34.0	35.6	26.5	24.0	23.3	24.0	0	24.2
10	44.1	42.2	29.8	24.0	25.5	24.0	0	24.5
11	53.2	46.6	32.8	24.0	27.6	24.0	0	24.7
12	60.3	48.6	35.4	24.0	29.5	24.0	0	24.8
13	64.9	47.9	37.8	24.0	31.0	24.0	0	24.9
14	66.5	44.9	45.2	24.0	32.1	24.0	0	25.0
15	65.4	40.3	52.8	24.0	32.9	24.0	0	25.0
16	61.6	39.2	57.8	24.0	33.4	24.0	0	25.0
17	55.2	37.9	59.4	24.0	33.2	24.0	0	24.9
18	46.8	36.0	56.8	24.0	32.4	24.0	0	24.8
19	37.8	33.9	50.0	24.0	31.5	24.0	0	24.6
20	29.2	31.2	38.1	24.0	30.1	24.0	0	24.4
21	24.6	28.4	28.4	24.0	28.4	24.0	0	24.2
22	23.4	27.3	27.3	24.0	27.3	24.0	0	24.1
23	22.4	26.3	26.3	24.0	26.3	24.0	0	24.1
24	21.4	25.3	25.3	24.0	25.3	24.0	0	24.0

Application of the RTSM—Detailed Example

Looking at the plenum temperatures, they are lower than might be expected. A review of the weights (UA for surfaces or $\dot{m}C_p$ for airflows) shows that the plenum air temperature is dominated by the return air, which holds the plenum air temperature relatively close to the room air temperature.

Now that the return air-plenum air temperatures are known, the heat gain from the plenum to the room can be determined, as can the heat gain to the return air. The heat gain to the room from the plenum is given by Equation 8.2:

$$q_{c,int} = UA \cdot \Delta t = UA \cdot (t_p - t_{rc}) = 18.74 \cdot (t_p - t_{rc})$$

The heat gain to the return air is

$$q_{ra} = C_s Q_s \Delta t = C_s Q_s (t_p - t_{rc}) = 178(t_p - t_{rc}) \quad (8.9)$$

These heat gains are summarized in Table 8.27. A comparison of the heat gains to the room from the plenum (last column of Table 8.27) and the heat gains from the roof to the room when the plenum was not explicitly considered (last column of Table 8.8),

Table 8.27 Heat Gains Associated with the Return Air Plenum

Hour	Heat Gain to Return Air, W	Heat Gain to Room from Plenum, W
1	-3	0
2	-9	-1
3	-15	-2
4	-18	-2
5	-21	-2
6	-24	-3
7	-22	-2
8	3	0
9	39	4
10	80	8
11	116	12
12	143	15
13	160	17
14	171	18
15	174	18
16	173	18
17	161	17
18	135	14
19	103	11
20	63	7
21	31	3
22	21	2
23	12	1
24	4	0

Load Calculation Applications Manual (SI), Second Edition

suggests that the amount of roof heat gain intercepted by the return air plenum is considerably higher than the 30% value assumed earlier. Near peak cooling load conditions, the heat gain to the room from the plenum is only about 20% of the roof heat gain.

8.5.2 Computation of Cooling Loads

Now that the return air plenum temperatures are known, the office cooling load can be calculated. There are a few minor differences associated with treating the return air plenum separately:

- In Section 8.3, the area of the walls in the room included the side walls of the return air plenum. Now, as the plenum is being treated separately, the wall areas are those shown in Table 7.15, based on the room inside.
- The roof heat gains are replaced with the plenum heat gains in Table 8.27.
- Because 3.6 L/s of the infiltration was allocated to the plenum, the cfm in the room will be reduced by 3.6 L/s.

The differing cooling loads and total room sensible cooling loads are summarized in Table 8.28.

In addition, the sensible cooling load on the system is also calculated, as illustrated in Table 8.29, by adding the zone sensible cooling load and the heat gain to the return air.

A comparison of the two approaches shows that the system sensible cooling loads are fairly similar but that the assumption that the return air plenum intercepts 30% of the roof heat gain tends to overpredict the cooling load in the room by about 10%. The actual percentage of the roof heat gain that the return air plenum intercepts, for this case, is significantly higher.

8.6 Summary

This chapter has presented an in-depth example of the calculation of cooling loads for a single room. Loads with and without venetian blinds were calculated and two different approaches for treating the return air plenum were demonstrated. One aspect of load calculations that was not explored is the possibly counterintuitive dependence of the cooling load on the month. For some zones, peak cooling loads will occur at months that are not peak temperature months but rather that represent peak solar heat gain conditions. In the northern hemisphere, the peak month would typically fall somewhere between July and December. A spreadsheet that automates much of the RTSM calculation, including the analysis of multiple months, is presented in Appendix B and included in the online supporting files accompanying this manual.

References

ASHRAE. 2013. *ASHRAE Handbook—Fundamentals*. Atlanta: ASHRAE.

Application of the RTSM—Detailed Example

Table 8.28 Room Sensible Cooling Load Components, W

Hour	Plenum Conduction	Infiltration	Total Cooling Loads
1	1	5	184
2	0	-2	148
3	-1	-9	114
4	-1	-15	83
5	-2	-20	58
6	-2	-23	39
7	-2	-23	52
8	1	-20	258
9	3	-12	534
10	7	1	690
11	10	18	802
12	13	39	906
13	15	60	1014
14	16	80	1101
15	17	94	1156
16	17	103	1258
17	16	104	1378
18	14	99	1300
19	12	88	1103
20	8	73	832
21	5	56	524
22	4	40	380
23	3	27	292
24	2	14	230

Load Calculation Applications Manual (SI), Second Edition

Table 8.29 System Sensible Cooling Loads, W

Hour	Zone Sensible	Calculated Gain to Return Air	System Sensible Cooling Load
1	184	-3	182
2	148	-9	138
3	114	-15	99
4	83	-18	65
5	58	-21	37
6	39	-24	15
7	52	-22	31
8	258	3	261
9	534	39	572
10	690	80	770
11	802	116	918
12	906	143	1049
13	1014	160	1173
14	1101	171	1272
15	1156	174	1330
16	1258	173	1431
17	1378	161	1539
18	1300	135	1436
19	1103	103	1207
20	832	63	895
21	524	31	555
22	380	21	401
23	292	12	305
24	230	4	234

Air Systems, Loads, IAQ, and Psychrometrics

Following calculation of the cooling and heating loads, an analysis must be carried out to specify the various parameters for selection of equipment and design of the air distribution system. The psychrometric processes involved are rigorously discussed in Appendix A, where it is shown that the psychrometric chart is a useful tool in visualizing and solving problems.

The complete air-conditioning system may involve two or more of the processes considered in Appendix A. For example, in the conditioning of a space during the summer, the air supplied must have a sufficiently low temperature and moisture content to absorb the total cooling load of the space. Therefore, as the air flows through the space, it is heated and humidified. If the system is closed-loop, the air is then returned to the conditioning equipment, where it is cooled and dehumidified and supplied to the space again. Outdoor air usually is required in the space; therefore, outdoor air (makeup air) must be mixed with the return air (recirculated air) before it goes to the cooling and dehumidifying equipment. During the winter months, the same general processes occur but in reverse. Notice that the psychrometric analysis generally requires consideration of the outdoor air required, the recirculated air, and the space load. Various systems will be considered that carry out these conditioning processes, with some variations.

9.1 Classical Design Procedures

The most common design problem involves a system where outdoor air is mixed with recirculated air. The mixture is cooled and dehumidified and then delivered to the space, where it absorbs the load in the space and is returned to complete the cycle. Figure 9.1 shows a schematic of such a system, with typical operating conditions indicated. The sensible and latent cooling loads were calculated according to procedures discussed in Chapters 5–7, and the outdoor air quantity was derived from indoor air quality considerations. The system, as shown, is generic and represents several different types of systems when they are operating under full design load. Partial load conditions will be considered later. The primary objective of the analysis of the system is to determine the amount of air to be supplied to the space, its state, and the capacity and operating conditions for the coil. These results can then be used in designing the complete air distribution system.

Example 9.1 Cooling and Dehumidification Process

Analyze the system of Figure 9.1 to determine the quantity and state of the air supplied to the space and the required capacity and operating conditions for the cooling and dehumidifying equipment. The desired room conditions are given at state 3 (the states are the circled numbers in Figure 9.1). Assume sea-level elevation.

Solution: Rigorous solutions to the various processes are covered in Appendix A. An approach with minor approximations will be shown here. The given quantities are shown and the states are numbered for reference on ASHRAE Psychrometric Chart 1 (ASHRAE 1992) and shown schematically in Figure 9.2.

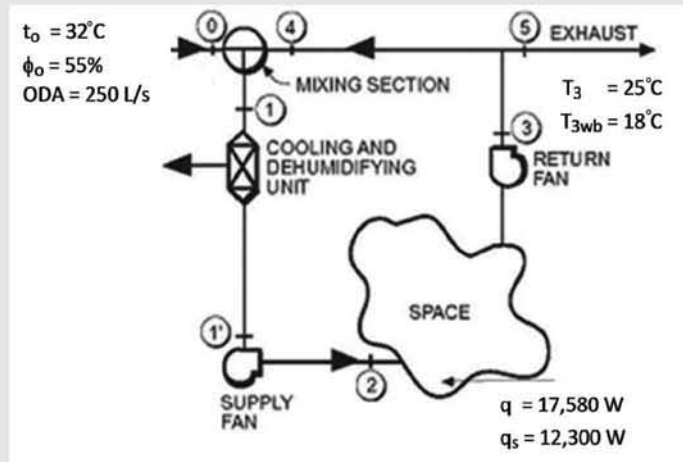


Figure 9.1 Cooling and dehumidifying system.

(Source: *Cooling and Heating Load Calculation Principles*, Figure 8.1).

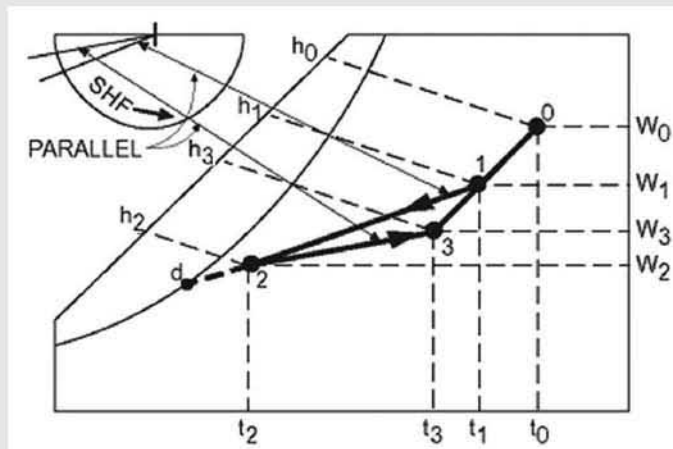


Figure 9.2 Psychrometric processes for Example 9.1.

Source: *Cooling and Heating Load Calculation Principles*, Figure 8.2).

Losses in connecting ducts and fan power will be neglected. First, consider the steady flow process for the conditioned space. The room sensible heat factor (RSHF) is

$$\text{RSHF} = \frac{12,300}{17,580} = 0.7.$$

To provide the desired room conditions, the state of the air entering the space must lie on the line defined by state 3 and the RSHF on ASHRAE Psychrometric Chart 1 (ASHRAE 1992). Therefore, state 3 is located as shown on Figure 9.2 and a line is drawn through the point parallel to the SHF = 0.7 line on the protractor. State 2 may be any point on the line and is determined by the operating characteristics of the equipment, desired indoor air quality, and by what will be comfortable for the occupants. A typical leaving condition for the coil would be at a relative humidity of 85% to 90%. The temperature t_2 is assumed to be 13°C and state 2 is determined. The air quantity required may now be found by considering processes 2–3 in Figure 9.2. Using Equation 9.1a,

Air Systems, Loads, IAQ, and Psychrometrics

$$q_s = (L/s)c_p(t_3 - t_2)/v_2 \quad (9.1a)$$

where L/s represents the airflow rate in L/s and q_s will be in Watts.

With c_p assumed constant at $1.02 \text{ kJ}/(\text{kg}\cdot^\circ\text{C})$ from Appendix A, Equation 9.1a becomes

$$q_s = 1.02 L/s(t_3 - t_2)/v_2 \quad (9.1b)$$

and further, when standard sea-level conditions are assumed, $v_2 = 0.82 \text{ m}^3/\text{kg}$,

$$q_s = 1.24 L/s(t_3 - t_2) \quad (9.1c)$$

Equation 9.1c is used extensively to compute air quantities and sensible heat transfer, even though v_2 is not usually equal to the standard value, even at sea level. However, the assumption of sea-level pressure and elevation is reasonable up to about a 750 m elevation. At that point, the error in the computed volume flow rate (L/s) or sensible heat transfer will be about 10%. The L/s will be about 10% low and sensible heat transfer will be about 10% high. The data for specific volume v from a proper psychrometric chart or from Table A.2 should be used for elevations above 750 m. To continue, $v_2 = 10.84 \text{ m}^3/\text{kg}$ from ASHRAE Psychrometric Chart 1 (ASHRAE 1992). Using Equation 9.1b,

$$L/s_2 = \frac{0.82(12,300)}{1.02(25 - 13)} = 807$$

Using Equation 9.1c, $L/s^2 = 827$.

Attention is now directed to the cooling and dehumidifying unit. However, state 1 must be determined before continuing. A mass balance on the mixing section yields

$$m_{a0} + m_{a4} = m_{a1} = m_{a2},$$

but it is approximately true that

$$L/s_0 + L/s_4 = L/s_1 = L/s_2$$

and

$$L/s_4 = L/s_1 - L/s_0 = 807 - 250 = 557,$$

and based on an energy balance, t_1 is given approximately by the following:

$$t_1 = t_0 \left(\frac{L/s_0}{L/s_1} \right) + t_4 \left(\frac{L/s_4}{L/s_1} \right)$$

$$t_1 = 32 \left(\frac{250}{807} \right) + 25 \left(\frac{557}{807} \right) = 27^\circ\text{C}$$

State 1 may now be located on line 3-0 of Figure 9.2 and ASHRAE Psychrometric Chart 1 (ASHRAE 1992). (Note that states 3, 4, and 5 all have the same conditions.) By using the graphical technique discussed in Appendix A, referring to Figure 9.2, and using L/s in place of mass flow rate, state 1 also may be found graphically:

$$\frac{\bar{31}}{30} = \frac{L/s_0}{L/s_1} = \frac{250}{807} = 0.3$$

Load Calculation Applications Manual (SI), Second Edition

$$\overline{31}(0.3) = \overline{30}$$

State 1 is located at approximately 27°C dB and 20°C wB. A line constructed from state 1 to state 2 on ASHRAE Psychrometric Chart 1 (ASHRAE 1992) then represents the process taking place in the conditioning equipment.

The coil may be specified in different ways, but the true volume flow rate entering the coil, L/s_1 , should be given. The mass flow rates m_{a1} and m_{a2} are the same; therefore, using Equation 9.2,

$$m_{a1} = m_{a2} = \frac{L/s_1}{v_1} = \frac{L/s_2}{v_2} \quad (9.2)$$

or

$$L/s_1 = L/s_2 \frac{v_1}{v_2}$$

$$L/s_1 = 807 \frac{0.865}{0.82} = 851 \quad ,$$

where v_2 is obtained from ASHRAE Psychrometric Chart 1 (ASHRAE 1992), Figure 9.2. Then the coil entering and leaving air conditions may be given as

$$t_1 = 27^\circ\text{C dB and } 20^\circ\text{C wB}$$

and

$$t_2 = 13^\circ\text{C dB and } 12^\circ\text{C wB,}$$

and the coil capacity may be left as an exercise for the application engineer. However, it is recommended that the coil capacity also be determined from the following:

$$q_c = m_{a1}(h_1 - h_2) = \frac{L/s_1(h_1 - h_2)}{v_1} \quad (9.3)$$

$$q_c = \frac{60(1740)(32.2 - 22.0)}{13.95}$$

$$q_c = 24,600 \text{ W}$$

The sensible heat factor for the cooling coil is found to be 0.64 using the protractor of ASHRAE Psychrometric Chart 1 (ASHRAE 1992). Then

$$q_{cs} = 0.64(24,600) = 15,744 \text{ W}$$

and

$$q_{cl} = 24,600 - 15,744 = 8856 \text{ W} \quad .$$

Alternately, the sensible load on the coil could be computed from Equation 9.1a:

$$q_{cs} = \frac{1.02(L/s_1)(t_1 - t_2)}{v_1}$$

$$q_{cs} = \frac{1.02(851)(27 - 13)}{0.865}$$

$$q_{cs} = 14,049 \text{ W}$$

and the latent load may then be determined by subtracting the sensible load from the coil load:

$$q_{cl} = 24,600 - 14,049 = 10,551 \text{ W}$$

The sum of q_{cs} and q_{cb} or q_c , is known as the *coil refrigeration load* (in contrast to the *space cooling load*). It is difficult to compute the coil latent load directly without the aid of a psychrometric chart or a computer routine. This problem is discussed further in Appendix A.

9.1.1 Fan Power

In an actual system, fans are required to move the air, and some energy from the fans is transferred to the air in the system. In addition, some heat may be lost or gained in the duct system. Referring to Figure 9.1, the supply fan is located just downstream of the cooling unit, and the return fan is upstream of the exhaust and mixing box. The temperature rise due to a fan is discussed in Appendix A, and data are given as a function of fan total efficiency and total pressure. At this point in the analysis, characteristics of the fan are unknown. However, an estimate can be made and checked later. Heat also may be gained in the supply and return ducts. The effect of the supply air fan and the heat gain to the supply air duct may be summed as shown on ASHRAE Psychrometric Chart 1 (ASHRAE 1992), Figure 9.3a, as process 1'-2. Likewise, heat is gained in the return duct from point 3 to point 4, and the return fan temperature rise occurs between points 3 and 4, as shown in Figure 9.3a. The condition line for the space, 2-3, is the same as it was before when the fans and heat gain were neglected. However, the requirements of the cooling coil have changed. Process 1-1' now shows that the capacity of the coil must be greater to offset the fan power input and duct heat gain.

Example 9.2 Sensible Heat Gain

Calculate the temperature rise of the air in a system like the one in Figure 9.1 and the effect on the system when the fan is a draw-through fan on the leaving side of the coil (Case A) and a blow-through fan behind the coil (Case B).

Solution: Assume the design total pressure difference across the fan is 500 Pa of water, the fan efficiency is 75%, and the motor efficiency is 85%. For these conditions, Table A.3 shows a temperature rise of the air of 0.5°C when the motor is outside the airstream. When the motor is in the airstream, the combined efficiency is $0.75 \cdot 0.85 = 0.64$. The temperature rise is then 0.6°C. These temperature differences apply to both Case A and Case B. For Case A, draw-through, state 1' is located at 0.5°C, or 0.6°C to the left of state 2 in Figure 9.3a. For Case B, blow-through, the state of the air entering the coil is located 0.5°C or 0.6°C to the right of state 1 in Figure 9.3a. Based on the solution of Example 9.1, the fan capacity is about 800 L/s. The shaft power input would then be about 0.5 kW. First, considering the draw-through fan configuration (Case A), the process from the fan inlet to the point where the air has entered the space appears as process 1'-2 in Figure 9.3a. All of the power input to the fan has been transformed into stored energy, which is manifested in the temperature rise. All of the energy input is a load on the space. With the motor outside the airstream, the additional load on the space is

Load Calculation Applications Manual (SI), Second Edition

$$q_f = 0.5 \text{ kW}$$

With the motor in the airstream,

$$q_f = \frac{0.5}{0.85} = 0.59 \text{ kW}$$

In the case of the blow-through fan configuration (Case B), the fan power is the same; however, the effect on the system is different. Most of the power results in a load on the coil, while a smaller part is a load on the space. It is customary to assign the entire load to the coil for simplicity. Figure 9.3b shows the fan effect in this case as process 1-1'. The additional loads assigned to the coil are the same values computed above. It is apparent in both cases that the fan energy eventually appears as a coil load.

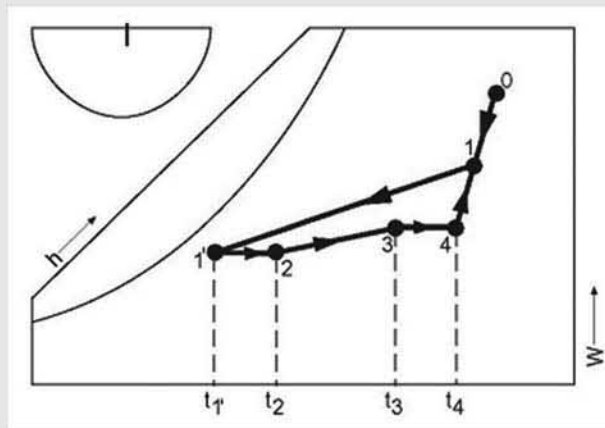


Figure 9.3a Psychrometric processes showing effect of fans and heat gain.

(Source: *Cooling and Heating Load Calculation Principles*, Figure 8.3).

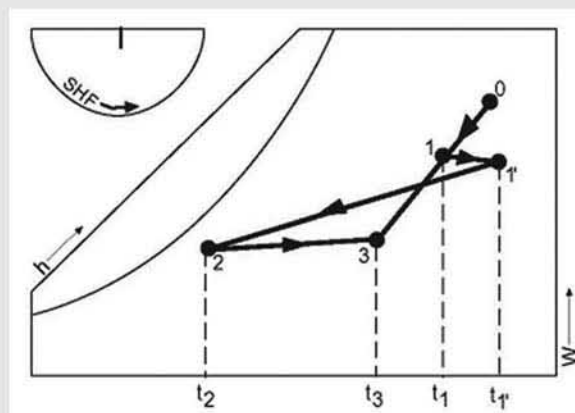


Figure 9.3b Fan effect with blow-through configuration.

(Source: *Cooling and Heating Load Calculation Principles*, Figure 8.3a).

9.1.2 Ventilation for Indoor Air Quality

Indoor air quality (IAQ) is closely related to the psychrometric analysis leading to system design because air quality is largely dependent on the amount of outdoor air brought into the conditioned space, usually through the cooling and heating system. This is the purpose of the outdoor air introduced in Example 9.1 above. For typical occupied spaces, the amount of clean outdoor air is proportional to the number of people in the space. ANSI/ASHRAE Standard 62.1-2013, *Ventilation for Acceptable Indoor Air Quality* covers this subject and is the recognized source of data for purposes of system design. For full details, Standard 62.1 should be consulted. One approach specified in the standard is the ventilation rate procedure. With this approach, if the outdoor air is of acceptable quality, the minimum required amount of outdoor air per person and per square meter are specified in Table 6-1 of the standard. Table 9.1 is excerpted from Table 6.2.2.1 of the standard. The per-person and per-square-meter values are added together to determine the total required ventilation flow rate. If the actual number of occupants is not known, the default occupant density given in Table 9.1 may be used. Using this default occupancy, the combined outdoor air rate given on the right-hand side of the table is the per-person required ventilation flow rate. When the occupancy is known, this should be used instead of the estimated density.

Example 9.3 Required Outdoor Air

An auditorium is designed for a maximum occupancy of 300 people and has a floor area of 240 m². Find the required outdoor airflow rate.

Solution: From Table 9.1 the minimum required outdoor airflow rate is

$$L/s_m = 300(2.5) + 240(0.3) = 822$$

The ventilation air rate necessary to offset the cooling or heating load will likely be greater than 2250 L/s. When the amount of air required to absorb the cooling load exceeds the minimum required ventilation air, it is generally desirable to recirculate and filter some of the air. Standard 62.1 gives full details for various conditions; a typical, somewhat idealized system will be presented here. A simple recirculating system is shown in Figure 9.4.

It is assumed that the ventilation system is a constant flow type, the outdoor air is acceptable by Table 9.1 standards, and ventilation effectiveness is 100%. The recirculating rate is

$$L/s_r = L/s_v - L/s_m,$$

where L/s_v is the ventilation rate required by the cooling load or some factor other than air quality. It is assumed that the minimum amount of outdoor air based on occupancy will supply the needed oxygen and will sufficiently dilute the contaminants (including carbon dioxide) generated by the occupants and the building materials.

There also could be a case where the required outdoor air exceeds the amount of air needed to absorb the load. In this case, the condition of the air entering the space must be located on the space condition line (see Appendix A) to satisfy both requirements.

9.1.3 Cooling and Heating Coils

The heat transfer surfaces, usually referred to as *coils* and mentioned in Example 9.1, are of primary importance in an air-conditioning system. These surfaces are usually of a finned-tube geometry, where moist air flows over the finned surface and a liquid or two-phase refrigerant flows through the tubes. The coil generally will

Load Calculation Applications Manual (SI), Second Edition

have several rows of tubes in the airflow direction, and each row will be many tubes high and perpendicular to the airflow. Coil geometry will vary considerably depending on application. Steam and hot-water heating coils usually will have fewer rows of tubes (1–4), less dense fins (2–3 fins per cm), and fewer circuits for fluid flow. Chilled-water and direct-expansion coils generally have more rows of tubes (4–8), more fins (3–6 fins per cm), and more circuits for fluid flow on the tube side. It will be shown later that the coil must match the characteristics of the space and outdoor

Table 9.1 Minimum Ventilation Rates in Breathing Zone

(Source: ANSI/ASHRAE Standard 62.1-2013)

Occupancy Category	People Outdoor Air Rate R_p		Area Outdoor Air Rate R_a		Default Values			Air Class
	cfm/Person	L/s · Person	cfm/ft ²	L/s · m ²	Occupant Density (see Note 4)	Combined Outdoor Air Rate (see Note 5)		
					#/1000 ft ² or #/100 m ²	cfm/Person	L/s · Person	
Office Buildings								
Office space	5	2.5	0.06	0.3	5	17	8.5	1
Reception areas	5	2.5	0.06	0.3	30	7	3.5	1
Telephone/data entry	5	2.5	0.06	0.3	60	6	3.0	1
Main entry lobbies	5	2.5	0.06	0.3	10	11	5.5	1
Public Assembly Spaces								
Auditorium seating area	5	2.5	0.06	0.3	150	5	2.7	1
Places of religious worship	5	2.5	0.06	0.3	120	6	2.8	1
Courtrooms	5	2.5	0.06	0.3	70	6	2.9	1
Legislative chambers	5	2.5	0.06	0.3	50	6	3.1	1
Libraries	5	2.5	0.12	0.6	10	17	8.5	1
Lobbies	5	2.5	0.06	0.3	150	5	2.7	1
Museums (children's)	7.5	3.8	0.12	0.6	40	11	5.3	1
Museums/galleries	7.5	3.8	0.06	0.3	40	9	4.6	1
Retail								
Sales (except as below)	7.5	3.8	0.12	0.6	15	16	7.8	2
Mall common areas	7.5	3.8	0.06	0.3	40	9	4.6	1
Barbershop	7.5	3.8	0.06	0.3	25	10	5.0	2
Beauty and nail salons	20	10	0.12	0.6	25	25	12.4	2
Pet shops (animal areas)	7.5	3.8	0.18	0.9	10	26	12.8	2
Supermarket	7.5	3.8	0.06	0.3	8	15	7.6	1
Coin-operated laundries	7.5	3.8	0.06	0.3	20	11	5.3	2

Note: This table is an excerpt from Table 6.2.2.1 of ANSI/ASHRAE Standard 62.1-2013, *Ventilation for Acceptable Indoor Air Quality*. Please consult the standard for necessary details for application of this data.

Air Systems, Loads, IAQ, and Psychrometrics

air loads and that selection of the proper coil is fundamental to good system design. Catalogs from manufacturers, computer simulation programs, and databases are very useful in this regard.

Although the design engineer may seek help from an application engineer in selecting a coil, it is important that the nature of coil behavior and the control necessary for off-design conditions be understood.

Heating Coils

Heating coils are much easier to design and specify than cooling coils because only sensible heat transfer is involved. The steam or water supplied to the coil usually must be controlled for partial-load conditions; thus, oversizing a coil, generally, is undesirable. Hot-water coils usually are preferable to steam coils, particularly when the load varies over a wide range. Steam and hot-water control is difficult when the flow rate must be reduced significantly.

Cooling and Dehumidifying Coils

The design of cooling and dehumidifying coils is much more difficult because of the transfer of both sensible and latent heat. Further, the sensible and latent loads on a coil usually do not vary in a predictable way during off-design operation. It is entirely possible that a coil that performs perfectly under design conditions will be unsatisfactory under partial load. An understanding of the coil behavior may prevent such an occurrence.

Figure 9.5 shows a cooling and dehumidification process for a coil. The process is not actually a straight line, but when only the end points are of interest, a straight line is an adequate representation. The intersection of the process line with the saturation curve defines the apparatus dew-point temperature t_{ad} . This temperature is the approximate dew point of the surface where the cooling fluid is entering the coil and where the air is leaving, assuming counterflow of the fluids.

The apparatus dew point is useful in analyzing coil operation. For example, if the slope of process 1-2' is so great that the extension of the process line does not intersect the saturation curve, the process probably is impossible to achieve with a coil in a single process and another approach will be necessary.

Process 1-2' in Figure 9.5 is an example of such a process. The relative humidity of the air leaving a chilled-water coil is typically about 90% and, based on experience, it is approximately true that

$$t_{ad} = \left(\frac{t_w + t_{wb}}{2} \right), \quad (9.4a)$$

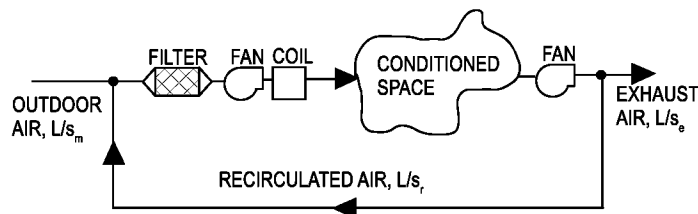


Figure 9.4 Schematic of recirculating system.

(Source: *Cooling and Heating Load Calculation Principles*, Figure 8.4).

Load Calculation Applications Manual (SI), Second Edition

where t_w is the entering water temperature and t_{wb} is the wet-bulb temperature of the air leaving the coil. This approximation can be used to estimate the required water temperature for a cooling process:

$$t_w \approx 2t_{ad} - t_{wb} \quad (9.4b)$$

In so doing, a designer might avoid specifying a coil for an impossible situation or one that requires an abnormally low water temperature.

To maintain control of space conditions at partial-load conditions, the flow rate of the air or cooling fluid (water or brine solution) in the coil must be regulated. In a well-designed system, both probably are under control. It is interesting to note how the leaving air condition changes in each case. The processes shown in Figure 9.6 are for a typical chilled-water coil in an air-conditioning system. Process 1-2 is typical of the performance with full flow of air but greatly reduced flow of water, while process 1-3 is typical of performance with full flow of water but greatly reduced flow of air. To generalize, as water flow is reduced, the leaving air condition moves toward point 2, and as airflow is reduced, the leaving air condition moves toward point 3. The conclusion is that by proper control of the flow rates of both fluids, a satisfactory air condition can be maintained under partial-load conditions.

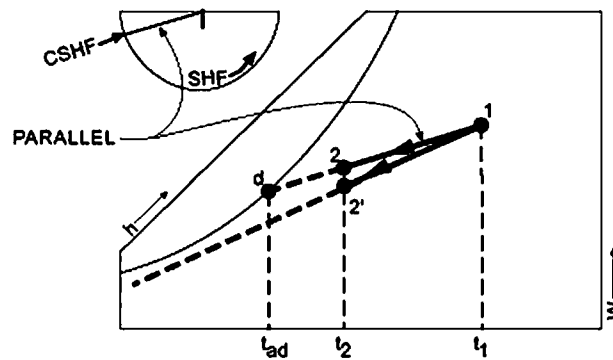


Figure 9.5 Comparison of coil processes.

Source: *Cooling and Heating Load Calculation Principles*, Figure 8.5).

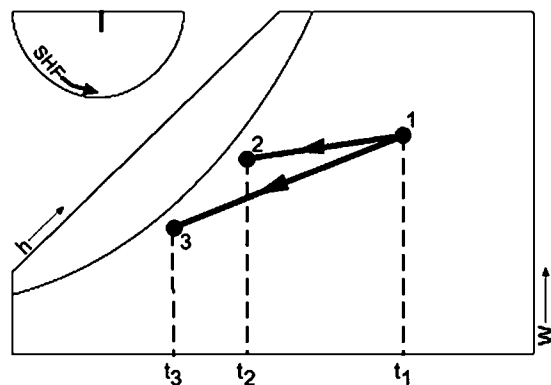


Figure 9.6 Comparison of coil processes with variable rates.

Source: *Cooling and Heating Load Calculation Principles*, Figure 8.6).

Bypass Factor

An alternate approach to the analysis of the cooling coil in Example 9.1 uses the so-called *coil bypass factor*. Note that when line 1-2 of Figure 9.5 is extended, it intersects the saturation curve at point d. This point represents the apparatus dew-point temperature of the cooling coil. The coil cannot cool all of the air passing through it to the coil surface temperature. This fact makes the coil perform in a manner similar to what would happen if a portion of the air were brought to the coil temperature and the remainder bypassed the coil entirely. A dehumidifying coil thus produces unsaturated air at a higher temperature than the coil temperature. Again referring to Figure 9.5, notice that in terms of the length of line d-1, the length of line d-2 is proportional to the mass of air bypassed, and the length of line 1-2 is proportional to the mass of air not bypassed. Because line d-1 is inclined, it is approximately true that the fraction of air bypassed is

$$b = \left(\frac{t_2 - t_d}{t_1 - t_d} \right) \quad (9.5)$$

and that

$$1 - b = \left(\frac{t_1 - t_2}{t_1 - t_d} \right) \quad (9.6)$$

The temperatures are dry-bulb values. Applying Equation 9.1b, the coil sensible load is

$$q_s = 1.02(L/s_1)(t_1 - t_d)(1 - b)/v_1. \quad (9.7)$$

Example 9.4 Bypass Factor

Find the bypass factor for the coil of Example 9.1, and compute the sensible and latent heat transfer rates.

Solution: The apparatus dew-point temperature obtained from ASHRAE Psychrometric Chart 1 (ASHRAE 1992) as indicated in Figure 9.2 is 8°C. Then from Equation 9.5 the bypass factor is

$$b = \frac{(13 - 8)}{(27 - 8)} = 0.26 \text{ and } 1 - b = 0.74$$

Equation 9.7 expresses the sensible heat transfer rate as

$$q_{cs} = \frac{1.02(851)(27 - 8)(0.74)}{0.865} = 14,109 \text{ W}$$

The coil-sensible heat factor is used to compute the latent heat transfer rate. From Example 9.1, the SHF is 0.64. The total heat transfer rate is

$$q_t = \frac{q_{cs}}{\text{SHF}} = \frac{14,109}{0.64} = 22,045 \text{ W}$$

and

$$q_{cl} = q_t - q_{cs} = 22,045 - 14,109 = 7,936 \text{ W}$$

It should be noted that the bypass factor approach often results in errors compared to the approach of Example 9.1. Accurate data for bypass factors are not generally available.

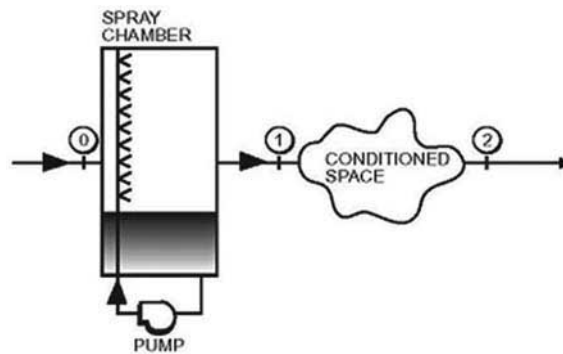


Figure 9.7 Simple evaporative-cooling system.

(Source: *Cooling and Heating Load Calculation Principles*, Figure 8.7).

9.1.4 Hot and Dry Environment

In Example 9.1, the outdoor air was hot and humid. This is not always the case, and State 0 can be almost anywhere on ASHRAE Psychrometric Chart 1 (ASHRAE 1992). For example, the southwestern part of the United States is hot and dry during the summer, and evaporative cooling often can be used to an advantage under these conditions. A simple system of this type is shown schematically in Figure 9.7.

The dry outdoor air flows through an adiabatic spray chamber and is cooled and humidified. An energy balance on the spray chamber will show that the enthalpies h_0 and h_1 are equal (see Appendix A); therefore, the process 0-1 is as shown in Figure 9.8.

Ideally, the cooling process terminates at the space condition line 1-2. The air then flows through the space and is exhausted. Large quantities of air are required, and this system is not satisfactory where the outdoor relative humidity is high. If the humidity ratio W_0 is too high, the process 0-1 cannot intersect the condition line. For comfort air conditioning, evaporative cooling can be combined with a conventional system as shown in Figure 9.9.

When outdoor makeup air is mixed with recirculated air without evaporative cooling, the ideal result would be state 1 in Figure 9.10. The air would require only sensible cooling to state 2 on the condition line. Second, outdoor air could be cooled by evaporation to state 0' in Figure 9.10 and then mixed with return air, resulting in state 1'. Sensible cooling would then be required from state 1' to state 2. Finally, the outdoor air could ideally be evaporatively cooled all the way to state 1". This would require the least power for sensible cooling, but the air supplied to the space would be 100% outdoor air. It must be recognized that controlling the various processes above to achieve the desired results is difficult.

9.1.5 Space Heating

The contrasting problem of space air conditioning during the winter months may be solved in a manner similar to Example 9.1. Figure 9.11 shows a schematic of a heating system.

It usually is necessary to use a preheat coil to heat the outdoor air to a temperature above the dew point of the air in the equipment room so that condensation will not form on the air ducts upstream of the regular heating coil. Figure 9.12 shows the psychrometric processes involved. The heating and humidification process 1-1'-2, where the air is first heated from 1 to 1', followed by an adiabatic humidification process from 1' to 2, is discussed in Appendix A.

Air Systems, Loads, IAQ, and Psychrometrics

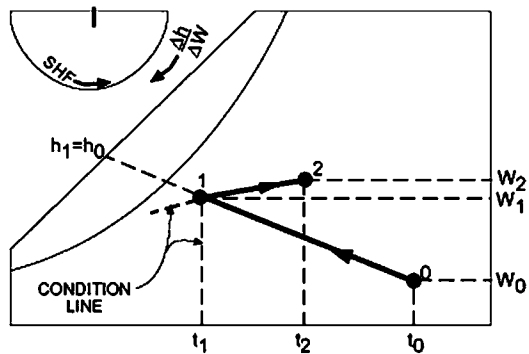


Figure 9.8 Psychrometric diagram for evaporative-cooling system of Figure 9.7.

(Source: *Cooling and Heating Load Calculation Principles*, Figure 8.8).

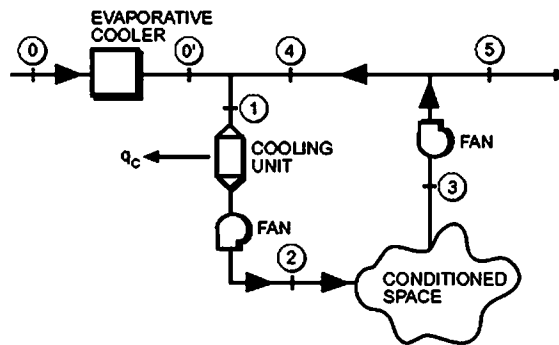


Figure 9.9 Combination evaporative/regular-cooling system.

(Source: *Cooling and Heating Load Calculation Principles*, Figure 8.9).

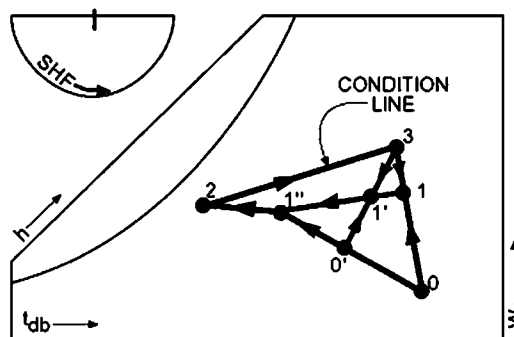


Figure 9.10 Psychrometric diagram of Figure 9.9.

(Source: *Cooling and Heating Load Calculation Principles*, Figure 8.10).

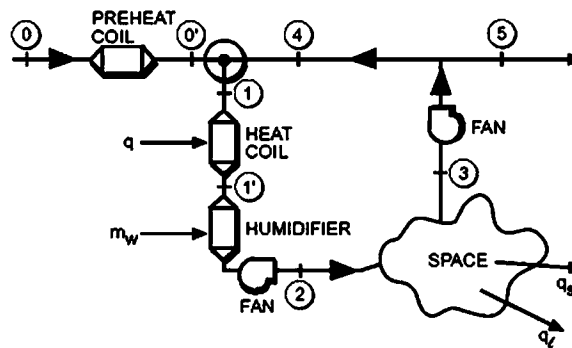


Figure 9.11 Heating system with preheat of outdoor air.

(Source: *Cooling and Heating Load Calculation Principles*, Figure 8.11).

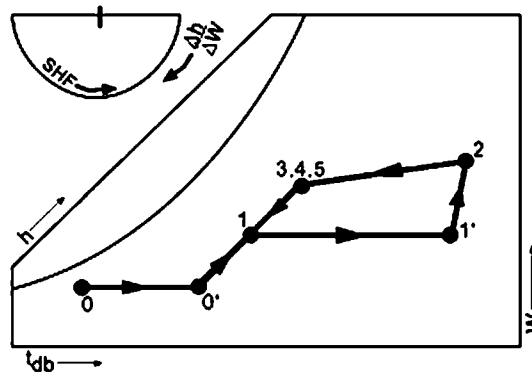


Figure 9.12 Psychrometric diagram of Figure 9.11.

(Source: *Cooling and Heating Load Calculation Principles*, Figure 9.12).

9.1.6 All Outdoor Air

There are situations where acceptable IAQ will require that all the ventilation air be outdoor air. Such a system would resemble Figure 9.13. Its psychrometric diagram could appear as shown in Figure 9.14. Outdoor air is cooled and dehumidified to state 1 when it enters the space, absorbs the cooling load, and is exhausted to the atmosphere. This system is analyzed in the same manner as Example 9.2 except there is no mixing of recirculated and outdoor air.

Example 9.5 Coil Specification

A space has a total cooling load of 73,000 W. The sensible portion of the load is 59,000 W. The space condition is 26°C dB and 50% relative humidity, and outdoor conditions are 35°C dB and 24°C wB with standard sea-level pressure. IAQ considerations require 6000 L/s of outdoor air. Determine the amount of air to be supplied to the space, the condition of the supply air, and the coil specification.

Air Systems, Loads, IAQ, and Psychrometrics

Solution: The condition line is first constructed on ASHRAE Psychrometric Chart 1 (ASHRAE 1992) using the RSHF.

$$\text{RSHF} = \frac{58,614}{73,268} = 0.8$$

The condition line appears as process 1-2 in Figure 9.14 and the extension of the line to the left. Point 1 is not known yet. Point 2 is the given space condition.

The quantity of outdoor air required is large and may be more than that required by the cooling load. Therefore, check to see what minimum amount of supply air will satisfy the cooling load. Assuming that a practical coil will cool air to about 90% relative humidity, this is given by recasting Equation 9.1b as

$$q_2 = 1.02 \text{ L/s}(t_2 - t_1)/v_1$$

or

$$\text{L/s}_{\min} = \frac{q_2 v_1}{1.02(t_2 - t_1)} = \frac{59,000(0.82)}{1.02(26 - 14)} = 3953,$$

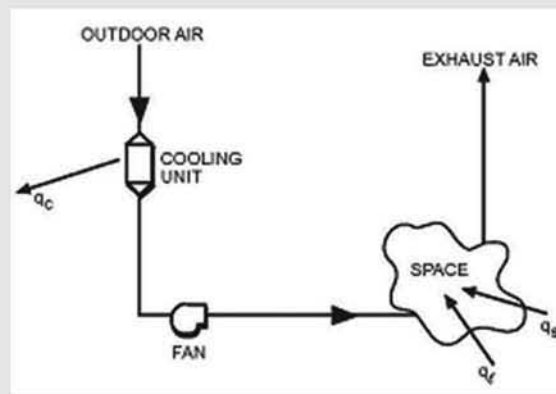


Figure 9.13 All-outdoor-air system.

(Source: *Cooling and Heating Load Calculation Principles*, Figure 8.13).

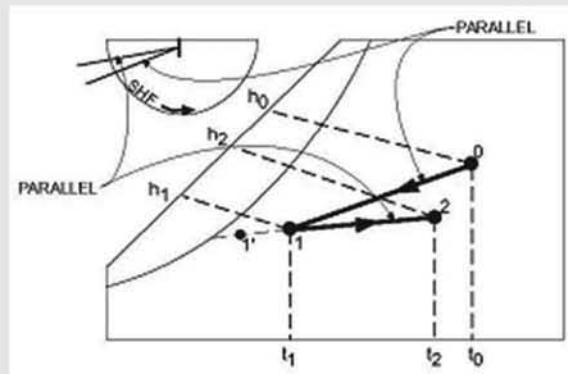


Figure 9.14 Psychrometric diagram of all-outdoor-air system.

(Source: *Cooling and Heating Load Calculation Principles*, Figure 8.14).

Load Calculation Applications Manual (SI), Second Edition

where the various properties are read from ASHRAE Psychrometric Chart 1 (ASHRAE 1992). Obviously, the required outdoor air is greater than that required by the load. Therefore, point 1 in Figure 9.14 must be located to accommodate 6000 L/s of outdoor air. Reconsider Equation 9.1b and solve for t_1 :

$$t_1 = t_2 - \frac{q_2 v_0}{1.02 \text{ L/s}}$$

The specific volume v_0 must be used because the amount of air to be supplied is based on 6000 L/s at outdoor conditions, $v_0 = 0.893 \text{ m}^3/\text{kg}$. Then,

$$t_1 = 26 - \frac{59,000(0.893)}{1.02(6000)} = 17.4^\circ\text{C}$$

Now, point 1 can be located on ASHRAE Psychrometric Chart 1 (ASHRAE 1992) and the entering air condition noted as about 17°C dB and 15°C wB. The volume flow rate of air at state 1 will be

$$\text{L/s}_1 = \text{L/s}_0 \left(\frac{v_1}{v_0} \right) = 6000 \left(\frac{0.835}{0.893} \right) = 5598$$

A line is now drawn from the outdoor condition at point 0 to point 1, the entering air state. This line represents the coil cooling process. Using Equation 9.3,

$$q_c = \text{L/s}(h_o - h_1)/v_o$$

$$q_c = \frac{6000}{0.893}(72 - 41) = 208,287 \text{ W}$$

The use of all outdoor air more than doubles the refrigeration load compared to no outdoor air at all. Referring to ASHRAE Psychrometric Chart 1 (ASHRAE 1992), the coil sensible heat factor (CSHF) = 0., and other operating parameters are the following:

Entering Air:	6000 L/s standard sea-level pressure 35°C dB 24°C wB
Leaving Air:	17°C dB 15°C wB

The coil sensible load could have been computed using Equation 9.1b and the total coil load then obtained using the CSHF.

9.2 Off-Design (Nonpeak) Conditions

The previous section treated the common space air-conditioning problem by assuming that the system was operating steadily at the design condition. Actually, the space requires only a part of the designed capacity of the conditioning equipment most of the time. A control system functions to match the required cooling or heating of the space to the conditioning equipment by varying one or more system parameters. For example, the quantity of air circulated through the coil and to the space may be varied in proportion to the space load, as in the variable-air-volume (VAV) system. Another approach is to circulate a constant amount of air to the space but divert some of the

Air Systems, Loads, IAQ, and Psychrometrics

return air around the coil and mix it with air coming off the coil to obtain a supply air temperature that is proportional to the space load. This is known as a *face and bypass system*. Another possibility is to vary the coil surface temperature with respect to the required load by changing the amount of heating or cooling fluid entering the coil. This technique usually is used in conjunction with VAV and face and bypass systems.

Figure 9.15a illustrates what might occur when the load on a VAV system decreases. The solid lines represent a full-load design condition, whereas the broken lines illustrate a part-load condition where the amount of air circulated to the space and across the coil has decreased. Note that the state of the outdoor air O' has changed and could be almost anywhere on the chart under part-load conditions. Because of the lower airflow rate through the coil, the air is cooled to a lower temperature and humidity. The room thermostat maintains the space temperature, but the humidity in the space may decrease. However, the process $2'-3'$ depends on the RSHF for the partial load. This explains why control of the water temperature or flow rate is desirable. Decreasing the water flow rate will cause point $2'$ to move upward and to the right to a position where the room process curve may terminate nearer to point 3.

The behavior of a constant-air-volume face and bypass system is shown in Figure 9.15b. The total design airflow rate is flowing at states 2, 3, and $3'$, but a lower flow rate occurs at state $2'$, leaving the coil. Air at states $2'$ and $1'$ is mixed downstream of the coil to obtain State 4. The total design flow rate and the enthalpy difference $h_3' - h_4$ then match the space load. Note that the humidity at state 4 may be higher or lower than necessary, which makes state $3'$ vary from the design value. At very small space loads, point 4 may be located very near state $1'$ on the condition line. In this case, the humidity in the space may become high. This is a disadvantage of a multizone face and bypass system. Control of the coil water flow rate can help to correct this problem.

A constant-air-volume system with water flow rate control is shown in Figure 9.15c. In this case, both the temperature and humidity of the air leaving the coil usually increase, and the room process curve $2'-3'$ may not terminate at state 3. In most cases, state $3'$ will lie above state 3, causing an uncomfortable condition in the space. For this reason, water control alone usually is not used in commercial applications but is used in conjunction with VAV and face and bypass systems, as discussed previously. In fact, all water coils should have control of the water flow rate. This also is important to the operation of the water chiller and piping system. The following example illustrates the analysis of a VAV system with variable water flow.

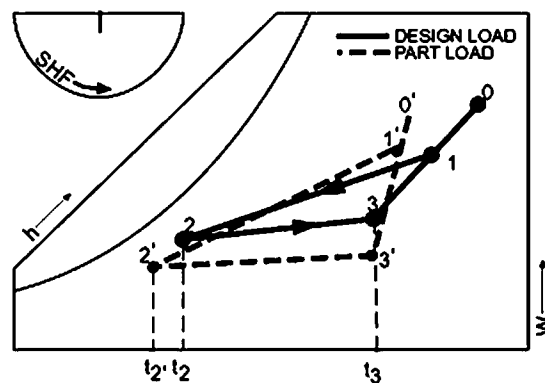


Figure 9.15a Processes for off-design VAV system operation.

Source: *Cooling and Heating Load Calculation Principles*, Figure 8.15a).

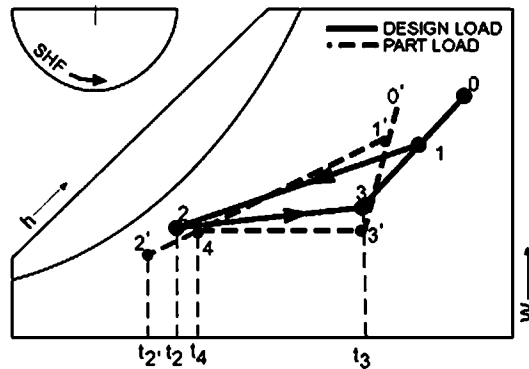


Figure 9.15b Processes for off-design face and bypass system operation.
(Source: *Cooling and Heating Load Calculation Principles*, Figure 8.15b).

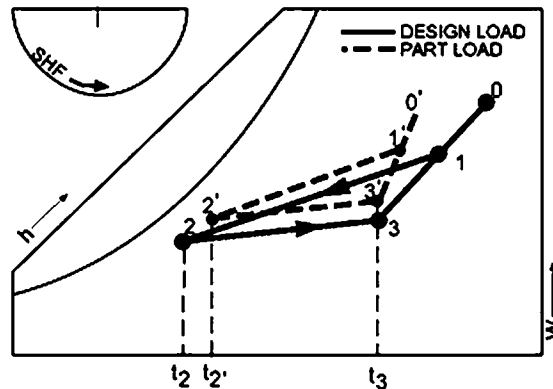


Figure 9.15c Processes for off-design variable water flow system operation.
(Source: *Cooling and Heating Load Calculation Principles*, Figure 8.15c).

Example 9.6
Coil for
VAV System

A VAV system operates as shown in Figure 9.16. The solid lines show the full-load design condition of 350 kW with a room SHF of 0.75. At the estimated minimum load of 50 kW with an SHF of 0.9, the airflow rate is decreased to 20% of the design value and all outdoor air is shut off. Estimate the supply air and apparatus dew-point temperatures of the cooling coil for minimum load, assuming that state 3 does not change.

Solution: The solution is best carried out using ASHRAE Psychrometric Chart 1 (ASHRAE 1992), as shown in Figure 9.16. Because the outdoor air is off during the minimum load condition, the space condition and coil process lines will coincide as shown by line 3-2'-d'. This line is constructed by using the protractor of ASHRAE Psychrometric Chart 1 with an SHF of 0.9. The apparatus dew point is seen to be 13°C, compared with 11°C for the design condition. The airflow rate for the design condition is given by Equation 9.1b:

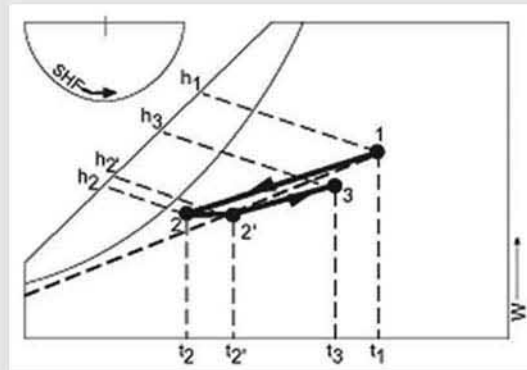


Figure 9.18 Psychrometric processes for Example 9.7.

(Source: *Cooling and Heating Load Calculation Principles*, Figure 8.18).

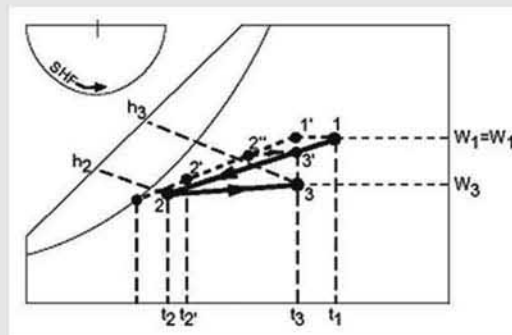


Figure 9.19 Psychrometric processes for Example 9.8.

(Source: *Cooling and Heating Load Calculation Principles*, Figure 8.19).

The volume flow rate of air entering the coil is from above:

$$L/s_1 = 1536 \frac{0.87}{0.83} = 1610$$

with air entering at 29°C dB and 21°C wB and air leaving at 12°C dB and 11°C wB. The reheat coil has a capacity of

$$q_r = \frac{1.02 L/s'_2 (t'_2 - t_2)}{v'_2} = \frac{1.02(1536)(16 - 12)}{0.83} = 7552 \text{ W}$$

9.2.2 Coil Bypass System

The following example relates to coil bypass control.

Example 9.8 Coil Bypass

A space is conditioned by a multizone unit using bypass control. The design operating condition for the space is shown in Figure 9.19 by process 2-3, where t_3 is thermostatically controlled at 24°C dB.

Consider a part-load condition where the space cooling load is one-third the design value with an RSHF of 0.9. Assume that the coil will operate with the same apparatus dew point as the design condition and the air will enter the coil at 24°C dB with the same humidity ratio as the design condition. The air leaving the coil will have a relative humidity of about 90%. Find the space condition and the coil bypass ratio.

Solution: The design operating condition is shown in Figure 9.19. These processes and the partial load coil process 1'-2' are then drawn on ASHRAE Psychrometric Chart 1 (ASHRAE 1992). The partial load condition line 2''-3' is not known at this point, but point 3' will lie on the 24°C dB temperature line and point 2'' will lie on process line 1'-2'. The design load is given by

$$q = m_2(h_3 - h_2)$$

and the partial load is

$$q_0 = \frac{m_2(h_3 - h_2)}{3}$$

Also, the partial sensible load is given by

$$q_{s0} = (\text{RSHF})q_0 = m_2 c_p (t'_3 - t''_2)$$

Then substituting for q_0 and noting that $t'_3 = t_3$,

$$t''_2 = t_3 - \frac{(\text{RSHF})(h_3 - h_2)}{3c_p}$$

$$t''_2 = 24 - \frac{0.9(48.2 - 36)}{3(1.02)} = 20.4^\circ\text{C dB}$$

Process 2''-3' can now be drawn on ASHRAE Psychrometric Chart 1 (ASHRAE 1992). The space condition is given by point 3' as 24°C dB and 18.5°C wB with a relative humidity of 60%. Note that this may be an uncomfortable condition for occupants; however, there is no practical way to avoid this with bypass control. The bypass ratio is

$$\text{BR} = \frac{\text{Amount of air bypassed at state 1}'}{\text{Amount of air cooled at state 2}'}$$

Because adiabatic mixing is occurring, the ratio is given by the length of the line segments from ASHRAE Psychrometric Chart 1 (ASHRAE 1992):

$$\text{BR} = \frac{2' - 2''}{2' - 1'} = 0.6$$

9.2.3 Dual-Duct System

The purpose of a dual-duct system is to adjust to highly variable conditions from zone to zone and to give accurate control. Figure 9.20 offers a schematic of such a system, showing one typical zone, and Figure 9.21 shows the processes on

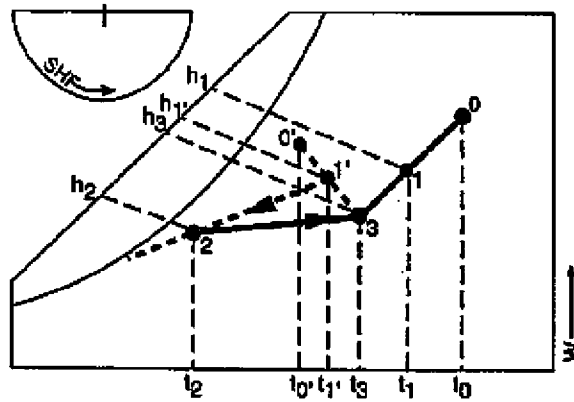


Figure 9.22 Psychrometric processes for economizer cycle.

(Source: *Cooling and Heating Load Calculation Principles*, Figure 8.22).

Figure 9.22. Assume that the condition line 2-3 does not change, but state 0 changes to state 0'. Theoretically, a mixed state 1' located anywhere on line 0'-3 could occur, but the air must be cooled and dehumidified to state 2. To do this, the coil apparatus dew point must be reasonable. Values below about 9°C are not economical to attain. Therefore, state 1' must be controlled to accommodate the coil. It can be seen in Figure 9.22 that moving state 1' closer to state 0' lowers the coil apparatus dew point rapidly and it soon reaches the condition where the coil process line will not intersect the saturation curve, indicating an impossible condition. It is obvious in Figure 9.22 that less energy is required to cool the air from state 1' to 2 than from state 1 to 2. There are many other possibilities that must be analyzed on their own merits. Some may require more or less outdoor air, humidification, or reheat to reach state 2.

References

- ASHRAE. 1992. *ASHRAE Psychrometric Chart 1*. Atlanta: ASHRAE.
- ASHRAE. 2013. ANSI/ASHRAE Standard 62.1-2013, *Ventilation for Acceptable Indoor Air Quality*. Atlanta: ASHRAE.
- Pedersen, C.O., D.E. Fisher, J.D. Spitler, R.J. Liesen. 1998. *Cooling and Heating Load Calculation Principles*. Atlanta: ASHRAE.

Heating Load Calculations

Before a heating system is designed, the maximum probable heat loss from each room or space to be heated must be estimated. There are three kinds of heat losses: (1) heat transmitted through walls, ceiling, floor, glass, or other surfaces; (2) heat required to warm outdoor air entering the space; and (3) the heat needed to warm or thaw significant quantities of materials brought into the space.

The actual heat loss problem is transient because the outdoor temperature, wind velocity, and sunlight are constantly changing. During the coldest months, however, sustained periods of very cold, cloudy, and stormy weather with relatively small variation in outdoor temperature may occur. In this situation, heat loss from the space will be relatively constant and, in the absence of internal heat gains, will peak during the early morning hours. Therefore, for design purposes, the heat loss usually is estimated based on steady-state heat transfer for some reasonable design temperature. Transient analyses often are used to study the actual energy requirements of a structure in simulation studies. In such cases, solar effects and internal heat gains are taken into account.

The practice of temperature setback has become a relatively common method of saving on heating energy costs. This control strategy causes a transient variation in the room temperature that may have an effect on the peak heating load and the comfort of the occupants. Such calculations should be done using the heat balance procedure described in Chapter 11.

In this chapter, two options for performing a steady-state heating load calculation are described:

1. It can be done with a cooling load calculation procedure, if the right assumptions are applied (Section 10.1).
2. It can be done as a separate, stand-alone steady-state calculation in a spreadsheet or by hand (the classic heat loss calculation described in Section 10.2).

10.1 Heating Load Using Cooling Load Calculation Procedures

In theory, any cooling load calculation procedure can also be used to calculate heating loads. It is simply a matter of differing assumptions. For heating load calculations, the differences are as follows:

1. There is no solar input, as the peak heating load is assumed to occur at night. If a dedicated cooling load calculation computer program is used, it may have an option that turns off the solar input. If not, it may be possible to turn off the solar input by setting the clearness to zero.
2. It is generally assumed that there are no internal heat gains (e.g., people, lights, equipment), and these may be set to zero by the user.
3. Constant outdoor temperatures are assumed; this may be done by setting the daily range to zero.
4. In cooling load calculations, it is often assumed that there is no net heat transfer to or from the ground via foundation elements. For heating load calculations, these losses should be included in the calculation. Calculation procedures are described in Section 10.2.

Load Calculation Applications Manual (SI), Second Edition

10.2 Classic Heat Loss Calculations

The general procedure for calculation of design heat losses of a structure is as follows:

1. Select the outdoor design conditions: temperature, humidity, and wind direction and speed (Chapter 4).
2. Select the indoor design conditions to be maintained (Chapter 4).
3. Estimate the temperature in any adjacent unheated spaces.
4. Select the transmission coefficients (Chapter 3) and compute the heat losses for walls, floors, ceilings, windows, doors, and foundation elements.
5. Compute the heat load caused by infiltration and any other outdoor air introduced directly to the space (Chapter 5).
6. Find the sum of the losses due to transmission and infiltration.

10.2.1 Outdoor Design Conditions

The ideal heating system would provide enough heat to match the heat loss from the structure. However, weather conditions vary considerably from year to year, and heating systems designed for the worst weather conditions on record would have a great excess of capacity most of the time. The failure of a system to maintain design conditions during brief periods of severe weather usually is not critical. However, close regulation of indoor temperature may be critical for some occupancies or industrial processes. Design temperature data are provided in Chapter 4, along with a discussion of the application of these data. Generally, it is recommended that the 99% temperature values given in the tabulated weather data be used. However, caution should be exercised and local conditions always investigated. In some locations, outdoor temperatures are commonly much lower and wind velocities higher than those given in the tabulated weather data.

10.2.2 Indoor Design Conditions

The main purpose of the heating system is to maintain indoor conditions that make most of the occupants comfortable. It should be kept in mind, however, that the purpose of heating load calculations is to obtain data for sizing the heating system components. In many cases, the system will rarely be called upon to operate at the design conditions. Therefore, the use and occupancy of the space is a general consideration from the design temperature point of view. Later, when the energy requirements of the building are computed, the actual conditions in the space and outdoor environment, including internal heat gains, must be considered.

The indoor design temperature should be selected at the lower end of the acceptable temperature range so that the heating equipment will not be oversized. Even properly sized equipment operates under partial load at reduced efficiency most of the time. Therefore, any oversizing aggravates this condition and lowers the overall system efficiency. A maximum design dry-bulb temperature of 21°C is recommended for most occupancies. The indoor design value of relative humidity should be compatible with a healthful environment and the thermal and moisture integrity of the building envelope. A maximum relative humidity of 30% is recommended for most situations.

10.2.3 Calculation of Transmission Heat Losses

Exterior Surface Above Grade

All above-grade surfaces exposed to outdoor conditions (e.g., walls, doors, ceilings, fenestration, and raised floors) are treated identically, as follows:

Heating Load Calculations

$$q = A \cdot HF \quad (10.1)$$

$$HF = U \Delta t \quad (10.2)$$

where HF is the heating load factor in W/m^2 .

Below-Grade Surfaces

An approximate method for estimating below-grade heat loss (based on the work of Latta and Boileau [1969]) assumes that the heat flow paths shown in Figure 10.1 can be used to find the steady-state heat loss to the ground surface, as follows:

$$HF = U_{avg}(t_{in} - t_{gr}) \quad (10.3)$$

where

U_{avg} = average U-factor for below-grade surface, $W/(m^2 \cdot K)$, from Equation 10.5 or 10.6

t_{in} = below-grade space air temperature, $^{\circ}C$

t_{gr} = design ground surface temperature, $^{\circ}C$, from Equation 10.4

The effect of soil heat capacity means that none of the usual external design air temperatures are suitable values for t_{gr} . Ground surface temperature fluctuates about an annual mean value by amplitude A , which varies with geographic location and surface cover. The minimum ground surface temperature, suitable for heat loss estimates, is therefore

$$t_{gr} = \bar{t}_{gr} - A \quad (10.4)$$

where

\bar{t}_{gr} = mean ground temperature, $^{\circ}C$, estimated from the annual average air temperature or from well-water temperatures, shown in Figure 17 of Chapter 34 in the *ASHRAE Handbook—HVAC Applications* (2011)

A = ground-surface temperature amplitude, $^{\circ}C$, from Figure 10.2 for North America

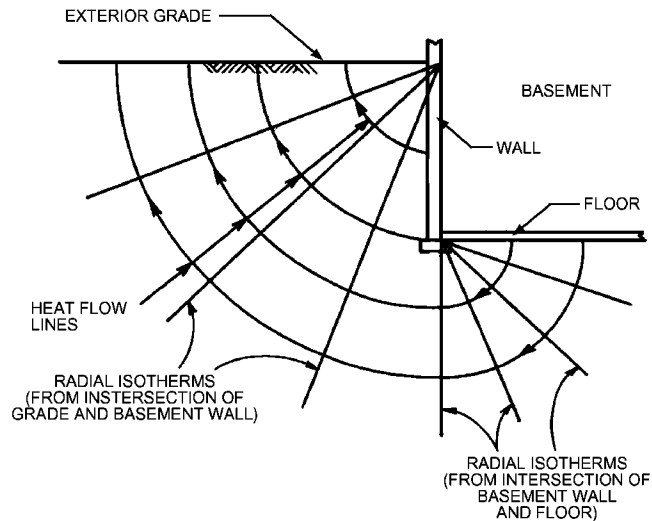


Figure 10.1 Heat flow from below-grade surfaces.

(Source: *ASHRAE Handbook—Fundamentals* [2013], Chapter 18, Figure 12).

Load Calculation Applications Manual (SI), Second Edition

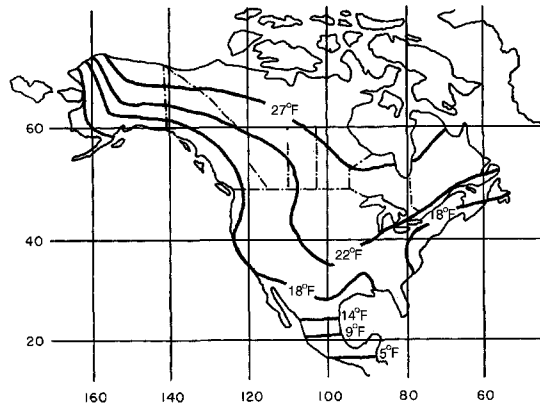


Figure 10.2 Ground temperature amplitudes for North America.
 (Source: ASHRAE Handbook—Fundamentals [2013], Chapter 18, Figure 13).

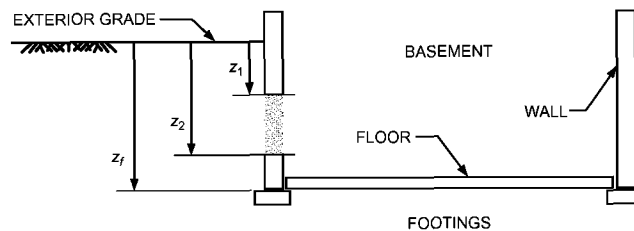


Figure 10.3 Below-grade depth parameters.
 (Source: ASHRAE Handbook—Fundamentals [2013], Chapter 18, Figure 14).

Figure 10.3 shows depth parameters used in determining U_{avg} . For walls, the region defined by z_1 and z_2 may be the entire wall or any portion of it, allowing partially insulated configurations to be analyzed piecewise.

The below-grade wall average U-factor is given by

$$U_{avg,bw} = \frac{2k_{soil}}{\pi(z_2 - z_1)} \cdot \left[\ln\left(z_2 + \frac{2k_{soil}R_{other}}{\pi}\right) - \ln\left(z_1 + \frac{2k_{soil}R_{other}}{\pi}\right) \right] \quad (10.5)$$

where

- $U_{avg,bw}$ = average U-factor for wall region defined by z_1 and z_2 , W/(m²·K)
- k_{soil} = soil thermal conductivity, W/(m·K)
- R_{other} = total resistance of wall, insulation, and inside surface resistance, (m²·K)/W
- z_1, z_2 = depths of top and bottom of wall segment under consideration, m (see Figure 10.3)

The value of the soil thermal conductivity k varies widely with soil type and moisture content. A typical value of 1.4 W/(m·K) has been used previously to tabulate U-factors, and R_{other} is approximately 10.259 (m²·K)/W for uninsulated concrete walls. For these parameters, representative values for $U_{avg,bw}$ are shown in Table 10.1.

The average below-grade floor U-factor (where the entire basement floor is uninsulated or has uniform insulation) is given by

Heating Load Calculations

Table 10.1 Average U-Factors for Basement Walls with Uniform Insulation

(Source: ASHRAE Handbook—Fundamentals [2013], Chapter 18, Table 22)

Depth, m	$U_{avg,bw}$ from Grade to Depth, W/(m ² ·K)			
	Uninsulated	R-0.88	R-1.76	R-2.64
0.3	2.468	0.769	0.458	0.326
0.6	1.898	0.689	0.427	0.310
0.9	1.571	0.628	0.401	0.296
1.2	1.353	0.579	0.379	0.283
1.5	1.195	0.539	0.360	0.272
1.8	1.075	0.505	0.343	0.262
2.1	0.980	0.476	0.328	0.252
2.4	0.902	0.450	0.315	0.244

Soil conductivity = 1.4 W/(m·K); insulation is over entire depth. For other soil conductivities and partial insulation, use Equation 10.5.

Table 10.2 Average U-Factors for Basement Floors

(Source: ASHRAE Handbook—Fundamentals [2013], Chapter 18, Table 23)

z_f (Depth of Floor Below Grade), m	$U_{avg,bf}$ W/(m ² ·K)			
	w_b (Shortest Width of Basement), m			
	6	7	8	9
0.3	0.370	0.335	0.307	0.283
0.6	0.310	0.283	0.261	0.242
0.9	0.271	0.249	0.230	0.215
1.2	0.242	0.224	0.208	0.195
1.5	0.220	0.204	0.190	0.179
1.8	0.202	0.188	0.176	0.166
2.1	0.187	0.175	0.164	0.155

Soil conductivity is 1.4 W/(m·K); floor is uninsulated. For other soil conductivities and insulation, use Equation 10.5.

$$U_{avg,bf} = \frac{2k_{soil}}{\pi w_b} \cdot \left[\ln\left(\frac{w_b}{2} + \frac{z_f}{2} + \frac{k_{soil}R_{other}}{\pi}\right) - \ln\left(\frac{z_f}{2} + \frac{k_{soil}R_{other}}{\pi}\right) \right] \quad (10.6)$$

where

w_b = basement width (shortest dimension), m

z_f = floor depth below grade, m (see Figure 10.3)

Representative values of $U_{avg,bf}$ for uninsulated basement floors are shown in Table 10.2.

At-Grade Surfaces

Concrete slab floors may be (1) unheated, relying for warmth on heat delivered above floor level by the heating system, or (2) heated, containing heated pipes or ducts that constitute a radiant slab or portion of it for complete or partial heating of the building.

Load Calculation Applications Manual (SI), Second Edition

The simplified approach that treats heat loss as proportional to slab perimeter allows slab heat loss to be estimated for both unheated and heated slab floors:

$$q = p \cdot HF \quad (10.7)$$

$$HF = F_p \Delta t \quad (10.8)$$

where

q = heat loss through perimeter, W

F_p = heat loss coefficient per meter of perimeter, W/(m·K) (Table 10.3)

p = perimeter (exposed edge) of floor, m

Surfaces Adjacent to Buffer Space

Heat loss to adjacent unconditioned or semiconditioned spaces can be calculated using a heating factor based on the partition temperature difference:

$$HF = U(t_{in} - t_b) \quad (10.9)$$

10.2.4 Infiltration

All structures have some air leakage or infiltration. This means heat loss will occur because the cold, dry outdoor air must be heated to the inside design temperature and moisture must be added to increase the humidity to the design value. Procedures for estimating the infiltration rate are discussed in Chapter 5.

Once the infiltration rate has been calculated, the resulting sensible heat loss, equivalent to the sensible heating load due to infiltration, is given by

$$q_s = Q\rho c_p(t_{in} - t_o) \quad (10.10)$$

where

Q = volume flow rate of the infiltrating air, m³/s

c_p = specific heat capacity of the air, J/(kg·K) (about 1000)

ρ = density of the infiltrating air, kg/m³ (about 1.2)

Assuming standard air conditions (15°C and sea-level conditions) for ρ and c_p , Equation 10.10 may be written as

$$q_s = 1230Q(t_{in} - t_o) \quad (10.11)$$

Table 10.3 Heat Loss Coefficient F_p of Slab Floor Construction

(Source: ASHRAE Handbook—Fundamentals [2013], Chapter 18, Table 24)

Construction	Insulation	F_p , W/(m·K)
200 mm block wall, brick facing	Uninsulated	1.17
	R-0.95 (m ² ·K)/W from edge to footer	0.86
100 mm block wall, brick facing	Uninsulated	1.45
	R-0.95 (m ² ·K)/W from edge to footer	0.85
Metal stud wall, stucco	Uninsulated	2.07
	R-0.95 (m ² ·K)/W from edge to footer	0.92
Poured concrete wall with duct near perimeter*	Uninsulated	3.67
	R-0.95 (m ² ·K)/W from edge to footer	1.24

*Weighted average temperature of the heating duct was assumed at 43°C during heating season (outdoor air temperature less than 18°C).

Heating Load Calculations

The infiltrating air also introduces a latent heating load given by

$$q_l = Q\rho(W_{in} - W_o)(2501 + 1.805t) \quad (10.12)$$

where

W_{in} = humidity ratio for the inside space air, g/kg

W_o = humidity ratio for the outdoor air, g/kg

t = average of indoor and outdoor temperatures, °C

For standard air and nominal indoor comfort conditions (15°C and 22°C, respectively), the latent load may be expressed as

$$q_l = 3040Q(W_{in} - W_o) \quad (10.13)$$

The coefficients 1230 in Equation 10.11 and 3040 in Equation 10.13 are given for standard conditions. They actually depend on temperature and altitude (and, consequently, pressure). Appendix A gives formulations based on temperature and altitude.

10.2.5 Heat Losses in the Air Distribution System

The losses of a duct system must be considered when the ducts are not in the conditioned space. Proper insulation will reduce these losses but cannot completely eliminate them. The losses may be estimated using the following relation:

$$q = UA_sDt_m \quad (10.14)$$

where

U = overall heat transfer coefficient, W/(m²·K)

A = outside surface area of the duct, m²

Dt_m = mean temperature difference between air in the duct and the environment, °C

When the duct is covered with 3 or 5 cm of insulation that has a reflective covering, the heat loss usually will be reduced sufficiently to assume that the mean temperature difference is equal to the difference in temperature between the supply air temperature and the environmental temperature. Unusually long ducts should not be treated in this manner, and a mean air temperature should be used instead.

It is common practice to estimate heat loss or gain to air ducts by simply assuming a small percentage of the sensible load. For well-insulated ducts, a 2% to 5% loss would be reasonable. It should be noted that heat loss from the supply air ducts represents a load on the space, while heat loss from the return air ducts represents a load on the heating equipment.

10.2.6 Auxiliary Heat Sources

The heat energy supplied by people, lights, motors, and machinery should always be estimated, but any actual allowance for these heat sources requires careful consideration. People may not occupy certain spaces in the evenings, on weekends, and during other periods, and these spaces generally must be heated to a reasonably comfortable temperature prior to occupancy. Therefore, it is customary to ignore internal heat gain in the heating load calculation for most spaces. Heat sources in industrial plants, if available during occupancy, should be substituted for part of the heating requirement. In fact, there are situations where so much heat energy is available that outdoor air must be used to prevent overheating of the space. However, sufficient heating equipment must still be provided to prevent freezing or other damage during periods when a facility is shut down.

10.3 Heating Load Calculation Example

This section gives a start-to-finish example of calculating the heating load for a single room. Rather than starting from building plans, determining U-factors, etc., we will compute the heating load for the office used as an example in Chapters 7 and 8, where there was a full discussion of issues such as determination of U-factors, areas, etc. That office is on the second floor. Since heat losses through foundation elements are often important for heating loads, we will consider the room both as a second-story room and as if it were moved to the first story and the existing floor was replaced with a slab-on-grade floor.

10.3.1 Room Description and Design Conditions

A more detailed description of the room can be found in Chapter 8; the description here extracts the relevant information from that chapter. Table 10.4 summarizes the exterior surfaces of the room. (Note that for the steady-state heating load calculation, the interior surfaces do not store and discharge heat, so they may be ignored for the calculation.) As described in Chapter 8, the walls and roof assumed an exterior surface conductance of 23 W/(m²·K). As shown in Table 3.4, this is consistent with summer design conditions. For winter, a value of 34 W/(m²·K) was taken. This value was used to compute the U-factors for the opaque surfaces. For the windows, the calculated value of 1.82 W/(m²·K) was used.

Selection of design conditions depends on the application; here the 99% annual heating design condition, -3.1 °C, will be used as the outdoor condition and 21°C will be used as the indoor condition. This gives a Δt of 24.1°C. For purposes of estimating latent heat losses, desired indoor conditions are chosen at 50% relative humidity. For outdoor conditions, the 99% outdoor humidity condition 1.3 grams of water vapor per kilogram of dry air will be used. Infiltration of 9.44 L/s based on 1 ach is assumed for this example.

10.3.2 Heating Load without Floor Losses

For the first part of this example, with the office located on the second floor and conditioned office space below, there is no net heat loss from the floor. In this case, the heating load is composed of heat losses from exterior, above-grade surfaces and infiltration. The heat losses from exterior, above-grade surfaces are determined with the heating factors defined in Section 10.2.3. Heating factors are computed with Equation 10.2 by multiplying the U-factors by the Δt of 24.1°C. The resulting heating factors are given in Table 10.5. The heat losses from each surface are then determined with Equation 10.1 and given in the last column of Table 10.5.

Table 10.4 Exterior Surfaces

Surface Name	Area, m ²	U, (W/m ² ·K)
Southeast brick	5.667	0.312
Southeast spandrel	1.487	0.386
Southeast window	3.716	1.873
Southwest brick	3.159	0.312
Southwest spandrel	1.487	0.386
Southwest window	3.716	1.873
Roof	12.077	0.182

Heating Load Calculations

The sensible infiltration heat loss may be computed using Equation 10.11:

$$q_s = 1230(9.44/1000 \text{ m}^3/\text{s})[21^\circ\text{C} - (-3.1^\circ\text{C})] = 280 \text{ W}$$

To compute latent infiltration heat loss from Equation 10.13, the indoor and outdoor humidity ratios must be determined. The indoor humidity was given as 50% relative humidity at 21°C. From the psychrometric chart, this is about 7.8 g/kg. The exterior humidity ratio was given as 1.3 grams of water vapor per kilogram of dry air. With 7000 grains per kilogram, this is equivalent to 1.3 g/kg. The latent infiltration heat loss may be computed using Equation 10.13:

$$q_s = 3040(9.44/1000 \text{ m}^3/\text{s})(7.8 - 1.3) = 187 \text{ W}$$

Totaling all of the heat losses, the total sensible heating load is 484 + 280 = 764 W. The total latent heating load is 187 W.

10.3.3 Heating Load with Slab-on-Grade Floor Losses

If the office is moved to the ground floor (while retaining its roof), the heating load would simply be increased by the heat loss through the slab-on-grade floor. The calculation procedure is described in Section 10.2.3 and requires the use of Equations 10.7 and 10.8. The exposed perimeter p of the office is the sum of the lengths of the southeast and southwest walls, or 7 m. The heat loss coefficient can be estimated using Table 10.3. The spandrel/brick wall construction does not obviously fit into any of the categories in Table 10.3. But given the range of constructions, a worse case might be the metal stud wall/stucco construction with an F_p of 2.07 W/(m·K). Then, from Equation 10.8, the heating factor for the slab-on-grade floor is

$$HF = 2.07 \text{ W/(m}\cdot\text{K)} \cdot 24.1^\circ\text{C} = 49.9 \text{ W/m}$$

and the heat loss from Equation 10.7 is

$$q = 7 \cdot 49.9 = 349 \text{ W}$$

So, with the slab-on-grade floor, totaling all of the heat losses, the total sensible heating load is 484 + 280 + 349 = 1113 W. The total latent heating load remains 187 W.

Table 10.5 Exterior, Above-Grade Surface Heat Losses

Surface	Area, m ²	U , W/(m ² ·K)	HF , W/m ²	q , W
Southeast brick	5.667	0.312	7.57	43
Southeast spandrel	1.487	0.386	9.46	14
Southeast window	3.716	1.873	45.08	168
Southwest brick	3.159	0.312	7.57	24
Southwest spandrel	1.487	0.386	9.46	14
Southwest window	3.716	1.873	45.08	168
Roof	12.077	0.182	4.41	53
Total	—	—	—	484

Load Calculation Applications Manual (SI), Second Edition

References

- ASHRAE. 2013. *ASHRAE Handbook—Fundamentals*. Atlanta: ASHRAE.
- ASHRAE. 2011. *ASHRAE Handbook—HVAC Applications*. Atlanta: ASHRAE.
- Latta, J.K., and G.G. Boileau. 1969. Heat losses from house basements. Housing Note No. 31, National Research Council of Canada, Division of Building Research, Ottawa, Ontario, Canada.

The heat balance processes introduced briefly in Chapter 2 are described in more detail in this chapter. The resolution of the simultaneous heat balance processes requires an iterative solution. It is not realistic to consider doing that without the aid of a computer. The heat balance concept is fundamental to both the heat balance method (HBM) and the radiant time series method (RTSM). To make the model useful, the concepts must be translated into mathematical form, then arranged into an overall solution scheme. This is done in this chapter.

In the following sections, the fundamentals of the HBM are discussed in the context of the outside face, inside face, and air-heat balances and wall conduction. The discussion is intended to present the physical processes in mathematical terms. This is followed by a brief discussion of the overall solution procedure.

In most cases, the surface heat balances are formulated on the basis of heat flux. The heat flux, which is defined as the rate of heat transfer per unit area (q/A) perpendicular to the direction of transfer, is denoted by the symbol q'' . The subscript on q'' shows the mode of heat transfer (conduction, convection, or radiation).

11.1 Outside Face Heat Balance

The heat balance at the outside face of an exterior zone wall is modeled with four heat exchange processes. Figure 11.1 shows this balance schematically.

The heat balance on the outside face is

$$q''_{\alpha sol} + q''_{LWR} + q''_{conv} - q''_{ko} = 0 \quad (11.1)$$

where

- $q''_{\alpha sol}$ = absorbed direct and diffuse solar (short-wavelength) radiation heat flux
- q''_{LWR} = net long-wavelength (thermal) radiation flux exchange with the air and surroundings

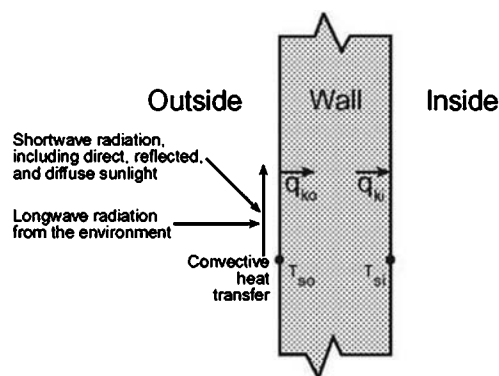


Figure 11.1 Schematic of surface heat balance.

(Source: *Cooling and Heating Load Calculation Principles*, Figure 2.1).

Load Calculation Applications Manual (SI), Second Edition

$$q''_{conv} = \text{convection flux exchange with outdoor air}$$
$$q''_{ko} = \text{conduction heat flux } (q/A) \text{ into the wall}$$

All terms are positive for net flux to the face except the conduction term, which traditionally is taken to be positive in the direction from outside to inside of the wall. Simplified procedures generally combine the first three terms by using the concept of a sol-air temperature.

The implementation of the HBM described here uses fundamental but simple solar, environmental, and outside convection models to calculate the terms of the outside heat balance where

- $q''_{a,sol}$ is calculated using the procedures from Appendix D
- $q''_{conv} = h_{co}(T_{air} - T_o)$, where h_{co} is the Yazdanian and Klems (1994) natural convection correlation (McClellan and Pedersen 1997), which is based on air and surface temperatures and is slightly more conservative than the ASHRAE constant coefficient¹ of $17.8 \text{ W/m}^2\cdot\text{K}$.
- q''_{LWR} is a standard radiation exchange formulation between the surface, the sky, and the ground. The radiation heat flux is calculated from the surface absorptance, surface temperature, sky and ground temperatures, and sky and ground view factors.
- The conduction term q''_{ko} is calculated using a transfer function method described in Section 11.2.

11.2 Wall Conduction Process

There are numerous ways to formulate the wall conduction process (*cf.* Spitler 1996), which is a topic that has received much attention over the years. Possible ways to model this process include the following:

- Numerical methods (e.g., finite difference, finite volume, and finite element methods)
- Transform methods
- Time series methods

The wall conduction process introduces part of the time dependence inherent in the load calculation process (Figure 11.2).

Figure 11.2 shows face temperatures on the inside and outside faces of the wall element and corresponding inside and outside heat fluxes. All four of these quantities are functions of time. The direct formulation of the process has the two temperature functions as input or known quantities and the two heat fluxes as outputs or resultant quantities.

In all simplified methods, including the RTSM formulation, the face heat transfer coefficients are included as part of the wall element. Then the temperatures in question are the indoor and outdoor air temperatures. This simplification hides the heat transfer coefficients and precludes changing them as airflow conditions change. It also precludes modeling the nonlinear aspects of internal longwave radiation exchange.

Because the heat balances on both sides of the element incorporate both the temperatures and heat fluxes, the solution technique must be able to deal with all quantities simultaneously. From a computational standpoint, the conduction transfer

1. The value of 3.1 represents the convective portion of the outside surface conductance under summer conditions given in Table 3.4. It is referred to here as the "ASHRAE" coefficient because the values in Table 3.4 have appeared in ASHRAE and predecessor societies' literature since the 1930s.

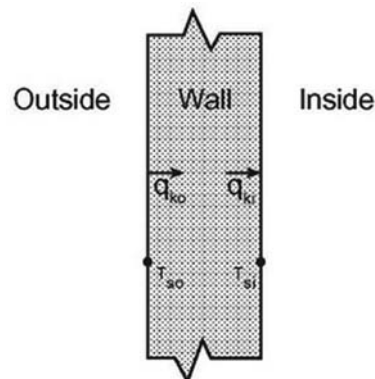


Figure 11.2 Conduction terms of the surface heat balance.

(Source: *Cooling and Heating Load Calculation Principles*, Figure 2.2).

function (CTF) procedure offers much greater computational speed than numerical methods with little loss of generality. It has therefore been used with the HBM. The CTF formulation relates the conductive heat fluxes to the current and past surface temperatures and the past heat fluxes. The general form for the inside heat flux is

$$q_{ki}''(t) = -z_o T_{i,t} - \sum_{j=1}^{nz} z_j T_{i,t-j\delta} + Y_o T_{o,t} + \sum_{j=1}^{nz} Y_j T_{o,t-j\delta} + \sum_{j=1}^{nq} \Phi_j q_{ki,i,t-j\delta} \quad (11.2)$$

and the outside heat flux is

$$q_{ko}''(t) = -Y_o T_{i,t} - \sum_{j=1}^{nz} z_j T_{i,t-j\delta} + X_o T_{o,t} + \sum_{j=1}^{nz} X_j T_{o,t-j\delta} + \sum_{j=1}^{nq} \Phi_j q_{ko,i,t-j\delta} \quad (11.3)$$

where

X_j = outside CTF, $j = 0, 1, \dots, nz$

Y_j = cross CTF, $j = 0, 1, \dots, nz$

Z_j = inside CTF, $j = 0, 1, \dots, nz$

Φ_j = flux CTF, $j = 0, 1, \dots, nq$

T_i = inside surface temperature

T_o = outside face temperature

q_{ko}'' = conduction heat flux on outside face

q_{ki}'' = conduction heat flux on inside face

The subscript following the comma indicates the time period for the quantity in terms of the time step σ (e.g., X_1 is applied to the temperature one time step earlier). The first terms in the series (those with subscript 0) have been separated from the rest to facilitate solving for the current temperature in the solution scheme.

The two summation limits, nz and nq , are dependent on the wall construction and somewhat dependent on the scheme used for calculating the CTFs. If $nq = 0$, the CTFs generally are referred to as *response factors*, but then theoretically nz is infinite. The values for nz and nq generally are set to minimize the amount of computation. Procedures for determining CTFs are cited by Spitler (1996), and one procedure for computing CTFs is described in detail by Hittle (1979).

Load Calculation Applications Manual (SI), Second Edition

11.3 Inside Face Heat Balance

The heart of the HBM is the internal heat balance involving the inside faces of the zone surfaces. This heat balance generally is modeled with four coupled heat transfer components, as shown in Figure 11.3:

1. Conduction through the building element
2. Convection to the room air
3. Shortwave radiant absorption and reflection
4. Longwave radiant interchange

The incident shortwave radiation comes from the solar radiation that enters the zone through windows and that is emitted from internal sources such as lights. The longwave radiant interchange includes the absorption and emittance from low-temperature radiation sources, such as zone surfaces, equipment, and people. The inside face heat balance for each face can be written as follows:

$$q''_{LWX} + q''_{SW} + q''_{LWS} + q''_{ki} + q''_{sol} + q''_{conv} = 0 \quad (11.4)$$

where

q''_{LWX} = net long-wavelength radiant exchange flux between zone surfaces

q''_{SW} = net shortwave radiation flux to surface from lights

q''_{LWS} = longwave radiation flux from equipment in zone

q''_{sol} = transmitted solar radiation flux absorbed at surface

q''_{ki} = conduction flux through wall

q''_{conv} = convection heat flux at zone air

The models for these heat exchange components will be described in the following sections.

11.3.1 Conduction, q_{ki}

This contribution to the inside face heat balance is the wall conduction term expressed by Equation 11.2. This represents the heat transfer behind the inside face of the building element.

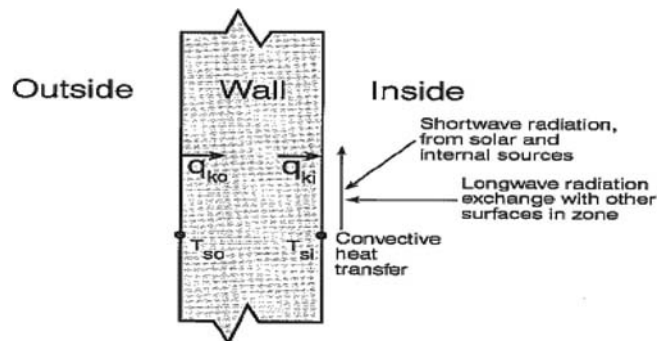


Figure 11.3 Inside face heat balance.

(Source: *Cooling and Heating Load Calculation Principles*, Figure 2.3).

11.3.2 Internal Radiation Modeling

Longwave (LW) Radiation Exchange Among Zone Surfaces, q_{LWX}

There are two limiting cases for internal longwave (LW) radiation exchange that are easily modeled:

1. The zone air is completely transparent to LW radiation.
2. The zone air completely absorbs LW radiation from the surfaces within the zone.

The limiting case of completely absorbing air has been used for load calculations and also in some energy analysis calculations. This model is attractive because it can be formulated simply using a combined radiation and convection heat transfer coefficient from each surface to the zone air. However, it oversimplifies the zone surface exchange problem. Accordingly, most heat balance formulations treat air as completely transparent.

Thus, the LW radiation exchange among the surfaces in the zone can be formulated directly. The HBM procedure in this manual uses a mean radiant temperature exchange formulation, which uses approximate view factors but retains very good accuracy (Liesen and Pedersen 1997).

Internal Furnishings

Furniture in a zone has the effect of increasing the amount of surface area and can participate in the radiant and convective heat exchanges. Furniture also adds thermal mass to the zone. These two changes affect the time response of the zone cooling load in opposite ways. The added area tends to shorten the response time, while the added mass tends to lengthen the response time. The proper modeling of furniture is an area that needs further research, but the heat balance formulation allows the effect to be modeled in a realistic manner by including the furniture surface area and thermal mass in the heat exchange process.

LW Radiation from Internal Sources

The traditional model for this source is to define a radiative/convective split for the heat introduced into a zone from equipment. The radiative part is then distributed over the surfaces within the zone in some prescribed manner. This, of course, is not a completely realistic model, and it departs from the heat balance principles. However, it is virtually impossible to treat this source in any more detail since the alternative would require knowledge of the placement and surface temperatures of all equipment.

Shortwave Radiation from Lights

The short-wavelength radiation from lights is distributed over the surfaces in the zone in some prescribed manner. In many cases, this is not a very large cooling load component.

11.3.3 Transmitted Solar Radiation

Currently available window data uses the solar heat gain coefficient (SHGC) as described by Wright (1995). This has the effect of lumping the transmitted and absorbed solar heat gains together. However, using the number of panes, window description, SHGC, and visual transmittance as a guide, a roughly equivalent window can be selected from Table 3.7, which gives fundamental properties such as angle-dependent transmittance, reflectance, and layer absorptances. With these properties available, a heat balance model can be made on the individual panes or the inside and outside faces of the window. The latter approach is described by Nigusse (2007). Transmitted solar radiation also is distributed over the surfaces in the zone in a pre-

Load Calculation Applications Manual (SI), Second Edition

scribed manner. It would be possible to calculate the actual position of beam solar radiation, but that would involve partial surface irradiation, which is inconsistent with the rest of the zone model that assumes uniform conditions over an entire surface.

The current procedures incorporate a set of prescribed distributions. Since the heat balance approach can deal with any distribution function, it is possible to change the distribution function if it seems appropriate.

11.3.4 Convection to Zone Air

The convection flux is calculated using the heat transfer coefficients as follows:

$$q''_{conv} = h_c(T_a - T_s) \quad (11.5)$$

The inside convection coefficients h_c presented in the *ASHRAE Handbook—Fundamentals* [2013] and used in most load calculation procedures and energy programs are based on very old natural convection experiments and do not accurately describe the heat transfer coefficients that are present in a mechanically ventilated zone. In previous calculation procedures, these coefficients were combined with radiative heat transfer coefficients and could not be readily changed. The heat balance formulation keeps them as working parameters. In this way, new research results can be incorporated into the procedures. It also will permit determining the sensitivity of the load calculation to these parameters.

11.4 Air Heat Balance

In heat balance formulations aimed at determining cooling loads, the capacitance of the air in the zone is neglected and the air heat balance is done as a quasi-steady balance in each time period. There are four contributors to the air heat balance: convection from the zone surfaces, infiltration and ventilation introduced directly into the zone, and the HVAC system air. The air heat balance may be written as

$$q_{conv} + q_{CE} + q_{IV} + q_{sys} = 0 \quad (11.6)$$

where

q_{conv} = convection heat transfer from the surfaces

q_{CE} = convective part of internal loads

q_{IV} = sensible load due to infiltration and direct zone ventilation air

q_{sys} = heat transfer to/from the HVAC system

11.4.1 Convection from Surfaces

The contribution of convection from surfaces is expressed using the convective heat transfer coefficient, as follows:

$$q_{conv} = \sum_{i=1}^{nsurfaces} h_{c,i} A_i (T_a - T_{s,i}) \quad (11.7)$$

11.4.2 Convective Parts of Internal Loads, q_{CE}

This component is the companion part of the radiant contribution from internal loads described previously. It is added directly into the air heat balance. Such a treatment also violates the tenets of the heat balance, since the surfaces producing the

internal loads exchange heat with the zone air through normal convective processes. However, the details required to include this component in the heat balance generally are not available, and its direct inclusion into the air heat balance is a reasonable approach.

11.4.3 Infiltration, q_V

Any air that enters by way of infiltration is assumed to be immediately mixed with the zone air. The determination of the amount of infiltration air is quite complicated and subject to significant uncertainty. Chapter 5 of this manual presents some procedures for estimating infiltration. In the HBM and RTSM procedures, the infiltration quantity is converted to a number of air changes per hour (ACH) and included in the zone air heat balance using the outside temperature at the current hour.

11.5 A Framework for the Heat Balance Procedures

To apply the heat balance procedures to calculating cooling loads, it is necessary to develop a suitable framework for the heat transfer processes involved. This takes the form of a general thermal zone for which a heat balance can be applied to its surfaces and air mass. A thermal zone is defined as an air volume at a uniform temperature plus all the heat transfer and heat storage surfaces bounding or inside of that air volume. It is primarily a thermal, not a geometric, concept and can consist of a single room, a number of rooms, or even an entire building. Generally, it parallels the HVAC system concept of the region that is controlled by a single thermostat. Note particularly, however, that such things as furniture are considered part of the thermal zone.

The heat balance procedure for load calculations needs to be flexible enough to accommodate a variety of geometric arrangements, but the procedure also requires that a complete thermal zone be described. Because of the interactions between elements, it is not possible to build up the zone behavior from a component-by-component analysis. To provide the necessary flexibility, a generalized 12-surface zone can be used as a basis. This zone consists of four walls, a roof or ceiling, a floor, and a thermal mass surface. Each of the walls and the roof can include a window (or skylight in the case of the roof). This makes a total of 12 surfaces, any of which may have zero area if it is not present in the zone to be modeled. Such a zone is shown schematically in Figure 11.4.

The 12-surface thermal zone model used in cooling load calculations requires that complex geometries be reduced to the following essential thermal characteristic:

- The equivalent area and approximate orientation of each surface
- The construction of each surface
- The environmental conditions on both sides of each surface

The 12-surface model captures these essentials without needlessly complicating the procedure. These surfaces provide the connections between the outside, inside, and zone air heat balances and constitute the minimum general set of surfaces that will accommodate a full heat balance calculation.

When using heat-balance-based procedures to calculate cooling loads for various building configurations and conditions, it is helpful to think in terms of the basic zone model and the three zone heat balances.

Load Calculation Applications Manual (SI), Second Edition

11.6 Implementing the Heat Balance Procedure

11.6.1 The Heat Balance Equations

The heat balance processes for the general thermal zone are formulated for a 24-hour steady periodic condition. The primary variables in the heat balance for the general zone are the 12 inside face temperatures and the 12 outside face temperatures at each of the 24 hours as described in the previous section. The first subscript i is assigned as the surface index, and the second subscript j as the hour index, or, in the case of CTFs, the sequence index. Then, the primary variables are

$T_{so,i,j}$ = outside face temperature, $i = 1, 2, \dots, 12; j = 1, 2, \dots, 24$

$T_{si,i,j}$ = inside face temperature, $i = 1, 2, \dots, 12; j = 1, 2, \dots, 24$

In addition, the variable q_{sysj} = cooling load, $j = 1, 2 \dots 24$.

Equations 11.1 and 11.3 are combined and solved for T_{so} to produce 12 equations applicable in each time step:

$$T_{so,i,j} = \frac{\sum_{k=1}^{nz} T_{si,j-k} Y_{i,k} - \sum_{k=1}^{nz} T_{so,i,j-k} X_{i,k} - \sum_{k=1}^{nq} \Phi_{i,k} q_{ko,i,j-k}}{X_{i,0} + h_{co,i,j}} + \frac{q''_{osol,i,j} + q''_{LWR,i,j} + T_{si,i,j} Y_{i,0} + T_{o,j} h_{co,i,j-k}}{X_{i,0} + h_{co,i,j}} \quad (11.8)$$

where

$Y_{i,k}$ = cross CTF, $k = 0, 1, \dots, nz$, $W/(m^2 \cdot K)$

$X_{i,k}$ = inside CTF, $k = 0, 1, \dots, nz$, $W/(m^2 \cdot K)$

$\Phi_{i,k}$ = flux CTF, $k = 1, 2, \dots, nq$, $W/(m^2 \cdot K)$

T_{si} = inside face temperature, °C

T_{so} = outside face temperature, °C

q''_{ko} = conductive heat flux (q/A) into the wall, W/m^2

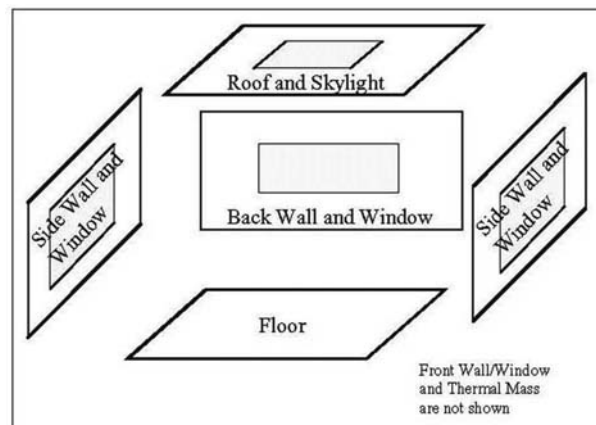


Figure 11.4 Schematic view of general heat balance zone.

(Source: *Cooling and Heating Load Calculation Principles*, Figure 10.1).

q''_{sol} = absorbed direct and diffuse solar (short-wavelength) radiant heat flux, W/m^2

q''_{LWR} = net long-wavelength (thermal) radiant flux exchange with the air and surroundings, W/m^2

Also, h_{co} is the outside convection coefficient, introduced by using Equation 11.5. This equation shows the need for separating the first term of the CTF series, $X_{i,0}$, because in that way the contribution of the current surface temperature to the conduction flux can be collected with the other terms involving that temperature. McClellan and Pedersen (1997) present alternative equations for the outside temperature, depending on the outside heat transfer model that is chosen.

Equations 11.2 and 11.4 are combined and solved for T_{si} to produce the next 12 equations for the inside surface temperatures:

$$T_{si,j} = \frac{T_{so,i,j} Y_{i,0} + \sum_{k=1}^{nz} T_{so,i,j-k} Y_{i,k} - \sum_{k=1}^{nz} T_{si,i,j-k} Z_{i,k} + \sum_{k=1}^{nq} \Phi_{i,k} q''_{k,i,j-k}}{Z_{i,0} + h_{ci,j}} + \frac{T_a h_{ci,j} + q''_{LWS} + q''_{LWX_{i,j}} + q''_{SW} + q''_{sol}}{Z_{i,0} + h_{ci,j}} \quad (11.9)$$

where

$Y_{i,k}$ = cross CTF for surface i, $k = 0, 1, \dots, nz$, $W/(m^2 \cdot K)$

$Z_{i,k}$ = inside CTF for surface i, $k = 0, 1, \dots, nz$, $W/(m^2 \cdot K)$

$\Phi_{i,k}$ = flux CTF for surface i, $k = 1, 2, \dots, nq$, $W/(m^2 \cdot K)$

T_{si} = inside face temperature, $^{\circ}C$

T_{so} = outside face temperature, $^{\circ}C$

T_a = zone air temperature, $^{\circ}C$

h_{ci} = convective heat transfer coefficient on the inside, obtained from Equation 11.5, $W/(m^2 \cdot K)$

Other heat flux terms are defined in Section 11.3. Note that in Equations 11.8 and 11.9 the opposite surface temperature at the current time appears on the right-hand side. The two equations could be solved simultaneously to eliminate those variables. Depending on the order of updating the other terms in the equations, this can have a beneficial effect on the solution stability.

The remaining equation comes from the air-heat balance, Equation 11.6. This provides the cooling load q_{sys} at each time step:

$$q_{sys} = q_{CE} + q_{IV} + q_{conv} \quad (11.10)$$

where

q_{CE} = convective part of internal loads, W

q_{IV} = sensible load due to infiltration and ventilation air, W

q_{sys} = heat transfer to/from the HVAC system, W

q_{conv} = convected heat transfer from zone surfaces, W

11.6.2 Overall HBM Iterative Solution Procedure

The iterative heat balance procedure is quite simple. It consists of a series of initial calculations that proceed sequentially, followed by a double iteration loop. This is shown in the following procedure:

Load Calculation Applications Manual (SI), Second Edition

1. Initialize areas, properties, and face temperatures for all surfaces, for all 24 hours.
2. Calculate incident and transmitted solar fluxes for all surfaces and hours.
3. Distribute transmitted solar energy to all inside faces, for all 24 hours.
4. Calculate internal load quantities, for all 24 hours.
5. Distribute longwave (LW), shortwave (SW), and convective energy from internal loads to all surfaces for all 24 hours.
6. Calculate infiltration and ventilation loads for all 24 hours.
7. Iterate the heat balance according to the following pseudo-code scheme:
 - For $Day = 1$ to $MaxDays$ (repeat day for convergence)
 - For $j = 1$ to 24 (hours of the day)
 - For $SurfaceIter = 1$ to $MaxSurfIter$
 - For $i = 1$ to 12 (surfaces)
 - Evaluate Equations 11.8 and 11.9
 - Next i
 - Next $SurfaceIter$
 - Next j
 - If not converged, $NextDay$
8. Display results.

It has been found that about four surface iterations ($MaxSurfIter$) are sufficient to provide convergence. The convergence check on the day iteration is based on the difference between the inside and the outside conductive heat flux terms q_k .

References

- ASHRAE. 2013. *ASHRAE Handbook—Fundamentals*. Atlanta: ASHRAE.
- Hittle, D.C. 1979. Calculating building heating and cooling loads using the frequency response of multilayered slabs. PhD thesis, Department of Mechanical and Industrial Engineering, University of Illinois at Urbana-Champaign.
- Liesen, R.J., and C.O. Pedersen. 1997. An evaluation of inside surface heat balance models for cooling load calculation. *ASHRAE Transactions* 103(2):485–502.
- McClellan, T.M., and C.O. Pedersen. 1997. An evaluation of inside surface heat balance models for use in a heat balance cooling load calculation procedure. *ASHRAE Transactions* 103(2):469–84.
- Nigusse, B.A. 2007. Improvements to the radiant time series method cooling load calculation procedure. PhD thesis, School of Mechanical and Aerospace Engineering, Oklahoma State University, Stillwater.
- Pedersen, C.O., D.E. Fisher, J.D. Spitler, and R.J. Liesen. 1998. *Cooling and Heating Load Calculation Principles*. Atlanta: ASHRAE.
- Spitler, J.D. 1996. *Annotated Guide to Load Calculation Models and Algorithms*. Atlanta: ASHRAE.
- Wright, J.L. 1995. Summary and comparison of methods to calculate solar heat gain. *ASHRAE Transactions* 101(2):802–18.
- Yazdanian, M., and J. Klems. 1994. Measurement of the exterior convective film coefficient for windows in low-rise buildings. *ASHRAE Transactions* 100(1):1087–96.

Appendix A

Psychrometric Processes—Basic Principles

Pychrometrics and psychrometric processes are used in the conversion of cooling and heating loads into equipment loads for system design and optimization. Psychrometrics enable the designer to determine air quantities and air conditions, which can be used for equipment selection and duct and piping design. This section deals with the fundamental properties of moist air and the basic processes used in HVAC systems. More detailed information is available in the *ASHRAE Handbook*, particularly the *Fundamentals* and the *HVAC Systems and Equipment* volumes.

There are two methods used to determine the properties of moist air. The calculations can be made using the perfect gas relations. Or, the various properties can be determined using a psychrometric chart, which is based on a somewhat more rigorous analysis. For all practical purposes, properties computed from the perfect gas relations agree very well with those read from a psychrometric chart. Many computer programs are available to compute the properties of moist air, and these programs may display a chart as well.

The psychrometric chart is a valuable visual aid in displaying the processes in the HVAC system. Figure A.1 is the abridged ASHRAE Psychrometric Chart 1 (ASHRAE 1992) for the normal temperatures of air-conditioning applications and for a standard barometric pressure of 101.325 kPa. Charts for other temperature ranges and other altitudes are also available. For example, ASHRAE Psychrometric Chart 4 (ASHRAE 1992) is for an elevation of 1500 m. The various properties may be identified on the chart where dry-bulb temperature is plotted on the horizontal axis and humidity ratio is plotted on the vertical axis. Chapter 1 of the *ASHRAE Handbook—Fundamentals* (2013) defines the various parameters and gives the various relations from which the properties may be computed. Local atmospheric pressure is an important fundamental property and depends on local elevation. This property will be discussed extensively in later sections. Other properties shown on the psychrometric chart are as follow:

- *Enthalpy*—given on the left-hand inclined scale with lines sloping downward to the right with units of kJ/kg.
- *Relative humidity*—shown by lines curving upward from the lower left to upper right and given in percent. The 100% line representing saturated air is the uppermost line.
- *Wet-bulb temperatures*—shown along the 100% relative humidity line in °C. Note that the wet-bulb temperature lines are nearly parallel with the enthalpy lines, indicating that enthalpy is mainly a function of wet-bulb temperature. Also, note that dry-bulb temperature equals wet-bulb temperature when the air is saturated, 100% relative humidity.
- *Specific volume*—shown by straight lines inclined downward from upper left to lower right. The lines are widely spaced; however, the change in volume is small across the chart and visual interpolation is adequate. Units are m³/kg.
- *Dew-point temperature*—not shown directly on the chart but can be easily determined at any state point by moving horizontally to the left to the 100% relative humidity line. The wet-bulb temperature at that point is the dew-point temperature in °C.

Load Calculation Applications Manual (SI), Second Edition

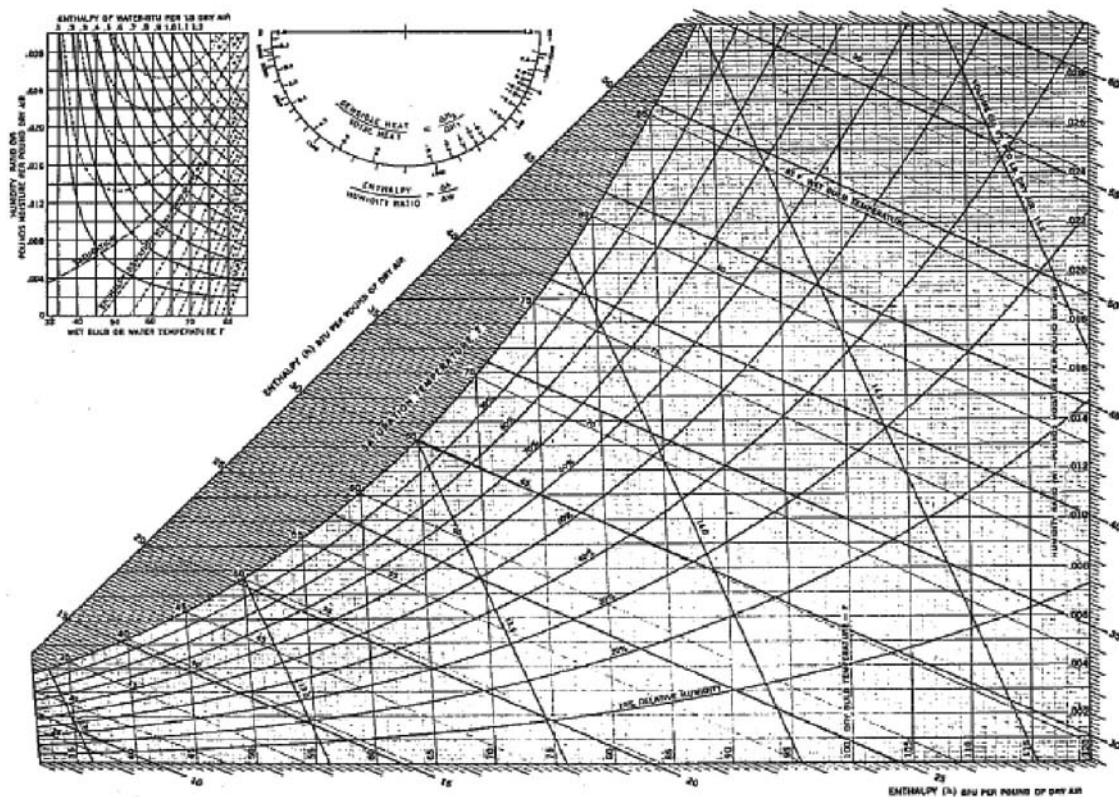


Figure A.1 ASHRAE Psychrometric Chart 1 (ASHRAE 1992).

A.1 Basic Data and Standard Conditions

The approximate composition of dry air by volume is as follows:

Nitrogen	0.78084
Oxygen	0.20948
Argon	0.00934
Carbon dioxide	0.00031
Neon, helium, methane, sulfur dioxide	
Hydrogen and other gases	0.00003

When the last group, considered to be inert, is included with the nitrogen, the resulting molecular weight is 28.965 and the gas constant is 287.055 J/(kg·K). This value of the gas constant is used with the perfect gas relations. The U.S. Standard Atmosphere is defined as follows (ASHRAE 2013):

- Acceleration due to gravity is constant at 9.80665 m/s².
- Temperature at sea level is 15°C.
- Pressure at sea level is 101.325 kPa.
- The atmosphere consists of dry air, which behaves as a perfect gas.

Moist air is a two-component mixture of dry air and water vapor. The amount of water vapor may vary from zero to a maximum amount dependent on pressure and

Appendix A: Psychrometric Processes—Basic Principles

temperature. The latter condition is referred to as *saturated air*. The molecular weight of water is 18.015 and the gas constant is 461.520 J/(kg·K), which is used with the perfect gas relations.

Local atmospheric pressure and temperature vary with altitude or elevation. Table A.1, taken from the *ASHRAE Handbook—Fundamentals* (2013), gives pressure and temperature as a function of altitude. The pressures are typical of local barometric pressure on the earth's surface at the elevations shown. However, the local temperatures on the earth's surface are influenced to a greater extent by climatic conditions, and other data should be used. For system design and load calculations, it is suggested that local weather data or the design temperatures from Chapter 4 of this manual be used. This same data gives the elevation for the various cities from which the local atmospheric pressure can be estimated. For elevations less than or equal to 10,000 m,

$$p = 101.325(1 - 2.25577 \cdot 10^{-5}Z)^{5.2559} \quad (\text{A.1})$$

where

- p = local atmospheric pressure, kPa
- Z = local elevation, m above sea level

The use of the proper local atmospheric pressure in calculations is very important to ensure accurate results.

A.2 Basic Moist Air Processes

The most powerful analytical tools of the air-conditioning design engineer are the conservation of energy (first law of thermodynamics) or energy balance, and the conservation of mass or mass balance. These conservation laws are the basis for the analysis of moist air processes. It is customary to analyze these processes by using the bulk average properties at the inlet and outlet of the device being studied. In actual practice, the properties may not be uniform across the flow area, especially at the outlet, and a considerable length may be necessary for complete mixing.

In this section we consider the basic processes that are a part of the analysis of most systems. The psychrometric chart will be used extensively to illustrate the processes.

Heat Transfer Processes in General

In almost all cases of design or analysis of heat transfer processes, the fluids such as moist air are flowing at a steady rate, often called *steady flow*. Therefore, the energy balance for a moist air-cooling process can be written

$$m_a h_1 = m_a h_2 + q + m_w h_w \quad (\text{A.2})$$

or

$$q = m_a (h_1 - h_2) - m_w h_w \quad (\text{A.3})$$

where

- q = heat transfer rate, kW
- m_a = mass flow rate of dry air, kg/s
- m_w = mass flow rate of water, kg/s
- h = enthalpy, kJ/kg_a or kJ/kg_w

The subscripts 1 and 2 refer to the entering and leaving air. Equation A.2 assumes that the system does not do any work and kinetic and potential energy changes are zero. Work will be considered later. It should be noted that the mass flow rate m_a is

Load Calculation Applications Manual (SI), Second Edition

for dry air and enthalpy h_a is based on a one-kilogram mass of dry air. The term $m_w h_w$, the energy of the liquid water, is often very small and can be neglected. It will be assumed zero for the following discussion and reintroduced later. As Equation A.2 is written, the heat transfer rate q is positive for heat transfer away from the airstream. If heating and humidification were being considered, the terms q and $m_w h_w$ would be on the opposite side of the equation and it would be written as follows:

$$q = m_a(h_2 - h_1) - m_w h_w \quad (\text{A.4})$$

In practice, the direction of the heat transferred is obvious by the nature of the problem. Equations A.2–A.4 are valid for any steady-flow heat transfer process, with the assumptions noted. The enthalpy difference $h_2 - h_1$ is made up of two parts:

$$h_2 - h_1 = c_p(t_2 - t_1) + \Delta h(W_2 - W_1) \quad (\text{A.5})$$

where

c_p = specific heat of moist air, kJ/(kg·K)

t = dry-bulb temperature, °C

W = humidity ratio, kg_v/kg_a

Δh = change in enthalpy required to vaporize or condense 1 kg of water, kJ/kg

The first term on the right-hand side of Equation A.5 represents the heat transferred to change the air temperature from t_1 to t_2 . This is referred to as *sensible heat transfer*. The other term in Equation A.5 represents the heat transferred to change the humidity ratio from W_1 to W_2 . This is referred to as *latent heat transfer*. Then, $h_2 - h_1$ is proportional to the total heat transfer, and Equation A.5 may be substituted into Equation A.4 to obtain

$$q = m_a(h_2 - h_1) = m_a[c_p(t_2 - t_1) + \Delta h(W_2 - W_1)] \quad (\text{A.6})$$

where the term $m_w h_w$ has been neglected.

It is customary to use the volume flow rate of moist air in L/s in design calculations rather than mass flow rate m_a . These two quantities are related by the specific volume v , another property shown on the psychrometric chart, as follows:

$$m_a = (\text{m}^3/\text{s})/v_a = \text{L}/\text{s}/(1000 \cdot v_a), \quad (\text{A.7})$$

where m_a is in kg/s. For unit simplicity, we use m³/s here, but flow rates in L/s are also common. The specific volume in m³/kg, computed or read from the psychrometric chart, is a very useful parameter. It is important that the volume flow rate, cfm, and specific volume v be specified at the same state or point on the psychrometric chart. The specific volume v_a may also be computed as follows using the ideal gas law:

$$v_a = (RT)/P_a \quad (\text{A.8})$$

where

R = gas constant for dry air, 0.287055, kJ/(kg·K)

T = absolute air temperature, $(t + 273.15)$, °K

P_a = partial pressure of dry air, kPa

The partial pressure of the air depends on the local barometric pressure and the humidity ratio of the moist air. For design purposes, partial pressure may be assumed equal to the local barometric pressure, which is proportional to the elevation above sea level (Table A.1). Table A.2 gives values of v_a for different elevations and temperatures, covering the range of usual design conditions. This data is useful in practical calculations.

Appendix A: Psychrometric Processes—Basic Principles

Table A.1 Standard Atmospheric Data for Altitudes to 30,000 ft

(Source: ASHRAE Handbook—Fundamentals [2013], Chapter 1, Table 1)

Altitude, m	Temperature, °C	Pressure, kPa
–500	18.2	107.478
0	15.0	101.325
500	11.8	95.461
1000	8.5	89.875
1500	5.2	84.556
2000	2.0	79.495
2500	–1.2	74.682
3000	–4.5	70.108
4000	–11.0	61.640
5000	–17.5	54.020
6000	–24.0	47.181
7000	–30.5	41.061
8000	–37.0	35.600
9000	–43.5	30.742
10,000	–50	26.436

Adapted from NASA (1976).

Table A.2 Specific Volume of Moist Air, m³/kg_a

(Source: Cooling and Heating Load Calculation Principles, Table D2)

Elevation, m	Dry-Bulb/Wet-Bulb Temperatures, °C					
	10/10	16/13	20/16	25/18	30/16	35/26
0	0.812	0.830	0.844	0.858	0.867	0.898
500	0.862	0.881	0.895	0.911	0.920	0.953
750	0.888	0.908	0.923	0.939	0.948	0.982
1500	0.973	0.995	1.011	1.029	1.039	1.076
2250	1.068	1.091	1.109	1.129	1.140	1.180
3000	1.174	1.199	1.219	1.241	1.253	1.297

The specific heat c_p in Equation A.6 is for the moist air but is based on 1 kg mass of dry air. So,

$$c_p = c_{pa} + W c_{pv} \quad (\text{A.9})$$

where

- c_{pa} = specific heat of dry air, 1.006 kJ/(kg·K)
- c_{pv} = specific heat of water vapor, 1.84 kJ/(kg·K)
- W = humidity ratio, kg/kg

Load Calculation Applications Manual (SI), Second Edition

The humidity ratio depends on the air temperature and pressure; however, for typical HVAC calculations, a value of 0.01 kg/kg is often used. Then,

$$c_p = 1.006 + 0.01(1.84) = 1.02 \text{ (kJ/(kg} \cdot \text{K))}$$

This value is used extensively in Chapter 9 where practical psychrometrics are discussed.

The enthalpy change Δh_w in Equations A.5 and A.6 is relatively constant in the range of air-conditioning processes, and a value of 2503 kJ/kg_v is often assumed. This value is representative of the enthalpy change for 1 kg of water changing from saturated vapor in the moist air to a saturated liquid when condensed.

Sensible Heating or Cooling of Moist Air

When air is heated or cooled without the loss or gain of moisture, the process yields a straight horizontal line on the psychrometric chart because the humidity ratio is constant. This type of process is referred to as *sensible* heating or cooling. Such processes can occur when moist air flows through a heat exchanger. Process 1-2 in Figure A.2 represents sensible heating, while the process 2-1 would be sensible cooling. The heat transfer rate for such a process is given by Equations A.3 or A.4 for heating.

$$q = m_a(h_2 - h_1) = m_a[c_p(t_2 - t_1) + \Delta h(W_2 - W_1)] \quad (\text{A.10})$$

Since there is no transfer of moisture, $W_2 - W_1 = 0$ and

$$q_s = m_a(h_2 - h_1) = m_a c_p(t_2 - t_1) \quad (\text{A.11})$$

where q_s denotes a sensible heat transfer process. Note that the heat transfer rate q_s is still proportional to the enthalpy change $h_2 - h_1$. Substituting Equation A.7 for m_a yields

$$q_s = (m^3/s)c_p(t_2 - t_1)/v_a \quad (\text{A.12})$$

When a constant value of 1.006 kJ/(kg_a·°C) is substituted for c_p in Equation A.12,

$$q_s = 1.006(m^3/s)(t_2 - t_1)/v_a \quad (\text{A.13})$$

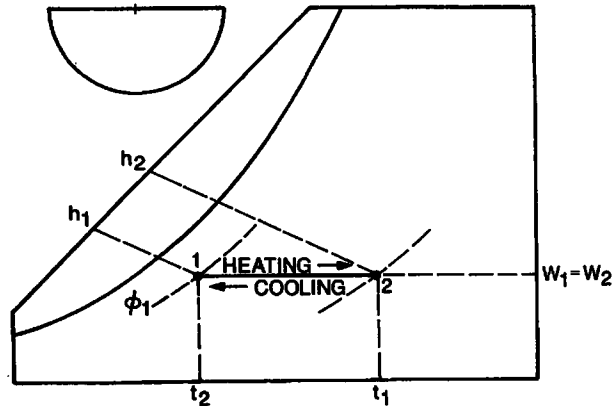


Figure A.2 Sensible heating and cooling process.

(Source: *Cooling and Heating Load Calculation Principles*, Figure D2).

Appendix A: Psychrometric Processes—Basic Principles

Further, when the standard value of $0.83 \text{ m}^3/\text{kg}$ is substituted for v_a in Equation A.6b,

$$q_s = 1.21 \text{ L/s}(t_2 - t_1) \quad (\text{A.14})$$

This is a commonly used relationship, but its limitations must be kept in mind. The constant may be easily adjusted using Table A.2 and Equation A.13. A slightly smaller constant of 1.2 is often used for heating conditions rather than 1.21; however, the difference is not significant. It is far more important to recognize that local atmospheric pressure or elevation has a greater effect. For example, the specific volume v of air at 1500 m elevation and 15°C is about $0.99 \text{ m}^3/\text{kg}$, and the constant in Equation A.14 would be 1.01—a significant difference of about 20%.

Example A.1 Sensible Heating

Find the heat transfer required to heat 750 L/s of atmospheric air at 16°C and 90% relative humidity to 49°C , without transfer of moisture to or from the air. Assume standard sea-level pressure.

Solution: Since this is a sensible heat transfer process, Equation A.12 or A.13 may be used to compute the heat transfer rate. Using A.6a,

$$q_s = (\text{m}^3/\text{s})c_p(t_2 - t_1)/v_a = 0.75 \cdot 1.006(49 - 16)/0.83 = 30 \text{ kW},$$

where v is from Table A.2 at zero elevation and $16^\circ\text{C}/13^\circ\text{C}$. Suppose this process took place at a location where the elevation above sea level was 1500 m. Using Table A.2, the specific volume v would be $0.995 \text{ m}^3/\text{kg}$. Then for 750 L/s at this high altitude using Equation A.6b:

$$q_s = 1.006(0.75)(49 - 16)/0.995 = 25 \text{ kW}$$

The specific volumes above could have been read from an appropriate psychrometric chart.

Cooling and Dehumidifying of Moist Air

When moist air is cooled to a temperature below its dew point, some of the water vapor will condense and leave the airstream. This process usually occurs with cooling coils and is one of the most important in HVAC design. Figure A.3 shows the process on the psychrometric chart. Although the actual process path will vary depending on the type of surface, surface temperature, and flow conditions, the heat and moisture transfer can be expressed in terms of the initial and final states. In the previous section, where heat transfer was discussed in general, the fact that some liquid water leaves the system as condensate was neglected. The condensate has some energy, although it is a small amount. The energy balance from Equation A.3 becomes

$$q = m_a(h_2 - h_1) - m_w h_w \quad (\text{A.15})$$

or

$$q = m_a[c_p(t_2 - t_1) + \Delta h(W_2 - W_1)] - m_w h_w \quad (\text{A.16})$$

For cooling, the last term on the right-hand side of Equations A.15 and A.16 is quite small compared to the other terms and can usually be neglected, as previously discussed. Then Equation A.16 is the same as Equation A.6. However, it is much more convenient in this case to use Equation A.15, neglect the last term, and read the enthalpies from a psychrometric chart.

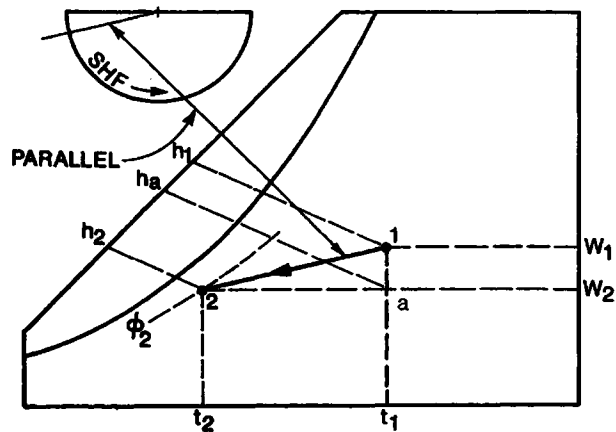


Figure A.3 Cooling and dehumidifying process.

(Source: *Cooling and Heating Load Calculation Principles*, Figure D3).

It was noted earlier that the change in enthalpy ($h_1 - h_2$) is made up of two parts, sensible and latent. This can be shown conveniently in Figure A.3. Imagine that the process follows the path 1-a-2 instead of path 1-2 as shown. The result is the same because

$$h_2 - h_1 = (h_a - h_1) + (h_2 - h_a) \quad (\text{A.17})$$

Path 1-a represents a latent heat transfer process and path a-2 represents a sensible heat transfer process. Both taken together represent the total heat transfer process. Therefore, this is a convenient way of determining the two quantities rather than using Equation A.16 to determine the separate quantities. When Equation A.15 is converted to the volume flow form, using Equation A.7, it becomes

$$q = (m^3/s)(h_1 - h_2)/v, \quad (\text{A.18})$$

where the term $m_w h_w$ has again been neglected and v may be obtained from a psychrometric chart, computed, or read from Table A.2. When a standard value of $0.83 \text{ m}^3/\text{kg}$ is used for v in Equation A.18 it becomes

$$q = 1.2(m^3/s)(h_1 - h_2) \quad (\text{A.19})$$

The sensible heat factor (SHF), sometimes called the sensible heat ratio (SHR), is defined as

$$\text{SHF} = q_s/q = \frac{(h_a - h_2)}{(h_1 - h_2)} \quad (\text{A.20})$$

where the enthalpy values are from Figure A.3. The SHF is also shown on the semicircular scale of Figure A.3. Use of this feature will be explained in an example.

Example A.2 Cooling

Moist air at 27°C db and 19°C wb is cooled to 14°C db and 80% relative humidity. The volume flow rate of the entering air is 1000 L/s (1 m³/s) and the condensate leaves at 16°C. Find the heat transfer rate. Assume standard sea-level pressure.

Appendix A: Psychrometric Processes—Basic Principles

Solution: Equation A.15 applies to this process, which is similar to Figure A.3. The term for the condensate will be retained to demonstrate how small it is. The following properties are read from ASHRAE Psychrometric Chart 1 (ASHRAE 1992): $v_1 = 0.865 \text{ m}^3/\text{kg}$, $h_1 = 53.8 \text{ kJ/kg}$, $W_1 = 10.5 \text{ g/kg}_{\text{da}}$ ($0.0105 \text{ kg/kg}_{\text{da}}$), $h_2 = 34.2 \text{ kJ/kg}$, and $W_2 = 8 \text{ g/kg}_{\text{da}}$ ($0.008 \text{ kg/kg}_{\text{da}}$). The enthalpy of the condensate is obtained from the thermodynamic properties of water, $h_w = 67.2 \text{ kJ/kg}$. The enthalpy of liquid water, the condensate, may also be closely estimated by

$$h_w = t_w - 4.18$$

Using Equation A.18 and retaining the condensate term,

$$q = (\text{m}^3/\text{s})(h_1 - h_2)/v - m_w h_w$$

The flow rate of the condensate m_w may be found from a mass balance on the water:

$$m_{v, \text{in}} = m_{v, \text{out}} + m_w$$

or

$$m_a W_1 = m_a W_2 + m_w$$

and

$$m_w = m_a(W_1 - W_2) = (\text{m}^3/\text{s})(W_1 - W_2)/v \quad (\text{A.21})$$

then

$$q = (\text{m}^3/\text{s})[(h_1 - h_2) - (W_1 - W_2)h_w]/v_1$$

$$q = 1[(53.8 - 34.2) - (0.0105 - 0.008)67.2]/0.865$$

$$q = 1.156(19.6 - 0.168)$$

The last term, which represents the energy of the condensate, is quite insignificant. For most cooling and dehumidifying processes this will be true. Finally, neglecting the condensate term, $q = 22.7 \text{ kW}$. A ton of refrigeration is 3.5 kW . Therefore, $q = 6.28 \text{ tons}$.

Note that the solution to Example A.2 is very difficult without a psychrometric chart or some other aid such as a computer program. The sensible heat transfer is easily computed using Equation A.11, but the latent heat transfer calculation requires the use of enthalpy or humidity ratio, Equations A.24 or A.23. These can be calculated from basic principles, but this is a tedious task. Therefore, one of the following three equations is recommended: A.15, A.16, or A.17. Note that the total heat transfer rate could be computed by $q = q_s/\text{SHF}$, where q_s is obtained from Equation A.11, and the SHF is obtained from a psychrometric chart. Psychrometric computer programs are very useful for problems of this type, particularly for elevations where charts are not available.

As discussed previously, the cooling and dehumidifying process involves both sensible and latent heat transfer, where sensible heat transfer is associated with the decrease in dry-bulb temperature and the latent heat transfer is associated with the decrease in humidity ratio. These quantities may be expressed as

Load Calculation Applications Manual (SI), Second Edition

$$q_s = m_a c_p (t_2 - t_1) \quad (\text{A.22})$$

and

$$q = m_a (W_2 - W_1) \Delta h \quad (\text{A.23})$$

By referring to Figure A.3, we may also express the latent heat transfer as

$$q_1 = m_a (h_1 - h_a) \quad (\text{A.24})$$

and the sensible heat transfer is given by

$$q_s = m_a (h_a - h_2) \quad (\text{A.25})$$

The energy of the condensate has been neglected. Recall that

$$m_a = (\text{m}^3/\text{s})/\nu$$

and obviously

$$q = q_s + q_1 \quad (\text{A.26})$$

The sensible heat factor SHF, defined as q_s/q , is shown on the semicircular scale of Figure A.3. The SHF is given on the circular scale by a line parallel to line 1-2, as shown, and has a value of 0.67 in Example A.2.

Heating and Humidifying Moist Air

This type of process usually occurs during the heating season when it is necessary to add moisture to conditioned air to maintain a healthful relative humidity.

Moist air may be heated and humidified in one continuous process. However, this is not very practical because the physical process would require spraying water on a heating element, resulting in a buildup of scale and dirt and causing consequent maintenance problems.

Warm air is also easier to humidify and can hold more moisture than cool air. Therefore, the air is usually heated, followed by an adiabatic humidification process. Sensible heating was previously discussed; adiabatic humidification will now be considered.

Adiabatic Humidification

When moisture is added to moist air without the addition of heat, the energy equation becomes

$$(h_2 - h_1)/(W_2 - W_1) = h_w = \Delta h/(\Delta W) \quad (\text{A.27})$$

It is important to note in Equation A.27 that h_1 and h_2 are the enthalpies of the moist air in kJ/kg, while h_w is the enthalpy of the water, liquid or vapor, used to humidify the air. The direction of the process on the psychrometric chart can vary considerably. If the injected water is saturated vapor at the dry-bulb temperature, the process will proceed at a constant dry-bulb temperature. If the water enthalpy is greater than the enthalpy of saturated vapor at the dry-bulb temperature, the air will be heated and humidified. If the water enthalpy is less than the enthalpy of saturated vapor at the dry-bulb temperature, the air will be cooled and humidified. Figure A.4 shows these processes.

One other situation is important. When liquid water at the wet-bulb temperature is injected, the process follows a line of constant wet-bulb temperature, as shown in Figure A.4. The quantity $\Delta h/\Delta W$ is also given on the semicircular scale of the psychrometric chart and is a great aid in solving humidification problems. This is demonstrated in Example A.3.

Appendix A: Psychrometric Processes—Basic Principles

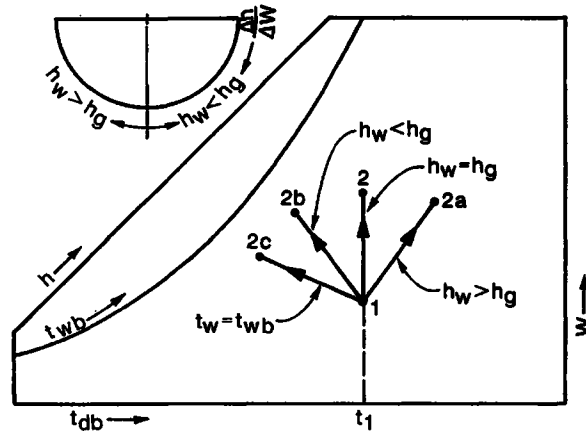


Figure A.4 Humidification processes without heat transfer.

(Source: *Cooling and Heating Load Calculation Principles*, Figure D4).

Example A.3 Heating and Humidification

Moist air at 16°C dB and 20% relative humidity enters a heater and humidifier at the rate of 800 L/s. It is necessary to heat the air followed by adiabatic humidification so that it leaves at a temperature of 46°C and a relative humidity of 30%. Saturated water vapor at 100°C is injected. Determine the required heat transfer rate and mass flow rate of the vapor. Assume standard sea-level pressure.

Solution: It is first necessary to locate the states, as shown in Figure A.5 from the given information and Equation A.27, using the protractor feature of the psychrometric chart. Process 1-a is sensible heating; therefore, a horizontal line to the right of state 1 is constructed. The $\Delta h/\Delta W$ scale on the protractor of the ASHRAE Psychrometric Charts (ASHRAE 1992) is designed so that (1) the path of a humidification process can be determined when $\Delta h/\Delta W$ is known or (2) if the process path is known, $\Delta h/\Delta W$ may be determined. For example, referring to Figure A.5, the complete process may be visualized as going from point 1 to point 2. When these two states are connected by a straight line and a parallel line transferred to the protractor, as shown, $\Delta h/\Delta W$ may be read and used in calculations as required. Also note that in the case of process a-2, an adiabatic process, $\Delta h/\Delta W$ equals h_w from Equation A.27. Therefore, because h_w is known (2675 kJ/kg), a parallel line can be transferred from the protractor to the chart to pass through point 2 and intersect the horizontal line from point 1, which represents the sensible heating process. Point a is thus determined: $t_a = 43^\circ\text{C}$. The heat transfer rate is then given by

$$q = m_a(h_a - h_1) = (m^3/s)c_p(t_a - t_1)/v_1 \quad (\text{A.28})$$

where

$$m_a = (m^3/s)/v_1 \quad (\text{A.29})$$

and h_1 and h_a are read from ASHRAE Psychrometric Chart 1 (ASHRAE 1992) as 38.8 and 67.9 kJ/kg, respectively.

Then,

$$q = (0.8) \cdot (49.1 - 21.8)/0.82 = 26.6 \text{ kW}$$

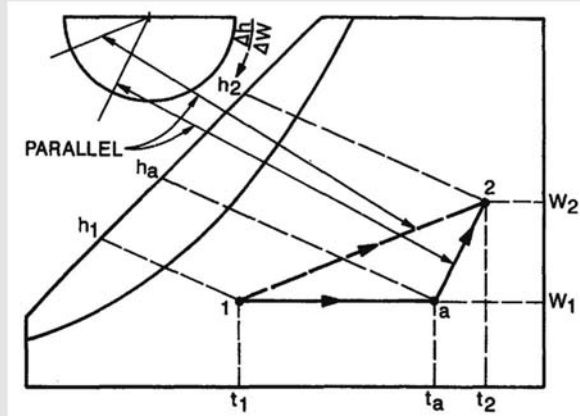


Figure A.5 Typical heating and humidifying process.

(Source: *Cooling and Heating Load Calculation Principles*, Figure D5).

or

$$q = (0.8) \cdot 1.02 \cdot (43 - 16) / 0.82 = 26.9 \text{ kW}$$

The mass flow rate of the vapor is given by a mass balance on the water:

$$m_{v1} + m_w = m_{v2}$$

$$m_a W_1 + m_w = m_a W_2$$

and

$$m_w = m_a (W_2 - W_1) \quad (\text{A.30})$$

where W_2 and W_1 are read from ASHRAE Psychrometric Chart 1 (ASHRAE 1992) as 0.0192 and 0.0022 kg/kg_{da}, respectively. Then,

$$m_w = (0.8 / 0.82) \cdot (0.0192 - 0.0022) \cdot 3600 = 59.7 \text{ kg}_w / \text{h}$$

which is saturated water vapor at 100°C.

Adiabatic Mixing of Two Streams of Moist Air

The mixing of airstreams is quite common in air-conditioning systems. The mixing process usually occurs under adiabatic conditions and with steady flow. An energy balance gives

$$m_{a1} h_1 + m_{a2} h_2 = m_{a3} h_3 \quad (\text{A.31})$$

where the subscripts 1 and 2 refer the airstreams being mixed and 3 refers to a mixed airstream. The mass balance on the dry air is

$$m_{a1} + m_{a2} = m_{a3} \quad (\text{A.32})$$

The mass balance on the water vapor is

$$m_{a1} W_1 + m_{a2} W_2 = m_{a3} W_3 \quad (\text{A.33})$$

Appendix A: Psychrometric Processes—Basic Principles

Combining Equations A.31 through A.33 gives the following result:

$$\frac{h_2 - h_3}{h_1 - h_3} = \frac{W_2 - W_3}{W_1 - W_3} = \frac{m_{a2}}{m_{a3}} \quad (\text{A.34})$$

The state of the mixed streams must lie on a straight line between states 1 and 2 as shown in Figure A.6. It may be further inferred from Equation A.34 that the lengths of the various line segments are proportional to the mass flow rates of the two streams to be mixed. So,

$$\frac{m_{a1}}{m_{a2}} = \frac{\overline{32}}{13}, \quad \frac{m_{a1}}{m_{a3}} = \frac{\overline{32}}{12}, \quad \frac{m_{a2}}{m_{a3}} = \frac{\overline{13}}{12} \quad (\text{A.35})$$

This fact provides a very convenient graphical procedure for solving mixing problems in contrast to the use of Equations A.31 through A.33.

It should be noted that the mass flow rate is used in the procedure; however, the volume flow rates may be used to obtain approximate results.

Example A.4 Mixing

One thousand L/s of air at 38°C dB and 24°C wB are mixed with 500 L/s (0.5 m³/s) of air at 16°C dB and 10°C wB. The process is adiabatic, at a steady flow rate and at standard sea-level pressure. Find the condition of the mixed stream.

Solution: A combination graphical and analytical solution is first obtained. The initial states are first located on ASHRAE Psychrometric Chart 1 (ASHRAE 1992) as illustrated in Figure A.6 and connected with a straight line.

Equations A.32 and A.33 are combined to obtain

$$W_3 = W_1 + \frac{m_{a2}}{m_{a3}}(W_2 - W_1) \quad (\text{A.36})$$

By using the property values from ASHRAE Psychrometric Chart 1 (ASHRAE 1992) and Equation A.7, we obtain

$$m_{a1} = \frac{0.5}{0.825} = 0.606 \text{ kg/s}$$

$$m_{a2} = \frac{1.0}{0.90} = 1.111 \text{ kg/s}$$

$$W_3 = 0.0053 + \frac{8333}{(4542 + 8333)}(0.013 - 0.0053) = 0.0103 \text{ lb}_v/\text{lb}_a$$

$$W_3 = 0.0052 + \frac{1.111}{(0.606 + 1.111)}(0.013 - 0.0052) = 0.0102 \text{ kg/kg}_{da}$$

The intersection of W_3 with the line connecting states 1 and 2 gives the mixture state 3. The resulting dry-bulb temperature is 29.5°C and the wet-bulb temperature is 19.5°C.

The complete graphical procedure could also be used where the actual lengths of the process lines are used:

$$\frac{\overline{13}}{\overline{12}} = \frac{m_{a2}}{m_{a3}} = \frac{1.111}{0.606 + 1.111} = 0.65$$

and

$$\overline{13} = 0.65(\overline{12})$$

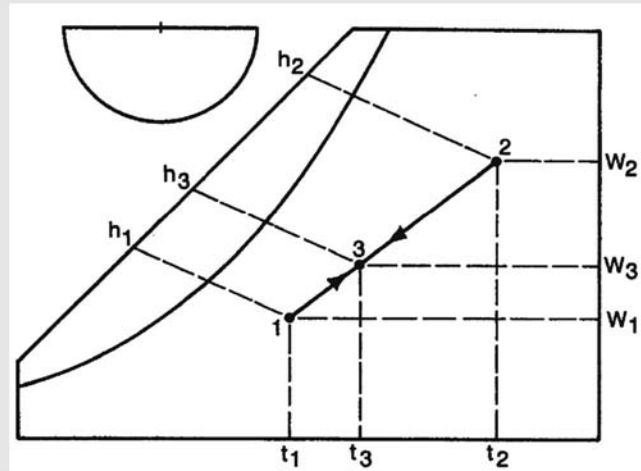


Figure A.6 Adiabatic mixing process.

(Source: *Cooling and Heating Load Calculation Principles*, Figure D6).

The lengths of line segments $\overline{12}$ and $\overline{13}$ depend on the scale of the psychrometric chart used. However, when length $\overline{13}$ is laid out along $\overline{12}$ from state 1, state 3 is accurately determined. If the volume flow rates (L/s) had been used in place of mass flow rates to determine the mixed condition,

$$\frac{\overline{13}}{\overline{12}} = \frac{1.0}{1.0 + 0.5} = 0.67$$

and

$$\overline{13} = 0.67(\overline{12})$$

In turn, this would result in some loss in accuracy in determining the mixed condition.

Evaporative Cooling

This type of process is essentially adiabatic, and the cooling effect is achieved through evaporation of water sprayed into the airstream. Therefore, the process is most effective when the humidity of the moist air is low. This is often the case at higher elevations and in desert-like regions.

The devices used to achieve this process are usually chambers with a sump from which water is sprayed into the airstream, with the excess water being drained back into the sump and recirculated. A small, insignificant amount of makeup water is required. When the makeup water is neglected, the energy equation becomes

$$h_1 = h_2, \tag{A.37}$$

which leads to the conclusion that the wet-bulb temperature is essentially constant. An evaporative cooling process is shown in Figure A.7. Example A.5 illustrates the process.

Appendix A: Psychrometric Processes—Basic Principles

Example A.5 Evaporative Cooling

One thousand L/s ($1.0 \text{ m}^3/\text{s}$) of atmospheric air at 38°C and 10% relative humidity are to be cooled in an evaporative cooler. The relative humidity of the air leaving the cooler is 50%. Determine the dry-bulb temperature of the air leaving the cooler, the required amount of makeup water, and the cooling effect. Assume standard sea-level pressure.

Solution: The process is shown in Figure A.7 and ASHRAE Psychrometric Chart 1 (ASHRAE 1992) can be used to determine the final temperature, the humidity ratios W_1 and W_2 , and specific volume v_1 by laying out the line 1-2. Then

$$\begin{aligned}t_2 &= 24^\circ\text{C} \\W_1 &= 0.0041 \text{ kg}_v/\text{kg}_a \\W_2 &= 0.0096 \text{ kg}_v/\text{kg}_a \\v_1 &= 0.887 \text{ m}^3/\text{kg}_a\end{aligned}$$

The flow rate of the make up water is given by Equation A.21:

$$m_w = m_a(W_2 - W_1)$$

where

$$m_a = (\text{L/s})/v_1 = (1.0)/0.887 = 1.127 \text{ kg}_a/\text{s}$$

$$m_w = 1.127(0.0096 - 0.0041) = 0.006 \text{ kg}_w/\text{s}$$

This is a volume flow rate of 0.006 L of water per second. The assumption of negligible makeup water is thus valid. Normally, one would use Equation A.15 to determine the cooling effect or heat transfer rate; however, in this case there is no external heat transfer. There has been an internal transformation of energy where sensible heat from the air has evaporated water, which has become part of the air-water vapor mixture. To evaluate the cooling effect one has to apply the conditioned air to a space to be conditioned. Suppose the air in this example is supplied to a room that is maintained at 30°C and 40% relative humidity.

$$q = m_a(h_r - h_2)$$

and from ASHRAE Psychrometric Chart 1 (ASHRAE 1992),

$$h_2 = 49.5 \text{ kJ/kg}_a$$

and

$$h_r = 57.3 \text{ kJ/kg}_a$$

then

$$q = 1.127(57.3 - 49.5) = 8.8 \text{ kW}$$

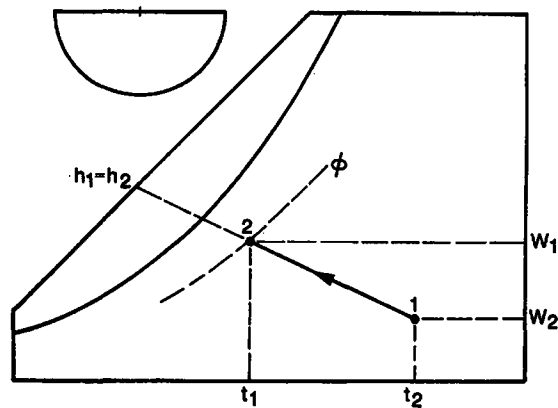


Figure A.7 Evaporative cooling process.

(Source: *Cooling and Heating Load Calculation Principles*, Figure D7).

Fog Condition

A constant pressure fog condition happens when the cooling process at constant pressure occurs in such a way that water droplets remain suspended in the air in a nonequilibrium condition after the dew point is reached. If all the condensed liquid remains suspended along with the remaining water vapor, the humidity ratio remains fixed. Energy and mass balance equations must be examined.

The fog condition exists when the condition is to the left of the saturation curve on the psychrometric chart, regardless of how that condition was attained. All that is inferred is that liquid water droplets remain suspended in the air rather than dropping out, as required by total equilibrium concepts. This two-phase region represents a mechanical mixture of saturated moist air and liquid water with the two components in thermal equilibrium. Isothermal lines in the fog region are coincident with extensions of thermodynamic wet-bulb temperature lines. As a rule, it is not necessary to make calculations in the fog region.

Conditioning a Space

Air must be supplied to a space at certain conditions to absorb the load, which generally includes both a sensible and a latent component. In the case of a cooling load, the air undergoes simultaneous heating and humidification as it passes through the space and leaves at a condition dictated by comfort conditions. Such a conditioning process is shown in Figure A.8.

The process 1-2 and its extension to the left are called the *condition line* for the space. Assuming that state 2, the space condition, is fixed, air supplied at any state on the condition line, such as at state 1, will satisfy the load requirements. However, as the point is moved, different quantities of air must be supplied to the space. In general, the closer point 1 is to point 2, the more air is required, and the converse is also true.

The sensible heat factor for the process can be determined using the circular scale by transferring a parallel line as shown in Figure A.8 and is referred to as the *room sensible heat factor (RSHF)*. The RSHF is dictated by the relative amounts of sensible and latent cooling loads on the space. Therefore, assuming that state 2—the space condition—is known, the condition line can be constructed based on the cooling load. State 1, which depends on a number of factors such as indoor air quality, comfort, and the cooling coil, then completely defines the amount of air required.

Appendix A: Psychrometric Processes—Basic Principles

Example A.6 Air Supply Rate

A given space is to be maintained at 25°C dB and 18°C wB. The total cooling load for the space has been determined to be 17.5 kW, of which 12.3 kW is sensible heat transfer. Assume standard sea-level pressure and compute the required air supply rate.

Solution: A simplified schematic is shown in Figure A.8. State 2 represents the space condition and state 1, at this point unknown, represents the entering air condition. By Equation A.20, the sensible heat factor is

$$\text{RSHF} = 12,300(17,500) = 0.7$$

The state of the air entering the space lies on the line defined by the RSHF on ASHRAE Psychrometric Chart 1 (ASHRAE 1992). Therefore, state 2 is located as shown on Figure A.8, and a line drawn through the point parallel to the RSHF = 0.7 line on the protractor. State 1 may be any point on the line and is determined by the operating characteristics of the equipment, desired indoor air quality, and by what will be comfortable for the occupants. For now, assume that the dry-bulb temperature t_1 is about 11°C less than t_2 . Then, $t_1 = 15^\circ\text{C}$ and state 1 is determined. The air quantity may now be found from

$$q = m_a(h_2 - h_1) = (\text{m}^3/\text{s})(h_2 - h_1)/v_1$$

and

$$(\text{m}^3/\text{s})_1 = \frac{qv_1}{(h_2 - h_1)}$$

From ASHRAE Psychrometric Chart 1 (ASHRAE 1992), $h_2 = 50.7 \text{ kJ/kg}_{\text{da}}$, $h_1 = 36 \text{ kJ/kg}_{\text{da}}$, and $v_1 = 0.825 \text{ m}^3/\text{kg}$. Thus,

$$(\text{m}^3/\text{s})_1 = \frac{17.5(0.827)}{(50.7 - 36)} = 0.98 = 980 \text{ L/s}$$

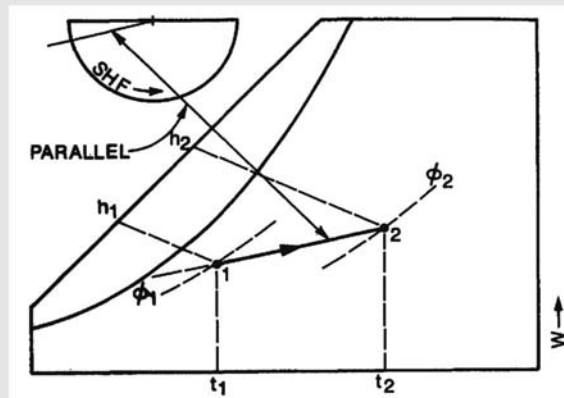


Figure A.8 Space-conditioning psychrometric process.

(Source: *Cooling and Heating Load Calculation Principles*, Figure D8).

Load Calculation Applications Manual (SI), Second Edition

Note that the volume flow rate at state 1 is not standard L/s but the actual L/s. It is sometimes desirable to give the volume flow rate as standard L/s. The actual airflow can be easily transformed by multiplying by the ratio of standard specific volume to actual specific volume:

$$\text{standard L/s}_1 = \text{L/s}_1(v_s/v_1)$$

$$\text{standard L/s}_1 = 980(0.83/0.827) = 983$$

In case this problem was being solved for some elevation where a psychrometric chart was not available, Equation A.12 or A.13 and Table A.2 would be convenient. Assume that the elevation is 2250 m above sea level and find L/s₁. From Equation A.12:

$$q_s = (\text{m}^3/\text{s})c_p(t_2 - t_1)/v_1$$

The specific volume, $v_1 = 1.129 \text{ m}^3/\text{kg}$ from Table A.2 and $c_p = 1.02 \text{ kJ}/(\text{kg}\cdot^\circ\text{C})$:

$$(\text{m}^3/\text{s})_1 = \frac{v_1 q_s}{(c_p)(t_2 - t_1)}$$

$$(\text{m}^3/\text{s})_1 = \frac{1.129(12.3)}{(1.02)(25 - 14)} = 1.24$$

A.3 Processes Involving Work and Lost Pressure

Air distribution systems have fans to circulate the air to the various conditioned spaces. The work energy or power input to a fan takes two forms as it enters the airstream. First, the useful effect is to cause an increase in total pressure at the fan outlet. The total pressure is the driving potential for the air to flow throughout the system. The second effect is not useful and is due to the inability of the fan to convert all the work input into total pressure, and the result is an increase in the air temperature, the same as if the air was heated. The fan total efficiency relates these quantities:

$$\eta_t = P_a/P_{SH} \quad (\text{A.38})$$

where

P_a = power delivered to the air, W

P_{SH} = shaft power input to the fan, W

The shaft power input may be expressed using the energy equation as

$$P_{SH} = m_a(h_2 - h_1) = m_a c_p(t_2 - t_1) \quad (\text{A.39})$$

Since no moisture transfer is present, the power input to the air is

$$P_a = m_a(P_{01} - P_{02})/\rho_a = \eta_t P_{SH} \quad (\text{A.40})$$

where

P_0 = total pressure for the air, kPa

ρ_a = air mass density, kg/m^3

Appendix A: Psychrometric Processes—Basic Principles

Combining Equations A.39 and A.40 results in

$$t_2 - t_1 = (P_{01} - P_{02}) / (\eta_t c_p \rho_a), \quad (\text{A.41})$$

which expresses the temperature rise of the air from the fan inlet to the point where the total pressure has been dissipated. It is assumed that the motor driving the fan is outside the airstream. When standard air is assumed, $(p_{01} - p_{02})$ is in Pa gage and η_t is expressed as a fraction, so Equation A.41 reduces to

$$t_2 - t_1 = 0.817(P_{01} - P_{02}) / \eta_t \quad (\text{A.42})$$

When the fan motor is located within the airstream, such as with a direct drive fan, η_t in Equation A.41 must be replaced with the product of the fan total efficiency and the motor efficiency. Table A.3 gives the air temperature rise for standard air as a function of fan efficiency and total pressure rise according to Equation A.42. Figure A.9 illustrates the effect of fans. Process 1-2 is for a draw-through-type fan installation where the air coming off the cooling coil experiences a rise in temperature before entering the space at state 2. Process 2-3 represents the space-conditioning process. Process 3-4 would be typical of the effect of a return air fan.

It should be noted that from the standpoint of load calculation, all the shaft power input to the fan eventually enters the airstream, because the energy represented by Equation A.39 is converted to energy stored in the air as the air flows through the ducts and into the space, where total pressure is approximately zero.

A.4 Heat Transfer in the Air Distribution System

It is common for some part of the air delivery or return system to be located outside of the conditioned space. Heat transfer to or from the system then has an effect on the psychrometric analysis and the cooling load, much like fans do, as dis-

Table A.3 Air Temperature Rise Caused by Fans, °C

(Source: *Cooling and Heating Load Calculation Principles*, Table D3)

Fan or Combined* Motor and Fan Efficiency, %	Pressure Difference, Pa										
	250	375	500	625	750	875	1000	1125	1250	1375	1500
50	0.4	0.6	0.8	1.0	1.2	1.4	1.6	1.8	2.0	2.2	2.5
55	0.4	0.6	0.7	0.9	1.1	1.3	1.5	1.7	1.9	2.0	2.2
60	0.3	0.5	0.7	0.9	1.0	1.2	1.4	1.5	1.7	1.9	2.0
65	0.3	0.5	0.6	0.8	0.9	1.1	1.3	1.4	1.6	1.7	1.9
70	0.3	0.4	0.6	0.7	0.9	1.0	1.2	1.3	1.5	1.6	1.8
75	0.3	0.4	0.5	0.7	0.8	1.0	1.1	1.2	1.4	1.5	1.6
80	0.3	0.4	0.5	0.6	0.8	0.9	1.0	1.1	1.3	1.4	1.5
85	0.2	0.4	0.5	0.6	0.7	0.8	1.0	1.1	1.2	1.3	1.4
90	0.2	0.3	0.5	0.6	0.7	0.8	0.9	1.0	1.1	1.2	1.3
95	0.2	0.3	0.4	0.5	0.6	0.8	0.9	1.0	1.1	1.2	1.3
100	0.2	0.3	0.4	0.5	0.6	0.7	0.8	0.9	1.0	1.1	1.2

*If fan motor is situated within the airstream, the combined efficiency is the product of the fan and motor efficiencies. If the motor is external to the airstream, use only the fan efficiency.

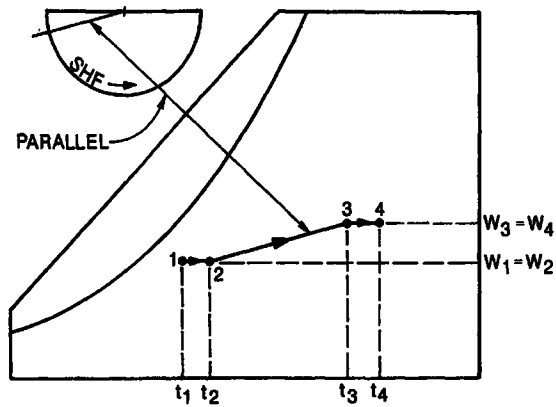


Figure A.9 Psychrometric processes showing effect of fans.
 (Source: *Cooling and Heating Load Calculation Principles*, Figure D9).

cussed in the previous section. Duct systems should be well insulated to minimize heat loss or gain. Indeed, an economic study would show that well-insulated ducts are very cost effective (ASHRAE 1989). However, in cases of high exposure and large temperature differences, it is desirable to estimate the heat loss/gain and the temperature rise/fall of the airstream. The physical problem is quite similar to a heat exchanger where an airstream flowing through a pipe is separated from still air by an insulated duct.

The following analysis may not always be practical. The intent is to discuss the problem fully so that a designer can adapt to a given situation. Heat transfer to the airstream is given by

$$q = m_a(h_2 - h_1) = m_a c_p(t_2 - t_1) \quad (\text{A.43})$$

and by the heat exchanger equation

$$q = UA\Delta t_m \quad (\text{A.44})$$

where

U = overall heat transfer coefficient, $\text{W}/(\text{m}^2 \cdot \text{K})$

A = surface area of the duct on which U is based, m^2

Δt_m = log mean temperature difference, $^\circ\text{C}$

When Equations A.43 and A.44 are equated and solved for the temperature rise,

$$t_2 - t_1 = \frac{UA\Delta t_m}{m_a c_p} \quad (\text{A.45})$$

some simplifications are in order. Since the anticipated temperature rise is small and the temperature in the surrounding t_o is constant,

$$\Delta t_m \approx t_o - t_1 \quad (\text{A.46})$$

As discussed previously,

$$m_a = (\text{m}^3/\text{s})/v_1$$

Appendix A: Psychrometric Processes—Basic Principles

and $c_p = 1.02 \text{ kJ}/(\text{kg}\cdot\text{K})$. It is usually most convenient to base U on the inside surface area of the duct, so

$$U_i = \frac{1}{(1/h_i) + R_d(A_i/A_m) + (1/h_o)(A_i/A_o)} \quad (\text{A.47})$$

where

- h_i = heat transfer coefficient inside the duct, $\text{W}/(\text{m}^2\cdot\text{K})$
- h_o = heat transfer coefficient outside the duct, $\text{W}/(\text{m}^2\cdot\text{K})$
- R_d = unit thermal resistance for the duct and insulation, $(\text{m}^2\cdot\text{K})/\text{W}$
- A_i = duct inside surface area, m^2
- A_o = duct outside surface area, m^2
- A_m = duct mean surface area, m^2

Again simplifications are in order. The outside heat transfer coefficient h_o will be about 9 to 11 $\text{W}/(\text{m}^2\cdot\text{K})$, depending on whether the insulation is foil-backed or not. The mean area A_m can be approximated by

$$A_m \approx (A_i + A_o)/2 \quad (\text{A.48})$$

The thermal resistance of metal duct can be neglected and only the insulation considered. For standard air, the inside heat transfer coefficient h_i can be approximated by a function of volume flow rate and duct diameter with

$$h_i = 0.8289(\text{m}^3/\text{s})^{0.8}/D^{1.8} = 0.0033 \text{ L/s}^{0.8}/D^{1.8} \quad (\text{A.49})$$

where D , the duct diameter, is in meters.

In the case of rectangular duct, Equation A.49 will be adequate when the aspect ratio is not greater than about 2:1. When duct velocity is compatible with typical low velocity duct design, h_i will vary from about 85 to 170 $\text{W}/(\text{m}^2\cdot\text{K})$ as L/s varies from 100 to 17,500.

Example A.7 Duct Losses

One thousand L/s of air flows in a 0.4 m diameter duct 30 m in length. The duct is metal with 50 mm of fibrous glass insulation and is located in an uncontrolled space where the air temperature is estimated to be 50°C on a design day. Estimate the temperature rise and heat gain for air entering the duct at 16°C , assuming standard air conditions.

Solution: Equations A.43 and A.45 may be used to solve this problem. The various parameters required are evaluated as follows:

$$\Delta t_m \approx t_o - t_1 = 50 - 16 = 34^\circ\text{C}$$

$$m_a = 1.0/0.83 = 1.2 \text{ kg/s}$$

where

- $v_l = 0.83 \text{ m}^3/\text{kg}$, for standard air
- $A_i = \pi(0.4) = 1.26 \text{ m}^2/\text{m}$
- $A_o = (0.5) = 1.57 \text{ m}^2/\text{m}$
- $A_m = (A_i + A_o)/2 = 1.41 \text{ m}^2/\text{m}$
- $h_o = 10.0 \text{ W}/(\text{m}^2\cdot\text{K})$
- $R_d = 1.23 (\text{m}^2\cdot\text{K})/\text{W}$

Load Calculation Applications Manual (SI), Second Edition

$$h_i = 0.8289(1.0)^{0.8}/(0.4)^{1.8} = 4.31 \text{ W}/(\text{m}^2\cdot\text{K})$$

Then the overall heat transfer coefficients U_i may be computed:

$$U_i = \frac{1}{1/4.31 + 1.25(1.26/1.41) + (1/10)(1.26/1.57)} = 0.71 \text{ W}/(\text{m}^2\cdot\text{K})$$

It should be noted that the insulation is the dominant resistance; therefore, the other thermal resistances do not have to be known with great accuracy. In fact, the inside and outside thermal resistance could be neglected and $U_i = 9 \text{ W}/(\text{m}^2\cdot\text{K})$.

The temperature rise is then given by Equation A.45:

$$t_2 - t_1 = \frac{30(1.26)(0.71)(34)}{1.02(1.2)1000} = 0.75^\circ\text{C}$$

And the heat gain to the air from Equation A.43 is:

$$q = 1.02(1.2)(0.75) = 0.92 \text{ kW}$$

which is sensible heat gain.

The previous example shows that it is generally unnecessary to compute the heat transfer coefficients h_i and h_o when the duct is well insulated. If the duct is not insulated or poorly insulated, the complete calculation procedure is necessary to obtain reliable results.

References

- ASHRAE. 1989. ASHRAE/IES Standard 90.1-1989, *Energy Efficient Design of New Buildings Except New Low-Rise Residential Buildings*. Atlanta: ASHRAE.
- ASHRAE. 1992. *ASHRAE Psychrometric Chart 1*. Atlanta: ASHRAE.
- ASHRAE. 2013. *ASHRAE Handbook—Fundamentals*. Atlanta: ASHRAE.
- NASA. 1976. U.S. Standard atmosphere, 1976. National Oceanic and Atmospheric Administration, National Aeronautics and Space Administration, and the United States Air Force. Available from National Geophysical Data Center, Boulder, CO.
- Pedersen, C.O., D.E. Fisher, J.D. Spitler, R.J. Liesen. 1998. *Cooling and Heating Load Calculation Principles*. Atlanta: ASHRAE.

Appendix B

Spreadsheet Implementation of the RTSM

Many approaches could be taken to implement the radiant time series method (RTSM) in a spreadsheet, depending on how the conduction time series factors (CTSFs) and radiant time factors (RTFs) are provided. For example, the RTSM could rely on pretabulated CTSFs and RTFs. Or it could rely on a separate computer program to generate custom CTSFs and RTFs. The implementation presented here instead relies on the Visual Basic for Applications (VBA) programming language that is embedded in Microsoft® Excel®. Programs for generating both CTSFs and RTFs are included with the sample spreadsheet *B-1_RTSM.xls* included in the online supporting files accompanying this manual (available at www.ashrae.org/lcam).

This chapter first gives an overview of the spreadsheet features (Section B.1), then presents an in-depth example of using the spreadsheet to compute the cooling loads for the office analyzed in Chapter 8 (Section B.2). Here, the spreadsheet will be used to automatically compute cooling loads for multiple months. Following the example presented in Section B.2, Sections B.3 to B.7 serve as a reference guide for the spreadsheet, defining input parameters, intermediate values, and results.

B.1 Overview

Basic features of the spreadsheet implementation of the RTSM procedure are described briefly as follows:

- A master input worksheet holds values of input parameters that are reasonably likely to stay constant for all or many zones in a building (e.g., location, design temperatures, lighting densities, etc.)
- A single worksheet is used for each zone. Each worksheet includes a range for zone input parameters, intermediate results, and monthly design day hourly cooling loads. Multiple zones can be represented by individual sheets in a workbook.
- The worksheets are designed in such a way that they can be used for a single design day analysis or automated computation of cooling loads for design days for each month of the year. The annual peak cooling loads for the building and individual zones are determined automatically.
- The CTSFs and RTFs are computed for each zone, in each worksheet, at the beginning of the load calculation by marching through each zone worksheet. The CTSF- and RTF-generating subprogram reads the input parameters from each spreadsheet and generates the coefficients by calling the VBA subprocedures.

Surface geometry and construction information:

- Construction surfaces require a keyword for identification of the type of constructions: *wall* for exterior and partition walls, *roof* for roofs, *floor* for floors, and *window* for windows. These keywords are used in the subprograms for collecting heat gains and cooling load contributions for each type of surface.
- A surface description includes geometric parameters for each surface: facing direction, tilt angle, and surface area. Inside surface conductances depend on the tilt angle of the surface; solar irradiation and sol-air temperatures depend on facing direction and tilt angle. The area is needed for many calculations.

Load Calculation Applications Manual (SI), Second Edition

- Inside surface longwave emissivity/absorptance is used in the RTF generation procedure for determining distribution and surface-to-surface interchange of long-wavelength radiation.
- Outside surface shortwave absorptance is used for sol-air temperature calculation.
- Two types of boundary conditions are used as identification keywords: *TOS* is used for outside boundary conditions, and *TA* is used for inside boundary conditions. For windows, the keyword *TOS* and the keyword *Window* (in the Surface Type row) are used to identify the surface and impose outdoor air temperature as the outside boundary condition.
- The number of layers includes the total number of layers for each surface, including the inside and outside surface film conductances. The layers are specified in order from outside to inside.
- This implementation expects the zone model to use one type of fenestration. A single normal solar heat gain coefficient (SHGC) is defined for all windows in a zone. Angular dependency of the SHGC is determined using tabulated angle correction factors and the normal SHGC internally in the subprogram. The reference FEN-CLASS angle correction factors are tabulated in a worksheet named *SHGCNEW*.

Weather information:

- The spreadsheet incorporates the ASHRAE design day weather database and allows users to select from thousands of locations around the world. The available data come from the same source as the PDFs on the accompanying online files. The master input worksheet uses an Excel function to select a location and then retrieve the monthly design weather data automatically for the master input worksheet. Each zone design day weather data cell location is linked to this master input worksheet range. However, for other locations, these equations may be overridden.

B.2 Office Example— RTSM Spreadsheet

This section presents a detailed example of use of the RTSM with a spreadsheet that supports building-level default inputs, multiple zones, and automated multimonth calculations. The office used as an example in Chapter 8 is revisited here.

Building Inputs

The spreadsheet implementation of the RTSM is included in the online supporting files accompanying this manual as *B-1_RTSM.xls*. It has been organized so that much of the building-related data are entered on a worksheet called *MASTER INPUT*, as shown in Figure B.1. This information is then propagated to the individual zone worksheets. If necessary, the individual zone worksheets can be edited so that they do not take all of their information from the master input worksheet. For example, different zones may have different heat gain schedules; those schedules can be changed on the individual zone worksheets.

The worksheet has been color-coded—most users should be first concerned with entering the information in the cells that are shaded and have a black font. Unshaded cells with a black font are default settings that advanced users might wish to change. Cells with a red font are automatically filled in when other settings are chosen. For example, choosing the location from the library will set the latitude, longitude, and other parameters. A user would only need to change these values if choosing a location that is not in the library.

Appendix B: Spreadsheet Implementation of the RTSM

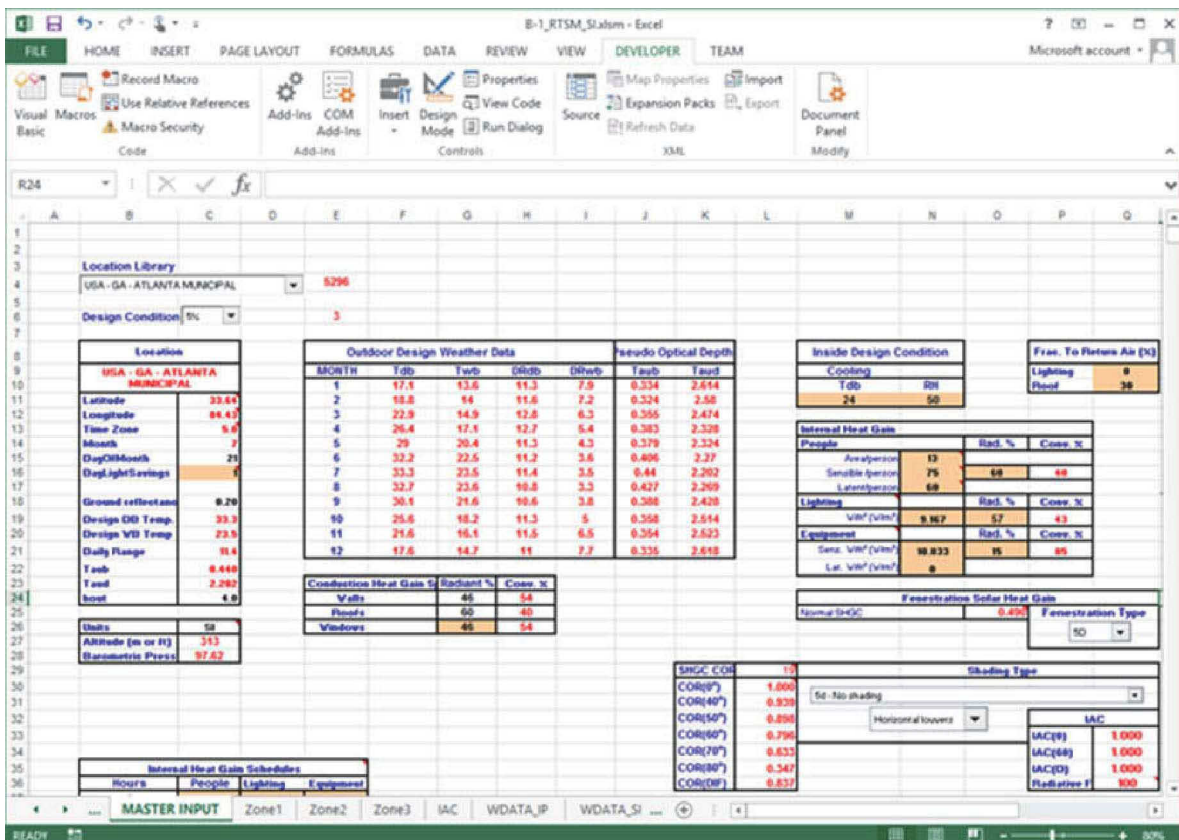


Figure B.1 The master input worksheet.

With the above in mind, building data can now be entered into the master input worksheet. Although any order can be followed, in this example we will enter the unit system, location data, inside design conditions, internal heat gain data, fenestration data, and miscellaneous data.

Unit System

The unit system—inch-pound (I-P) or international system (SI)—is something that should be set at the beginning; the default is I-P units. This is set by simply typing *IP* or *SI* in cell C26. Changing from one unit system to the other will result in location information, if chosen from the location library, changing units correctly (i.e., the design temperatures will change correctly from one set of units to the other). However, other user entries, such as internal heat gains and building dimensions, will keep the same numeric value. This example will use SI units.

Location Data

There are two ways to enter location data—either use the library of locations from the dropdown menu (covering cells B4 through D4) or enter the data manually. The first method is by far the easiest, but in the event that the user wishes to use a location not available as part of the database, manual entry is required. Figure B.2 shows the location dropdown menu being used to select Atlanta Municipal design conditions. In conjunction with the location, the user must select the 0.4%, 2%, 5%, or 10% design condition from the dropdown box in cell C6. Selecting the location and design conditions sets the latitude (C11), longitude (C12), time zone (C13), altitude (C27), and corresponding barometric pressure (C28). It also sets the monthly design dry-bulb temperature, mean

Load Calculation Applications Manual (SI), Second Edition

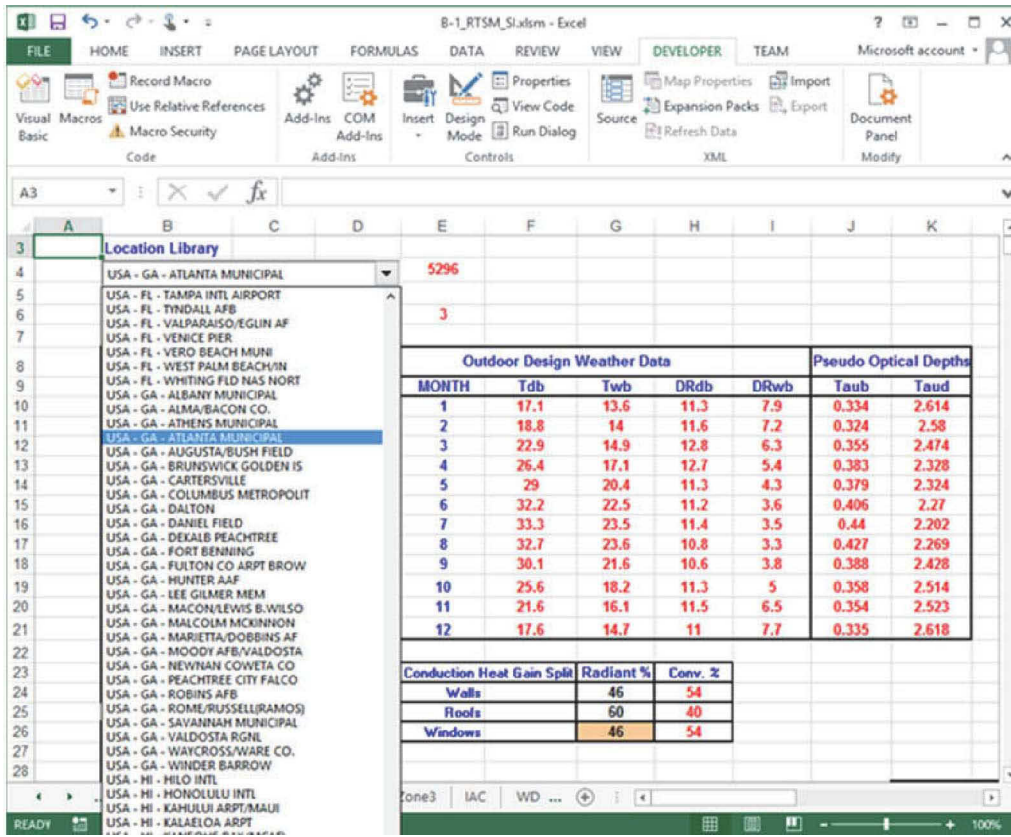


Figure B.2 Location selection from the location library.

coincident wet-bulb temperature, daily ranges, and optical depths in cells F10:K21. The spreadsheet is set to automatically calculate peak cooling loads for every month, so the month input (C12) is usually not needed.

Note that the selected weather conditions are the monthly design conditions, not the annual design conditions. For example, *Atlanta 5%* represents a collection of weather data. For each month, the value given represents the 5% cumulative frequency of occurrence for that month. The Atlanta July 5% condition gives a peak dry-bulb temperature of 33.3°C. The Atlanta annual 1% condition gives a peak dry-bulb temperature of 33.1°C. For this example, we will use the Atlanta 5% monthly design conditions.

If a location that is unavailable in the location library is needed, the user may input the data manually. This would involve entering inputs in the relevant cells that would replace the VLOOKUP functions that extract data from the location library.

Indoor Design Conditions

Selection of indoor design conditions was discussed briefly in Chapter 4. Here, we will choose 24°C and 50% relative humidity. These are set in cells M11 and N11.

Internal Heat Gains and Schedules

Information about internal heat gains and schedules may be set in cells N15:O22 and C37:E60, respectively. These might be thought of as default values for the zones in the building. Peak heat gain rates and schedules are quite likely to vary throughout the building, but entering the information here on a per-unit-area basis will give a default setting for all zones that can be changed as needed.

Appendix B: Spreadsheet Implementation of the RTSM

Internal Heat Gain			
People		Rad. %	Conv. %
Area/person	13		
Sensible /person	75	60	40
Latent/person	60		
Lighting		Rad. %	Conv. %
W/ft ² (W/m ²)	9.167	57	43
Equipment		Rad. %	Conv. %
Sens. W/ft ² (W/m ²)	10.833	15	85
Lat. W/ft ² (W/m ²)	0		

Figure B.3 Internal heat gain inputs on master input worksheet.

People are specified on an area-per-person basis coupled with sensible and latent heat gain per person. Here, we will set the peak occupancy to 12.1 m² per person, with each person having a sensible heat gain of 73 W and a latent heat gain of 59 W. This corresponds to moderately active office work adjusted for a typical male/female ratio, as shown in Table 6.1. This peak occupancy rate is then adjusted on an hour-by-hour basis according to the schedule of fractions in cells C37:C60.

Peak lighting and equipment heat gains are specified in cells N19, N21, and N22 on a watt-per-square-foot basis. Lighting heat gain has been set at 9.11 W/m² and equipment sensible heat gain has been set at 1 W/m². We have assumed no equipment latent heat gain, as would be expected for office equipment. Like occupant heat gains, the peak values are modified by the fractional schedules given in cells D37:E60.

In addition to setting peak heat gain levels and schedules for each heat gain type, the radiant and convective fractions are set for each heat gain type. From Table 6.1, the occupant sensible heat gain is taken as 60% radiative. For pendant lighting, a value of radiative fraction, 57%, is chosen from Table 6.3. For equipment, it is anticipated that there will be a range of office equipment, fan-cooled and non-fan-cooled. Taking an intermediate value between the two options (10% radiative for fan-cooled, 30% radiative for non-fan-cooled) given in Table 7.10, we choose 15% radiant. These selections are shown in Figure B.3.

People, lighting, and equipment schedules are set in cells C37:E60. For purposes of making the load calculation, some reasonable assumptions must be made about the schedule of operation. Here, we have assumed that the building will be fully in operation from about 7:30 a.m. to 5:30 p.m. and, as a result, the people, lighting, and equipment fractions are set to be 1 for hours 9–17 and 0.5 for hours 8 and 18. During the remainder of the day, it is assumed that there will be no occupants present but that lighting and equipment will have about 10% of their peak heat gain due to some lights and equipment remaining on and/or being in standby condition.

Load Calculation Applications Manual (SI), Second Edition

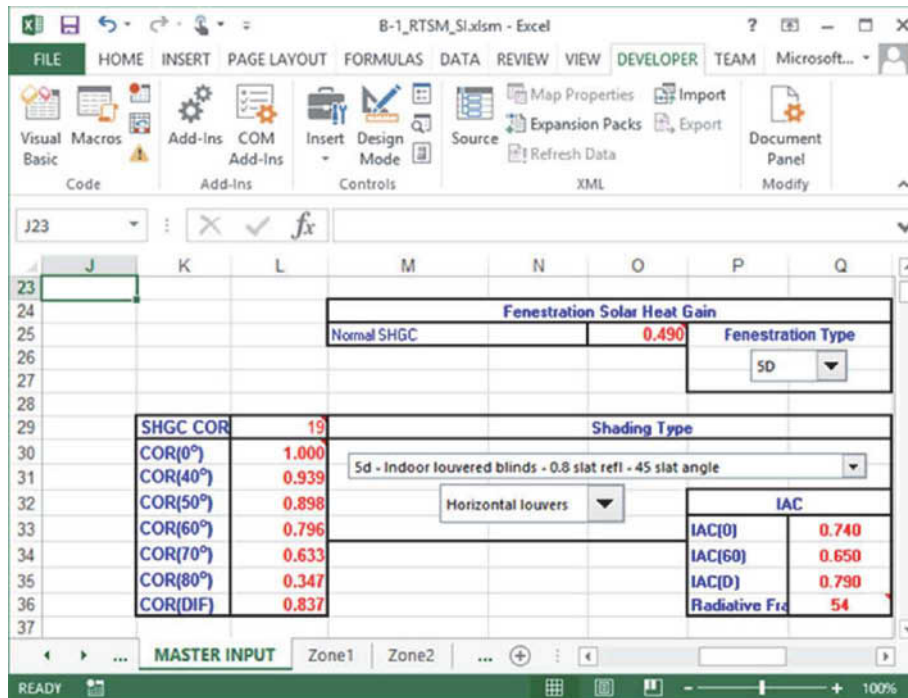


Figure B.4 Fenestration and shading inputs.

Fenestration Details

The windows have a normal SHGC of 0.49; this is set in cell O25. Initially, we will assume no interior shading, so the interior attenuation coefficients (IACs), set in cells Q33:Q35, are 1, and the radiative fraction is 100%. Based on the example in Chapter 8, the closest fenestration type is 5D; this is selected with the dropdown menu near cell P26. This has the effect of setting the SHGC in cell O25 and the SHGC angle correction factors shown in cells K30:K36.

Internal shading is set in the dropdown boxes near cells M31:Q32. After choosing a new fenestration type, the shading type will initially be “no shading”; then, using the dropdown menu, other internal shading options can be set as shown in Figure B.4. Choosing a shading option sets the IACs and radiative fraction in cells Q33:Q36.

Fraction to Return Air

Finally, there are two additional cells that are used to set estimates of the fraction of heat gains that go directly to the return air from lighting and, for the second floor, the roof. For lighting, the fraction to return air is taken from Table 6.3, where 100% of the lighting heat gain due to pendant luminaires is estimated to go to the room. For the roof heat gain, the actual percentage that goes to the return air depends on the surface and return air temperatures—quantities that cannot readily be determined by the RTSM alone. Therefore, an estimate of 30% is made here. As shown in Section 8.5, it is possible to make an estimate using a relatively simple, quasi-steady-state heat balance. Those results suggest that the percentage of roof heat gain that goes to the return air should be close to 80%. However, we will use 30% here for consistency with Section 8.3.

Appendix B: Spreadsheet Implementation of the RTSM

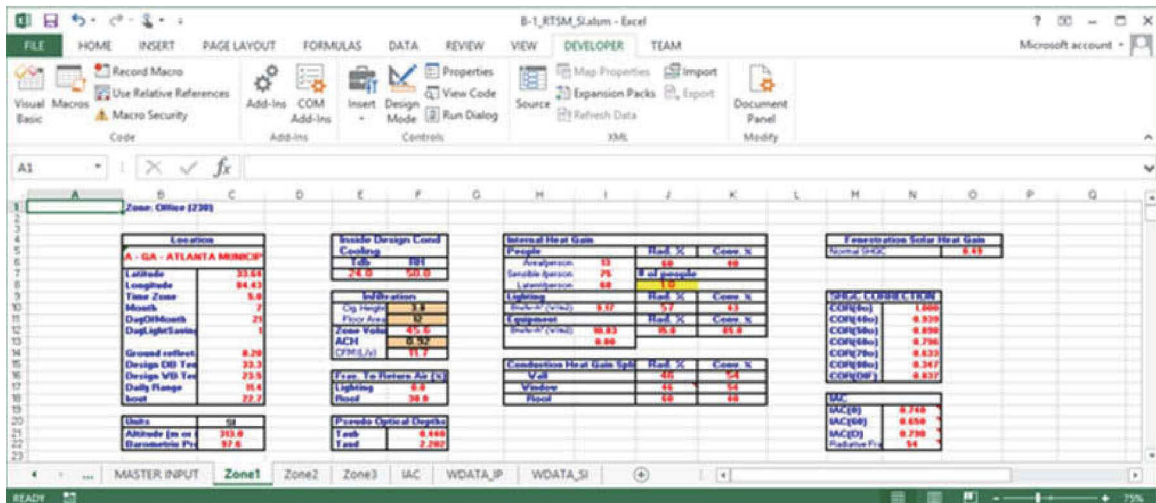


Figure B.5 Zone input as derived from the master input worksheet.

In the spreadsheet, if the user clicks on the Zone 1 tab, the worksheet shown in Figure 8.11 will be shown. In the first 23 rows shown in Figure B.5, almost all of the information is taken directly from the master input worksheet. One exception is the infiltration information, found in cells F10:F14. Here, the zone ceiling height, floor area, and ACH are entered in order to determine the infiltration rate.

In some cases, not all of the input derived from the master input sheet will be suitable, in which case the data from the master input sheet can be manually overridden by simply typing in a new value.

However, as shown in Figure B.4, some of the inputs, particularly the occupancy, may not be suitable for a conference room. It is expected that the peak occupancy loading will be more than 1.9 people. As an estimate, consider a peak occupancy load of 12 people. To override the information taken from the master input worksheet, simply enter the number 12 in cell J8.

Scrolling down, as is shown in Figure B.6, all of the information is input for each surface:

- *Surface ID* (spreadsheet row 25) is an index number used to keep track of each surface.
- *Surface Name* (row 26) is for the user's use in identifying each surface.
- *Surface Type* (row 27) is used for identifying the heat gain types when summing different categories of heat gain and for identifying whether sol-air temperature (for opaque surfaces) or air temperature (for windows) is used as the outside boundary condition.
- *Facing Direction* (row 28) is the direction the outside of the surface faces, in degrees clockwise from north.
- *Tilt Angle* (row 29) is the degrees the angle is tilted above horizontal; a horizontal surface would have a tilt angle of 0°; a vertical surface would have a tilt angle of 90°.
- *Area* (row 30) is the surface area in square feet or square meters.
- *Emissivity In* (row 31) is the emissivity/absorptivity of the surface on the inside for thermal (longwave) radiation. This is used in RTF generation.
- *Sol Abs. Out* (row 32) is the absorptivity of the surface on the outside to solar radiation. This entry is ignored for windows.

Load Calculation Applications Manual (SI), Second Edition

Surface ID	1	2	3	4	5	6	7	8	9	10	11
Surface Name	SE Brick	SE Spand	SV Brick	SV Spand	E Part	N Part	SE Window	SV Window	Roof	Floor	Furniture
Surface Type	Wall	Wall	Wall	Wall	Wall	Wall	Window	Window	Roof	Floor	Furniture
Facies Dir.	150.0	150.0	240.0	240.0	330.0	60.0	150.0	240.0	0.0	0.0	0.0
Tilt Angle	90.0	90.0	90.0	90.0	90.0	90.0	90.0	90.0	0.0	180.0	180.0
Area	7.8	3.5	4.4	3.5	10.3	8.4	3.7	3.7	12.0	12.0	12.0
Emissivity In	0.90	0.90	0.90	0.90	0.90	0.90	0.90	0.90	0.90	0.90	0.90
Sol. Abs. Out	0.90	0.90	0.90	0.90	0.90	0.90	0.00	0.00	0.90	0.90	0.90
Boundary Cond.	TOS	TOS	TOS	TOS	TA	TA	TOS	TOS	TOS	TA	TA
Number of Lay	7	6	7	6	5	5	5	5	4	7	3
Layer1	F01	F01	F01	F01	F02	F02	F01	F01	F01	F03	F02
Layer2	M01	F09	M01	F09	G01	G01	V03	V03	F13	F16	G05
Layer3	M02	F04	M02	F04	F04	F04	F20	F20	M6	F05	F02
Layer4	I07	I07	I07	I07	G01	G01	V03	V03	F03	F08	
Layer5	G01	G01	G01	G01	F02	F02	F02	F02		M18	
Layer6	M02	F02	M02	F02						F17	
Layer7	F02		F02							F03	
Layer8											
Layer9											
Layer10											
Window Geometries											
Window Height							1.95	1.95			
Window Width							1.91	1.91			
Horiz. Projection							0.00	0.00			
PH							0.91	0.91			
RV							0.00	0.00			
Vert. Projection							0.00	0.00			
PV							0.00	0.00			
RV							0.00	0.00			

Figure B.6 Zone input—the surface details.

- *Boundary Condition* (row 33) indicates whether the surface is an interior or exterior surface. If it is an interior surface, its properties are only used for computing RTFs. If it is an exterior surface, its properties are used both for computing RTFs and for computing heat gains.
- *Number of Layers* (row 34) indicates how many layers of material will be specified in rows 35–44.
- For windows, the *Window Height* and *Window Width* (rows 47 and 48) are needed in order to compute the shading. The horizontal projection and vertical projection dimensions in rows 50–54 correspond to Figure D.2 in Appendix D of this manual.

With general inputs for the building entered on the master input worksheet and zone-specific inputs entered on the Zone 1 input sheet, it is possible to perform a cooling load calculation for the office. Figure B.7 shows two buttons that will perform cooling load calculations:

- *Annual Building Cooling Load* will perform a cooling load calculation for all zones for all months of the year.
- *Monthly Building Cooling Load (Select Month)* will perform a cooling load calculation for all zones for the month specified in cell C14.

Setting the month in cell C14 to 7 (July) and clicking the *Monthly Building Cooling Load* button results in a cooling load calculation for the month of July.

Appendix B: Spreadsheet Implementation of the RTSM

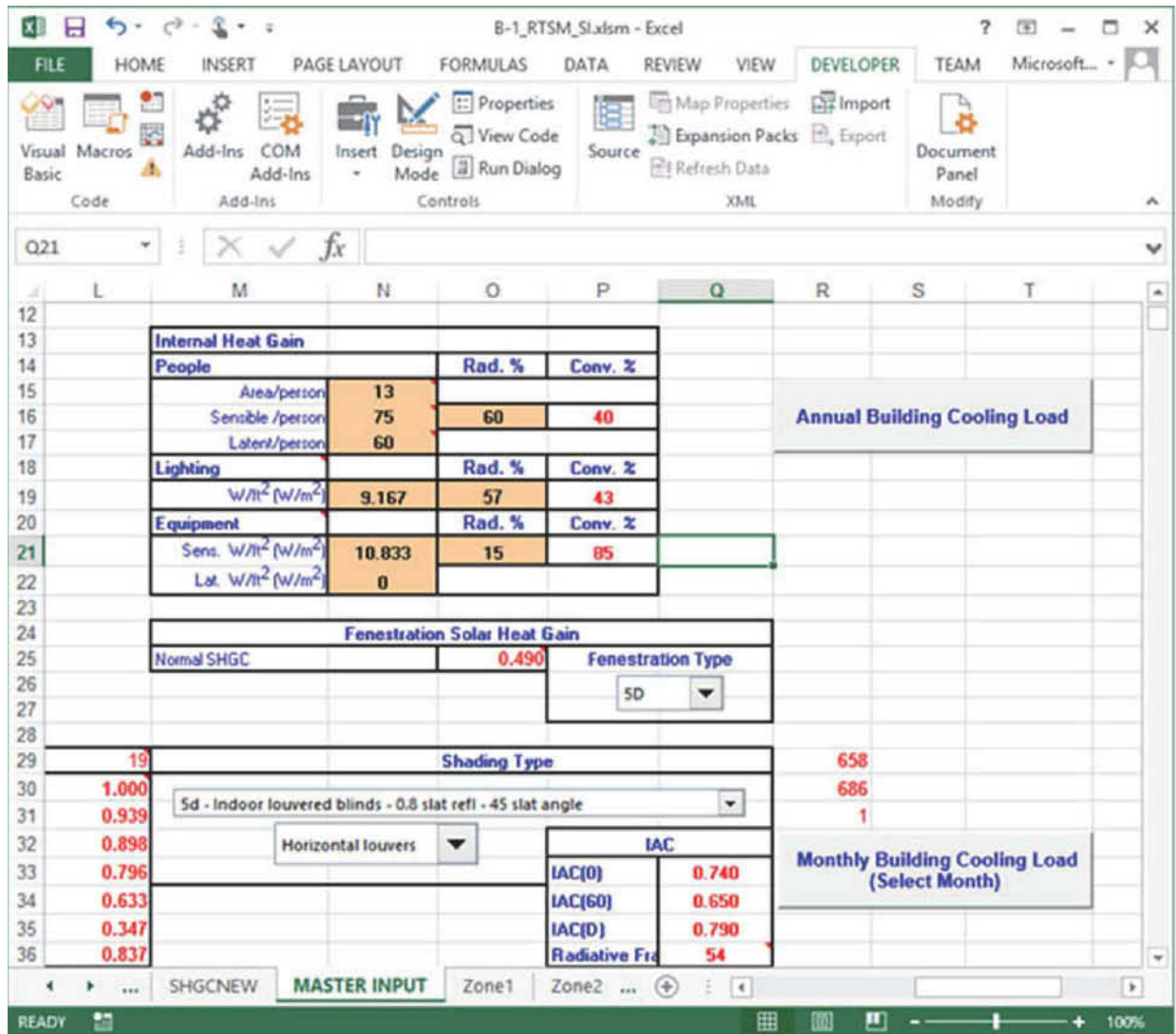


Figure B.7 The master input worksheet showing buttons for cooling load calculations.

Returning to the Zone 1 worksheet and scrolling down from the input section, the reader can see the intermediate calculations, starting with beam radiation and diffuse radiation incident on each surface, as shown in Figure B.8. The reader can inspect the spreadsheet equations—Figure B.8 shows one of the equations for finding the beam radiation incident on a surface. The *Solar_Beam* function is VBA code and the reader can see this code too. (In Excel 2003, this is done from the Tools menu by choosing Macro, then Visual Basic Editor. In Excel 2013, this is done by choosing the Developer tab, then the Visual Basic icon. In Excel 2013, the Developer tab is not shown by default, so the user must first choose the options button from the File tab, choose Customize Ribbon and check Developer under the list of Main tabs. Open the module *Solar* then scroll down or search to find the function *Solar_Beam*, as shown in Figure B.9).

Scrolling down further in the spreadsheet, one can follow all of the steps of the RTSM procedure:

Load Calculation Applications Manual (SI), Second Edition

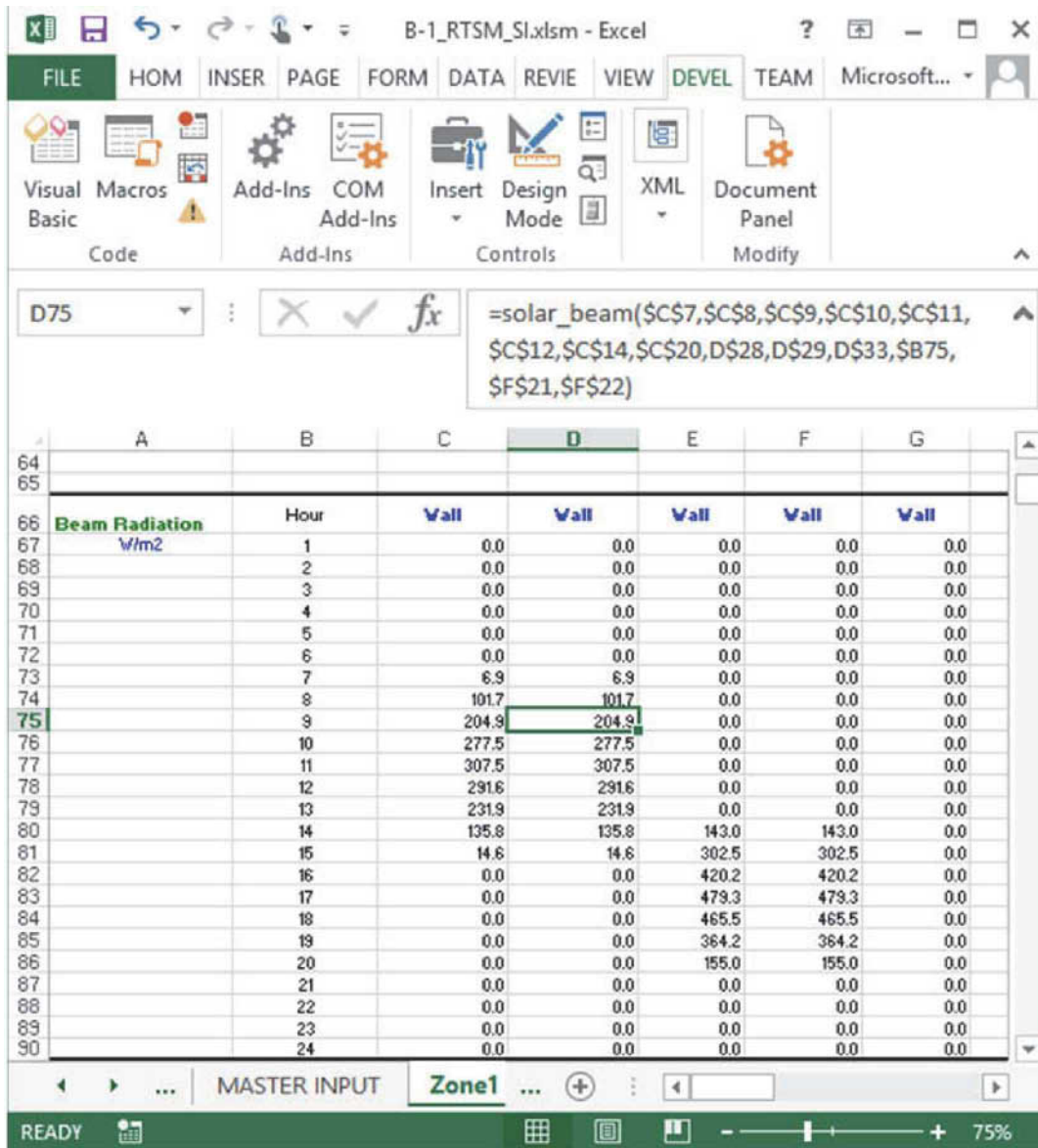


Figure B.8 The Zone 1 worksheet that shows the beginning of the intermediate calculations.

1. Compute beam (rows 67:90) and diffuse (rows 94:117) incident radiation on each surface.
2. Compute sol-air temperature for each surface (rows 121:144).
3. Determine U-factor (row 148) and CTSFs for each construction (rows 149:172). The CTSFs are calculated by VBA subroutines that execute when one of the cooling load calculation buttons is pressed. The CTSFs are written directly to these cells by the VBA code.
4. Conduction heat gains are calculated (rows 178:201).
5. For windows, determine sunlit area fraction (rows 205:228).
6. For windows, determine beam (rows 233:256) and diffuse (rows 261:284) solar heat gains.
7. Based on user-defined schedules and peak heat gains, find hourly sensible and latent internal heat gains (rows 290:313).
8. Determine hourly infiltration loads (rows 319:342).

Appendix B: Spreadsheet Implementation of the RTSM

9. Sum heat gains from different types of surfaces (e.g., walls) and split all heat gains into radiative and convective portions (rows 348:371).
10. Compute solar and nonsolar RTFs (rows 375:398). Like the CTSFs, they are calculated by VBA subroutines and written directly to the appropriate cells.
11. Apply the RTFs to the radiant heat gains and compute cooling loads due to radiant and convective heat gains (rows 403:428).
12. Sum all cooling loads on a component basis and find sensible and latent totals for each hour (rows 433:456).

The end results, as they appear in the spreadsheet, can be seen in Figures B.10 and B.11.

It is entirely possible, though, that the peak cooling load will not occur in July. To examine this possibility, the spreadsheet's other cooling load button (*Annual Building Cooling Load*) will calculate the cooling loads for 12 monthly design days. It will automatically write 1, 2, etc. in cell C12 of the master input worksheet and calculate the cooling loads for each month. For each day that the cooling load calculation is performed, it will perform the same 11-step procedure described above, writing into the same cells. When it is done, rows 67:456 will have the loads and intermediate variables for the last month calculated, which is December. For each month, the cooling load components and totals will be given in rows 464:751. The month and hour with the highest zone sensible cooling load will be summarized in row 757, as shown in Figure B.13. In addition, rows 72:359 of the master input worksheet contain totals for all zones analyzed, and the peak cooling load for the entire building is found in row 365.

As may be noted from Figure B.13, the peak sensible cooling load for the office does not occur in the hottest month (July), but rather in September; the difference is about 10%. A check of row 365 of the master input worksheet shows that the building (at this point, really only three zones, not the entire building) has its peak cooling load occurring in July. So, were these three zones representative of the entire building, it would be likely that the equipment would be sized based on July loads. But, the airflow to the office would be sized based on the September peak. The user should be aware, though, that the differences can be more sizable, and zone peak cooling loads can occur in any month of the year.

B.3 Description of Input Parameters

Before describing the individual parameters, it should again be noted that the entire spreadsheet can operate in I-P or SI units. This is controlled by entering either *IP* or *SI* in cell C26 of the master input worksheet. All other unit-dependent inputs are interpreted based on this cell.

B.3.1 Master Input Worksheet Parameters

Tables B.1 to B.8 describe or define the input parameters in the master input worksheet, giving the cell locations, and a brief note on the use and, in some cases, the source of the data.

B.3.2 Input Parameters in the Zone Sheets

All of the input parameters described in the master input worksheets are passed directly to the zone sheets by linking the corresponding cells in the zone worksheet to the master input worksheet cell locations. IMPORTANT: These values can be overridden at the zone level by replacing the equation link to the mas-

Load Calculation Applications Manual (SI), Second Edition

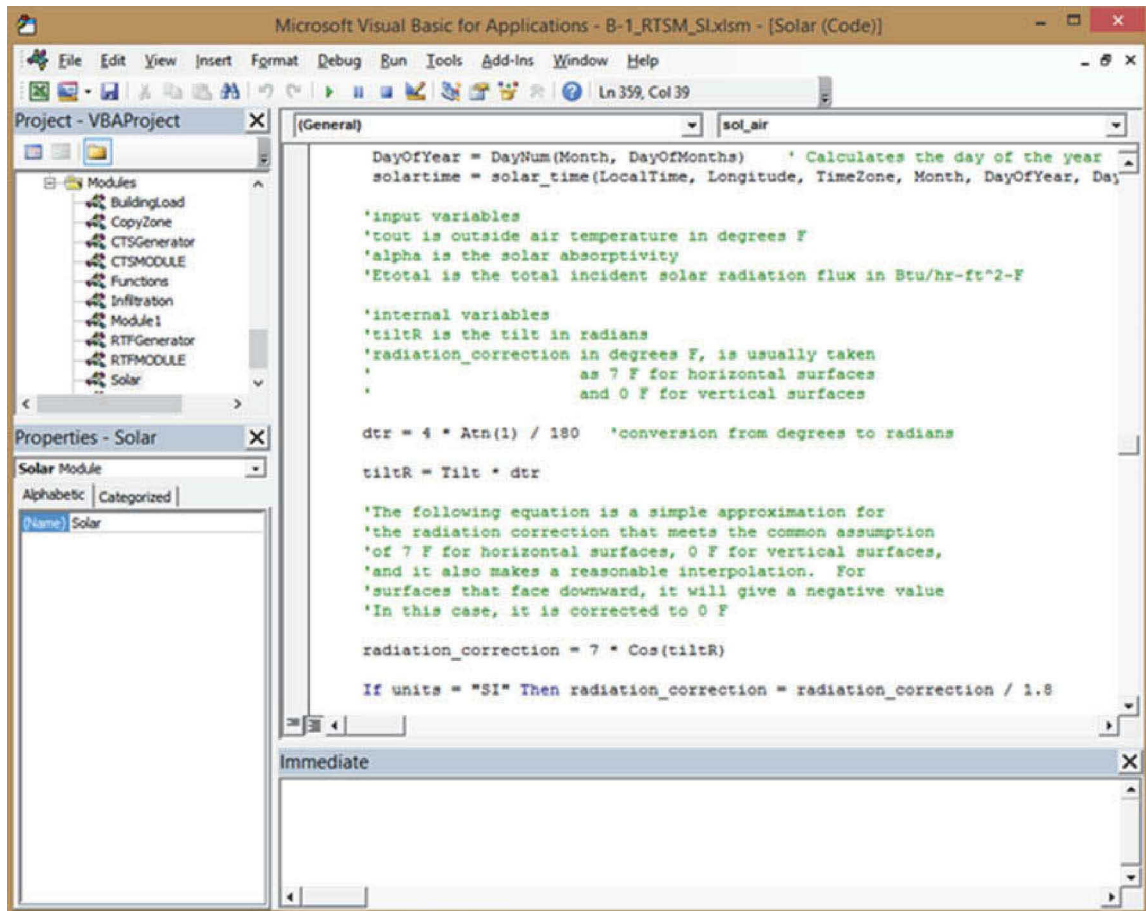


Figure B.9 Visual basic editor showing *Solar_Beam* function in solar module.

ter input worksheet with the actual value. The cell locations for these parameters in the zone sheets are not necessarily the same as in the master input worksheet. The zone-specific input parameters such as the zone geometry, orientations, construction fabrics, and window geometries are specified in each zone. The descriptions of the input parameters are outlined in Tables B.9–B.19.

B.4 Intermediate Results on Zone Worksheets

The intermediate results that appear in the zone worksheets are described briefly in Tables B.20–B.22.

B.5 Results: Zone Design Day Cooling Load

The hourly cooling loads for each design day and for each zone are summarized on the zone worksheet, as summarized in Table B.23. The zone cooling loads are summarized for the 24 hourly values of the design day. The hourly values are summarized by heat gain type.

Appendix B: Spreadsheet Implementation of the RTSM

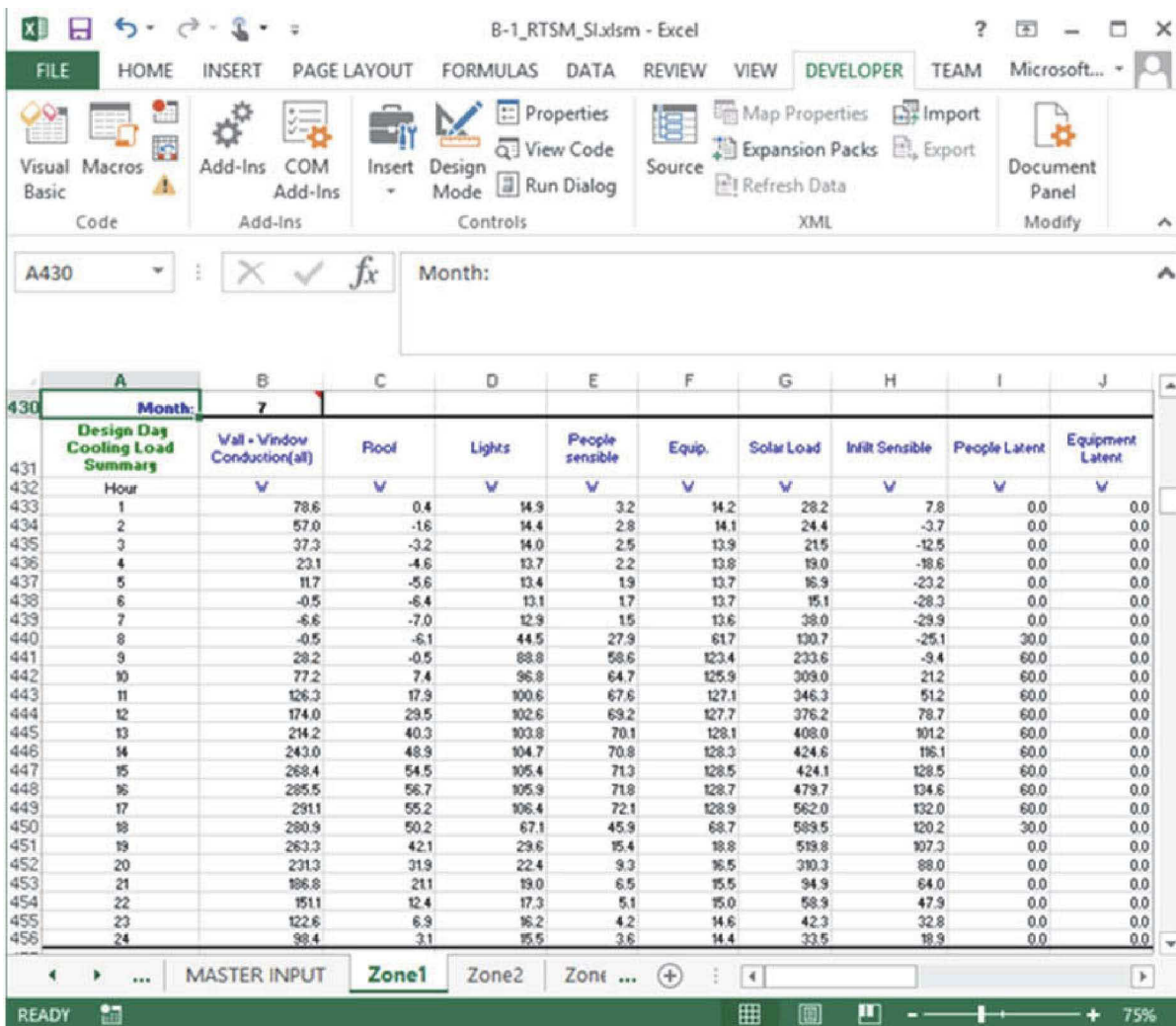


Figure B.10 Cooling loads for July design day, first part.

B.6 Results: Zone Monthly-Hourly Cooling Loads

When all 12 months are run, the zone hourly cooling loads given in Table B.23 are summarized for each of the 12 months, making a total of 288 hourly values, as shown in Table B.24. Then the zone peak cooling is determined by selecting the maximum value of the 288 hourly cooling loads. The cooling load components corresponding to the zone peak cooling load are summarized in the zone worksheets in the cell range A757:U757.

B.7 Results: Building Monthly-Hourly Cooling Loads

Building cooling loads, summed for all zones, for each hour of each monthly design day are summarized, by heat gain component, in the master input worksheet. The 288 hourly total zone cooling loads are added component by component to determine the building monthly-hourly cooling loads summary as shown in Table B.25.

Load Calculation Applications Manual (SI), Second Edition

	Infiltr Latent	Zone Sensible	Zone Latent	Zone Total	Lighting to return Air	Roof Heat Gain To Return Air	Sub Total To Return Air	Total Cooling Load
430								
431								
432								
433	-99.6	147.2	-99.6	47.6	0.0	-1.3	-1.3	46.4
434	-119.0	107.4	-119.0	-11.7	0.0	-1.9	-1.9	-13.5
435	-133.2	73.4	-133.2	-59.8	0.0	-2.4	-2.4	-62.2
436	-142.8	48.6	-142.8	-94.2	0.0	-2.8	-2.8	-97.0
437	-149.8	28.9	-149.8	-120.9	0.0	-3.2	-3.2	-124.1
438	-157.5	8.4	-157.5	-149.1	0.0	-3.4	-3.4	-152.5
439	-159.8	22.5	-159.8	-137.2	0.0	-3.6	-3.6	-140.8
440	-152.6	233.1	-122.6	190.5	0.0	-3.2	-3.2	97.4
441	-129.2	522.8	-69.2	454.5	0.0	-0.7	-0.7	453.9
442	-75.8	702.3	-15.8	686.6	0.0	3.9	3.9	690.5
443	-17.6	837.1	42.4	879.5	0.0	9.7	9.7	889.2
444	42.3	957.9	102.3	1060.2	0.0	15.5	15.5	1075.7
445	96.3	1065.7	156.3	1222.0	0.0	20.6	20.6	1242.6
446	135.1	1136.4	195.1	1331.5	0.0	24.3	24.3	1355.8
447	169.9	1180.6	228.9	1409.5	0.0	26.3	26.3	1435.8
448	196.2	1262.8	246.2	1509.0	0.0	26.6	26.6	1535.6
449	179.0	1347.7	239.0	1586.7	0.0	25.1	25.1	1611.8
450	146.0	1222.6	176.0	1398.6	0.0	21.9	21.9	1420.5
451	111.9	996.3	111.9	1108.2	0.0	17.3	17.3	1125.5
452	64.1	709.8	64.1	773.9	0.0	11.9	11.9	785.8
453	9.3	407.9	9.3	417.2	0.0	6.6	6.6	423.8
454	-24.4	307.6	-24.4	283.2	0.0	2.7	2.7	285.6
455	-54.1	239.7	-54.1	185.5	0.0	0.6	0.6	186.1
456	-80.1	187.4	-80.1	107.4	0.0	-0.5	-0.5	106.9

Figure B.11 Cooling loads for July design day, second part.

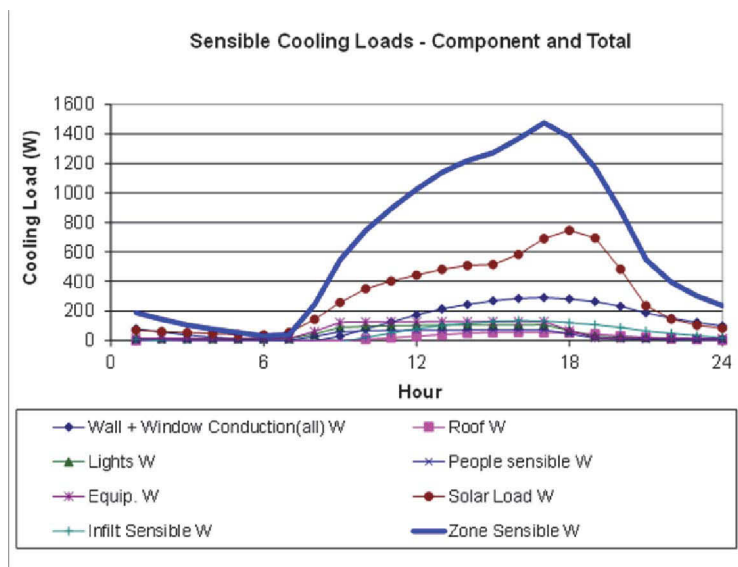


Figure B.12 Zone sensible cooling loads for July 21.

Appendix B: Spreadsheet Implementation of the RTSM

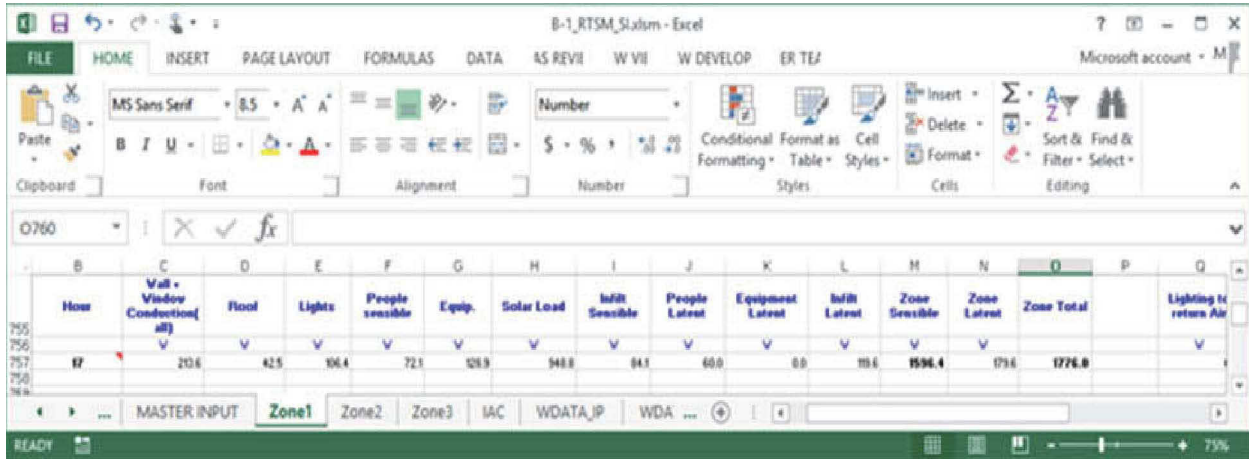


Figure B.13 Summary of peak cooling load, which occurs in September.

Table B.1 Site: Location and Design Weather Conditions

Parameter	Cell	Units	Description and Notes
Latitude	C11	degrees	Local latitude: northern hemisphere positive, southern hemisphere negative
Longitude	C12	degrees	Local longitude: west of the prime meridian, positive; east of the prime meridian, negative
Time zone	C13	hours	Standard time zone of the location: hours west of GMT positive, hours east of GMT negative. Example: Atlanta is in NAE, 5 hours west of GMT; the value of the time zone parameter is 5
Month	C14	—	Month of the year: Jan.=1, Feb.= 2, ...
Day of month	C15	—	Design day of the month (default 21)
Daylight savings	C16	—	1: Daylight savings time is used at this location. 0: Daylight savings time is not used at this location.
Ground reflectance	C18	—	Reflectance of the ground, see Table D.2
Design dB temperature	C19	°F (°C)	Peak design day temperature of the month
Design wB temperatures	C20	°F (°C)	Mean coincident wet-bulb temperature of the month
Daily range	C21	°F (°C)	Design daily dry bulb temperature range of the month
taub	C22	—	Clear-sky optical depth for beam irradiance
taud	C23	—	Clear-sky optical depth for diffuse irradiance
h _{out}	C24	Btu/h·ft ² ·°F (W/m ² ·K)	Outside surface combined conductance, Table 3.4

Load Calculation Applications Manual (SI), Second Edition

Table B.2 Units and Site: Altitude and Barometric Pressure

Parameter	Cell	Units	Description and Notes
Units	C26	—	Units of measurement either I-P or SI
Altitude	C27	ft (m)	Site local elevation from sea level
Barometric pressure	C28	psi (kPa)	Local atmospheric pressure (from weather data)

Table B.3 Conduction Heat Gain: Radiative and Convective Fractions

Parameter	Cell	Units	Description and Notes
Walls	G24:H24	%	Radiative and convective fractions, Table 7.10
Roofs	G25:H25	%	Radiative and convective fractions, Table 7.10
Windows	G26:H26	%	Radiative and convective fractions, Table 7.10

Table B.4 Inside Design Conditions

Parameter	Cell	Units	Description and Notes
dB temperature, cooling	M11	°F (°C)	Room air design dry-bulb temperature
Relative humidity	N11	%	Room air design relative humidity

Table B.5 Fractions to Return Air

Parameter	Cell	Units	Description and Notes
Lighting	Q9	%	Fraction of lighting heat gain that goes to the return air
Roof	Q10	%	Fraction of roof conduction heat gain that goes to return air

References

- ASHRAE. 2013. *ASHRAE Handbook—Fundamentals*. Atlanta: ASHRAE.
- Gueymard, C.A. and D. Thevenard. 2009. Monthly average clear-sky broadband irradiance database for worldwide solar heat gain and building cooling load calculations. *Solar Energy* 83:1998–2018.
- Thevenard, D. and C.A. Gueymard. 2010. Updating the ASHRAE climatic data for design and standards. *ASHRAE Transactions* 116(2):444–59.

Appendix B: Spreadsheet Implementation of the RTSM

Table B.6 Internal Heat Gains

Parameter	Cell	Units	Description and Notes
People			
Area/person	N15	ft ² /person (m ² /person)	Occupancy density in unit area per person
Sensible/person	N16	[Btu/h(W)]/person	Rate of sensible heat gain per person, Table 6.1
Latent/person	N17	[Btu/h(W)]/person	Rate of latent heat gain per person, Table 6.1
Radiant fraction	O16	%	Radiant fraction of the people sensible heat gain, Table 6.1
Convective fraction	P16	%	Convective fraction of people sensible heat gain
Lighting			
Heat gain rate	N19	W/ft ² (W/m ²)	Rate of lighting heat gain per unit floor area
Radiant fraction	O19	%	Radiant fraction of lighting heat gain, Table 6.3
Convective fraction	P19	%	Convective fraction lighting heat gain
Equipment			
Sensible heat gain rate	N21	W/ft ² (W/m ²)	Equipment peak sensible heat gain
Latent heat gain rate	N22	W/ft ² (W/m ²)	Equipment peak latent heat gain, Chapter 6
Radiant fraction	O21	%	Radiant fraction of equipment sensible heat gain, Chapter 6
Convective fraction	P21	%	Convective fraction equipment sensible heat gain, Chapter 6

Load Calculation Applications Manual (SI), Second Edition

Table B.7 Fenestration Solar Heat Gain

Parameter	Cell	Units	Description and Notes
Normal solar heat gain coefficient (SHGC)	O25	—	SHGC at zero incidence angle
Interior attenuation coefficients (IAC): Tables 3.9a through 3.9g		—	Interior attenuation coefficients for interior shades
IAC ₀	Q33	—	IAC at 0° incidence angle
IAC ₆₀	Q34	—	IAC at 60° incidence angle
IAC _D	Q35	—	IAC for diffuse irradiation
Radiative fraction	Q36	%	Radiative fraction of solar heat gains, see Table 7.10 and Tables 3.9a to 3.9g
SHGC Correction: Table 3.8			
Coef1	L30	—	SHGC correction at 0° incident angle
Coef2	L31	—	SHGC correction at 40° incident angle
Coef3	L32	—	SHGC correction at 50° incident angle
Coef4	L33	—	SHGC correction at 60° incident angle
Coef5	L34	—	SHGC correction at 70° incident angle
Coef6	L35	—	SHGC correction at 80° incident angle
Coef7	L36	—	Diffuse SHGC correction

Table B.8 Internal Heat Gain Schedules

Parameter	Cell	Units	Description and Notes
People heat gain schedule	C37:D60	—	Hourly people occupancy fractions
Lighting heat gain schedule	D37:D60	—	Hourly lighting use fractions
Equipment heat gain schedule	E37:D60	—	Hourly equipment use fractions

Appendix B: Spreadsheet Implementation of the RTSM

Table B.9 Location and Design Weather Conditions

Parameter	Cell	Units	Description and Notes
Latitude	C7	degrees	Local latitude: northern hemisphere positive, southern hemisphere negative
Longitude	C8	degrees	Local Longitude: west of the prime meridian, positive; east of the prime meridian, negative
Time zone	C9	—	Standard time zone of the location: hours west of GMT positive, hours east of GMT negative. Example: Atlanta is in NAE, 5 hours west of GMT; value of time zone
Month	C10	—	Month of the year: Jan.=1, Feb.= 2, ...
Day of month	C11	—	Design day of the month (default 21)
Daylight savings	C12	—	1: Daylight savings time is used at this location 0: Daylight savings time is not used at this location
Ground reflectance	C14	—	Ground reflectance, Table D.2
Design dB temperature	C15	°F (°C)	Peak design day temperature of the month
Design wB temperature	C16	°F (°C)	Mean coincident wet-bulb temperature of the month
Daily range	C17	°F (°C)	Design daily dry bulb temperature range of the month
h_{out}	C18	Btu/h·ft ² ·°F (W/m ² ·K)	Outside surface combined conductance, Table 3.4
Taub	F21	—	Clear-sky optical depth for beam irradiance
Taud	F22	—	Clear-sky optical depth for diffuse irradiance

Table B.10 Units and Site: Altitude and Barometric Pressure

Parameter	Cell	Units	Description and Notes
Units	C20	—	Units of measurement either I-P or SI
Altitude	C21	ft (m)	Site local elevation from sea level
Barometric pressure	C22	psi (kPa)	Local atmospheric pressure from weather data

Table B.11 Zone Infiltration

Parameter	Cell	Units	Description and Notes
Ceiling height	F10	ft (m)	Ceiling height of the zone
Floor area	F11	ft ² (m ²)	Zone inside floor area
Zone volume	F12	ft ³ (m ³)	Zone volume
Air changes per hour (ACH)	F13	ach	Air changes per hour of the zone
Rate	F14	cfm (m ³ /s)	Infiltration rates

Load Calculation Applications Manual (SI), Second Edition

Table B.12 Inside Design Conditions

Parameter	Cell	Units	Description and Notes
dB temperature, cooling	E7	°F (°C)	Room air design dry-bulb temperature
Relative humidity	F7	%	Room air design relative humidity

Table B.13 Fraction to Return Air

Parameter	Cell	Units	Description and Notes
Lighting	F17	%	Fraction of the lighting heat gain picked by the return airstream
Roof	F18	%	Fraction of the roof conduction heat gain picked by the return airstream

Table B.14 Conduction Heat Gain: Radiative and Convective Fractions

Parameter	Cell	Units	Description and Notes
Walls	J16:K16	%	Radiative and convective fractions, Table 7.10
Roofs	J17:K17	%	Radiative and convection fractions, Table 7.10
Windows	J18:K18	%	Radiative and convection fractions, Table 7.10

Appendix B: Spreadsheet Implementation of the RTSM

Table B.15 Internal Heat Gains

Parameter	Cell	Units	Description and Notes
People			
Area/person	I6	ft ² /person (m ² /person)	Occupancy density in unit area per person
Sensible/person	I7	[Btu/h(W)]/ person	Rate of sensible heat gain per person, Table 6.1.
Latent/person	I8	[Btu/h(W)]/ person	Rate of latent heat gain per person, Table 6.1.
Radiant fraction	J6	%	Radiant fraction of the people sensible heat gain, Table 6.1
Convective fraction	K6	%	Convective fraction of people sensible heat gain
Lighting			
Heat gain rate	I10	W/ft ² (W/m ²)	Rate of lighting heat gain per unit floor area
Radiant fraction	J10	%	Radiant fraction of lighting heat gain, Table 6.3
Convective fraction	K10	%	Convective fraction lighting heat gain
Equipment			
Sensible heat gain rate	I12	W/ft ² (W/m ²)	Equipment peak sensible heat gain
Latent heat gain rate	I13	W/ft ² (W/m ²)	Equipment peak latent heat gain, Chapter 6
Radiant fraction	J12	%	Radiant fraction of equipment sensible heat gain, Chapter 6
Convective fraction	K12	%	Convective fraction equipment sensible heat gain, Chapter 6

Table B.16 Fenestration Solar Heat Gain

Parameter	Cell	Units	Description and Notes
Normal solar heat gain coefficient (SHGC)	O5	—	SHGC at zero incidence angle
Interior attenuation coefficients (IAC): Tables 3.9a through 3.9g		—	Interior attenuation coefficients for interior shades
IAC ₀	N19	—	IAC at 0° incidence angle
IAC ₆₀	N20	—	IAC at 60° incidence angle
IAC _D	N21	—	IAC for diffuse irradiation
Radiative fraction	N22	%	Radiative fraction of solar heat gains, see Table 7.10 and Tables 3.9a to 3.9g
SHGC Correction: Table 3.8			
Coef1	N10	—	SHGC correction at 0° incident angle
Coef2	N11	—	SHGC correction at 40° incident angle
Coef3	N12	—	SHGC correction at 50° incident angle
Coef4	N13	—	SHGC correction at 60° incident angle
Coef5	N14	—	SHGC correction at 70° incident angle
Coef6	N15	—	SHGC correction at 80° incident angle
Coef7	N16	—	Diffuse SHGC correction

Load Calculation Applications Manual (SI), Second Edition

Table B.17 Internal Heat Gain Schedules

Parameter	Cell	Units	Description and Notes
People schedule	C290:C313	—	Hourly people occupancy fraction
Lighting schedule	F290:F313	—	Hourly lighting use fraction
Equipment schedule	H290:H313	—	Hourly equipment use fraction

Table B.18 Zone Geometry, Surface Construction, and Properties

Parameter	Cell	Units	Description and Notes
Surface ID	C26:V26	—	Zone surface number, assigned sequentially, starting with 1
Surface type	C27:V27	—	Name of surfaces: the following key words are utilized: <i>wall</i> for exterior and internal surfaces, <i>window</i> for fenestrations, <i>roof</i> for roofs, <i>floor</i> for floor, and <i>furniture</i> for furnishings
Facing	C28:V28	degrees	Surface facing direction measured clockwise from north
Tilt angle	C29:V29	degrees	Surface tilt angle from the horizontal
Area	C30:V30	ft ² (m ²)	Surface area
LW emissivity in	C31:V31	—	Inside surface emissivity/absorptivity
SW absorption out	C32:V32	—	Outside surface absorptance to shortwave radiation, (i.e., solar)
Boundary conditions	C33:V33	—	Boundary conditions: <i>TOS</i> for exterior surfaces, <i>TA</i> for partition surfaces. The key difference is that <i>TOS</i> surfaces are used both for computing the response of the zone and for computing net heat gain to the zone. <i>TA</i> surfaces are only used for computing the response of the zone—they store and release energy but have no net heat gain.
Number of layers	C34:V34	—	Number of layers in each construction including the inside and outside combined conductance
Layer code	C35:V44	—	Surface construction layers code. To be selected from the worksheets <i>Layers IP</i> or <i>Layers SI</i> for I-P and SI units, respectively. See Table 7.5. Users may add their own construction layer codes into the spreadsheet worksheets <i>Layers IP</i> and <i>Layers SI</i> . New layers may be entered there with a layer code of no more than three characters—letters and numbers only.

Table B.19 Window Geometry

Parameter	Cell	Units	Description and Notes
Window height	C47:V47	ft (m)	Window height
Window width	C48:V48	ft (m)	Window width
Horizontal Projection			
P _H	C50:V50	ft (m)	Overhang depth, Figure D.3
R _H	C51:V51	ft (m)	Overhang distance from the window, Figure D.3
Vertical Projection			
P _V	C53:V53	ft (m)	Fin vertical projection depth, Figure D.3
R _W	C54:V54	ft (m)	Fin lateral distance from the window, Figure D.3

Appendix B: Spreadsheet Implementation of the RTSM

Table B.20 Zone Intermediate Results, Part I

Parameter	Cell	Units	Description and Notes
Beam Radiation			
Surface type	C66:V66	—	Key words used to identify surfaces: <i>wall, window, roof, floor, and furniture</i>
Beam radiation	C67:V90	Btu/h·ft ² (W/m ²)	Beam irradiation, calculated using the procedure given in Appendix D, Equation D.21. Each column represents a zone surface.
Diffuse Radiation			
Surface name	C93:V93	—	Surface names linked to the zone inputs
Diffuse radiation	C94:V117	Btu/h·ft ² (W/m ²)	Diffuse irradiation, calculated using the procedure given in Appendix D, Equations D.22–D.25. Each column represents a zone surface.
Sol-Air Temperature			
Surface name	C120:V120	—	Surface names linked to the zone inputs
Other side temperature	C121:V144	°F (°C)	Sol-air temperatures for exterior surfaces, room air temperature for partition surfaces, and outdoor air temperatures for fenestration
CTSFs			
Surface type	C147:V147	—	Key words used to identify surfaces: <i>wall, window, roof, floor and furniture</i>
U-factor	C148:V148	Btu/h·ft ² ·°F (W/m ² ·K)	Air-to-air U-factors of surfaces
CTSFs	C149:V172	—	Conduction time series factor of each construction in the zone
Conduction Heat Gains			
Surface type	C177:V177	—	Key words used to identify surfaces: <i>wall, window, roof, floor, and furniture</i>
Conduction heat gain	C178:V201	Btu/h (W)	Conduction heat gain computed using Equation 7.1 or 7.2
Sunlit Area Fraction			
Surface name	C204:V204	—	Surface names linked to the zone inputs
Sunlit area fraction	C205:V228	—	Sunlit area fraction. Accounts for area of the window shaded by the overhang and/or fins. For use with direct solar heat gain calculation. Uses Equation D.30
Window Beam Solar Heat Gain			
Surface name	C232:V232	—	Surface names linked to the zone inputs
Beam solar heat gain	C233:V256	Btu/h (W)	Beam solar heat gain for each fenestration, Equation 7.4a
Window Diffuse Solar Heat Gain			
Surface name	C260:V260	—	Surface names linked to the zone inputs
Diffuse solar heat gain	C261:V284	Btu/h (W)	Diffuse solar heat gain for each fenestration, Equation 7.4b

Load Calculation Applications Manual (SI), Second Edition

Table B.21 Zone Intermediate Results, Part II

Parameter	Cell	Units	Description and Notes
Internal Heat Gains			
People schedule	C290:C313	—	Fraction of the peak people heat gains
Sensible heat gain	D290:D313	Btu/h (W)	Sensible heat gain due to occupancy, Table 6.1
Latent heat gain	E290:E313	Btu/h (W)	Latent heat gain due to occupancy, Table 6.1
Lighting schedule	F290:F313	—	Fraction of the peak lighting heat gains
Lighting heat gain	G290:G313	Btu/h (W)	Sensible heat gain due to lighting, Equation 6.1 and Table 6.2
Equipment schedule	H290:H313	—	Fraction of the peak equipment heat gain
Sensible equipment heat gain	I290:I313	Btu/h (W)	Sensible heat gain due to equipment, Equations 6.2 to 6.6 and Tables 6.4 to 6.12
Latent equipment heat gain	J290:J313	Btu/h (W)	Latent heat gain due to equipment, Tables 6.5a to 6.5e
Infiltration Heat Gain			
Outdoor air temperature	C319:C342	°F (°C)	Outdoor air temperature
Sensible heat gain	D319:D342	Btu/h (W)	Sensible heat gain due to infiltration, Equation 5.4
Latent heat gain	E319:E342	Btu/h (W)	Latent heat gain due to infiltration, Equation 5.5
Heat Gain Summary			
Walls conduction heat gain	B348:B371	Btu/h (W)	Radiative heat gain due to conduction for walls
	C348:C371	Btu/h (W)	Convective heat gain due to conduction for walls
Roof conduction heat gain	D348:D371	Btu/h (W)	Radiative heat gain due to conduction for roofs
	E348:E371	Btu/h (W)	Convective heat gain due to conduction for roofs
Window conduction heat gain	F348:F371	Btu/h (W)	Radiative heat gain due to conduction for windows
	G348:G371	Btu/h (W)	Convective heat gain due to conduction for windows
Diffuse solar heat gain	H348:H371	Btu/h (W)	Diffuse solar heat gain radiative component
	I348:I371	Btu/h (W)	Diffuse solar heat gain convective component
Lighting sensible heat gain	J348:J371	Btu/h (W)	Sensible heat gain radiative component due to lighting
	K348:K371	Btu/h (W)	Sensible heat gain convective component due to lighting
People sensible heat gain	L348:L371	Btu/h (W)	Sensible heat gain radiative component due to equipment
	M348:M371	Btu/h (W)	Sensible heat gain convective component due to equipment
Equipment sensible heat gain	N348:N371	Btu/h (W)	Sensible heat gain radiative component due to people
	O348:O371	Btu/h (W)	Sensible heat gain convective component due to people
Beam solar heat gain	P348:P371	Btu/h (W)	Beam solar heat gain radiative component for fenestrations
	Q348:Q371	Btu/h (W)	Beam solar heat gain convective component for fenestrations

Appendix B: Spreadsheet Implementation of the RTSM

Table B.22 Zone Intermediate Results, Part III

Parameter	Cell	Units	Description and Notes
Fraction to Return Air			
Lighting sensible heat gain to return airstream	S348:S371	Btu/h (W)	Lighting sensible heat gain radiative component to return air
	T348:T371	Btu/h (W)	Lighting sensible heat gain convective component to return air
Roof conduction heat gain to return airstream	U348:U371	Btu/h (W)	Roof conduction heat gain radiative component to return air
	V348:V371	Btu/h (W)	Roof conduction heat gain convective component to return air
RTF Coefficients			
Non-solar RTF	B375:N398	—	RTF coefficients
	S375:U398	—	RTF coefficients
Solar RTF	P375:P398	—	RTF coefficients
Cooling Loads Summary			
Cooling load due to walls conduction heat gain	B405:B428	Btu/h (W)	Cooling loads due to walls conduction heat gain radiative component
	C405:C428	Btu/h (W)	Cooling loads due to walls conduction heat gain convective component
Cooling load due to roof conduction heat gain	D405:D428	Btu/h (W)	Cooling loads due to roof conduction heat gain radiative component
	E405:E428	Btu/h (W)	Cooling loads due to roof conduction heat gain convective component
Cooling load due to window conduction heat gain	F405:F428	Btu/h (W)	Cooling load due to windows conduction heat gain radiative component
	G405:G428	Btu/h (W)	Cooling load due to windows conduction heat gain convective component
Cooling load due to diffuse solar heat gain	H405:H428	Btu/h (W)	Cooling load due to diffuse solar heat gain radiative component
	I405:I428	Btu/h (W)	Cooling load due to diffuse solar heat gain convective component
Cooling load due to lighting heat gain	J405:J428	Btu/h (W)	Cooling load due to lighting heat gain radiative component
	K405:K428	Btu/h (W)	Cooling load due to lighting heat gain convective component
Cooling load due to people heat gain	L405:L428	Btu/h (W)	Cooling load due to equipment heat gain radiative component
	M405:M428	Btu/h (W)	Cooling load due to equipment heat gain convective component
Cooling load due to equipment heat gain	N405:N428	Btu/h (W)	Cooling load due to people heat gain radiative component
	O405:O428	Btu/h (W)	Cooling load due to people heat gain convective component
Cooling load due to beam solar heat gain	P405:P428	Btu/h (W)	Cooling load due to beam solar heat gain radiative component
	Q405:Q428	Btu/h (W)	Cooling load due to beam solar heat gain convective component
Cooling Load to Return Air			
Lighting sensible heat gain to return airstream	S405:S428	Btu/h (W)	Cooling load due to lighting heat gain radiative components to return air
	T405:T428	Btu/h (W)	Cooling load due to lighting heat gain convective components to return air
Roof conduction heat gain to return airstream	U405:U428	Btu/h (W)	Cooling load due to roof conduction heat gain radiative component to return air
	V405:V428	Btu/h (W)	Cooling load due to roof conduction heat gain convective component to return air

Load Calculation Applications Manual (SI), Second Edition

Table B.23 Design Day Cooling Load Summary

Parameter	Cell	Units	Description and Notes
Hour	A433:A456	—	Hours of the day
Walls	B433:B456	Btu/h (W)	Cooling loads due to conduction for walls
Roofs	C433:C456	Btu/h (W)	Cooling loads due to conduction for roofs
Lighting	D433:D456	Btu/h (W)	Cooling loads due to lighting heat gain
People sensible	E433:E456	Btu/h (W)	Cooling loads due to people sensible gain
Equipment sensible	F433:F456	Btu/h (W)	Cooling loads due to equipment sensible gain
Solar heat gain	G433:G456	Btu/h (W)	Cooling loads due to solar heat gain
Infiltration sensible	H433:H456	Btu/h (W)	Cooling loads due to sensible infiltration heat gain
People latent	I433:I456	Btu/h (W)	Cooling loads due to people latent heat gain
Equipment latent	J433:J456	Btu/h (W)	Cooling loads due to equipment latent heat gain
Infiltration latent	K433:K456	Btu/h (W)	Cooling loads due to infiltration latent heat gain
Zone total sensible	L433:L456	Btu/h (W)	Cooling loads of the zone due to sensible heat gain
Zone total latent	M433:M456	Btu/h (W)	Cooling loads due to latent heat gain
Zone total	N433:N456	Btu/h (W)	Cooling loads of the zone
Lighting cooling load to return air	P433:P456	Btu/h (W)	Cooling loads due to lighting to return air
Roof cooling load to return air	Q433:Q456	Btu/h (W)	Cooling loads due to roof heat gain to return airstream
Cooling load to return air	R433:R456	Btu/h (W)	Cooling loads due to lighting and roof conduction heat gains to return airstream
Total cooling load	T433:T456	Btu/h (W)	Total system cooling load of the zone

Appendix B: Spreadsheet Implementation of the RTSM

Table B.24 Zone Hourly Cooling Load Summary

Parameter	Cell	Units	Description and Notes
Month	A464:A751	—	Month of the year: Jan. = 1, Feb. = 2, ...
Hour	B464:B751	—	Hour of the day: 1...24
Walls	C464:C751	Btu/h (W)	The zone hourly cooling loads due to conduction for walls
Roofs	D464:D751	Btu/h (W)	The zone hourly cooling loads due to conduction for roofs
Lighting	E464:E751	Btu/h (W)	The zone hourly cooling loads due to lighting heat gain
People sensible	F464:F751	Btu/h (W)	The zone hourly cooling loads due to people sensible gain
Equipment sensible	G464:G751	Btu/h (W)	The zone hourly cooling loads due to equipments sensible gain
Solar heat gain	H464:H751	Btu/h (W)	The zone hourly cooling loads due to solar heat gain
Infiltration sensible	I464:I751	Btu/h (W)	The zone hourly cooling loads due to sensible infiltration heat gain
People latent	J464:J751	Btu/h (W)	The zone hourly cooling loads due to people latent heat gain
Equipment latent	K464:K751	Btu/h (W)	The zone hourly cooling loads due to equipment latent heat gain
Infiltration latent	L464:L751	Btu/h (W)	The zone hourly cooling loads due to infiltration latent heat gain
Zone total sensible	M464:M751	Btu/h (W)	The zone hourly cooling loads of the zone due to sensible heat gain
Zone total latent	N464:N751	Btu/h (W)	The zone hourly cooling loads due to latent heat gain
Zone total cooling load	O464:O751	Btu/h (W)	The zone hourly cooling loads of the zone
Lighting cooling load to return air	Q464:Q751	Btu/h (W)	The zone hourly cooling loads due to lighting to return air
Roof cooling load to return air	R464:R751	Btu/h (W)	The zone hourly cooling loads due to roof heat gain to return air
Total cooling load to return air	S464:S751	Btu/h (W)	The zone hourly cooling loads due to roof and lighting heat gain to return air
Total zone system cooling load	U464:U751	Btu/h (W)	The zone total hourly system cooling loads

Load Calculation Applications Manual (SI), Second Edition

Table B.25 Building Monthly-Hourly Cooling Load Summary

Parameter	Cell	Units	Description and Notes
Month	A70:A357	—	Month of the year: Jan.=1, Feb.= 2, ...
Hour	B70:B357	—	Hour of the day: 1...24
Walls	C70:C357	Btu/h (W)	The building total hourly cooling loads due to conduction through exterior walls
Roofs	D70:D357	Btu/h (W)	The building total hourly cooling loads due to conduction through roofs
Lighting	E70:E357	Btu/h (W)	The building total hourly cooling loads due to lighting heat gain
People sensible	F70:F357	Btu/h (W)	The building total hourly cooling loads due to people sensible gain
Equipment sensible	G70:G357	Btu/h (W)	The building total hourly cooling loads due to equipment sensible gain
Solar	H70:H357	Btu/h (W)	The building total hourly cooling loads due to solar heat gain
Infiltration sensible	I70:I357	Btu/h (W)	The building total hourly cooling loads due to sensible infiltration heat gain
People latent	J70:J357	Btu/h (W)	The building total hourly cooling loads due to people latent heat gain
Equipment latent	K70:K357	Btu/h (W)	The building total hourly cooling loads due to equipment latent heat gain
Infiltration latent	L70:L357	Btu/h (W)	The building total hourly cooling loads due to infiltration latent heat gain
Zone sensible	M70:M357	Btu/h (W)	The building total hourly cooling loads due to sensible heat gain
Zone latent	N70:N357	Btu/h (W)	The building total hourly cooling loads due to latent heat gain
Zone total	O70:O357	Btu/h (W)	The building total hourly cooling loads
Lighting load to return air	Q70:Q357	Btu/h (W)	The building total hourly cooling loads due to lighting to return air
Roof load to return air	R70:R357	Btu/h (W)	The building total hourly cooling loads due to roof heat gain to return air
Load to return air	S70:S357	Btu/h (W)	The building total hourly cooling loads due to roof and lighting heat gain to return air
Total building load	U70:U357	Btu/h (W)	The building total hourly system cooling loads

Appendix C

Calculation of CTSFs and RTFs

This appendix briefly describes the calculation of conduction time series factors (CTSFs) and radiant time factors (RTFs). Only a brief description of the procedures is given here. For details, the reader is referred to the original papers by Spitler and Fisher (1999) and Nigusse (2007) for CTSF generation and Nigusse (2007) for RTF generation using a reduced heat balance method (HBM).

C.1 CTSF Generation

The CTSFs are normalized periodic response factors. That is, they are equivalent to the periodic response factors defined by Spitler et al. (1997) divided by the U-factor of the construction. In the 2001 and 2005 editions of the *ASHRAE Handbook—Fundamentals* (ASHRAE 2005), they were referred to as *conduction time factors*. In order to reduce ambiguity for the acronym CTF, the term *conduction time series factor* (CTSFS) has been adopted.

Periodic response factors (PRFs) can be generated by converting tabulated or otherwise-computed CTF coefficients (Spitler and Fisher 1999), using a frequency response regression method (Chen and Wang 2005) or using a one-dimensional numerical method (Nigusse 2007). For this manual, a one-dimensional implicit finite volume method (FVM) has been implemented in visual basic for application (VBA). The FVM routines use six uniform control volumes per layer with a fixed 60-second time step. The periodic response factors are generated by exciting the construction with a unit triangular temperature pulse and computing the resulting heat flux until the response drops below a set limit. The hourly response factors are changed into periodic response factors by summing the corresponding terms as described by Spitler et al. (1997). Then the PRFs are converted to CTSFs by dividing by the U-factor. For further details, see Nigusse (2007).

C.2 CTSF Generation—Spreadsheet Implementation

In the spreadsheet *C-1_CTSFgen.xls*, included in the supporting files accompanying this manual (online at www.ashrae.org/lcam) and shown in Figure C.1, the user enters the layer codes, from outside to inside, in Cells B5:B14. The spreadsheet comes with thermal properties of the material layers from Table 7.5, but the reader may add more to either the sheet *LAYERS IP* or the sheet *LAYERS SI*. Both sheets have a button that will translate and copy the layers from one sheet to the other sheet. The actual computation is done in SI units; users entering in *LAYERS IP* should click on the button to translate and copy their layers to the other worksheet.

Once the layers are entered, clicking on the *GENERATE CTSF* button will cause the spreadsheet to calculate the CTSFs and U-factors, and the CTSFs will be plotted as shown in Figure C.2.

C.3 RTF Generation

As part of ASHRAE RP-1326 (Spitler 2009), a reduced heat balance procedure was developed to generate RTFs. This algorithm has been implemented in the radiant time series method (RTSM) spreadsheets used in Chapters 7 and 8. The RTF coefficients are determined by exciting the thermal zone model with a

Load Calculation Applications Manual (SI), Second Edition

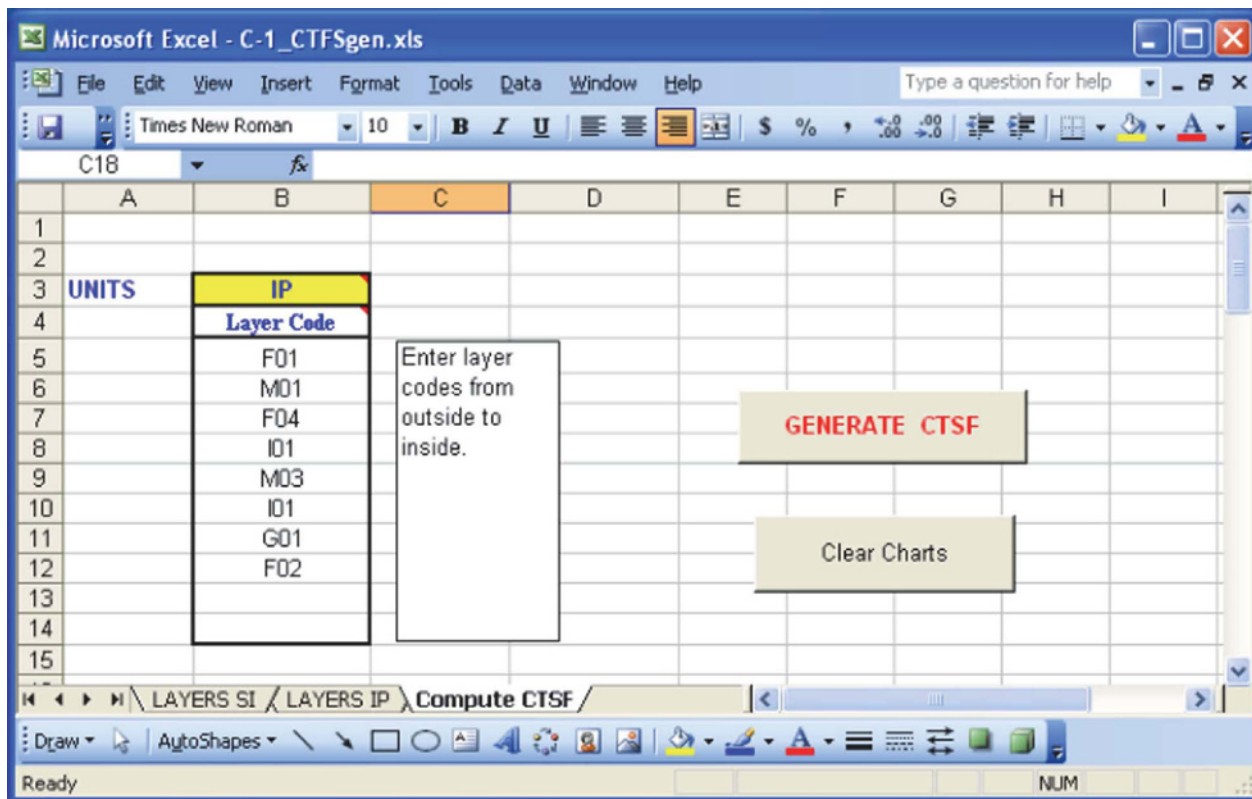


Figure C.1 CTSF generation spreadsheet inputs.

radiant pulse and monitoring the resulting cooling loads. Solar and nonsolar RTFs are obtained by adjusting the distribution of the radiant pulse. Full details may be found in Nigusse (2007). The spreadsheet *C-2_RTFgen.xls* implements this algorithm in VBA code.

C.4 RTF Generation—Spreadsheet Implementation

This section describes a spreadsheet implementation of the RTF generation procedure. This may be considered an excerpt from the full RTSM spreadsheets discussed in Chapter 8 and Appendix B. Therefore, the inputs are similar to what is described in Chapter 8 and Appendix B. The following input information is required:

1. A zone description consisting of geometric parameters: tilt angles, facing directions, and surface areas.
2. Construction information: layer codes for each material layer in each construction. Additional layers can be specified in the *LAYERS IP* and *LAYERS SI* spreadsheets, as discussed above, for the CTSF generation spreadsheet.

The spreadsheet in Figure C.3 (*C-2_RTFgen.xls*) shows the input data for the RTF generation. These input parameters are described in the previous section. Clicking the *GENERATE RTF* button calls the VBA subroutines to read the input parameters, compute the solar and nonsolar RTFs, and return them to the worksheet as shown in Figure C.4.

Appendix C: Calculation of CTSFs and RTFs

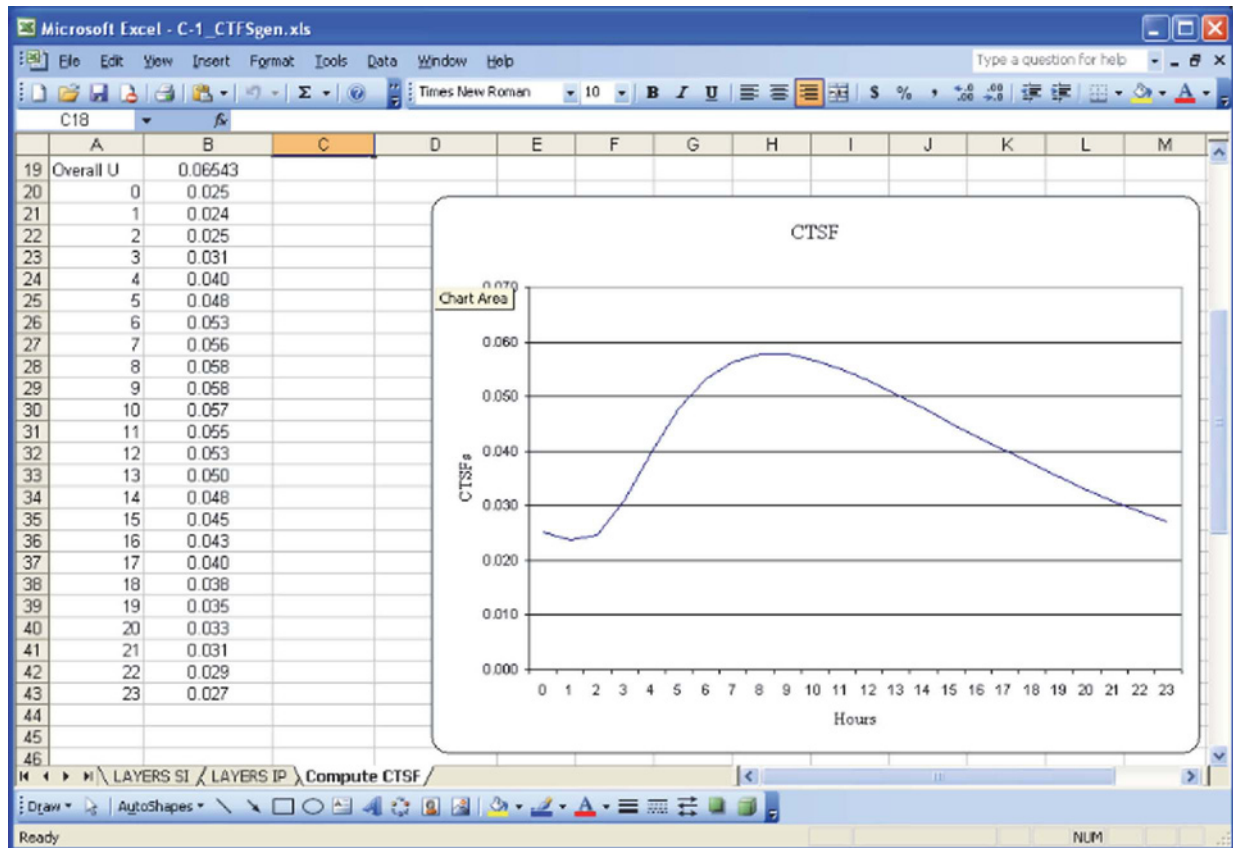


Figure C.2 CTSFs generated by spreadsheet.

The user can add more surfaces to the zone in columns M, N, etc. by following the format in columns C:L. Currently, only 20 surfaces per zone are allowed, though that limit could be changed in the VBA code. Notes on input, also relevant to adding additional surfaces, are as follows:

1. Surface ID numbers should be assigned sequentially.
2. Surface name is at the discretion of the user.
3. Facing angle is degrees clockwise from north.
4. Tilt angle is degrees above horizontal.
5. Surface area is in square feet (I-P) or square meters (SI).
6. Longwave emissivities are used to estimate radiation distributions.
7. All boundary conditions should be set to *TA*.
8. The number of layers, including surface conductances, should be set. Then, in the following rows, layers are specified from the outside to the inside.

Additional layers can be added into the *LAYERS IP* or *LAYERS SI* worksheets. Then, using the *unit conversion* button, the layers for the other worksheet will be synchronized.

References

Chen, Y., and S. Wang. 2005. A new procedure for calculating periodic response factors based on frequency domain regression method. *International Journal of Thermal Sciences* 44(4): 382–92.

Load Calculation Applications Manual (SI), Second Edition

- Nigusse, B.A. 2007. Improvements to the radiant time series method cooling load calculation procedure. PhD thesis, School of Mechanical and Aerospace Engineering, Oklahoma State University, Stillwater.
- Spitler, J.D., D.E. Fisher, and C.O. Pedersen. 1997. Radiant time series cooling load calculation procedure. *ASHRAE Transactions* 103(2):503–15.
- Spitler, J.D., and D.E. Fisher. 1999. Development of periodic response factors for use with the radiant time series method. *ASHRAE Transactions* 105(1):491–509.
- Spitler, J.D. 2009. Application manual for non-residential load calculations. RP-1326, Final Report. Atlanta: ASHRAE.

Surface ID	1	2	3	4	5	6	7	8	9	10
Surface Name	SouthS	SouthW	EastS	EastW	NorthS	WestS	WestW	Roof	Floor	Furniture
Facing	180.0	180.0	270.0	90.0	0.0	90.0	270.0	0.0	0.0	0.0
Tilt Angle	90.0	90.0	90.0	90.0	90.0	90.0	90.0	0.0	180.0	180.0
Area	12.5	12.54	12.5	0.0	25.1	12.5	0.0	41.8	41.8	20.9
LW Emissivity In	0.9	0.9	0.9	0.9	0.9	0.9	0.9	0.9	0.9	0.9
Boundary Cond	TA	TA	TA	TA	TA	TA	TA	TA	TA	TA
Number of Layers	6	3	5	3	5	5	3	6	6	3
Layer1	A0	E0	E0	E0	E0	E0	E0	E0	E0	E0
Layer2	A3	W1	E1	W1	E1	E1	W1	F20	E5	E7
Layer3	B3	E0	B1	E0	B1	B1	E0	C14	E4	E0
Layer4	B1	E1	E1	E1	E1	E1	E1	E4	C14	
Layer5	E1	E0	E0	E0	E0	E0	E0	E5	F20	
Layer6	E0							E0	E0	

Figure C.3 Input parameters for RTF generation.

Appendix C: Calculation of CTSFs and RTFs

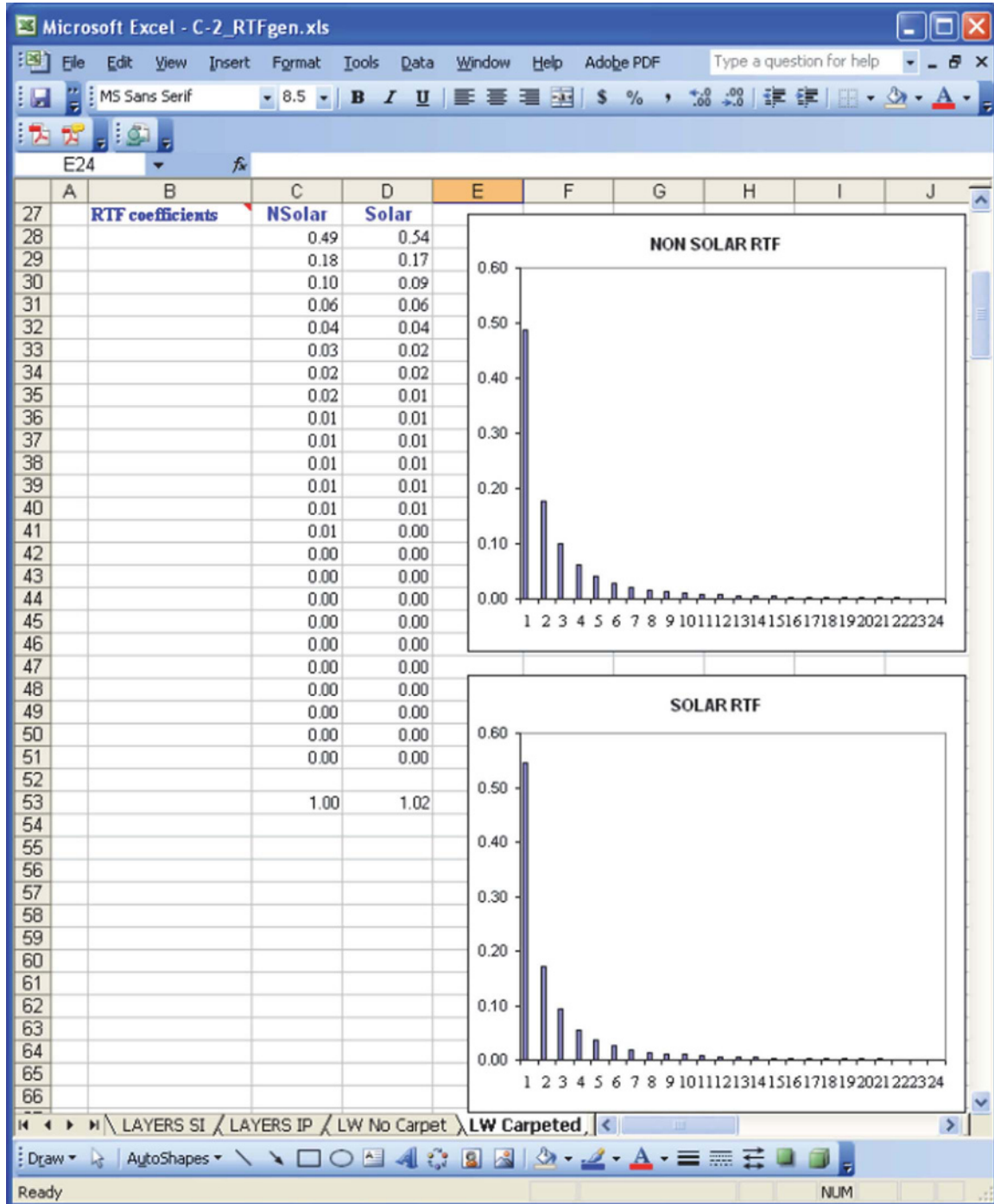


Figure C.4 Sample RTF output.

Appendix D

Solar Radiation and Heat Gain

This appendix briefly describes the calculation of solar irradiation (solar radiation flux) and sol-air temperature under clear-sky conditions. It is essentially a synopsis of the calculation procedures given in Chapter 14 of the *ASHRAE Handbook—Fundamentals* (2013). (Chapter 14 of the Handbook covers the subject in more detail, and the reader is referred to this chapter for a more thorough treatment.)

Solar irradiation incident on a surface is of interest for determining heat gains of fenestration in both the radiant time series method (RTSM) and the heat balance method (HBM). For the HBM, it is also used directly as part of the surface heat balance. For the RTSM, it is used to calculate sol-air temperature. The first step in determining solar irradiation incident on a surface is to determine the relevant angles, as described in Section D.1. With these angles determined, the revised ASHRAE clear-sky model (Thevenard 2009) can be used to calculate the incident solar irradiation, as shown in Section D.2. If exterior shading devices are present, the reduction in direct or beam irradiation must be determined as explained in Section D.3. Finally, if needed, sol-air temperatures can be determined as described in Section D.4.

D.1 Solar Angle Calculations

The earth's rotational position relative to the sun can be characterized with the apparent solar time (AST) (the sun is due south or due north at an AST of noon). The AST will be different from the local time at most locations for several reasons:

- When daylight saving time is in effect, the local standard time (LST) is one hour behind (or one hour less) than the local daylight saving time.
- LST is determined for the standard meridian in each time zone (Eastern Standard Time corresponds to the 75°W meridian, Central Standard Time corresponds to the 90°W meridian, Mountain Standard Time corresponds to the 105°W meridian, and Pacific Standard Time corresponds to the 120° W meridian). In general, the local standard meridian corresponds to the number of hours that the time zone is different from coordinated universal time (UTC), multiplied by 15°. The U.S. Central standard time zone is six hours behind UTC; the standard meridian is $-6 \cdot 15^\circ = -90^\circ$. Likewise, the Central European Time zone is one hour ahead of UTC; the standard meridian is $1 \cdot 15^\circ = 15^\circ$.
- The earth's orbital velocity varies slightly throughout the year, and the resulting difference in rotational position is given by the equation of time (ET). The ET (in minutes) can be read from Table D.1 for the twenty-first day of each month, or it can be related to the day of the year n by

$$ET = 2.2918[0.0075 + 0.1868 \cos(\Gamma) - 3.2077 \sin(\Gamma) - 1.4615 \cos(2\Gamma) - 4.089 \sin(2\Gamma)] \quad (D.1)$$

$$\Gamma = 360^\circ \frac{(n-1)}{365} \quad (D.2)$$

The formulation given in Equations D.1 and D.2 is based on that given by Spencer (1971), and it appears in the above version in Chapter 14 of the *ASHRAE Handbook—Fundamentals* (2013). For the examples used in this book, we use a slightly more convenient formulation given by Duffie and Beckman (1980):

Load Calculation Applications Manual (SI), Second Edition

$$ET = 9.87 \sin(2B) - 7.53 \cos(B) - 1.5 \sin B \quad (D.3)$$

where

$$B = 360^\circ \frac{(n-81)}{364} \quad (D.4)$$

The AST in hours is related to the LST, ET in minutes, the local standard meridian (LSM) in degrees, and the local longitude (LON) in degrees as follows:

$$AST = LST + ET/60 + (LSM - LON)/15 \quad (D.5)$$

With the AST known, the computation of the angles shown in Figure D.1 can proceed.

The hour angle H , in degrees, is calculated from the AST as follows:

$$H = 15(AST - 12) \quad (D.6)$$

The earth's pole is not orthogonal to the plane formed by the earth's orbit around the sun; it is tilted at an angle of 23.45° . As the earth rotates around the sun, the declination angle (that is, the angle between the earth's pole and a vector from the earth to the sun) varies. The declination in degrees can be read from Table D.1 for the twenty-first day of each month, or it can be related to the day of the year n by:

$$\delta = 0.3963723 - 22.9132745 \cos(\Gamma) + 4.0254304 \sin(\Gamma) - 0.387205 \cos(2\Gamma) + 0.05196728 \sin(2\Gamma) - 0.1545267 \cos(3\Gamma) + 0.08479777 \sin(3\Gamma) \quad (D.7)$$

where Γ is as defined in Equation D.2. Chapter 14 of the *ASHRAE Handbook—Fundamentals* (2013) gives a simpler formulation (Cooper 1969):

$$\delta = 23.45 \sin\left(360^\circ \frac{n+284}{365}\right) \quad (D.8)$$

The solar altitude angle β is related to the latitude angle L of the location, the declination angle δ , and the hour angle H :

$$\sin \beta = \cos L \cos \delta \cos H + \sin L \sin \delta \quad (D.9)$$

The solar azimuth angle measured from the south is given by

$$\cos \phi = \frac{\sin \beta \sin L - \sin \delta}{\cos \beta \cos L} \quad (D.10)$$

Table D.1 Approximate Astronomical Data for the 21st Day of Each Month

(Source: *ASHRAE Handbook—Fundamentals* [2013], Chapter 14, Table 2)

Month	Jan	Feb	Mar	Apr	May	Jun	Jul	Aug	Sep	Oct	Nov	Dec
Day of year	21	52	80	111	141	172	202	233	264	294	325	355
E_o , W/m ²	1410	1397	1378	1354	1334	1323	1324	1336	1357	1380	1400	1411
Equation of time (ET), min	-10.6	-14.0	-7.9	1.2	3.7	-1.3	-6.4	-3.6	6.9	15.5	13.8	2.2
Declination δ , degrees	-20.1	-11.2	-0.4	11.6	20.1	23.4	20.4	11.8	-0.2	-11.8	-20.4	-23.4

Appendix D: Solar Radiation and Heat Gain

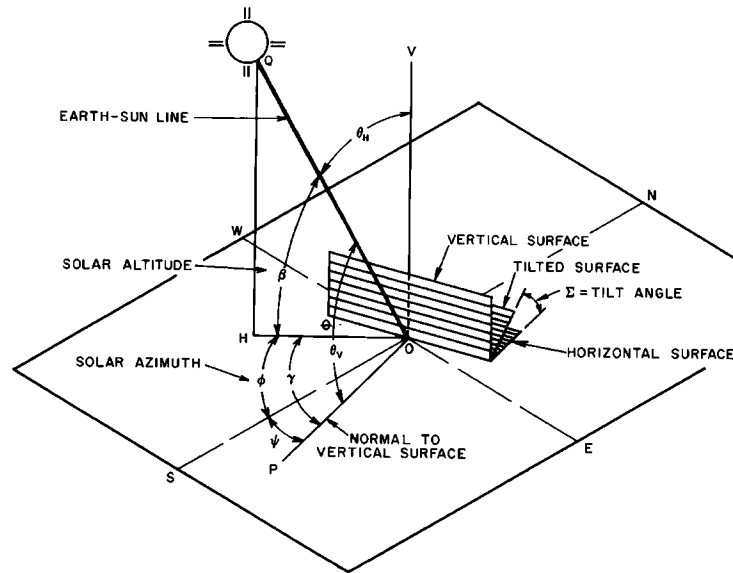


Figure D.1 Solar angles.

(Source: *ASHRAE Handbook—Fundamentals* [2013], Chapter 14, Figure 3).

When measured from the south, the solar azimuth angle is positive in the afternoon and negative in the morning. As this formulation is really derived for use in a northern-hemisphere application, a more general expression, giving solar azimuth angle in degrees clockwise from north, may be desirable:

$$\cos \phi = \frac{\sin \delta \cos L - \cos \delta \sin L \cos H}{\cos \beta} \quad (\text{D.11})$$

Note that, when using Equation D.10, the sign of the angle should be set after taking the inverse cosine, depending on whether it is before or after noon. On the other hand, when using Equation D.11, the inverse cosine function (regardless of the programming environment) does not distinguish between, for example, in the northern hemisphere, $\cos(\phi) = 0.9$, meaning 154.16° in the morning and $\cos(\phi) = 0.9$, meaning 205.84° in the afternoon.

Likewise, in the southern hemisphere, the solar azimuth angle is positive in the morning, zero at noon, and negative in the afternoon. Again, the inverse cosine function cannot differentiate between 45° (morning) and 315° (afternoon). A general correction can be applied by checking to see if the hour angle H is greater than zero. If so, then let

$$\phi = 2\pi - \phi \text{ (in radians) or } \phi = 360^\circ - \phi \quad (\text{D.12})$$

The surface azimuth angle ψ is defined as the angle between OS and OP in Figure D.1, with surfaces facing west of south having positive surface azimuth angles and surfaces facing east of south having negative surface azimuth angles. When the solar azimuth is defined in terms of the angle clockwise from due north, the surface azimuth should also be defined in terms of the angle clockwise from due north. As long as the convention is the same for both the solar azimuth and the surface azimuth, the difference between the two, γ , is given by

$$\gamma = \phi - \psi \quad (\text{D.13})$$

Load Calculation Applications Manual (SI), Second Edition

If the solar-surface azimuth angle is greater than 90 or less than -90, the surface is shaded. The angle of incidence θ , the angle between the sun's rays and the normal to the surface, is given by

$$\cos \theta = \cos \beta \cos \gamma \sin \Sigma + \sin \beta \cos \Sigma \quad (\text{D.14})$$

where Σ is the tilt angle of the surface, $\Sigma = 0^\circ$ corresponds to a horizontal surface, and $\Sigma = 90^\circ$ corresponds to a vertical surface.

D.2 ASHRAE Clear-Sky Model

The ASHRAE clear-sky model (Thevenard and Gueymard 2013) is used to estimate beam and diffuse irradiation incident on any surface for clear-sky conditions. Note that the term “clear sky” represents a theoretical maximum of total solar irradiation. In most locations, this means an absence of clouds, but in some locales, the sky may still be hazy. Once the solar angles have been determined, the next step is to determine the solar irradiation outside the earth's atmosphere; the extraterrestrial solar irradiation varies over the year because of the earth's elliptical orbit. The extraterrestrial solar irradiation is given by

$$E_o = E_{SC} \left\{ 1 + 0.033 \cos \left[360^\circ \frac{(n-3)}{365} \right] \right\} \quad (\text{D.15})$$

where E_{SC} is the extraterrestrial solar constant, 1367 W/m².

The earth's atmosphere attenuates the extraterrestrial solar irradiation. This attenuation depends on the path length through the atmosphere and the turbidity of the atmosphere. Thevenard and Gueymard (2010) developed a widely applicable model with data available for the entire set of ASHRAE design weather data. Use of the model is summarized here; for a more detailed description, see Gueymard and Thevenard (2009) and Chapter 14 of the *ASHRAE Handbook—Fundamentals* (2013).

First, the relative air mass m is computed depending on the solar altitude angle β :

$$m = 1 / \left[\sin \beta + 0.50572(6.07995 + \beta)^{-1.6364} \right] \quad (\text{D.16})$$

Then the beam optical depth τ_b and diffuse optical depth τ_d are determined for the specific location and month of interest from the design weather data in the accompanying online files. Table 4.1 and Tables 4.4 through 4.8 contain these data for sample locations. With these values, the air mass exponents ab and ad may be computed:

$$ab = 1.454 - 0.406\tau_b - 0.268\tau_d + 0.021\tau_b\tau_d \quad (\text{D.17})$$

$$ad = 0.507 + 0.205\tau_b - 0.080\tau_d - 0.190\tau_b\tau_d \quad (\text{D.18})$$

Once the optical depths and air mass exponents have been determined, the beam normal irradiance (solar radiation flux perpendicular to the rays from the sun) is calculated:

$$E_b = E_o e^{-\tau_b m^{ab}} \quad (\text{D.19})$$

The diffuse horizontal irradiance is calculated as follows:

$$E_d = E_o e^{-\tau_d m^{ad}} \quad (\text{D.20})$$

Appendix D: Solar Radiation and Heat Gain

D.3 Solar Irradiation on Surfaces

The shortwave-beam (direct) solar radiation $E_{t,b}$ (W/m^2) incident on a surface is given by

$$E_{t,b} = E_b \cdot \cos\theta \quad (\text{D.21})$$

Diffuse irradiation incident on a surface from the sky is calculated in two different ways, depending on the tilt of the surface. The diffuse solar irradiation on a vertical surface is given by the following:

$$E_{t,b} = Y \cdot E_d \quad (\text{D.22})$$

$$\begin{aligned} Y &= 0.45 && \text{for } \cos\theta < -0.20 \\ Y &= 0.55 + 0.437\cos\theta + 0.313\cos^2\theta && \text{for } \cos\theta \geq -0.20 \end{aligned} \quad (\text{D.23})$$

where Y is the ratio of diffuse solar radiation on vertical surfaces to a horizontal surface. For nonvertical surfaces, the diffuse irradiation is given by the following:

$$E_{t,d} = E_d(Y \sin\Sigma + \cos\Sigma) \quad \text{if } \Sigma \leq 90^\circ \quad (\text{D.24})$$

$$E_{t,d} = E_d Y \sin\Sigma \quad \text{if } \Sigma > 90^\circ \quad (\text{D.25})$$

where Σ is the surface tilt angle.

The ground-reflected diffuse solar irradiation is given by

$$E_{t,r} = (E_b \sin\beta + E_d) \rho_g \left(\frac{1 - \cos\Sigma}{2} \right) \quad (\text{D.26})$$

where ρ_g is the ground reflectivity (which may be estimated from Table D.2). Finally, for an unshaded surface, the total solar irradiation is

$$E_t = E_{t,b} + E_{t,d} + E_{t,r} \quad (\text{D.27})$$

D.4 Exterior Shading of Fenestration

Exterior shading of windows by overhangs or other devices can have a significant effect on solar heat gains. In many cases, the geometry can be represented as shown in Figure D.3, with the horizontal and vertical dimensions of the shading device sufficiently large so that the shadow has only horizontal and vertical components on the window. For these cases, the analysis given below is sufficient. In other cases, a procedure such as that described by Walton (1979) might be used.

Prior to calculating the shadow dimensions, the solar altitude angle β and the surface solar azimuth angle γ will have already been calculated with Equations D.9 and D.13. As shown in Figure D.2, the profile angle Ω for the horizontal projection is given by

$$\tan \Omega = \frac{\tan(\beta)}{\cos(\gamma)} \quad (\text{D.28})$$

The shadow width S_W and the shadow height S_H of the horizontal overhang are given by the following

$$S_W = P_V \cdot |\tan \gamma| \quad (\text{D.29})$$

Table D.2 Solar Reflectances of Foreground Surfaces

(Source: ASHRAE Handbook—Fundamentals [2013], Chapter 14, Table 5)

Foreground Surface	Reflectance
Water (near normal incidences)	0.07
Coniferous forest (winter)	0.07
Asphalt, new	0.05
weathered	0.10
Bituminous and gravel roof	0.13
Dry bare ground	0.2
Weathered concrete	0.2 to 0.3
Green grass	0.26
Dry grassland	0.2 to 0.3
Desert sand	0.4
Light building surfaces	0.6
Snow-covered surfaces:	
Typical city center	0.2
Typical urban site	0.4
Typical rural site	0.5
Isolated rural site	0.7

Source: Adapted from Thevenard and Haddad (2006).

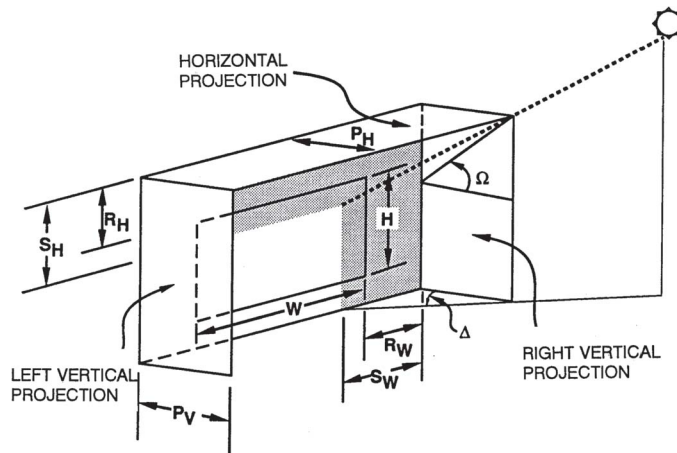


Figure D.2 Shading for vertical and horizontal projections.

(Source: ASHRAE Handbook—Fundamentals [2013], Chapter 15, Figure 16).

$$S_H = P_H \cdot \tan \Omega \quad (D.30)$$

where P_V and P_H are the horizontal and vertical projection distances shown in Figure D.2.

The fenestration sunlit and shaded areas can then be calculated:

$$A_{SL} = [W - (S_W - R_W)] \cdot [H - (S_H - R_H)] \quad (D.31)$$

Appendix D: Solar Radiation and Heat Gain

Row	Field	Value
5	Latitude Angle	33.64
6	Longitude Angle	84.43
7	Site Name	USA - GA - ATLANTA MUNICIPAL
8	Design Conditions	5%
9	Facing Direction	0.0, 45.0, 90.0, 135.0, 180.0, 225.0, 270.0, 315.0
10	Tilt Angle	0.0, 90.0
11	Time Zone	5, NAE
12	DayLightSavings	1
13	Months	1, 2, 3, 4, 5, 6, 7, 8, 9, 10
14	DayOfMonth	21
15	UnitsOfMeas	IP
16	Peak Temperature	62.8, 65.9, 73.3, 79.5, 84.3, 90, 91.9, 90.9, 86.3, 78
17	Daily Range	20.4, 21.0, 23.0, 22.8, 20.3, 20.2, 20.5, 19.4, 19.1, 20.3
18	Taub	0.334, 0.324, 0.355, 0.383, 0.379, 0.406, 0.44, 0.427, 0.388, 0.358
19	Taud	2.614, 2.58, 2.474, 2.328, 2.324, 2.27, 2.202, 2.269, 2.428, 2.514

Figure D.3 Solar input data.

$$A_{SH} = A - A_{SL} \quad (D.32)$$

where A is the total fenestration surface area and R_W and R_H are dimensions shown in Figure D.3.

The sunlit window area fraction $A_{SL,F}$ is calculated from the ratio of the sunlit area to the total window area as follows:

$$A_{SH,F} = A_{SL}/A \quad (D.33)$$

D.5 Sol-Air Temperature Calculation

Sol-air temperature is the outdoor air temperature that, in the absence of all radiation heat transfer, gives the same rate of heat flowing into the surface as would the combination of incident solar radiation, radiant energy exchange with the sky and other outdoor surroundings, and convective heat exchange with outdoor air. The sol-air temperature T_{SA} is given by the following:

$$T_{SA} = T_o + \frac{\alpha E_t}{h_o} - \frac{\epsilon \Delta R}{h_o} \quad (D.34)$$

where

T_o = outdoor air temperature, °C

α = surface solar absorptance

h_o = combined outside surface conductance, W/(m²·K)

E_t = total solar irradiation on the surface, W/m²

Load Calculation Applications Manual (SI), Second Edition

ΔR = difference between the radiation emitted by a blackbody at the outdoor air temperature and the actual thermal radiation incident on the surface from the sky and surroundings, W/m^2

ε = surface emissivity

The total solar irradiation is computed from the beam, diffuse, and reflected components calculated using Equation D.27.

The third term of Equation D.34 is effectively a correction for the fact that the sky and surroundings are not at the local air temperature. For horizontal surfaces that view the sky, this correction is taken as 4 K. For vertical surfaces, where the view to the sky and the higher temperature surroundings may be approximately equal, the correction is usually taken to be 0 K.

The value of the parameter α/h_o depends on surface color. A value of 0.026 is appropriate for a light-colored surface with a solar absorptance of 0.6 and a summer surface conductance of 22.7, whereas 0.3 represents the usual maximum value for this parameter (i.e., for a dark-colored surface with a solar absorptance of 0.9 and summer surface conductance of 22.7). Values for the combined conductance h_o , which depends on wind speed, are given in Table 3.4 in Chapter 3.

D.6 Spreadsheet Implementation

This section describes a spreadsheet implementation of the solar irradiation and sol-air temperature calculations for the eight cardinal directions and a horizontal surface. Solar irradiation and sol-air temperatures are calculated for the 21st day of each month under clear-sky and design cooling conditions.

The spreadsheet *D-1 solar.xls*, included in the supporting files accompanying this manual (online at www.ashrae.org/lcam), initially opens with a screen (shown in Figure D.3) showing a summary of preexisting input data. Clicking on the button labeled *Solar Intensity & Sol-Air Temperature* will bring up the input dialog box shown in Figure D.4.

There are five categories of inputs as shown in the user form in Figure D.4.

All input parameters have default values provided, though they may be completely irrelevant to the user's situation. The user may select either SI or I-P units. Local time or solar time, which controls the basis on which solar irradiation and sol-air temperature are tabulated, may also be chosen. Beyond that, almost all the rest of the parameters may be set automatically by selecting one of the climate/design day combinations. For other locations, all parameters may be specified individually by typing their values in the appropriate field. The parameters are summarized in Table D.3.

The solar irradiation and sol-air temperature calculations use the equations given in this chapter. The input parameters are described in Table D.3. The default values have the units of the default unit system, which is I-P.

Once all of the parameters are set, clicking on *OK* will create a new worksheet, which will hold a series of tables of solar irradiation values and sol-air temperatures. Choosing 0.4% conditions for Gage, Oklahoma, for example, will give tables for which Figure D.5 is a small excerpt.

How does this work? While a complete explanation is beyond the scope of this manual, interested readers may explore the Visual Basic for Applications (VBA) source code. (In Excel 2003, this is done from the Tools menu by choosing *Macro*, then *Visual Basic Editor*.) In Excel 2013, this is done by choosing the Developer tab,

Appendix D: Solar Radiation and Heat Gain

Solar Intensity and Sol_Air Temperature Calculation [X]

General

Select Time: Local Time Solar Time

Select Units System: SI IP

Location

Site Name: USA - GA - ATLANTA MUNICIPAL

Latitude: 33.64

Longitude: 84.43

Time Zone: 5 NAE

Design Conditions: 5%

Hemisphere: North South

Of Greenwich Meridian: West East

Surface Parameters

Facing: 0, 45, 90, 135, 180

Tilt Angle: 90

Date

Month: all

Day: 21

Daylight Savings Time: Yes No

Solar Parameters

taub: 0.334, 0.324, 0.355

taud: 2.614, 2.58, 2.474, 2

Ground Reflectance: 0.2

Sol-air Temperature Parameters

Design Temperature: 62.8, 65.9, 73.3, 79.5 °F

Daily Range: 20.4, 21, 23, 22.8, 20 °F

Absorptance Out: 0.9

Surf. Conductance Out: 3 Btu/hr-ft² °F

Figure D.4 Solar irradiation and sol-air temperature calculation input user form interface.

Load Calculation Applications Manual (SI), Second Edition

Table D.3 Input Parameter Descriptions

Input Parameters	Default Values	Note
Location	Atlanta, Georgia	A combo-box allows selecting the location. This sets most of the other parameters below.
Design Condition	5%	A combo-box allows the user to select the desired monthly design conditions (0.4%, 2%, 5% or 10%)
Latitude	33.64	When a location is selected, the corresponding latitude is retrieved.
Longitude	84.43	When a location is selected, the corresponding longitude is retrieved.
Time zone	5.0	When a location is selected, the corresponding time zone is retrieved.
Facing direction	0, 45, 90, ..., 315	The eight cardinal directions. Users can edit the facing directions to other values. The angles are measured clockwise from true north.
Tilt angle	90	For all walls except the roof. By default the roof is considered horizontal.
Month	All	The 12 months of the year. Users can specify the months by using integer values 1, 2, or 3, ..., 12. A single month can also be specified.
Day	21	Users can specify the day of the month.
Daylight savings time	Yes	Enforces daylight savings time.
Taub	Atlanta, Georgia	$\tau_{a,b}$ is retrieved from the ASHRAE design day database sheet when a location is selected by the user.
Taud	Atlanta, Georgia	$\tau_{a,d}$ is retrieved from the ASHRAE design day database sheet when a location is selected by the user
Ground reflectance	0.2	Table D.2.
Design temperature	Atlanta, Georgia	The peak design temperature is retrieved from the ASHRAE design day database sheet (featured on the CD that accompanies the <i>ASHRAE Handbook—Fundamentals</i> (2013) (<i>WDATA_SI</i> or <i>WDATA_IP</i>) when a location is selected by the user.
Daily range	Atlanta, Georgia	The design day daily range is retrieved from the ASHRAE design day database sheet (featured on the CD that accompanies the <i>ASHRAE Handbook—Fundamentals</i> (2013) (<i>WDATA_SI</i> or <i>WDATA_IP</i>) when a location is selected by the user.
Absorptance	0.9	Outside surface short-wavelength absorptance.
Conductance	22.7	Outside conductance.

then the Visual Basic icon. In Excel 2013, the Developer tab is not shown by default, so the user must first choose the options button from the File tab, choose “Customize Ribbon” and check Developer under the list of Main tabs.)

References

- ASHRAE. 2013. *ASHRAE Handbook—Fundamentals*. Atlanta: ASHRAE.
- Cooper, P.I. 1969. The absorption of radiation in solar stills. *Solar Energy* 12(3):333–46.
- Duffie, J.A., and W.A. Beckman. 1980. *Solar Engineering of Thermal Processes*, New York: John Wiley & Sons.
- Gueymard, C.A. and D. Thevenard. 2009. Monthly average clear-sky broadband irradiance database for worldwide solar heat gain and building cooling load calculations. *Solar Energy* 83(11):1998–2018.
- Spencer, J.W. 1971. Fourier series representation of the position of the sun. *Search* 2(5):172.
- Thevenard, D. 2009. *Updating the ASHRAE climatic data for design and standards (RP-1453)*. ASHRAE Research Project, Final Report. Atlanta: ASHRAE.

Appendix D: Solar Radiation and Heat Gain

Sol-Air Temperature (F) for June 21, 36.3°N Latitude, 99.78°W Longitude, Time Zone: NAC Daylight Savings Time
 USA - OK - GAGE/SHATTUCK, 0.4% Design Condition, Surface Color: alpha/ho = 0.3

Local Time	Air Temp.	N	NE	E	SE	S	SW	W	NW	Horiz
1.0	79.2	79.2	79.2	79.2	79.2	79.2	79.2	79.2	79.2	72.2
2.0	77.3	77.3	77.3	77.3	77.3	77.3	77.3	77.3	77.3	70.3
3.0	75.9	75.9	75.9	75.9	75.9	75.9	75.9	75.9	75.9	68.9
4.0	74.9	74.9	74.9	74.9	74.9	74.9	74.9	74.9	74.9	67.9
5.0	74.1	74.1	74.1	74.1	74.1	74.1	74.1	74.1	74.1	67.1
6.0	73.3	73.3	73.3	73.3	73.3	73.3	73.3	73.3	73.3	66.3
7.0	73.1	86.5	101.1	100.2	84.4	74.7	74.7	74.7	74.7	71.3
8.0	73.9	95.5	130.1	134.6	106.2	78.6	78.6	78.6	78.6	89.3
9.0	76.7	95.3	139.0	151.2	124.0	84.7	84.4	84.4	84.4	112.0
10.0	81.9	93.9	138.9	157.4	137.6	93.0	92.1	92.1	92.1	136.2
11.0	86.8	99.9	131.8	153.8	144.0	108.7	99.2	99.2	99.2	157.5
12.0	91.4	105.7	120.7	142.7	143.4	122.2	105.8	105.3	105.3	174.1
13.0	95.0	109.9	110.8	126.2	136.0	131.1	114.4	110.3	109.9	184.5
14.0	97.5	112.4	112.4	113.2	123.1	134.4	133.5	120.9	113.1	188.0
15.0	99.5	114.2	113.9	113.9	114.6	132.7	148.2	144.1	122.9	185.2
16.0	100.5	114.0	113.5	113.5	113.5	125.9	156.5	162.6	140.2	175.9
17.0	99.9	111.9	111.1	111.1	111.1	114.5	157.0	173.4	153.3	160.5
18.0	97.9	114.4	106.6	106.6	106.6	107.1	149.0	174.1	159.3	140.2
19.0	95.8	117.1	101.6	101.6	101.6	101.6	134.1	163.1	155.8	118.1
20.0	92.5	110.9	95.2	95.2	95.2	95.2	111.8	134.5	134.1	96.0
21.0	88.5	88.5	88.5	88.5	88.5	88.5	88.5	88.5	88.5	81.5
22.0	85.9	85.9	85.9	85.9	85.9	85.9	85.9	85.9	85.9	78.9
23.0	83.4	83.4	83.4	83.4	83.4	83.4	83.4	83.4	83.4	76.4
24.0	81.1	81.1	81.1	81.1	81.1	81.1	81.1	81.1	81.1	74.1

Solar Irradiation (Btu/hr-ft²) for July 21, 36.3°N Latitude, 99.78°W Longitude, Time Zone: NAC Daylight Savings Time
 USA - OK - GAGE/SHATTUCK, Ground Reflectance: rho_g = 0.2

Local Time	N	NE	E	SE	S	SW	W	NW	Horiz
1.0	0.0	0.0	0.0	0.0	0.0	0.0	0.0	0.0	0.0
2.0	0.0	0.0	0.0	0.0	0.0	0.0	0.0	0.0	0.0
3.0	0.0	0.0	0.0	0.0	0.0	0.0	0.0	0.0	0.0
4.0	0.0	0.0	0.0	0.0	0.0	0.0	0.0	0.0	0.0
5.0	0.0	0.0	0.0	0.0	0.0	0.0	0.0	0.0	0.0
6.0	0.0	0.0	0.0	0.0	0.0	0.0	0.0	0.0	0.0
7.0	24.2	52.6	52.2	23.1	3.4	3.4	3.4	3.4	8.5

Figure D.5 Tables for Gage, Oklahoma.

Thevenard, D., and C. Gueymard. 2013. *Updating climatic design data in the 2013 ASHRAE Handbook—Fundamentals (RP-1613)*. ASHRAE Research Project RP-1613, Final Report. Atlanta: ASHRAE.

Thevenard, D., and K. Haddad. 2006. Ground reflectivity in the context of building energy simulation. *Energy and Buildings* 38(8):972–80.

Walton, G.N. 1979. The application of homogeneous coordinates to shadowing calculations. *ASHRAE Transactions* 85(1):174–80.

Appendix E

Treatment of Thermal Bridges

Both cooling load calculation procedures described in this manual use one-dimensional transient conduction analysis procedures with precomputed conduction transfer functions (for the heat balance method [HBM]) or conduction time series factors (for the radiant time series method [RTSM]). In both cases, the first step is to describe the wall, roof, or floor as a series of one-dimensional homogeneous layers. For cases with thermal bridges, a method to determine an equivalent wall made up of one-dimensional homogeneous layers is needed. Karambakkam et al. (2005) proposed an approximate one-dimensional procedure for dynamic modeling of thermal bridges, and validation of the model was reported by Nigusse (2007).

E.1 Equivalent Homogeneous Layer Model

The equivalent homogeneous layer (EHL) model (Karambakkam et al. 2005) is suitable for walls with a single composite layer (e.g., steel studs and insulation). The model determines the thermal characteristics of the homogeneous layer such that both the overall wall resistance and the composite layer's thermal mass are maintained. The first step, then, is to determine the total thermal resistance of the actual construction, as discussed in the next section.

The EHL has the following properties:

- Thickness is the same as the thickness of the composite layer.
- Conductivity is determined from the resistance of the EHL required to maintain the overall thermal resistance of the wall and the thickness of the composite layer.
- Density is the volume-weighted average of the densities of the composite layer materials.
- Specific heat is determined from a mass-weighted average of the specific heats of the composite layer materials.

The accuracy of the EHL model in duplicating the actual construction depends on the accuracy of the steady-state thermal resistance or R-value. Nigusse (2007) showed that the EHL model predicted peak conduction heat gain within $\pm 3\%$ of experimental results for seven walls with experimental measurements when the experimentally measured R-value was used to determine the EHL properties. However, methods for estimating steady-state R-values, discussed in the next section, introduce additional error. Using the recommended methods for estimating R-values, the error of the EHL model rose to $\pm 8\%$ of the experimentally measured peak conduction heat gain for six of the seven walls. The seventh wall had an error in predicted peak conduction heat gain of 19%, due to an error of more than 11% in the *ASHRAE Handbook—Fundamentals* (2005) method for estimating the R-value.

E.2 Steady-State R-Value

The *ASHRAE Handbook—Fundamentals* (2013) provides a range of procedures for estimating R-values and U-factors for walls with thermal bridge elements: the isothermal planes method, the parallel path method, the zone method, and the modified zone method. The reader is referred to pages 27.3–27.7 of the *ASHRAE Handbook—Fundamentals* (2013). One additional method that should be considered for walls with steel studs was recently published by Gorgolewski (2007) and is described briefly as follows.

Load Calculation Applications Manual (SI), Second Edition

Gorgolewski (2007) gives a semi-empirical correlation for computing the steady-state R-value of light frame steel stud walls. This procedure uses a weighted average of the isothermal plane and parallel-path method R-values. (The two methods bound the possible range of R-values.) The weighting parameter p is calculated from a semi-empirical correlation that depends on the geometry of the steel frame and R-values determined by the isothermal and parallel-path methods. For SI units,

$$p = 0.8(R_{min}/R_{max}) + 0.44 - 0.1(w/40) - 0.2(600/s) - 0.04(d/100) \quad (E.1)$$

where

R_{min} = is the R-value of the steel stud construction calculated with the isothermal plane method, $\text{ft}^2 \cdot \text{°F} \cdot \text{h/Btu}$ ($\text{m}^2 \cdot \text{K/W}$)

R_{max} = is the R-value of the steel stud construction calculated with the parallel path method, $\text{ft}^2 \cdot \text{°F} \cdot \text{h/Btu}$ ($\text{m}^2 \cdot \text{K/W}$)

w = steel stud flange width, in. (mm)

s = the studs center-to-center spacing, in. (mm)

d = depth of the stud, in. (mm)

With the weighting parameter determined, the R-value is then given by

$$R_T = pR_{max} + (1 - p)R_{min} \quad (E.2)$$

Once the overall wall R-value has been determined, the EHL properties may be determined, as described next.

E.3 EHL Step-by-Step Procedure

The EHL model (Karambakkam et al. 2005) relies on accurate knowledge of the air-to-air or surface-to-surface R-value and the geometry of the actual construction. The step-by-step procedure for calculating the EHL model wall for cases with a single composite layer is described as follows:

1. Determine the overall resistance of the actual construction based on one of the methods listed in the previous section. For use with the RTSM, the overall resistance should include the surface resistances on both sides of the construction. For use with the HBM, where variable convection and radiation coefficients are a possibility, an estimate of the surface resistances under peak heat gain conditions should be made.
2. Compute the effective equivalent resistance of the homogenous layer based on the actual overall resistance determined in the previous step. The EHL resistance is the difference between the actual thermal resistance and the sum of the homogeneous layer resistances in the actual construction and is given by the following:

$$R_{Hom} = R_T - \sum_{i=1}^N R_i \quad (E.3)$$

where

R_T = the steady-state, overall air-to-air thermal resistance of the construction, ($\text{m}^2 \cdot \text{K/W}$)

R_i = the thermal resistance of the i th homogeneous layer in the construction, ($\text{m}^2 \cdot \text{K/W}$)

R_{Hom} = the thermal resistance of the equivalent homogeneous layer, ($\text{m}^2 \cdot \text{K/W}$)

N = the number of homogeneous layers in the actual construction

Note that the summation does not include the composite layer.

Appendix E: Treatment of Thermal Bridges

3. Thermal conductivity of the EHL is obtained by dividing the thickness of the EHL with the resistance of the EHL. The thickness of the EHL is equal to the thickness of the composite layer or the total thickness minus the thickness of the homogeneous layers:

$$X_{Hom} = X_{Tot} - \sum_{i=1}^N X_{Sl,i} \quad (E.4)$$

The conductivity is then the thickness divided by the resistance:

$$k_{Hom} = \frac{X_{Hom}}{R_{Hom}} \quad (E.5)$$

where

- X_{Tot} = the overall thickness of the actual construction, mm
- X_{Hom} = the thickness of the equivalent homogeneous layer, mm
- $X_{Sl,i}$ = the thickness of the i th single homogeneous layer in the construction, mm
- k_{Hom} = the thermal conductivity of the EHL, W/(m·K)

4. Density of the EHL is determined from densities of the components of the composite layers and the corresponding volume fractions. The product sum of the volume fraction and densities of the components in the composite layer yields the EHL density and is given by the following:

$$\rho_{Hom} = \sum_{i=1}^M y_i \rho_i \quad (E.6)$$

where

- y_i = the volume fraction of i th component in the composite layer(s)
- ρ_i = the density of the i th component in the composite layer(s), kg/m³
- ρ_{Hom} = the density of the EHL, kg/m³

The constituents' volume fraction in the composite layer is determined from the geometry of the composite layer.

5. The specific heat of the homogeneous layer is determined from the product sum of the specific heat, densities, and volume fractions of the constituents of the composite layers:

$$C_{p,Hom} = \sum_{i=1}^M y_i \rho_i C_{pi} / \rho_{Hom} \quad (E.7)$$

where

- C_{pi} = specific heat of the i th component in the composite layer(s), kJ/(kg·K)
- $C_{p,Hom}$ = specific heat of the EHL, kJ/(kg·K)

Once the thickness and thermophysical properties of the EHL have been determined, the EHL model wall can be input and analyzed as if it were made up of homogeneous layers.

Example E.1 Steel Stud Wall

The EHL wall model is demonstrated using a generic-type steel stud wall as shown in Figure E.1 with 400 mm center-to-center stud spacing and 89 mm deep studs with 38 mm flange width and 1.5 mm thickness. The thermophysical properties of the construction layer materials are given in Table E.1. The problem to be solved is to find the properties of the EHL.

Solution: *Step 1: Calculation of the overall steady-state resistance.* The Gorgolewski (2007) procedure is used to estimate the steady-state, surface-to-surface, overall R-value of the steel stud wall. This procedure requires calculation of the overall resistances using the isothermal plane method and parallel path method.

The isothermal plane method combines in parallel the resistances of the elements of the composite layer and then sums the resistances of each layer in the construction. The resistance of the composite layer is given by the following:

$$R_{CL} = \frac{1}{\frac{A_{f,metal}}{R_{metal}} + \frac{A_{f,insulation}}{R_{insulation}}} = 0.432 \text{ (m}^2\cdot\text{K)/W} \quad (\text{E.8})$$

where

$A_{f,metal}$ = area fraction of the metal stud

$A_{f,insulation}$ = area fraction of the insulation

R_{metal} = resistance of the metal stud

$R_{insulation}$ = resistance of the insulation

The individual layer resistances and the combined resistance of the composite layer are given in Table E.2; the total resistance of the construction using the isothermal plane method is given in the last line of the table—this is the R_{min} value.

The parallel path method computes the total resistances (see Table E.3) for heat transfer through the insulation path and metal stud path separately and then adds them together in parallel:

$$R_{max} = \frac{1}{\frac{A_{f,metal}}{R_{mp}} + \frac{A_{f,insulation}}{R_{ip}}} = 4.126 \text{ (m}^2\cdot\text{K)/W} \quad (\text{E.9})$$

With R_{max} and R_{min} computed, Equation E.1 can be used to determine the weighting parameter, p :

$$p = 0.8(2.292/4.126) + 0.44 - 0.1(38/40) - 0.2(600/400) - 0.04(89/100) = 0.454$$

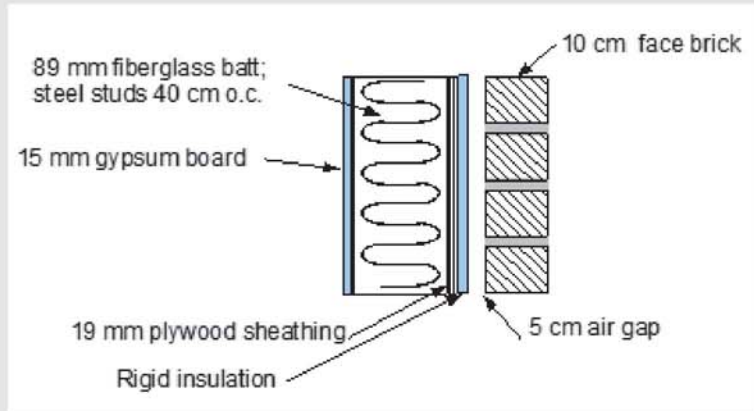


Figure E.1 Steel stud wall with exterior brick finish.

Appendix E: Treatment of Thermal Bridges

Table E.1 Thermophysical Properties of the Layers for Example E.1

Name	Density, lb _m /ft ³	Specific Heat, Btu/lb _m ·°F	Conductivity, Btu·in./h·ft ² ·°F	Thickness <i>L</i> , in.	Resistance, ft ² ·°F·h/Btu
Outside air film					0.250
Brick	119.9	0.189	5.00	4.0	0.804
Clear air cavity	0.1	0.241	1.73	2.0	1.136
Rigid insulation	5.3	0.230	0.32	2.0	6.168
Plywood	34.0	0.290	0.80	0.8	0.987
Metal	474.5	0.120	314.3	3.5	0.011
Insulation	0.9	0.170	0.27	3.5	12.97
Gypsum	49.9	0.261	1.11	0.6	0.532
Inside air film					0.688

Table E.1 Thermophysical Properties of the Layers for Example E.1

Table E.2 Layer Resistances—Isothermal Plane Method

Layers	Name	Resistance, (m ² ·K)/W
1	Outside film	0.044
2	Brick	0.142
3	Clear air cavity	0.200
4	Rigid insulation	1.086
5	Plywood	0.174
7	Metal/insulation	0.432
8	Gypsum	0.094
9	Inside film	0.121
Sum	All	2.292

Table E.3 Layer Resistances—Parallel Method

Layers	Name	Insulation Path Resistances, (m ² ·K)/W	Metal Path Resistances, (m ² ·K)/W
1	Outside film	0.044	0.044
2	Brick	0.142	0.142
3	Clear air cavity	0.200	0.200
4	Rigid Insulation	1.086	1.086
5	Plywood	0.174	0.174
7	Metal / insulation	2.284	0.002
8	Gypsum	0.094	0.094
9	Inside film	0.121	0.121

Load Calculation Applications Manual (SI), Second Edition

Then, Equation E.2 can be used to find the total resistance:

$$R_T = 0.454 \cdot 4.126 + (1 - 0.454)2.292 = 3.124 \text{ (m}^2\text{·K)/W}$$

Step 2: Calculation of the equivalent layer thermal resistance. The EHL resistance is given by Equation E.3:

$$R_{Hom} = R_T - \sum_{i=1}^N R_i \quad (\text{E.3})$$

$$R_{Hom} = 3.124 - 1.860 = 1.264 \text{ (m}^2\text{·K)/W}$$

Step 3: Calculation of the EHL thermal conductivity. The thermal conductivity of the equivalent layer is calculated using Equation E.5:

$$k_{Hom} = \frac{0.089}{1.264} = 0.0704 \text{ W/(m·K)}$$

Step 4: Calculation of the equivalent layer (composite layer) density. The volume fraction of the metal in the composite layer is determined from the metal stud parameters given in the problem description as follows:

$$y_{steel} = \frac{(89 + 2 \cdot 38) \cdot 1.5}{89 \cdot 400} = 0.007$$

Similarly, for the insulation section in a two-component composite layer, the volume fraction is given by

$$y_{insulation} = 1 - \frac{(89 + 2 \cdot 38) \cdot 1.5}{89 \cdot 400} = 0.993$$

The density of the equivalent layer is given by Equation E.6:

$$\rho_H = 7600 \cdot 0.007 + 14 \cdot 0.993 = 67.1 \text{ kg/m}^3$$

Step 5: Calculation of the equivalent layer (composite layer) specific heat. Using the volume fraction of the steel and insulation determined in step 4, the specific heat of the composite layer is determined as follows:

$$c_p = \frac{(7600 \cdot 0.50 \cdot 0.007 + 14 \cdot 0.71 \cdot 0.993)}{67.1} = 0.54 \text{ kJ/(kg·K)}$$

The thermophysical properties of the wall layers are summarized in Table E.4, with the EHL shown in bold.

Finally, once the EHL properties have been computed, conduction transfer functions or conduction time factor series can be readily computed using the layer-by-layer description.

Appendix E: Treatment of Thermal Bridges

Table E.4 Thermophysical Properties of the EHL Wall for Example E.1

Layers	Thickness, L, mm	Conductivity, W/(m·K)	Density, kg/m ³	Specific Heat, kJ/(kg·K)	Resistance, (m ² ·K)/W
Outside air film					0.044
Brick	100	0.72	1920	0.79	0.142
Clear air cavity	50	0.25	1.6	1.01	0.200
Rigid insulation	50	0.046	85	0.96	1.086
Plywood	19	0.12	540	1.88	0.174
EHL	89	0.07	67	0.54	1.264
Gypsum	0	0.16	800	1.09	0.094
Inside air film					0.121

References

- ASHRAE. 2004. ANSI/ASHRAE/IES Standard 90.1-2004, *Energy Standard for Buildings Except Low-Rise Residential Buildings*. Atlanta: ASHRAE.
- ASHRAE. 2005 *ASHRAE Handbook—Fundamentals*. Atlanta: ASHRAE.
- ASHRAE. 2013. *ASHRAE Handbook—Fundamentals*. Atlanta: ASHRAE.
- Gorgolewski, M. 2007. Developing a simplified method of calculating U-values in light steel framing. *Building and Environment* 42(1):230–36.
- Karambakkam, B.K., B. Nigusse, and J.D. Spitler. 2005. A one-dimensional approximation for transient multi-dimensional conduction heat transfer in building envelopes. *Proceedings of the Seventh Symposium on Building Physics in the Nordic Countries, The Icelandic Building Research Institute, Reykjavik, Iceland* 1:340–47.
- Nigusse, B. 2007. Improvements to the radiant time series method cooling load calculation procedure. PhD dissertation, School of Mechanical and Aerospace Engineering, Oklahoma State University, Stillwater.

Appendix F

Treatment of Uncontrolled Spaces

This appendix briefly describes treatment of unconditioned and/or uncontrolled spaces such as return air plenums, attics, crawlspaces, and attached garages. Whether for nonresidential buildings or residential buildings, the physics are the same. In either case, an estimate of the space air temperatures in the uncontrolled spaces is often needed to determine the heat flow between the conditioned space(s) and unconditioned space(s). There are several possible approaches:

- For heating load calculations, a simple conservative estimate that uninsulated, uncontrolled spaces are at the outdoor temperature may be sufficient.
- Using a steady-state heat balance, estimate the temperature at each desired condition (i.e., the heating design condition and each hour of the day for cooling load calculations). In some cases, it might be sufficient to estimate a single temperature for cooling load calculations; however, the temperature of an uncontrolled space will generally change throughout the day. This approach has the advantage of being feasible for manual or spreadsheet calculation. For cooling load calculations, it has the disadvantage of ignoring heat storage in the building fabric.
- Using a transient heat balance (i.e., the heat balance method [HBM]), compute the temperature of the uncontrolled space at each hour of the day for cooling load calculations. This approach can also be used for heating load calculations, but with the typical assumptions used in heating load calculations, it is effectively a steady-state calculation.

In considering which approach to use, three factors should be considered:

1. The importance of the heat transfer between the conditioned space and the uncontrolled space. Specifically, if the conductance between the two spaces is relatively small (i.e., if the surface dividing the two spaces is well insulated) and if the likely heat transfer between the two spaces is small relative to other heat gains, the simpler steady-state heat balance is probably appropriate.
2. The construction of the building, specifically the thermal mass, may be important in considering whether a transient heat balance is needed. If there is significant thermal mass between the outside and the uncontrolled space, a steady-state heat balance may be inadequate.
3. The likely space air temperature variation in the uncontrolled space over a cooling load calculation day may be important. If it is small, then the steady-state heat balance may be appropriate, regardless of other factors.

For example, consider an attic space in a conventionally constructed wood frame house. The space air temperature variation is large under most cooling load conditions, but the thermal mass of the surface between the outside and the uncontrolled space (composite shingles and plywood deck) is relatively small, so an hourly steady-state heat balance would be acceptable. Furthermore, if the attic floor is well insulated, the heat transfer rate will be relatively small, again suggesting that a steady-state heat balance will be adequate.

As another example, consider the space between an uninsulated 100 mm thick concrete roof deck and a suspended acoustical tile ceiling. Although such a construction could not be recommended from an energy perspective, it does serve as a good example of the need for a transient heat balance. In this case, the conductance between the unconditioned space and the conditioned space is high. There is significant thermal mass in the surface

separating the outside and the uncontrolled space (the 100 mm thick concrete roof deck), and a high space air temperature variation would be expected. So, a transient heat balance would be recommended in this case, unless the distance from the roof deck to the acoustic tile was small relative to the length and width of the roof. If the distance is small, it would be much simpler to treat the roof deck, air space, and acoustical tile as the layers of the exterior roof construction. On the other hand, if the distance is not small relative to the length and width of the roof deck, the side walls of the space might make an important contribution to the temperature, and, therefore, a transient heat balance would be recommended.

If a transient heat balance is necessary, the engineer should use a computer program that implements the HBM and that allows space air temperatures computed for uncontrolled spaces to be used as other side boundary conditions for conditioned spaces. For the majority of cases, a steady-state heat balance is adequate. An example follows.

Example F.1 Unheated Mechanical Room

A small mechanical room in a building is unheated. A plan view of the building is shown in Figure F.1 with the mechanical room labeled; the rest of the building is conditioned. Additional information about the building is given below.

The U-factors and areas are summarized in Table F.1. Additional building details are as follows:

- Under design heating conditions, the outdoor air is at -12°C and the conditioned space is at 21°C .
- The building is 3.66 m high and has a flat roof.
- The steel building is built on a concrete slab, which is uninsulated. The perimeter heat loss coefficient F_p is taken from Table 10.3 as $2.07 \text{ W}/(\text{m}\cdot\text{K})$.
- Infiltration in the uncontrolled mechanical room may be assumed to be 30 L/s.
- Atmospheric pressure is 101.325 kPa; specific volume of air at -12°C is $0.74 \text{ m}^3/\text{kg}$; c_p is $1.003 \text{ kJ}/(\text{kg}\cdot\text{K})$.

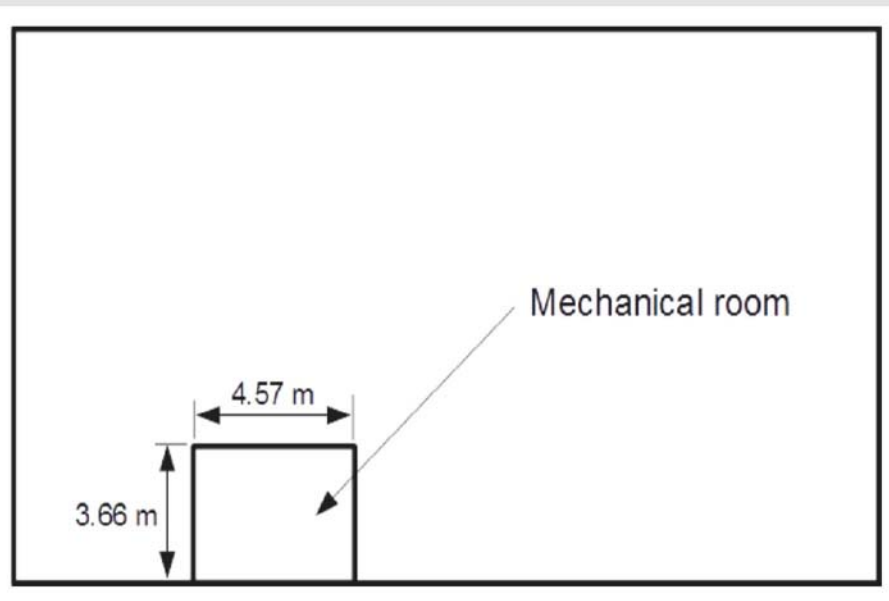


Figure F.1 Plan view of building with uncontrolled mechanical room.

Appendix F: Treatment of Uncontrolled Spaces

Under design heating conditions, find the temperature in the mechanical room and the heat loss from the conditioned space to the mechanical room.

Solution: A steady-state heat balance is performed by balancing all of the heat flows into and out of the mechanical room. These include conduction heat transfer from the conditioned space into the mechanical room, conduction heat transfer from the mechanical room to the outside, and infiltration heat loss.

Conduction Heat Transfer from the Conditioned Space into the Mechanical Room. As stated in Chapter 10, for above-grade surfaces, conduction heat losses are formulated in terms of a heating factor HF and the surface area A (Equations 10.1 and 10.2):

$$q = A \cdot HF$$

$$HF = U \Delta t$$

where HF is the heating load factor in W/m^2 .

Combining the two equations,

$$q = UA \cdot \Delta t \quad (F.1)$$

For the walls between the conditioned space and the mechanical room, the heat transfer from the conditioned space to the mechanical room is

$$q_{cs-mr, walls} = UA_{iw} \cdot (t_{iw} - t_b) \quad (F.2)$$

where

t_{in} = the inside air temperature, °C

t_b = the mechanical room air temperature, °C

UA_{iw} = the overall heat transfer coefficient for the interior walls, W/K

In addition, there will be a similar expression for heat transfer through the doors:

$$q_{cs-mr, doors} = UA_{id} \cdot (t_{in} - t_b) \quad (F.3)$$

where UA_{id} is the overall heat transfer coefficient for the interior doors in W/K.

There will also be a small amount of heat transfer from the conditioned space to the mechanical room via the slab, but we will neglect that.

Table F.1 U-Factors and Areas for Example F.1

Surface	$U, W/(m^2 \cdot K)$	A, m^2	$UA, W/K$
Roof	0.227	16.7	3.8
Exterior wall	0.397	12.8	5.1
Exterior (man) doors	3.407	3.9	13.3
Wall between conditioned space and mechanical room	0.454	41.5	18.8
Door between conditioned space and mechanical room	2.271	2.0	4.5

Conduction Heat Transfer from the Mechanical Room to the Outside. Similarly, for the wall between the mechanical room and the outside, the heat transfer is

$$q_{mr-o, wall} = UA_{ow} \cdot (t_b - t_o) \quad (F.4)$$

where t_o is the outdoor air temperature in °C.

Again, there will also be heat transfer through the doors, and there will be a similar expression for this:

$$q_{mr-o, doors} = UA_{od} \cdot (t_b - t_o) \quad (F.5)$$

where UA_{od} is the overall heat transfer coefficient for the exterior doors in W/K.

Likewise, for heat transfer through the roof,

$$q_{mr-o, roof} = UA_{or} \cdot (t_b - t_o) \quad (F.6)$$

where UA_{or} is the overall heat transfer coefficient for the roof in W/K.

The heat loss from the slab is given in Chapter 10 as the following (Equations 10.7 and 10.8):

$$q = p \cdot HF$$

$$HF = F_p \Delta t$$

where

q = heat loss through perimeter, W

F_p = heat loss coefficient per foot of perimeter, W/(m·K) (Table 10.3)

p = perimeter (exposed edge) of floor, m

Combining the two equations, the heat loss from the mechanical room to the outside via the slab is

$$q_{mr-o, slab} = p \cdot F_p (t_b - t_o) \quad (F.7)$$

Infiltration Heat Loss. For sea-level conditions, the infiltration heat loss is given by Equation 9.1c, which adapted to our situation, is

$$q_{infiltration} = 1.24(L/s)(t_b - t_o) \quad (F.8)$$

Heat Balance with No Internal Heat Gains. Assuming for now that there are no internal heat gains from equipment, a steady-state heat balance on the mechanical room air can be expressed in words as “the heat transfer rate into the mechanical room is equal to the heat transfer rate out of the mechanical room.” Or, as

$$q_{cs-mr, walls} + q_{cs-mr, doors} = q_{mr-o, walls} + q_{mr-o, doors} + q_{mr-o, roof} + q_{mr-o, slab} + q_{infiltration} \quad (F.9)$$

Then, substitute Equations F.2–F.8 into F.9 and solve for t_b :

$$t_b = \frac{UA_{iw}t_{in} + UA_{id}t_{in} + UA_{ow}t_o + UA_{od}t_o + UA_{or}t_o + pF_p t_o + 1.24(L/s)t_o}{UA_{iw} + UA_{id} + UA_{ow} + UA_{od} + UA_{or} + pF_p + 1.24(L/s)} \quad (F.10)$$

Appendix F: Treatment of Uncontrolled Spaces

Substituting in numerical values,

$$t_b = \frac{18.8 \cdot 21 + 4.5 \cdot 21 + 5.1 \cdot (-12) + 13.3 \cdot (-12) + 3.8 \cdot (-12) + 5 \cdot 2.07 \cdot (-12) + 1.24 \cdot 30 \cdot (-12)}{18.8 + 4.5 + 5.1 + 13.3 + 3.8 + 5 \cdot 2.07 + 1.24 \cdot 30}$$

$$t_b = -3.6^\circ\text{C} \quad .$$

The heat loss from the conditioned space to the mechanical room is determined by summing the heat transfer rates expressed in Equations F.2 and F.3:

$$q = UA_{iw} \cdot (t_{in} - t_b) + UA_{id} \cdot (t_{in} - t_b) = 18.8 \cdot (21 - [-3.6]) + 4.5 \cdot (21 - [-3.6]) \quad (\text{F.11})$$

$$q = 405 \text{ W}$$

F.1 Additional Heat Transfer Paths

Other types of spaces, such as return air plenums, may have heat gains from lighting or equipment, airflows from other spaces, etc. The general approach is as illustrated above, though additional terms may be introduced into Equations F.9 and F.10. One such example can be found in Section 8.5 of Chapter 8.

Appendix G

Correction Factor for High-Conductance Surface Zones

The radiant time series method (RTSM) generally performs as desired for a simplified cooling load calculation procedure—it has a small but acceptable amount of overprediction of peak cooling loads compared to the heat balance method (HBM). However, as shown previously by Rees et al. (1998), for zones with a significant amount of single-pane glass, the RTSM can overpredict the peak cooling load by as much as 37%. To a lesser degree, zones with significant amounts of double-pane glazing (Nigusse 2007) have overprediction as high as 14%. In theory, this could also be the case for other high-conductance surfaces, such as tents.

Nigusse (2007) developed a correction for zones that can be applied to the RTSM. It has been tested for a very wide range of test zones and can be applied to all zones or only to zones where significant overprediction is expected. The correction factor takes the form of a dimensionless conductance that is computed from the zone geometry, inside combined conductance, and overall U-factor of the fenestration. In addition, a slightly different value of radiative fraction is recommended for window solar heat gain.

G.1 Computation of Dimensionless Conductance

The dimensionless loss conductance is derived by Nigusse (2007). In the simplest form, for a room with one window, the dimensionless loss conductance is given as the following:

$$U^* = \frac{U_{window}}{h_{i,window}} \cdot \frac{A_{window}}{A_{room}} \tag{G.1}$$

where

- U_{window} = U-factor for the window, W/(m²·K)
- $h_{i,window}$ = inside surface conductance for the window, W/(m²·K); a typical value for a vertical window is 8.29 W/(m²·K) from Table 3.4
- A_{window} = window surface area, m²
- A_{room} = total interior surface area of the room, including furniture, m²

For a room with M windows, the dimensionless heat loss conductance would be given by the following:

$$U^* = \left(\frac{1}{A_{room}} \sum_{j=1}^M \frac{U_j A_j}{h_{i,j}} \right) \tag{G.2}$$

where

- U_j = U-factor for the j th window, W/(m²·K)
- $h_{i,j}$ = inside surface conductance for the j th window, W/(m²·K) (see Table 3.4)
- A_j = j th window surface area, m²
- A_{room} = total interior surface area of the room including furniture, m²

For windows with interior shades, the U-factor would include the resistance of the shade and the air gap. For zones with two exterior façades, the dimensionless loss conductance, depending on the glazing fraction, may range from 0.01 to 0.14.

G.2 Splitting Heat Gains into Radiative and Convective Portions

In Chapter 7, Section 7.7 describes the procedure for splitting the heat gains into radiative and convective portions and Table 7.10 gives the recommended splits. When using the correction factor, the procedure is identical, except that the recommended radiative fraction for solar heat gain through fenestration without interior shading is 0.9 instead of 1.0. Table G.1 is an excerpt from Table 7.10, showing the modified values of radiative and convective fraction.

G.3 Correction of the Radiant Time Factor Series

The heat loss is accounted for by correcting the first terms of the solar and nonsolar radiant time factor series (RTF series). The corrected terms, for solar and nonsolar radiant time factors, are given by the following:

$$r_{s,0,c} = (r_{s,0} - U^*) \quad (G.3)$$

$$r_{ns,0,c} = (r_{ns,0} - U^*) \quad (G.4)$$

where

- U^* = dimensionless loss conductance of the space
- $r_{s,0}$ = the first term of the solar radiant time factors
- $r_{ns,0}$ = the first term of the nonsolar radiant time factors
- $r_{s,0,c}$ = the corrected first term of the solar radiant time factors
- $r_{ns,0,c}$ = the corrected first term of the nonsolar radiant time factors

Once the first terms of the two RTF series have been corrected, they are used as described in Chapter 7 (Equation 7.7) to determine cooling loads from the radiative heat gains.

Example G.1 Correction Factor

As an example, consider the office used as an example in Section 8.2, with one significant modification: here, the double-pane windows have been replaced with single-pane windows. In order to determine the correction factor, we need to determine the UA of the windows, the interior surface conductance of the windows, and the total room interior surface area.

- The window U-factor, for single-pane windows, may be determined by summing the resistances of the three layers:
 - The exterior surface conductance for summer conditions from Table 3.4 is $22.7 \text{ W/m}^2 \cdot ^\circ\text{C}$ and the corresponding resistance is $0.044 \text{ m}^2 \cdot ^\circ\text{C} \cdot \text{W}$.
 - The single pane of glass, taking the conductivity as $56.8 \text{ W}/(\text{m}^2 \cdot \text{K})$ from Table 3.1, has a resistance of $0.018 \text{ (m}^2 \cdot \text{K)}/\text{W}$.
 - The interior surface conductance, from Table 3.4, is $8.29 \text{ W}/(\text{m}^2 \cdot \text{K})$, and the corresponding resistance is $0.12 \text{ (m}^2 \cdot \text{K)}/\text{W}$.
 - The sum of the three resistances is $0.182 \text{ (m}^2 \cdot \text{K)}/\text{W}$, and the U-factor is $5.49 \text{ W}/(\text{m}^2 \cdot \text{K})$.

Table G.1 Recommended Radiative/Convective Splits for Internal Heat Gains

Heat Gain Type	Recommended Radiative Fraction	Recommended Convective Fraction	Comments
Solar heat gain through fenestration without interior shading	0.9	0.1	

Note: See Table 7.10 for all other heat gain types.

Appendix G: Correction Factor for High-Conductance Surface Zones

- The total window area, as given in Table 8.2B, is 7.43 m².
- The total interior surface area, including exterior walls, interior partitions, windows, ceiling, floor, and furniture, at or below the level of the dropped ceiling is approximately 74.69 m².

The interior surface conductance for the windows is 8.29 W/(m²·K); this was originally taken from Table 3.4 and used to find the U-factor for the window.

Using Equation G.1, with the understanding that both windows have the same U-factor and same interior conductance, so the window area is simply taken as the total window area, the dimensionless loss conductance is

$$U^* = \frac{5.49}{8.29} \cdot \frac{7.43}{74.69} = 0.066$$

The dimensionless loss conductance is subtracted from the first value of the radiant time factors (RTFs). For this zone, the first value of the solar RTFs corresponding to the current hour is 0.53; rounding the dimensionless loss conductance to two decimal places, the new value is 0.53 – 0.07 = 0.463. Likewise, the first value of the nonsolar RTFs is 0.51, and subtracting the dimensionless loss conductance gives a value of 0.44. In addition, the radiative fraction of the window solar heat gain is decreased to 90%, as shown in Table G.1. When these three changes are made and the cooling load calculation is re-run, the peak cooling load is decreased by 4.0%. The hourly cooling loads calculated with and without the correction for losses are shown in Figure G.1. The loads calculated without the correction are labeled *Standard RTSM*; those with the correction are labeled *Improved RTSM*.

The correction is not very significant with this amount of single-pane windows. This zone has two exposed façades, and 39% of the façade area is window. If the zone description is modified so that 95% of the façade area were glazed, the dimensionless loss conductance would increase to 0.173. Using the correction factor would give a peak cooling load that was 12% lower, as shown in Figure G.2.

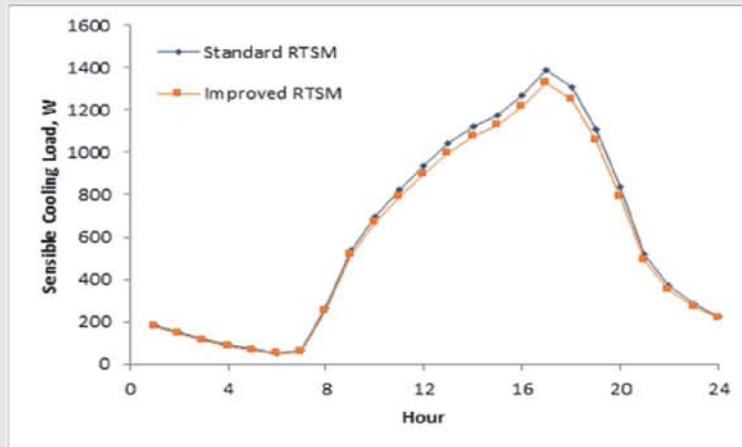


Figure G.1 Comparison of sensible cooling loads, with and without consideration of losses; 39% of the facade is glazed.

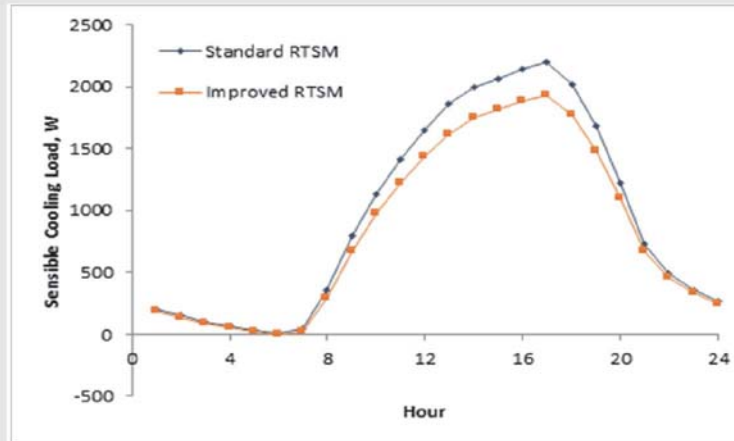


Figure G.2 Comparison of sensible cooling loads, with and without consideration of losses; 95% of the facade is glazed.

References

- Nigusse, B. 2007. Improvements to the radiant time series method cooling load calculation procedure. PhD dissertation, School of Mechanical and Aerospace Engineering, Oklahoma State University, Stillwater.
- Rees, S.J., J.D. Spitler, and P. Haves. 1998. Quantitative comparison of North American and U.K. cooling load calculation procedures—Results. *ASHRAE Transactions* 104(2):47–61.

INDEX

Index Terms

Links

A				
adiabatic humidification	232	274	275	
adiabatic mixing	243	276	278	
air density	107			
air distribution system	125	221	251	282
air system	235			
altitude	169	199	251	265
	267	271	304	322
	325			
angle correction factors	41	166	183	193
	288			
appliances	129	172		
ASHRAE headquarters building	177	185		
ASHRAE/IES Standard	90	131		
atmospheric boundary layer	112			
atmospheric pressure	265	267	271	304
	342			
attic	184	341		
 B				
ballast	131	151		
basement	19	184	248–9	
below grade	98	247	249	
buffer space	250			
building materials	24	116		
bypass factor	231			
 C				
clear sky model	199	321	324	
coefficients	111			
coil bypass system	241			
computers	139	181	207	

Index Terms

Links

conduction heat gain	13	20	22	155
	159	165-6	169	171-2
	179	184	196	199
	203	215	305	308
	311	333		
conduction heat transfer	15-7	19	27	215
	339	343-4		
conduction time series factors	20	158-9	164-5	176
	193	196	287	295
	308	315-7		
conductivity	16-7	29	38	87
	248-9	333	335	337-8
	348			
conference room	177	181	191	193
	214	252-3	293-4	348
convection heat transfer	21	259-60		
convective fraction	129	131	135	172
	291	305	348	
cooling coil	106	116	224-5	229
	231	238	240	271
	280	283		
cooling load	11-5	19	27	29
	91	95	106	129
	132	135	137	150
	151	155-7	159	166
	171-2	174	179-80	182
	192-3	196	199	204
	209-10	218	221	225
	227	234	235	240
	242	245	259	260
	261	263	280	281
	283	287	294	296
	297	300	302	311-2
	316	318	333	339
341	347-50			
cracks	105-7	115-6	118-20	124-5
crawlspace	341			
curtain wall	115-7	125	177	185

Index Terms

Links

D				
daily range	96–7	157	245	
daily temperature range	95–6			
declination	169	322		
dehumidifying coil	229	231		
density	19–20	29	40	107
	109	131	227	282
	306	333	335	337–8
design conditions	11	14	19–21	41
	91–5	97	100–4	157
	176	196	229	236
	246	252	268	289
	290	305		
dew point	229	232	238	241–3
	271			
door	116	118	120–2	124
	127	137		
draperies	41			
dry-bulb temperature	11	91	246	265
	268	273–4	277	281
	305			
E				
economizer	241	244		
enthalpy	92	238	265	267–8
	270	272–4		
equation of time	169	321		
equipment	11	14	23	27
	87	129	136–7	142
	151	171–3	181	184
	200	203–4	207	221–2
	224	232	236	241
	245–6	251	259	265
	281	291	306–7	311–3
	344–5			
equivalent homogeneous layer	333	335	338	
evaporative cooling	232	278–9		

Index Terms

Links

F				
fan power	222	225–6		
fenestration	29	41	87	156
	159	166	172	175
	179	184	192	196
	246	288–9	292	308
	321	326	347–8	
fog condition	280			
furniture	171	173–4	191–2	259
	261	308	347	349
G				
ground temperature	256			
H				
heat balance	11–5	20	26–7	38
	129	155	171	214
	216	245	255–63	315
	321	333	341	343–4
	347			
heat balance method (HBM)	11–5	20	23	25
	38	41	129	155–6
	255–8	261	263	315
	321	333–4	341–2	347
heat gain	13	20	22	41
	94	129	131	135–7
	139	150–2	155	156
	158–9	162	164–70	172–3
	179	181–2	185	194–7
	200	203	209	214–20
	225	251	259	264
	285–6	288–91	293	302
	305	308	311–2	333–4
	347–8			
heating coil	227	229	232	
heating conditions	113	271	343	
heating design conditions	41			

Index Terms

Links

heating load	11	14-5	19	29
	41	91	97	106-7
	197	221	227	245-6
	250-3	265	341	343
hospital equipment	129	139		
humidification	92	107	229	232
	243	268	274-5	280

I

index	165	262	293	
indoor air quality	106	221-2	227	234
	243	280-1		
indoor design conditions	91	246	290	
infiltration	14	27	95	105-6
	109	111	113	115
	117-25	127	171-2	184
	196	203-4	207	215-6
	218	246	250	252-3
	260-1	263	296	304
	311-3	342	344	
input parameters	179	287	298	300
	316	318	328	
insulation	19-20	29	40-41	87
	164	191-2	196	215
	248-9	251	285-6	333
	336-8			
interior attenuation coefficient	41	89		
internal heat gain	13-4	129	139	155
	157	166	171-3	176
	179	184	192	196
	200	203	245-6	251
	289-91	296	307	344

L

laboratory equipment	139			
lamps	130-1	151		
latent heat gain	129	291	306	311-3

Index Terms

Links

latitude	91 322	168	185	288
leakage	113 127	116 250	118	122
lighting	23 171–2 210 305–7	27 184 215–6 311–3	129–31 200 287 345	135–6 203–4 291
longitude	168	185	288	
luminaires	131	135		
M				
mechanical room	214	342–5		
mixing	12 234	21 243	223 267	225 276–8
moist air	227 280	265–72	274–6	278
motors	172	251		
N				
neutral pressure level	107	113	116	
O				
occupants	19–20 184 227 291	129 192 243	150 200 245–6	171–3 222 281
office	207			
office equipment	129	139	172	291
optical property data	41			
outdoor air	19 113 216 234–6 251	21 165 221 238	25 167 227–8 241	106 196 232 245–6 342
outdoor design conditions	91	246		

Index Terms

Links

P

people	23	27	120	122-3
	129	136	150	203-4
	227-8	245	251	258
	291	293	306-7	311-3
	185	192		
pilaster	185	192		
plenum	131	135	151	177
	184-5	192	204	210
	214-9	341	345	
plenum fraction	132			
pressure	92	105-13	116	120-2
	125-6	131	142	223
	225	236	251	265-8
	271-2	275	277	279-83
	304	342		
pressure coefficients	111	126		
pressurization	107	113	116	
psychrometric chart	221-5	231-2	235-6	238
	240	242-3	253	265
	267-8	270-1	273-5	278
	280-1			
psychrometrics	14	265	270	
R				
radiant	13	37		
radiant time factors	13	135	155	172-4
	176-7	17-84	193	209
	287-8	293	296-7	315-6
	318-9	348-9		
radiant time series method (RTSM)	11-4	20	23	37
	41	129	135	155-7
	172	175	184-5	193
	207	209-10	214	220
	255	261	264	287-8
	295	315-6	318	321
radiation heat transfer	333-4	339	347	350
	21	23	27	327

Index Terms**Links**

radiative fraction	129	131	136	207
	291	347-9		
reflectance	22-3	41	87	89
	196	259		
reheat system	240			
relative humidity	91	196	222	229
	232	235	242-3	246
	252	265	271-2	274-5
	279	290	305	
resistance	15-20	25	29-30	38
	40-1	108-9	156	164
	173	192	215	248
	285-6	333-8	347-8	
return	204	341		
return air plenum	151	177	184-5	192
	210	214-7	345	
revolving door	121-4	127		
roof	15	19	21	29
	37	41	87	111
	158-9	166	172	176
	183	185	191-3	196
	204	207	210	214-6
	218-9	261	287	305
	308	311-3	333	341
	342	344		
RTF	184	287-8	318	
R-value	17-8	333-4	336	

S

sensible cooling	184	209-10	219	232
	270	350		
sensible heat factor	106	216	222	224
	231	238	272-4	280-1
sensible heat gain	129	203	286	291
	306	311-3		
sensible heating	250	253	270	274-5

Index Terms

Links

shading	41	167–8	170–2	179
	185	193	199	203
	207	214	294	321
	326	348		
shortwave fraction	131			
single-pane glass	347			
slab-on-grade	19	252–3		
sol-air temperature	25	155	157	159
	165	183	193	196
	215–6	256	287–8	293
	295	308	321	327–9
solar	259			
solar angle	199	321	323	
solar heat gain coefficient	41	159	162	167–8
	170	172	183–4	191
	193–4	199	259	288
solar irradiation	21	157	183	287
	321	327–9		
solar radiation	19	23	25–6	41
	95	135	157	159
	165	169	173–4	193
	196	209	258–9	293
	321	327		
solar time	96–7	169	196	199
	321	328		
space heating	232			
spandrel	177	185	192–3	
specific heat	19	29	139	250
	268–9	333	335	337–8
specific volume	223	236	250	265
	268	271	279	282
	342			
splitting heat gain	171	348		
spreadsheet	155	157	159	164
	173–4	179	182–4	193
	196	220	245	287–8
	293	295	316–7	328
	341			

Index Terms

Links

ssure	116			
stack effect	105	107–10	113	125
standard conditions	106	251		
studs	159	192	333–5	
surface conductance	24–6	37	155–7	196
	252	287	317	327
	347–9			
surface heat balance	26	155	255	257
	264	321		
swinging door	120			
T				
thermal bridges	15	29	159	183
	192	333		
thermal conductivity	29	38	87	248
	335	338		
thermal property data	29			
transmission heat loss	246			
transmittance	22–3	41	89	159
	162	168	170	184
	259			
U				
U-factors	19	29	41	87
	184	196	248	252
	333	342		
uncontrolled spaces	184	214	341	
V				
venetian blinds	185	203	207	210
	219			
ventilation	106	113	127	227
	234	243	260	263
W				
wall	15–21	24–6	29–30	40–1
	98	106	109–11	113

Index Terms

Links

wall (*Cont.*)

115-7	124-5	127	156	
158-9	164-5	168	172-3	
175-7	179-80	183	185	
192-3	196	203	215-6	
218	245-6	248-9	252-3	
255-8	261-2	287	296	
305	308	311-3	333-6	
338	342-4	349		
wet-bulb temperature	95	230	265	274
	277-8	280		
wind effect	107	109		
wind speed	95	97	109	111-2
	125			
window	23	25	29	41
	105-6	116	118-9	124-5
	127	159	161-2	166-8
	170-4	177	179	183
	185	191	193	197
	199	203	207	214
	246	252	258-9	261
	264	287-8	293	296
	300	305	308	325
	327	347-9		